ENVIRONMENTAL CHANGE AND CATASTROPHIC FLOODING IN THE VOIDOMATIS AND AOOS BASINS, NORTHWEST GREECE

By

Robertson Henry Blacker Hamlin

Submitted in accordance with the requirements for the degree of Doctor of Philosophy

The University of Leeds
School of Geography

August, 2000

The candidate confirms that the work submitted is his own and that appropriate credit has been given where reference has been made to the work of others

CONTAINS

PULLOUT

ACKNOWLEDGEMENTS

The last three or four years have been full of highs and lows, joys and frustrations, happiness and anger. It is only with the support and help of colleagues, friends and family that I have been able to produce this thesis and emerge from all of these experiences feeling a sense of success and achievement.

I would like to thank my supervisors, Jamie Woodward and Adrian McDonald, for their sound advice and comments. I also thank everyone in the Graphics Unit, whose high standard of work has been of great benefit. Stuart Black has been kind to offer his advice with much of my analytical work and interpretations. I must also thank Simon Robinson, Mark Bateman, and Danien Lanforth for their help with laboratory analyses. I am grateful to Eleni Kotjalopolou and Takis Karkanas for their advice regarding Boila, and Phil Ashworth for passing on relevant literature. I also want to say a huge thanks to Pete Downs, whose inspiring teaching and vibrant approach to research got me started on this thing in the first place.

Fellow postgrads have helped continuously throughout my work. I must thank George Christopoulos for making my trip to Athens a pleasure and for helping me navigate the maze that is Greek bureaucracy. In terms of others, thanks to all those who have made me smile over the last few years: Jackie, Alma, Ruth, Dave, Suzie, Gary, Sarah and everyone else! Most important of all are my long-term office mates Steve Mardon and Claire Sedgwick. Steve has been a true and solid friend, always prepared to help, and regularly cheering me up with lines like "I do" and "Blimey". Claire has helped me with practically everything: fieldwork, writing, interpretations, and hockey skills!

The time I spent in Zaghori was wonderful. The landscape of the region is simply magnificent, and made even more special by the incredible hospitality and kindness of the local people. Special thanks go to all the people of Aristi, and in particular Nicos, Aphroidite and Alexandra, who made Claire and I feel so welcome during the field visits.

I would like to pay a special tribute to my cousin Larry Hamlin, who died mid-way through my PhD studies. I was inspired by his love and respect for the natural world, and in particular the beauty of mountain areas. His encouragement of my work in Baffin Island and latterly in Greece meant a great deal to me. I still find myself thinking about him now, and by doing so his influence remains with me today.

I feel very lucky to have such a caring family, who have been a huge help in so many ways. Mum, Dad and Lue, and adopted (!) family members Maureen and Martin, you have all been a great support, thank you. Finally of course there is Claire, who has brought so much joy and happiness to my life over the last 3 or 4 years. Her love means more to me than I can possibly explain here. She quite simply makes everything I do worthwhile.

ABSTRACT

Catastrophic floods are important events, particularly in the Mediterranean region, where they cause damage to life and property and have major effects on the landscape. Unfortunately, their violence and rarity means that investigating them using conventional hydrological monitoring is often not possible. This study uses palaeoflood hydrological techniques to extend flood records and further our understanding of the occurrence and effects of catastrophic floods in the Mediterranean region. Research has focused on the Voidomatis and Aoos basins; two steepland catchments in northwest Greece. Periods of catastrophic flooding are placed within the context of long-term environmental variability and landscape change, so that the environmental controls on catastrophic flooding, and the effects they have had in the development of these river systems can be fully understood.

The late Quaternary behaviour of the Voidomatis River has primarily been controlled by climatic conditions. Uranium-series dating results show that major phases of aggradation took place during the cold stages of the Late Pleistocene. Climatic amelioration in the Late-glacial and the Holocene periods reduced sediment supply and induced progressive incision until the last c. 1000 years or so, when prominent vertical accretion in the contemporary floodplain has occurred. Late Quaternary variations in fine-grained fluvial sediment sources are explored using a quantitative fingerprinting technique. These provenance data are shown to be valuable for reconstructing long-term changes in river activity.

Analyses of palaeoflood slackwater deposits provides evidence for the occurrence of two distinct periods of Late Pleistocene catastrophic flooding, at around 21 ka and 17 cal ka. Fine sediment provenance data enable a detailed analysis of catchment conditions at the time of these flood events. Glacial meltwater discharges and general climatic and hydrological instability during the last glacial-interglacial transition were important factors in generating these floods.

Palaeoflood information obtained from boulder berms and overbank floodplain sedimentation are combined with the short duration gauged data to develop a record of high magnitude flooding spanning the last 200 years. Catastrophic flooding is shown to reoccur at least every 40 to 50 years. Boulder berms record a decrease in the magnitude of extreme floods over this period, in response to hydrological changes induced by climatic warming following the end of the Little Ice Age (c. 1850 AD).

This is one of the first extensive applications of palaeoflood hydrology in the Mediterranean region. High magnitude floods over long timescales are shown to play an important role in the late Quaternary development and contemporary operation of these mountain catchments. This study illustrates the potential value of palaeoflood hydrological techniques to flood prone regions of the Mediterranean, where systematic hydrological data are inadequate for understanding and predicting extreme flood events.

CONTENTS

LIST OF FIGURES

Chapter 1

Chapter 2

Chapter 3

Chapter 5

Chapter 6

Chapter 7

LIST OF TABLES

Chapter 1

Chapter 2

Chapter 3

Chapter 4

Chapter 5

Chapter 6

Chapter 7

Chapter 8

LIST OF SYMBOLS

$C_{D'}$	Adjusted drag coefficient (from Fig. 3 in Helley, 1969, p. G4)
C_L	Lift coefficient (0.178)
D	Mean water depth (m)
F_D	Drag force (N/m^2)
F_L	Lift force (N/m^2)
F_R	Resisting force (N/m^2)
MR_D	Drag turning moment (from Helley, 1969, p. G4)
MR_L	Lift turning moment (from Helley, 1969, p. G4)
N	Newtons
Q	Mean water discharge (m^3/s)
S	Water surface slope and channel slope (these are usually assumed to be equal in palaeohydrology)
W	Channel width (m)
d	Particle diameter (mm, unless noted)
d_S	Shortest particle axis (mm, unless noted) (often referred to as c-axis)
d_I	Intermediate particle axis (mm, unless noted) (often referred to as b-axis)
d_L	Longest particle axis (mm, unless noted) (often referred to as a-axis)
d_{50}	Median particle diameter
g	Acceleration due to gravity (9.807 m/s)
n	Manning's resistance coefficient
q_c	Critical water discharge per unit channel width
τ	Bed shear stress (N/m^2)
τ^*	Sheilds' dimensionless shear stress
v	Mean flow velocity (m/s)
v_b	Bottom or bed velocity (m/s)
ω	Unit stream power (N/m/s)
γ	Specific weight of water (9 807 N/m^3)
γ_s	Specific weight of particles (25 970 N/m^3)
μ	Coefficient of static friction (0.7)
χ	Low-frequency mass-specific magnetic susceptibility
$\%\chi_{fd}$	Frequency-dependant magnetic susceptibility

LIST OF ACRONYMS

FFMI	Flash Flood Magnitude Index of Beard (1975)
OKB	Old Klithonia Bridge
OIS	Oxygen Isotope Stage
OISst	Oxygen Isotope Substage
OSL	Optically-Stimulated Luminescence
PSI	Palaeostage Indicator
STD	Standard Deviation
SWD	Slackwater Deposit
XRD	X-ray Diffraction
XRF	X-ray Fluorescence

1. INTRODUCTION

1.1 RIVER SYSTEMS AND ENVIRONMENTAL CHANGE

River catchments are one of the most important components of the physical environment, but they are sensitive systems, in which process and form can rapidly alter in response to environmental change (Schumm, 1977; Knighton, 1998). Climatic variations, changing vegetation characteristics, tectonic movements, and anthropogenic activity can all have profound effects on the behaviour of streams and rivers. This is important, because human activities are often dependent upon fluvial environments, which are heavily utilised in many ways, including navigation, agriculture and resource exploitation (Penning-Rowsell *et al.*, 1986; Boon *et al.*, 1992; Newson, 1997; Smith and Ward, 1998). There are often high population densities around river channels and floodplains, as these areas may offer a constant supply of water and generally constitute the most fertile and accessible parts of the landscape (Smith and Ward, 1998). For human development to be successful and sustainable adjacent to river environments, it is important that the dynamics of rivers are well understood. Continuing and increasing levels of human modifications to river catchments and the prospect of global warming mean that the ability to reliably predict river response to environmental modifications is increasingly important (Knighton, 1998).

For many years geomorphologists have sought to explain how river systems have developed through the geological and historical past. Early philosophies focused catastrophic explanations of landform development, until the 19th century when notions of uniformitarianism and gradualism became more prominent (Knighton, 1998). In his classic cycle of erosion, Davis (1899) suggested that landforms develop gradually through time, driven by physical processes acting to slowly reduce relief. However, in the latter part of the 20th century there has been increasing realisation that rivers are dynamic systems, influenced by numerous controlling factors which are variable through time, and thus simple progressive change is unlikely to have occurred. Whilst rivers may seek to establish a form which is adjusted to the prevailing hydrological and sedimentological conditions (i.e. an equilibrium state) (Chorley, 1962), there can be numerous disturbances which can induce a change in form. Brunsden and Thornes (1979) describe how such disturbances can be of a sudden 'pulsed' nature, such as extreme flood events, or of a more progressive 'ramped' nature, such as variations in climate. Disturbances leave the river in a state of disequilibrium, with adjustment requiring a certain length of time (the 'relaxation time') before equilibrium can be re-established.

However, because rivers are evidently sensitive systems that undergo frequent disturbances, it has been argued that genuine equilibrium states are rarely established (Bull, 1979; Phillips, 1992; Ferguson, 1993). Instead, rivers are characterised by variability and

dynamism. In addition, it has become widely recognised that fluvial response to environmental disturbances can be complex through space and time, controlled by the variable interaction of numerous physical parameters, thresholds, sensitivities and modes of adjustment (Schumm, 1973, 1977; Brunsden and Thornes, 1979; Petts, 1979; Phillips, 1991). Whether disturbances to river systems have important effects is partly determined by whether thresholds are exceeded or not. Schumm (1973, 1977) identifies two types:

i) intrinsic thresholds, where inherent features of geomorphic systems evolve to a critical state where adjustment occurs, and;

ii) extrinsic thresholds, where changes result from sufficient external disturbance by factors such as natural- and human-induced environmental change.

As extrinsic controls such as climate and land-use are fundamental driving mechanisms behind changes in the fluvial environment, it is important that they are understood (Knighton, 1998).

There have been many studies of river system responses to environmental change, focusing on different geographical areas, different physical processes and forms, and different timescales. For example, it has been shown that the last glaciation had dramatic effects on many rivers, causing major changes in geometry, sediment load and hydrological regime (Lewin *et al.*, 1995a; Knox, 1995). Over historical timescales, it is known that only quite modest climatic shifts (1 - 2°C change in mean annual temperature and ≤10 - 20% mean annual precipitation) have resulted in major changes in the frequency and magnitude of flooding (Knox, 1993; Ely, 1997). Over the last few thousand years, and particularly the last few centuries, human-induced changes in catchment environments have had profound effects on river systems. Direct disturbance such as dam construction, gravel extraction and river channelisation, and wider changes in land-use, particularly forest clearance and urbanisation, have all greatly disrupted river behaviour and sediment yields (e.g. Wolman, 1967; Petts, 1979; Brookes, 1987).

Environmental changes, whether natural or anthropogenic, impact on river systems by changing their hydrological regime and/or sediment load, which can in turn result in major changes in fluvial activity and form. With widespread human development associated with rivers and floodplains, understanding these environment-river linkages has become an important issue. An appreciation of the historical dimension of rivers and the ability to analyse (and hence anticipate) change over time are two of the main ways that geomorphology can make an effective contribution to sustainable river basin management (Macklin and Lewin, 1997; Knighton, 1998).

1.2 MEDITERRANEAN RIVER ENVIRONMENTS

Rivers in the Mediterranean basin have many characteristics that predispose them to being particularly sensitive and fragile environments in comparison to many parts of the world (Woodward, 1995). The region contains extensive outcrops of soft sedimentary rocks, whose slopes are easily eroded and modified by hydrological processes. The high relief of the

Mediterranean basin means that hillslopes and river channels tend to have steep gradients, which accentuate erosive forces (Woodward, 1995). Additionally, the region is prone to intense storms (Wainwright, 1996) and flashy, high magnitude flood events which can accomplish major channel change (Poeson and Hooke, 1997). These characteristics have made the effects of environmental change on Mediterranean river systems particularly prominent. In general terms climatic oscillations over the Pleistocene and Holocene have resulted in alternating periods of hillslope sediment production and river alluviation, followed by slope stability and valley incision (e.g. Vita-Finzi, 1969; Lewin *et al.* 1991; Fuller *et al.*, 1996; Harvey, 1996; Rose and Meng, 1999). More minor, recent climatic changes have also had significant effects, changing the characteristics of river sedimentation (Ballais, 1995; Grove, 1997) and the frequency and magnitude of flood events (Benito *et al.*, 1996). Alongside these climatic changes, Mediterranean river environments have experienced a exceptionally long history of anthropogenic disturbances. Human-induced environmental change can be traced back to Neolithic agriculture around 8000 BC (Macklin *et al.*, 1995), and since then large-scale vegetation destruction and land misuse, which accelerated rapidly in classical times, have been shown to have stimulated considerable alterations in river forms and processes (van Andel *et al.*, 1986, 1990). The Mediterranean is also a zone of active tectonic movements (Dewey *et al.*, 1973; Bailey *et al.*, 1993), which can also play a major role in the behaviour of the region's rivers (Harvey and Wells, 1987; Collier *et al.*, 1995; Kuzucuoglu, 1995). This combination of dynamic and capricious environmental conditions with fragile and sensitive river systems means that an understanding of fluvial responses to environmental change is likely to be of particular importance for managing rivers in the Mediterranean region. This is exemplified by the fact that two of the most serious environmental problems facing the region, increasing evidence for land degradation and catastrophic flooding (Poeson and Hooke, 1997), both revolve around concerns regarding changes in the characteristics of river catchments over time.

Considerable research and debate has focussed on the serious problem of land degradation and desertification in certain parts of the Mediterranean region (e.g. Brandt and Thornes, 1996). Whilst the inherent fragility of parts of the Mediterranean landscape undoubtedly results in a natural vulnerability to erosion (Woodward, 1995), there is considerable evidence for human activity having increased the extent and intensity of land degradation (Grennon and Batisse, 1989; Dedkov and Mozzherin, 1992; Milliman and Syvitski, 1992). In comparison to land degradation, comparatively little is known about the problem of catastrophic floods, their occurrence and effects, and whether or not environmental changes are making these events larger and more frequent.

1.3 CATASTROPHIC FLOODING IN THE MEDITERRANEAN REGION

There are many important human and physical consequences of catastrophic floods (Baker, 1993). The operation and form of river systems as a whole can be dramatically altered (Mayer

and Nash, 1987), with large water and sediment discharges resulting in loss of life and property within the valley floor (Figure 1.1). Furthermore, there has been increasing concern about an unusually large number of catastrophic floods reported in and around the Mediterranean region over the last few years (Table 1.1).

FIGURE 1.1 A catastrophic flood during the summer 1996 in the mountains north of Pisa, Tuscany, Italy. The flood occurred due to >45 mm of rain falling in under 4 hours. During its peak stages the flood washed away cars and other large debris (left image), and killed 14 people. After the event, the erosion and sedimentation caused by the flood were particularly clear. Many mountain roads were destroyed, leaving villages cut off for several days. Buildings and cars caught in the path of the flood had been partially buried by flood sediments (right image). *(Source: ITV Television "The Raging Planet").*

TABLE 1.1 Examples of recent catastrophic floods in the Mediterranean region. *(Sources: [1]Benito et al., 1998; [2]López-Avilés, 1998; [3]Poesen and Hooke, 1997; [4]Johnstone, 1997; [5]http://news.bbc.co.uk/)*

Location	Date	Deaths	Other known effects
Northeast Spain[1]	1994	9	
Po River, NW Italy[2]	November 1994	100	
Central Spain[1,2]	August 1995	10	
Morocco[3,4]	August 1995	136	Extensive destruction and land degradation
Tuscany, Italy[2]	June 1996	14	Villages and roads destroyed
Biescas, Spanish Pyrenees[1]	August 1996	87	Campsite swept away
Central Greece[5]	January 1997	3	Widespread economic damage
Alicante, eastern Spain[1]	1997	5	$75 million losses
Badajoz, Spain and Portugal[1,3]	1997	34	$300 million losses
Nr. Naples, Italy[3]	May 1998	> 100	
Athens, Greece[5]	March 1998		Roads blocked, evacuations, major damage and economic costs
Northwest Turkey[5]	May 1998	> 10	Thousands left homeless

Unfortunately, there is a serious lack of data on high magnitude flood events in the Mediterranean, as systematic measurements of rainfall and discharge are of a poor spatial coverage and records typically only cover a few decades (Poeson and Hooke, 1997). Such limited and short gauged records are inadequate to properly assess the occurrence of rare, catastrophic floods. Unfortunately, data is most scarce in the type of river catchments that are most prone to catastrophic floods. Following Macklin *et al.* (1995), four main types of Mediterranean river environment can be identified:

1. Steepland river systems.

2. Alluvial fans.
3. Basin and range environments.
4. Coastal alluvial plains and deltas.

Due to widespread mountainous relief in the Mediterranean basin (Figure 1.2), steepland river systems drain the majority of the region (Macklin *et al.*, 1995). These are the areas mostly likely to produce extreme discharges, yet they have the shortest and most infrequent gauged records. It is also unfortunate that the dynamics of mountain rivers tend to be less well understood (Jarrett, 1990a), and until recently in the Mediterranean most fluvial geomorphological research had been conducted on alluvial fans or in basin and range environments (Lewin *et al.*, 1995b). Not only is the occurrence and production of catastrophic floods in the Mediterranean poorly understood, but their geomorphic importance and effects on the mountain river systems in the region also remains unclear (Poesen and Hooke, 1997). However, with growing populations the demands on the resources of mountain areas are increasing (Grennon and Batisse, 1989; Jarrett, 1990a), and thus the environmental variables controlling fluvial processes such as high magnitude flooding in these areas need to be understood. This requires the assimilation of long term flood records and investigation of the historical and longer-term responses of these steepland catchments to environmental change (Jeftić *et al.*, 1996; Smith and Ward, 1998).

In the absence of historical or documentary records, sedimentary evidence for floods may offer a valuable opportunity to extend flood records (Lewin *et al.*, 1995b). Fortunately, flood deposits are frequently well preserved in steepland catchments (Jarrett, 1990a). As they document floods which occurred prior to direct measurement or observation, they are frequently termed 'palaeoflood deposits', with 'palaeoflood hydrology' being used to describe this type of investigation (Baker, 1987). Palaeoflood deposits have been extensively studied in the United States and Australia (Kochel and Baker, 1982; Baker *et al.*, 1983a; Baker and Pickup, 1987; Knox, 1988, 1993), and there are only a few recent examples of this type of research in the Mediterranean region (Benito *et al.*, 1998; Greenbaum *et al.*, 1998; Lopez-Aviles, 1998). However, the value and applicability of palaeoflood hydrology to further our knowledge of the operation of Mediterranean mountain rivers requires more extensive study.

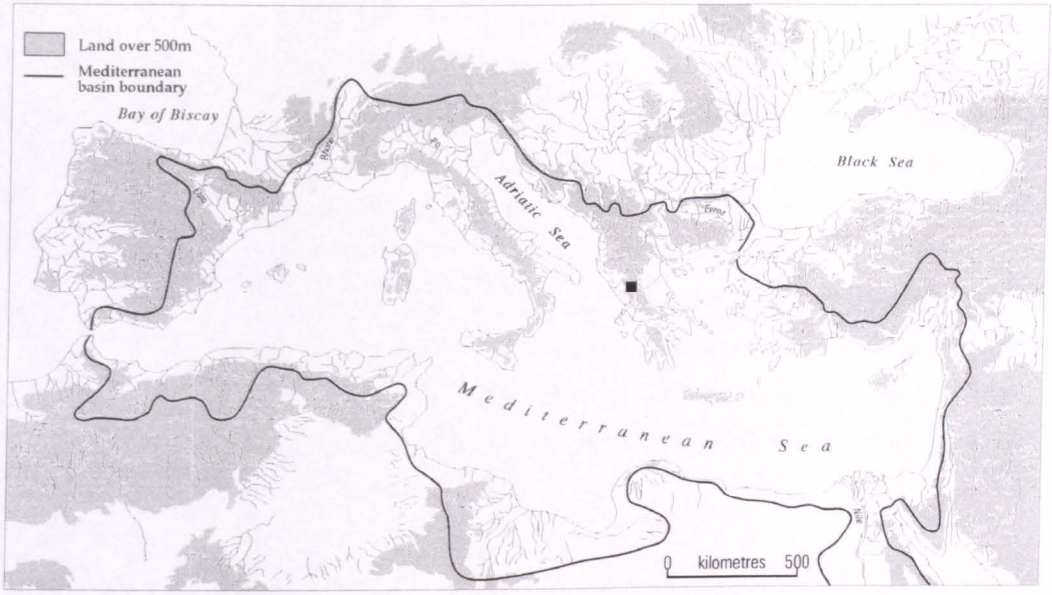

FIGURE 1.2 Relief and river drainage network of the Mediterranean basin. The 500 m contour is used as a divide between uplands and lowlands in Milliman and Syvitivki's (1992) classification of world rivers (Woodward, 1995). The location of the Voidomatis and Aoos basins in Epirus, northwest Greece is shown (identified by ▪) *(Modified slightly from: Macklin et al., 1995)*

1.4 THESIS AIMS, SCALE AND OBJECTIVES

The overall aim of this thesis is to investigate the occurrence of catastrophic flooding within the context of environmental variability and landscape change, focusing on two mountain catchments in the Mediterranean basin. This will further knowledge on the production, temporal variability and geomorphic effects of extreme flood phenomena, with the results from these two study catchments having wider implications for Mediterranean mountain catchments in general. Spatial and temporal scales need to be carefully considered in geomorphological studies (Schumm and Lichty, 1965). The spatial and temporal scope of this study is outlined below, followed by a detailed definition of the research objectives.

1.4.1 Spatial Scale and selection of study area

The Voidomatis (384 km^2) and Aoos (665 km^2) catchments in Epirus, northwest Greece have been selected for this study (Figure 1.2). These catchments share a common watershed and are situated on the western side of the Pindus Mountain range. They have many of the characteristic features of steepland Mediterranean river systems (*sensu* Macklin *et al.*, 1995), with high gradient hillslopes and coarse cobble- to boulder-bed channels. This fluvial setting is conducive to catastrophic flooding due to flashy storm hydrographs, rainfall intensified by local orographic effects, and, in the northern parts of the Mediterranean, significant volumes of spring snowmelt. Catchments of this type were therefore appropriate for this study. The Voidomatis and Aoos Rivers flow through a number of deep bedrock canyons, which are often ideal settings for the

preservation of geomorpholoigcal evidence for catastrophic flood events (Kochel and Baker, 1982, 1988, Baker and Kochel, 1988). Whilst palaeoflood evidence has previously not been specifically investigated on these rivers, there does exist a valuable background of research into the alluvial history of the Voidomatis basin (Lewin *et al.*, 1991), upon which this study builds. There is also a considerable volume of local and regional palynological data (e.g. Tzedakis, 1993, 1994; Turner and Sánchez Goñi, 1997; Willis, 1997) and archaeological evidence (e.g. Higgs *et al.*, 1967; Bailey 1997a, 1997b) which have been used to reconstruct changes in the palaeoenvironment of these catchments over time. Both catchments are large enough to offer a wide choice of potential study sites whilst maintaining their steepland character. The selection of two rivers provides the opportunity to incorporate any between-catchment variability in catastrophic flood occurrence.

1.4.2 Temporal Scale

High magnitude flood events can be important processes in the operation of river systems over various temporal scales, ranging from large scale, persistent landscape changes caused by Late Pleistocene floods (e.g. Baker and Bunker, 1985; Bull, 1988; Coxon *et al.*, 1996) to the more immediate effects which can be observed after contemporary events (e.g. Harvey, 1984a; Carling, 1986; Inbar, 1987). However, attempting to study flooding over the entire late Quaternary was beyond the scope of this study, due to logistical considerations, the nature of the stratigraphic record and the availability of dating techniques. To investigate the occurrence of catastrophic flooding through changing environmental conditions, this study focuses on two specific time periods that were identified as being important:

1.4.2.1 The last 200 years

As gauged flow records in the Mediterranean are generally very short (typically 30 - 40 years at best), it is important to extend these flood records so that rare, catastrophic flood phenomena can be more fully understood. The last 200 years is a suitable timescale over which to extend stream records, in an attempt to improve the reliability of extreme flood recurrence and magnitude estimations, and to provide data to assess the geomorphic significance of these events in Mediterranean steepland rivers. This period also encompasses environmental changes that are of great significance to the present and future management of European river catchments. During the middle part of the last millennium Europe experienced a series of cold episodes which are collectively referred to as the 'Little Ice Age' (Grove, 1988; Bradley and Jones, 1992). The most recent cold Little Ice Age period saw particularly severe conditions from c.1700-1850, after which there has been a general warming in climate (Bradley and Jones, 1992). This climatic variation has been shown to have caused major changes in flood hydrology (Knox, 1984, 1988; Benito *et al.*, 1996; Ely, 1997). The magnitude of temperature and rainfall variations over this time are comparable to those predicted for approximately the next 40 years (Knox, 1993; Houghton, 1997), and therefore the study of extreme floods over this timescale

may provide a useful analogue for the effects of future climate change on flood occurrence (Rumsby and Macklin, 1996). The last 200 years has also seen major anthropogenic disturbance of upland landscapes in the Mediterranean (McNeil, 1992), and such human influences need to be evaluated along with climatic changes to understand their potential role in catastrophic flood occurrence.

1.4.2.2 The Late Würm (c. 25 - 10 ka)

This is the most recent period of major climatic transition from full glacial to interglacial conditions. Many mountain environments in the Mediterranean supported small valley and cirque glaciers at the Last Glacial Maximum (LGM) (Messerli, 1967) and the last glaciation had profound impacts on many Mediterranean river systems (Lewin *et al.*, 1995a). Following the LGM, there was major climatic amelioration until the onset of the warm Holocene at c. 10ka (Thouveny *et al.*, 1994). This change from glacial to interglacial conditions was therefore a period of large-scale hydrological, climatic and geomorphological instability and adjustment (Knox, 1995). High magnitude flooding is likely during such climatic transitions (Knox, 1988, 1993; Ely *et al.*, 1993), particularly considering the extensive meltwater discharges which resulted from the decay of mountain glaciers and snowpacks after the LGM in the Mediterranean region (e.g. Zonneveld, 1996; Zonneveld and Boessenkool, 1996). Such extreme floods may have played an important role in the landscape changes which occurred during this latter part of the Pleistocene, with rivers in the in the Mediterranean experiencing large changes in the sedimentation style (e.g. Lewin *et al.*, 1991; Roberts, 1995; Maas *et al.*, 1998).

1.4.3 Research objectives

There are four key objectives for this study in the Voidomatis and Aoos basins:

- To investigate changes in catchment characteristics and river activity in response to environmental variations over the Late Pleistocene and Holocene, encompassing both the last 200 years and the Late Würm. This will build on the work of Lewin *et al.* (1991) by mapping new areas, and applying recently developed methods for dating and interpreting alluvial stratigraphy. This will provide a well-constrained history of long-term changes in river behaviour, which can be compared with the occurrence of catastrophic flood events.
- Numerous studies have shown that, in complement to Quaternary dating techniques, detailed analyses of alluvial sediment composition can provide valuable information on catchment conditions and sediment sources (Foucault and Stanley, 1989; Woodward *et al.*, 1992; Rose and Meng, 1999). This study aims to develop a quantitative sediment fingerprinting technique (*sensu* Peart and Walling, 1986; Woodward and Walling, 1995), which can be used to investigate the variations in fluvial fine sediment sources over the Late Pleistocene and Holocene. Where possible this will be used in conjunction with geochronological data to provide a closer link between changes in the catchment environment and river activity and flood sedimentation.

- To investigate the occurrence of catastrophic flood events over the Late Würm, and:

  a) Establish the timing of catastrophic floods over this period, and the environmental conditions associated with their generation.

  b) Elucidate the likely geomorphological effects of these catastrophic flood events in the context of changes in river behaviour over this period.

- To establish a history of catastrophic flood events over the last 200 years by combining evidence from systematic gauged hydrological data and the geomorphological record of palaeoflood deposits. These data will used in three ways:

  a) To investigate temporal variability in the frequency and magnitude of extreme flood events, and to establish whether or not they are becoming larger and more frequent.

  b) To determine the environmental controls associated with extreme flood occurrence by assessing the influence of meteorological processes (synoptic conditions), climatic shifts, and anthropogenic landscape disturbances.

  c) To consider the significance of catastrophic flood events in the recent geomorphological development of these river systems.

1.5 THESIS OUTLINE

Chapter 2 provides information on the key principles and issues involved in this research. Palaeoflood hydrological techniques are reviewed and assessed, and the potential applications of long-term flood records are outlined. A detailed discussion of Mediterranean river environments is also presented. *Chapter 3* describes the characteristics of the Voidomatis and Aoos basins, placing them in regional context, and paying particular attention to the local flood hydrology. *Chapter 4* presents the approaches and methods that have been used in this study, including data sources and acquisition, field techniques and analytical procedures. *Chapter 5* describes the development of the quantitative fingerprinting procedure, and presents data to assess the validity of the technique. *Chapter 6* documents the Late Pleistocene and Holocene development of the Voidomatis River basin, and discusses potential linkages between environmental changes and river behaviour. *Chapter 7* then discusses the occurrence and effects of catastrophic floods over the Late Würm, evaluating the environmental controls on their generation and their effects on the development of the Voidomatis River. *Chapter 8* addresses similar issues, but over the last 200 years and for both the Voidomatis and Aoos Rivers. The extended flood records are also used to assess recent trends in the occurrence of catastrophic floods that are relevant to contemporary management issues such as flood control and prediction. *Chapter 9* presents the conclusions of this study, discusses the benefits and limitations of the research approach, and identifies some areas for future study.

2. PALAEOFLOOD HYDROLOGY: TECHNIQUES AND APPLICATIONS FOR THE MEDITERRANEAN REGION

Catastrophic floods are important events in the Mediterranean region, as they cause damage to life and property and have major effects on the landscape. Unfortunately, their violence and rarity means that investigating them using conventional hydrologic monitoring is often not possible. Nonetheless, sound estimates of their frequency and magnitude are needed for structural designs and risk analyses, and for assessing their geomorphic importance in shaping Mediterranean valleys. In addition, the environmental controls on their frequency and magnitude need to be understood so that the variability in the flood producing system can be incorporated into current and future predictions of extreme flood recurrence. By extending conventional gauged records, palaeoflood hydrology offers an opportunity to assess the occurrence and variability of catastrophic flooding.

This chapter reviews current knowledge of palaeoflood hydrology and then discuses its potential application in Mediterranean environments. This review has guided the direction and the structure of this study by identifying gaps in our understanding and appropriate data collection methods. It provides a basis for study area selection, as well as for the development of a research methodology (Chapter 4). It also facilitates an analysis and discussion of the results (Chapters 5 to 8) in the light of current knowledge. Sections 2.2 and 2.3 provide a working guide to some of the most useful palaeoflood reconstruction techniques, outlining research procedures and assessing their reliability. Section 2.4 then describes the ways in which palaeoflood data may be used to redress uncertainty regarding low frequency high magnitude floods. Finally, section 2.5 describes the significance of catastrophic flooding as an environmental phenomenon in the Mediterranean region.

2.1 INTRODUCTION TO PALAEOFLOOD HYDROLOGY

2.1.1 Definitions

Palaeoflood hydrology is the study of past or ancient flood events that occurred prior to the time of human observation or direct measurement by modern hydrologic procedures (Baker, 1987, p. 79). This differentiates it from flood analysis based on either systematic (i.e. measured) or historical data. Palaeoflood hydrology studies generally aim to determine either the timing and/or magnitude of palaeoflood events, hence such research is frequently termed *palaeoflood reconstruction.*

A *flood* has been defined by Ward (1978) as:

> "a natural body of water which rises to over flow land which is not normally submerged."

However, there are less widely accepted definitions of *catastrophic flooding* in the geomorphological literature. Abrahams and Cull (1979) describe how, from a geomorphological perspective, a flood is catastrophic by virtue of its magnitude, not directly its frequency. They propose an arbitrary definition of a flood with a peak discharge equal to or greater than four times the discharge of the mean annual flood. Erskine (1993, 1994) and Erskine and Livingstone (1999) have also considered this problem in New South Wales and found a ratio of at least 10 times greater is more appropriate, as such floods totally destroy the pre-flood channel whereas smaller floods do not cause such extensive or persistent landscape changes in these environments. However, this does not overcome the problem of defining what constitutes a catastrophic flood in ungauged or poorly gauged catchments, where the mean annual flood discharge (and perhaps also the event discharge) cannot be reliably determined. This problem often arises for mountain catchments in the Mediterranean, so a more qualitative definition is required for this study. A number of more general definitions of catastrophic floods have been proposed:

> "events of extremely rare occurrence that produce a major modification of fluvial morphology" (Baker, 1977);
>
> "devastating high magnitude low frequency flow events" (Mayer and Nash, 1987);
>
> "those floods at the large and rare end of the range" (Baker, 1993);
>
> "large perturbations of the magnitude-frequency distribution of flood flows" (Erskine and Saynor, 1996);

In line with these definitions, a catastrophic flood in this study is considered to be any flood event that is of exceptional magnitude relative to ordinarily observed flows. Such floods will have had the potential to produce widespread and long lasting morphological change, although the use of the term *catastrophic* in this study primarily refers to the exceptional magnitude (and often low frequency) of these events. Thus for the purposes of this study, a catastrophic flood does not necessarily have to involve the loss of life and property.

2.1.2 The importance of palaeoflood hydrology studies

Flooding is a fundamental physical process, having implications ranging from cultural and economic, to hydrologic and geomorphic. World-wide human and economic losses as a result of floods are staggering. Data released by the Office of US Foreign Disaster Assistance (1996, in Smith and Ward 1998) for 835 floods that occurred outside the USA since 1964, show that over 130,000 people have been killed, 70 million made homeless and that over US$ 91 billion was incurred in economic costs. In addition, floods may exert a major control on agricultural practices (Penning-Rowsell *et al.*, 1986; Smith and Ward, 1998), and whole landscapes may be reshaped by their effects (e.g. Baker and Bunker, 1985). Baker (1993, p. 402) describes flooding as:

> "...arguably the most pervasive, diverse and destructive of all natural hazards."

He goes on to emphasise that,

> "...we are suffering increasing damage to life and property from catastrophic floods."

It can be argued that the most serious flood phenomena are catastrophic events. Unfortunately, systematic records are rarely long enough to provide adequate data to assess their likelihood of occurrence or temporal and spatial variability (Costa, 1978a; Jarrett, 1991). Thus catastrophic floods present an unenviable problem for catchment management. They present the greatest flood risk, yet they are the hardest to predict. Estimates of their magnitude and frequency are the most commonly needed for engineering design and floodplain management (Jarrett, 1991), but they are the least well documented flow events in conventional data. Perhaps it is not surprising that a perception exists among much of the public that large floods essentially occur randomly, and that we have little hope of predicting their occurrence (Zawada, 1997). However, recent advances in techniques for obtaining palaeoflood data offer the potential to overcome some of the uncertainty surrounding catastrophic flows (Baker, 1987; Stedinger and Baker, 1987). Palaeoflood hydrology can provide quantitative flood information over the long timescales (10^2 – 10^4 years) required to understand rare catastrophic events. Thus conventional stream records can be extended and flow records constructed for ungauged catchments. The resulting long flood records are potentially of great value for investigating and predicting floods. Three main problems may be addressed by collecting palaeoflood data: -

1. Uncertainty regarding flood-frequency estimations, especially the 100- or 200-year flood, which is difficult where systematic records are short or absent (Zawada, 1997).
2. Uncertainty regarding the effects of environmental change on flood frequency and magnitude. Longer-term hydrological data can give greater insight into the complexity and variability of the flood-producing system (Jarrett, 1991).
3. Uncertainty regarding the relative importance of rare catastrophic floods in landscape evolution. Extreme events, occurring beyond the systematic flood record, may play a fundamental role in the operation of certain river systems (Baker, 1977; Gupta, 1983), however the lack of conventional data on the long-term occurrence of these floods precludes a direct diagnosis of their geomorphic significance.

These applications of palaeoflood information are illustrated in more detail in section2.4. They are particularly pertinent in view of increasing development and population pressure in flood-prone areas (Zawada, 1997; Smith and Ward, 1998). Indeed, as Hirschboeck (1987, p. 51) states:

> "The challenge awaits both hydroclimatologists and geomorphologists to continue to sort out the numerous variables which control the occurrence and impact of catastrophic flooding."

2.1.3 Evidence used for palaeoflood reconstruction

Several techniques have been used to provide palaeoflood records:

1. Flood transported gravel and boulders deposited as coarse-grained overbank deposits in boulder berms, bars or splays provide evidence of particularly high magnitude palaeofloods (e.g. Costa, 1978b, 1984; Knox, 1979, 1988, 1993). These have the potential to both be dated (e.g. Macklin *et al.*, 1992a) and to be used in palaeocompetence assessments (e.g. Costa, 1983; Williams, 1983).
2. Palaeoflood slackwater deposits (SWDs) provide long and detailed records of multiple large flood events (e.g. Baker *et al.*, 1983a; Ely and Baker, 1985; Baker and Kochel, 1988; Gillieson *et al.* 1991), and can be dated techniques such as radiocarbon. In addition, their height can be used as a palaeostage indicator (PSI) for palaeodischarge determinations (the SWD-PSI approach) (Baker, 1987).
3. Fine-grained floodplain sedimentation which has accumulated due to overbank deposition of fines by successive flood events, and can therefore be used as a record of palaeoflood events (e.g. Knox, 1987; Wells, 1990; Macklin *et al.*, 1992b).
4. The dimensions of former channels and the sedimentological characteristics of associated point bars and bed sediments can be used to reconstruct changes in the magnitude of floods with a 1 to 2 year recurrence (Knox, 1979, 1984, 1985, 1988). This is based on the fact that the magnitude of floods with a 1 to 2 year frequency strongly controls channel cross section capacity and point bar height (Wolman and Leopold, 1957). Whilst this has provided a good deal of valuable palaeoflood data (*cf.* Knox, 1984, 1985, 1988), it is generally only applicable for alluvial channels and for the documentation of high-frequency flood events (Baker, 1989).
5. Investigating damage to woody floodplain vegetation that has been caused by large floods can yield useful data (Sigafoos, 1964). This may include corrasion scars caused by transported debris, or adventitious sprouts growing from part of a tree that has been removed by a flood (Sigafoos, 1964; Hupp, 1987, 1988; Gottesfeld, 1996). More intricate evidence may also be of value, such as eccentric tree ring growth since the tilting of a tree (Hupp, 1987, 1988), or abnormal tree ring micromorphology ("flood rings") due to flood effects (Yanowsky, 1983). These features may be dated by dendrochronology. However, botanical approaches may be problematic as many flood damage features may only be recordered in the tree at certain times during the growing season, or only in certain species (Yanosky, 1982, 1983; Gottesfeld, 1996).
6. Evidence for the truncation of tributary debris fans or old river terraces of known age can be used to estimate extreme flood recurrence intervals (Costa, 1978a; Jarrett and Costa, 1988).
7. Evidence of palaeofloods such as bedrock notches, silt, scour and debris (trash) lines can be valuable palaeostage indicators, and are often integrated into SWD-PSI studies (e.g. Ely and Baker, 1985; Baker, 1987; Partridge and Baker, 1987; Wohl *et al.*, 1994).

These different techniques will clearly be of varying value depending on the study environment and the timescale and flood magnitude of interest. The following sections of this chapter describe some of these methods in more detail. In particular, the use of boulder deposits, slackwater deposits and floodplain sedimentation are developed further, as they have the greatest potential for reconstructing catastrophic palaeofloods.

2.2 COARSE-GRAINED FLOOD DEPOSITS

2.2.1 Water-flood boulder deposits

In rivers with an availability of coarse-grained sediments, floods of exceptionally high magnitude are capable of transporting boulders and gravels out of the channel, leaving an unusual deposit of particularly coarse-grained sediments on the floodplain (e.g. Scott and Gravlee, 1968; Ritter, 1975; Carling, 1986; Cenderelli and Cluer, 1998). Such deposits may be investigated as evidence of low-frequency high-magnitude flood events (Knox, 1979, 1988; Jarrett, 1990b). The most characteristic and distinctive deposits are *boulder berms*. These are open-framework coarse gravels and boulders deposited across or adjacent to the river channel (Costa, 1984), forming an often large linear deposit (e.g Figure 2.1). Berms are fairly thick (>2 m), have steep sides and considerable surface relief (Macklin *et al.*, 1992a). Other water-flood deposits such as splays, sheets and in particular boulder bars may also be used to reconstruct floods. Bars can be very similar to berms (e.g. Cenderelli and Cluer, 1998), although they tend to be thinner and flatter with less distinct or steep margins, and may have a coarse sand matrix below a clast-supported surface armouring (Costa and Jarrett, 1981; Macklin *et al.*, 1992a; Wohl, 1992b). Often coarse-grained flood deposits remain exposed on the floodplain surface, although through time they may become buried by alluvium of a finer texture to form boulder or gravel lenses within alluvial stratigraphy (e.g. Costa, 1974a, 1978b; Ritter, 1975; Knox, 1979, 1988; Brookes, 1987). In either situation, they have been shown to provide a valuable source of palaeoflood data.

The precise mechanics of deposition for features such as boulder berms has long been uncertain (Costa, 1984). Ritter (1975) suggested from field observations in southern Illinois that gravels may be deposited overbank as a result of either rolling up lateral channel bars or by being lifted momentarily into suspension. More recently, Carling (1987, 1989) has demonstrated how berms may form at points of flow separation during catastrophic discharges, such as in the shear flow zone inside channel bends or at areas of channel expansion. He has also emphasised how berm formation may be associated with hydraulic jumps during large floods, with clasts swept through the jump and deposited in the calmer conditions immediately downstream (Carling, 1995). There may of course be other important mechanisms, such as intense secondary circulations, macroturbulence, or deposition left from elevated bedform waves (Scott and Gravlee, 1968; Costa, 1984; Cenderelli and Cluer, 1998).

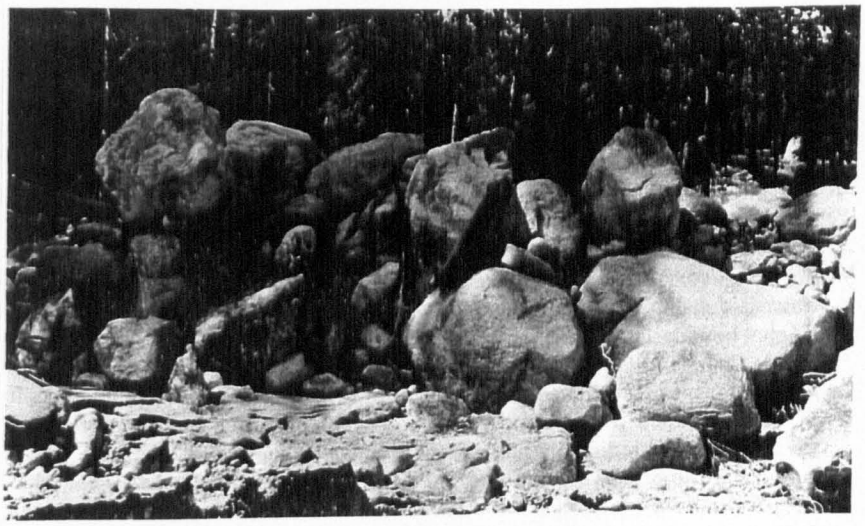

FIGURE 2.1 An example of a boulder berm formed following a dam-break flood on the Fall River, Colorado. Backpack sitting on boulder in left-centre of photograph for scale. *(Source: Costa, 1984)*

2.2.2 Differentiation of Water Floods and Debris Flows

If boulder deposits are to be used as palaeoflood evidence, it is fundamental that their origin can be confidently ascribed to deposition by water floods, rather than other processes such as debris flows that may also deposit near channel boulders (Costa and Jarrett, 1981). A debris flow is a rather different process, which is not necessarily associated with flooding (Costa and Jarrett, 1981). Discharge estimates made from boulder deposits are likely to be excessive if they were deposited by debris flows, and therefore flood control measures taken on the basis of such data may be designed inappropriately (Costa and Jarrett, 1981).

2.2.2.1 Different types of water and sediment flows

Water floods and debris flows are distinctly different types of flow. The nature of a moving fluid is affected by its sediment concentration, with water floods and debris flows being end members of a continuum of a wide range of sediment-water mixtures (Costa, 1984). Water floods have comparatively low sediment concentrations (Table 2.1) and behave as Newtonian fluids, in that they show a linear relationship between shear stress and the rate of strain (Costa, 1988). They represent the normal flood flows in most channels (Costa, 1984, 1988). Conversely, debris flows have very high sediment concentrations (Table 2.1), to the extent that solid particles and water move together as a single viscoplastic body where sediment entrainment is irreversible (Costa, 1988). Spanning the transition between these two flow types are hyperconcentrated flows (Table 2.1), which are water floods heavily enriched with sediment. They behave in a less Newtonian fashion with increasing sediment concentration, although like water floods, the sediment and water remain separate parts of the flow. Whilst the deposits from hyperconcentrated flows show many similarities to those of water floods, they may be thicker and exhibit a greater occurrence of reverse grading (Cenderelli and Cluer, 1998). Boulder berms

may often result from such sediment charged floods (Carling, 1987), and therefore the key discrimination to make here is between completely non-Newtonian debris flow deposits and Newtonian to transitional water laid flood deposits. For palaeoflood deposits, the most reliable way to do this is on the basis of the sedimentological and morphological differences which exist between the deposits from these two types of process (Costa, 1984).

TABLE 2.1 General rheologic classification of water and sediment flows in channels[a] *(Adapted from: Costa, 1988).*

Flow Type	Sediment Concentration	Bulk Density (g/cm^3)	Shear Strength ($dyne/cm^2$)	Fluid Type
Water flood	1-40% by wt. 0.4-20% by vol.	1.01-1.33	0-100	Newtonian
Hyperconcentrated flow	40-70% by wt. 20-47% by vol.	1.33-1.80	100-400	Transitional: Newtonian to non-Newtonian ?
Debris flow	70-90% by wt. 47-77% by vol.	1.80-2.30	>400	Non-Newtonian: viscoplastic ?

[a] Assumes silt and clay content <10%

2.2.2.2 Sedimentological and morphological criteria for discrimination

1. Debris flow deposits are characterised by a matrix of silts and clays surrounding the boulders (Costa, 1984, 1988), whereas berms and other flood deposits are commonly clast-supported and free of a fine-grained matrix (Mears, 1979; Costa, 1984; Cenderelli and Cluer, 1998). Whilst it is possible for the matrix of debris flows to be washed away, some remnant can normally be found. The presence or absence of this matrix is probably the most useful diagnostic feature.
2. The geometry of elongate flood deposits such as berms tends to be aligned approximately parallel to the channel or valley, and may often be located at zones of flow separation downstream of sudden changes in channel geometry (Carling, 1987; 1989). Deposition by a debris flow will tend to be far less localised or selective, with its downslope progress marked by distinctive lateral levees which may be preserved along the entire length of the flow, often containing large matrix-supported boulders (Costa, 1984). A steep fronted terminal lobe then marks the end of a debris flow.
3. The clast fabrics of debris flow deposits normally show random orientations, but flood deposits will tend show a more consistent alignment parallel or perpendicular to the direction of flow (Carling, 1987; Costa, 1988).
4. Due to the deposition of levees and lobes by debris flows, the largest rocks appear to be at the surface and edges of a deposit (Costa and Jarrett, 1981), whereas flood deposits have large clasts throughout.
5. Water-flood deposited berms typically have a noticeable trough on their distal side between the often quite steeply sloping berm margin and an upper floodplain surface or valley side (Carling, 1989).

6. Although flood sediments may only be moderately to poorly sorted, they are generally far better sorted than in debris flow deposits which are poorly to extremely poorly sorted (Costa and Jarrett, 1981; Costa, 1988).
7. Unlike debris flow deposits, water-deposited sediments may show some form of bedding and roughly horizontal imbrication of clasts (Costa, 1984).
8. Debris flow deposits may often show reverse grading, although normal fining-upwards is also possible (Costa and Jarrett, 1981; Costa, 1984). Unfortunately, flood deposits and in particular boulder berms may also exhibit reverse grading (Costa, 1974, 1984; Cenderelli and Cluer, 1998), and therefore this may not be a reliable differentiating factor.

Ideally, an assemblage of these diagnostic characteristics and their wider geomorphological context should be used to ascertain the genesis of the deposit (Costa and Jarrett, 1981), and whether the sediments may be of use for palaeoflood reconstruction.

2.2.3 Dating approaches

The majority of previous studies of coarse-grained flood deposits have concentrated on either determining the discharges that deposited the sediments or on evaluating their distribution and geomorphic significance. This may partly reflect the fact that these deposits are not necessarily easy to date. However, without a geochronology it is impossible to investigate the occurrence and magnitude of catastrophic floods *over time*, and hence impossible to analyse for temporal trends and likely effects of environmental change on flood occurrence. A variety of dating methods have been used and their suitability largely depends on whether or not the clasts have been buried by fine-grained alluvium. If buried, dating has normally been achieved by radiocarbon dating of organics preserved within or beside the flood deposits (e.g. Costa, 1978b; Brookes, 1987; Jarrett and Costa, 1988; Knox, 1988, 1993). If the boulders remain on the surface it may be possible to find radiocarbon samples within the deposit (e.g. Helley and LaMarche, 1973; Grimm *et al.*, 1995), but more often the approach is taken to date the length of time the boulders have been exposed since deposition. Hence attempts have been made to date flood deposits by lichenometry (Gregory, 1976; Macklin *et al.*, 1992a; Merrett and Macklin, 1999) and dendrochronology (Helley and LaMarche, 1973; Grimm *et al.*, 1995). Both techniques have the potential to provide valuable age estimates, as long as the validity of the assumptions made are carefully considered (as discussed for lichenometry in section 4.4.2).

2.2.4 Determination of palaeodischarge

Two main approaches have been used. Firstly, the coarse-grained deposits may be used as palaeostage indicators (PSIs), and discharge calculated from Manning's equation, slope-area methods (section 2.3.3.2) or step-backwater programs (section 2.3.3.3) (e.g. Mears, 1979; Grimm *et al.*, 1995). Whilst there is evidence to support the use of coarse sediments as PSIs (*cf.* Carling, 1987), it is probable that they are not as reliable as fine-grained slackwater sediments (Williams and Costa, 1988). Therefore, the majority of previous work has favoured a second

approach, which involves applying sediment transport equations to relate the size of boulders within the deposit to the scale of flow which deposited them (e.g. Bradley and Mears, 1980; Costa, 1983; Williams, 1983). A fundamental assumption is that all sizes of sediment are available for transport, thus the size of the largest particles in the deposit reflects the flow competence, and is not restricted by an absence of any larger particles in the area (Costa, 1983; Maizels, 1983). In theory, two main approaches to coarse-sediment transport may be taken. Firstly, focus may be give to the erosional *velocity* required to move sediment particles of a certain size (e.g. Helley, 1969; Bradley and Mears, 1980). Alternatively, competency calculations may be based on the required stream depth and slope to produce a given *tractive force* (e.g. Baker and Ritter, 1975; Carling, 1983).

To illustrate these approaches, two of the most widely used methods are briefly summarised here. Firstly, Costa (1983) used four different methods to reconstruct both velocity and depth as shown in Table 2.2, which includes both theoretical and empirical relationships. For his coarse sediment transport data set, Costa averages the results obtained from the four sets of equations, to obtain a single mean value for flow velocity and depth for each particle. By regressions of the combined velocity results, he obtained a single equation for the relationship between particle size and velocity, which he recommends for use in steep channels. (*All notations used in this section are defined in a master list at the beginning of the thesis*):

$$v = 0.18d_l^{0.487} \tag{2.1}$$

A similar relationship was found with depth, which varies systematically with channel slope. Flow width is obtained by fitting a water surface width to a surveyed cross section at the point of the deposit so that the calculated average depth is obtained. Discharge can then be calculated by the continuity equation:

$$Q = vDW \tag{2.2}$$

assuming that there have been stable channel cross sections and that steady, uniform flow prevailed during the flood (Maizels, (1983).

An alternative approach is taken by Williams (1983) who extrapolates a zone of possible sediment transport fitted to primarily empirical observations for unit stream power, bed shear stress and mean flow velocity. He uses the lower boundary of these to extrapolate the equations presented below, representing a minimum estimate of flow strength required to move a particle of certain size:

$$\omega = 0.079d_l^{1.3} \quad (10 \le d_l \le 1500\text{mm}) \tag{2.3}$$

$$\tau = 0.17d_l^{1.0} \quad (10 \le d_l \le 3300\text{mm}) \tag{2.4}$$

$$v = 0.065d_l^{0.05} \quad (10 \le d_l \le 1500\text{mm}) \tag{2.5}$$

Using equations 2.3 - 2.5, depth and discharge can be calculated by manipulating equation 2.2 and the conventional adaptation of the DuBoys relationship, where D is assumed to be a close surrogate for the hydraulic radius:

$$\tau = \gamma DS \tag{2.6}$$

Again, width may be determined from measured cross sections.

TABLE 2.2 Velocity and depth reconstruction methods used by Costa (1983). All notations used in this section are defined in a master list at the beginning of the thesis.

Velocity (m/s)	Depth (m)
1. Helley (1969)[1]	1. Manning: $0.040 \le n \le 0.124$;
$v_b = 3.276\left[\frac{(\gamma_s - 1)d_L(d_s + d_I)^2 MR_L}{C_D d_s d_L(MR_D) + 0.178\ d_I\ d_L\ MR_L}\right]^{0.5}$	$D = \left[\frac{v\ n}{\sqrt{S}}\right]^{1.5}$
2. Bradley and Mears (1980): $F_D + F_L = F_R$;	2. Unit stream power
$v_b = \left[\frac{z(\gamma_s - \gamma)d_I\ g\ \mu}{\gamma(C_L + C_D')}\right]^{0.5}$	$\omega = 0.009\ d^{1.686}$;
	$D = \frac{\omega}{\gamma\ S\ v}$
3. U.S. Bureau of Reclamation (in Costa, 1983)	3. Shields (1936): $0.013 \le \tau^* \le 0.032$;
$v_b = 5.9(d_I)^{0.5}$	$D = \frac{\tau^*\ d_I(\gamma_s - \gamma)}{\gamma\ S}$
4. Costa (1983)[2]: from data set ($5mm \le d_I \le 3200mm$)	4. Relative smoothness: $0.05m < d < 0.6m$;
$v = 0.20\ d_I^{0.455}$	$\frac{v}{(8g\ D\ S)^{0.5}} = 1.16 + 2.03\ \log\frac{D}{d_I}$

[1]Computed velocity in feet per second
[2]Uses the mean of the 5 largest intermediate axes. Particle axis in mm, all others in m.

Whilst other methods and relationships have been suggested (e.g. Carling, 1983, 1986), many of these are site-specific and not suitable for general application (Komar, 1987). Subsequent work has therefore commonly adopted or combined the ideas of Costa (1983) or Williams (1983) (e.g. Knox, 1988, 1993; Wohl, 1992a, 1992b; Maas, 1998). Such equations have the advantage that they are quick and simple to apply. However, the reliability of these approaches, in particular that of Costa (1983), has been questioned, with suggestions that his equation frequently overestimates discharge and does not provide a satisfactory representation of flow hydraulics (Carling, 1986; Komar, 1988, 1989; Reid and Frostick, 1987). Potentially important factors such as grain density and in particular the general sorting and size characteristics of the bedload as a whole may be very important factors, but are not considered by Costa's approach (Komar, 1988, 1989). In addition, Costa utilised Shields' (1936) equation to calculate depths, which has been shown to be unsuitable for steep slopes or coarse bed materials (Baker and Ritter, 1975; Bathurst *et al.*, 1983).

In view of these problems, it is worth considering alternative equations available from the wealth of literature on coarse bedload transport. Bathurst *et al.* (1987) developed relationships between particle size characteristics and water discharge per unit flow width. With relevance to uniform bed load sizes they empirically derived:

$$q_c = 0.15g^{0.5} d_l^{1.5} S^{-1.12} \quad (2.7)$$

This was established based on grain sizes <44 mm diameter, which means that the relationship would have to be extrapolated for larger particles. Nevertheless, this approach has the advantage that it does not directly require knowledge of depth, which is hard to determine for steep violent flows (Bathurst *et al.*, 1987). However, this equation still does not incorporate hiding and exposure effects due to bedload sorting which may be of fundamental importance (Komar, 1988, 1989; Reid and Frostick, 1987a). In response to this problem, Bathurst (1987) developed his ideas to include non-uniform bedload entrainment. Komar (1987, 1988) has also proposed equations that incorporate bedload sorting. However, applying such equations is problematic as they all inevitably require some reference bedload grain size (usually d_{50}), and also sometimes a measure of the bedload grain size range. It remains unclear how to measure these representatively when faced with horizontally sorted or armoured deposits (Komar, 1989), both of which are common in coarse bedload streams. The decision of where to measure bedload is further complicated by the fact that it is rarely possible to establish where the boulders were entrained (Carling and Tinkler, 1998). Additionally, if a berm was deposited decades or centuries previously, the character of the bedload may have changed considerably over the intervening time period, so modern bed load measurements would not be reliable representation of those at the time of transport.

Overall, it seems clear that as yet there is no widely acceptable method for estimating palaeodischarges from coarse-grained flood deposits. This may be partly explained by the fact that our knowledge of catastrophic flow processes is limited due to the difficulties in observing or measuring these events. Thus considerable uncertainty remains about the fluvial transport of boulders (Carling and Tinkler, 1998). Many would argue that flow-competence evaluations are only capable of providing very rough discharge estimates, as we often rely on extrapolating by orders of magnitude from measurements taken during lower discharges (Komar, 1988). Such limitations have lead some authors to refrain from making any calculations, and to merely use d_l as a palaeodischarge proxy (e.g. Macklin *et al.*, 1992a; Merrett and Macklin, 1999). However, by not providing discharge estimates such results are incompatible with many hydrological and engineering purposes. The approaches of Costa (1983) and Williams (1983) are simplistic, but they have been found to be applicable in some studies. In particular, Williams' minimum entrainment equations may provide useful conservative estimates of palaeodischarge. Ultimately, it would seem that independent assessment of the reliability of predicted discharges is essential for selecting the appropriate equations and ensuring that the results provide valid

estimates. If reasonable correspondence is found, the judicious application of palaeocompetence approaches could provide valuable flood magnitude estimates.

2.3 FINE-GRAINED FLOOD DEPOSITS

2.3.1 Palaeoflood slackwater deposits (SWDs)

Slackwater deposits typically consist of silt, sand, and occasionally gravel, which are rapidly deposited from suspension during large floods in sheltered areas, where flow velocities suddenly decrease and reverse eddying predominates. This differentiates them from the coarse-grained deposits discussed above, as although berms can also be deposited in slackwater flow zones, the term palaeoflood slackwater deposit (SWD) is reserved for fine-grained sediments deposited out of suspension at high-levels during floods. If well protected from erosion, SWDs may often occur as stacked sediment sequences resulting from periodic flood sedimentation by numerous high magnitude events (Baker *et al.*, 1983a). An impressive example of a deep slackwater sequence is the deposits at Arenosa Shelter, a large alcove cut into cliffs bordering the Pecos River in west Texas (Patton and Dibble, 1982). Here over 10 metres of slackwater sediments are preserved from numerous flood events, interbedded with archaeology and aeolian sediments (Figure 2.2 and Figure 2.3).

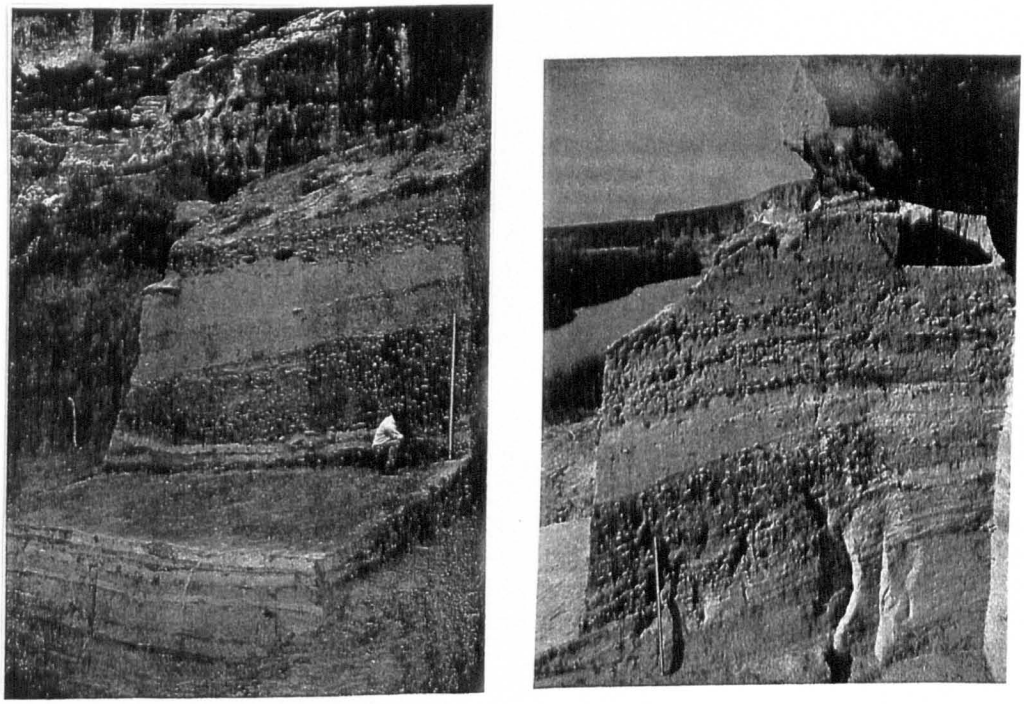

a) b)

FIGURE 2.2 a) Front view of the slackwater deposits preserved in the Arenosa Shelter in west Texas. Thin, fine-grained layers are clearly visible at the bottom of the picture (strata 12 - 18) below thick cultural layers (strata 9 - 11), with thicker and coarser SWD units near the top of the sequence. The picture can be correlated with the right-hand stratigraphic column in Figure 2.3. b) A section through the SWDs, showing that the deposits are not planar, but sloping and increasing in thickness towards the channel. The survey rod is 2.25 m long. (Source: Patton and Dibble, 1982).

The first main use of SWDs in palaeohydrology was as indicators of catastrophic Pleistocene flooding of the Channeled Scabland in eastern Washington from Glacial Lake Missoula (Bretz, 1929; Baker and Bunker, 1985). Over the last two decades SWDs been increasingly studied in the USA (e.g. Kochel and Baker, 1982, 1988; Patton and Dibble, 1982; Ely and Baker, 1985; O'Connor *et al.*, 1994; Ely, 1997), Australia (e.g. Baker *et al.*, 1983b; Baker and Pickup, 1987; Gillieson *et al.*, 1991; Wohl, 1992a; Saynor and Erskine, 1993), and more recently in India (Kale *et al.*, 1994), Israel (Greenbaum *et al.*, 1998, in press), South Africa (Hattingh and Zawada, 1996; Zawada, 1997) and Spain (Benito *et al.*, 1998). Stacked SWD sequences may provide quasi-continuous records of high magnitude floods, which may be preserved for thousands of years. As these sequences may be dated over long timescales (see section 2.3.2), and used as palaeostage indicators (see section 0), SWDs may potentially yield the most complete and accurate determinations of palaeoflood age and discharge (Baker, 1987).

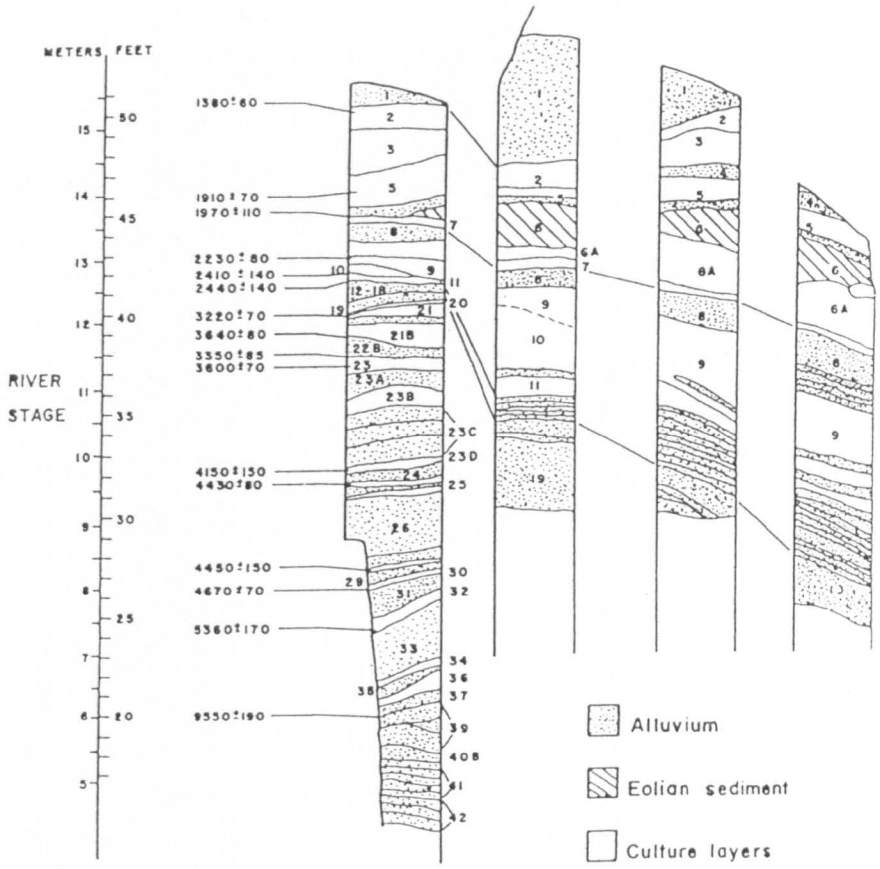

FIGURE 2.3 Composite stratigraphy of Arenosa Shelter, compiled from four different excavated trenches. Radiocarbon dates from the cultural layers are shown on the left-hand side. River stage is relative to the low water elevation of the Pecos River during the excavations. *(Source: Patton and Dibble, 1982).*

2.3.1.1 SWD deposition and preservation

SWDs occur in a variety of settings, the most common being tributary mouths (Table 2.3) (Baker *et al.*, 1983a). The process of slackwater sedimentation at tributary mouths has been studied in detail from field evidence (Kochel and Baker, 1982, 1988) and flume observations (Kochel and Ritter, 1987; Baker and Kochel, 1988). The common requirements for all SWD study sites are that they provide an area sheltered from the main flow that allows sufficient sediment deposition and also protects the SWDs from subsequent erosion. The majority of studies have therefore concentrated on bedrock controlled gorges cut in resistant lithologies, which are likely to contain many of the potential sites listed in Table 2.3. These valleys tend to be fairly narrow and therefore experience large increases in stage during floods, leaving SWDs more protected from regular channel scour and fill processes (Baker and Pickup, 1987). In addition, such rivers also have a fairly stable channel geometry which favours preservation (Ely and Baker, 1985; Wohl *et al.*, 1994). Arid or semi-arid environments are conducive to excellent SWD preservation due high suspended sediment concentrations and low rates of bioturbation and rainwash (Saynor and Erskine, 1993); however, more humid environments may also provide valid SWD study areas (Kochel and Baker, 1988; McQueen *et al.*, 1993).

2.3.2 Establishing a flood record from slackwater sediment sequences

The layers of sediment deposited by individual floods can be distinguished on the basis of sedimentary features such as abrupt vertical changes in grain size, preserved buried palaeosols, colour changes, and fine silt caps or basal layers (Baker *et al.*, 1983a; Ely and Baker, 1985; Kochel and Baker, 1988; Ely, 1997). Thus the precise number of floods recorded in the SWDs can often be identified. Where possible, correlation of these flood units with other SWDs in the catchment can add further confidence to the palaeoflood record obtained (Baker, 1989). Dating of the flood units allows a chronology of flood events to be constructed from the SWDs. Dating may be achieved in a variety of ways, though radiocarbon (^{14}C) analysis (section 4.4.3) has been by far the most commonly used method. For example, the ^{14}C dates from the cultural layers at Arenosa Shelter, which separate the flood units, provide reliable time brackets for the palaeoflood events (Figure 2.3) (Patton and Dibble, 1982). Dating of fine organic debris, such as leaves and twigs, incorporated within a flood deposit may also be valuable, as these have been shown to yield ^{14}C dates very close to the actual flood age (Baker *et al.*, 1985; Ely *et al.*, 1992).

^{14}C does not provide the only means of dating SWDs. In particular, luminescence techniques (section 4.4.5) may offer considerable potential, although so far their application is limited. In northern Australia, Gillieson *et al.* (1991) successfully dated SWDs by means of thermoluminescence (TL). In addition, Murray (1996) has presented impressive results using optical luminescence techniques to date a 2000-year sequence of flood deposits, showing good correspondence with ^{14}C dates. For particularly recent SWDs, ^{137}Cs dating (section 4.4.1) has been used to provide an indicator for sediments that post-date 1950 (Ely *et al.*, 1992).

TABLE 2.3 Summary of the main locations where slackwater deposits are found *(Adapted from Baker, 1987).*

Type of site	Local hydraulic conditions	Examples	Specific comments
Tributary mouths	Backflooding of main channel flow up tributary results in reverse eddying and a rapid decrease in competence	Kochel and Baker (1982, 1988); Baker *et al.*, (1983a); Baker and Pickup, (1987)	Deposition is favoured in small tributaries that have low erosive power and debouch their peak flows before the main channel. Other ideal conditions are tributary junction angles close to 90° and a fairly low main channel gradient.
Abrupt channel expansion	Deposition occurs downstream in zones of flow separation	Patton *et al.*, (1979); Ely and Baker (1985)	Deposits accumulate near valley walls, lateral to main channel
Abrupt channel constriction	Deposition occurs upstream due to a backwater effect	Patton *et al.*, (1979)	Requires a very large flood for constrictions to generate backflooding to this extent.
Caves and rockshelters	Deposition occurs in the floor/mouth of the cave where flow velocities will suddenly decrease	Patton and Dibble (1982); O'Connor *et al.*, (1994)	Excellent preservation due to minimal erosion or bioturbation. Minimum stage of the flood is well known from the height of the cave lip, which must have been overtopped by the flood.
Protruding bedrock spurs, boulders or talus	Reverse eddies during large floods in the lee of these protrusions cause a sharp decrease in velocity	Ely and Baker (1985); Partridge and Baker (1987)	Protrusions protect deposits from subsequent erosion by separating the flow.
Slackwater terraces, benches or levees	Large, high vertical accretion deposits. These often occur in combination with irregular protrusions or channel expansions.	Ely and Baker (1985); Wohl (1992a); Benito *et al.* (1998)	These are different from normal overbank deposits as they receive flood sediments far less regularly than near channel floodplain areas.
Channel-margin alcoves	Deposition occurs in eddy zone	Patton *et al.*, (1979); Partridge and Baker (1987)	Generally small bedrock niches
Outside of ingrown bedrock meander bends	Extreme floods adopt a straighter thalweg, hence eddies form at meander bends	Patton and Boison (1986)	Well preserved if bedrock overhangs the depositional sequence.

2.3.3 The use of slackwater deposits in determining palaeodischarge

The principle of using SWDs to estimate palaeodischarge is relatively simple, in that floodwaters must have reached a stage at least equivalent to that of the slackwater sediment that they deposited. However, as this section will show, this approach involves various important assumptions and complications that demand careful consideration

2.3.3.1 Fundamental assumptions

The main assumptions of this approach are that:

1. The elevation of the upper surface of the SWD approximates to peak flood stage, and can therefore be used as a palaeostage indicator (PSI).

2. The channel geometry of the study reach has remained stable since the deposition of the SWDs. Channel bank and bed stability, with insignificant scour or fill are important (Baker, 1987).

Bedrock channels therefore provide the most suitable settings, as they tend to have stable channel cross sections and are resistant to channel downcutting. Once these assumptions have been satisfied, a variety of mathematical approaches can be used to determine palaeodischarge, and these are described in the following two sections.

2.3.3.2 The slope-area method

Until the early 1980s the slope-area method, which fits a modelled flow through a reach to PSIs (for details see Chow, 1959; Dalrymple and Benson, 1967), was used to estimate palaeodischarge (e.g. Patton and Dibble, 1982; Baker *et al.*, 1983a). Whilst this was developed for uniform flow conditions, it was thought to provide reasonable estimates of flow in open non-uniform channel conditions where there were no extreme variations in channel geometry through the downstream reach (Baker *et al.*, 1983a). However, more recently its limitations have been realised. One of the most serious problems results from the fact that channel cross sections, which are needed to characterise the reach, may only be surveyed at the points where the PSIs are located. Thus discharge is often overestimated because SWDs are normally located at points of channel expansion or separation (Table 2.3), meaning that the cross sections tend not to be representative of the reach as a whole (O'Connor and Webb, 1988). Many other problems have been found with the slope-area method for calculating large discharges, such as significant errors in both field measurements and selection of the roughness coefficient (Quick, 1991). These are exacerbated for steep gradient mountain streams (Jarrett, 1987).

2.3.3.3 Computerised step-backwater models

The need for more accurate modelling of high discharge flow conditions has lead to the use of open channel flow step-backwater models. These are based on the principle of energy conservation, in that the total potential and kinetic energy at a cross section downstream must equal that at an upstream section minus any energy losses between sections due to friction, turbulence or flow separation (Ely and Baker, 1985; O'Connor and Webb, 1988; Benito, 1997). From this principle, a one dimensional energy loss equation for gradually varied flow is used (Chow, 1959; Chadwick and Morfett, 1993). There are various computer models available to carry out the step-backwater procedure, many of which are very similar. HEC-2 was developed by the US Army Corps of Engineers (for details see Feldman, 1981; Hydraulic Engineering Centre, 1982), and has been the most widely used model in palaeoflood studies (e.g. Ely and Baker, 1985; Baker and Pickup, 1987; Partridge and Baker, 1987; Wohl, 1992a; O'Connor *et al.*, 1994; Benito, 1997). Whilst some two- or three-dimensional modelling approaches are possible, they have not been extensively tested and their added complications are not necessarily worthwhile for merely fitting PSI-based water surfaces (Miller and Cluer, 1998). The input

variables for HEC-2 are surveyed cross sections and reach lengths, energy loss coefficients characterising roughness and channel expansion/contraction, initial conditions (estimated water surface elevation and energy slope), surveyed heights of palaeostage indicators relative to the channel bed, and an understanding of the dominant flow regime (subcritical or supercritical) (Martínez-Goytre *et al.*, 1994). Water surface profiles are calculated for a designated discharge, and then adjusted on an iterative basis until an energy balance profile is obtained that approximates to the flood water elevation indicated by the palaeostage evidence (e.g. Figure 2.4) (Ely and Baker, 1985; Wohl, 1992). It is important that the cross sections are obtained accurately, as they, along with the initial estimated discharge, tend to be the primary controlling factors (Ely and Baker, 1985).

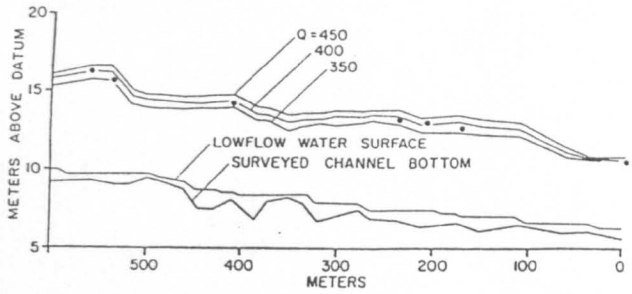

FIGURE 2.4 Step-backwater generated flow profiles. Note how a 'best-fit' discharge of 400 m^3s^{-1} is shown, with upper and lower brackets of 350 to 450 m^3s^{-1}. *(Source: O'Connor and Webb, 1988).*

The advantage of the step-backwater procedure over the slope-area method is that the cross sections do not have to be located only at points of palaeostage indicators, but instead may be located regularly to take account of all significant variations in channel geometry (Ely and Baker, 1985). However, there are limitations and problems. For example, estimation of the roughness coefficient (Manning's n) is difficult for large flood events (Trieste and Jarrett, 1987). Often a value is subjectively chosen, with n normally expected to be in the range of 0.025-0.040 for confined bedrock canyons during large floods (Carling and Grodek, 1994). Fortunately, studies have found that calculations are actually rather insensitive to changes in n (O'Connor and Webb, 1988; Benito, 1997). Of greater importance is determining whether flow was sub- or supercritical. It is thought that supercritical flow in natural channels cannot be sustained over significant time or space (Jarrett, 1984, 1987; Trieste, 1992). However, this subject is poorly understood, and the fact that supercritical flow has been observed during exceptional flood events (e.g. Reid and Frostick, 1987b), means that it may have been possible during palaeoflood events (Martínez-Goytre *et al.*, 1994). It is also important to appreciate that HEC-2 is only a one-dimensional model, and therefore a uniform energy slope is considered for each cross section (Benito, 1997). The model will therefore not take account of ineffective flow areas or superelevation of the water surface. In addition, the model is for gradually varied flow,

and therefore cannot accommodate major changes in flow velocity or areas of complex hydraulics such as tortuous channel bends (Ely and Baker, 1985).

Some of these limitations in the HEC-2 approach may explain why computed water surface profiles are not always consistent with slackwater deposit elevations. For example, Partridge and Baker (1987) computed water surface profiles for palaeostage indicators from a large flood in 1952 (Figure 2.5). The computed discharges show an extremely wide range from 2500 m^3s^{-1} to 4500 m^3s^{-1}. Such variation was undoubtedly due to some of the limitations of HEC-2 discussed above. However, some of the most serious problems may come from more fundamental theoretical shortcomings, as discussed in the following two sections.

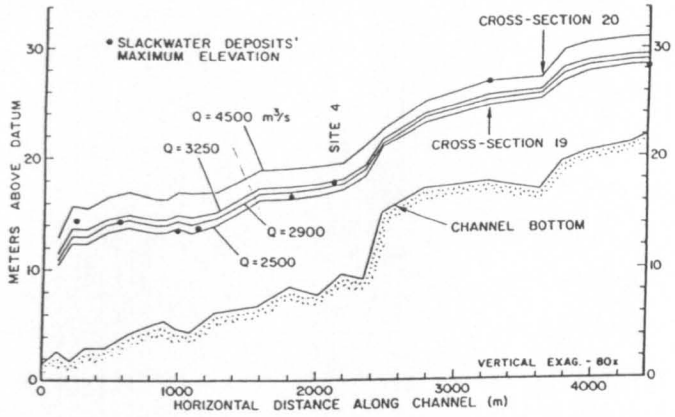

FIGURE 2.5 Water surface profiles computed for palaeostage indicators (PSI) from the 1952 flood event on the Salt River, Arizona. The PSI at cross section 19 is high due to complex hydraulics at that site. The actual gauged discharge was 3144 m^3s^{-1}. *(Source: Partridge and Baker, 1987).*

2.3.3.4 Complications related to erosion and sediment transport

A fundamental assumption of the HEC-2 approach is that neither the channel geometry nor the height of river bed level have changed since SWD deposition (section 2.3.3.1). However, in practice this may be unrealistic, especially for catastrophic floods. Such flows are renowned for their erosive power and ability to entrain sediment (Baker and Costa, 1987), and both modification of channel cross sections and channel scour are likely. Such channel change would cause inaccurate calculation of palaeodischarges for pre-existing SWDs (Jarrett, 1987), and also has serious implications for a single event if sediments are deposited before the majority of channel change has taken place (see Quick, 1991). An additional concern raised by Quick (1991) relates to the fact that all these flow models assume clear water floods. However, large floods are characterised by high sediment transport, as stream power and boundary shear stress are at a maximum. Bagnold (1966) has shown that active sediment transport absorbs one third of the total streampower, leaving less power to move water (Quick, 1991). However, models such as HEC-2 only consider energy losses associated with channel roughness (Manning's *n*)

and channel expansions and contractions (Bentio, 1997), and may therefore overestimate flood discharges.

2.3.3.5 Are SWDs valid palaeostage indicators?

SWDs are normally considered to provide a good approximation of peak flood stage (see section 2.3.3.1). However, sediments deposited by floods probably only provide minimum palaeostage indicators (PSIs), as some floodwater must have been higher to facilitate their deposition (Baker, 1987; Gillieson *et al.*, 1991). Ely and Baker (1985) found that the SWD-PSI method only underestimated discharges by 15% due to deposits being lower than peak stage. However, other studies have documented SWDs at much lower heights than the actual flood stage (e.g. Patton and Dibble, 1982, Fig. 4). It therefore seems important to fully understand the nature of slackwater sediment deposition. Such sedimentation processes have been investigated (e.g. Kochel and Ritter, 1987; Baker and Kochel, 1988), although the full implications for palaeodischarge reconstruction may not have been recognised.

The common assumption is that SWDs, approximating to peak palaeoflood stage, provide a 'censoring level' (Baker and Pickup, 1987; O'Connor *et al.*, 1994; Wohl *et al.*, 1994), with a larger flood being required to overtop the previous layer of sediments and deposit a subsequent flood unit above. This notion of slackwater sedimentation is outlined in Figure 2.6. Here Flood 1 is a high magnitude flood that gives a thick slackwater deposit with a planar surface approximating to peak palaeoflood stage. All lower floods (e.g. Floods 2 and 3) cannot overtop it, and are therefore not recorded in the sequence. They result in inset deposits that are less likely to be preserved (Wohl *et al.*, 1994). It is not until a flood of larger magnitude than Flood 1 occurs (Flood 4) that another slackwater sediment layer is deposited. Surveyed heights for PSIs may be taken of the upper slackwater horizons, points A, B, C and D on Figure 2.6.

What may be more realistic is the scenario outlined in Figure 2.7. This suggests that deposition from each successive flood event does not actually fill the slackwater area completely. Flood 1 deposits a band of sediment that thickens down-tributary due to lower areas being under slackwater for a longer period and coarser material being deposited in the lower parts. This type of sedimentation accommodates deposition from subsequent floods, even if they are of a lower peak stage (Floods 2 and 3), thus producing the typical sequence of SWDs. This pattern of coarsening and widening with proximity to the main channel has been noted in the field (Kochel and Baker, 1982; McQeen *et al.*, 1993). Contemporary slackwater deposition observed by the author in the Voidomatis basin during winter floods in 1996 showed backwaters depositing a gently sloping layer of sediment which would 'pinch out' at a point approximating to the peak stage (Figure 2.8). This sloping surface was related to the propagation of low amplitude waves up the slackwater zone (Figure 2.8). Such sloping sediment surfaces and wave motions in the slackwater zone were also the dominant style of sedimentation observed in the flume experiments of Kochel and Ritter (1987) (Figure 2.9). This style of sedimentation is

clearly not restricted to tributary mouths either, but has also been observed in rockshelter SWDs (Figure 2.2b) (Patton and Dibble, 1982).

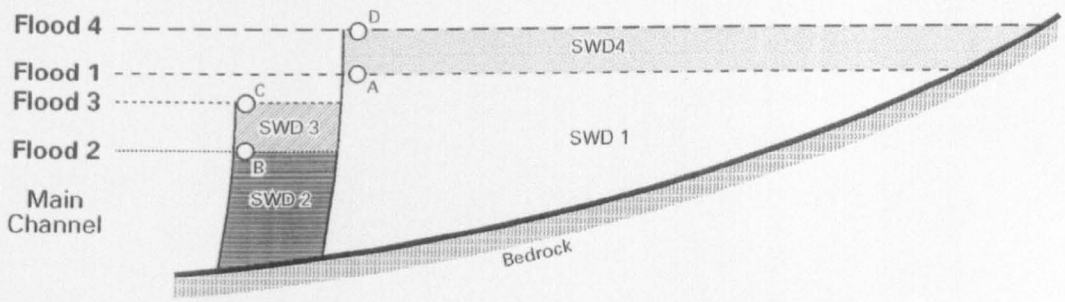

FIGURE 2.6 An 'idealised' picture of slackwater sediment deposition. Floods are numbered in relative chronological order.

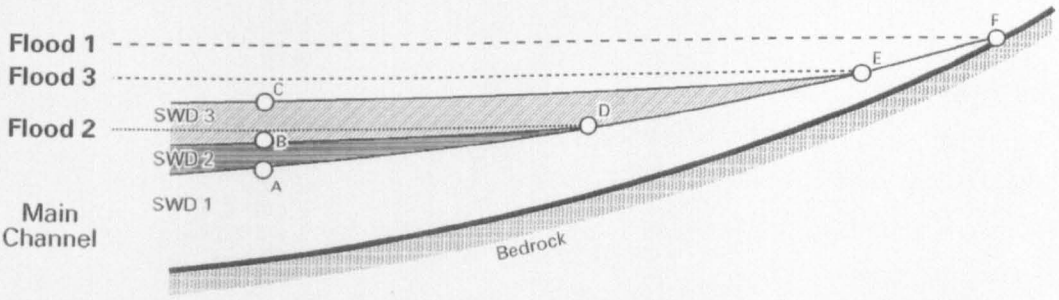

FIGURE 2.7 An alternative schematic of slackwater sediment deposition. Floods are numbered in relative chronological order.

FIGURE 2.8 Contemporary deposition of slackwater sediments at a tributary mouth in the Lower Vikos Gorge, Voidomatis River, northwest Greece in November 1996. Low amplitude waves were propagating up the slackwater zone. The mouth of the tributary is approximately 4 m wide.

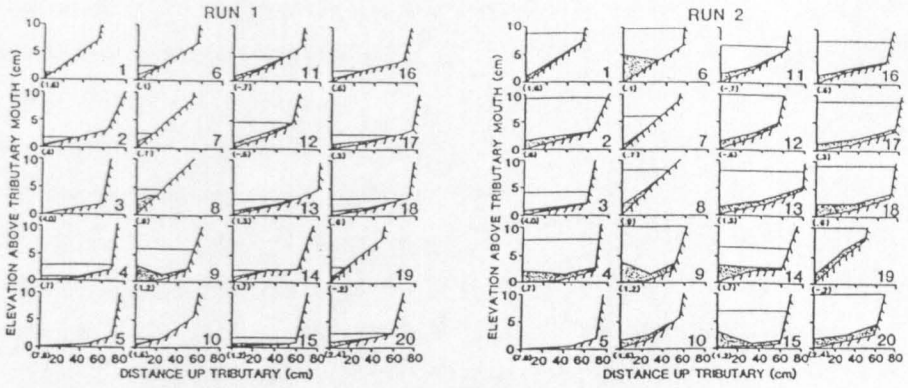

FIGURE 2.9 Tributary cross sections from the flume investigations of slackwater deposition. Run 1: Low flow, low slope. Run 2: High flow, low slope. Numbers 1 to 20 refer to tributary mouth sites of varying geometry. *(Source: Kochel and Ritter, 1987).*

There is therefore considerable evidence that Figure 2.7 is a realistic model. This has important implications for palaeodischarge reconstructions in terms of where to measure the palaeostage. If the palaeostage heights were surveyed at points A, B and C in Figure 2.7, the largest flood (Flood 1) would actually show the lowest stage, with the smaller flood (Floods 2 and 3) showing considerably higher stages. This would give meaningless estimates from the HEC-2 procedure. At points A, B and C the height of the slackwater deposit is largely reliant on the antecedent conditions at deposition. Whilst a higher deposit is a more recent one, it does *not* necessarily represent a larger flood. The only meaningful palaeostage indicators are at the point where the deposits 'pinch-out' up-tributary. This will especially be the case where the tributary has a significant slope (often the case in bedrock canyons), as the sloping nature of the slackwater deposit may be accentuated. The pinch-out points D, E and F (Figure 2.7) give reasonable indicators of peak palaeoflood stage. This again agrees with field and flume observations (Figure 2.8 and Figure 2.9).

Whilst some authors have tried to survey to pinch-outs (e.g. McQueen *et al.*, 1993), past studies in general do not provide details on exactly where SWD-PSI heights were surveyed, and thus it is not necessarily clear whether misinterpretations have been made. Certainly with fragmented SWDs where 'pinch-outs' cannot be found, careful consideration should be given as to whether the site is suitable for the SWD-PSI method at all. An alternative approach can be to use sedimentary parameters such as sediment thickness, grain size and the degree of cross-bedding to provide a relative measure of palaeoflood magnitude (Kochel and Baker, 1988; Benito *et al.*, 1998). However, such approaches cannot provide palaeodischarge estimates.

2.3.4 Perspective on palaeoflood slackwater deposits

The above discussion regarding palaeodischarge determination using SWDs serves to highlight the need to thoroughly investigate the deposits and their setting to see if they conform to the two

key assumptions outlined in section 2.3.3.1. A careful assessment of any phases of aggradation, incision or channel change since SWD deposition will be required, which is probably best achieved through studying the extent and age of alluvial units along the river (Baker, 1987). This may enable a reconstruction of the cross section at the time of flooding through establishing the rate of downcutting or the periods of high, aggraded river levels.

The style of deposition of the SWDs needs to be understood if reliable discharge calculations are to be made. Some deposits may not conform to the frequently assumed planar units, but instead slope towards the channel. Thus horizontal trends in sedimentary units should be investigated, and where units are sloping 'pinch-outs' must be used as PSIs.

Where the assumptions are valid, models such as HEC-2 are useful, as, although they need improvement, they currently provide the best means of estimating palaeodischarge from SWDs. In cases where the assumptions cannot be confidently satisfied, step-backwater procedures are likely to be misleading and inappropriate.

Aside from the various possibilities for discharge reconstructions, SWD sequences are uniquely useful because they can provide a detailed record of multiple high magnitude flood events over timescales of centuries and millennia. Bedrock gorge environments are likely to be most conducive to their preservation, especially where there are small high-level tributary mouths and rockshelters cut in the gorge walls.

2.3.5 Floodplains as a source of palaeohydrological data

Just as SWDs result from high magnitude floods, such floods are also likely to deposit fine-grained overbank sediments over stabilised floodplain areas where fine sediments are accumulating. Fine-grained overbank floodplain sediments are not generally classed as SWDs, as they are not normally found in such high-level sheltered ineffective flow zones. Instead, overbank floodplain deposits are typically found in corridors adjacent to the channel. They are prone to reworking via lateral channel instability and large flood events, and therefore don't tend to be preserved for such long periods of time. This may explain why there have been relatively few studies that have used overbank floodplain sediments for palaeoflood reconstruction. Nevertheless, over shorter timescales they can provide valuable and near continuous data on large flood events (e.g. Knox, 1987; Wells, 1990; Macklin *et al.*, 1992b). Thus fine-grained floodplain accretion may be a frequently overlooked source of palaeohydrological information. Large floods recorded in fine-grained alluvium may show distinct textural characteristics, the most common being units which reverse the overall fining upward sequence typical in fine-grained alluvium (Knox, 1987; Walling *et al.*, 1997). This is due to larger floods transporting sediment of a given grain size to higher surfaces than is normally possible by more frequent floods of smaller magnitude (Knox, 1987). Hence interpretations of palaeoflood magnitude may be possible from particle size characteristics. If this sedimentological information could be combined with reliable chronological control, either

through ^{14}C (e.g. Wells, 1990), or perhaps through other radiometric methods such as levels of unsupported ^{210}Pb or ^{137}Cs (section 4.4.1), valuable flood information could obtained from fine-grained alluvium (e.g. Walling *et al.*, 1997).

2.4 APPLICATIONS OF PALAEOFLOOD DATA

The preceding two sections have outlined some of the most valuable palaeoflood reconstruction techniques. When applied judiciously, such approaches can provide a detailed record of flood events over long timescales. This section describes the three principle reasons for obtaining these long flood records.

2.4.1 Extending flood records and improving flood frequency estimations

> "It is incumbent upon the hydrologist to ensure that in applying statistical, deterministic and/or empirically derived flood-prediction models, every attempt should be made to verify independently the flood predictions by incorporating geological/geomorphological evidence of past flows. By ignoring this evidence, conventional flood prediction will remain a partially speculative process and be subject to the criticism that it does not attempt to understand the flood-producing system." (Zawada, 1997, p.111).

Zawada's remarks highlight one of the most important potential applications of palaeoflood data. By their nature, low frequency high magnitude floods are difficult to assess on the basis of systematic (i.e. measured) data (Costa, 1978a; Lane, 1987; Jarrett, 1991). Even when systematic records are exceptionally long, perhaps spanning more than 100 years, they still provide little means of assessing the variability of catastrophic floods, which may only occur once a century or less. Moreover, in many areas it is far more common to find much shorter systematic records, of the order of several decades (Jarrett, 1991; Zawada, 1997). Thus the hydrologist is often in the unenviable situation of having to calculate the 100- or 200-year flood on the basis of a flow record which is on average 30 years long (Zawada, 1997). The problem may be exacerbated in mountain areas, where a considerable number of catchments may remain ungauged (Jarrett, 1990a), leaving scant information on which to base flood frequency estimates. Even if gauging stations are present, violent catastrophic flows may damage gauging equipment and erode weirs, resulting in gaps in gauged records (Zawada, 1997). These factors therefore present a considerable problem for the prediction of extreme floods, with standard techniques often having to rely on extrapolations well beyond the length of the systematic record or on hypothetical models which lack real experience or verification (Ely *et al.*, 1991). However, extreme flood predictions are precisely the data required for flood risk analyses (Enzel *et al.*, 1991) and by engineers in the design of dams, bridges and other structures within the floodplain (Baker *et al.*, 1987). It is therefore of fundamental importance that the recurrence intervals and magnitudes of extreme floods are properly assessed, as an estimate which is too low may result in the loss of life, whilst an estimate that is too great results in over-design of structures, generating extremely high and unnecessary economic costs (Costa, 1978a).

Palaeoflood information has the potential to help hydrologists overcome these problems by extending the systematic flood record or providing flood data for ungauged sites. This is particularly pertinent in view of developments in the techniques available for palaeoflood reconstruction which have been discussed earlier in this chapter (Stedinger and Baker, 1987), which mean that the approach is increasingly well prepared to move beyond the research stage into applied work (Baker, 1987). The value of incorporating palaeoflood data into extreme flood predictions can be illustrated with reference to work on the Pecos River in Texas (Patton and Baker, 1977; Baker *et al.*, 1979; Kochel, 1988a). Whilst the river has a relatively long streamflow record beginning in 1900, it includes 2 catastrophic floods in 1954 and 1974 which appear as outliers (Figure 2.10). This results in a dilemma for water resources planners using conventional flood frequency analysis. Extrapolating the systematic data without these outliers included gives a recurrence interval for the 1954 event of millions of years (Curve A in Figure 2.10), which is clearly improbable. However, including the outliers gives a recurrence interval of just 86 years (Curve A in Figure 2.10) (Kochel, 1988a), and the steep frequency curve makes the 100-year flood an enormous discharge, which would result in gross over design in engineering projects (Baker *et al.*, 1979). This unrealistically low recurrence interval is clearly an artefact of the length of the gauged record. Using the SWD-PSI method (section 2.3) with the deposits at Arenosa Shelter (Figure 2.2 and Figure 2.3) palaeoflood discharge and age data can be incorporated into the flood frequency plot by determining recurrence intervals as described by Patton and Dibble (1982) and Kochel (1988a) (curve C in Figure 2.10). This revealed that the 1954 and 1974 events had a recurrence interval with a lower limit of 2000 years (Patton and Dibble, 1982; Kochel, 1988a), and the palaeoflood data greatly refines flood frequency estimations between 100 and 1000 years (Patton and Baker, 1977).

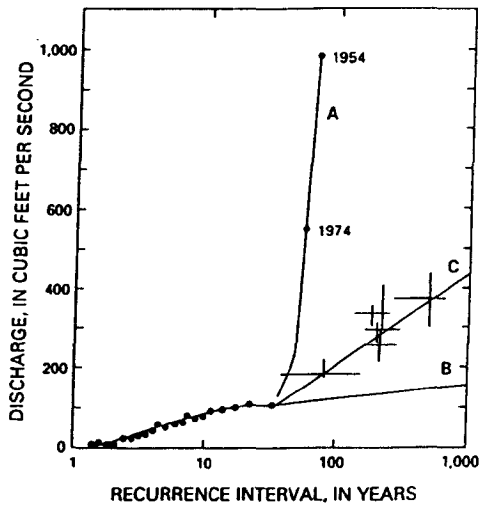

FIGURE 2.10 Flood frequency curves for the Pecos River near Comstock, Texas. Curve A is the frequency curve based on the systematic data including the 1954 and 1974 events, whilst curve B is based on the same data excluding these two extremely large floods. Curve C is constructed from the analysis of palaeoflood data. Vertical bars display discharge uncertainty, and horizontal bars the recurrence-interval uncertainty for the palaeoflood data. *(Source: modified from Patton and Baker, 1977, in Jarrett, 1991).*

Realisation of the potential value of incorporating palaeoflood data in flood frequency analysis has lead to considerable developments of more sophisticated techniques for incorporating these types of data with systematic and historical records (e.g. Stedinger and Cohn, 1986; Lane, 1987). In particular, the use of maximum likelihood estimators (MLEs) has shown how palaeoflood data can be of tremendous value for flood frequency analysis (Stedinger and Cohn, 1986; Baker, 1989), as demonstrated by the successful combination of systematic and palaeoflood data for the Colorado River in Arizona (Figure 2.11) (Ely *et al.*, 1991; O'Connor *et al.*, 1994). One of the countries most often cited for using historical and palaeoflood information is China, as most of their systematic records are too short for design applications (Hua, 1987). They have carried out a survey of historical flood marks, flood documentation and flood sedimentation to improve their knowledge of extreme floods (Luo, 1987; Shi *et al.*, 1987), and such data have played a role in spillway designs for major dams, including the massive Gezhouba and Three Gorges projects (Baker *et al.*, 1987; Hua, 1987). In the U.S.A., palaeoflood data have been used to assess the design of existing dams, which are usually based on the Probable Maximum Flood (PMF). For example, Baker *et al.* (1987) compare the maximum floods determined by various different approaches for rivers in central Arizona (Table 2.4). Their palaeoflood investigations covered the last 1000 to 2000 years, and show that over this time maximum floods have been between 64 and 74% less than the PMF. This shows that accommodating high PMFs may be resulting in over design and great extra expense. Thus flood data over thousands of years can be of considerable importance in providing evidence of the type of flows that are possible in a geographical setting (Zawada, 1997), hence allowing planners to assess the validity of their extreme flood estimates. Consequently, national institutions in the U.S. have recognised the potential value of palaeohydrological techniques in assessing the size of possible floods (*cf.* U.S. National Research Council, 1985).

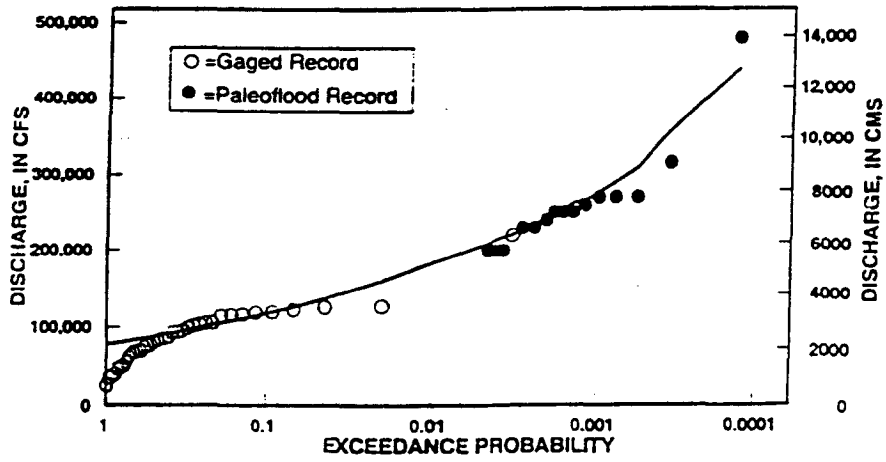

FIGURE 2.11 Log-Pearson Type III flood frequency distribution of the combined gauged and palaeoflood data from the Colorado River near Lees Ferry (O'Connor *et al.*, 1994). The exceedance probabilities were estimated using maximum likelihood techniques, based on only those floods with discharges greater than 100,000 cfs (2830 m^3s^{-1}). *(Source: Ely et al., 1991).*

TABLE 2.4 Flood peaks in central Arizona determined by several methods; discharges in m^3/s. *(Source: Baker et al., 1987a).*

Location	Maximum Observed Systematic Flood	Maximum Observed Historic Flood	Maximum Palaeoflood	Theoretical PMF
Salt River near Roosevelt	2900	2900	4600	12900
Verde River above Horseshoe Dam	2830	4250	5400	21000

In Zawada's quote at the beginning of this section, it is also implied that the hydrologist requires a comprehension of flood generation. Fundamental to this is understanding how the magnitude and frequency of large floods responds to changes in the environment, as described in the following section. Flood frequency assessments make the assumption that the data set is 'stationary', in that the entire period of record is a relevant reference to the environmental conditions of today and the future (Zawada, 1997). However, changes in climate, land-use, vegetation and other catchment conditions often drastically alter flood response, thus introducing 'non-stationarity' (Baker, 1987). This problem must be taken into account when considering the length of record relevant to contemporary flood predictions (Webb and Baker, 1987).

2.4.2 Investigating the effects of environmental change on flood frequency and magnitude

> "Assessing climatic or hydrologic variability with systematic hydrologic data is difficult, if not impossible...[but] because floodplain management policies are based on the estimated magnitude of large floods, generally the 100-year flood, potential effects of climatic variability might need to be considered...Palaeohydrologic data provide a means to assess past climatic variability in water-resources planning." (Jarrett, 1991, p. 112-3).

As discussed by Jarrett, the response of flood regime to climatic changes can be properly assessed by extending hydrological records with palaeoflood data. There are, of course, other environmental variables that can affect flood frequencies and magnitudes, in particular land-use change (Webb and Baker, 1987). However, climate is often the principal factor (Jarrett, 1991), both through direct hydrological effects and indirect effects on vegetation dynamics (Knox, 1984).

A number of comprehensive palaeoflood studies have demonstrated how flood regimes have shown considerable variation in relation to climatic change over past centuries and millennia (e.g. Knox, 1984, 1985, 1988, 1993; Ely *et al.*, 1993; Ely, 1997). Knox's extensive work on the Mississippi River is useful to demonstrate this intricate relationship between floods and climate. Knox (1984) shows variations in the annual flood series through four climatic periods from 1867 to 1980 (Figure 2.12). The four climatic periods were identified on the basis of independent studies that indicated the dates of distinct changes in the characteristics of large-scale atmospheric circulation patterns. Flood magnitudes show systematic variation linked to

climatic conditions (Figure 2.12), with the periods dominated by prevailing meridional circulation patterns experiencing much larger floods than those of prevailing zonal circulation. It is important to note that the highest magnitude floods, those that may be catastrophic, exhibited the most significant variations, suggesting that they are particularly sensitive to climatic change (Figure 2.12). This example demonstrates the potential importance of understanding flood hydroclimatology, in the sense that flood events should be viewed within a history of climatic fluctuations, during which variability in large-scale atmospheric circulation may have had an important control over flood hydrology (Hirschboeck, 1988). The link between atmospheric circulation and large floods is widely recognised, along with the particular importance of the relative strength of meridional flow in producing heavy storms at mid-latitudes (Knox, 1984; Haydon, 1988; Hirschboeck, 1987, 1988; Rumsby and Macklin, 1994; Ely, 1997). The Mississippi example therefore provides a classic demonstration of the problem of non-stationarity in flood predictions. Which 100-year flood values should be taken from this record? Is it appropriate to treat the last 100 years as a single stationary data set knowing the systematic variation within it? Or, are these variations simply part of a longer-term dynamic equilibrium? Unfortunately, even a long systematic record such as this cannot fully answer these questions. If we are to predict future floods, we need to properly understand flood variability. Hence the need for palaeoflood data.

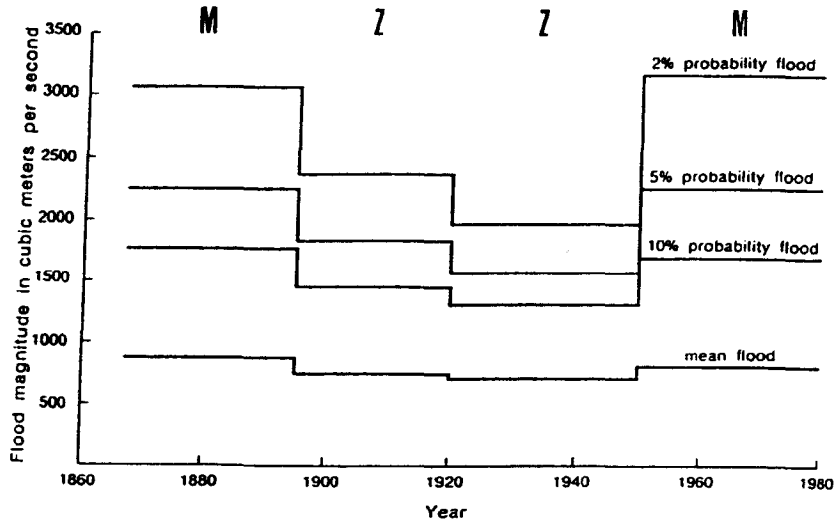

FIGURE 2.12 Climatic influence on magnitudes of floods of a given recurrence probability for the Mississippi River at St. Paul, Minnesota. M (for prevailing meridional circulation) and Z (for prevailing zonal circulation) label the prevailing large-scale atmospheric circulation. *(Adapted from Knox, 1984).*

Knox (1988, 1993) has presented data for high magnitude palaeofloods in the Upper Mississippi over approximately the last 5000 years, based on coarse-grained deposits preserved in alluvium (Figure 2.13). Considerable variations are evident. During a warm, dry period from

approximately 4500 to 3300 years BP, the largest palaeofloods did not exceed the magnitude of a modern flood with a 50-year recurrence probability. Conversely, after about 3300 years BP a shift to cooler and wetter conditions brought more frequent large floods that equalled or exceeded a modern 500-year event (Figure 2.13). The most extreme floods in the record are between about AD 1250 to 1450, a period of climatic transition from the medieval warm period to the cooler Little Ice Age. The most startling implication of these results is the great sensitivity of large floods to climatic fluctuations, as all of these variations were associated with mean annual temperature changes of only about 1-2 °C and mean annual precipitation changes of less than 10-20 % (Knox, 1993). It should be noted that climate-related temporal variations in extreme flood occurrence akin to those presented by Knox have also been identified in other areas, such as the southwestern U.S. (*cf.* Ely *et al.*, 1993; Ely, 1997).

Palaeoflood data such as these have two main implications. Firstly, the sensitivity of large floods to relatively small climatic variations over timescales of centuries or less means that it may be hard to justify the assumption of stationarity in standard flood frequency techniques (Knox, 1993). Palaeoflood hydrology provides the opportunity to assess the variability of large floods over different climatic periods, and provides data that enable the current flood regime to be viewed within a context of past natural variations. This therefore provides a far better understanding of the flood producing system and the variability of rare, high-risk catastrophic floods.

Secondly, it is important to recognise that the scale of changes which have brought about the large variations in flood frequency and magnitude in records such as Figure 2.13 are generally *smaller or comparable to* climate changes predicted by global circulation models as a result of increased atmospheric greenhouse gas concentrations (Knox, 1993). This therefore adds considerable weight to the commonly held belief that one of the most significant impacts of future climate changes will be in altering the character of extreme events (Ely *et al.*, 1993). Since systematic records do generally not cover a period long enough to encompass climate change of this scale, palaeoflood investigations provide one of the few means of assessing the potential impacts of postulated future climate change on flood occurrence.

A challenge for the future is that different hydroclimatic regions may have shown differences as well as similarities in flood response to climate change (Ely, 1997). Whilst some impressive palaeoflood data sets exist for parts of the U.S., many parts of the world, including the Mediterranean basin, still have little long-term flood data with which to assess past and future flood variability (section 2.5.4). However, in an era of anticipated climate change (Houghton, 1997), it is of increasing importance to have good quality data regarding possible hydrological changes, and in particular changes in flood regime (Meko *et al.*, 1991; Jetfić *et al.*, 1996). It can be argued that engineering design should incorporate possible hydrologic variability, and the siting of hazardous waste sites must be safe from the maximum possible flood for hundreds to thousand of years (e.g. Foley *et al.*, 1984). Modelling climate change

requires reference data such as palaeoflood analysis to validate predictions (Ely *et al.*, 1993; Zawada, 1997). Thus, the overall implication of both this and the previous section, is that the continued application of palaeoflood analysis can reduce the uncertainty in flood estimation and water resources planning (Jarrett, 1991), and consequently reduce risk to life and property.

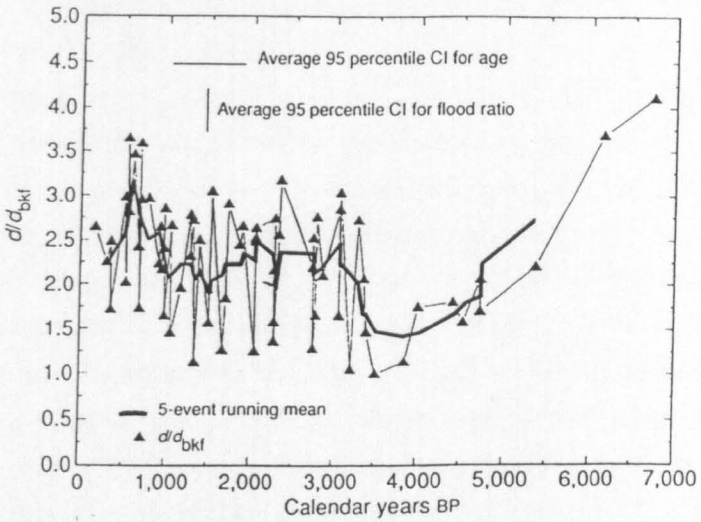

FIGURE 2.13 Palaeoflood record of Holocene overbank floods in the Upper Mississippi. The flood magnitude is taken as a flood ratio of palaeoflood depth (d) to the corresponding bankfull stage water depth (d_{bkf}). A flood ratio of 2.0 corresponds to modern floods expected about once every 30 - 50 years, whereas a flood ratio of 3.0 relates to modern floods expected about once every 500 - 1000 years. *(Adapted from: Knox, 1993).*

2.4.3 Investigating the geomorphological significance of high magnitude flood events

> "The effects of floods on the modes of operation of stream subsystems range from minimal to profound. The occurrence of infrequent but extremely large flow events also raises intriguing questions about the operation of fluvial systems over time spans of centuries or millennia." (Bull, 1988, p. 157.)

Bull's quote raises two important points for this section. Firstly, the effects of floods can be extremely variable, both in space and time. Secondly, rare catastrophic flood events may play an important role in river system dynamics. A view of the way a river behaves will depend upon the time scale that is considered (Schumm and Lichty, 1965). By studying contemporary fluvial processes in a river system, the role of rare floods might easily be overlooked, yet in certain circumstances such events may be of paramount geomorphological importance (Baker, 1977; Brunsden and Thornes, 1979; Gupta, 1983). In many situations, river systems may have inherited their form from a previous period, when the flood regime was considerably different (e.g. Rose *et al.*, 1980). Bull's quote therefore serves to highlight the value that palaeoflood data may hold for the geomorphologist, providing long-term information on the frequency and magnitude of extreme events that may be used to explain fluvial form (Baker and Costa, 1987; Baker *et al.*, 1988; Lewin, 1989; Baker and Kale, 1998). Such data are unlikely to be properly

represented in short systematic records or by field measurements, which are extremely difficult during high discharges (Baker and Pickup, 1987). This section considers the geomorphological effects that high magnitude floods may have, and considers how our understanding of geomorphological systems can be furthered through palaeoflood studies.

A discussion of the geomorphic effects of catastrophic floods must inevitably consider the relative importance of forces of varying magnitude and frequency, which has been a long running debate in geomorphology. This is epitomised by the two primary philosophies regarding earth history: catastrophism and uniformitariatism. Both philosophies have held sway at different times, with recent decades seeing increasing attention paid to the occurrence of occasional but persistent landscape changes (see Knighton (1998) p. 279 for details). However, a major recent issue has been the different various ways of defining geomorphic work. Wolman and Miller (1960) considered the amount of sediment load to be representative of the amount of work achieved. This lead them to conclude that over time, the bankfull discharge, occurring every 1 - 2 years, would be most important in controlling channel morphology. Whilst extreme events could transport large volumes of sediment, they were considered too rare to have the dominant impact on the fluvial system. Conversely, Wolman and Gerson (1978) proposed that the relative importance of different events is represented by their effectiveness in forming the landscape and the length of recovery time following such events. This approach is in keeping with recognition of the importance of geomorphic thresholds (Schumm, 1973, 1979; Bull, 1979). Their view of formative events and effectiveness allowed for the fact that in certain situations, fluvial landforms exhibit high thresholds of competence which can only be significantly modified by extreme events capable of overcoming the high resistance to change. Neither of these two views of geomorphic work are necessarily incorrect. In alluvial rivers channel margins are relatively erodible and hence flows of moderate magnitude and frequency are often responsible for shaping the channel (as described by Wolman and Miller, 1960; Leopold *et al.*, 1964). However, in areas of higher competence thresholds where sediment transport and channel modification is more episodic, ideas of formative events suggested by Wolman and Gerson (1978) may be more appropriate in recognising the greater importance of more extreme flood events.

The renewed interest regarding extreme events and landform development is demonstrated by examining Miller and Gupta (1999), a recent volume on fluvial geomorphology, where over half the papers discuss large floods as being important geomorphic factors. This is not a recent phenomenon, as over 20 years ago the importance of extreme events in geomorphology was receiving considerable recognition (e.g. Brunsden and Thornes, 1979). Large floods have high shear stresses and stream powers and hence have the potential to be the agent of extensive landscape change (Baker and Costa, 1987; Komar, 1988). In alluvial channels, where channel bed and margins are non-cohesive, the power of a flood can be dissipated by modification of channel margins and through sediment transport (Baker, 1984,

1988). However, flood power is amplified in non-alluvial rivers, where resistant channel boundaries mean that there tends to be an increasing disparity between sediment availability and erosive capability as the flood increases. Where these rivers flow through bedrock gorges, they accommodate extreme discharges by very large increases in stage, resulting in stream power, shear stress and macroturbulence all being extremely high (Baker, 1984, 1988; Baker and Costa, 1987; Baker and Kale, 1998). When these reach a level that exceeds the resistance of the channel boundary, major geomorphic response may result (Baker, 1977).

There are however numerous factors that control the effects of high magnitude events in different settings. Some locations experience a wide variety of long lasting effects of high magnitude floods, ranging from channel incision, scour and widening, to extensive boulder deposition and channel aggradation (Table 2.5). Conversely, in other areas the effects may be minimal or the landscape soon recovers back to its pre-flood state (e.g. Gupta and Fox, 1974; Magilligan *et al.*, 1998). The factors that control whether a river's form is strongly affected by extreme floods can be divided into *catchment (extrinsic) factors* and *channel (intrinsic) factors.*

TABLE 2.5 Examples of the major geomorphic effects of extreme floods. Boulder sizes refer to the b-axes.

Geomorphic Effects	Environment	Location	Reference(s)
Excavation of a wide superflood channel through the destruction of terraces. Large boulders as big as 3.4 m scattered over the channel and floodplain.	Tropical river prone to intense storms	Yallahs River, eastern Jamaica	Gupta (1975, 1983)
Channel scour and widening, with scour holes as deep as 2 m formed. Extensive deposition of coarse sediment (including large 1.5 m boulders) in prominent riffles, bars and berms. Valley meanders shaped according largest floods.	Upland bedrock streams	Elm and Blieders Creeks, central Texas	Baker (1977); Patton and Baker (1977)
In bedrock gorges large boulder berms are formed and bedrock shows many signs of intense erosion (potholes, scour, scabland appearance). Drastic and abrupt changes in channel course and pattern. Alluvial reaches show a large outer channel adjusted to extreme floods within which are flood-sculpted bars.	Alluvial and bedrock reaches, with tropical monsoon climate.	Narmada River, central India	Baker and Kale (1998); Gupta *et al.* (1999)
Intense reworking of the valley floor by stripping and scouring, resulting in an increased planimetric braided pattern. Transport of very coarse bedload. Massive deposition of fines with formation of new delta at river mouth.	Mountainous bedrock and braided river, Mediterranean climate	Jordan River Basin, eastern Mediterranean	Inbar (1987)
Widespread scour in upper fan and channel widening through bank collapse. Fresh head cut gullies on farmland. Debris flows due to undercutting. Geometry of channel shaped to the extreme event. Extensive downfan deposition.	Alluvial fan complex, semi-arid Mediterranean environment	Area of the Rambla Honda, southeast Spain	Harvey (1984a)
Severe bedrock erosion and extensive boulder transport, boulder berms formed, and over 1 m of aggradation in lower energy reaches. Major peat landslides due to undermining of slopes.	Upland cobble-boulder bed streams	Northern Pennines, U.K.	Carling (1986)
Severe erosion and enlargement of the channel through the destruction of in-channel benches. The river bed is temporarily aggraded by over 2m due to the liberated sediment forming a bedload wave.	Bedrock confined river reaches	Hunter Valley, New South Wales, Australia	Erskine (1994); Erskine and Livingtone (1999)
Incision of sandur deposits forming outwash terrace sequences and relic flood channels.	Glacial outwash areas	Tekapo Valley, N.Z.	Maizels (1987)

Extrinsic factors are the flood generating processes. Catastrophic floods are likely to be of great geomorphological importance when floods of exceptional magnitude compared to the mean annual discharge occur frequently (Gupta, 1983; Kochel, 1988). Thus the steeper the flood frequency curve (i.e. greater flood variability) the more likely that the river will be adjusted to catastrophic floods (Baker, 1977; Abrahams and Cull, 1979). On the other hand, rivers with relatively flat flood frequency curves may conform more closely to the Wolman and Miller (1960) concept (Figure 2.14). A useful quantitative measure of flood variability is the Flash Flood Magnitude Index (FFMI) of Beard (1975) which can be used to compare the extreme flood 'potential' for different basins (Figure 2.14) (see Beard, 1975; Baker, 1977). Many factors may determine the flood variability of a catchment. Climate will obviously play a major role, with extreme flood occurrence likely in areas which experience intense convective or frontal storms which may be enhanced by orographic forcing (Hirshboeck, 1988). However, drainage basin physiography will also play a major role, with a propensity for predominant overland flow encouraging rapid delivery of precipitation inputs to the channel (Baker, 1977). This would be encouraged by a catchment of high relief, high drainage density, thin soils and low vegetation density (Kochel, 1988b). A roughly circular or balloon shaped watershed morphometry also encourages a steep flood hydrograph by concentrating runoff (Patton, 1988).

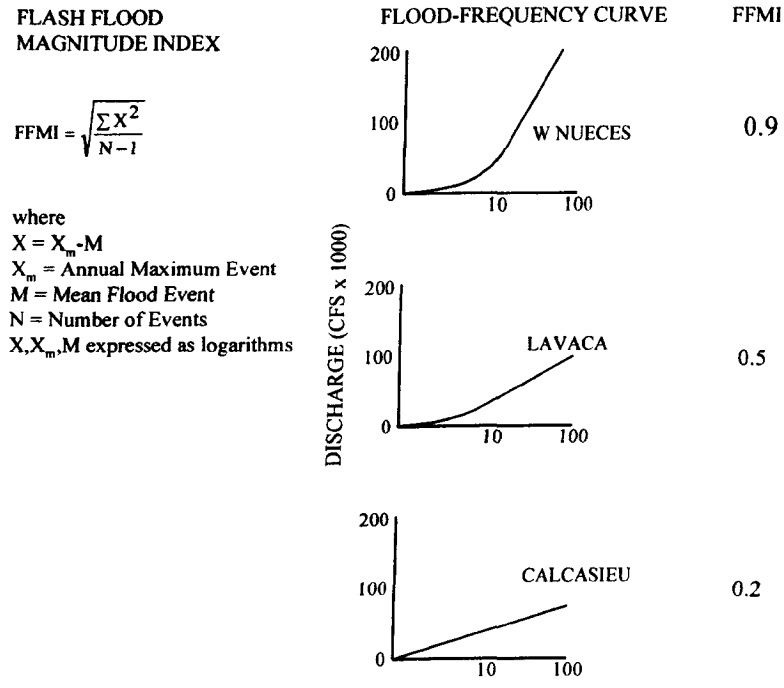

FIGURE 2.14 Computation of the Flash Flood Magnitude Index (FFMI) of Beard (1975). Flood frequency curves and FFMIs are shown for three locations in Texas. West Nueces River is the most prone to catastrophic floods, and therefore has the greatest potential for a geomorphology controlled by extreme floods. *(Source: Baker, 1977).*

Extrinsic catchment controls determine flood potential, but for extreme flood-affected river forms to be widespread and stable through time, favourable intrinsic channel characteristics are required (Baker, 1977; Patton and Baker, 1977; Gupta, 1983). The calibre of the river's sediment is of great importance here. Where a river is supplied with coarse gravels and boulders, the valley floor is likely to display forms attributable to extreme floods, since these are the only flows able to overcome intrinsic thresholds of competence. These forms are likely to be stable over time, as lower magnitude, post-flood flows will lack the ability to significantly modify these forms (Gupta, 1983; Gupta *et al.*, 1999). Coarse bedload is likely in areas of resistant geology where the host bedrock breaks down to produce large fragments, especially in mountain streams where sediment calibre has not yet been attenuated by downstream fining. In contrast, alluvial rivers exhibit highly contrasting recovery times, with the ability to quickly readjust their form to lower flows following the effects of an extreme flood (e.g. Costa, 1974b; Gupta and Fox, 1974). The depth of flood flow is another intrinsic factor to consider, because as previously discussed, narrow channel geometry generates large increases in stage during a flood, which in turn generate a high flood power (Baker and Costa, 1987). The temporal ordering of extreme events must also be considered when assessing geomorphic effects (Wolman and Gerson, 1978). If a river is reshaped by a catastrophic flood and then experiences flood of similar magnitude soon after, the second event may have negligible effects as forms would already be fully adjusted to such a flow (Kochel, 1988b).

Although the concept of defining one single formative dominant discharge can be attractive, it is important to realise that this may be an oversimplification. Where rivers do depart from the Wolman and Miller (1960) concept, it is becoming increasingly apparent that a combination of a range of different flood magnitudes are of primary importance. For example, Gupta *et al.* (1999) discuss how the Narmada River in India has a channel-in-channel physiography, with high-magnitude floods maintaining a large outer channel and smaller post-flood flows transporting sand to build insets against the flood-widened banks. Rivers in New South Wales have been shown to gradually build in-channel benches through moderate magnitude events, which are episodically destroyed by catastrophic floods that excavate a wide outer channel (Erskine, 1994; Erskine and Livingtone, 1999). In this region, Nanson (1986) has shown how other rivers build their floodplains by vertical accretion affected by frequent floods, which is periodically catastrophically stripped by higher magnitude flows. Thus floods of different magnitude may each have their role to play in shaping and maintaining the valley floor morphology. The resulting landscape may be viewed as a mosaic of various features that owe their formation to floods of different magnitude.

Whilst there is increasing evidence of the importance of extreme events, both Baker (1988) and Baker and Kale (1998) stress that there remains a need to further our knowledge of catastrophic flood effects. Palaeoflood data provide one of the most promising means of doing this (Kochel, 1988b). A wider palaeohydrological appraisal of the genesis of fluvial landforms

such as terraces and scour features is also required to complement these data. The chronology of these features may be compared to the palaeoflood records, to see what correspondence there is between extreme flood events and fluvial forms (Baker *et al.*, 1988). A further advantage of using palaeoflood data is that they provide information on how the flood regime may have changed in relation to environmental change (section 2.4.2). Some areas may have inherited forms from a previous climatic period when the magnitude of large floods was very different (e.g. Rose *et al.*, 1980; Coxon, 1996; Benito, 1997). In such instances it would be impossible to confidently explain the landscape without palaeohydrological data. This is also of relevance to the future, as changes in flood regime due to climatic change may affect the stability of land in the valley floor (Knox, 1985; Newson, 1992). If procedures such as river engineering (e.g. bank protection) or restoration design (e.g. re-establishing river meanders) are to be sustainable, possible changes in sediment transfers or the erosive capability of the river must be anticipated in the design process (Brookes, 1995). The dynamic relationship between flood frequency and magnitude and landscape change therefore needs to be understood.

To conclude this section, it is clear from this brief review of flood effects, that they are complex in space and time. Whilst the formative discharge in non-cohesive alluvial channels may be fairly well understood (*cf.* Leopold *et al.*, 1964), the situation is far more complex in rivers which less readily adjust their forms. Such rivers tend to exhibit slow recovery times and therefore may owe their morphology to a series of flood events over centuries or millennia. Without a palaeoflood record it may be difficult to determine accurately the sensitivity of the landscape to extreme floods and climate change, or the typical landscape recovery times following extreme floods. Palaeoflood data, combined with wider geomorphological investigation, provide the opportunity to correlate long-term changes in flood regime to the development and behaviour of these episodically changing rivers. Thus rather than taking a snapshot view at the current point in time, rivers can be treated and studied as the temporally and spatially dynamic systems that they are.

2.5 MEDITERRANEAN RIVER ENVIRONMENTS

This section introduces the characteristics of rivers in the Mediterranean region. Catastrophic floods frequently occur in this region, thus the case for applying palaeoflood hydrology to decrease the uncertainty regarding their occurrence and effects is discussed. This involves not only a discussion of contemporary Mediterranean river environments, but also their Late Quaternary geomorphological development, so that the long-term effects of catastrophic floods on Mediterranean landscapes can be considered along with the issue of modern flood hazards.

2.5.1 Contemporary river systems in the Mediterranean basin

The watershed of all but the very large rivers draining into the Mediterranean Sea demarcates the extent of the Mediterranean basin (Figure 1.2). A striking feature of the region is the large

proportion of mountainous areas. With the exception of some parts of the North African fringe, nearly all of the Mediterranean Basin exhibits narrow coastal plains backed by extensive mountainous areas (Woodward, 1995). As a result of this mountainous physiography many of the rivers flow for a relatively short distance from source to outlet to the sea. With the obvious exception of the Nile, many Mediterranean watersheds extend only 100 - 200 km from the coastline (Figure 1.2). This means that many catchments in the Mediterranean have high channel gradients and steep slopes (Woodward, 1995; Poesen and Hooke, 1997). Other common landscape features can be recognised in the region, though geology often controls their occurrence. In areas of hard limestones, rivers of cobble-to boulder-bed nature often flow through rock gorges with steep rock slopes. In contrast, areas of erodible Tertiary sedimentary rocks may display a more intricate, dendritic drainage and heavily dissected terrain.

The rivers of the Mediterranean basin are inevitably strongly influenced by the characteristic regional climate of hot dry summers and cool wet winters. Thus many rivers have a seasonal flow regime, particularly in their headwater reaches, with the great majority of the annual discharge occurring between October and May. Whilst the dry season may vary from practically year long to almost non-existent, and annual precipitation totals from less than 200 mm to greater than 1500 mm (Grenon and Batisse, 1989), it is noteworthy that there are examples of intense rainfall events from all over the region (see Wainwright, 1996). This propensity for dramatic storm downpours, combined with rapid runoff generation by steep slopes and river gradients, means that flashy flood hydrographs are common in many Mediterranean rivers (Grennon and Batisse, 1989; Poeson and Hooke, 1997).

In their recent review paper, Poesen and Hooke (1997) identified two key environmental problems regarding Mediterranean river catchments that are becoming of increasing concern: -

1. Land degradation, in terms of soil erosion and desertification.
2. Catastrophic floods and their destructive effects.

These problems attest to the sensitive and dynamic nature of these river systems. These problems are sometimes interlinked, as extensive erosion may be caused by catastrophic floods, and conversely land degradation may affect flood generation by altering infiltration and runoff. These problems are therefore considered here in turn.

2.5.1.1 Land degradation in the Mediterranean

There are numerous examples of serious erosion in the Mediterranean basin and the associated problems of decreasing soil fertility and crop productivity (e.g. Benito *et al.*, 1992; Ruiz-Flaño *et al.*, 1992; Brandt and Thornes, 1996). The problem is multi-layered, as not only are Mediterranean environments naturally vulnerable to processes of erosion (Woodward, 1995), but there is also a long history of human disturbance of the landscape through widespread

deforestation and farming, which may have increased erosion rates by orders of magnitude (Dedkov and Mozzherin, 1992; Milliman and Syvitski, 1992).

Numerous different factors control erosion rates in Mediterranean environments, including rainfall intensities and topography (Inbar, 1992; Poesen and Hooke, 1997), lithological resistance (Woodward, 1995), and land use and vegetation (Kosmas *et al.*, 1997). Mountain catchments are particularly sensitive to erosion (Milliman and Syvitski, 1992; Woodward, 1995). Precipitation amounts and intensities are enhanced by orographic effects, thus making rainfall events more erosive. Slopes are particularly steep and experience more rapid runoff than more vegetated low-lying areas. Mass movements are important erosional processes in the mountains, encouraged by steep slopes and earthquakes (Ergenzinger, 1992). In addition, mountain areas are very sensitive to human disturbance, in particular to increases in grazing intensities (Poesen and Hooke, 1997). A further problem has been the terracing of mountain slopes. Although soil erosion was reduced where these structures were maintained (van Andel *et al.*, 1986), terraces are frequently being abandoned as they are unsuitable for modern agricultural machinery, leading to serious land degradation (Grenon and Batise, 1989; Ruiz-Flaño *et al.*, 1992). Geology remains an important factor in mountain degradation, with often intensely selective erosion having focused on upland basins of softer Tertiary lithology (Woodward, 1995).

Irreversible land degradation, in the form of badlands, typifies the erosion problems of the Mediterranean basin. Although fully developed badlands occupy only 5% of southern Europe (De Ploey, 1989), they are a stark reminder of the potentially devastating erosion that may occur in this regional setting. It should also be noted that the lithologies conducive to badland formation are widespread in the Mediterranean basin, and additional areas of semi-badland landscapes have been identified (Woodward *et al.*, 1992; Woodward, 1995). Most badlands are located on or near major mountain ranges, especially where active tectonic uplift encourages gullying and stream incision (Poesen and Hooke, 1997). Considerable uncertainty surrounds the processes that have lead to badland formation, as different badland areas show highly variable erosion rates (Benito *et al.*, 1992). They certainly result from both water erosion and mass movements, with erosion being encouraged by large rainfall events (Sirvent *et al.*, 1997). The intense gully erosion and network extension has often been attributed to historical human disturbance of slopes composed of unconsolidated silt-rich Tertiary lithology, in particular through decreasing vegetation cover (Woodward, 1995). However, the estimated age of Mediterranean badlands range from 2,700 to 40,000 years (De Ploey, 1992), and hence some may not necessarily be a feature of recent slope disturbance (Wise *et al.*, 1982).

The overriding importance of water erosion in the Mediterranean (Sala, 1983; Grenon and Batisse, 1989; Poesen and Hooke, 1997) means that land degradation problems are inextricably linked to hydrological and fluvial processes. It should be recognised that in some parts of the Mediterraenean, the most intense erosion is accomplished by extremely large

rainfall and flood events (Inbar, 1987; Ergenzinger, 1988; Sala, 1988; Wainwright, 1996). Therefore the problem of catastrophic floods may in some situations be closely linked to land degradation.

2.5.1.2 Catastrophic flooding in the Mediterranean

Steep slopes, high gradient mountainous catchments, thin soils, and a tendency for intense rainfall events are all factors that suggest the Mediterranean basin could be prone to catastrophic flooding. The maximum observed floods database of Rodier and Roche (1984) indicates that in southern Europe maximum floods have been of greater magnitude than those in northern Europe for small and moderate sized basins (10-3000 km^2), although the flood magnitudes tend to converge for very large rivers (Figure 2.15).

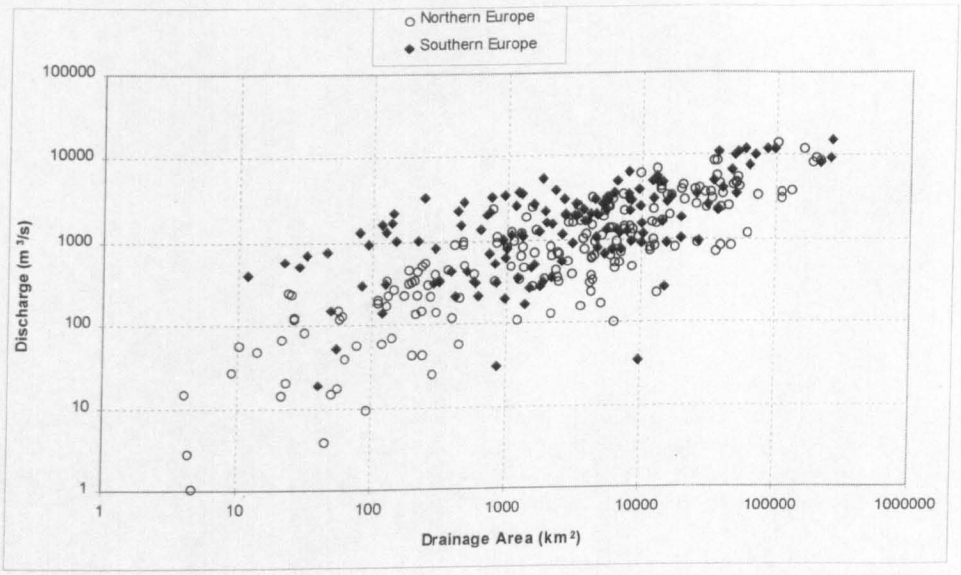

FIGURE 2.15 A comparison of the maximum observed floods in drainage basins of northern and southern Europe. Southern European countries for which data are available are: Albania, Bulgaria, French basins draining into the Mediterranean, Italy, Portugal, Spain, Turkey and the former Yugoslavia. *(Data from Rodier and Roche, 1984).*

Figure 2.16 shows further evidence for Mediterranean countries being prone to extreme floods. This is a map of an extreme flood magnitude index, which was calculated by dividing each maximum observed flood by its drainage area and calculating the mean value for countries in the database of Rodier and Roche (1984). Therefore, countries with a higher index have experienced larger extreme floods per unit area, those floods that are likely to have been most catastrophic. The areas most prone to such extreme flooding tend to be in the Mediterranean Basin. In particular, Italy and the portion of France that drains into the Mediterranean have seen the most intense flooding, with Albania and Tunisia also having very high indices (Figure2.16). With the exception of the UK, northern Europe has in comparison experienced less extreme flooding in the past. There is some variability over the Mediterranean region as a whole, which

probably reflects the differing climatic and physiographic characteristics. Nevertheless, it is clear from both Figure 2.15 and Figure 2.16 that the Mediterranean basin contains regions which are particularly prone to catastrophic flooding.

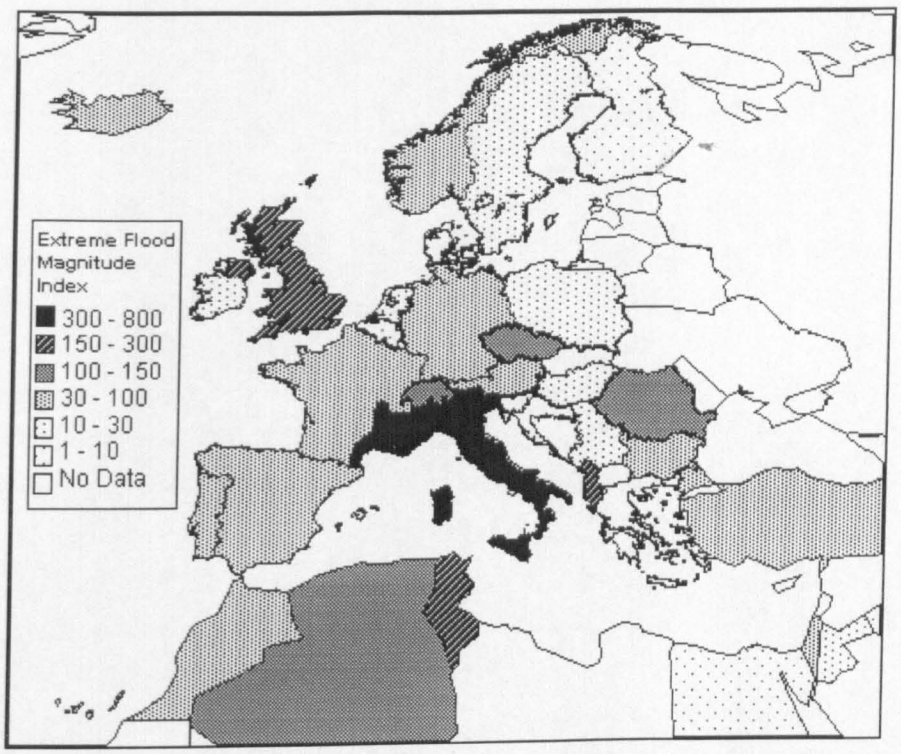

FIGURE 2.16 Map of an extreme flood magnitude index for the Mediterranean region and northern Europe. The index is a measure of the magnitude of the largest observed floods in a country in proportion to the drainage area that produced them. Therefore, the countries with a higher index experience larger extreme floods per unit area. France has been divided so that the area draining into the Mediterranean Sea is shown separately. *(Data from Rodier and Roche, 1984).*

There are numerous examples of catastrophic floods in the Mediterranean that have resulted in devastating fatalities, casualties and destruction (Table 1.1). Many of the major floods have been in the mountain areas, such as the Pyrenees or the Italian Apennines (Poesen and Hooke, 1997). The issue is becoming of increasing concern, as the last five years have seen a large number of these catastrophic events (Table 1.1). Many historical records also show a recent increase in flood frequency (Poesen and Hooke, 1997). It is as yet unclear to what extent this may be a genuine departure from the normal flood regime, and to what extent climatic or land use changes may have induced these catastrophes. However, both anthropogenic disturbance such as urbanisation (Sala and Inbar, 1992), and climatic changes relating to the variability of atmospheric circulation (Benito *et al.,* 1996) have been attributed as causes of increased flooding.

The propensity for catastrophic flooding in the Mediterranean basin presents a major problem for floodplain and water resources management. Estimates of the frequency and magnitude of large floods are important, but are difficult because adequate systematic

hydrological records are lacking (Poesen and Hooke, 1997; Benito *et al.*, 1998). Precipitation and gauging stations are often of low spatial resolution, and may only have several decades of measurements which is too short to record such rare extreme events. In other instances such records may be completely absent, especially in the flood-prone mountain areas. The Mediterranean region has seen a near exponential increase in dam construction over the last century (Schwartz *et al.*, 1990). In Spain, for example, dam spillways must be designed to the 500-year capacity flood (Poesen and Hooke, 1997), but this would be difficult to determine with any accuracy on the basis of a short systematic record. To address the deficiencies of the systematic record, various attempts have been made to investigate regional flood frequency models (e.g. Mimikou and Gordios, 1989; Ferrari *et al.*, 1993) and regional maximum flood envelope curves (e.g. Mimikou, 1984a, 1984b, 1987). From these, flood estimates may be predicted from catchment characteristics, with the former aimed at predicting mean annual floods and the latter at maximum floods. However, both approaches again suffer from the problem that they are based on a gauged data set that is inadequate both in terms of duration and spatial density to properly represent catastrophic floods. Maximum floods from envelope curves only have a return period equivalent to the length of the flood record (Mimikou, 1987).

A further problem with the short records is that they provide scant means of assessing possible temporal variability in the flood record relating to climatic or land use changes. The feature of non-stationarity that is becoming increasingly evident in other areas of the world (section 2.4.2) may be prevalent in the Mediterranean (Benito *et al.*, 1998), especially considering the significant climatic fluctuations and anthropogenic effects which have taken place in the past (Poesen and Hooke, 1997). Unlike the substantial work in the United States (Hirschboek, 1987, 1988, 1991), little is known about the flood hydroclimatology of the Mediterranean region, in terms of the climatic configurations that produce floods of various magnitudes and frequencies. One of the few studies of this type is Benito *et al.* (1996), who overcame the problem of short systematic records by using historical flood data to examine flood hydrological processes in Spain. However, much remains to be learnt about the flood producing system and its spatial and temporal variability across the Mediterranean basin, so that improved flood predictions and warnings can be made.

2.5.2 Geomorphological impact of catastrophic floods in the Mediterranean

A number of studies have demonstrated the devastating and persistent effects that catastrophic floods can have on Mediterranean landscapes (see Harvey (1984a) and Inbar (1987) in Table 2.5). These observations suggest that some Mediterranean rivers do not conform to the Wolman and Miller (1960) concept (section 2.4.3), but instead are principally controlled by extreme events. This is supported by Ergenzinger (1988), who found that low frequency high magnitude events carry out the most geomorphic work in the Buonamico Basin, Italy. Other authors have also noted episodic erosion through time occurring during large rainfall and flood events (Sala,

1988; Tropeano, 1991; Batalla and Sala, 1995; Wainwright, 1996; López-Avilés, 1998). However, there is still little detailed knowledge of the geomorphic effects of big floods in the Mediterranean (Poesen and Hooke, 1997). Because these events may play a major role in sediment transfers, it is important that their effects are understood to enable informed catchment management decisions. To understand the geomorphological effects of rare, catastrophic floods through time, demands a consideration of their role in the longer-term evolution of Mediterranean valleys. This provides the time frame necessary to assess their effects through changing environmental conditions, so that if extreme flooding does increase with future climatic change, the effects on the stability of Mediterranean landscapes could be properly assessed. The potential role of catastrophic floods in the evolution of Mediterranean valleys is discussed in the following section.

2.5.3 Pleistocene and Holocene river development in the Mediterranean

The long-term development of rivers in the Mediterranean has been influenced by three key environmental variables: active tectonics, climate change and anthropogenic disturbance (*cf.* Macklin *et al.*, 1995). All of these have been active and variable in the Mediterranean over the late Quaternary, and hence studies of Mediterranean river system development over the Pleistocene and Holocene tend to focus on one, two or all of these as being controlling factors (*cf.* Lewin *et al.*, 1995a). Research in this area started with geomorphological investigations linked to archaeological projects in Epirus, northern Greece in the 1960s (e.g. Higgs and Vita-Finzi, 1966). The publication of *The Mediterranean Valleys* (Vita-Finzi, 1969) was the culmination of extensive research around the Mediterranean by Claudio Vita-Finzi (e.g. Vita-Finzi, 1963, 1964), in which he proposed a general model of late Quaternary alluviation for Mediterranean rivers. This outlined a twofold valley sequence, consisting of a Late Pleistocene "Older Fill" alluviation phase, followed by incision, then a Late Holocene "Younger Fill" alluviation c. 300 - 1600 AD which was also succeeded by incision (Vita-Finzi, 1969). Climate was cited as the cause of these apparently synchronous phases of alluviation (Vita-Finzi, 1969). Vita-Finzi (1976) refined the model slightly, suggesting that latitudinal position might distort the exact timing of alluviation, although the Older Fill – Younger Fill model was retained. This basic model was supported by some results from Greece (e.g. Bintliff, 1975). However, others criticised it almost immediately for the fact that the field evidence and data were inadequate to support the bold generalisations made (Butzer, 1969). The strict twofold climatically controlled alluviation model and chronology conflicted with subsequent evidence which pointed to anthropogenic causes as being important (e.g. Davidson, 1980; Wagstaff, 1981). Data presented by van Andel and co-workers (Pope and van Andel, 1984; van Andel *et al.*, 1986, 1990) further highlighted how Vita-Finzi's model suffered from attempting to relate poorly dated periods of alluviation to a limited climatic record.

Over the last decade advances in dating techniques have enabled far more accurate and reliable chronologies of river activity to be established (e.g. Lewin *et al.*, 1991; Fuller *et al.*, 1996, 1998; Rose and Meng, 1999; Rose *et al.*, 1999). This has coincided with the publication of well-constrained high-resolution climatic records for southern Europe (e.g. Paterne *et al.*, 1986; Thouveny *et al.*, 1994). Developments in dating techniques such as optical luminescence and uranium-series have meant that the timescale of study can be extended, so that theories of climatic controls can be tested through repetitions of climatic cycles (Rose and Meng, 1998). This has generated increasing recognition of the fundamental role climate plays in controlling river behaviour (e.g. Harvey, 1984b, 1996; Grossman and Gerson, 1987; Lewin *et al.*, 1991; Macklin *et al.*, 1994; Roberts, 1995; Fuller *et al.*, 1996, 1998; Maas, 1998; Rose and Meng, 1999; Rose *et al.*, 1999). Recent studies have found that, over the Late Pleistocene, periods of river aggradation have coincided with cold phase climate which brought increased sediment supply and runoff, whilst warmer periods either experienced negligible river activity or incision stimulated by hillslope stability and sediment starvation (e.g. Figure 2.17) (Fuller *et al.*, 1996, 1998; Maas, 1998; Rose and Meng, 1999).

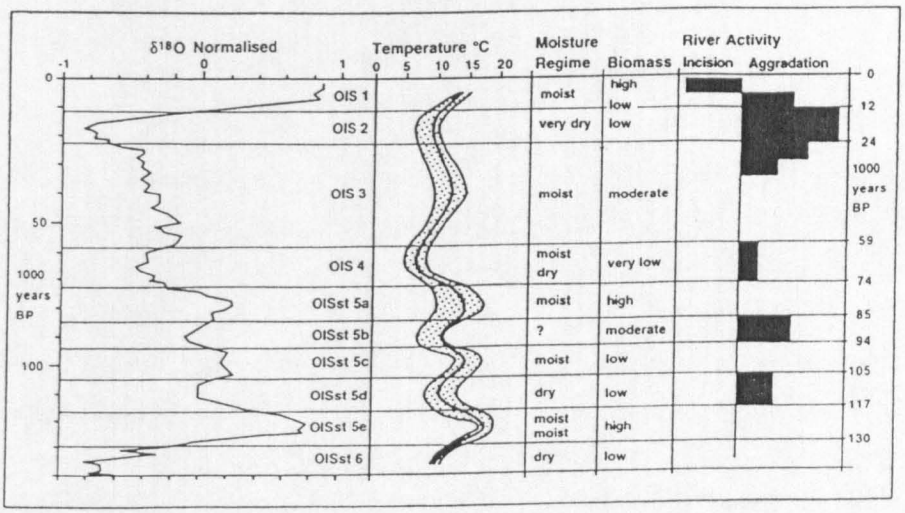

FIGURE 2.17 Palaeoenvironment and river activity in small catchments over the last 140 ka in north-eastern Mallorca, Spain. *(Source: Rose and Meng, 1999)*

The influence of climatic change is complicated in the Holocene due to the increasing likelihood of anthropogenic landscape disturbances. Previous research around the Mediterranean has shown that both climatic and human factors may have been important influences on Holocene river behaviour. Holocene sedimentation on alluvial fans in Turkey has been attributed to changes in moisture and temperature regimes (Roberts, 1983, 1995), and Fuller *et al.* (1996, 1998) also consider climate to be primary geomorphic control, as of course, did Vita-Finzi (1969). Conversely, many studies, often located in catchments with a long history of cultural

disturbance preserved in archaeological records, have shown a strong correspondence between anthropogenic activity, landscape degradation and valley floor alluviation (Wagstaff, 1981; Pope and van Andel, 1984; van Andel *et al.*, 1986, 1990; Abbott and Valastro, 1995; Hunt and Gilbertson, 1995). Settlement in new areas, slope clearance and the neglect of terraces have all been cited as factors which have driven fluvial sedimentation on valley floors (Pope and van Andel, 1984; van Andel *et al.*, 1986, 1990). However, there has been no general consensus regarding which factor has been the prime geomorphic stimulus. This probably reflects the varying intensity, and hence significance, of anthropogenic disturbance between different study areas. However, an overall lack of synchrony between Holocene alluvial records (Maas, 1998) suggests that although climate may have remained important, human induced land use changes have had a strong control over Holocene river behaviour in the Mediterranean.

It must be also be borne in mind that climatic variations and anthropogenic disturbances may have occurred within a framework of changes in other extrinsic controls, particularly tectonic activity. In certain settings, active tectonics may be a fundamental control on river development (e.g. Alonso and Garzón, 1994; Kuzucuoglu, 1995; King *et al.*, 1997), and in other instances the combined effects of climate and tectonics are particularly evident (e.g. Harvey and Wells, 1987; Frostick and Reid, 1989; Mather *et al.*, 1995). In these situations, it can be difficult to establish causation with confidence (*cf.* Macklin *et al.*, 1995).

In summary, it is important to emphasise that there is spatial variability in the importance of different extrinsic controls on Mediterranean river behaviour, particularly over the Holocene when anthropogenic factors may increase in significance. Site specific catchment histories and physiographies and regional tectonic variations mean that differences in the precise timing and controls of river activity across the region should perhaps be expected. Nevertheless, increased research over the last 10 years has clearly served to highlight the very close interplay between climatic variations and Mediterranean landscapes over the Middle and Late Pleistocene, resulting in many similarities in modes of river development across the region.

Considering the frequency and effectiveness of catastrophic floods in the Mediterranean, it seems appropriate that they should be considered as a factor in long-term river system development. Studies have often referred to high magnitude flooding as a potentially important process in stimulating phases of aggradation and incision in and around the Mediterranean (e.g. Grossman and Gerson, 1987; Frostick and Reid, 1989; Rose and Meng, 1999). However, a detailed demonstration of their long-term effects will only be possible when knowledge of the age and sedimentological characteristics of different valley floor landforms can be compared with long-term flood records. Generally it is only the landforms that have been documented so far, and there remains a need to develop long-term flood records so that the role of large floods in the development of Mediterranean landscapes may be assessed. Considering the discussion in section 2.4.3, this may be particularly relevant to steep mountain catchments of

resistant geology and coarse sediment where the Wolman and Miller (1960) concept may be inappropriate, and instead extreme floods may influence long-term river development.

2.5.4 Long-term flood records in the Mediterranean

There is clearly a pressing need in the Mediterranean for long-term flood records, both to assess the variability and occurrence of catastrophic floods to enable more informed management, and to improve our understanding of their long-term geomorphological effects (*cf.* Poesen and Hooke, 1997). Unfortunately, such data are sparse, and Table 2.6 shows the few significant studies to date. Perhaps the most comprehensive study is that of Benito *et al.* (1996), who found marked variability in historical flood records, which they ascribed to a sensitivity of flood frequency and magnitude to climatic change. AD 1400 – 1500 and AD 1850 – 1910 were identified as periods of extensive high-magnitude floods, corresponding to transitional climatic conditions. Braudel (1972) documents exceptional flooding of the Rhone Valley in the 16th century, which has been observed in some records in other areas (see Pavese *et al.*, 1992; Benito *et al.*, 1996). These records clearly show strong evidence of the non-stationarity that may be prevalent in Mediterranean flood records. Most records also show an increased flood frequency with time, however, this may largely be an effect of increased reporting (Poesen and Hooke, 1997). Nearly all of these records are documentary, which inherently means potentially incomplete records and non-homogenous error through time (Pavese *et al.*, 1992). In addition, it is often difficult to estimate flood magnitude reliably from historical data (Benito *et al.*, 1996), and such records must be treated with caution.

With current knowledge it is difficult to assess catastrophic flood variability or propensity over the Mediterranean basin as a whole. Whilst some large data sets exist for the Iberian Peninsula, long-term flood records are scant for the eastern Mediterranean. As catastrophic floods have occurred across the Mediterranean region, there is clearly a need to develop long-term flood records in those areas where such information is absent. In view of the potential shortcomings of historical data, geological palaeoflood evidence could be a valuable source of information. Palaeoflood techniques are just beginning to be applied in the Mediterranean region (Benito *et al.*, 1998; Greenbaum *et al.*, 1998, in press; López-Avilés, 1998; Maas, 1998), and show considerable promise for providing long-term quantitative data on flood frequency and magnitude.

TABLE 2.6 Long-term flood records in the Mediterranean basin.

Reference	Location	Timescale	Data type
Braudel (1972)	Rhone Valley	1500 - 1600 AD	Historical
Benito *et al.* (1996)	Spain	Mainly 1000 - 1900 AD	Historical
López-Avilés (1998)	Guadalope River, Spain	Mainly 1300 – 1996 AD	Historical & geological
Maas (1998)	Aradena Gorge, Crete	Since c. 1847 AD	Geological
Molina Sempere *et al.* (1994)	Segura River, SE Spain	826 – 1990 AD	Historical
Pavese *et al.* (1992)	Italy	500 BC – 1870 AD (R. Tiber) 1160 – 1670 AD (R. Tanaro)	Historical

2.6 SUMMARY

Rivers in the Mediterranean basin are characterised by small and steep catchments prone to intense rainfall during storms. These characteristics contribute to the propensity for catastrophic floods on these rivers, which have resulted in widespread damage to life and property and also extensive geomorphological change in Mediterranean valleys. Catastrophic floods are therefore one of the major environmental problems facing the Mediterreanean basin. They are also linked to a second major problem, that of land degradation, due to the intense erosion which may take place during these events. However, the lack of systematic hydrological data for much of the Mediterranean, and as yet few published long-term flood records, means that at present relatively little is known about these low frequency high magnitude floods.

Palaeoflood hydrology provides an opportunity to extend the flood records by exploiting preserved geomorphological evidence of flood events. Coarse-grained deposits such as boulder berms and bars, and fine-grained deposits such as slackwater deposits are all good evidence of catastrophic flood events. Such deposits may be dated by various methods to provide flood records over thousands of years. Palaeodischarge reconstructions are considerably more complex, requiring a careful assessment of the assumptions made in the techniques, ideally combined with independent confirmation of some results. In particular, incorporating a wider geomorphological investigation of valley floor features such as terraces and scour features would be valuable for assessing the stability of valley floor geometry over the period since deposition of the palaeoflood sediments. However, when investigated judiciously, both types of deposit can provide valuable quantitative data regarding catastrophic flood events. By doing so, three main areas of hydrologic and geomorphic uncertainty can be addressed:

1. Estimations of the frequency and magnitude of extreme flood events.
2. Predictions of the response of catastrophic floods to environmental change.
3. Our understanding of the geomorphological effects of catastrophic floods and their impact on landscape stability in Mediterranean river environments.

Reducing such uncertainties would be of considerable value to water-resources planning and floodplain management in the Mediterranean region, especially for the mountain areas that are particularly prone to catastrophic flooding and erosion problems.

This review therefore forms an important foundation for the present study. Gaps in current knowledge have been established, and it has been described how these could be addressed through the application of palaeoflood techniques as part of a wider geomorphological approach. Thus by providing the context of current knowledge regarding catastrophic floods and Mediterranean rivers, this chapter acts as a guide for the direction and structure that this study adopts.

3. THE VOIDOMATIS AND AOOS BASINS, EPIRUS, NORTH-WEST GREECE

This chapter describes the characteristics and regional setting of the Voidomatis and Aoos river basins. While both the physical and human attributes of this study area are considered, particular attention is given to those features important for flood hydrology and geomorphology. Previous authors have described the Voidomatis basin (Woodward, 1990; Bailey *et al.*, 1997), but very little information on the characteristics of the Aoos basin has been published in English. Section 3.1 provides a description of the geography, geology and regional geomorphology of Epirus, including background information on previous geological and geomorphological research in the region. In section 3.2 the physiography of the study basins are considered in detail. Later sections consider specific aspects of the catchments, namely vegetation and vegetational changes (section 3.3), the historic local human activities and land-use change (section 3.4), the climate and flood hydrology of the two rivers (section 3.5).

3.1 INTRODUCTION TO EPIRUS

3.1.1 Regional setting

The Voidomatis (384 km^2; 39.9° N, 20.75° E) and Aoos (665 km^2; 40.1° N, 20.8° E) River basins are situated adjacent to each other in northwest Greece (Figures 3.1 and 3.2), where they drain from the western flanks of the Pindus Mountains. Downstream of their confluence the Aoos flows northwest into Albania (where it is termed the Vjose) until it flows into the southern Adriatic Sea near the Straits of Otranto, more than 150 km further downstream. The Pindus is one of the largest mountain ranges in the Mediterranean region, extending northwards from central Greece into Albania and Macedonia. This region of northwest Greece, known as Epirus, is dominated by the imposing relief of the Pindus range. The foothills rise almost immediately from the Ionian Sea coastline, and further inland the highest peaks and karst plateaux of the Pindus are found, aligned parallel to the present coastline in a belt trending NNW-SSE. The Voidomatis and Aoos catchments are located within some of the highest terrain of Epirus, in the mountainous district known as Zaghori. The highest peak in the Pindus, Mount Smólikas (2637 m), lies on the northern watershed of the Aoos Basin (Figure 3.2). The line of mountains called the Gamila Massif, which form the watershed between the Voidomatis and Aoos catchments, are only just lower than Mount Smólikas with peaks of up to 2497 m. The study basins therefore constitute some of the most mountainous parts of Greece, characterised by rugged karst plateaux, and steep mountain gorges, peaks and passes which rise dramatically above lower-lying sedimentary basins. This relief has a profound influence over the characteristics of the

area, not only in terms of regional geomorphology, but also the climate, hydrology, vegetation, economy and cultural activities. Understanding this regional landscape requires an appreciation of the active tectonic history of the area, as described in the following section.

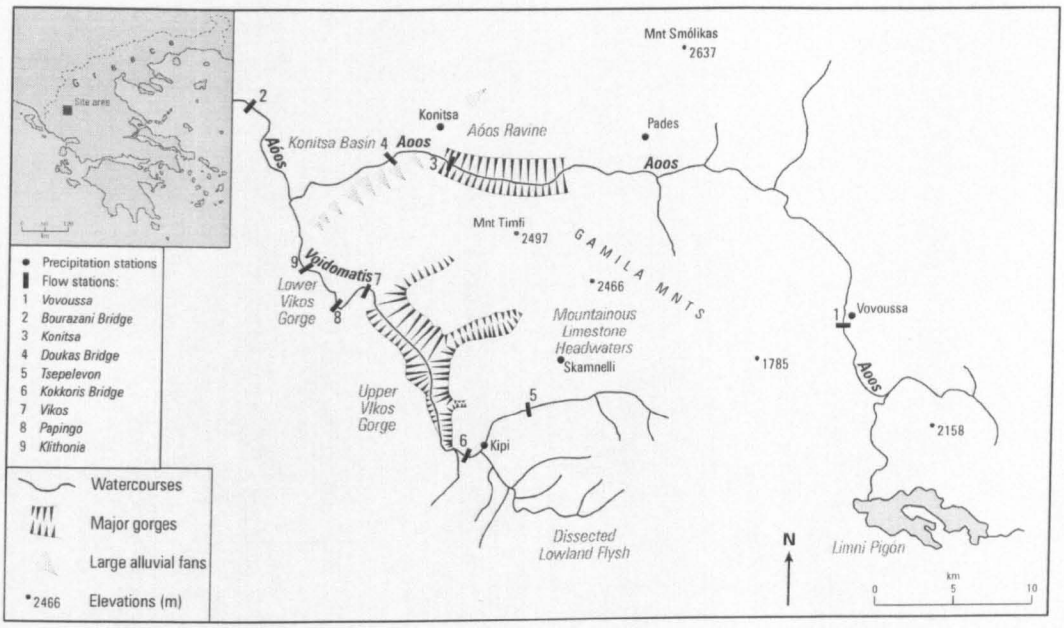

FIGURE 3.1 Map of the Voidomatis and Aoos Basins. More physiographic detail for each catchment is shown in Figure 3.8 and Figure 3.15. The stations recording precipitation and streamflow are also shown here, and data from these sites are discussed later in this chapter. The nature of the hydrological records is described in section 4.2.

3.1.2 Regional tectonics, geology and geomorphology

The Pindus Mountains and much of Epirus are a distal segment of the Alpine Mountain system that stretches through central and southern Europe (Everett *et al.*, 1986). The region lies at the heart of the most tectonically active part of the Mediterranean Basin (Figure 3.3). This activity results from close proximity to active plate margins, not only with the meeting of the African and Eurasian Plates (Figure 3.4), but also due to numerous smaller microplates which may behave differently to the larger continental units (Dewey *et al.*, 1973). Much of Greece is experiencing extension and subsidence due to subduction of the Aegean Plate beneath the Ionian Plate and an accreting margin at the southern end of the Pindus (Figure 3.4). However, Epirus continues to experience long-term compression and tectonic uplift (King *et al.*, 1997). Determinations of local uplift rates and seismic activity are difficult because the juxtaposition of geological structures and formations that exist in northwest Greece mean that it is difficult to explain fully microearthquake activity (King *et al.*, 1983). However, tectonic activity is comparable to regions such as Japan, New Zealand and parts of the Middle East, where uplift rates of between metres and tens of metres per millennia are well established (Bailey *et al.*,

1993). Tectonic events such as the disastrous earthquake in Turkey during the summer of 1999 are stark reminders of the crustal instability in the eastern Mediterranean.

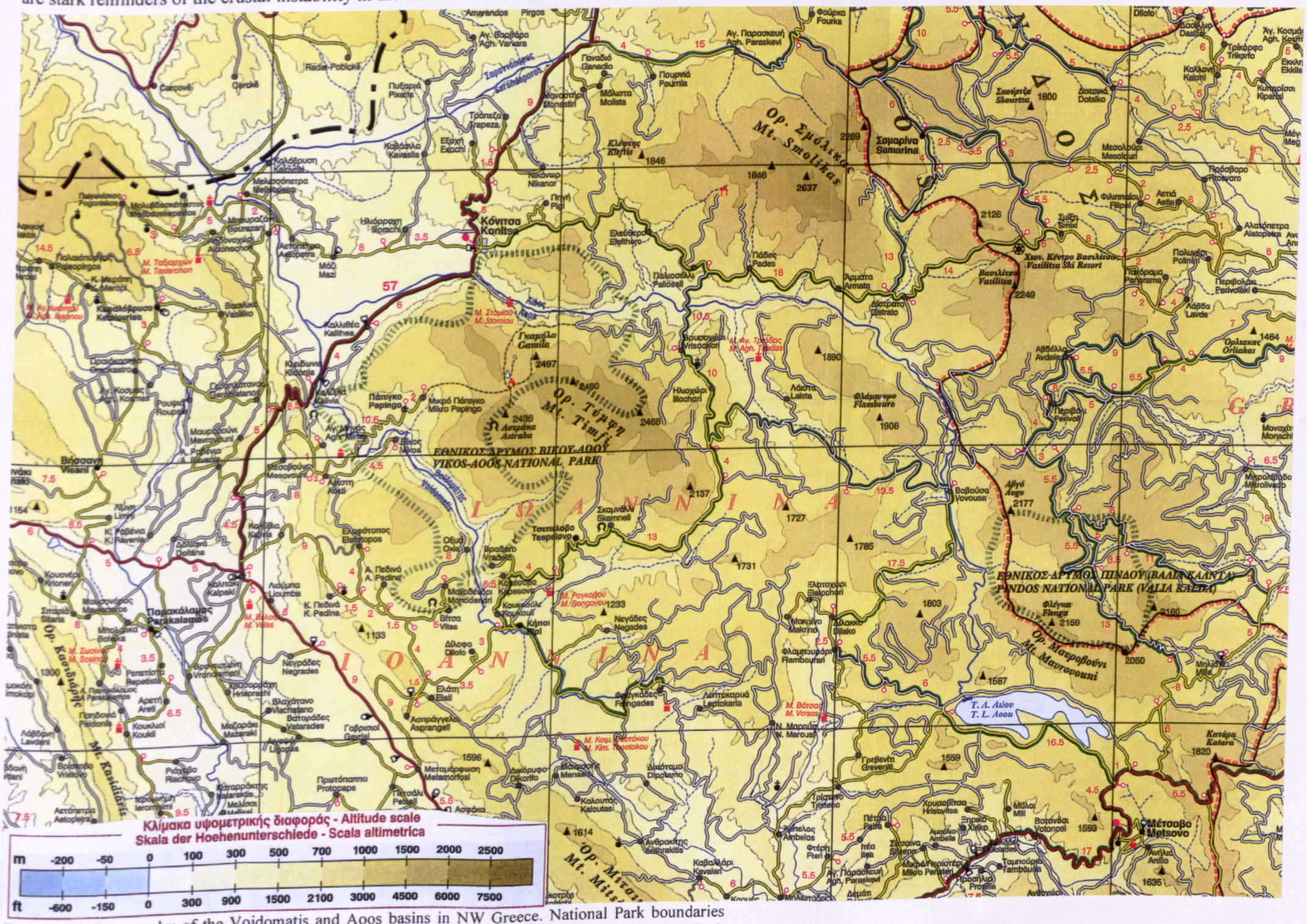

FIGURE 3.2 Topography of the Voidomatis and Aoos basins in NW Greece. National Park boundaries (dashed green lines), roads (solid green, yellow and white lines) and settlements are also shown. Each grid square is 15 km across, and north is directly upwards. *(Source: R.E.S.A., 1995)*

The compressional tectonics of Epirus have resulted in a series of overlapping lithofacies belts which trend NNW-SSE at right-angles to the general direction of compression and parallel to the present Ionian coastline (Woodward, 1990). The Voidomatis and Aoos catchments lie near the divide between a lower lying frontal zone (Ioanian Geological Zone) and further to the northeast the highest mountains of the Pindus range (Pindos Geological Zone). This

compressional alignment developed during the Cretaceous and Tertiary (Smith and Moores, 1974), and has had a strong control over the geological development of Epirus.

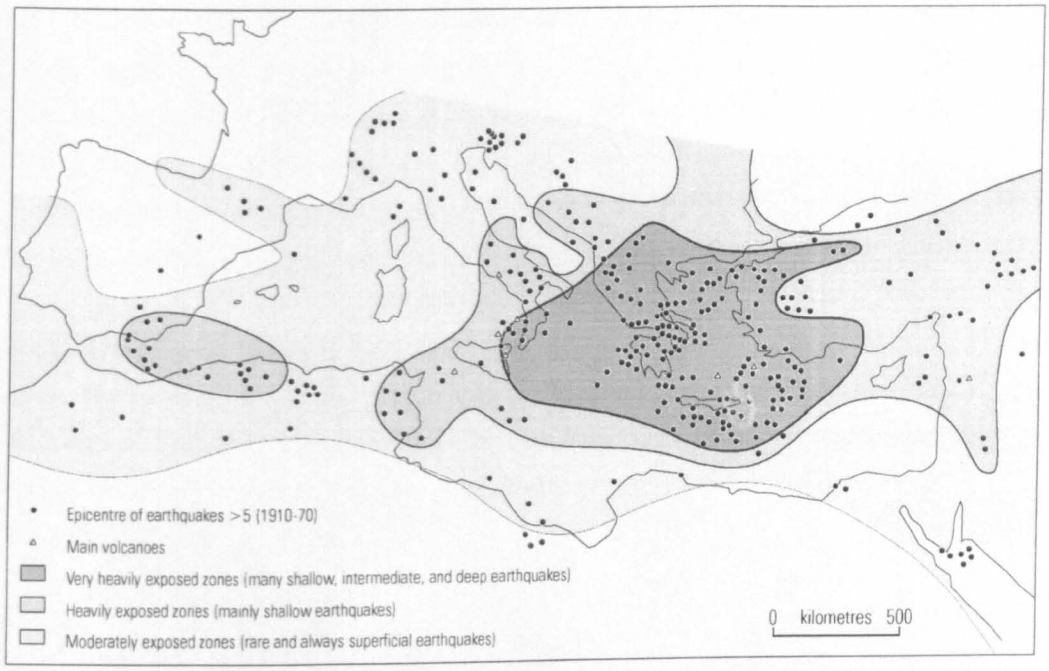

FIGURE 3.3 Present day seismicity and volcanism in the Mediterranean basin *(after Grenon and Batisse, 1989).*

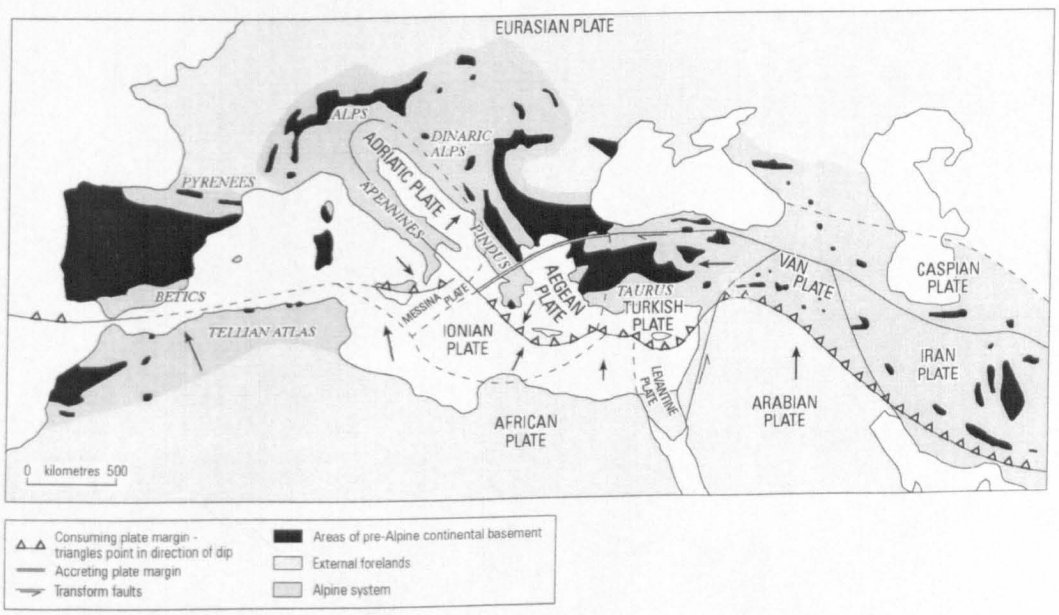

FIGURE 3.4 The present large scale lithospheric plate configuration of the Mediterranean basin together with the distribution of the pre-Alpine continental basement. Arrows refer to plate motions relative to the Eurasian plate *(after Macklin et al., 1995; and based on Dewey et al., 1973 and Windley 1984).*

The regional lithology can be simplified into four key groups: (i) limestones, (ii) flysch and flysch-like siliceous deposits, (iii) igneous material, (iv) Plio-Pleistocene alluvium, lake and fan

deposits (Figure 3.5) (King *et al.*, 1997). From the early Mesozoic Era until the Late Eocene, limestones accumulated across the entire area in the shallow water platforms of the Tethyan Ocean (Clews, 1989; King *et al.*, 1997). This calcareous deposition was interrupted by mid-Eocene times with the initiation of the Pindus Thrust, which remained active until the Oligiocene (40 - 26 Ma) and resulted in the formation of the Pindus Mountains (Clews, 1989). This emergence of more land and associated sub-aerial erosion brought increased deposition of clastic siliceous 'flysch' sediments by the Late Eocene, reflecting a change in the position of Greece from oceanic to continental margin (King *et al.*, 1997). The flysch strata are turbidite deposits of mudstone, siltstone and sandstone, whose great thickness, ranging from c. 1000 m in the west to c. 4000 m in Eprius (Richter *et al.*, 1978), reflects the enormous input of sediment from the newly uplifted mountains. This major period of flysch sedimentation ended in Epirus at the end of the Eocene, and over the Hellenides continued no later than the early Miocene, when the onset of major tectogenesis uplifted the flysch above base level to the point that it now unconformably overlies the limestone strata (Richter *et al.*, 1978; Clews, 1989).

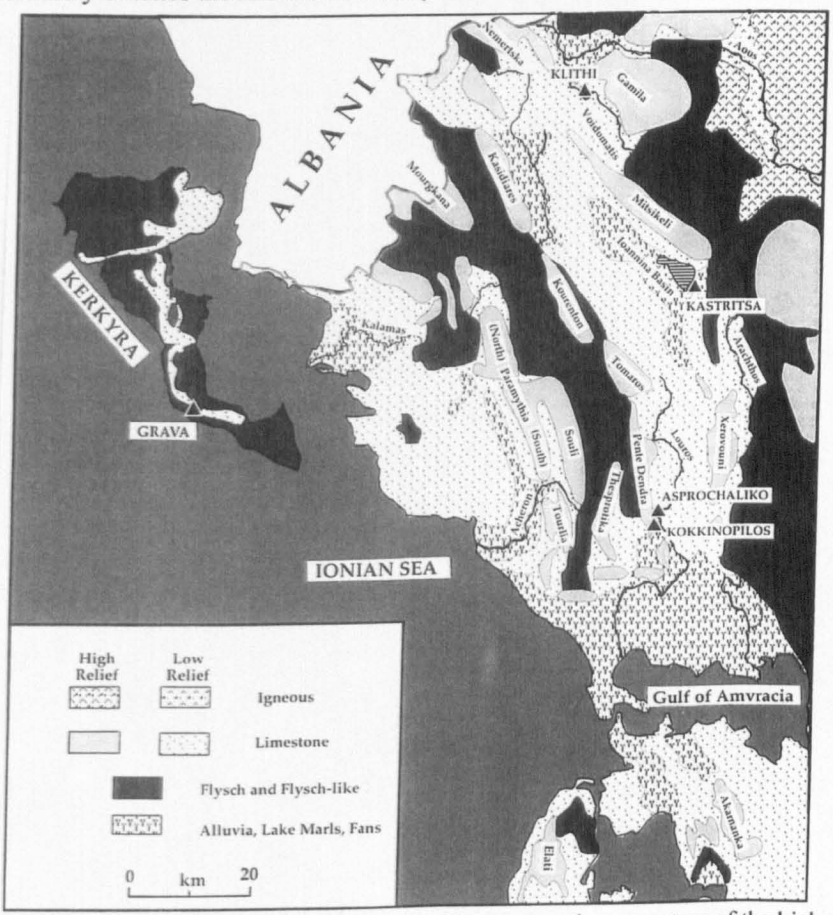

FIGURE 3.5 Simplified geology of northwest Greece. The non-continuous nature of the high relief limestone ridges is due to local regions of extension and subsidence that punctuate these steepland tracts. The locations of principal Palaeolithic sites are also shown. (*Source: King et al., 1997).*

This flysch uplift is of prime importance in understanding the regional geomorphology of Epirus. The deposition of Late Eocene flysch is illustrated in Figure 3.6a. The effect of

compression (Figure 3.6b) causes the flysch basins to be preferentially uplifted, bounded by narrow limestone ridges (anticlines) associated with the most active fault structures (King*et al.*, 1997). The weaker flysch suffers more rapid sub-aerial weathering, leaving the limestone ridges as the highest topography (Figure 3.6b). Only relict patches of flysch remain on many of the karst plateaux. This explains the large-scale features of the Epirus landscape, with alternating high limestone ridges and plateaux separated by somewhat lower-lying flysch basins. This structure is visible in Figure 3.5, with the limestone ridges and flysch basins aligned at right-angles to the direction of compression. High limestone ranges such as the Gamila and Mitiskeli rise prominently from interspersed low-relief basins such as those around Ioannina, Doliana and Konitsa, which act as long-term sedimentary sinks (Bailey*et al.*, 1997). There is little doubt that long-term evolution of the drainage networks in the area has also been strongly influenced by tectonic activity (Collier *et al.*, 1995; Macklin *et al.*, 1995). For example, this is particularly clear from the path of the Louros River that drains southward between the Xerovouni and Pente Dendre limestone horsts towards the Gulf of Amvracia (Figure 3.5). Additionally, river incision following tectonic uplift associated with either regional compression or local faulting has lead to the development of spectacular limestone gorges on a number of the rivers of Epirus (section 3.2). In some river basins, such as the Kalamas, tectonic influences may have been the dominant control on the broad pattern of fluvial erosion and sedimentation right through into the Holocene (King *et al.*, 1997). However, for other rivers in Epirus, such as the Voidomatis, it is known that important climate- and human-induced changes in river behaviour are superimposed onto the regional tectonic framework (Lewin *et al.*, 1991; Bailey *et al.*, 1997).

The Late Cenozoic uplift of the flysch represented in Figure 3.6b also explains the general instability of the flysch lithology in the Epirus region, which shows many signs of intense erosion in headwater flysch basins (section 3.2.1.2). It is tempting to attribute such degradation to anthropogenic disturbance of these erodible slopes. However, a variety of evidence shows that this chronic erosion has been occurring over long periods of the Late Quaternary, with the underlying primary cause being tectonic uplift (Bailey*et al.*, 1993). This is evidenced by high levels of flysch in Pleistocene and early-Holocene alluvial fills in Epirus (Lewin *et al.*, 1991; Bailey *et al.*, 1993), and evidence for intense erosion of the Kokkinopilos red beds over tens of thousands of years (Bailey *et al.*, 1992).

Igneous rocks also occupy an extensive part of northeast Epirus in the area of the Aoos basin (Figure 3.5). The main igneous outcrops are of Pindos Ophiolite, which is believed to have been emplaced during mid-Mesozoic times (Smith *et al.*, 1979; Jones and Robertson, 1991). The Pindos Ophiolite is thought to be continuous at depth with the Vourinos and Kastoria Ophiolites beneath the Meso-Hellenic molasse trough (see Jones and Robertson, 1991), and perhaps also with the Othris and Koziakas ophiolites which outcrop further south (Smith*et al.*, 1979).

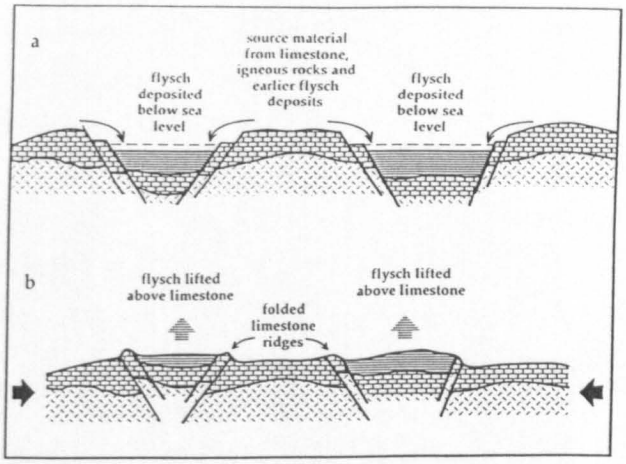

FIGURE 3.6 Simplified illustration of the relation of flysch to limestone areas. This structural configuration produces the typical mixture of horsts and grabens found throughout Epirus *(Source: King et al., 1997; concepts from Aubouin, 1965).*

3.1.3 Palaeolithic Archaeology in Epirus and the Klithi Project

In this introductory section it is important to recognise that much of current knowledge regarding the physical geography of Epirus stems from research into the Palaeolithic archaeology of the region. This research is particularly pertinent to geomorphologists, as it has sought to investigate the interactions between environmental and landscape conditions and human activities in the Palaeolithic. Eric Higgs directed the first generation of fieldwork in Epirus during the mid-1960s. Higgs identified and investigated numerous Palaeolithic sites, including finds eroding out of the red-beds at Kokkinopilos, and preserved in the rockshelters at Asprochaliko and Kastritsa (see Figure 3.5 for locations) (Higgs, 1963, 1966, Higgs and Vita-Finzi, 1966; Higgs *et al.,* 1967). He became increasingly fascinated by the influence of palaeoenvironment and palaeogeography on the Palaeolithic economies of the region, and developed a now famous theory of seasonal transhumance between archaeological sites. Although there were many shortcomings in Higgs' work, it established the importance of analysing regional and environmental contexts for interpreting the occupation of Palaeolithic sites (Bailey, 1997c).

With the challenge of establishing more substantiated links between the archaeology and palaeoenvironment of Epirus, a second generation of research, lead by Geoff Bailey, began in 1979. This involved the re-examination of Higgs' sites, and excavation of new sites. Discovery of the large Klithi rockshelter in the Lower Vikos Gorge of the Voidomatis (Figure 3.7), brought a new thrust of research in the area. Klithi has proved to be the richest Palaeolithic site in Greece, with excavations from 1983 to 1988 recovering over one million bones and flints. This large multi-disciplinary body of research has recently been formally assimilated through the publication of the Klithi volumes (Bailey, 1997a, 1997b). Whilst investigation of

the site itself was intensive, a remarkable amount of work was done into the nature of the wider environment and landscape of the Voidomatis and the Epirus region, particularly for the time of occupation at Klithi, which occurred between about 16 ka and 10 ka. This off-site work included investigations of regional tectonics (King and Bailey, 1985; King *et al.*, 1997), Palaeolithic geography (Sturdy *et al.*, 1997), vegetational history (Willis, 1992a, b, c, 1997; Turner and Sánchez Goñi, 1997), and most pertinent to this study, the investigation of river environments and sedimentation histories during the late Quaternary (Bailey *et al.*, 1990; Lewin *et al.*, 1991). The results of the alluvial investigations are described in section 6.2, and provide an important context upon which this study builds. It is largely thanks to the extensive study of the Palaeolithic of Epirus that a broad basis of knowledge exists regarding Quaternary environmental change and landscape dynamics in the region.

FIGURE 3.7 The Klithi rockshelter in the Lower Vikos Gorge of the Voidomatis basin. The low stone wall built beneath the rockshelter can be seen. The location of the rockshelter is shown in Figure 3.5

3.2 PHYSIOGRAPHY AND LOCAL GEOLOGY OF THE STUDY CATCHMENTS

3.2.1 The Voidomatis basin

Although only 384 km^2, the Voidomatis catchment contains a remarkable diversity of landscape features. This is in no small part due to the large altitudinal range of over 2000 m within the catchment. The modern channel has a steep average slope (0.016) over its c. 40 km length from the headwater streams to its downstream confluence with the River Aoos. Following Lewin *et al.* (1991), five major physiographic units can be identified. These are described in turn.

3.2.1.1 The glaciated mountainous Tsepelovon district

The northeastern watershed of the Voidomatis straddles the highest limestone peaks and plateaux of the Gamila Massif (Figure 3.8). The limestone mineralogy is very pure calcite with only small amounts of quartz and iron oxide. Directly below these peaks lies the mountain headwater region in the district of Tsepelovon, where numerous features of Pleistocene glaciation are preserved. Most immediately striking are extensive areas (c. 7 km^2) of glacially modified and transported sediments which have been deposited in well preserved moraine features (Figure 3.8) (Woodward, 1990; Woodward *et al.*, 1995; Smith *et al.*, 1998). This till is largely composed of the pure local limestone, but also includes a small but significant proportion of flysch. In addition to glacial moraines, other classic evidence of glaciations such as cirques, hanging valleys, glacial troughs and glacio-fluvial features such as kame terraces can all be identified (Bailey *et al.*, 1997). Glacial features of this nature are evident in many other parts of the Mediterranean region (Messerli, 1967), including Corsica (Conchon, 1986), the Italian Apennines (Palmentola *et al.*, 1990) and southwestern Turkey (Birman, 1968).

3.2.1.2 The headwater flysch terrain

To the south east of the catchment in the region of Kipi and Negades lies a large area of Late Eocene flysch (Figure 3.8). The flysch mineralogy is dominated by quartz with significant feldspar and clay mineral components. The area has a distinctive terrain of heavily dissected short ridge and valley forms (Figure 3.10) which support the highest drainage density of any area of the catchment at 0.84 km/km^2 (Woodward, 1990). This landscape of active gully erosion, unstable slopes and only partial vegetation cover has been described as 'semi-badland' (Woodward, 1995). The flysch is composed of fine-grained quartzite-rich sandstones that are intercalated between finer, more fissile siltstones (Figure 3.9). It is highly vulnerable to erosion and can produce large quantities of fine sediment. High intensity storms have particularly severe impacts upon this fragile headwater landscape. Rapid runoff is delivered to the high density 'pinnate' (modified dendritic) drainage network (Bloom, 1991), which forms a highly effective sediment transport system during peak flows (Bailey *et al.*, 1997).

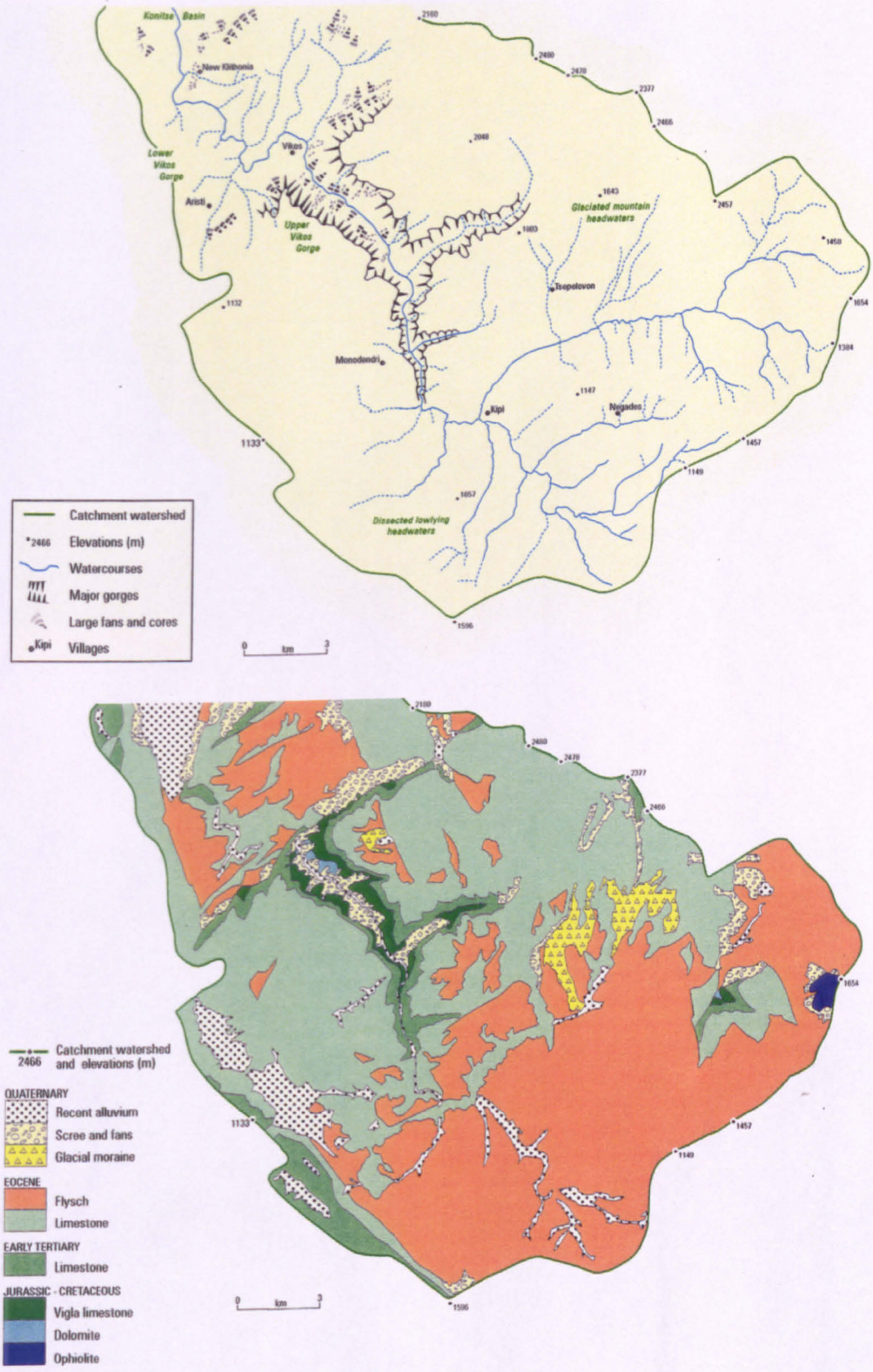

FIGURE 3.8 Physiography and geology of the Voidomatis basin, showing the region south of 40°N. *(After: IGME, 1968, 1970; Lewin et al., 1991).*

FIGURE 3.9 An exposure of the flysch lithology on the Aristi-Papingo road in the Voidomatis Basin.

FIGURE 3.10 The flysch landscape in the upper parts of the Voidomatis Basin.

3.2.1.3 The Upper Vikos Gorge

Tectonic uplift of the central limestone block of the Voidomatis, and subsequent river incision, has lead to the Voidomatis cutting down through the tablelands of Mount Gamila to produce the Upper Vikos Gorge (Figure 3.8). This dramatic karst canyon is in places almost 1000 m deep, yet only about 2500 m across. From its narrowest point to the east of Monodendri the gorge widens progressively downstream, and colluvial deposits mantling the sides of the gorge become increasingly common (Figure 3.8). At its downstream point near the village of Vikos this colluvium is practically continuous, forming large talus cones which extend close to the channel (Figure 3.11). This leaves only a narrow, gently meandering valley floor area where colluvial debris is interdigitated with alluvial terrace surfaces and elongate overbank boulder deposits. Near the mouth of the canyon is the Vikos spring, which supplies a year long flow of water through the Voidomatis downstream of this point. Upstream the Voidomatis is seasonal, having a dry bed for most of the summer months.

Here the Voidomatis displays a steep, narrow channel and a very rough boulder-bed, with the calibre of well-rounded in-channel clasts exceeding 2 m at some localities (Figure 3.12). These characteristics are indicative of very high stream powers (Bailey *et al.*, 1997) which can be expected in bedrock gorge environments during extreme flood discharge events.

3.2.1.4 The Lower Vikos Gorge

The Lower Vikos Gorge is less deep (the gorge walls are 150 - 200 m high), and generally narrower (typically 150 - 250 m wide) than the Upper Vikos Gorge. In contrast to the straight or gently meandering planform of the Upper Gorge channel, in the Lower Gorge the Voidomatis displays a series of deeply incised meander bends (Figure 3.8 and Figure 3.13). This may reflect slower tectonic uplift than in the main gorge upstream, allowing progressive lateral fluvial erosion of the gorge walls as well as vertical incision (Bailey *et al.*, 1997). The meandering pattern is accompanied by large flat lateral gravel bars, deep pools and quite steep, shallow gravely riffles which are particularly prominent during low flows. Although the gorge walls are narrower in the Lower Gorge, the valley floor area is generally wider than the Upper Gorge due to a much smaller volume of colluvium intruding into near channel areas. Instead, in some reaches the floodplain tends to occupy nearly the entire gorge floor, with significant areas of alluvial sediment storage in stabilised floodplain segments. The channel is, on the whole, significantly wider than in the Upper Gorge (10 - 25 m compared to 8 - 15 m), with a finer bedload, characterised by coarse gravels and cobbles. Unlike the main canyon, bedrock is rarely exposed around the channel bed, suggesting that vertical incision is proceeding at a slower rate along this reach of the Voidomatis (Bailey *et al.*, 1997). Flysch beds lie above the Lower Gorge (Figure 3.8), and tributaries draining from these areas bring significant volumes of fine-grained flysch material into the main channel, particularly during storm events. Debris flows are also locally important.

FIGURE 3.11 View of the Upper Vikos Gorge from Vikos village looking up valley from the downstream end of the canyon.

FIGURE 3.12 The Voidomatis channel bed in the Upper Vikos Gorge. There are numerous rounded and imbricated boulders over 1 m in diameter, which have been transported by high magnitude flood events.

FIGURE 3.13 The mid-reaches of the Lower Vikos Gorge in the region of the Aristi-Papingo bridge, looking downstream towards the Konitsa basin. The deeply incised meanders and dense deciduous hollyoak forest that characterise this physiographic area are clear from this view.

3.2.1.5 The Konitsa basin

From the mouth of the Lower Vikos Gorge at the Old Klithonia Bridge, the Voidomatis flows out onto the Konitsa basin, the final physiographic unit before its confluence with the Aoos (Figure 3.14). The Konitsa basin is a fault-controlled graben of Tertiary age (Bailey *et al.*, 1997) which acts as a large sedimentary sink for the Voidomatis, Aoos and other smaller mountain catchments. Large debris fans have developed along the margins of the basin, running steeply down from the mountain front. The basin supports relatively intensive agriculture aided by river-fed irrigation schemes. The river bisects the triangular plain with a gently meandering channel that flows around large, alternating lateral gravel bars (Figure 3.14). It flows within a floodplain which is rarely more than 200 m wide, having become steeply entrenched in Pleistocene alluvial deposits whose terrace surfaces are in places over 10 m above the modern floodplain.

3.2.2 The Aoos basin

At 665 km^2, the Aoos River basin is over 70% larger than the Voidomatis, and has a significantly different geological configuration and physiography. However, the Aoos drains a similarly large altitudinal range to the Voidomatis, and also has a relatively steep gradient (0.013) over its c. 75 km length from the headwaters to the Konitsa basin. Five main physiographic areas can again be identified.

FIGURE 3.14 View from the southern end of the Konitsa basin, looking north. The outlet of the Voidomatis from the Lower Vikos Gorge is on the far right of the photo, from which the Voidomatis bisects the basin, wandering towards its confluence with the Aoos in the distance.

3.2.2.1 Lake Pigon and the steep headwater region near Metsovo

The most upstream watershed of the Aoos catchment extends to the north of the town of Metsovo (Figure 3.15). This headwater region upstream of Vovoussa is the narrowest part of the catchment, being less than 10 km across in places, and bounded on either side by mountain ridges whose peaks reach beyond 2000 m asl. The area is underlain by Eocene flysch and some ophiolite, and is quite densely vegetated. Numerous very steep tributaries drain from the narrow mountain valleys into the main Aoos channel and the large Lake Pigon (c. 20 km^2). On one of these tributaries is the Aoos Springs hydroelectric station (Figure 3.15), that began operating in 1991. This uses the power provided by the springs of the Aoos with a fall of water of 680 m and average annual production of 200 GWH (M.I.C.C., 1994). Smaller hydroelectric plants are present on the Aoos near Vovoussa, Armata and Elefthero (Figure 3.15), however, these are normally small weirs and are minor in comparison to the Aoos Springs station.

3.2.2.2 The ophiolite terrain between Vovoussa and Distrato

Between Vovoussa and Distrato, the lithology of the Aoos catchment is mostly Pindos Ophiolite (Figure 3.15). The ophiolite is largely composed of ultrabasic rocks, mainly harzburgities and some dunites, locally intensely serpentinized, and in small veins is traversed by pyroxenite and gabbro (IGME, 1987). Although fairly extensive logging is currently in operation, the area is quite remote, supporting dense forest. The valley floor at Vovoussa is less than 15 m wide,

hemmed in by the steep surrounding mountains. However, downstream to Distrato the valley floor broadens with a floodplain up to 100 m across. These wider reaches appear to be aggrading with large in-channel gravel benches. Unlike the seasonal headwaters of the Voidomatis, the Aoos headwaters have continual flow during the summer, which, at least in part, must be due to the regulation of summer flow by Lake Pigon. On the north limits of the ophiolite terrain is Mount Smólikas (2637 m), whose slopes support many Pleistocene glacial features and sediments.

3.2.2.3 The flysch mid-reaches around Pades

Downstream of Distrato to the beginning of the Aoos Ravine the river flows over a c. 10 km wide outcrop of flysch, where the valley floor continues to widen, being up to 200 m across in places (Figure 3.15). Here the Aoos exhibits a regularly meandering planform, with some very sinuous bends downstream of Elefthero (Figure 3.15). Stream density is lower than in the headwater areas, with valley-side drainage mainly being achieved by four large tributaries (Figure 3.15). The flysch mid-reaches of the Aoos represent a zone of significant alluvial sediment storage before the valley floor narrows and the river becomes more confined through the Aoos Ravine.

3.2.2.4 The Aoos Ravine

As the underlying geology changes from flysch to dolomite, the resistant valley sides become much steeper to form the Aoos Ravine (Figure 3.15). The dolomite is grey with thin intercalations of black chert. The ravine walls are c. 500 m high, and typically 1.5 km apart. The high Gamila peaks lie directly to the south, where limestone-derived glacial deposits akin to those in the Voidomatis are present (Figure 3.15). The river straightens in the ravine, and has a channel width of some 20 - 30 m. The most distinct difference of the Aoos Ravine to the gorges of the Voidomatis is that it has minimal storage of both alluvial sediment in the valley floor or colluvial sediment mantling the gorge walls. The only significant sedimentation features are near-channel splays, bars and berms of boulders and gravel (Figure 3.16). This may reflect more resistant bedrock or more efficient fluvial sediment transport in the Aoos Ravine.

3.2.2.5 The Konitsa Basin braidplain

In contrast to the predominantly single thread Voidomatis channel on the Konitsa basin (section 3.2.1.5), the Aoos bifurcates and widens to form a braidplain more than 1 km wide, a channel pattern which is maintained until the downstream confluence with the Voidomatis (Figure3.15). The river exhibits many braided features such as confluence-diffluence units and dynamic mid-channel bars. Gravel extraction is ongoing and important in this area.

Konitsa is one of the largest towns in Epirus, and is located on a large alluvial fan in a zone of active faulting. It is particularly vulnerable to earthquakes, which during the 1990s damaged or destroyed many buildings.

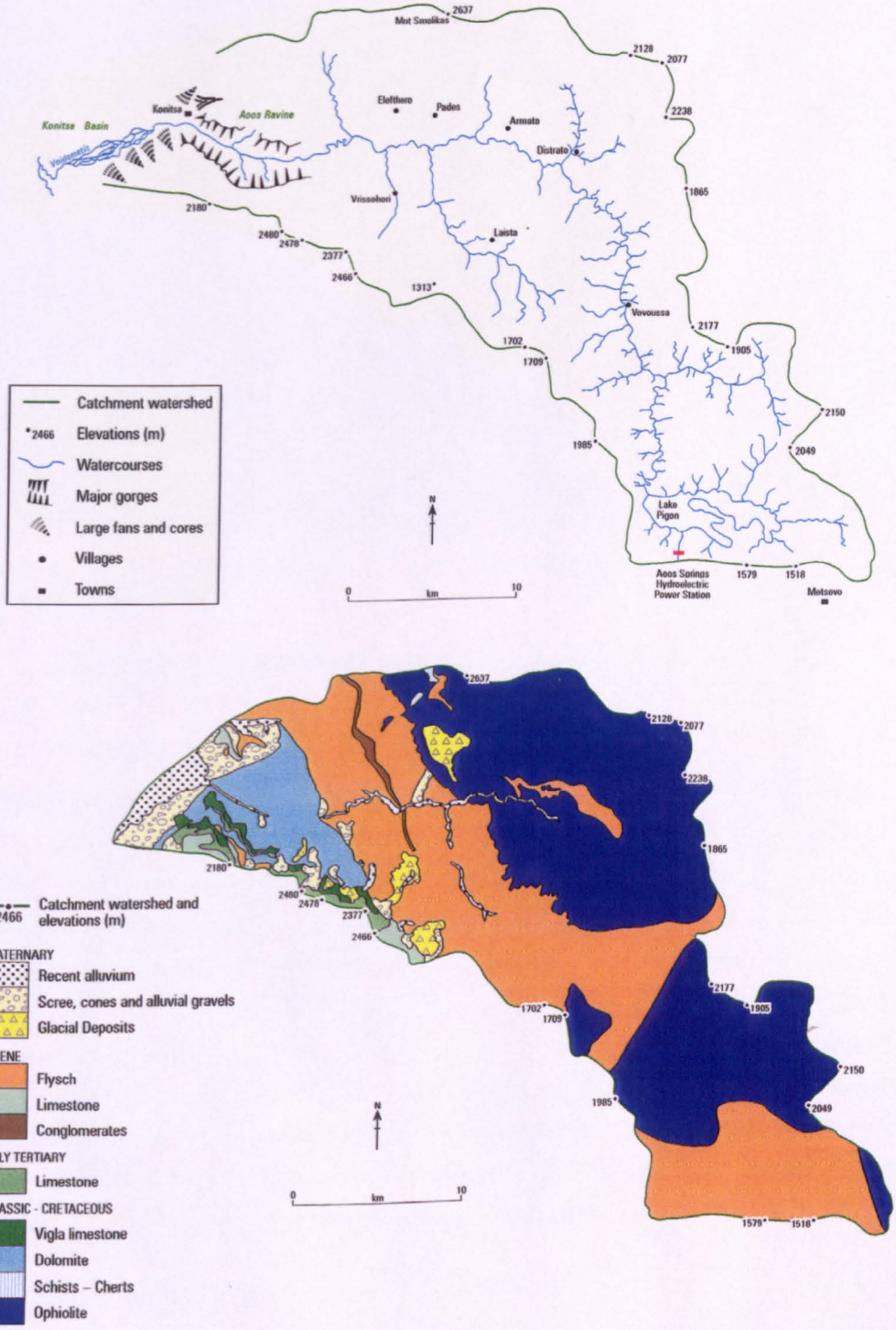

FIGURE 3.15 Physiography and geology of the Aoos basin. *(Source: IGME, 1987; HMGS, 1985).*

FIGURE 3.16 The Aoos Ravine approximately 1 km upstream from its outlet onto the Konitsa basin. The view is looking downstream.

3.3 PAST AND PRESENT VEGETATION IN NORTHWEST GREECE

3.3.1 Present day vegetation

Epirus is vegetationally one of the most diverse regions of the Balkan Peninsula (Bailey *et al.*, 1997). Away from the coast dense deciduous forests dominate the foothill regions of the Pindus, with species such as hornbeam (*Ostrya carpinifolia*), oak (*Quercus frainetto*), and hazel varieties (e.g. *Carpinus betulus, Corylus avellana*). In lower-lying basins or hillsides close to human settlements and roads, the forest vegetation has been suppressed by grazing and burning, leaving large shrubby areas of maquis and garrigue. At higher altitudes (particularly above 1000 m asl), deciduous forests give way to more uniform evergreen conifer communities, with species such as fir (*Abies*) and black pine (*Pinus nigra*). Higher regions of the Pindus have alpine grasslands above the treeline, whose elevation appears to be strongly influenced by human activities (Bailey *et al.*, 1997). The gorges of Epirus such as the Vikos and Aoos are botanically very rich with a great diversity of tree and herb flora.

3.3.2 Vegetational history

Northwest Greece is blessed with a wealth of proxy-environmental records based on palynological evidence. This is partly due to interest in the local palaeoenvironment sparked by the Palaeolithic investigations, but also because of extremely long and well preserved pollen

records which exist in lake sediments at a number of locations (Figure 3.17 and Table 3.1). Most prominent of these is the record from Lake Ioannina, located 30 km to the south of the Voidomatis basin. This exceptionally thick sedimentary sequence covers the last four interglacial-glacial cycles, a timescale of over 400,000 years (Tzedakis, 1993, 1994) (Table 3.1). The broad pattern shown by the Ioannina record is a switching between forest during warm periods, characterised by species such as *Quercus* (oak), *Ulmus* (elm) and *Zelkova* (Caucasian elm), and an open steppe-like vegetation during cold periods dominated by herb taxa such as *Artemisia* (wormwood) and *Chenopodiaceae* (goosefoot) (Tzedakis, 1993, 1994). Although some 350 km east in Macedonia, the even longer record from Tenaghi Philippon (Wijmstra, 1969; Wijmstra and Groenhart, 1983) also provides information on general palaeoclimatic changes in the eastern Mediterranean. Both the Ioannina and Tenaghi Philippon records show a broad correspondence with deep-sea oxygen isotope records (Tzedakis, 1993, 1994; Tzedakis *et al.*, 1997), and have played an important part in reconstructing palaeoenvironments in and around southern Europe since the previous interglacial (Van Andel and Tzedakis, 1996).

Whilst undoubtedly of great value, the Ioannina record reflects a large pollen catchment, containing regional and far-travelled sources. Thus its vegetational record integrates the vegetation of Epirus as whole, from the peaks of the Pindus to the Ionian coastal zone (Turner and Sánchez Goñi, 1997). To provide more local data for specific parts of Epirus, four records from much smaller lake basins have been constructed by Willis (1992a, 1992b, 1992c, 1997) and Turner and Sánchez Goñi (1997) (see Figure 3.17 and Table 3.1). The records provide high resolution pollen data for the Lateglacial and Holocene period. Following the open vegetation of the last glacial, they all show a rapid and sustained expansion of woodland during the Lateglacial and Early Holocene, initiated as early as 15,000 ^{14}C years BP at Lakes Tseravinas and Ziros. Such rapid expansions would have been aided by the presence of mountain refugia of temperate tree taxa during periods of severe climate (Willis, 1992b, 1997). Woodland communities continued to develop and diversify during the warm, moist early-Holocene. However, from the mid-Holocene onwards, human activities had a major impact upon the vegetational systems of Epirus. At around 6000 ^{14}C years BP the pollen records show the beginning of woodland decline, and although tree species show short periods of slight recovery, they have overall suffered a persistent decrease to produce the contemporary vegetation characteristics, marked by much larger proportions of shrub and herb species (Willis, 1992a, b, c, 1997; Turner and Sánchez Goñi, 1997). The decline resulted initially from landscape disturbance by Neolithic people (Willis, 1992c, 1997) and was then accentuated by widespread Bronze Age settlement and slope clearance that occurred throughout the Balkans. Thus the influence of both climate- and human-induced changes in vegetation characteristics have been inferred in Epirus. The palaeoclimate and vegetational dynamics of the region are discussed further in Chapter 6 when considering their impact upon long-term river system development.

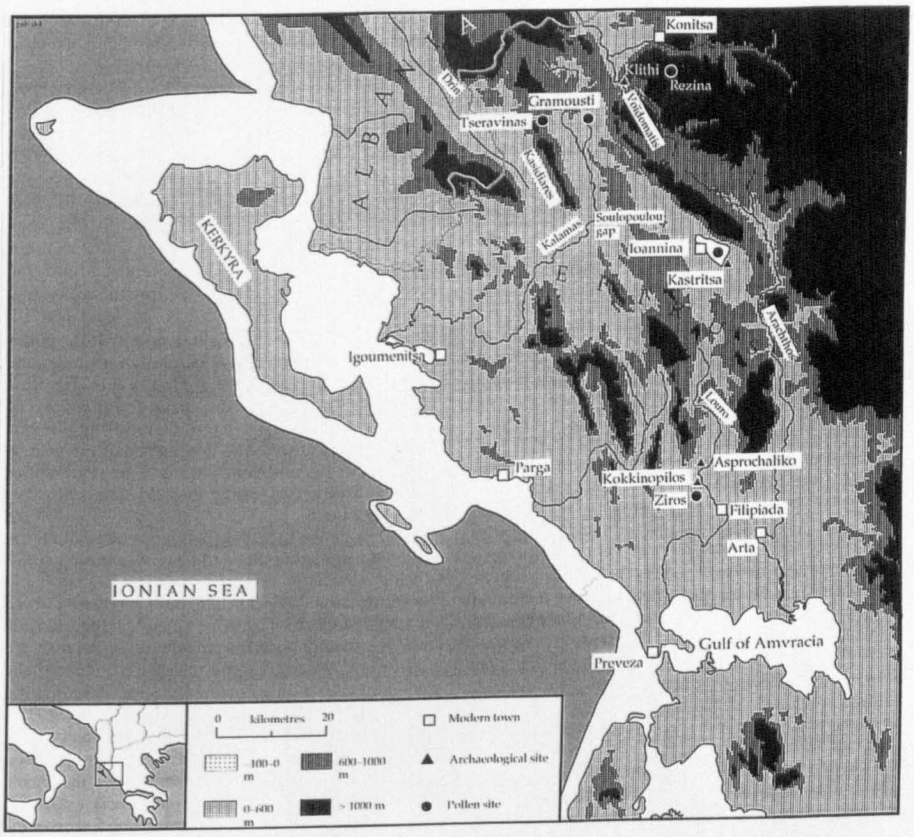

FIGURE 3.17 Map of pollen record study sites in the study region. The pollen sites are summarised in Table 3.1. *(Source: Turner and Sánchez Goñi, 1997).*

TABLE 3.1 List of the principal pollen records published from the study region. The site locations are shown in Figure 3.17.

Site	Reference (s)	Timescale covered	Core Depth
Ioannina basin and other Greek sites	Bottema (1974)	The last c. 50,000 years BP	> 10 m
Ioannina Core 249	Tzedakis (1993, 1994)	The last c.423,000 years	230.0 m
Lake Gramousti	Willis (1992a, 1992c, 1997)	Late glacial and Holocene (c. 14,000 to c. 1000 years BP)	18.45 m
Rezina Marsh	Willis (1992b, 1992c, 1997)	The last c. 10,000 years BP	12.42 m
Lake Tseravinas	Turner and Sánchez Goñi (1997)	Late glacial and Holocene (From c.15,300 years BP)	16.50 m
Lake Ziros	Turner and Sánchez Goñi (1997)	Similar to Lake Tseravinas	13.68 m

3.4 HUMAN ACTIVITIES AND THEIR ENVIRONMENTAL IMPACTS

3.4.1 Human settlement in Epirus

The turbulent history of Epirus is briefly summarised in Table 3.2 (for further details see Hammond, 1967; McNeill, 1992). As discussed in section 3.3.2, significant effects on the landscape of Epirus were brought about by human activities as early as Neolithic times (c. 6000 years BP), and afterwards due to further activities in the Bronze Age. This section deals with

human activities that are recorded in historical documentary evidence. The nature of the historical record means that more recent events are documented in far greater detail. Therefore, whilst human-induced environmental changes have taken place for thousands of years, this section concentrates on a historical period covering the last few centuries. This is important because it has been a dynamic period in the region's history, where mountain areas such as the Zaghori experienced considerable population fluctuations that impacted upon the natural environment.

TABLE 3.2 Table of chronology for selected major human activities in Epirus. *(Source: McNeill, 1992; M.I.C.C., 1994).*

Palaeolithic Age	Humans appear in Epirus. Hunter-gatherer economies.
1900 – 1550 BC	The first Greeks (Thesprotes) settle.
1550 – 1200/1100 BC	Mycenean objects found across Epirus.
400 – 300 BC	First steps towards political systems, the first signs of building and urban planning
297 – 272 BC	Reign of King Pyrrhus. Continued construction evidenced at Dodona.
168 BC	Romans conquer Epirus. Destruction and massacre.
1205 – 1449 AD	The Medieval Despotate of Epirus. Region established as semi-autonomous entity under the Byzantine Empire.
1449	Ottoman Rule, surrender to the Turks.
1500 – 1600 AD	Ioannina prospers and flourishes and the region sees a beginning of increases in mountain settlement.
1600 – 1780 AD	Continued growth of population in mountains.
1789 – 1822 AD	Ali Tepelenlis is Pasha of Ioannina. Road building and protection of overland trade. Military activities.
1822 AD	Death of Ali Pasha. There followed a period of poor public order and decreased trade. Spread of diseases through Epirus.
1820-1880 AD	Many mountain villages overpopulated and busy. Much pressure on surrounding land.
1897 AD	Epirus becomes politically Greek following the Greco-Turkish War
1880 - present	Progressive decline in mountain village populations.
1930 - 1960	Height of logging and fuel wood deforestation in central Zaghori.

Population changes of mountain villages in the area of the Voidomatis and Aoos basins are shown Figure 3.18. This shows the high populations of villages during the 19th century, with population growth seeming to have been particularly great for Laista and Vovoussa, villages in the Aoos basin (Figure 3.15). Populations probably experienced initial growth during the 15th to 18th centuries, either in response to Ottoman oppression and more common disease in the lowlands, or due to the introduction of maize to Epirus (Table 3.2) (McNeill, 1992). Village populations were therefore probably high in the 17th century. These were either sustained or grew during the jurisdiction of Ali Pasha (Table 3.2), where improved roads and agricultural expansion, combined with continued disease in the lowlands, meant that people chose to live in more mountainous areas (McNeill, 1992). Busy village life appears to have continued until the 1880s, when population decline began (Figure 3.18). This was probably caused by the detrimental effects of village overpopulation, and out-migration due to the Greco-Turkish War of 1897 (Table 3.2). During the 20th century, the two World Wars took their toll on village populations, with lows in 1920s and 1950s, overlain on a continued general decreasing trend

relating to the 20th century phenomenon of rural depopulation (Figure 3.18). In general, population trends in the towns of Zaghori have been similar (Figure 3.19), although a temporary decline occurred in the early 19th century, probably due to social unrest following the death of Ali Pasha (Table 3.2). Overall it is clear that the last two centuries have seen vast changes in the size (and prosperity) of human settlements in Zaghori, where villages are now largely populated by the remaining elderly generations. The population pressure on the region during the 19th century is believed to have had a considerable impact on the local environment and landscape, as discussed in the following section.

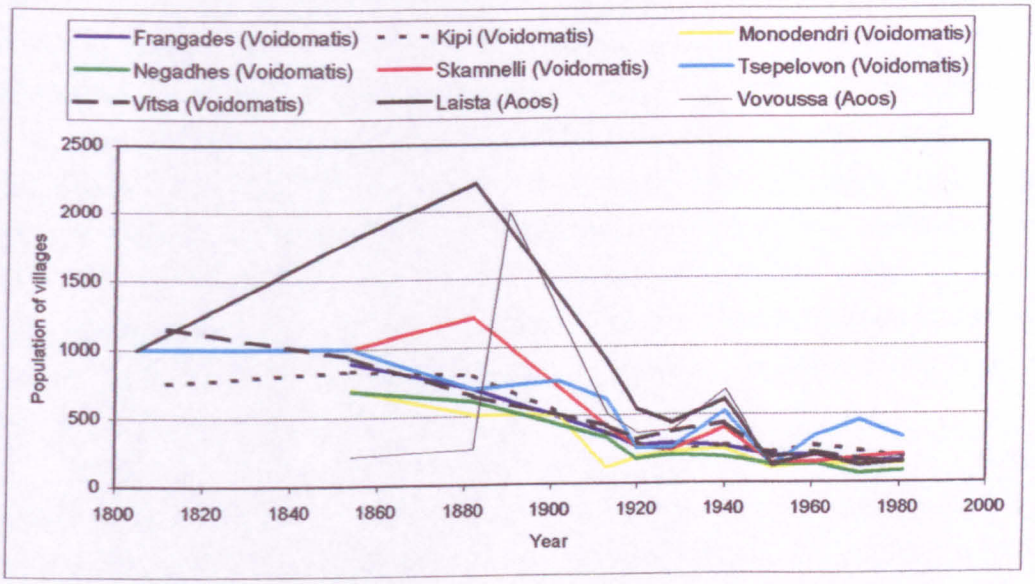

FIGURE 3.18 The population of selected villages in the Voidomatis and Aoos basins, 1805-1981. The location of most of these villages is shown in Figure 3.1, Figure 3.8 and Figure 3.15 *(Source: McNeill, 1992 and references therein).*

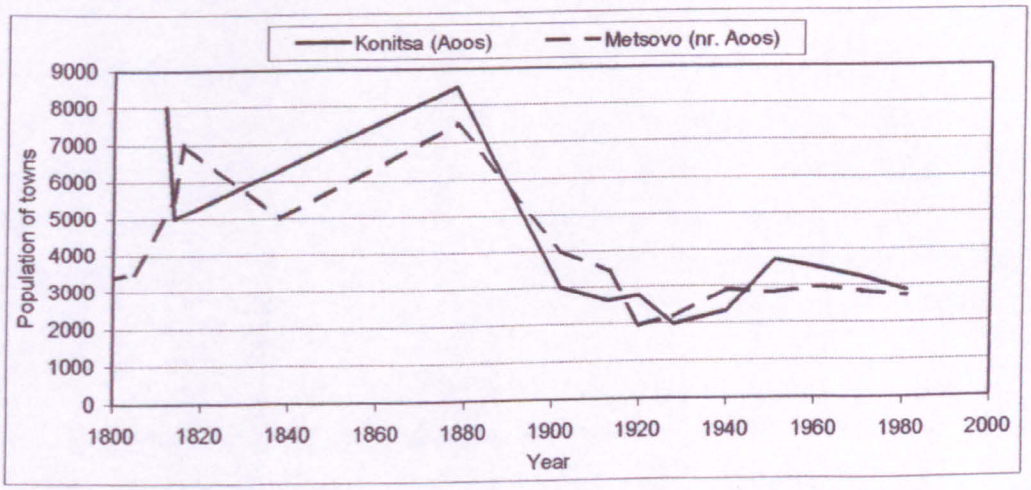

FIGURE 3.19 The population of the towns of Konitsa and Metsovo (1735-1981), whose locations are shown on Figure 3.15. *(Source: McNeill, 1992 and references therein).*

3.4.2 Historical land-use changes

As a result of the 19th century concentration of population in the mountains, Epirus experienced considerable deforestation and soil erosion (McNeill, 1992). Shepherds would burn large areas of forest to promote grass growth for pasture. Overgrazing meant that forest cover was largely unable to re-establish, whilst logging and the collection of firewood exacerbated the problem. For example, documented historical evidence from the early 19th century describes the shoulders of the Aoos at its entrance to the Konitsa plain to be covered in fir, and the mountains to the east of Konitsa to be covered in woodland (see McNeill, 1992). Today, however, the shoulders of the Aoos at this point are mostly covered in scrub, and large parts of the surrounding mountains display only stunted kermes oak. Soil erosion problems came hand in hand with the process of deforestation in many parts of Greece, particularly on the less resistant flysch terrain (van Andel *et al.*, 1986; 1990). This sometimes severe erosion continued into the 20th century due to depopulation and land abandonment and the demand for firewood persisting through to the 1940s. By the 1950s, erosion problems were recognised as one of the greatest concerns for the future of Greek development (FAO, 1959). Although soil erosion remains a serious environmental issue (section 2.5.1), the landscape may have experienced something of a respite since the 1960s due to a decline in rural depopulation, logging and fuel wood collection, and a major decline in sheep and goat numbers (Figure 3.18).

Whilst the effects of population pressure on the environment of Epirus have undoubtedly been serious, it is certainly not true that the entire regional landscape has been degraded. More remote areas, which were too steep to be cultivated and less accessible by road, appear to have suffered less, experiencing only slight land-use changes. In Zaghori there remain large expanses of heavily forested terrain relatively unscathed by human actions, particularly in mountain headwater regions. It is probable that the rugged terrain of much of the Voidomatis and Aoos basins meant that they were somewhat less severely impacted upon than other, more accessible regions of Epirus.

3.4.3 Recent developments

In 1973, The Vikos-Aoos National Park was founded, encompassing the majority of the Voidomatis basin and the Aoos Ravine (M.I.C.C., 1994). The National Park aims to protect the natural beauty and heritage of the region. A threat to the area arose in 1970 with series of proposed dams on the Voidomatis, including one that would have been constructed in the centre of the Upper Vikos Gorge. The establishment of the National Park should prevent such development.

3.5 CLIMATE, HYDROLOGY AND FLOODING

The climate of Epirus is transitional between central Europe and the Mediterranean, with considerable spatial variability due to the contrasts in aspect and relief (Bailey *et al.* 1997). In

the Voidomatis and Aoos basins the climate closely resembles a Mediterranean regime, but with distinctive Alpine characteristics due to the high local relief. This section describes the climate and hydrology of the study basins, making use of hydrological records that have been compiled by the author (described in section 4.2).

3.5.1 Temperature

Epirus has a high annual temperature range of between 40 to 45°C (Furlan, 1977), with hot summers and freezing winters. The relief imposed by the Pindus Mountains exerts a strong control over the regional temperature. The lower-lying Ionian coastal zone (Figure 3.17) has mean July temperatures some 5 to 10°C warmer than in the Pindus Mountains where the average is between 15 and 20°C (Woodward, 1990). Cloud cover tends to be at its lowest in July (Furlan, 1977), so it is frequently the hottest month of the year. In winter the effect of relief is even more intense, with average January temperatures in the mountains of Zaghori ranging from -2.5 to -5°C (Furlan, 1977). Frosts are common from October to May, especially during the harsh winter months.

3.5.2 Precipitation

All areas of the Voidomatis and Aoos basins receive high mean annual precipitation, typically ranging between 1100 to 1700 mm, as shown in Figure 3.20. Spatial variations between stations reflect their different location and relief within each catchment. For both the Voidomatis and Aoos, the stations in the headwaters (Skamnelli and Vovoussa) are the wettest, with those in the mid-section (Kipi and Pades) and lower section (Konitsa and Papingo) having progressively less annual precipitation (see station locations in Figure 3.1). In particular, Skamnelli, the highest of all these stations, receives 1702 mm yr^{-1}, suggesting that the shared watershed over the Gamila Massif is probably the wettest area in each catchment. Topography and relief have a large effect on weather patterns in the Mediterranean (HMSO, 1962; Furlan, 1977), and particularly so over Zaghori, where orographic uplift of air is a key factor in generating the high annual rainfall.

The Mediterranean character of the climate is reflected in the considerable seasonality in the annual precipitation regime (Figure 3.21), with typically 70% of the annual precipitation falling between October and March and less than 10% in the summer months. November and December are typically the wettest months of the year, with monthly precipitation often in excess of 200 mm, whilst July and August are the driest, averaging less than 50 mm for each month. During the summer there is a contracted circumpolar vortex associated with the intensification and expansion of the Azores anticyclone eastwards/north-eastwards towards the Alps (HMSO, 1962). This situation is rarely disturbed, and thus the Mediterranean largely experiences subsidence relating to a subtropical upper tropospheric high (Perry, 1981). September to October is a period of transition, with the onset of the wet winter weather brought by a drop in mean pressure and the invasion of cyclonic activity associated with the southward intrusion of cold air (HMSO, 1962; Furlan, 1977). Precipitation during the winter generally

occurs due to the meridional transport of cold air, with depressions along a meandering polar front bringing large amounts of rain (Furlan, 1977; Perry, 1981), which over the Voidomatis and Aoos basins is strongly aided by orographic effects. The winter appears to die away more slowly than it began. The spring-summer transition often occurs in an irregular fashion with stutters and 'false starts' (HMSO, 1962), with the dry summer conditions being fully established by June (Figure 3.21).

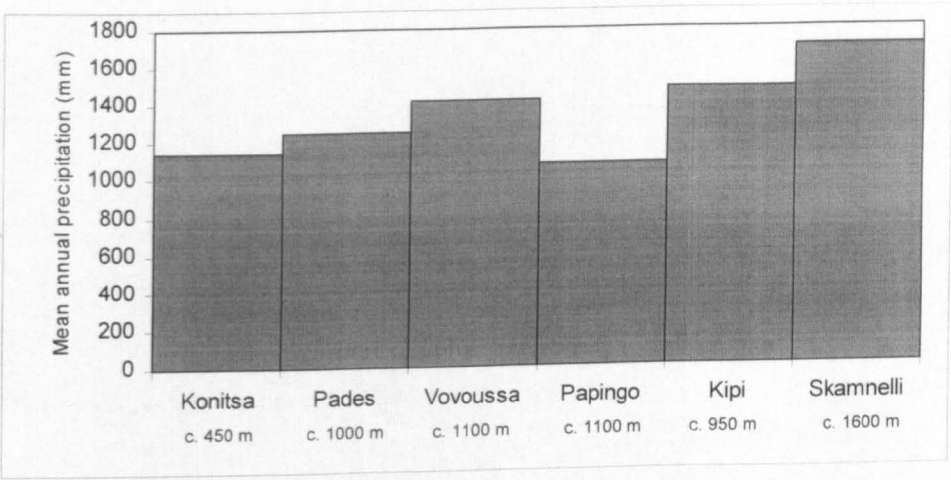

FIGURE 3.20 Mean annual precipitation for stations in the Voidomatis and Aoos basins. Locations are shown on Figure 3.1. The approximate altitude of the stations above sea level is shown. The nature of these records is described in section 4.2.

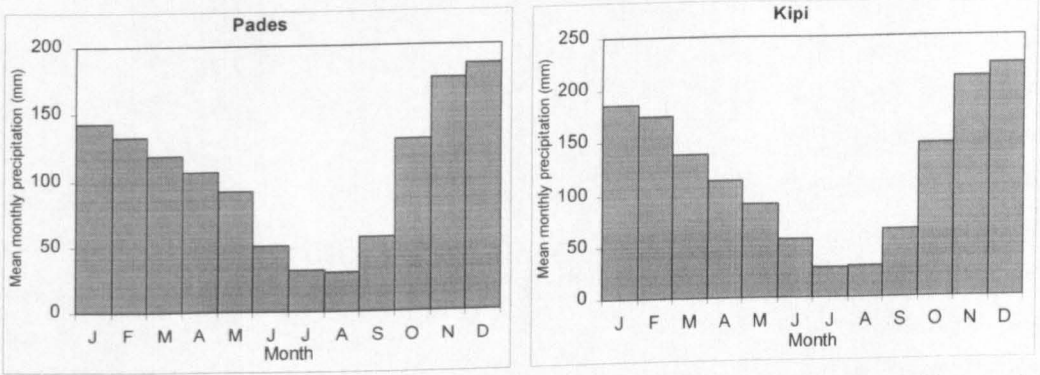

FIGURE 3.21 The precipitation regime at Pades and Kipi (locations shown in Figure 3.1), to illustrate the seasonality in precipitation. Calendar years are shown, with months abbreviated to their starting letter. The nature of these records is described in section 4.2.

The Voidomatis and Aoos basins can experience intense precipitation, as illustrated in Table 3.3. The most severe storms have occurred in the winter months, such as the exceptionally high precipitation experienced over the New Year period of 1970-71 (Table 3.3). However, storms are not limited to the winter, as heavy rains occur in both autumn and summer (Table 3.3). Although summers are very dry compared to winters, they receive some rainfall (Figure 3.21), much of which is due to intense precipitation falling during short duration thunderstorms.

Vovoussa (Figure 3.1) has the highest daily totals on record, suggesting that the headwater region of the Aoos receives the most intense storms in the area. However, high intensity precipitation is common at all stations, with the average number of days each year with >40 mm rainfall varying from 3 times a year at Papingo to 7 times each year at Skamnelli. These data demonstrate a propensity for severe and intense storms in the study area. Whilst these storms may originate from convective weather systems, their severity is undoubtedly aided by orographic effects.

TABLE 3.3 A selection of days of most extreme precipitation within the Voidomatis and Aoos Basins, including examples for different times of the year. The nature of these records is outlined in Table 4.1.

Station	Date	Precipitation (mm)
Vovoussa	31/12/1970 to 1/1/1971	315.3
Pades	31/12/1970 to 1/1/1971	261.9
Vovoussa	23/10/1970	183.5
Kipi	23/10/1970	117.7
Vovoussa	5/12/1976	118.7
Skamnelli	19/9/1977	53.6
Vovoussa	15/9/1978	79.4
Kipi	17/6/1983	42.4
Papingo	1/6/1989	52.3

3.5.3 River flow

The River Aoos at Konitsa station (Figure 3.1) has an average discharge of 47.8 m^3s^{-1}, but displays considerable seasonal variations (Figure 3.22). As would be expected, the annual flow regime largely reflects the seasonality of rainfall, with summer discharges approximately 15% of those in winter. However, there are some distinct differences between the annual rainfall regimes (Figure 3.21) and the annual flow regime at Konitsa (Figure 3.22). Firstly, there appears to be a lag between the return of wetter weather in October and the rise in river levels during November and December, which may be caused by replenishment of moisture deficits in the catchment following the drier summer period. In addition, there are also differences earlier in the year as flow levels remain high until May yet precipitation tends to become progressively less through the spring. In fact, the Aoos has some of its highest flows during April, even though this does not tend to be one of the wettest months. This is probably caused by the input of spring snowmelt that is significant enough to maintain high river levels until May. Snow falls every year across both the Voidomatis and Aoos basins, with the mountain station of Skamnelli receiving an average of 13 days of snowfall each year. Freezing winter temperatures mean that snow may not melt until spring, with the highest peaks of the northern Pindus Mountains known to have had snow cover until the end of June (Furlan, 1977).

The most complete flow record for the Aoos are daily stage data at Bourazani Bridge (downstream of the Voidomatis confluence) and Doukas Bridge (near Konitsa) (see Figure 3.1 and section 4.2). Rating equations have been used to convert these stage records to discharge, as described in section 4.2.2. The resulting flow records, displayed in Figure 3.23 and Figure 3.24,

show the quite flashy nature of the Aoos, particularly during winter and spring. Each winter normally sees several periods of high river levels and flooding. An important feature of the Bourazani Bridge records is that from 1963 onwards there appears to be a smooth gradual increase in river stage during the summer and autumn, which is characteristic of reservoir release. This is believed to mark the start of controlled water release from Lake Pignon (Figure 3.15), and thus the lack of summer flow in 1961 and 1962 in Figure 3.23 probably represents a period of zero release allowing lake levels to rise immediately after dam closure. The effect is slightly different at Doukas Bridge, where there is less of a steady rise but more of a general maintenance of summer flow.

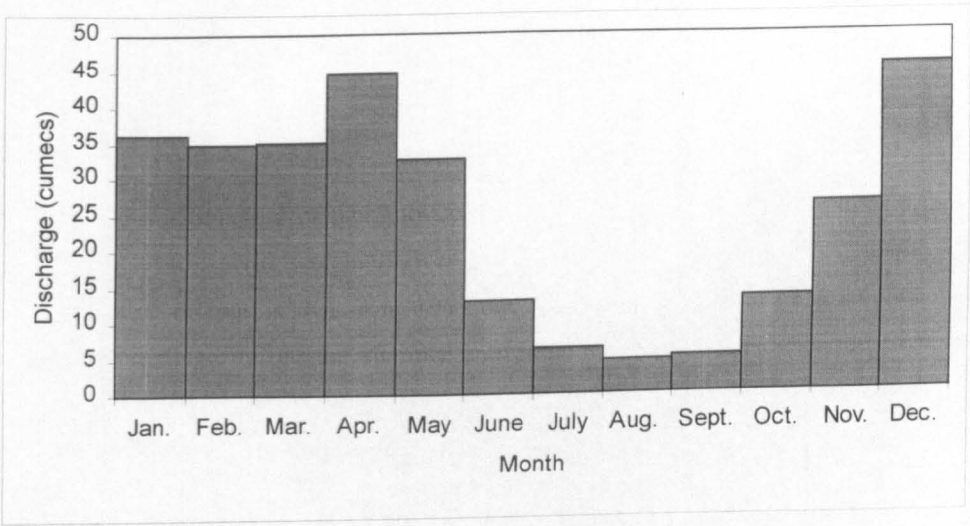

FIGURE 3.22 Mean monthly discharge on the River Aoos at Konitsa station, 1963-1987.

There are other marked differences between the Doukas and Bourazani Bridge records. Surprisingly, despite being further downstream, Bourazani Bridge records flashier hydrographs. This is probably due to the input of the Voidomatis flows downstream of Doukas Bridge (Figure 3.1). In fact, the Voidomatis is the only significant input of stream water between Doukas Bridge and Bourazani Bridge, and accounts for the much higher flood discharges at Bourazani Bridge. This means that it is possible to estimate the flow of the Voidomatis itself by subtracting the discharge at Doukas Bridge from that at Bourazani, as shown in Figure 3.25. This provides a very useful guide to the flow of the Voidomatis, especially with regard to flood events, as there is no directly gauged data for this river (section 4.2). Figure 3.25 shows that the Voidomatis displays a very flashy regime, with greater flow variability than the Aoos at Doukas Bridge. Another difference is the much higher extreme flood discharges on the Voidomatis, which exceed 900 m^3s^{-1} on four occasions, whilst a discharge of 450 m^3s^{-1} has never been exceeded at Doukas Bridge. The Voidomatis flood, estimated at 1627 m^3s^{-1}, that occurred on the 31st December 1970 (due to intense rainfall listed in Table 3.3), was a particularly high magnitude

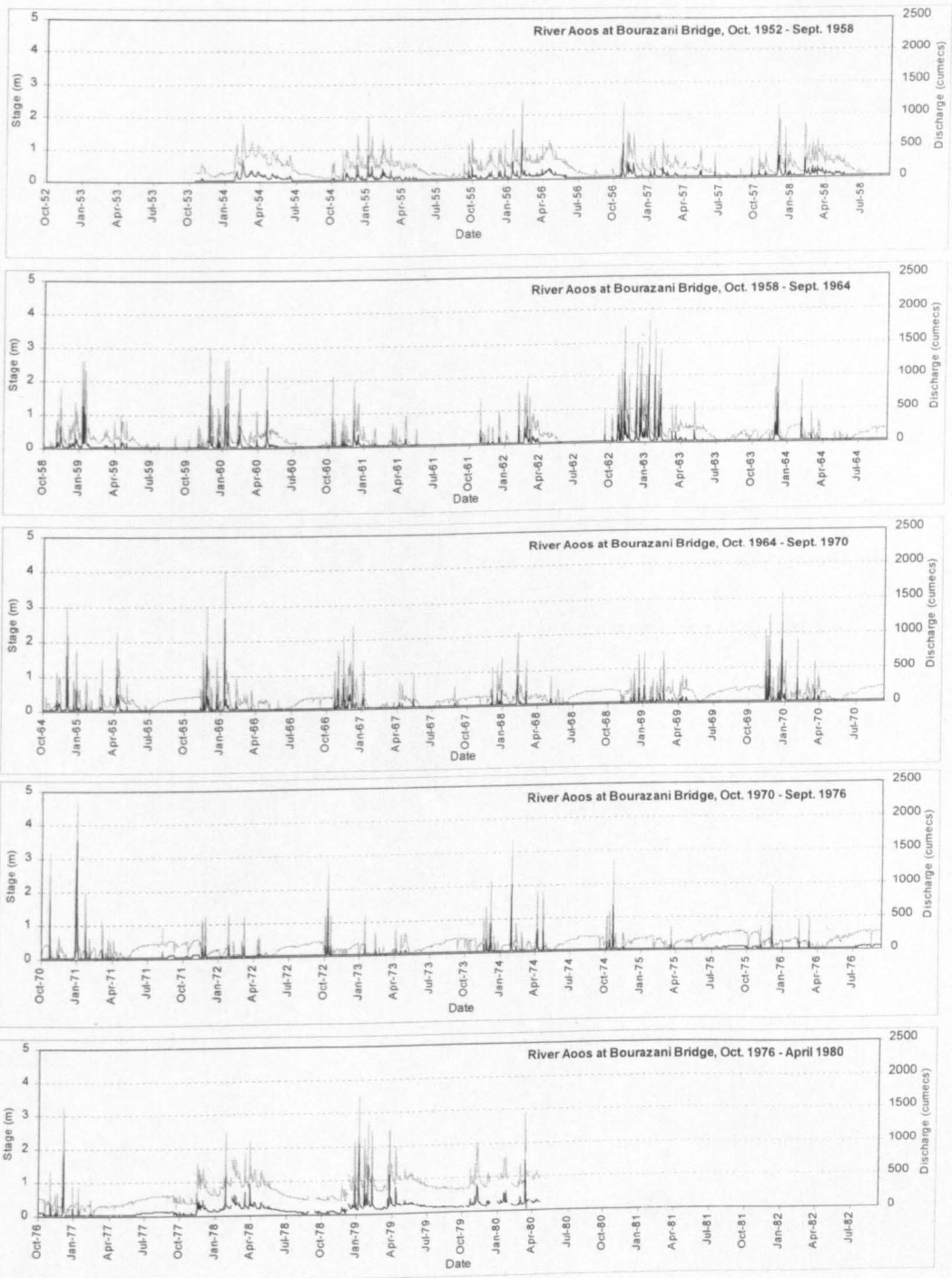

FIGURE 3.23 Daily stage (grey line) and discharge (black line) for the River Aoos at Bourazani Bridge, October 1953 to April 1980.

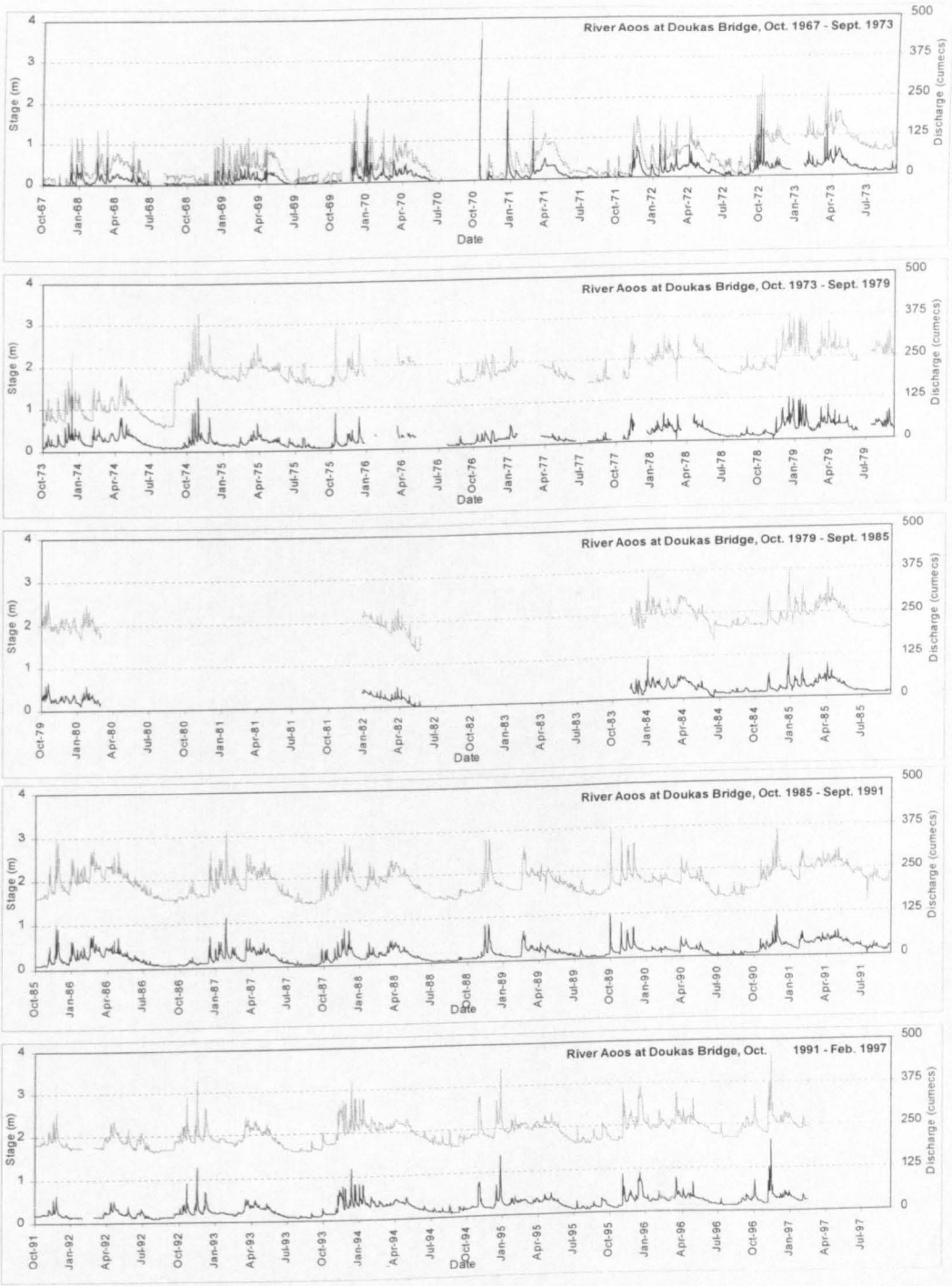

FIGURE 3.24 Daily stage (grey line) and discharge (black line) for the River Aoos at Doukas Bridge, October 1967 to February 1997. Note that for certain periods such as the early 1980s data are not available.

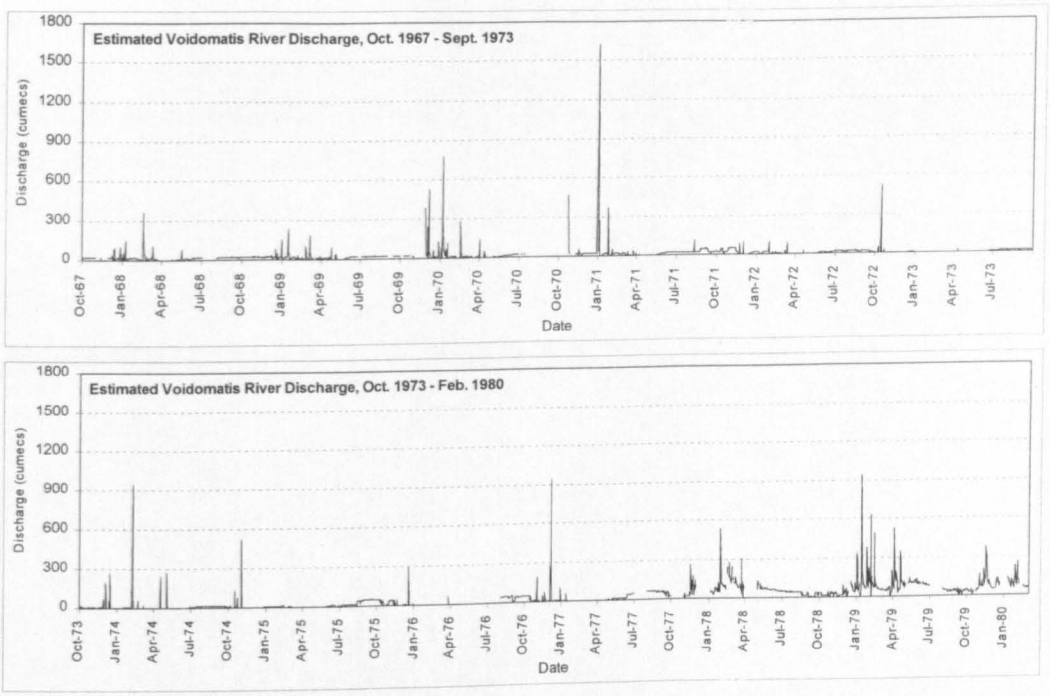

FIGURE 3.25 Estimated discharge of the Voidomatis River from October 1967 to February 1980, determined by subtracting the discharge at Doukas Bridge from that at Bourazani Bridge.

event. These higher discharges on the Voidomatis are surprising considering that the area of Aoos at 665 km^2, is over 70% greater than the Voidomatis (384 km^2), and would be expected to produce larger floods. There are various reasons for this irregularity. Regulation of the Aoos discharge in the headwaters at Lake Pigon and the Aoos Springs HEP station probably moderates flooding on the Aoos to some degree. In addition, basin morphometry may be a factor. Compared to the narrow, elongate Aoos watershed (Figure 3.15), the Voidomatis has a 'balloon' shaped morphometry (Figure 3.8) which favours the generation of extreme floods because more runoff is delivered simultaneously to the main channel than in elongate catchments (Patton, 1988). It is also likely that the high drainage density of the extensive flysch terrain in the Voidomatis (Figure 3.8 and section 3.2.1.2) serves to deliver water very rapidly to the main channel.

A more detailed view of the storm hydrograph characteristics is presented in Figure 3.26, which shows the response of the Aoos and Voidomatis to heavy rainfall during the winter period of 1st December 1969 to the 11th January 1970. This demonstrates how both rivers (and particularly the Voidomatis) exhibit very rapid, large increases in discharge in response to storm precipitation, with very short lag times (peak flow may occur on the same day as the onset of the storm) and steep, short receding limbs. This reflects rapid surface runoff and efficient delivery of water to the channel, and is indicative of a tendency for sudden, high magnitude flooding (i.e. catastrophic flooding). An independent measure of the propensity for catastrophic flooding is the Flash Flood Magnitude Index (FFMI) developed by Beard (1975) (see section 2.4.3). The closer to 1 the FFMI is, the more prone the river is likely to be to catastrophic

flooding (see Figure 2.14). All of the stations have fairly high FFMIs, suggesting that low-frequency, high-magnitude events are an important feature at all three stations. However, the FFMI for the Voidomatis of 0.76 is particularly high, suggesting that catastrophic flooding may be a relatively frequent phenomenon, and that these high magnitude events may be particularly important geomorphological events in the dynamics of the Voidomatis River (Baker, 1977).

Further discussion of the systematic hydrological data is presented in Chapter 8. However, from this section it is apparent that high magnitude flooding is an important feature of the streamflow and general hydrology of these rivers.

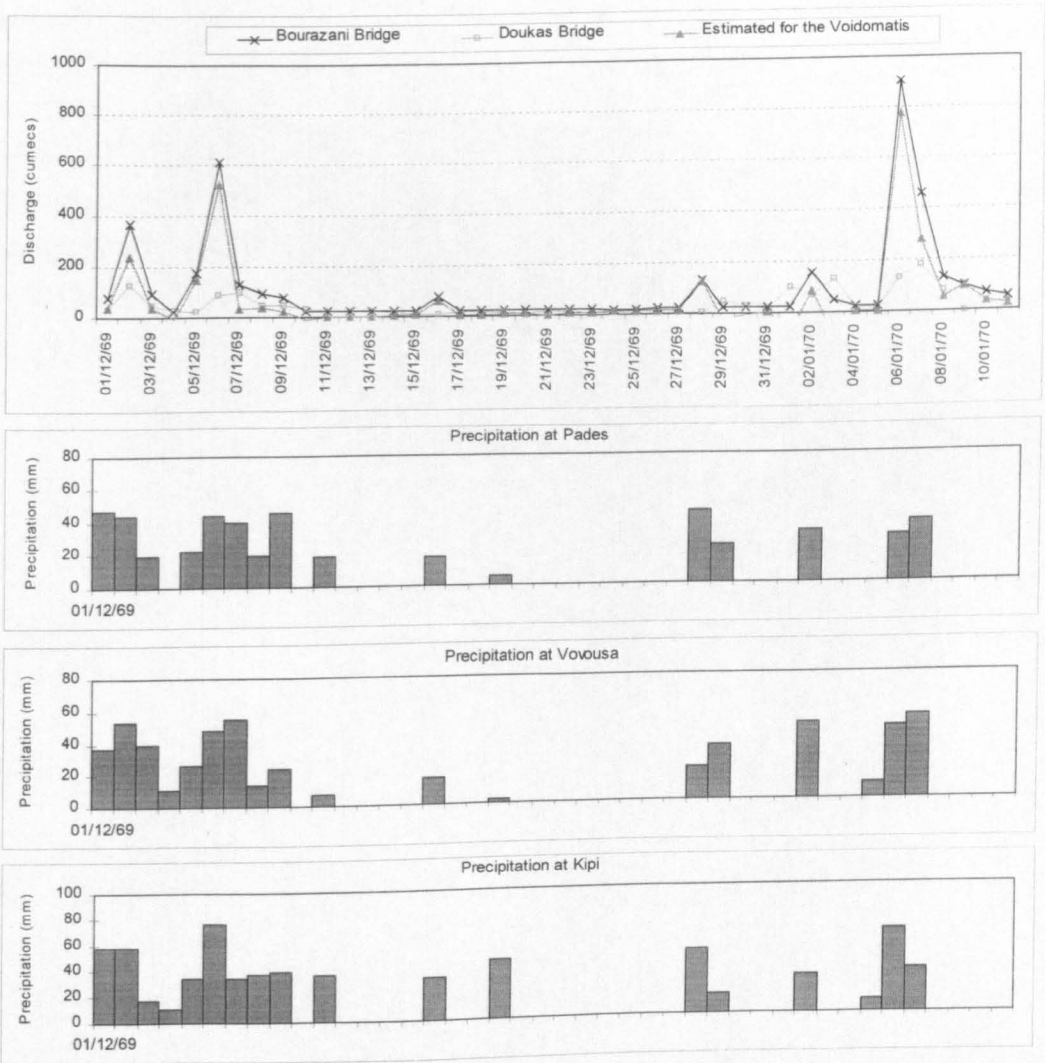

FIGURE 3.26 Comparison of precipitation and discharge records for the Aoos and Voidomatis rivers over the period 1st December 1969 to 11th January 1970. The comparison shows the rapid, flashy response of both rivers to large inputs of precipitation.

TABLE 3.4 Flood data and Flash Flood Magnitude Index (FFMI) (Beard, 1975) determined from discharge records for the Aoos and Voidomatis Rivers.

Station	Mean Annual Maximum Flood (m^3s^{-1})	Maximum Flood on Record (m^3s^{-1})	FFMI
Doukas Bridge	139	432	0.42
Bourazani Bridge	701	1779	0.51
Voidomatis (estimated)	650	1627	0.76

3.6 SUMMARY

This chapter has described the contemporary characteristics and environmental history and context of the Voidomatis and Aoos basins and the region of Epirus. Active tectonics and geology play a fundamental role in the regional landscape, having produced the characteristic arrangement of high limestone ridges and contrasting, less resistant flysch basins. Over the Pleistocene and Holocene, both climatic changes and human activities have had major impacts on the landscape. The modern day catchments have a Mediterranean style annual climatic and hydrological regime, although the high local relief means that winters are particularly cold and wet. Both rivers are prone to high magnitude flash flooding during winter, in response to intense storm precipitation. This is particularly evident in the Voidomatis basin.

4. RESEARCH APPROACH, METHODS AND TECHNIQUES

This chapter provides a description of the project methodology. The research approach, methods and techniques are outlined in section 4.1. Sections 4.2 and 4.3 provide further detail regarding the assimilation of systematic hydrological records and the collection of field data. The analytical techniques employed in this study are then described in two sections, 4.4 addressing the dating techniques, and 4.5 the laboratory determinations of sediment properties. Considerable attention is given to the dating methods used in this study, as a sound comprehension of their theory and application is fundamental to the interpretation of results that follow in subsequent chapters. Finally, a brief summary is provided in section 4.6.

4.1 RESEARCH APPROACH

4.1.1 Introduction

A range of information sources have been required to meet the research objectives outlined in Chapter 1 and these are summarised in Figure 4.1. The valley floor alluvial stratigraphy has been investigated to enable the timing and effects of catastrophic palaeofloods to be evaluated within a history of landscape dynamics and fluvial responses to environmental change. The investigation of catastrophic flooding has focused on two specific timescales; i) the Late Würm (c. 25 - 10 ka), and ii) the last 200 years (section 1.4.2). A single source of flood information cannot provide high-resolution data over such contrasting timescales. Therefore, the research approach utilises a range of flood evidence, selecting the available information sources and analytical methods most appropriate for the timescale of interest (Figure4.1). The investigation of alluvial deposits has combined dating analyses with fine-grained sediment provenance data, which provide an additional tool for interpreting the sedimentary evidence of river activity.

This section introduces the main techniques used in this study. Further details are given in sections 4.2 to 4.5.

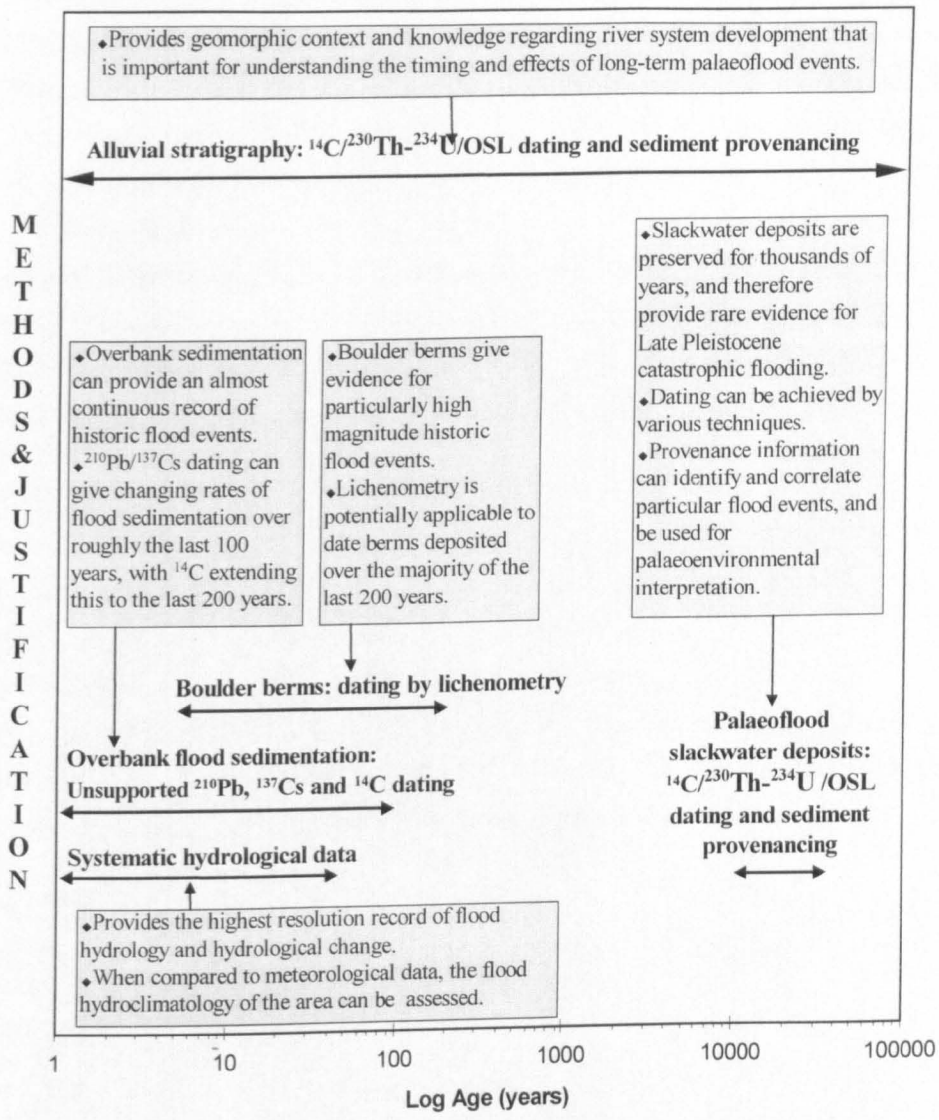

FIGURE 4.1 Summary diagram of project information sources.

4.1.2 Long-term river system development

There are three principal reasons why an assessment of the occurrence and impact of long-term catastrophic flooding requires knowledge of river system development:

1. To reconstruct palaeoflood magnitudes from flood deposits it is often important to assess whether the channel geometry and bed level height have remained stable since the depositing flood occurred (see section 2.3.3). An investigation of valley floor alluvial stratigraphy allows evidence for intervening aggradation, incision and cross-section change to be assessed (Baker, 1987).
2. To investigate the geomorphological effects of catastrophic flood events, it is important to determine the nature and timing of major changes in the form and behaviour of the river. Once this alluvial history is established, it can be compared to the palaeoflood records to

investigate possible linkages between flood events and longer-term river system development.

3. There is a more general need to develop an understanding of the relationships between environmental change and landscape dynamics. This allows the geomorphological influence of high magnitude flooding to be understood in conjunction with other factors, such as changing sediment supply and slope stability.

Investigation of flood deposits alone would therefore be insufficient for this study. Valley floor alluvial units have been dated using radiocarbon (^{14}C), uranium-series disequilibria ($^{230}Th/^{234}U$ method) and optically-stimulated luminescence (OSL), and in conjunction with this the fine-grained fraction has been analysed for provenance characteristics, as outlined in section 4.1.5.

4.1.3 Catastrophic flooding over the Late Würm

Palaeoflood slackwater deposits (SWDs) have the potential to provide long and detailed records of multiple large flood events (section 2.3). On the basis of previous dating results (*cf.* Bailey *et al.*, 1986; Macklin *et al.*, 1997), SWDs in the Voidomatis basin are believed to be of Late Pleistocene age, and provide information on catastrophic floods over this time period (Figure 4.1). As for valley floor alluvial units, ^{14}C, $^{230}Th/^{234}U$ and OSL dating analyses have been carried out in combination with fine sediment provenancing (section 4.1.5). Attempts at palaeodischarge reconstruction are described with the field results in Chapter 7.

4.1.4 Catastrophic flooding over the last 200 years

Three data sources have been used to reconstruct a flood history for this timescale (Figure 4.1):

4.1.4.1 Systematic hydrological data

Gauged flow records are the obvious starting point for investigating flooding over the last two centuries, as these provide the most reliable and detailed flood records available. Both gauged flow and precipitation records have been obtained from Greek Government authorities (see section 4.2). However, whilst these provide the highest resolution data, the records are of quite short duration, most extending for 20 or 30 years, with the oldest records dating back to the mid-1950s (section 4.2). In the absence of documentary evidence, wall marks or folk laws recording large historic flood events, palaeoflood hydrological techniques provide a means of extending the flood record to cover the last 200 years necessary to assess catastrophic flooding. Two types of palaeoflood evidence have been used (Figure 4.1):

4.1.4.2 Boulder berms

These are open-framework coarse gravels and boulders deposited across or adjacent to the river channel (Costa, 1984), which often form a fairly thick (>2 m) linear deposit with steep sides and considerable surface relief (Macklin *et al.*, 1992a). The use of these deposits in palaeoflood reconstruction has been reviewed in section 2.2. Lichenometry has been used to date berms

deposited over the last 200 years, utilising abundant *Aspicilia calcaria (L.) Mudd* populations. The methods of field identification of berm deposits and palaeodischarge reconstruction are described with the field results in Chapter 8.

4.1.4.3 Overbank flood sedimentation

The accumulation of fine-grained sediments deposited over the floodplain during periods of inundation provides a useful record of palaeoflood events (section 2.3.5). Radiometric dating using unsupported Lead-210 (^{210}Pb) and Ceaseium-137 (^{137}Cs) combined with ^{14}C has enabled a chronology of overbank flood sedimentation to be constructed for the last two centuries.

4.1.5 Determination of sediment sources to identify changes in the fluvial environment

In addition to the field studies and geochronological work described above, analyses have been carried out to determine the source of fine sediment within fluvial deposits. Previous work by Woodward *et al.* (1992) demonstrated the potential for using the properties of deposited fine sediment to investiagte the temporal variability of catchment sediment sources. They showed that, in the Voidomatis River, the provenance of fine sediments has been strongly influenced by the prevailing environmental conditions. Therefore, further sediment provenancing work has been carried out in this study, primarily to reconstruct catchment scale environmental conditions at the time when sediments were deposited. The approach taken here was to build on the work of Woodward *et al.* (1992) in three ways:

1. developing more robust, *quantitative* determinations of fine-grained sediment provenance by applying recently developed quantitative 'fingerprinting' techniques (Peart and Walling, 1986; Walling and Woodward, 1995);
2. using the quantitative fingerprinting technique to provide more detailed provenance information on a larger number of the potential fine sediment sources which exist in the Voidomatis basin. This could not have been achieved by Woodward *et al.* (1992) who used more traditional, qualitative mineralogical analyses;
3. establishing the provenance of the fine-grained flood palaeoflood slackwater deposits, which were not explored by Woodward *et al.* (1992).

Details of the sediment fingerprinting work are given in Hamlin *et al.* (in press) and are described here in Chapter 5. Fingerprinting requires the analysis of the sediments for a number of chemical and/or physical properties. The selection of these techniques and the adopted laboratory procedures are described later in this chapter (section 4.5).

4.2 SYSTEMATIC HYDROLOGICAL DATA

4.2.1 Data Collection

Precipitation and streamflow data were collected from two Government sources in Athens, the records obtained being summarised in Table 4.1 and Table 4.2. The Public Power Corporation

(PPC) held many of the local precipitation records. They also had a large number of river discharge records, although these generally cover a short timespan with no more than a few recordings per month (Table 4.2). The Ministry of Physical Planning (MPP) (Department of Environmental and Public Works) holds a smaller number of records from other stations, with two daily stage records being of particular value. Unfortunately, both institutions insist that the data must be copied by hand on the premises, and this limited the volume of data that could be obtained. Nevertheless, a large data set of both precipitation and streamflow records was collected. In addition to the Government data, long duration temperature, precipitation and pressure records have also been obtained from the World Climate Disk (1992) (Table 4.3).

TABLE 4.1 Precipitation data obtained from Greek authorities. The station locations of are shown in Figure 3.1.

Station	Source	Length of record	Type of data
Konitsa	MPP	1951-1981	Mean monthly precipitation, daily values for periods of extreme precipitation†.
Kipi	PPC	1967-1992	As above, in addition the number of days per month with some snowfall was recorded.
Pades	PPC	1967-1992	As above
Vovoussa	PPC	1967-1992	As above
Papingo	PPC	1971-1992	As above
Skamnelli	PPC	1973-1992	As above

†A day of "extreme precipitation" was normally defined as greater than 40 mm of precipitation at one of the stations. 40 mm was a common enough amount to occur reasonably regularly yet large enough to represent very heavy storm precipitation. Precipitation preceding and following a large storm was also recorded.

TABLE 4.2 Flow data obtained from Greek authorities. The station locations of are shown in Figure 3.1.

Station	River	Source	Length of record	Type of data
Konitsa	Aoos	PPC	1963-1987	Calculated mean monthly discharge
Konitsa	Aoos	PPC	1964-1993	Fairly regular daily discharge
Vovoussa	Aoos	PPC	1961-1993	Fairly regular daily discharge
Kokkoris Br.	Voidomatis	PPC	1961-1980	Occasional daily discharge
Tspelevon	Voidomatis	PPC	1970-1987	Occasional daily discharge
Klithonia	Voidomatis	PPC	1970-1971	Occasional daily discharge
Papingo	Voidomatis	PPC	1970-1971	Occasional daily discharge
Vikos	Voidomatis	PPC	1970-1971	Occasional daily discharge
Bourazani Br.	Aoos	MPP	1953-1980	Daily stage
Bourazani Br.	Aoos	MPP	1953-1962	Limited daily stages and discharge
Doukas Br.	Aoos	MPP	1967-1997	Daily stage
Doukas Br.	Aoos	MPP	1953-1967	Limited daily stages and discharge

TABLE 4.3 Data obtained from the World Climate Disk (1992).

Station	Length of record	Type of data
Athens (Observatory)	1858-1990	Mean monthly temperature
Athens (Observatory)	1858-1991	Mean monthly precipitation
Various latitudes and longitudes	1873-1991	Mean monthly sea level pressure

4.2.2 Stage-Discharge Relationships

The daily stage records obtained from the MPP for Bourazani Bridge and Doukas Bridge represent the most comprehensive flow records available for the study area. However, to make this data amenable to common hydrological analyses required converting stage to discharge. Fortunately, a number of simultaneous stage-discharge readings exist for both stations, which can be used to construct stage-discharge relationships (or rating curves). Most stage-discharge relationships involve a single best fit line through the simultaneous stage-discharge data, which normally takes the form of a simple power regression (Shaw, 1988). However, both of the stations in this study exhibited some complexities that required adaptation of this standard form. At Bourazani Bridge, the data appeared to separate into two groups above and below about 0.5 m stage, each of which exhibited a very different stage-discharge trend. This occurs because the cross section at this station has a small, narrow inner channel about 0.5 m deep, where stage responds very differently to increases in discharge compared to the channel occupied above 0.5 m flow depth which is much broader (MPP, pers. comm. 1997). As recommended by Shaw (1988), two different power regressions were fitted to each of these groups (Figure 4.2), and the different rating equations used for each stage range (Table 4.4). As some of the stage-discharge readings included negative stage values, 0.2 m was added to all stage data to permit the calculation of the power regression, and is therefore also included in the rating equation.

At Doukas Bridge the stage-discharge data do closely fit a single power regression (Figure 4.3). However, the complication here arises due to apparent non-stationarity in the position of the channel bed at this station. This is shown in Figure 4.4, where both the annual minimum and mean stage saw systematic upward shifts in the early 1970s, whilst the discharge at the nearby Konitsa station (Figure 3.1) shows that there were no systematic increases in the minimum or average flow on the Aoos River over this period. The stages at Doukas Bridge show two distinct increases over time. The most pronounced is between the hydrological years 1973-74 and 1974-75, where minimum stage increases by about 1 m (Figure 4.4). This has been caused by a sudden change in the stage reading form 31st August 1974 of 0.63 m to 1.64 m the next day, which is clearly visible as an abrupt and prominent change in Figure 3.24. This has not been caused by a genuine flow increase as for many days before and after these dates there is little or no change in stage (Figure 3.24). Instead, it is likely that this has resulted either from replacement or adjustment of the stage board, with it being left in a position some 1 m higher than before. This explains the consistently higher minimum and average stage after this date (Figure 4.4). A second change occurred several years before this, when between 1971-72 and 1972-73 the stage again has increased systematically by about 0.5 m (Figure 4.4). This appears to have occurred around October 1972 (Figure 3.24), after which the minimum stage never again falls below 0.5 m. Whilst this might partly be due to hydrological variability, this increase seems beyond the range of variation in minimum stage during earlier years (c. 0.25 m), and may therefore have been caused by some raising of the riverbed at this time. As the simultaneous

stage-discharge readings were taken before the 1970s, these systematic changes in cross section and stage board position must be accounted for in the rating equations to ensure that the discharge record is internally consistent. Therefore, from the 1st October 1972 0.25 m is subtracted from the stage readings, and from the 1st September 1974 a further 1.0 m subtracted (Table 4.4). This resulting discharge record (Figure 3.24) shows similar values to that at the nearby Konitsa station (Appendix I), and therefore these stage corrections are believed to be valid.

Although there were complications in constructing both stage discharge relationships, it is believed that the rating equations provide an acceptably accurate means for stage-discharge conversion. Although the number of simultaneous stage-discharge recordings would ideally be larger, the fitted lines for both stations show very good R^2 values, and thus form a valid method of stage-discharge conversion.

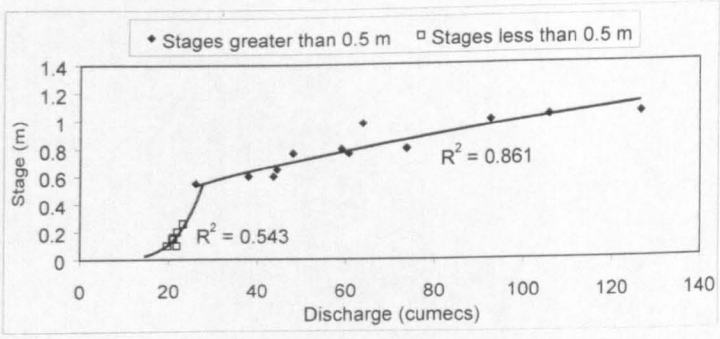

FIGURE 4.2 Stage-discharge relationship for Bourazani Bridge.

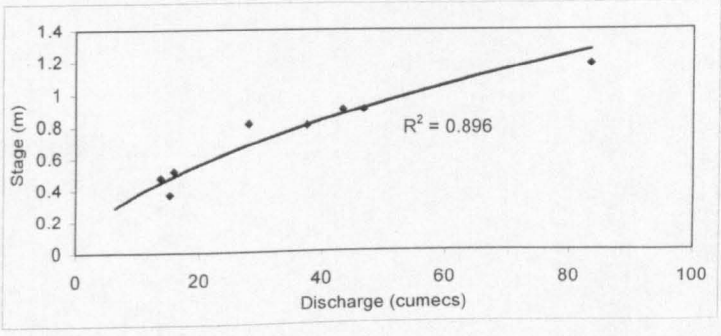

FIGURE 4.3 Stage-discharge relationship for Doukas Bridge.

TABLE 4.4 Stage-discharge (rating) equations determined for Bourazani Bridge and Doukas Bridge. The form of the equations is explained in the text.

Station	Conditions	Equation†
Bourazani Bridge	Stages of 0.5 m or less	$Q = 93.741\ (H + 0.2)^{1.852}$
	Stages greater than 0.5 m	$Q = 26.245\ (H + 0.2)^{0.109}$
Doukas Bridge	From the start of record until end Sept. 1972	$Q = 51.645\ (H)^{1.560}$
	From 1st Oct. 1972 until end Aug. 1974	$Q = 51.645\ (H - 0.25)^{1.560}$
	From 1st Sept. 1974 onwards	$Q = 51.645\ (H - 1.25)^{1.560}$

†where Q is discharge in m^3s^{-1} and H is stage in m.

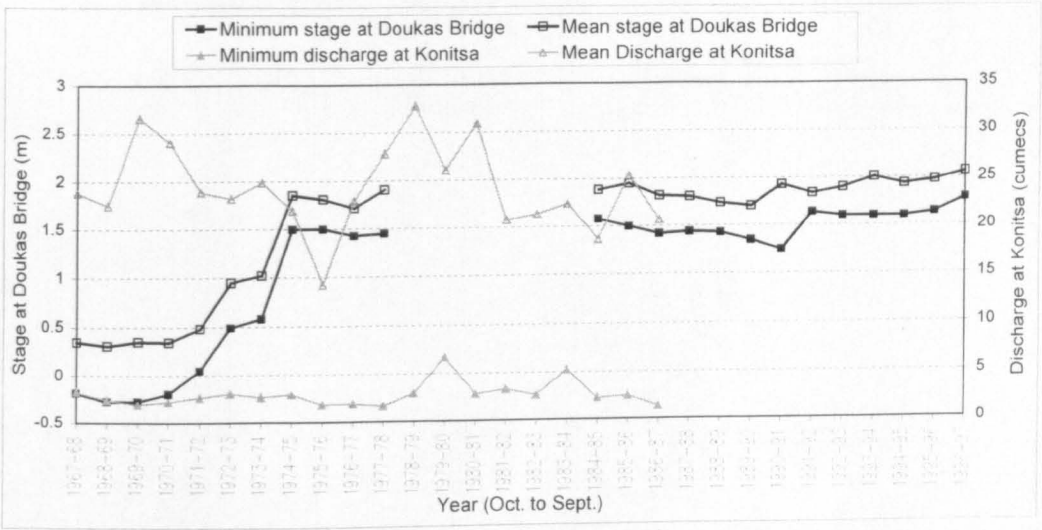

FIGURE 4.4 Comparison of minimum and average annual stage at Doukas Bridge with minimum and average discharge at the nearby Konitsa station (Figure 3.1) for hydrological years (Oct. to Sept.) 1967-68 to 1996-97. The stage record for Doukas Bridge between 1977-78 and 1984-85 is unreliable, and has therefore been omitted.

4.3 FIELDWORK APPROACH

4.3.1 Selection of study sites

Deposits of interest were identified by means of a reconnaissance survey. Much of the Aoos basin proved to be inaccessible and those areas that could be accessed often lacked suitable deposits. As a result, only boulder berms were investigated in the Aoos. All other work was carried out in the Voidomatis basin.

To investigate the long-term alluvial history of the catchment, five study reaches were selected where a number of terraces were preserved. These are numbered 1, 2, 3, 4, and 6 in Figure 4.5. Geomorphological mapping and surveying terrace heights from the channel bed established stratigraphic height relationships between terraces, and hence an idea of relative chronology within each reach could be ascertained. This was preferred to investigating widely distributed terrace fragments where no relative height relationships can be made.

Three SWD sites were identified for study (Figure 4.5), where there was good stratigraphic context and field evidence suggested a Late Pleistocene age (e.g. located well above the current channel in sheltered areas conducive for long-term preservation).

Boulder berms only seemed to occur in the large deep gorges of each catchment. Therefore one long 'boulder berm reach' reach at the bottom end of each major gorge was selected, their locations shown in Figure 4.5 and Figure 4.6. Additional berms were identified in study reach 6 in the Voidomatis basin (Figure 4.5).

The site for investigating overbank sedimentation was chosen within study reach 3 in Figure 4.5, where fine-grained floodplain sediments were accumulated to over 2 m depth, and a radiocarbon date at the bottom of the unit gave an initial approximation of sedimentation rate.

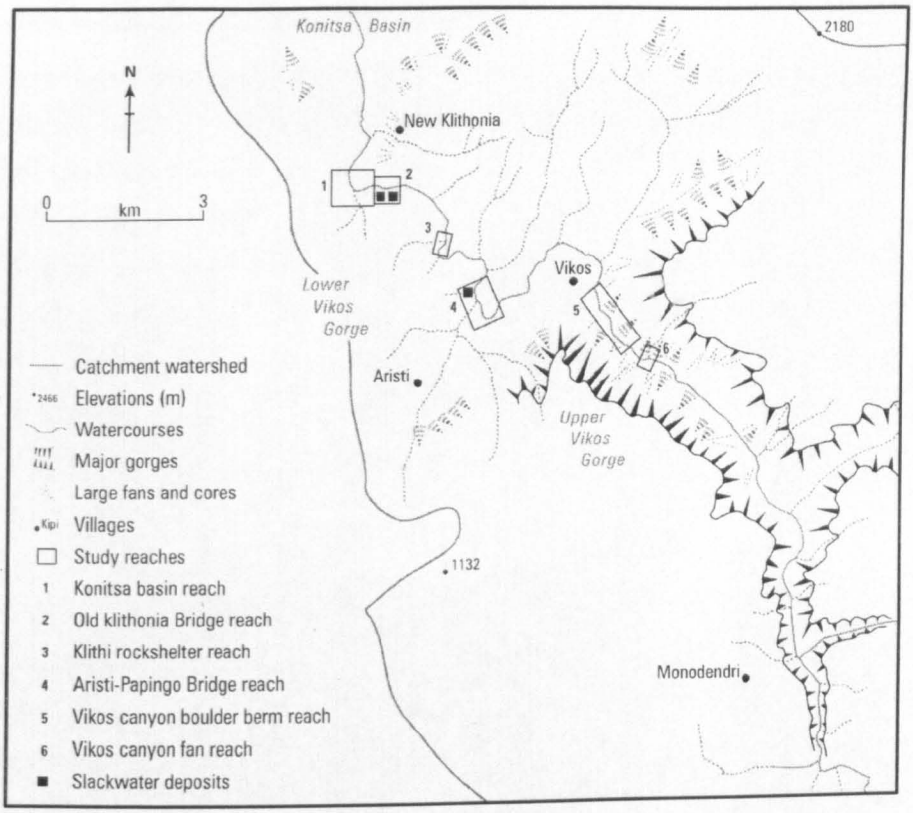

FIGURE 4.5 Location of study sites in the Voidomatis basin.

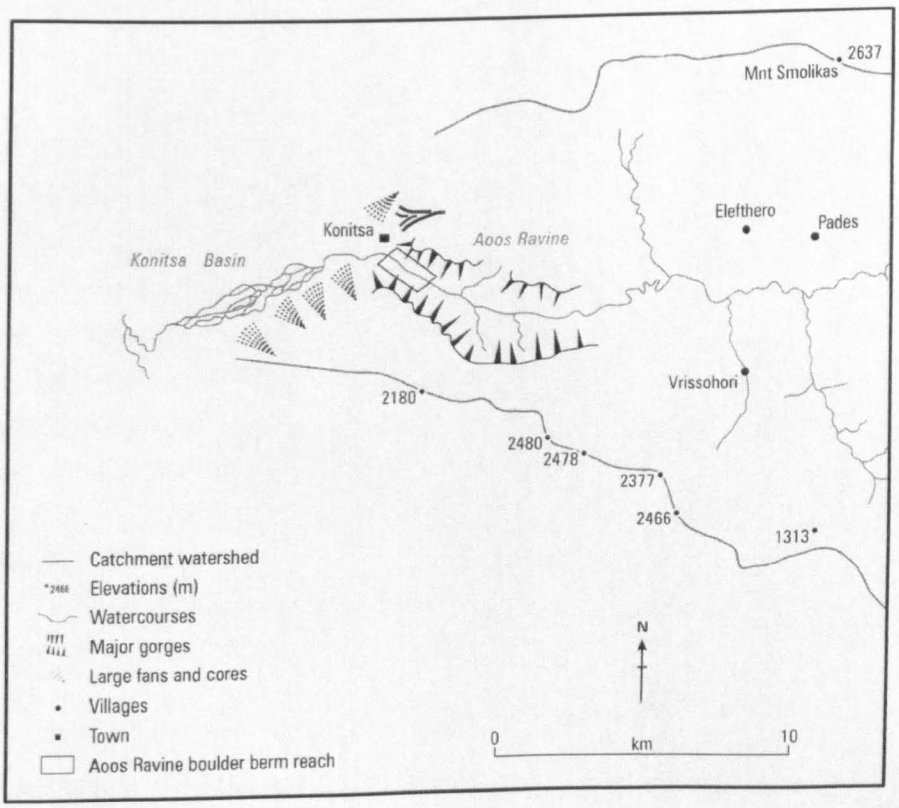

FIGURE 4.6 Location of study site in the Aoos basin.

4.3.2 Geomorphological mapping and surveying

Geomorphological mapping onto air photographs was carried out in most reaches to determine the presence, extent and location of different alluvial units and terrace surfaces. This was complemented by surveying to verify mapping accuracy and to determine stratigraphic height relationships between different deposits. With no available altitude benchmarks in the area, heights had to be surveyed relative to the deepest part of the channel bed. This is satisfactory for establishing within-reach height relationships. However, care should be taken when comparing heights between reaches, as different valley floor characteristics could lead to the sediments being deposited and preserved at different heights above the bed. Surveying was carried using a Vickers CTS manual theodolite, which is accurate to within approximately ±5 cm over 150 m.

4.3.3 Sampling strategy

4.3.3.1 Collection of alluvial fine-sediment samples

Sediment samples were required for the characterisation and provenancing of valley fill sediments and SWDs. At least 2 samples were collected from exposures beneath each terrace, totalling 19 samples in all. As the <2 mm fraction was required for analysis, only the fine-grained matrix in alluvial units containing coarse gravels and boulders was collected. Some of these coarse-grained alluvial units were cemented in their upper horizons by secondary calcite, which would effectively act as contamination, altering the characteristics of the sediment. To avoid this problem, care was taken to ensure that samples were collected from the lower, unconsolidated part of the sediments which were free from alteration by secondary calcite (*cf.* Woodward *et al.*, 1992). Care was also taken to avoid sampling sediments that appeared to be heavily weathered, showing signs such as discoloration, palaeosols or bioturbation.

The SWDs were logged in detail, noting texture (according to Table 4.5) contacts between units, colour changes, sedimentary structures and any evidence of weathering. Samples for provenancing were carefully collected from each individual sedimentary unit, resulting in 79 samples from the three SWD sites (Figure 4.5). To assess current river sediment characteristics, 8 samples of in-channel contemporary fines were collected from random locations within the catchment during winter and summer field visits. In all cases, samples were collected from several locations within the exposed deposit to allow for heterogeneity in sediment characteristics

The collection of samples for dating are described with the relevant dating technique in section 4.4.

4.3.3.2 Collection of catchment source materials for fine sediment provenancing

Geological samples (bedrock, glacial deposits and soils) were collected at random locations throughout the catchment to characterise potential fine sediment sources. These are described with the fingerprinting procedure in section 5.2.1.

TABLE 4.5 Grain size scales used for sedimentary logging in the field, taken from Wentworth (1922) and Friedman and Sanders (1978). The correct application of these scales was confirmed by microscopic analysis of sediments described in the field to ensure that grain sizes has been allocated the correct textural description. Phi values are not appropriate for the pebble, gravel and boulder textural ranges used in this study.

Textural description	Grain size range	
	Metric	ϕ (phi)
Boulders	> 256 mm	> -8.0
Cobbles	64 – 256 mm	-6.0 – -8.0
Pebbles	2 – 64 mm	-1.0 – -6.0
Very coarse sand	1 – 2 mm	0 – -1.0
Coarse sand	0.5 – 1 mm	1.0 – 0
Medium sand	250 – 500 microns	2.0-1.0
Fine sand	125 – 250 microns	3.0 – 2.0
Very Fine sand	63 – 125 microns	4.0 – 3.0
Very Coarse silt	31 – 63 microns	5.0 – 4.0
Coarse silt	16 – 31 microns	6.0 – 5.0
Medium silt	8 – 16 microns	7.0 – 6.0
Fine silt	4 – 8 microns	8.0 – 7.0
Clay	< 7 microns	< 8.0

4.4 DATING TECHNIQUES

This section covers both the theoretical aspects of the main dating techniques used in this study, and also the specific sampling and analytical methods used. The dating techniques are summarised in Table 4.6.

4.4.1 Lead-210/Caesium-137

Lead-210 (^{210}Pb) and Caesium-137 (^{137}Cs) are both radionuclides which may become adsorbed to river sediments, and be used to date their progressive accumulation on floodplains. Whilst they lend themselves to being used in combination, the dating theory behind each of them is quite different, and is therefore discussed separately here.

4.4.1.1 ^{210}Pb Dating

^{210}Pb is part of the uranium (^{238}U) decay series (Robbins, 1978). Decay of the intermediate isotope ^{226}Ra (half life of 1622 years), which occurs naturally in the earth's crust, results in the inert gas ^{222}Rn (radon, half life of 3.83 days). ^{222}Rn diffuses out of the lithosphere and is transported into the atmosphere by means of turbulence and advection (Robbins, 1978), where it decays through a series of short-lived isotopes to produce ^{210}Pb. ^{210}Pb becomes rapidly attached to natural aerosols, and may subsequently return to the earth's surface, mainly through precipitation, but also due to dry deposition (Oldfield and Appleby, 1984b). Thus ^{210}Pb fallout is essentially a natural process, which can be considered as having occurred at a constant rate through time (He and Walling, 1996). Fallout leads to ^{210}Pb being incorporated onto sediment particles at the earth's surface. ^{210}Pb originating from atmospheric fallout is often termed

unsupported ^{210}Pb, differentiating it from the small amount of supported ^{210}Pb which is produced from the *in situ* decay of ^{226}Ra within the sediments themselves (Faure, 1977). Dating is based on levels of the unsupported component, which once adsorbed on to the sediment will decay exponentially at a rate determined by its half-life of 22.26 years (Oldfield and Appleby, 1984b). The half-life of ^{210}Pb means that dating is possible over potentially the last 100-150 years, depending on the strength of the unsupported ^{210}Pb signal.

TABLE 4.6 Summary of dating techniques used in this study.

Dating method	Applicable timescale	Type of sample required	Basis of technique
^{137}Cs	Approx. the last 40 years	Sediment core.	Measurement of ^{137}Cs in deposits can indicate various periods in recent history e.g. the time of peak weapons testing (1963) and the Chernobyl accident (1986).
Uranium-series disequilibrium: unsupported ^{210}Pb	Approx. the last 100 years.	Sediment core.	Utilises the radioactive decay of natural fallout ^{210}Pb incorporated in sediments.
Lichenometry	Environment and species dependent; c. last 500 years (Innes, 1985)	Measurement of lichen thalli.	The assumption that the size of lichen thalli growing on a surface will be directly related to substrate age (Beshel, 1961, 1973).
Radiocarbon (^{14}C)	Normally no greater than 45 ka	Preserved organic material.	Utilises the radioactive decay of ^{14}C within dead organic material.
Uranium-series disequilibrium: ^{230}Th/^{234}U	c. 3 - 350 ka	Carbonate concretions, secretions and precipitates.	The gradual growth of daughter nuclide ^{230}Th towards equilibrium with parent ^{234}U at a predictable rate after the formation of a carbonate deposit.
Optically-Stimulated Luminescence (OSL)	c. 0.1 - 100 ka	Buried sediment held in an opaque tube.	Luminescence signal of sediment is assumed to be zeroed by sunlight upon deposition, from which time it will increase at a predictable rate due to radiation received from the surrounding sediment.

The application of ^{210}Pb dating of sediment has increased greatly over the last few decades. One of the most common uses has been for dating lacustrine sedimentation (e.g. Robbins and Edgington, 1975; Farmer, 1978; Oldfield and Appleby, 1984b; Douglas *et al.*, 1994), but it has recently been applied to the analysis of floodplain sediments (Popp *et al.*, 1988; Walling and He, 1994; He and Walling, 1996; Rowan *et al.*, 1999). Whilst the determination of ^{210}Pb is relatively simple, controversy has surrounded the choice of dating model which calculates the distribution of unsupported ^{210}Pb with depth. Dating models rely on the validity of certain key assumptions associated with them, principally:

1. Can the supply of unsupported ^{210}Pb (^{210}Pb flux) be assumed to have been constant over the last 100-200 years? This assumption is often made, as ^{210}Pb flux will be largely controlled by

the regional meteorology, which over this timescale is likely to have remained fairly similar (Oldfield and Appleby, 1984b).

2. Can a constant sedimentation rate be assumed? Whilst this can be true for certain depositional environments, in many locations this may not be the case.

Appleby and Oldfield (1978) have proposed a constant rate of supply (CRS) model, which assumes a constant ^{210}Pb flux, but does not assume a constant sedimentation rate. They have shown that this appears to provide more accurate results for dating lake sediments than other models such as the constant flux constant sedimentation rate (CFCS) model or the constant initial concentration (CIC) model (Robbins, 1978; Oldfield and Appleby, 1984b). More recently, it has been suggested by Walling and He (1994), and He and Walling (1996), that such models are less suitable for dating floodplain sediments as they do not take account of possible unsupported ^{210}Pb supply from fluvial sediment deposition. They propose a constant initial concentration-constant sedimentation rate (CICCS) model, which calculates a mean sedimentation rate based only on the unsupported ^{210}Pb supplied from sediment deposition (i.e. excess unsupported ^{210}Pb).

Whichever model is chosen, dating should ideally be supported by other independent techniques, such as alternative dating methods (Oldfield and Appleby, 1984b) or magnetic analysis (Oldfield and Appleby, 1984a) to evaluate the validity of the approach taken. Dating in combination with ^{137}Cs was therefore adopted to complement the ^{210}Pb dating in this study.

4.4.1.2 Cs-137 dating

Whereas ^{210}Pb is essentially a natural radionuclide, ^{137}Cs is completely anthropogenic in origin. It was introduced into the atmosphere by nuclear weapons testing during the middle and latter part of the 20th century, and fallout via precipitation occurred rapidly and on a global scale, making ^{137}Cs a potentially valuable marker of sediment age. Whilst some ^{137}Cs was released by early nuclear tests before 1950, significant levels of global fallout recorded in sediments are generally thought to have started in 1954 (Wise, 1980; Walling and He, 1997). Over the following decade fallout was particularly high, with a peak at 1958-9 and an overall maximum in 1963 (Figure 4.7) (Ritchie and McHenry, 1990; Walling and He, 1993). 1963 was the year of the Nuclear Test Ban Treaty, since when fallout has steadily decreased apart from very small increases in the early 1970s (Ritchie and McHenry, 1990). In some areas, principally in parts of Europe and its surroundings, an additional peak of ^{137}Cs fallout occurred in 1986 due to the Chernobyl accident in 1986 (Figure 4.7) (Rowan *et al.*, 1993).

Fallout ^{137}Cs is rapidly and strongly adsorbed by soils and sediments, primarily onto the clay and organic particles (Walling and He, 1997). However, ^{137}Cs dating can be successfully carried out on sediments that are almost entirely sands and silts (Ely *et al.*, 1992). Once adsorbed, the ^{137}Cs is known to be very stable (Ritchie and McHenry, 1990), and therefore its mobility will be almost entirely due to physical processes of particle redistribution.

Consequently, ^{137}Cs has been used for dating fluvial deposits (e.g. Ritchie *et al.*, 1975; Popp *et al.*,1988; Ely *et al.*, 1992; Walling and He, 1994, 1997), and lake sediment sequences (e.g. Ritchie *et al.*, 1973; Robbins and Edgington, 1975; Rowan *et al.*, 1993; Walling and He, 1993). Dating may involve determining the depth of post-fallout sedimentation, which is often approximated as post-1950 (Popp *et al.*,1988; Ely *et al.*, 1992), or identification of the major peaks in fallout (Figure 4.7), in particular the maximum at 1963 (Ritchie *et al.*, 1975; Ritchie and McHenry, 1990; Walling and He, 1994). Dating of the post-1950 sediment may become increasingly problematic as the 30.17 year half-life of ^{137}Cs means that in some cases this lower signal may become increasingly hard to detect (Ritchie and McHenry, 1990). In a similar fashion to their work on ^{210}Pb, Walling and He (1993, 1997) have proposed models that determine the excess ^{137}Cs inventory of catchment derived sediments, but such models suffer from the fact that they assume a constant sedimentation rate, which in many cases may be unrealistic.

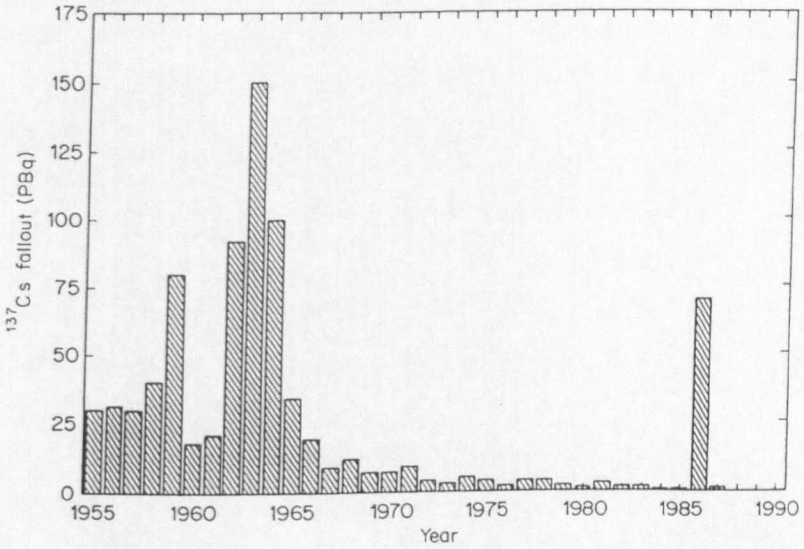

FIGURE 4.7 Atmospheric fallout of ^{137}Cs in the northern hemisphere (source: data from Cambray *et al.*, 1987, in Rowan *et al.*, 1993).

4.4.1.3 Sample collection and analysis

A 62 cm core was collected in two 31 cm sections from a section of fine-grained floodplain alluvium located with the study reach 3 in Figure 4.5. A rigid plastic drainpipe was sliced down the middle to give an open corer with a semi-circular cross section. This was hammered into the sediments and then carefully excavated. The whole core was wrapped tightly with waterproof tape and stored in a refrigerator before analysis. An X-ray photograph of the core was taken before analysis to investigate sedimentary structures, although the sediments were found to be relatively homogenous. The core was sliced in 1 cm increments in the laboratory, and analysed

for radionuclides using a Canberra Broad Energy Germanium Detector (75% relative efficiency) at PRIS, University of Reading. The selection of the unsupported ^{210}Pb dating model is discussed with the analytical results in section 8.4.

4.4.2 Lichenometry

4.4.2.1 Theoretical background

Lichenometry, originally developed by R.E. Beshel in the 1950s, is based on the assumption that the size of lichen thalli growing on a surface will be directly related to substrate age (Beshel, 1950 (translated, 1973), 1961). It has been most commonly applied in glacial environments, in particular for the dating of Late- and Neoglacial moraines (e.g. Carrarra and Andrews, 1972; Miller, 1973; Matthews, 1975,1977; Mottershead, 1980; Davis, 1985). As discussed by Locke *et al.* (1979), some early lichenometric work involved questionable and inconsistent techniques and received some criticism regarding the applicability of lichen size as a measure of substrate age (e.g. Jochimsen, 1973; Worsley, 1981). However, continued development of the technique has shown that it remains a valuable dating tool, over a time range where many other techniques are not applicable (Table 4.6). Of particular importance here is that lichenometry is very useful for dating coarse-grained alluvial deposits. It has been applied successfully in fluvial environments in northern Britain (Harvey, *et al.*, 1984, Macklin *et al.*, 1992a, Merret and Macklin, 1998a, 1999), Australia (Gregory, 1976), Iceland (Thompson and Jones, 1986), Norway (Innes, 1985b, p.237-8) and in Crete (Maas *et al.*, 1998). The technique is believed to be appropriate for coarse-grained flood deposits as Gregory (1976) showed that most lichen are destroyed by transport during floods and that anomalous large lichen are easily recognised on reworked material.

Several key assumptions underlie the lichenometric technique: i) the surface is lichen free upon stabilisation of the substrate, and that any transport has resulted in the removal or death of previously growing lichen, ii) that lichen colonisation begins immediately after exposure (unless rates of colonisation are known), iii) that larger thallus (lichen body) size indicates greater age, and iv) consequently the largest lichens will indicate substrate age, as smaller thalli are either late colonisers or slower growing individuals. It is critical that growth rates of lichen are relatively uniform within the study region, and hence possible micro-environmental effects on growth rates are minimal. It has been suggested that numerous environmental factors can affect lichen growth (see Innes (1985) for summary), and in particular aspect (Armstrong, 1975,1977), substrate lithology (Brodo, 1973), moisture availibility (Innes, 1985c), altitude (Miller, 1973) and pollution may be important. Lichenometry can only be used successfully if such effects do not induce significantly different rates of lichen growth between measurement sites.

4.4.2.2 Fieldwork procedure: lichen measurement and growth curve construction

This study used measurements of *Aspicilia calcaria (L.) Mudd*, a commonly occurring white crustose lichen which is found on rock surfaces throughout the region (Figure 4.8). It was observed to grow in the radial fashion suitable for lichenometry. The longest axis of the lichen thalli was measured in accordance with previous recommendations (e.g. Innes, 1985b; Easton, 1995), as it has been shown to be less susceptible to micro-environmental effects (Innes, 1985a, 1985b, 1986). Measurement to the nearest millimetre was achieved using vernier callipers. Coalescing or dead lichens were not measured. Any anomalous thalli (*cf.* Innes, 1985b) on older reworked clasts incorporated in the berms were easily identified due to exceptional lichen cover on a single clast. Such lichen were not measured. A local lichen growth curve was constructed by the indirect method, measuring the largest lichens growing on independently dated surfaces (see section 8.3.2).

The largest lichens growing on the surface of clasts within the boulder berms were then measured, ensuring that at least the largest 10 individuals were recorded. The entire berm was always searched. Comparison of lichen sizes on berms with the growth curve enables an age estimate to be calculated (section 8.3). Although early work took the single largest lichen as a measure of substrate age (e.g. Webber and Andrews, 1973), this seems prone to producing irregular and inconsistent results (Innes, 1985b, 1986). An averaging procedure was therefore adopted here in accordance with Matthews (1975) and Innes (1985a, 1985b), using the mean of the five largest lichens as a measure of age.

FIGURE 4.8 An individual of *Aspicilia calcaria (L.) Mudd*, growing on a rock surface in Epirus.

4.4.3 Radiocarbon (^{14}C)

As ^{14}C dating is so well established, only a brief review is presented here. For more details the reader may refer to the reviews of Aitken (1990) and Pilcher (1991a).

4.4.3.1 Theoretical background

^{14}C is formed in the atmosphere by neutrons produced by cosmic rays interacting with stable isotopes, primarily ^{14}N (Faure, 1977):

$$ {}^{1}_{0}n + {}^{14}_{7}N \rightarrow {}^{14}_{6}C + {}^{1}_{1}H \qquad (4.1) $$

where n is the neutron and H is the emitted proton. The ^{14}C is a radioactive isotope of carbon, which through time will decay back to ^{14}N by the emission of beta (β^-) particles:

$$ {}^{14}_{6}C \rightarrow {}^{14}_{7}N + \beta^- \qquad (4.2) $$

In the atmosphere ^{14}C is rapidly oxidised to carbon dioxide ($^{14}CO_2$), which is subsequently mixed and transferred throughout the atmosphere, the hydrosphere (as dissolved carbonate), and the biosphere, as ^{14}C is absorbed by plants and animals through tissue building (Lowe and Walker, 1997). The concentration ratio of ^{14}C to non-radioactive carbon (^{12}C and ^{13}C), which is about one in a million million, is in an approximate equilibrium state throughout these three carbon reservoirs, and this equilibrium has broadly remained constant through time (Aitken, 1990). However, when plants or animals die, the ^{14}C contained within their tissue will continue to decay as shown in Equation 4.2, but it will no longer be replenished by absorption of ^{14}C by the organism. Therefore, assuming that the decay rate of ^{14}C is known, and that the ^{14}C activity in living tissue is known, the time elapsed since the death of the organism can be determined by the measurement of the remaining ^{14}C activity. It is hence possible to date a wide variety of material, including charcoal, wood, seeds, cloth, hide, peat, ivory, bones, shells, carbonate deposits, or sediments and soils (by virtue of humic acids or calcium carbonate). However, due to a variety of potential analytical problems different materials offer varying reliability (for details see Faure, 1977; Aitken, 1990; Attendorn and Bowen, 1997).

The half-life of ^{14}C was previously thought to be 5568 ±30 years (Libby, 1955), until it was more accurately determined as 5730 ±40 years (Godwin, 1962). However, due to the large number of dating analyses previously carried out using the Libby half-life, it is still used this for all ^{14}C dating to ensure the comparability of results (Mook, 1986). Ages calculated using the Libby half-life are termed 'conventional radiocarbon ages' (Stuiver and Polach, 1977). From this value the decay curve for radiocarbon may be determined (Figure 4.9). It is important to note that by 45 ka the decay curve has become of very low gradient (Figure 4.9), and hence it is only possible to date beyond this age with particularly sensitive equipment. This is often considered the approximate time limit of the technique (Table4.6), although dates older than 30 ka must be treated with caution, as the effect of any contamination is magnified.

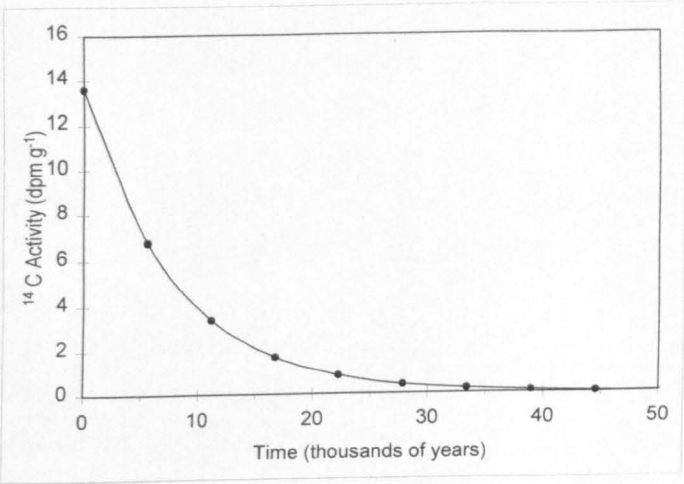

FIGURE 4.9 The ^{14}C decay curve, using the Libby half-life (5568 years), and the best estimate of the specific activity of ^{14}C in equilibrium with the atmosphere of 13.56 ±0.07 dpm g^{-1} (Karlen *et al.*, 1966).

Two main types of radiocarbon analysis are commonly available. Firstly, *conventional ^{14}C laboratories* measure the ^{14}C activity by either scintillation counting or gas counting and compare this with a decay curve such as Figure 4.9 to determine the age. A modern reference standard is used to determine the initial ^{14}C concentration ratio, which is usually the modern activity level of NBS oxalic acid prepared by the American Bureau of Standards. This allows comparability between laboratories and also avoids the problem of artificially high atmospheric ^{14}C activity since approximately 1950 (see below). ^{14}C dates are reported as ^{14}C years before present, where "present" = 1950 (Stuiver and Polach, 1977). The second main type of analysis is achieved through *Accelerator Mass Spectrometry (AMS dating)*. This involves separating ^{14}C from other atoms of similar atomic mass by the deflection of the particles though a very high voltage magnetic field (Aitken, 1990). The principal advantage of AMS is that it can date very small samples or samples with very low carbon content (Hedges, 1991). The development of AMS has been particularly valuable for establishing SWD chronologies, typically utilising small charcoal samples (Baker, 1987).

The analytical precision of ^{14}C dating is represented by quoted errors which reflect statistical uncertainties associated with the randomness of radioactive decay and the measurement of the decay curve, and also counting uncertainties for conventional dates and measurement uncertainties for AMS (Aitken, 1990; Picher, 1991b; Lowe and Walker, 1997). These are normally reported as ± 1 standard deviation (68% probability), however, is generally better procedure to double these to 2 sigma values for discussion purposes (Pilcher, 1991a).

4.4.3.2 Calibration problems

It is now well known that ^{14}C activity in the atmosphere has not remained constant over time. This problem has been compounded by the fact that the variation of ^{14}C activity has not been systematic over time, and hence researchers have had to develop empirical relationships for age

corrections (Pilcher, 1991b). This can be achieved through high-precision studies of ^{14}C in long tree ring sequences, which have shown irregular fluctuations in ^{14}C activity extending back to 11.4 ka dendro BP (Becker and Kromer, 1993; Stuiver *et al.*, 1993). Until recently, calibration has not been possible over longer timescales, including the Last Glacial period which is often of particular interest to Quaternary scientists (Pilcher, 1991b). However, recent work by Bard *et al.* (1990, 1992, 1993) has used both AMS ^{14}C and mass spectrometric $^{230}Th/^{234}U$ dating (see section 4.4.4) on corals offshore of Barbados and Mururoa in an attempt to calibrate the ^{14}C timescale over the last c. 30 ka. Their results show that the ^{14}C ages are systematically younger than the true ages, with the exception of a short period over the last 2.5 ka (Figure 4.10). Their data agree well with combined dating of cave speleothem (Holmgren *et al.*, 1994), as well as dendrochronological records and data from Greenland ice cores (Lowe and Walker, 1997).

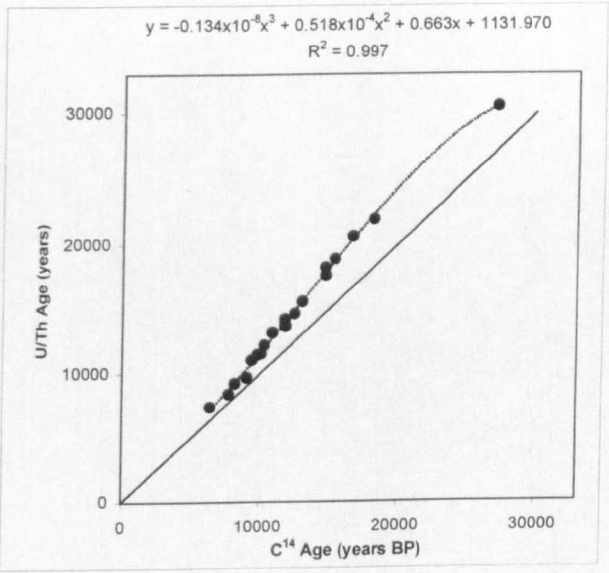

FIGURE 4.10 U-Th ages plotted against ^{14}C ages for corals off Barbados and Mururoa. Error bars are not shown, but these are very small, rarely approaching as much as 5% (Bard *et al.*, 1990, 1992). The dotted line and equation above the chart are the results of a 3rd order polynomial regression which was fitted to the data to facilitate the calibration of ^{14}C ages > c. 11 ka to calendar years. *(Data from Bard et al., 1990, 1992).*

4.4.3.3 Sample collection and analysis

During the inspection and logging of sedimentary sections care was taken to identify and collect any preserved organics which appeared suitable for ^{14}C dating. The only suitable material found was charcoal, which was carefully removed from the sediments with a trowel and collected using polythene bags and aluminium foil.

Beta Analytic Inc., of Miami, Florida carried out the ^{14}C analysis. Pretreatment of the charcoal involved dispersion in deionized water, followed by hot HCL acid washes to eliminate carbonates, alkali washes (NaOH) to remove secondary organic acids, and a final acid wash to neutralise the solution. Conventional radiometric analysis was carried out by synthesising

sample carbon to benzene (92% C), and the ^{14}C content was measured in a scintillation spectrometer. AMS results were derived from the reduction of sample carbon to graphite (100% C), and the sample was sent for AMS measurement at one of six collaborating facilities (Beta Analytic Inc, pers. comm., 1997). All results are reported as both the "Conventional Radiocarbon Age" in "years BP", and as a calibrated age in "cal AD", "cal BC" or "cal years" to allow comparison with other dating results. It should however be recognised that calibration does not necessarily make the results more accurate (Pilcher, 1991a), as it may incorporate additional potential errors. Ages within the dendrochronological calibration timescale were calibrated by Beta Analytic Inc. according to the results in Stuiver *et al.* (1993), Talma *et al.* (1993) and Vogel *et al.* (1993). Ages beyond this calibration range were calibrated by a third order polynomial trendline fitted to the U/Th and ^{14}C data of Bard *et al.* (1990, 1992), as shown in Figure 4.10.

4.4.4 Uranium-series disequilibrium: $^{230}Th/^{234}U$ dating

4.4.4.1 Theoretical background

Uranium-series disequilibrium dating methods utilise the radioactive decay series of ^{238}U, ^{235}U and ^{232}Th (the daughter nuclide of ^{236}U, which is no longer found in nature) (Smart, 1991). Such elements are common throughout the lithosphere. In undisturbed rocks, a state of equilibrium in the decay series has normally been reached whereby the nuclides are decaying at a similar rate to their production by the decay of parent nuclides (Lowe and Walker, 1997). However, this equilibrium can be disturbed by various mechanisms such as weathering, sediment deposition, mineral precipitation from aqueous solutions, and volcanic activity (Faure, 1977; Smart, 1991; Attendorn and Bowen, 1997). This can result in certain parts of the decay series being removed from the material, initiating a state of disequilibrium. Sometime later the material will be reformed, for example by the precipitation of a mineral, and if it then remains undisturbed, it is possible to date its formation by determining the extent to which the radionuclides have returned towards equilibrium (Ivanovich *et al.*, 1992). This forms the basis of uranium-series disequilibrium dating techniques. Of course, the process of decay equilibrium disturbance has to be understood so the correct approach can be taken. Upon disturbance, U and its weathering products are relatively soluble in water, whereas other daughter nuclides, in particular Th, are insoluble and are therefore tend to be adsorbed onto clay minerals, hydroxides or other solid particles (Bischoff and Fitzpatrick, 1991; Smart, 1991). This leads to the separation (or fractionation) of U from its decay products. This fractionation offers two main types of dating approach:

1. Sediments accumulating in lakes or ocean floors will be rich in Th which has been adsorbed and coprecipitated with the sediments, and low in U which remains in solution. Dating of these sediments can be achieved by measuring the amount of decay of the excess of Th compared to U (Smart, 1991). They have therefore been termed daughter excess (DE)

methods. This has most commonly be applied to the dating of marine sediments (e.g. Broecker and Ku, 1969; Kominz *et al.*, 1979).

2. Carbonate precipitated from solution or secreted by organisms will be rich in U, but low in daughter products such as Th which were not held in solution. Such material can therefore be dated by the gradual increase of daughter nuclides compared to the amount of the U parent over time, and are termed daughter deficient (DD) methods. They may be used in the dating of speleothems (e.g. Gascoyne *et al.*, 1983; Gordon, *et al.*, 1989), corals (e.g. Bard *et al.*, 1990, 1992; Hoang and Taviani, 1991), and a wide variety of terrestrial carbonate deposits (e.g. Ku *et al.*, 1979; Hillaire-Marcel and Causse, 1989), often through measurement of the $^{230}Th/^{234}U$ ratio. In this study $^{230}Th/^{234}U$ dating has been adopted for the dating of carbonate concretions within alluvial sediments. Although this is a less usual application of the technique, it has considerable potential (Ku *et al.*, 1979), and has been shown by previous work to provide valuable age estimates for dating alluvial deposits (Pope and van Andel, 1984; Black *et al.*, 1998; Maas, 1998).

4.4.4.2 $^{230}Th/^{234}U$ dating: applicable timesale and assumptions

The $^{230}Th/^{234}U$ method is based on the initial deficiency in ^{230}Th compared to ^{234}U. The half-life of ^{230}Th is 75,200 years, which normally restricts the dating range to the last 350 ka (approximately five times the half-life) (Table 4.6). To use this ratio for dating, a number of assumptions are invoked: -

1. The decay coefficients for the decay process are accurately known.
2. The activity of the nuclides must be measurable to a high level of precision, which in part requires U to be present in measurable quantities (Ivanovich *et al.*, 1992).
3. Ideally there should be no ^{230}Th within the carbonate at the time of deposition (Smart, 1991).
4. Following deposition, the material should exhibit closed system behaviour, with no loss or gain of nuclides (Lowe and Walker, 1997). Open system behaviour is possible with carbonate concretions (Smart, 1991), and therefore testing dates to see if they are consistent with both other dating techniques and their stratigraphic position is important (Ivanovich *et al.*, 1992). In addition, physical evidence of recrystallisation, solution, secondary precipitation, weathering, or high porosity can all be indicative of open system behaviour (Smart, 1991), and hence such samples were avoided.
5. It is assumed when applying the technique for dating alluvial deposits that the calcite has formed quickly after the deposition of the sediments and therefore provides a valid estimate of *minimum age* for the deposit. This assumption has been shown to be valid in previous research using carbonate deposits where detailed dating of stratigraphic sequences enables assessment of dating reliability (e.g. Bischoff *et al.*, 1988; Bischoff and Fitzpatrick, 1991).

4.4.4.3 Sample collection and analysis

The exposed surface of the cemented sediments was removed by lump hammer and chisel, as it was more likely to have experienced some post-formation disturbance. This allowed a sample of 100 - 200 g of sediment to be taken containing a substantial quantity of undisturbed calcite cement, showing no evidence of open-system behaviour (see assumption 4 above). Samples exhibiting large calcite crystals were avoided, as these are likely to have formed more slowly and are less likely to satisfy assumption 5. Where possible, samples were collected from an area where stratigraphic height relationships had been determined and dates from other techniques were available, thus allowing further assessment of the possibility of open-system behaviour.

Uranium-series radionuclides were measured by high-resolution alpha spectrometry and ICP-MS at Lancaster University. Uranium and thorium isotopes were separated on ion-exchange resins and electrodeposited onto stainless steel planchets (see Black *et al.*, 1997 and Kuzucuoglu *et al.*, 1998). Corrections were made for decay of excess ^{234}U and detrital ^{230}Th, on the assumption that these were present at precipitation of the calcite deposits. The need to correct for excess ^{234}U is due to the fact that ^{234}U is preferentially released into solution compared to ^{238}U, and therefore the decay of excess ^{234}U may increase the $^{230}Th/^{234}U$ ratio through time by contributing to the ^{230}Th activity (Smart, 1991; Attendorn and Bowen, 1997). Correction for detrital ^{230}Th, on the other hand, arises from the fact that carbonate concretions often contain a significant proportion of detrital particles, often derived from the local sediment (Schwarcz and Gascoyne, 1984). Detritus will introduce non-carbonate ^{238}U, ^{234}U, and in particular ^{230}Th to the sample (Bischoff and Fitzpatrick, 1991; Ivanovich *et al.*, 1992), which will disrupt the true $^{230}Th/^{234}U$ ratio. Attempts at correction have often involved trying to separate the allochtonous detrital fraction from the authogenic carbonate phase by partial dissolution (leaching) of the sample. However, a reliable leaching procedure is very difficult to maintain (Luo and Ku, 1991), with the detritus not neccessarily being resistant to attempts at selective leaching (Bischoff and Fitzpatrick, 1991). Therefore, a correction for the detrital component was made from isochron plots after successive total dissolutions were performed on subsamples using the methods of Bischoff and Fitzpatrick (1991). In all cases the slopes of the isochrons are best determinations by a method of least squares fitting which takes account of the errors in both variables (after York, 1969). An example is shown in Figure 4.11. The isochron essentially plots the authigenic carbonate fraction (x-axis) against the detrital fraction (y-axis). The isochron depicts the mixing of these two components to enable the authogenic $^{230}Th/^{234}U$ ratio to be determined and hence its age estimated. As described by Bischoff and Fitzpatrick (1991), the isochron line will rotate with time from an initial slope of zero, to a slope of unity (the equiline) where equilibrium between ^{238}U and ^{230}Th has been achieved (after 350kyr). A close degree of fit of the points along the isochron line is an indicator of homogeneity and closed system behaviour (Bischoff and Fitzpatrick, 1991; Lowe and Walker, 1997), and implies that a single phases of uranium uptake occurred during a relatively short period of time (S.

Black, pers. comm. 1997). The isochron plot is therefore particularly valuable, not only for correcting for the detrital component, but also for assessing the validity of the dating assumptions.

Errors on the dates are quoted at 2 sigma probability, and are calculated as a measure of counting uncertainties in the determination of nuclide concentrations (Smart, 1991). Analysis of the standard material A-THO, a sample of rhyolitic obsidian from Iceland, was used to monitor quality control by comparison with published results (Williams *et al.*, 1992).

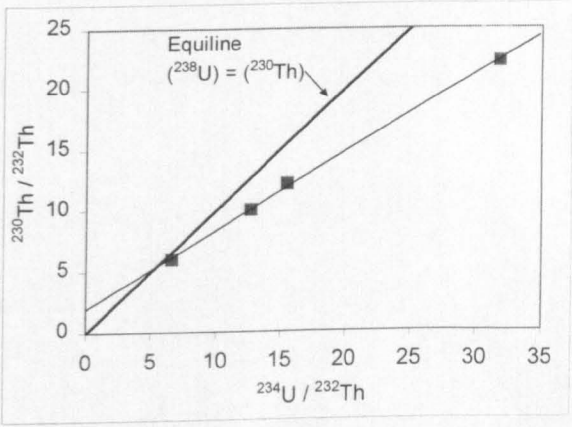

FIGURE 4.11 An isochron plot used in the age determination of cemented alluvium in the Voïdomatis Basin (sample #2). Error bars are smaller than the plotted points. The R^2 for the isochron line is 0.999.

4.4.5 Optically-Stimulated Luminescence (OSL)

4.4.5.1 Theoretical background

Luminescence dating of sediments has become firmly established over the last few decades (Aitken, 1992; Duller, 1996). Although a variety of techniques exist, they all rely on a similar theoretical basis. As has been mentioned in section 4.4.4, rocks, sediments and soils contain commonly occurring radioactive isotopes, which include ^{238}U, ^{230}Th and ^{40}K. The decay of these isotopes results in the continuous emission of alpha (α), beta (β) and gamma (γ) particles to the surrounding material (Lowe and Walker, 1997). Gamma radiation is the most mobile, penetrating through sediments for tens of centimetres (Bailiff, 1992). Naturally occurring minerals such as quartz and feldspars within buried sediments will gradually acquire this energy through time, and this behaviour can be used to estimate the age of sediment deposition. α, β and γ radiation interacts with their crystalline structure, freeing electrons from their normal atomic sites (Huntley *et al.*, 1985). Due to the imperfect nature of these crystalline structures, the freed electrons become trapped within such minerals, where they may remain indefinitely to accumulate through time (Bailiff, 1992). Exposure of the sediment to sunlight can result in the rapid emission of the stored electrons. This release of energy is termed *luminescence*, and arises from the recombination of the electron charge (Smith *et al.*, 1990). The process of charge

removal is often termed 'zeroing' or 'bleaching', and is crucial in the resetting the luminescence signal prior to the burial of sediments upon deposition. Once buried, the quartz and feldspars will begin to re-accumulate a luminescence signal, containing a greater radiation dose (often termed Equivalent Dose (ED) or Palaeodose) with increased time since burial. Thus determination of the ED facilitates age estimation. However, the ED will increase more rapidly through time with higher concentrations of U, Th and K in the surrounding medium. Therefore the second parameter which must be known is a measure of the strength of this environmental radiation, which is often measured as the annual dose. This can be determined through sample analysis for U, Th and K concentrations or by on-site measurements of the radiation dose emitted from the surrounding sediment. The age of the sample can subsequently be calculated by:

$$\text{Luminescence Age (years)} = \frac{\text{Equivalent Dose (ED)}}{\text{Annual Dose}} \tag{4.3}$$

It is in the determination of ED that different techniques have been developed to stimulate the luminescence signal. Thermoluminescence (TL) was the first widely used luminescence dating method, freeing the trapped electrons by progressive heating in the laboratory. Further details on TL can be found in the reviews of Aitken (1985, 1990) and Wintle (1991). Whilst TL can be applicable for the dating of Quaternary sediments, it suffers from the fact that zeroing of the TL signal requires a relatively long duration of light exposure and may not always be complete (Bailiff, 1992). This lead to the recent development of optically-stimulated luminescence (OSL) dating. OSL determines the ED using laser illumination which only measures electrons from the most light-sensitive traps within the mineral crystal lattice (Huntley *et al.*, 1985). OSL is therefore more suitable for dating fluvial sediments (Fuller *et al.*, 1994, 1996), where there may not have been sufficient light exposure to zero the TL signal, either during erosion, transport or deposition. Optical luminescence techniques have been successfully applied in the dating of Late Pleistocene and Holocene alluvium (e.g. Macklin *et al.*, 1994; Perkins and Rhodes, 1994; Fuller *et al.*, 1996, 1998; Murray, 1996), and results have shown good agreement with ^{14}C results (Macklin *et al.*, 1994; Murray, 1996). One of the main advantages with luminescence is that the sediment itself is being dated, and not some potentially erroneous marker of minimum or maximum sediment age, such as the organics used in radiocarbon dating.

4.4.5.2 The OSL dating approach: technique selection, time range and errors

A number of different wavelengths of light have been used for OSL, including monochromatic green light (OSL) and also infra-red wavelengths (the latter being referred to as infra-red stimulated luminescence (IRSL)). OSL dating of quartz was selected for this study. The use of quartz overcomes the potential problem with feldspars of anomalous fading (Wintle, 1977), where the mineral can gradually lose some of its dose through time due to instability in the feldspar charge storage mechanism, resulting in an underestimate of age (Bailiff, 1992).

The upper time limit for OSL is controlled by the length of time taken to saturate the sediments with radiation dose (Lowe and Walker, 1997), plus the stability of the luminescence signal (Duller, 1996). It is therefore quite variable, but is often at least 100 ka (Huntley *et al.*, 1985). The lower limit, whilst originally thought to be roughly 1000 years, has been progressively lowered to approximately 100 years by recent developments (e.g. Smith *et al.*, 1990; Stokes, 1992; Murray, 1996). This is controlled by the need for a sufficient OSL signal to have accumulated and a low residual luminescence to have been present (Duller, 1996).

The error term associated with OSL dates incorporates systematic uncertainties with the determination of the annual dose and errors associated with the ED determination, such as calibration of laboratory radiation (Lowe and Walker, 1997; M.Bateman, pers. comm. 1997). Inaccuracy in the determination of palaeomoisture content can also strongly affect the annual dose received from the surrounding material (Wintle, 1991).

4.4.5.3 Sample collection and analysis

Sediment sections were cleaned using a trowel prior to sampling. Sediment was collected in aluminium tubes approximately 6 cm in diameter and 25 cm long. The tube was inserted horizontally into the sediments using a lump hammer, and then carefully excavated. Both ends of the tube were immediately taped up using thick opaque duct tape. The depth of burial and the sample's location within the section log were recorded. Samples were preferably taken from sandy units that were likely to have high quartz content, and from near the top of sedimentary units, as this sediment should have received greater light exposure upon deposition. As a portable γ-ray spectrometer was unavailable, samples were taken from 20 cm above and below the OSL tube for U, Th and K analysis, to assess for heterogeneity in the surrounding material

Dating was carried out by the Sheffield Centre for International Drylands Research (SCIDR) at the University of Sheffield. The % moisture was determined, and an uncertainty range of ± 5% used in annual dose calculations. The concentrations of U, Th, and K were determined by ICP, and converted to effective dose rates using the coefficients given by Aitken (1985). The dose contribution from the sediments above and below the tube, attenuated by distance, was also calculated (Aitken, 1985), along with the contribution from cosmic sources (as in Prescott and Hutton, 1994). Quartz was extracted as outlined in Bateman and Catt (1996) and Thomas *et al.*, (1997), and the 90 - 125 μm fraction selected (M.Bateman, pers. comm. 1997). The OSL was measured using a standard Risø reader fitted with a filtered halogen lamp (Bøtter-Jensen and Duller, 1992). Samples were dosed with a calibrated strontium-90 beta source, and heated prior to measurement to remove the unstable signal generated by laboratory irradiations (M. Bateman, pers. comm. 1997). The multiple aliquot ED was calculated using the additive growth method (Mejadahl, 1987), with numerous aliquots being stimulated by the same dose. Single aliquot ED determinations were also carried out according to Duller (1994) and

Clarke (1996). These act as valuable bleaching tests, both independently and in comparison with the multiple aliquot determinations. Ages were subsequently calculated using Equation 4.3.

4.5 LABORATORY ANALYSIS OF SEDIMENT PROPERTIES

4.5.1 Selection of analytical techniques

4.5.1.1 Sediment fingerprinting purposes

Quantitative sediment fingerprinting (described in Chapter 5) requires analytical data that satisfy the following:

1. They must provide quantitative information amenable to statistical analysis.
2. There should be a reasonably large number of different sediment properties measured to provide a 'composite fingerprint' (Walling *et al.*, 1993).
3. All source and target samples must be analysed for all properties.
4. If possible, the data should include at least two different types of sediment property, with differing environmental behaviour, as this is more likely to yield reliable fingerprinting results (Hutchinson, 1995; Collins *et al.*, 1998).

Trace element geochemical analysis by X-ray fluorescence (XRF) and magnetic susceptibility were chosen for this study. Both of these techniques can yield a considerable number of quantitative measurements and are therefore very suitable for fingerprinting.

4.5.1.2 Determination of other sedimentary characteristics

Two other principal types of sample analysis have been carried out. Firstly, X-ray diffraction (XRD) analysis was used to support and assess the fingerprinting results by determining the broad the broad mineralogical composition of certain samples. Secondly, detailed grain size analysis of fine-grained (<2 mm) alluvial sediment was carried out to quantify textural differences between sedimentary deposits, principally the SWDs where such textural information can be valuable for interpreting the sequence of flood events (e.g. Partridge and Baker, 1987; Saynor and Erskine, 1993). Grain size data can also be useful for characterising valley floor alluvium (Hooke *et al.*, 1990).

4.5.2 X-ray fluorescence (XRF)

4.5.2.1 Theoretical background and analytical procedure

XRF is suitable for providing fingerprinting data as it can rapidly and accurately measure a wide range of elements, whilst avoiding the need for extraction procedures that are required for most other types of geochemical analysis (Fairchild *et al.*, 1988). The technique is based on the principle that when a sample is exposed to high energy primary X-rays, secondary X-ray radiation is emitted with wavelengths and intensities determined by the elements present.

Wavelength dispersive XRF (the most common technique) was used in this study, with measurements carried out on an ARL 9400 spectrometer. The X-ray tube in the XRF spectrometer produces primary radiation which has sufficient energy to ionise the sample, displacing electrons from the inner shells of atoms (Fitton, 1997). As outer electrons replace the vacancy in the inner shell, they release energy by emitting secondary (fluorescent) X-ray photons (Lewis and McConchie, 1994). The machine's detector measures the discrete wavelength and intensity of this secondary radiation, which is determined by the elemental composition of the sample. This allows quantitative sequential analysis in the range of 1ppm to 100% (Fitton, 1997). Standard geological reference materials were analysed first, from which calibration curves were constructed. Fluorescent emission from the samples can then be compared to the calibration curves to determine elemental concentrations. The detection limit for most elements is 10 ppm or less (Fitton, 1997).

XRF has the potential to measure both major elements (those in excess of 0.1%) such as Si, Ti, Al, Fe, Ca, Mg, and trace elements (less than 0.1%) such as Ba, Cu, Ni, Pb, Sr and Zn. Whilst either would have differentiated the catchment source types, trace elements were chosen for two main reasons: i) the sample preparation is simpler, avoiding the more complex preparation of fused discs that major element analysis requires; and ii) a larger number of elements could be established by trace element analysis. The concentrations of the following trace elements were determined: Ba, Cr, Cu, La, Ni, Nd, Pb, Rb, Sr, V, Y, Zn, and Zr. Standard reference materials were run throughout the analysis to monitor analytical precision. The error associated with the measurements is variable, but is often quoted at ± 2%, which is perfectly adequate for fingerprinting purposes. Further discussion of the potential analytical errors associated with XRF can be found in Fairchild *et al.* (1988). Perhaps more important for fingerprinting than analytical accuracy, is that the analysis is precise (i.e. reproducible). To assess analytical precision, 10% of the pellets were analysed twice for the same trace elements.

4.5.2.2 Sample preparation

XRF analysis requires a solid sample which must be ground to a fine powder, as irregular or too coarse particle sizes can affect the emission of fluorescent radiation, particularly at longer wavelengths (Fitton, 1997). For the unconsolidated sediments, the <2 mm size fraction was chosen for grinding and subsequent analysis as it covers a large proportion of the fine sediments which would be deposited out of suspension during floods (typically sands and silts).

All samples were initially air-dried. If necessary, sediment samples were gently desegregated using an agate pestle and mortar, and then the >2 mm grains were removed by passing the sample through a nylon mesh. Whole rock samples must be reduced to <2 mm crumbs before grinding. They were therefore cut to less than 40 mm long pieces using a hydraulic splitter, and these pieces then crushed to <2 mm using a hand held hammer and an enclosed steel mortar and pestle.

Grinding of the < 2mm rock and sediment samples to a fine powder was achieved using a Tema® mill with an agate bowl and rings. Where only small samples were avaliable (<60 g), the sample had to be ground by hand in an agate mortar and pestle. All samples were ground to at least less than 125 μm. Excessive sample grinding was avoided as this can increase the contamination risk (McAlister, 1996).

Trace element XRF analysis uses the sample in the form of a pressed pellet. 15g of powdered sample was accurately weighed into a plastic cup, and then mixed thoroughly with a specific amount of PVA glue solution. This mixture was emptied into the presser and a weight of 10 tons was applied. The pellet was then carefully removed and left to dry in a low temperature oven. Where 15 g of sample was unavailable, a smaller pellet was made with 8 g of sample. The 15 g pellet is stronger and more robust, and therefore preferred where possible. However, analysis of the two pellet sizes made from the same powder showed them to be highly consistent. Two international reference standards were prepared by the same method to check the consistency and reliability of the results.

4.5.3 Magnetic susceptibility

4.5.3.1 Theoretical background

There are many potential uses of magnetic data in environmental studies, as magnetic minerals are persistent and conservative in a wide range of depositional environments (Oldfield, 1983), and measurements are fast, convenient, non-destructive and cost effective (Oldfield, 1991; Dearing, 1994). Magnetic analyses are regularly employed for the study of soils, the atmosphere, or river, lake and marine sediments (Thompson and Oldfield, 1986; Oldfield and Thompson, 1986). Of particular note here is their value in studies of palaeohydrology, with core correlation and sediment influx, magnetic differentiation (for pedogenesis and weathering), and sediment source identification all being major research areas (see Oldfield, 1983, 1991).

Two common magnetic measurements were taken here to complement the geochemical data, these being mass-specific magnetic susceptibility (χ) and percentage frequency-dependant susceptibility ($\%\chi_{fd}$). The magnetic characteristics of a material are determined by the combined configuration of all electron motions in its atoms (Dearing, 1994). Magnetic susceptibility is defined as "a measure of the ease with which a material can be magnetised" (Thompson and Oldfield, 1986, p. 25). This is essentially measuring magnetic hysteresis: the variation of magnetisation of a sample with exposure to an applied field (Robinson, 1997). In most natural samples χ is largely determined by the concentration of ferrimagnetic minerals, and particularly magnetite (Fe_3O_4) (Thompson and Oldfield, 1986), though is also sensitive to changes in magnetic grain size. $\%\chi_{fd}$ however is reliant upon the concentration of ultrafine (<0.03μm) superparamagnetic ferrimagnetic minerals within the sample (Dearing, 1994).

4.5.3.2 Analytical procedure

Measurements were taken using a Bartington MS2 Magnetic Susceptibility Meter with the MS2B single sample dual frequency sensor. χ was first measured at a low frequency (0.46 KHz), giving a dimensionless volume susceptibility (κ). Mass specific susceptibility (χ) was calculated by dividing κ by sample mass. χ is expressed in S.I. units of $10^{-8} m^3 kg^{-1}$. Calculation of $\%\chi_{fd}$ requires measurements at two different frequencies, both low (χ_{lf}) and high (χ_{hf}). Whilst χ_{lf} reflects the total susceptibility of the sample, χ_{hf} essentially unaffected by any ultrafine superparamagnetic minerals (Robinson, 1997), thus allowing the determination of χ_{fd}. The samples were therefore measured again at a high frequency (4.6KHz), placing them into the sensor in the same orientation as before. The frequency-dependant component of susceptibility was then calculated by:

$$\%\chi fd = \{(\chi lf - \chi hf) / \chi lf\} \times 100 \quad (4.4)$$

4.5.3.3 Sample preparation

All samples were initially air dried in the laboratory and sediments were disaggregated gently using an agate pestle and mortar. The >1mm grains were then removed from the sediment samples by passing them through a nylon mesh. The rejected coarser grains are likely to be of low susceptibility and are therefore not only of less interest, but also if included might make the samples too weakly magnetic for accurate measurement. The powders prepared for XRF analysis (see section 4.5.2) were used to determine the susceptibility of the whole rock samples. $10cm^3$ plastic pots were filled with a weighed amount of sample that was wrapped and packed in clingfilm to immobilise the particles. An empty pot was also prepared as a blank to assess any magnetic effects of the plastic, from which the sample readings could be corrected.

4.5.4 X-ray diffraction (XRD)

4.5.4.1 Theoretical Background

XRD enables mineral identification with only fairly simple sample preparation (Lewis and McConchie, 1994). There are numerous applications within sedimentology, in particular involving the analysis of clay minerals, carbonates and silica minerals (Hardy and Tucker, 1988). The technique is based on the principle that X-rays are diffracted by the atomic layers in mineral crystals. A tube produces X-rays, which are collimated into a divergent beam and aimed at the sample. A goniometer holds and rotates the sample through a range of angles at a regular speed. The diffracted X-rays are measured by a detector and other forms of radiation (e.g. fluorescent X-rays) are removed by a pulse height analyser. As each different mineral has a unique and distinct set of atomic layer spacings (*d* spacings), the measurement of diffracted X-rays can be used to identify the minerals present in the sample (Lewis and McConchie, 1994).

4.5.4.2 Analytical procedure

XRD measurements were carried out on a Phillips PW 1840. Instrument conditions depended on the sample being analysed, however, angles of 10 to 70° 2θ were used for a broad mineral scan, with typical power settings of 40 kV and 30 mA. Minerals were identified on the basis of the diffraction peaks. Some semi-quantitative estimates of mineralogy were made on the basis of: a) the intensity of the diffraction pattern representing the concentration of the mineral in the sample (Hardy and Tucker, 1988); and b) by comparing the peak heights to that of the 100% composition peak (Lewis and McConchie, 1994).Quantitative analysis is difficult for XRD, and was not attempted here.

4.5.4.3 Sample preparation

Samples were crushed and ground as for XRF (see section 4.5.2). Additional grinding by mortar and pestle was carried out where necessary to reduce the sample to a very fine powder (ideally 5-10 μm). 2 - 3g of sample was mounted in an aluminium cavity mount holder. The cavity mount was then fitted into the diffractometer and suitable instrument conditions were set.

4.5.5 Grain size determination

Samples analysed included the palaeoflood slackwater sediments, fine-grained alluvium (including the fine-grained matrix from coarser alluvial units), and contemporary channel fines.

A wide variety of different analytical procedures have been used in the past to determine grain size distributions (for details see McManus, 1988). In this study, samples were analysed using a Coulter® LS™230 laser diffraction particle size analyser. The machine utilises the fact that different grain sizes scatter a directed beam of light in different ways, and hence if this scatter, or diffraction can be detected, the grain size can be determined. The machine can determine grain sizes from 2 mm down to sub-micron diameters by virtue of PIDS (Polarisation Intensity Differential Scattering) measurements. The sediments were sieved to >2 mm, and then the 1 - 2 mm fraction was screened off and weighed. This was done because long, narrow shaped grains may pass through a 1 mm mesh, but may actually be considerably larger, and can damage the machine. Subsequently the <1 mm fraction was also weighed, and then analysed on the Coulter® LS™230, quality control being maintained through the analysis of internal reference standards. To avoid problems of aggregation, samples were dispersed on a watchglass before analysis with a small amount of 5% calgon (a dispersant) and then washed into the machine with calgon. The data for the 1 - 2 mm and <1 mm fractions were integrated using the Coulter® LS™230 software.

4.6 SUMMARY

This chapter has described the techniques that have been used to reconstruct the nature and timing of catastrophic flooding within the Voidomatis and Aoos Basins. Systematic records,

boulder berms and floodplain sedimentation provide data for the last 200 years, and palaeoflood slackwater deposits for the Late Würm (c. 25-10 ka). However, the analysis of flood deposits alone does not allow a satisfactory interpretation of their occurrence, magnitude or geomorphic effects. Therefore, an investigation of the valley floor alluvial stratigraphy has also been undertaken to establish the Late Pleistocene and Holocene alluvial history of Voidomatis basin, and the nature of environmental controls on river activity.

Numerous dating techniques have been employed over the two timescales: i) lichenometry, ^{210}Pb, ^{137}Cs over the last 200 years; and ii) $^{230}Th/^{234}U$, ^{14}C and OSL over the Late Pleistocene. The combined application of these techniques presents the opportunity for cross-verification of dating results. Of particular importance is the inclusion of quantitative fine sediment fingerprinting into the project, which provides a large amount of extra information for the interpretation of fluvial deposits.

5. A QUANTITATIVE SEDIMENT FINGERPRINTING TECHNIQUE FOR APPLICATION TO LATE PLEISTOCENE AND HOLOCENE ALLUVIAL DEPOSITS

This chapter describes and assesses the quantitative sediment fingerprinting procedure that has been used to determine the provenance of fine-grained (<2 mm) alluvial sediments of various ages in the Voidomatis basin. This work has been conducted primarily for the purpose of using sediment provenance information to aid in the reconstruction of catchment scale environmental conditions when these river sediments were deposited. The deposits of interest are palaeoflood slackwater sediments and valley fill alluvium, which have been laid down during the Late Pleistocene and Holocene (section 4.1). Although the sediment provenance results are presented more fully in Chapters 6 and 7 (in combination with the relevant geochronological and sedimentological information), it is firstly important to consider the nature of the fingerprinting approach that has been employed and this is described in detail in this chapter. Section 5.1 outlines the broader context for sediment provenance research, and describes the principles of the quantitative fingerprinting approach. In addition, this section details the rationale for using fine sediment provenancing in this study. Section 5.2 describes the fingerprinting procedure that has been used and section 5.3 assesses the reliability of the results. All analytical data used in the fingerprinting are provided in Appendix II-VI.

5.1 BACKGROUND TO SEDIMENT PROVENANCING

Information on sediment provenance is a fundamental requirement for many geological and geomorphological investigations. Provenance data have been used to calibrate models of tectonic uplift and displacement, to investigate the formation of sedimentary sequences and for large-scale palaeogeographic reconstructions (Haughton *et al.*, 1991). Within process geomorphology provenance information has proved to be of considerable value in elucidating catchment sediment dynamics, providing information on temporal and spatial variations in sediment sources (e.g. Yu and Oldfield, 1989; Walling and Woodward, 1995; Collins *et al.*, 1998). These studies have focused mainly on either tracing the source of contemporary suspended sediment (e.g. Walling *et al.*, 1979; Walling and Woodward, 1992, 1995) or on fine-grained sediments deposited in lake basins and estuaries (e.g. Yu and Oldfield, 1989, 1993; Dearing, 1992; Hutchinson, 1995). They have demonstrated that the source of sediment from catchment areas of contrasting land use and/or lithology can be established (e.g. Walling and Woodward, 1995).

Many provenance studies have employed qualitative or semi-quantitative methods to identify sediment source areas or types (e.g. Wood, 1978; Walling *et al.*, 1979; Oldfield *et al.*, 1985; Woodward *et al.*, 1992). More recently, however, techniques for obtaining more robust, quantitative constraints of fine sediment source have been developed. These 'quantitative fingerprinting' approaches (Peart and Walling, 1986) assume that the physical and chemical properties of the sediment of interest directly reflect the relative contributions from catchment source areas. Certain physical and chemical properties are firstly selected to differentiate the source area materials (e.g. soils, sediments, bedrock etc.), and a multivariate mixing model is then used to determine the relative contribution of each individual source type (e.g. Yu and Oldfield, 1989; Walling *et al.*, 1983). A wide variety of approaches have been employed to establish sediment provenance, including geochemistry (Passmore and Macklin, 1994; Collins *et al.*, 1997a, 1997b, 1998), mineral magnetics (Walling *et al.*, 1979; Yu and Oldfield, 1989, 1993; Dearing, 1992; Hutchinson, 1995; Foster *et al.*, 1998), radionuclide concentrations (Walling and Woodward, 1992; Olley *et al.*, 1993; Hutchinson, 1995), SEM analysis (de Boer and Crosby, 1995), mineralogy (Wood, 1978; Woodward *et al.*, 1992), sediment colour (Grimshaw and Lewin, 1980) and particle-size distributions (Kurashige and Fusejima, 1997). The advantage of the recently developed multivariate fingerprinting approach is that it has the potential to provide objective, quantitative provenance data in contexts where there are a large number of diverse potential fluvial sediment sources (e.g. Walling and Woodward, 1995; Collins *et al.*, 1997a, 1998). Such information cannot be obtained using more traditional qualitative mineralogical analyses.

Over Late Pleistocene and Holocene timescales, the flux and provenance of fine-grained fluvial sediment will be influenced by environmental controls such as climate variations, vegetation dynamics, land use change or tectonic activity. Changes in these factors will modify the characteristics of the catchment, and the nature of sediment delivery to the river over time. The provenance of the fine sediment within fluvial deposits can therefore provide information regarding the characteristics of the catchment environment at the time of deposition (Woodward *et al.*, 1992; Passmore and Macklin, 1994). Thus data on changes in Late Pleistocene and Holocene fine sediment provenance may provide valuable information regarding fluvial responses to catchment-wide environmental changes (Hamlin *et al.*, in press). Indeed, previous work in the Voidomatis basin by Woodward *et al.* (1992) demonstrated that the <63 micron fraction of the fluvial sediment load has exhibited very different mineralogical characteristics over the Late Quaternary. Most importantly, they found a much greater proportion of limestone-derived minerals in alluvial sediments deposited during the Last Glacial compared to those in the contemporary system. Furthermore, Lewin *et al.* (1991) showed a similar increase in limestone within the gravel fraction of alluvial deposits in the Voidomatis basin (section 6.2). These provenance changes have been attributed to increased supply of limestone derived sediments during the cold glacial climate (Lewin *et al.*, 1991; Woodward *et al.*, 1992).

The provenance of *fine-grained* (<2 mm) sediments has been investigated in this study because, of the total sediment load, this is the most appropriate fraction to use for the investigation of *catchment-wide* environmental conditions. Coarse-grained sediments (gravels, cobbles and boulders), are less mobile and transported more episodically than the fine fraction, and, at a given location, are likely to be less representative of catchment scale sediment dynamics. Instead, their provenance is more strongly controlled by local coarse sediment supply (Woodward *et al.*, 1992). In contrast, the fine fraction can be transported quickly and over large distances during flood events, and will therefore be sensitive to both spatial and temporal changes in sediment delivery and transport. In addition, fine sediment provenance data from dated alluvial fills provide important context for the slackwater sediments, which do not contain coarse-grained material. The use of fine sediments means that the provenance data from the two types of deposit are directly comparable.

Quantitative fine-sediment provenance data may of course serve various other purposes for this study. For example, they can be used to identify and correlate specific fluvial deposits, in particular individual flood units within the slackwater deposits. Sediments deposited by different floods have commonly been identified by sedimentary features (see section 2.3.2), but previous work has shown that this can be difficult, as such features are not always evident or conclusive (Hattingh and Zawada, 1996). This problem may be particularly serious for Late Pleistocene deposits (e.g. Baker and Bunker, 1985), which may have been modified by bioturbation or weathering. However, sediment provenance data can alleviate this problem by detecting changes in provenance characteristics between sedimentary units. Saynor and Erskine (1993) demonstrated this by employing heavy mineral analysis to qualitatively differentiate flood sediments from those that contained a proportion of locally derived colluvium.

The application of the quantitative fingerprinting technique over long (10^2 - 10^5 years) timescales also presents an opportunity to advance methods for investigating alluvial stratigraphy. Previous work has discussed the potential value of provenance data for interpreting long-term river behaviour (Woodward *et al.*, 1992; Passmore and Macklin, 1994), and investigations of changing sediment delivery to lakes has enabled reconstruction of historical changes in catchment environments (Oldfield *et al.*, 1985; Yu and Oldfield, 1989, 1993; Dearing, 1992). Building on these promising results, recent years have seen an increasing number of geomorphological investigations into the source of Holocene floodplain deposits (e.g. Passmore and Macklin, 1994; Collins *et al.*, 1997b; Rowan *et al.*, 1999; Schell *et al.*, in press). It is also worth remembering that pre-Quaternary geologists have for many years made extensive use of various provenance techniques for investigating large-scale geological sequences. However, catchment scale provenancing covering timescales from modern environments back into the Late Pleistocene remains rare, particularly for quantitative fingerprinting. Given the potential value of such long-term fingerprinting data, it is of

considerable importance to investigate the viability of using quantitative fingerprinting as a tool for interpreting long-term river behaviour.

5.2 SEDIMENT FINGERPRINTING PROCEDURE

The fingerprinting methodology used in this study builds on previous approaches (e.g. Yu and Oldfield, 1989, 1993; Walling *et al.*, 1993; Walling and Woodward, 1995; Collins *et al.*, 1997a, 1998) and has three key stages:

1. Identification of potential sediment sources (section 5.2.1).
2. Selection of a suite of variables that together differentiate unequivocally all the potential sediment sources (section 5.2.2).
3. Use of the composite fingerprint with a multivariate mixing model to determine quantitatively the relative contribution of each source group to the fine sediment in the fluvial deposits (section 5.2.3).

5.2.1 Stage 1: Identification of potential sediment sources

The fingerprinting procedure aimed to determine the contribution of different geological sources in the Voidomatis basin to the preserved fluvial sediments. Using geological maps (Figure 3.8), air photographs, field data and XRD information, seven distinct geological source groups were identified (Table 5.1). In addition, alluvium is also taken to be a potential source, thus allowing for the possible incorporation of reworked sediments. These alluvium source samples were only taken from Late Pleistocene deposits, as most of the target samples were deposited during the Late Pleistocene (SWDs and older terraces), and more recent alluvium would not have been present during this time. The lithologies that most commonly outcrop in the catchment, namely limestone and flysch, demanded a larger number of source samples to ensure that they were adequately represented (Table 5.1). The collection of only a single dolomite sample was due to difficulty in differentiating it from limestone in the field, and its generally limited outcrop in the catchment (Figure 3.8).

TABLE 5.1 List of geological source groups used in the fingerprinting analysis. † This is calculated using the area of the Voidomatis catchment shown in Figure 3.x, where N/A refer to unavailable as these sources are not shown on the geology maps. Colluvium, which as not used as a source here, occupies a further 4.8% of the catchment area.

Geological Source Group	Number of samples	Area in catchment †	
		(km^2)	(%)
Limestone	13	173.0	46.7
Till	4	7.0	1.9
Flysch	18	150.1	40.5
Dolomite enriched flysch	2	N/A	N/A
Dolomite	1	0.5	0.1
Ophiolite	3	1.0	0.3
Terra Rossa	4	N/A	N/A
Alluvium	7	21.4	5.8

5.2.2 Stage 2: Selection of a suite of variables that together differentiate unequivocally all the potential sediment sources.

It is fundamental to any provenancing methodology that the potential sediment sources can be adequately characterised and discriminated. Figure 5.1 shows plots of a variety of the geochemical and mineral magnetic fingerprinting parameters for the 52 source samples collected. These show that many of the parameters are capable of distinguishing some or all of the different lithological sources. For example, the Cr v Ni plot shows very tight clustering of the different source groups. In particular, the ophiolite has much higher values compared to other sources, as would be expected for this igneous material. Other parameters show different behaviour between the source groups. The Ba v Sr plot shows a good separation of the different sources, but here high values are found in different groups. The dolomitic materials, as expected, are high in Ba, whilst the limestone, till and alluvium are characterised by higher Sr concentrations than the flysch or terra rossa. It is noticeable that Sr splits the limestone samples into two groups, with the younger Eocene limestone having higher Sr concentrations than the underlying Tertiary and Jurassic-Cretaceous limestone strata (Figure 3.8). The Rb v V plot again shows a promising separation of the different sources. However, these elements do show two separate groupings for the flysch, which occurs due to the solid sandstone flysch beds having lower values than the more fissile siltstone layers which are intercalated between them (see Figure 3.9 for a view of the flysch lithology). Zr and low-frequency magnetic susceptibility (χ) appear to differentiate some source groups better than others. The magnetic susceptibility clearly discriminates the terra rossa, and to a lesser extent the ophiolite, but other sources have fairly similar values. Zr neatly separates the limestone, alluvium, and till at low values, and the flysch is also discriminated from these groups although there is a considerable range in the flysch values. However, not all of the parameters are as efficient as these. For example, the La v Zn plot shows that although the limestone and terra rossa are separated at low and high values respectively, all the other sources have quite similar values and might not be distinguishable using these elements. These bivariate plots provide a useful means of exploring the effectiveness of various parameters in differentiating between the source groups. It is important that the parameter combination selected for the fingerprinting procedure most efficiently discriminates between the different source groups. To ensure that this is done in an objective and reliable manner, a range of statistical procedures have been employed in three steps, as described below.

5.2.2.1 Nonparametric Krushkal Wallis H-test to determine which parameters successfully differentiate the source groups.

The Krushkal Wallis H-test is appropriate for this purpose as it can determine whether there is a significant difference between three or more groups of data. A nonparametric test such as this was required because the data were found to have neither uniform distributions nor equal

variances, thus making parametric tests unsuitable. Before carrying out the tests, all analytical data were initially made dimensionless by dividing the values for each parameter by the maximum recording. This was done to normalise the data and thereby ensuring that each parameter exerted an equal influence in the fingerprinting calculations (Verrucchi and Minisale, 1995).

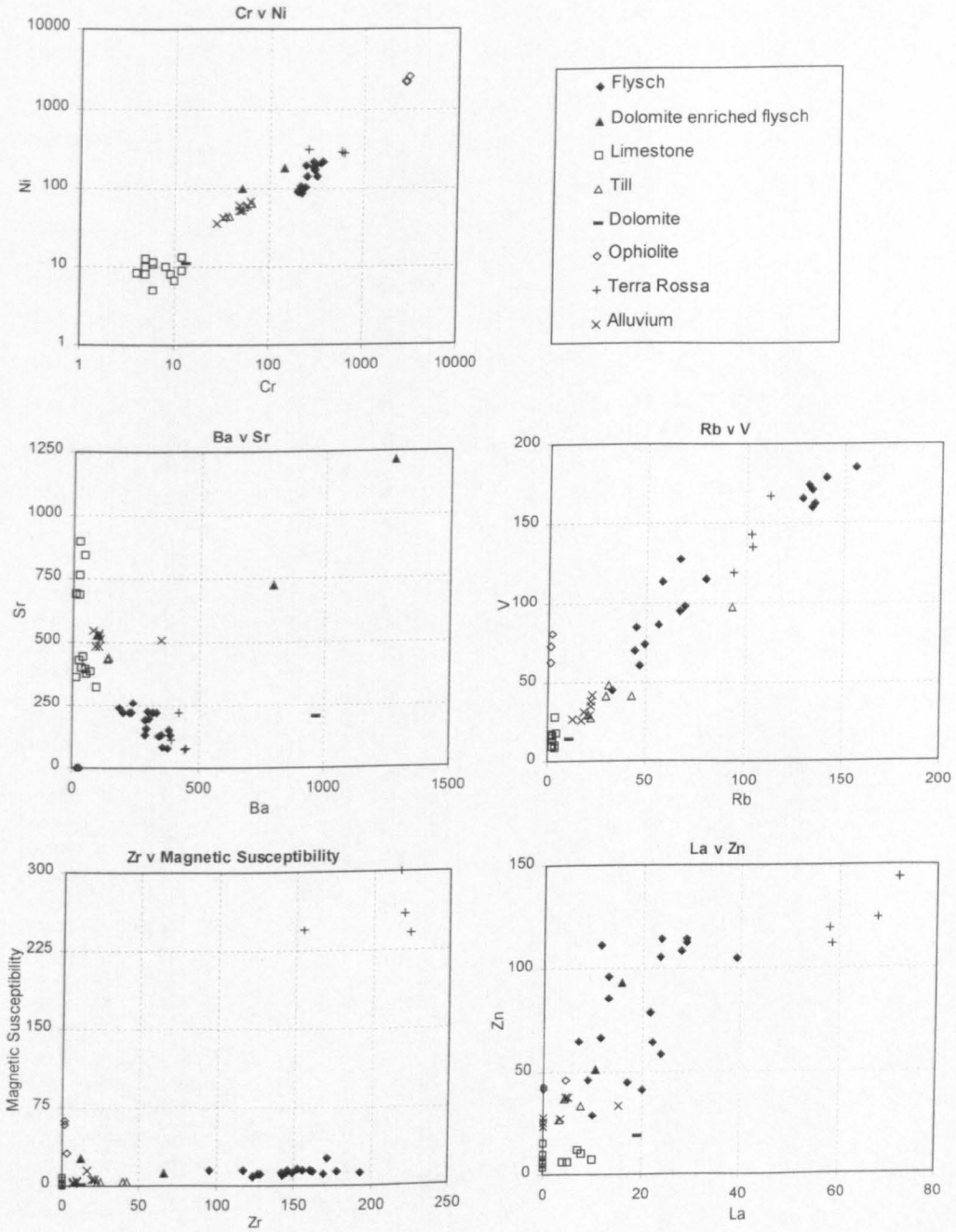

FIGURE 5.1 Scatter plots of selected fingerprinting parameters for different source groups. The plots of Chromium (Cr) v Nickel (Ni), Barium (Ba) v Strontium (Sr), Rubidium (Rb) v Vanadium (V) and Zirconium (Zr) v magnetic susceptibility all show reasonably good differentiation of the source groups. In contrast, the plot of Lanthanum (La) v Zinc (Zn) shows a far less successful discrimination of the different sources. The Cr v Ni plot is shown using logarithmic scales due to the large values for ophiolite. All geochemical data are in ppm, whilst magnetic susceptibility is in 10^{-8} m^3 kg^{-1}.

With the exception of frequency-dependant magnetic susceptibility ($\%\chi_{fd}$), all parameters produce values for H_{calc} which are greater that H_{crit} at the 99.9% significance level (Table 5.2). This means that for all parameters apart from $\%\chi_{fd}$ there is a 99.9% probability that the differences between the mean parameter values for each source group are not attributable to random variation. This exceptionally high level of significance is due to the distinct differences in the fingerprinting parameters between the geological source groups, which is necessary to produce accurate fingerprinting results. The H-value of 14.30 for $\%\chi_{fd}$ is less than H_{crit} at the 99.9% significance level (Table 5.2), as it is not so successful at differentiating the sources, due to the low concentration of ultrafine superparamagnetic grains in these samples. This problem with $\%\chi_{fd}$ was experienced by Lees (1997), who also found that it was a less valuable fingerprinting parameter. Frequency dependant magnetic susceptibility is therefore rejected at this point. In contrast, low-frequency magnetic susceptibility provided effective discrimination and has been shown to be the most reliable mineral magnetic parameter in experimental evaluations of quantitative fingerprinting procedures (Lees, 1997). All the geochemical (XRF) parameters and the low-frequency magnetic susceptibility pass the test and are used in the next stage.

TABLE 5.2 Results of Krushkal-Wallis H-tests on the different parameters used to differentiate geological sources. Critical values are shown below. A calculated value greater than the critical value indicates that the null hypothesis can be rejected, and the parameter does statistically significantly differentiate source groups.

Parameter	H-value
Barium (Ba)	45.18
Chromium (Cr)	46.65
Copper (Cu)	38.22
Lanthanum (La)	39.29
Neodymium (Nd)	38.82
Nickel (Ni)	46.67
Lead (Pb)	45.46
Rubidium (Rb)	44.98
Strontium (Sr)	44.96
Vanadium (V)	43.61
Yttrium (Y)	47.55
Zinc (Zn)	45.11
Zirconium (Zr)	47.78
Mass- specific magnetic susceptibility (χ)	43.02
% frequency dependant magnetic susceptibility ($\%\chi_{fd}$)	14.30

H_{crit} = 14.07 (95%), 24.32 (99.9%).

5.2.2.2 Assessment of the reproducibility and long-term stability of the parameters.

To produce accurate results it is important to establish that the geochemical and magnetic data are reliable and reproducible. Thus, repeat analyses of the same sample aliquot were carried out

on a random 10% selection from the total sample set. The replicate data were divided by their mean, and a weighting (1 minus the standard deviation) was calculated (Table 5.3). This provides an assessment of the reproducibility of analytical measurements (Collins*et al.*, 1997a). Table 5.3 shows that all elements show very good reproducibility with the exception of La, and in particular Nd.

It is well known that under certain conditions, some trace elements can be prone to alteration in sediments, often due to diagenetic effects (e.g. Farmer and Lovell, 1984). However, a combination of trace elements has been selected for this study that would be expected to remain stable in this environment over the timescale of interest. Nevertheless, both La and Nd are Light Rare Earth Elements (LREE), and known to be prone to long-term instability in sediments. This could be a problem as their concentrations in old alluvial sediments may have been altered. For reasons of poor reproducibility and possible long-term instability, La and Nd were both therefore discarded at this stage.

TABLE 5.3 Weightings for geochemical parameters used to differentiate geological sources. A higher weighting indicates greater analytical reproducibility.

Parameter	Weighting
Sr	0.976
χ	0.972
Zn	0.958
Ni	0.956
Zr	0.950
Y	0.947
Cr	0.934
Rb	0.930
Cu	0.927
Ba	0.860
V	0.829
Pb	0.822
La	0.572
Nd	0.219

5.2.2.3 Multivariate Discriminant Analysis (MDA) to select the composite fingerprint parameters.

From the twelve parameters that passed the preceding stages, MDA was used to select a parameter combination capable of successfully differentiating all the source samples. Stepwise selection was achieved by the minimisation of Wilk's lambda, through the parameter with the smallest lambda value being selected at each step. Lambda values close to zero indicate that within-group variability is small compared to total variability, therefore the most useful parameters and hence composite signatures will be associated with low lambda values.

The results of this process are shown in Table 5.4. Note that due to the very high efficiency of the parameters in differentiating the source groups, very low lambda values are obtained early in the selection process. With only the first four parameters all the source

samples are correctly classified (Table 5.4). This could be used as the composite fingerprint. However, a larger numbers of parameters will improve the reliability of the results, given the large number of source groups in this study (Table 5.1). With successive parameters added, there is a continued decrease in Wilk's lambda (Table 5.4), which demonstrates the improved discrimination that a larger composite fingerprint affords. Nine parameters (Table 5.4) were therefore selected as the composite fingerprint for this study. The addition of further parameters (Cu, Ni, Pb or Zn) was not necessary, as the value of Wilk's lambda has been minimised to such an extent that they could not make the fingerprint significantly more efficient (Table5.4). These results show how the XRF and low-frequency magnetic susceptibility data have allowed effective differentiation of a range of diverse catchment sources. This could not have been achieved using standard mineralogical analyses such as XRD. This demonstrates the value of using a number of fingerprinting parameters in combination to differentiate catchment sediment sources. Table 5.5 lists the rank order of each fingerprinting parameter according to the different source groups. This shows the contrasting behaviour of the different parameters between the diverse range of sediment source types, which is also apparent in some of the plots shown in Figure 5.1. Such variations in rank ordering between the parameters included in the composite fingerprint improve its ability to discriminate between individual sources (Walling *et al.*, 1993; Walling and Woodward, 1995).

TABLE 5.4 Results of Multivariate Discriminant Analysis (MDA) selection of the composite fingerprint.

Parameter	Wilk's lambda	% of samples correctly classified
Cr	0.00789	75.00
χ	0.0000809	75.00
Zr	0.00000449	98.08
Ba	0.000000418	100.00
Sr	0.000000106	100.00
Y	0.0000000679	100.00
Rb	0.0000000312	100.00
Cu	0.0000000141	100.00
V	0.00000000963	100.00

TABLE 5.5 Ranking of the mean parameter values for each source group from highest (1) to lowest (8) for all nine tracers included in the composite fingerprint. The mean parameter values on which these rankings are based are shown in Table 5.6.

Fingerprint property	Limestone	Till	Flysch	Dolomite enriched flysch	Dolomite	Ophiolite	Terra Rossa	Reworked alluvium
Ba	7	6	4	1	2	8	3	5
Cr	8	5	3	4	7	1	2	6
Cu	8	4/5	3	2	7	6	1	4/5
Rb	7	4	2	3	6	8	1	5
Sr	2	4	5	1	6	8	7	3
V	7/8	5	2	4	7/8	3	1	6
Y	7	4/5	2	3	4/5	8	1	6
Zr	8	4	2	3	6	7	1	5
χ	7	6	4	3	8	2	1	5

5.2.3 Stage 3: Use of a multivariate mixing model to determine quantitatively the relative contribution of each source group to the fine sediment in the fluvial deposits.

A similar mixing model approach to that employed by Walling *et al.* (1993) is used here. In a linear mixing model it is assumed that the analytical data from the sediment samples are attributable to the relative contributions of the different source groups: -

$$B_t = \sum_{s=1}^{S} V_{st} P_s \tag{5.1}$$

subject to the following set of linear constraints:-

$$\sum_{s=1}^{S} P_s = 1 \tag{5.2}$$

$$0 \leq P_s \leq 1 \tag{5.3}$$

while minimising the error term,

$$E = \sum_{t=1}^{T} \left\{ \left[B_t - \left(\sum_{s=1}^{S} V_{st} P_s \right) \right] / B_t \right\} W_t \tag{5.4}$$

where P_s is the fraction of sediment derived from source type s, V_{st} is the average value of fingerprint property t for source type s, S is the number of source types, B_t is the deposit fine sediment sample value for fingerprint property t, W_t is the weighting for fingerprint property t (Table 5.3), and T is the number of fingerprint properties considered. At the start, the source contributions P_s are set equal and the error term E is calculated. Changes in P_s are carried out that minimise E. This proceeds until no further reduction of E is possible, the change is then halved, and the procedure repeated until the optimum estimate (minimum E) for relative source contributions is achieved (Walling *et al.*, 1993). The values of P_s are therefore used provide the sediment source results as a percentage value. The results for the flysch and dolomite enriched flysch source groups for each sample were amalgamated to obtain a single value for the flysch lithology.

Part of the mixing model procedure can be illustrated by comparing the fingerprinting results to the raw XRF and mineral magnetics data. If the mixing model is operating correctly, those samples predicted to be dominated by a certain lithology should exhibit similar geochemical and magnetic characteristics to that source type. It has been shown that main sediment sources have a number of distinctive characteristics. For example, the limestone is high in Sr, but low in most other parameters (Table 5.6). The till is similar to the limestone, with a slightly less pure trace element geochemistry reflecting the incorporation of a minor flysch component (Table 5.6). The flysch, in contrast, shows relatively high concentrations of Ba, Cr, Rb, V, and Zr, and has a higher magnetic susceptibility (Table 5.6). As an example of these contrasts and the mixing model process, Figure 5.2 and Figure 5.3 show the output for two samples; one alluvial fine matrix sample predicted to have a high limestone and till content (V65a), and one SWD sample from the Boila rockshelter predicted to have a high flysch content (OKB1.9). These are compared to the Cr, Sr and χ data, which depict some of the clear

differences between these major source groups. Comparison of the data for both samples shows that the fingerprinting predictions are consistent with the geochemical and mineral magnetic signatures, thus providing a simple qualitative check that the mixing model is producing sensible results.

TABLE 5.6 Mean source material fingerprint properties for the 8 source groups. Geochemical data are shown in ppm, whilst magnetic susceptibility (χ) is in 10^{-8} m^3 kg^{-1}. The % coefficient of variance is also shown.

Fingerprint property		Limestone	Till	Flysch	Dolomite enriched flysch	Dolomite	Ophiolite	Terra Rossa	Reworked alluvium
Ba	**Mean**	**38**	**118**	**302**	**1034**	**964**	**25**	**429**	**132**
	% C.V.	59.3	22.1	20.7	32.9	-	18.4	6.2	71.8
Cr	**Mean**	**7**	**48**	**265**	**97**	**13**	**2831**	**454**	**47**
	% C.V.	38.6	29.3	18.8	66.7	-	4.5	37.8	26.7
Cu	**Mean**	**9**	**24**	**35**	**56**	**16**	**19**	**89**	**24**
	% C.V.	34.9	6.6	48.2	57.0	-	3.5	27.1	18.8
Rb	**Mean**	**3**	**26**	**88**	**68**	**11**	**1**	**103**	**19**
	% C.V.	28.7	20.4	48.6	52.7	-	41.6	7.1	19.2
Sr	**Mean**	**538**	**482**	**178**	**971**	**203**	**0**	**121**	**514**
	% C.V.	38.3	10.6	31.2	35.3	-	0.0	57.2	4.9
V	**Mean**	**14**	**36**	**120**	**69**	**14**	**72**	**141**	**33**
	% C.V.	37.2	27.1	38.2	57.0	-	12.3	14.4	18.9
Y	**Mean**	**4**	**11**	**23**	**15**	**11**	**0**	**63**	**9**
	% C.V.	65.3	6.1	22.0	35.9	-	0.0	17.0	11.6
Zr	**Mean**	**0**	**32**	**148**	**39**	**12**	**2**	**204**	**13**
	% C.V.	0.0	30.2	16.2	97.0	-	39.9	16.2	43.7
χ	**Mean**	**1.5**	**3.6**	**12.8**	**19.1**	**1.4**	**50.1**	**261.3**	**5.6**
	% C.V.	133.9	4.3	28.6	52.6	-	33.5	10.4	72.3

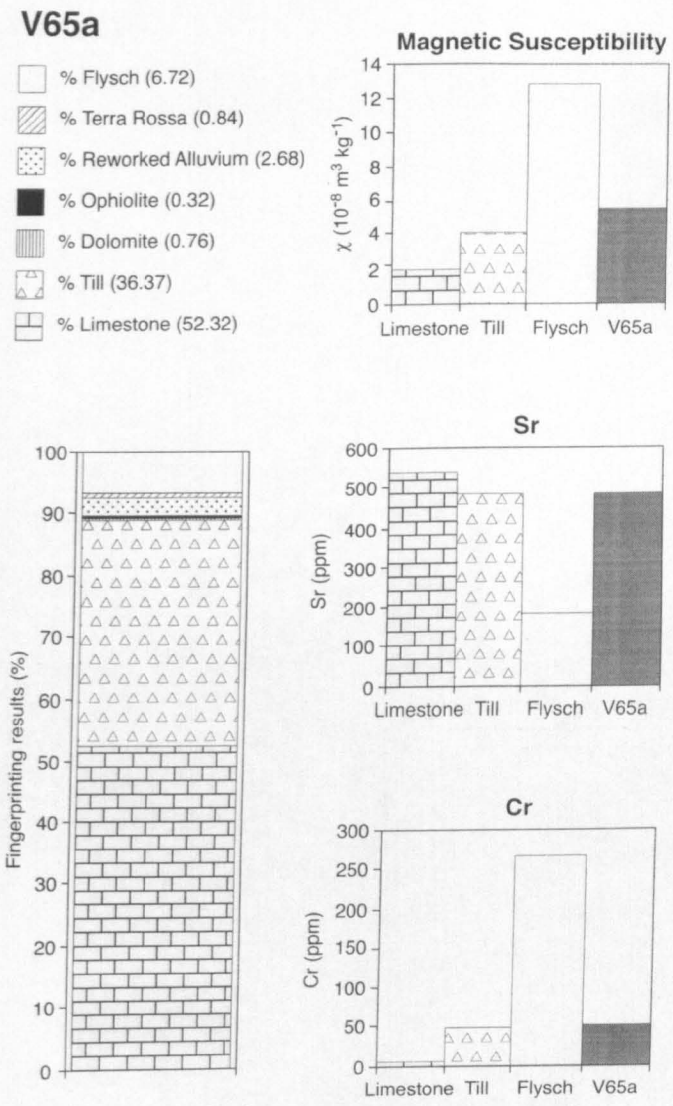

FIGURE 5.2 Comparison of fingerprinting results (stacked bar chart) with geochemical and magnetic data for sample V65a (standard bar charts) which was taken from the fine-grained matrix of a coarse-grained alluvial unit.

5.3 RELIABILITY OF FINGERPRINTING RESULTS

It is important to assess the reliability of the fingerprinting results. Initial inspection of the results for the alluvial fill and slackwater sediments (which are presented in the following two chapters) showed that the most extensive source materials within the catchment (limestone, flysch and till) dominate the fingerprinting predictions. This suggests that the results are realistic. However, the difference between the measured and predicted parameter values can be used to obtain a mean relative error. In this study these are typically ± 10-15%, which is only slightly larger than recent work on contemporary suspended sediments (c. ± 10%) reported by Collins *et al.* (1997a, 1998). This is encouraging when one considers some of the potential problems involved in obtaining such provenance data for Pleistocene sediments. However, this

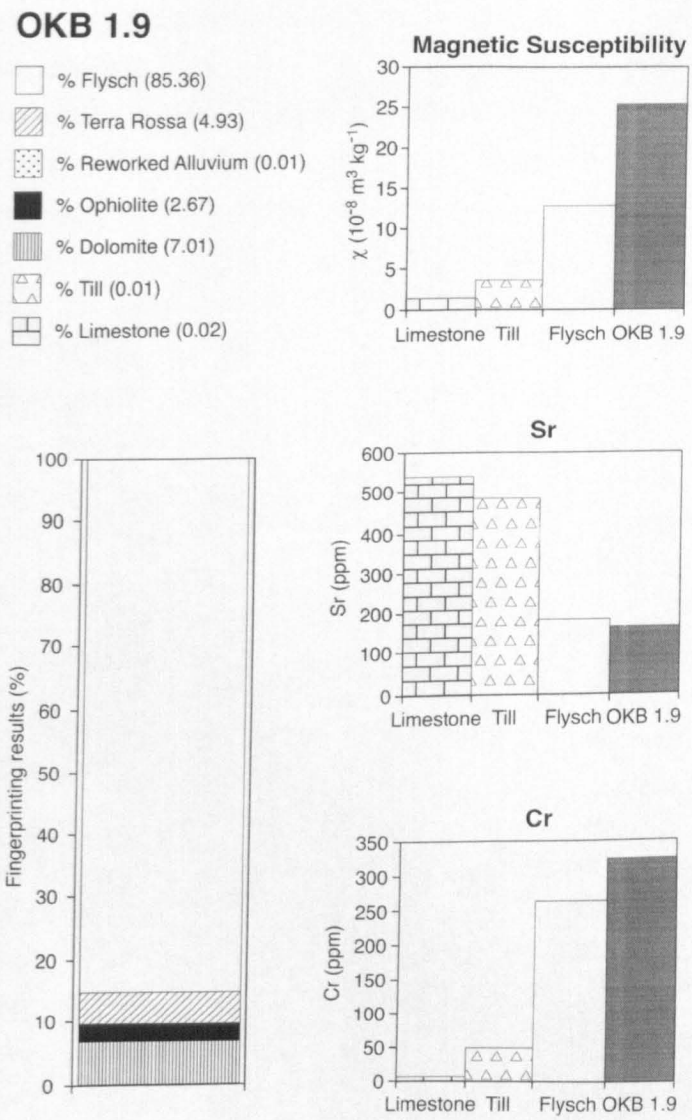

FIGURE 5.3 Comparison of fingerprinting results (stacked bar chart) with geochemical and magnetic data for sample OKB1.9 (standard bar charts), which was taken from the Boila rockshelter SWDs.

is only a very simplistic method of error estimation, and there is currently considerable interest in the development of improved techniques to provide more robust estimates of fingerprinting uncertainty (e.g. Goodwill and Rowan, in press). In this study the reliability of the results have been tested through independent mineralogical validation, sensitivity analysis of the fingerprinting calculations, and an inspection of the results from duplicate field samples. These are described in turn.

5.3.1 Mineralogical validation

The results can be tested by comparing the fingerprinting predictions with independent mineralogical data determined by XRD. The distinctive characteristics of the main sediment sources (Table 5.6) reflect their mineralogical differences. The limestone has relatively simple

geochemical and mineral magnetic characteristics as it is composed largely of calcite with small amounts of quartz (Woodward *et al.*, 1992). The till is similar to the limestone, being dominated by calcite but including a little more quartz and feldspar. In contrast, high concentrations of many trace elements in the flysch, and its higher magnetic susceptibility, can be explained by a mineralogy dominated by quartz, with a significant amount of feldspar and various clay minerals. As an example, Figure 5.4 shows the mineralogical data for the two samples whose fingerprinting results are displayed in and Figure 5.3. For V65a the mineralogy is dominated by calcite (75%), with some quartz (20%) but very little clays or feldspar, thus supporting the fingerprinting predictions of approximately 90% limestone and till (Figure 5.2). The agreement of the data is also encouraging for OKB1.9, which has a high quartz content (58%) and a significant amount of feldspar and clays, which is consistent with the high flysch content predicted for this sample (Figure 5.3). Thus in both cases, mineralogical information fully supports the fingerprinting predictions, suggesting that the source ascription is both accurate and reliable.

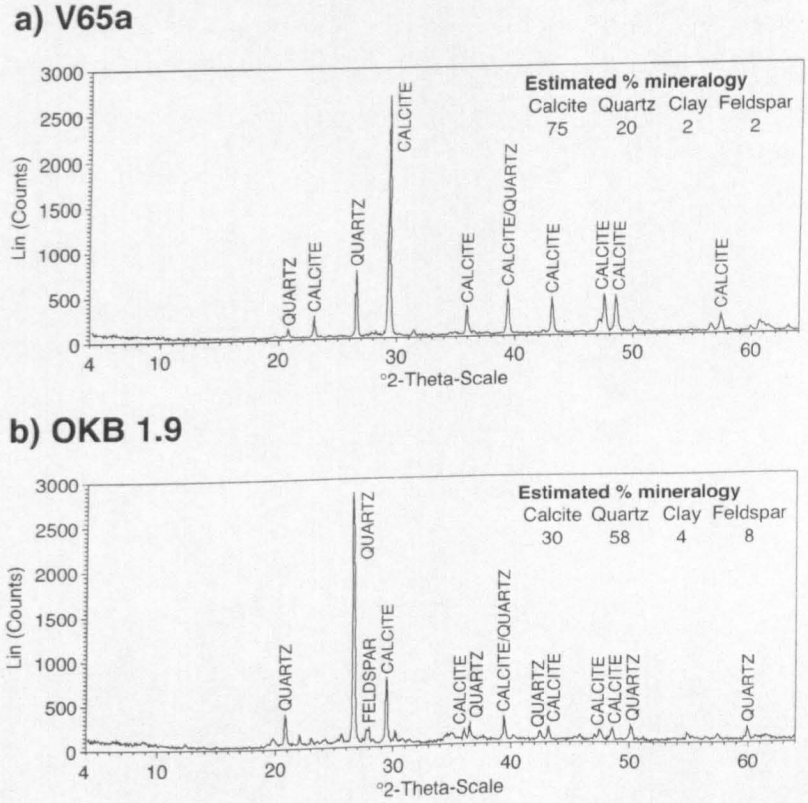

FIGURE 5.4 Mineralogical characteristics of samples V65a and OKB1.9. The fingerprinting results for these samples are shown in Figure 5.2 and Figure 5.3.

5.3.2 Sensitivity analysis of fingerprinting calculations

To assess the sensitivity of the fingerprinting calculation procedure, the provenance of 66 samples was determined using three different variations of the technique (Table 5.7). The variability between these is depicted in Figure 5.5, which shows the mean standard deviation between cases for each source group's percentage contribution. Dolomite, ophiolite and reworked alluvium are less variable between cases than other sources, although this is at least partly because they are found in lower overall proportions, and hence the lower difference between the predictions is to be expected. More importantly, Figure 5.5 demonstrates that the mean standard deviation is typically less than 4% when considering all cases. Cases 1 and 3 showed the most variation. However, even when considered alone the mean standard deviations are only slightly higher (Figure 5.5). This indicates a very low degree of variation between the different cases, which shows that the fingerprinting procedure is robust, and not sensitive to the specific nature of the input data or analytical decisions made by the researcher. For many samples, there is no discernible difference between the different cases, and certainly the principal sources identified do not change significantly. Thus the procedure appears to be both objective and reproducible.

TABLE 5.7 The different fingerprinting calculations carried out to assess the sensitivity of the overall procedure.

Run number	Parameters available for selection	Resulting composite fingerprint	Data made dimensionless by dividing by maximum value
CASE 1†	All	Ba, Cr, Cu, Rb, Sr, V, Y, Zr, χ	Yes
CASE 2	All	Ba, Cr, Cu, Rb, Sr, V, Y, Zr, χ	No
CASE 3	Only geochemical	Ba, Cr, Cu, Ni, Pb, Rb, Sr, V, Y, Zn, Zr	No

† The calculating conditions used for the actual fingerprinting procedure described in section 5.2.

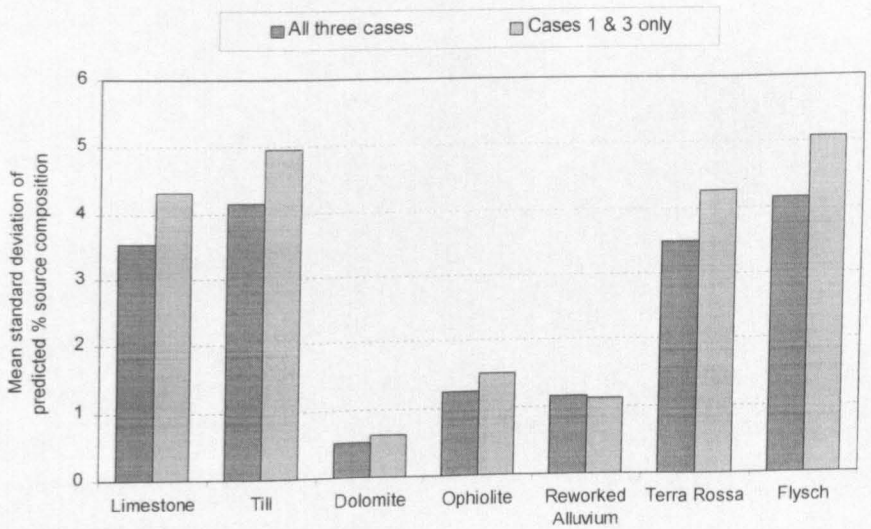

FIGURE 5.5 Graph showing the variability in fingerprinting source ascription when using the different conditions shown in Table 5.7.

5.3.3 Inspection of duplicate sample results

Duplicate target samples were taken from some of the valley fill alluvial units in order to assess the potential significance of sampling and analytical error on the fingerprinting results. If field sampling, laboratory analysis and statistical procedures introduced no error into the overall fingerprinting process, duplicate samples collected from the same unit should show the same provenance signatures. The results of these duplicate analyses are shown in Figure 5.6. Whilst a certain amount of heterogeneity is to be expected, these results are encouraging, as on the whole the duplicate samples show very similar provenance characteristics, suggesting that the effects of sampling and analytical procedures on the results are minimal. The exceptions are the KB 10 m unit and particularly the A-P Bridge 14 m unit, which show significant between-duplicate differences, which may have been caused by some primary or secondary heterogeneity in sediment characteristics within this unit or anomalous analytical results. However, these are the only duplicates to show significant variation. Furthermore, the entire duplicate data set have been analysed using a robust analysis of variance (ANOVA) to estimate the significance of sampling and analytical errors following the approach outlined by Ramsey *et al.* (1992). An ANOVA program (Ramsey, 1998) was used to separate the two fundamental components of variance between the duplicate field samples; variance due to genuine provenance differences and variance due to measurement errors. If measurement variance comprises roughly no more than 20% of the total variance for a certain source group, the fingerprinting procedure can be considered to provide a valid description of the genuine provenance variance of this source (Ramsey *et al.*, 1992). The results of this analysis are shown in Figure 5.7, which demonstrates that for all source groups except till, the fingerprinting process adequately determined the natural pattern of variation in geological composition of the Voidomatis sediments. Provenance variance is close to 100% for limestone, flysch and terra rossa, which is particularly encouraging as these are major sediment sources within the basin. The reliable determinations for these source groups will be helped by the fact that they are very well discriminated from other source groups, as demonstrated in Figure 5.1. The less satisfactory results for till suggest that this source is either less reliably quantified by the fingerprinting procedure, or that it exhibits greater within-unit variability than the other source types. The till composition may be somewhat harder to predict accurately, as it is a mixture of glacially-entrained limestone and flysch, and could therefore have less distinct sedimentary characteristics than other source types. However, the measurement variance only just breaches 20%, so the results can certainly still be considered meaningful.

In summary, this consideration of variation between duplicate samples indicates that the errors associated with field sampling and analytical procedures are acceptably small, and the results of the fingerprinting procedure do provide a valid representation of the differences in provenance between different alluvial deposits.

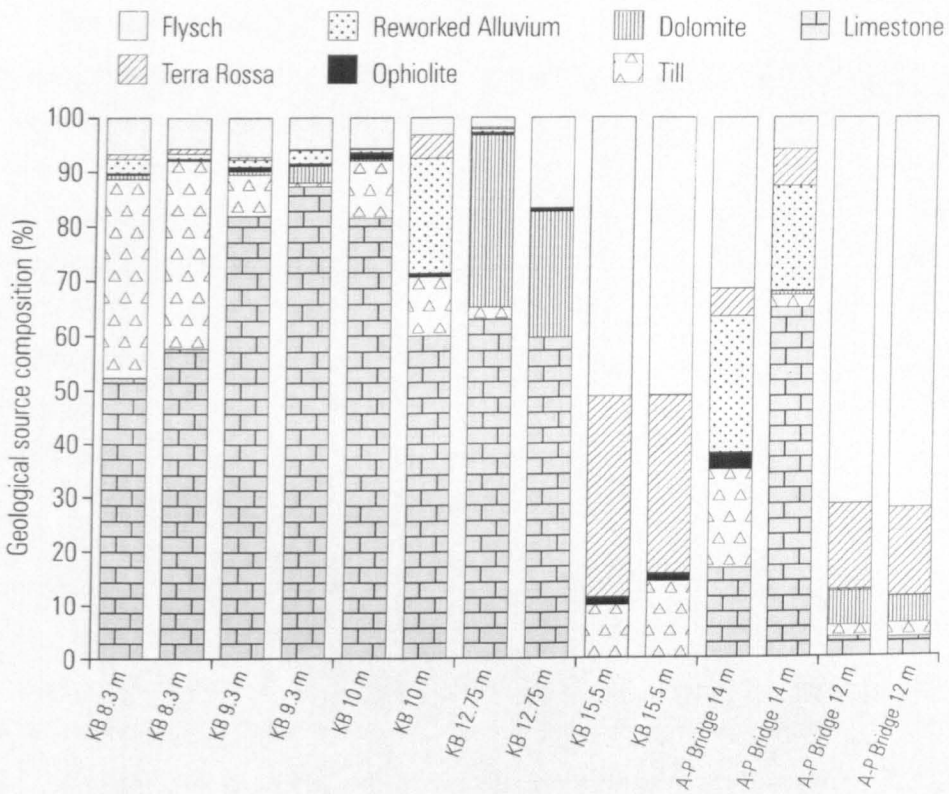

FIGURE 5.6 Comparison of quantitative sediment fingerprinting results for the duplicate samples taken from each Late Pleistocene alluvial unit. The x axis labels identify the alluvial unit by its height above the channel bed and its study reach location, as described in section 6.3. KB = Konitsa basin study reach. A-P Bridge = Aristi-Papingo bridge study reach.

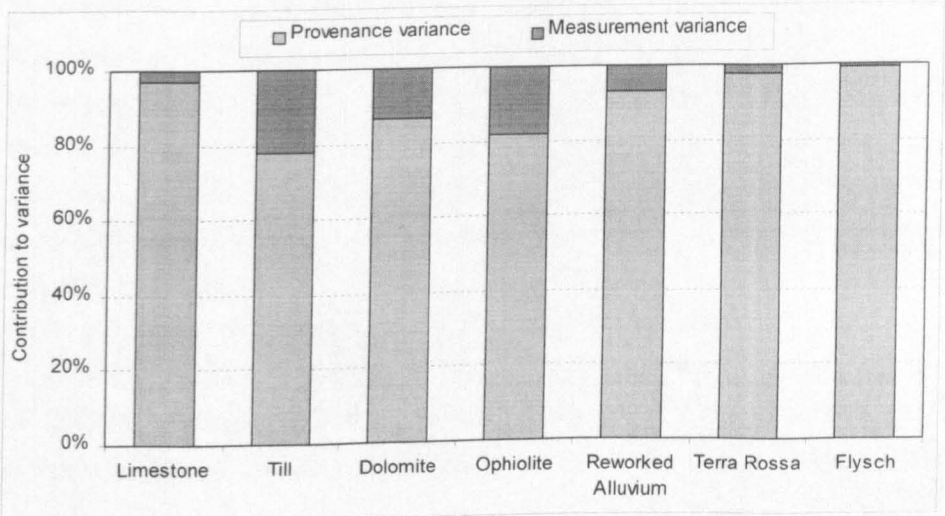

FIGURE 5.7 The percentage contribution of provenance and measurement variance to total variance for the fingerprinting results of duplicate samples taken from alluvial fill deposits.

5.3.4 Discussion of fingerprinting reliability

A rigorous assessment of data quality is vital if sound interpretations are to be made. Assessing the reliability of quantitative sediment fingerprinting is complex, as it involves many different analytical and statistical procedures. The above three sections have shown different ways to assess the reliability of the data. The overall impression from these reliability assessments is encouraging. Fingerprinting outputs compare very well with independent mineralogical investigations, suggesting that the results are a valid representation of the geological constituents of the sediment. It has been shown that the fingerprinting predictions are not sensitive to variations in the specific nature of the input data, indicating that the procedures are objective and robust. Inspection and analysis of the results from duplicate samples has shown that sampling and analytical errors are small, and that the fingerprinting procedure provides a valid determination of the provenance characteristics of different alluvial sediments. The apparent consistency and reliability of the fingerprinting results is undoubtedly strengthened by the very clear differences between the source group characteristics. The fingerprinting parameters differentiated the sources at the 99.9% confidence level (section 5.2.2.1), and in combination the parameters showed highly effective discrimination of source types (section 5.2.2.3) as evidenced by extremely low lamda values (Table 5.4). This extremely efficient discrimination of the source types, and the positive results found in tests of the fingerprinting procedure, indicate that the fingerprinting data can be used with confidence in the following chapters to investigate variations in sediment provenance between different alluvial deposits.

Nevertheless, there are two potential problems associated with fingerprinting Late Pleistocene fine sediment in the Voidomatis basin, which need to be considered:

1. Diagenetic processes are a potential source of inaccuracy when sediments are of Late Pleistocene age, as *in situ* weathering processes could alter the physical and chemical characteristics of sediment preserved in fluvial deposits, and thus distort the primary provenance signature (Collins *et al.*, 1997b). However, such effects have been minimised through careful sampling of alluvial deposits to avoid weathered sediments, as well as choosing geologically stable fingerprinting parameters (section 5.2.2.2). However, further work could explore the significance of diagenetic effects in more detail through mineral magnetic and/or microscopic analysis.
2. Some provenance studies have chosen to correct for the effects of grain size on the fingerprinting results (e.g. Walling and Woodward, 1992; Collins *et al.*, 1998). However, it is difficult to correct for potential grain size effects when many of the principal sediment sources are bedrock. Therefore, analysis of a standardised fine sediment fraction (powdered <2 mm for XRF, <1 mm for magnetics) was judged to be appropriate.

5.4 SUMMARY

This chapter has described the procedures used to obtain quantitative data on the provenance of fine sediments deposited during and since the Late Pleistocene. The procedure involves the use of a number of statistical analyses to select a combination of parameters that effectively differentiate all of the potential sources, and subsequently applies a mixing model to quantitatively determine the contribution of each source to the fluvial deposit in question. The use of nine parameters (Cr, χ, Zr, Ba, Sr, Y, Rb, Cu and V) in combination was selected as the most suitable composite fingerprint for sediment in the Voidomatis basin. The fingerprinting procedure has been used to determine the provenance of valley fill sediments and the palaeoflood slackwater deposits, and these results are presented in the following two chapters. The approach has the advantage that through the use of objective and robust statistical procedures it provides quantitative provenance data for all of the diverse potential sediment sources in the catchment. Such information could not be obtained using more traditional mineralogical analyses, which could not adequately characterise the large number of diverse source types or provide quantitative sediment source data. Tests have been presented for assessing the validity and precision of fingerprinting results. It has been shown that some sources such as limestone, flysch and terra rossa may be predicted with greater reliability than others such as till. However, overall the fingerprinting procedure has been shown to give reliable and robust results, which are not seriously affected by sampling or analytical errors.

6. LATE QUATERNARY ENVIRONMENTAL CHANGE AND RIVER DEVELOPMENT IN THE VOIDOMATIS BASIN

This chapter investigates the environmental and geomorphological changes that have taken place in the Voidomatis River over the Late Pleistocene and Holocene. Section 6.1 provides a background to the aims and objectives of this chapter. Previous research on the alluvial history of the Voidomatis basin by Lewin *et al.* (1991) is summarised in section 6.2. The new field observations and dating results obtained in this study from various alluvial fills are presented in Section 6.3. Additional information on the genesis of these deposits is presented in section 6.4, through an interpretation of quantitative fingerprinting data from the fine-grained component of the alluvial fills. Section 6.5 considers the implications of this new data in comparison to previous alluvial record established for the area, to describe the current understanding of the alluvial stratigraphy. In section 6.6 the data are used to elucidate the nature of environmental controls on the development of the Voidomatis River over the Late Quaternary. These findings are summarised at the end of the chapter.

6.1 INTRODUCTION

To assess the geomorphic importance of very large palaeofloods, a sound chronology of valley floor sedimentation and incision must first be established (section 4.1). The timing of catastrophic palaeoflood events can then be placed within the context of long-term environmental change, river activity and landscape development (especially the valley floor), to understand their overall geomorphic importance in this environment. This chapter presents field evidence and geochronological and sedimentological results that enable the Late Pleistocene and Holocene environmental and landscape history of the Voidomatis basin to be established. By doing so, this provides an opportunity to extend previous work in the area by Lewin *et al.* (1991) in the light of recent developments in the application of dating techniques such as uranium-series and optically stimulated luminescence (OSL) (section 4.4.5), and advances in techniques for provenancing Late Quaternary fine sediments (Hamlin *et al.*, in press). The history of alluviation in Mediterranean rivers has long been debated with many studies presenting different arguments regarding the relative importance of climatic, tectonic and anthropogenic controls (see section 2.5.3). However, there is an emerging trend from recent studies that climate has been the overriding control on Mediterranean river activity over the Late Pleistocene in many systems (section 2.5.3). It has been shown that in many Mediterranean catchments extensive river aggradation occurred during cold phase Late Pleistocene environments, separated by periods of incision or subdued river activity during warmer phases (e.g. Lewin *et al.*, 1991; Fuller *et al.*, 1996, 1998; Maas, 1998; Rose and Meng, 1999; Rose *et*

al., 1999). Therefore, this chapter not only provides important environmental and geomorphological context for the palaeoflood investigations, but also provides new data of relevance to the ongoing debate on the extrinsic controls on Mediterranean river behaviour.

6.2 PREVIOUS FIELD INVESTIGATIONS OF LEWIN *ET AL.* (1991)

The renewed research into Palaeolithic human activity in Epirus by Geoff Bailey and his co-workers in the 1980s meant that there was increasing interest in Late Quaternary environments and landscapes in the region (section 3.1.3). Occupation of Klithi and other rockshelters found in the valleys of Epirus was thought to be strongly influenced by environmental conditions, including the changing nature of valley floor environments during the Late Pleistocene. This provided an ideal setting for geomorphological investigations of changes in river activity and sedimentation during the Late Quaternary. The alluvial sediments of the Voidomatis were studied during the 1980s, with a varied programme of sedimentological investigations (see Bailey *et al.*, 1990; Lewin *et al.*, 1991; Woodward *et al.*, 1992; Woodward *et al.*, 1994; Woodward *et al.*, 1995; Macklin *et al.*, 1997). Five major alluvial units were initially identified by means of stratigraphic and morphological relationships, clast lithological analysis and sourcing of the fine (<63 μm) fraction by means of mineralogy (Table 6.1; Woodward *et al.*, 1992). In addition, dating of the alluvial units was achieved through the application of TL, ESR and ^{14}C dating (Lewin *et al.*, 1991; Debenham, 1997). The Kipi unit (> 150 000 years), is much older than the other units, having been deposited before the incision of the gorges within which the modern Voidomatis flows. The high occurrence of igneous clasts (44%) suggests that these sediments were deposited at a time when the watershed of the Voidomatis was configured differently, probably extending further to the east to encompass a larger area of the ophiolite terrain that is now largely drained by the Aoos River (Woodward, 1990). The most extensive alluvial fill in the catchment was named the Aristi unit (c. 28,200 (± 7000) to 24,300 (± 2600) years), which is composed of matrix-rich cobble gravels and occasional boulder sized clasts (Table 6.1). Subsequent investigation of soil development on these units identified at least two different phases of Late Pleistocene Aristi-type sedimentation, the more recent at c. 28,200 (± 7000) to 24,300 (± 2600) years, and an earlier phase of sedimentation with a minimum age of c. 85,000 years, estimated by means of a soil weathering index (Woodward *et al.*, 1994). These Aristi sediments were believed to have been deposited during glacial Late Pleistocene climates by a wide, aggrading braided channel, with the latter phase of Aristi sedimentation corresponding to the severest climatic phase of the Late Würm (Lewin *et al.*, 1991; Macklin *et al.*, 1997). In contrast to the Aristi unit, the Vikos unit (c. 24,300 (± 2600) to 19,600 (± 3000) years) only occupies a small proportion of the valley floor, and thus represents a quite minor phase of aggradation. Nevertheless, it is sedimentologically distinctive from the Aristi unit, primarily on the basis of higher flysch and ophiolite occurrences in the clast lithological assemblage (Table 6.1). In contrast to the pre-Holocene units, the younger Klithi unit was

composed predominantly of fine-grained overbank sediments. Whilst this unit was shown to be composite in nature, its deposition was dated to the last 1000 years (Lewin *et al.*, 1991). The deposition of the Klithi sediments was thought to have occurred following anthropogenic disturbance of catchment vegetation, which lead to the erosion of large volumes of sediments from the less resistant flysch terrain (Lewin *et al.*, 1991; Woodward *et al.*, 1992). More details on the Late Quaternary changes in sediment fluxes are described by Woodward *et al.* (1992) and the palaeoenvironmental implications of these results is considered at greater length in Macklin *et al.* (1997). This work demonstrated considerable changes in the sedimentation style of the Voidomatis River over the Late Quaternary, influenced by both long-term climatic changes and latterly by anthropogenic landscape disturbances.

TABLE 6.1 Alluvial units in the Voidomatis basin identified by Lewin *et al.* (1991). *(After: Lewin et al., 1991).*

Alluvial unit	Terrace surface height above river bed (m)	Max. thick-ness (m)	Clast lithological composition % (8-256 mm) Lt = Limestone Fl = Flysch Ft = Flint Ig = Igneous				Coarse (C)/fine sediment (F) member ratio	Fluvial sedimentation style	Age (BP)
			Lt	Fl	Ft	Ig			
Present channel	-	-	73	27	0.5	0.2	C > F	Incising, confined meandering gravel-bed river. Low suspended sediment load	< 30
Klithi	x = 3.2 σ = 0.7 Range = 1.8 – 4.5	4.5	69	30	1	0.1	C < F	Aggrading, high sinuosity gravel bed river. High suspended sediment load.	1000 ± 50
Vikos	x = 6.8 σ = 1.7 Range = 3.9–9.7	8.3	82	13	0.6	4	C > F	Incised, wandering gravel bed river. Low suspended sediment load.	24,300 ± 2600 - 19,600 ± 3000
Aristi	x = 12.4 σ = 3.9 Range = 6.7– 25.9	25.9	95	3	2	0.1	C > F	Aggrading, low sinuosity coarse sediment river system. High suspended sediment load.	28,200 ± 7000 - 24,300 ± 2600
Kipi	56	22.9	19	37	0.9	44	C > F	Aggrading (?) low sinuosity, coarse sediment river system	>150,000

6.3 LOCATION, STRATIGRAPHY AND CHRONOLOGY OF PRESERVED ALLUVIAL FILL SEDIMENTS

The long-term development of the Voidomatis River was assessed following a catchment wide reconnaissance survey of the valley floor stratigraphy and detailed examination of five small

(<1 km long) study reaches (Figure 4.5). The sedimentological and geochronological results from these field investigations are presented in this section.

6.3.1 Types of alluvial fill sediments in the Voidomatis basin

Throughout the basin, alluvial fills generally display two distinctive types of lithofacies:

1. High units with terraces typically at 8 - 16 m above the modern channel are quite frequently preserved, especially in wider gorge sections where there has been less reworking. These alluvial units are composed of well-rounded medium to coarse gravels and some small boulders held in a fine-grained sandy matrix. They tend to mantle the edges of the valley floor, where these areas are not covered by colluvial deposits. These are akin to the Aristi sediments documented by Lewin *et al.* (1991).
2. Near channel areas almost always contain much lower units whose surface is approximately 2 - 4.5 m above the modern channel. These have a contrasting lithofacies, composed of fine to medium gravel with a sandy matrix overlain by often extensive depths (> 2 m) of fine-grained bedded sands and silts. These sediments correspond to the Klithi unit described by Lewin *et al.* (1991). This is the type of lithofacies being deposited by the contemporary Voidomatis River through both vertical, and to a lesser extent, lateral accretion.

These two types of lithofacies represent distinctly different styles of sedimentation. The coarse-grained type are former in-channel gravels which have been abandoned by subsequent channel migration and/or incision, whilst the fine-grained lithofacies are overbank flood sediments. Geomorphological mapping, surveying and section logging in five study reaches allowed a more detailed investigation of these different valley fills.

6.3.2 Konitsa Basin Reach

This reach is located immediately downstream of the Lower Vikos Gorge where the Voidomatis river opens out to flow into the Konitsa basin (identified in Figure 4.5 and shown in Figure 3.14). Widening of the valley floor at this point has facilitated good preservation of alluvial sediments. Both lithofacies types are evident. Five high (15.5 - 8.5 m) coarse-grained units, and three lower (4.5 - 2.0 m) predominantly fine-grained units were identified (Figure 6.1). All but one of the coarse-grained units contained an exposed calcite-cemented upper layer, from which samples were taken for uranium-series dating (section 4.4.4). These samples yielded Late Pleistocene ages, culminating in a depositional phase which ended at c. 25,000 ± 2000 years (Figure 6.1). The dates provide a minimum age for the deposits, with the calcite cement assumed to have formed soon after the depositional phase of the alluvial sediments (i.e. the detrital material) (section 4.4.4.). This assumption is consistent with the observed U-Th isochrons which show very good correlations ($R^2 > 0.98$) indicating that the cement probably formed during a short time period. A example of the isochrons is shown in Figure 4.11, showing the close fit of the isochron line, a feature that was exhibited in all the U-Th analyses in this study (see Appendix IX).

These dating results provide clear evidence that the high, coarse grained lithofacies observed around the Voidomatis basin can be subdivided into at least four separate phases of aggradation over the Late Pleistocene, when channel bed was between 8 and 15.5 m higher than present. It is possible that there may have been a fifth sedimentation phase represented by the 11 m surface (Figure 6.1). However, with no exposures (or dating results) for these sediments, it uncertain whether they represent a separate sedimentation phase, or if they merely constitute an incisional surface within the 12.75 m unit, formed during Late Pleistocene lowering and westward migration of the river channel.

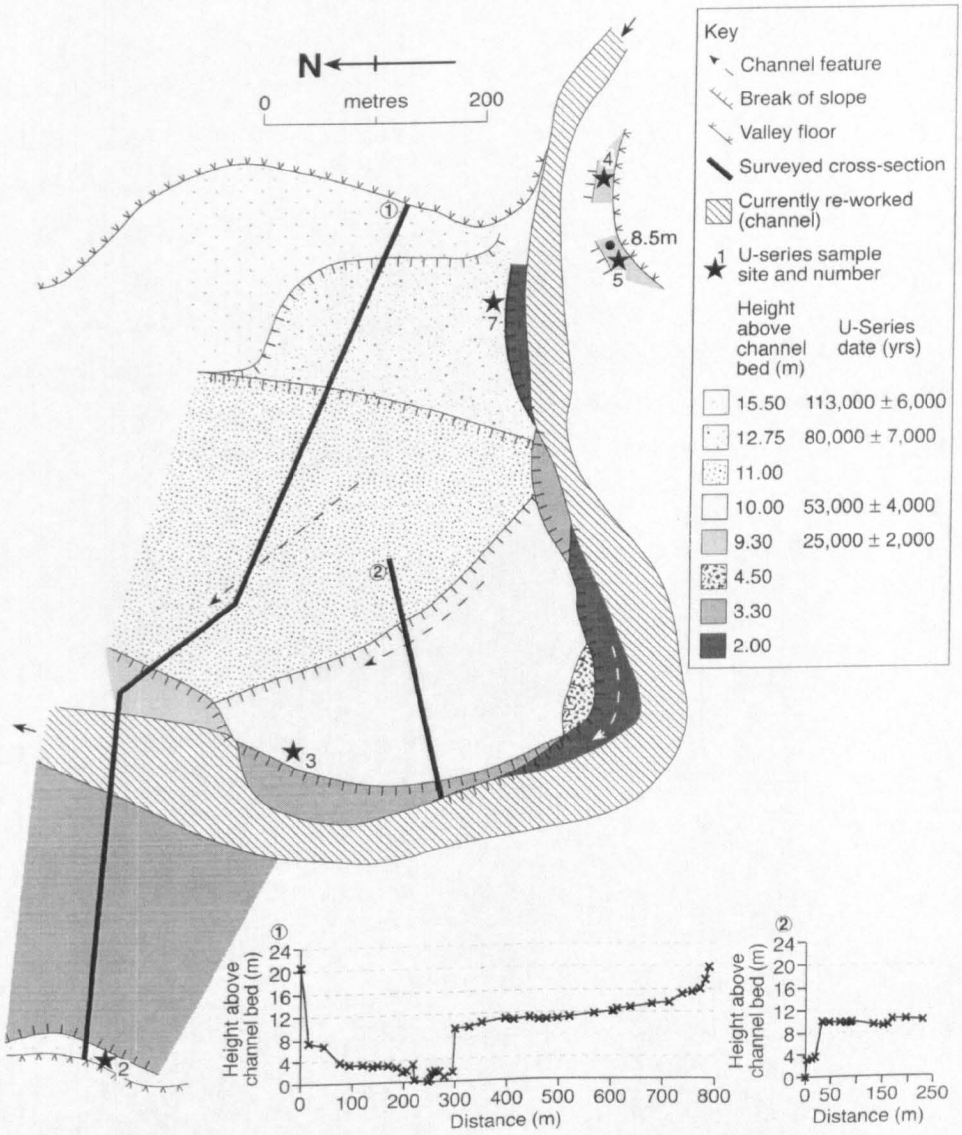

FIGURE 6.1 Geomorphological map and topographic survey results from the Konitsa Basin reach on the Voidomatis River. Mean heights above channel bed and uranium-series dating results are given in the key. Uranium series samples 1, 6 and 8 are discussed in subsequent sections.

The sedimentology of the exposed Late Pleistocene deposits is remarkably similar. They have a distinctive yellow-cream colour, ranging from Munsell classification 2.5Y 7/4 to 2.5Y 8/2,

which is in stark contrast to the typically much darker coloured colluvial sediments in the Voidomatis basin. Figure 6.2 shows the section through the oldest unit in the reach (113,000 ± 6000 years), where the pale coloured alluvial sediments are resting on, and partially covered by weathered angular colluvium which is much more orange and brown. Exposures such as this often reveal a depth of at least 3 m of rounded alluvial gravels in a sandy matrix (e.g. Figure 6.2). Clast lithology is dominated by limestone (c. 95%) (Lewin *et al.*, 1991). The gravels are poorly sorted, with typical b-axes ranging from 1.5 to 15 cm, but occasional boulder sized clasts do occur. These gravels are almost always horizontally bedded or massive, although imbrication is well developed in places where there is less fine matrix and the gravels are not too spherical in shape. It is likely that all of these Late Pleistocene gravel units were laid down by a wide braided river system, which at times occupied almost the entire valley floor. These gravels have been deposited over an extensive area (as much as 800 m wide in Figure 6.1), that could not be accomplished by a single thread channel. Additionally, the exposure in Figure 6.2 shows a small palaeochannel sand body some 3 m wide, which represents a small anabranch stream, a relic feature of a braided channel pattern. The Voidomatis catchment was glaciated during the Late Pleistocene (section 3.2.1.1), and in common with many contemporary glaciated catchments, the valley floor appears to have been occupied by an extensive glaciofluvial outwash terrain (Lewin *et al.*, 1991).

FIGURE 6.2 Section through the 15.5 m alluvial unit exposed at the western end of cross section 1 on Figure 6.1. A channel-fill sand body can be seen just above J.C. Woodward's head. The alluvial sediments are notably pale in colour, resting on, and covered by partially weathered angular colluvium which is darker in colour.

No datable material could be found within the lower (4.5 - 2.0 m) units. The nature of these lower, fine-grained units is discussed at greater length later in this chapter. At the upstream end of this reach is the Old Klithonia Bridge, where a number of alluvial units and palaeoflood slackwater deposits are preserved. These are detailed in the following study reach.

6.3.3 Old Klithonia Bridge Reach

This reach is located at the mouth of the Lower Vikos Gorge, at the upstream end of the terrace sequence described in the previous section. Upstream of the bridge the gorge is less than 100 m wide (Figure 6.3), with near vertical bedrock walls. The valley floor sequence here is notable for the absence of the lower, fine-grained lithofacies. Instead, segments of high, coarse-grained units are preserved at the edge of the valley floor, inside which is a floodplain of fresh, coarse gravel bars that are partially vegetated by large plane trees. The two major coarse-grained alluvial units that have been preserved are on the southern side (left bank) of the valley, and their respective surfaces are c. 8.3 m above the channel bed. One of these units underlies the Boila rockshelter sequence, and the other at cross section 2 has slackwater sediments directly below and several metres above it (Figure 6.3 and Figure 6.4). The sedimentology of these gravel units is identical to those described in the Konitsa Basin. However, the section shown in Figure 6.4 clearly shows preferential calcite cementation of the upper metre or so of the unit, which, due to erosion of the lower sediments, now stands proud in section to form a prominent 'cemented balcony'. This feature is common in many of these Pleistocene lithofacies in the Voidomatis basin. Samples from each of the two cemented units, and a third from a small notch containing cemented gravels preserved on the right hand side of the valley, were taken for uranium-series dating (Figure 6.3).

The dating results for the left-bank unit downstream of the Old Klithonia Bridge was quoted in section 6.3.2 (25,000 ± 2000 years), and a minimum age of 24,000 ± 2000 years for the unit below the Boila rockshelter indicates that these two deposits almost certainly originate from the same sedimentation phase. Lewin *et al.* (1991) dated slackwater sediments found beneath the gravel unit downstream of Old Klithonia Bridge (Figure 6.4a). A tooth from a deer mandible was dated by ESR (using the linear, continuous U-uptake model; by R. Grün) and produced ages of 24,300 ± 2600 (571c), 25,000 ± 500 (571a) and 26,000 ± 1900 (571b) (Lewin *et al.*, 1991). Considering the uncertainty around the uranium-series date for the gravel unit, any of these ESR dates could be the true age, however the oldest is used here and shown on Figure 6.4a, as it fits most sensibly with the date for the overlying gravel. The close similarity between the ESR dates and the uranium-series gravel unit date (which is a minimum age) indicates that the coarse-grained sedimentation at c. 25,000 years was a fairly rapid process.

The notch of gravel on the right hand side was dated to 56,000 ± 5000 years, which overlaps with the date for the 10 m unit in the Konitsa basin reach (Figure 6.1), so the 2 units are possibly coeval.

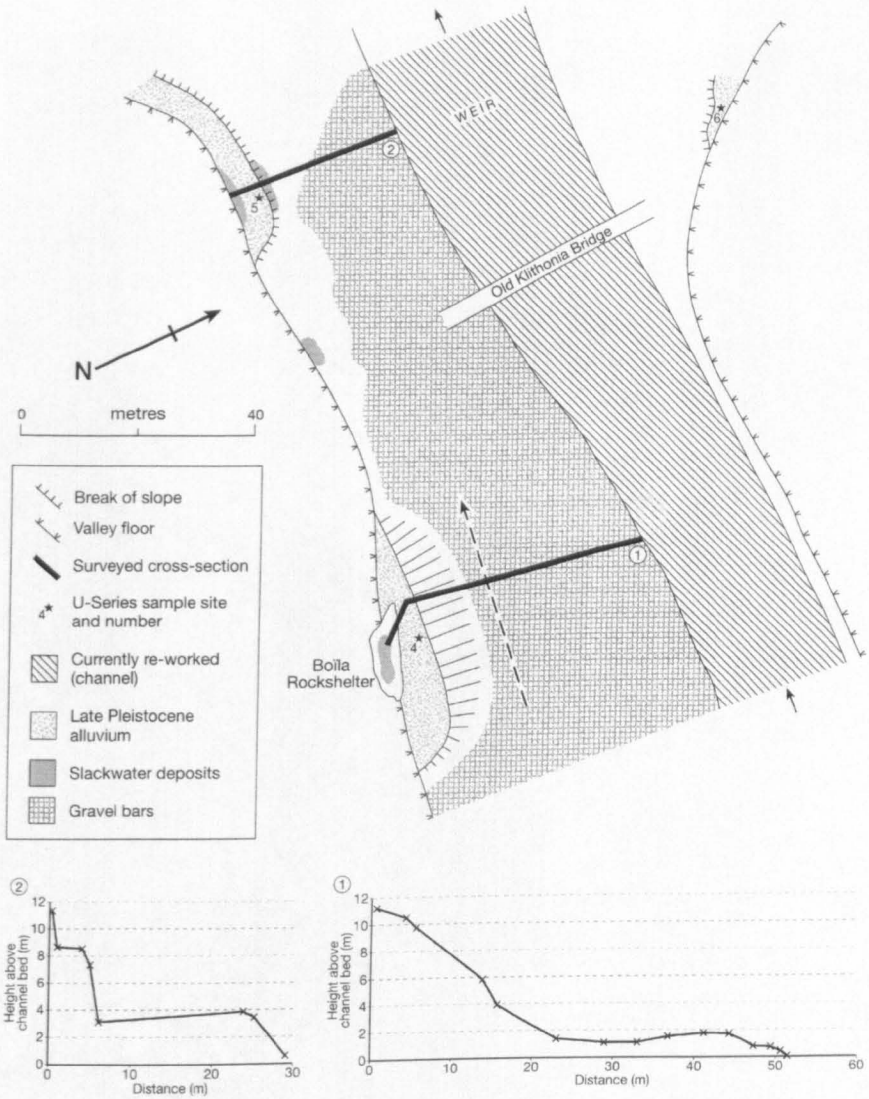

FIGURE 6.3 Geomorphological map and topographic survey results from the Old Klithonia Bridge reach. All cross sections are shown viewing the section from the upstream direction.

6.3.4 Klithi Rockshelter Reach

In the central part of the Lower Vikos Gorge, the valley fill sequence was investigated in a small reach just less than 500 m downstream of the Klithi rockshelter (Figure 4.5). No high, coarse-grained units have been preserved at this point, but instead the lower, fine-grained alluvial fill is an important feature (Figure 6.5). On both sides of the channel the unit surfaces are c. 3.7 m above the channel bed, with over 2.5 m of fines and pebbles resting on top of a gravel base (Figure 6.6). This lithofacies association is common in meandering river systems (e.g. Jackson, 1978), with the gravels representing former bars and in-channel gravel, whilst the fines are overbank flood deposits. The fines are buff to dark drown (10YR 5/3) fine sands and coarse silts that are quite thickly bedded in units typically c. 10 cm deep which often fine upwards (Figure 6.6). The gravels below them are flat-bedded and of a medium to fine calibre and reasonably

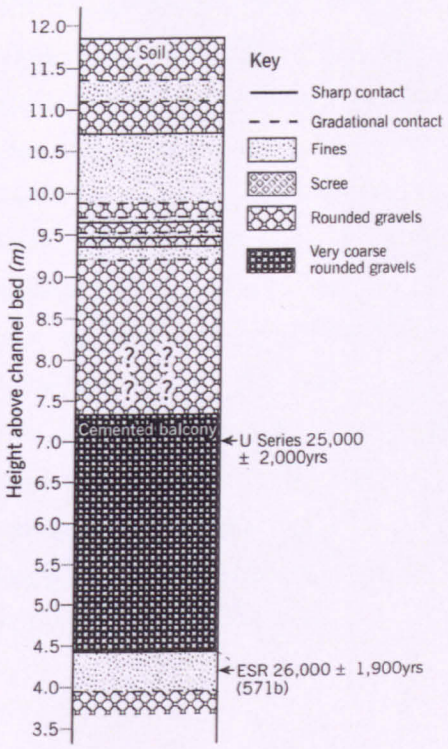

a)

b)

FIGURE 6.4 a) Section of the alluvial sediments preserved just downstream of Old Klithonia Bridge, at cross section 1 on Figure 6.3. The alluvial unit mapped at this point corresponds to the coarse-grained sediments that lie between c. 4.5 - 7.5 m above the channel bed. Slackwater sediments lie beneath these gravels, and have been dated by R. Grün using ESR methods (discussed further in section 6.3.3). b) Photograph of this section, showing the coarse-grained unit and its 'cemented balcony', with the lower SWDs having been excavated at the base. A less distinct cemented balcony can also be seen in Figure 6.2.

well sorted, typically with a b-axis of 50 mm. These gravels are virtually clast supported with small amounts of sandy matrix. On the inside of the meander bend at cross section 1 are two small lower surfaces (Figure 6.5), which are probably features of recent lateral migration and incision.

Dating the main fine-grained fill in this reach was possible by conventional ^{14}C analysis of charcoal from a well preserved hearth buried c. 1.6 m from the top of the section at point A on Figure 6.5. This yielded a date of AD 1420 – 1650 (Beta – 109186) (Figure 6.6). The ^{14}C date is reliable as the hearth is so well preserved that it precludes the possibility that the charcoal could be older reworked material (*cf.* Blong and Gillespie, 1978; Baker *et al.*, 1983b). The hearth represents a former land surface, with the fines above having been deposited by vertical accretion after this time. Dating of a floodplain core from this site by unsupported ^{210}Pb and ^{137}Cs (described in section 8.4) has shown that the upper horizons of these fines have accumulated over recent decades. This agrees with a ^{14}C date of 'modern' (OxA-1747) obtained by Lewin *et al.* (1991) from a similar exposure in this area, which suggested that vertical accretion was still occurring on these surfaces. The base of these fines at 220 cm depth (Figure

6.6) was sampled for dating by OSL, resulting in ages of 2040 ± 600 years for single aliquot measurement and 2960 ± 400 years using multiple aliquots (Shfd97086). The lack of correspondence between these two measurements suggests that these sediments may not have been fully bleached prior to burial. The single aliquot date is probably the most accurate, but should be viewed as a *maximum* age estimate. The problems associated with OSL dating in the Voidomatis basin are discussed in more detail in section 7.3.3, where further evidence demonstrates that the OSL ages are not reliable. However, previous dates in the Voidomatis basin do suggest that this vertical accretion of fine sediments was in progress significantly earlier than the date for the hearth. Bailey *et al.* (1986) and Gowlett *et al.* (1997) reported ^{14}C dates from charcoal found in fine-grained alluvium of 1000 ± 300 years BP (cal AD 690-1290) (OxA-191) and 800 ± 200 years BP (cal AD 1020-1400) (OxA-192). These dates could correspond to the older fine-grained sediments below the hearth in Figure 6.6a. All of these dating results combine to imply that this fine-grained sedimentation has probably been ongoing for the last 1000 years or more.

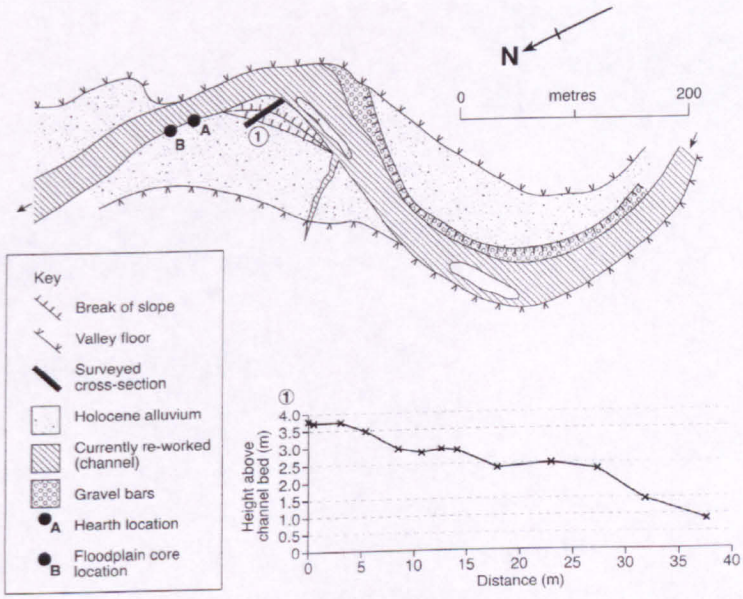

FIGURE 6.5 Geomorphological map and topographic survey results from the Klithi Rockshelter reach. The cross section is shown viewing the section from the upstream direction.

Approximately 500 m upstream of this reach, exposed on the right bank path c. 100 m upstream of the Klithi rockshelter, well-cemented, rounded limestone gravels are present, plastered against the valley side on a bedrock strath, approximately 18 m above the current channel. This area could not be mapped due to dense vegetation cover, but uranium-series dating of a sample from this limited exposure yielded an age of 74,000 ± 6000 years.

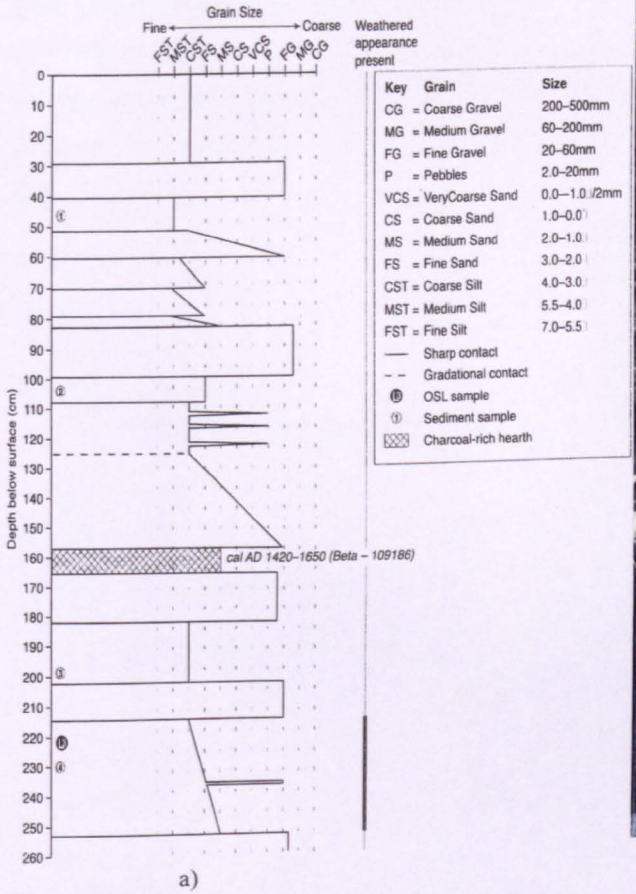

a)

b)

FIGURE 6.6 a) Section log of the alluvial sediments at site A on Figure 6.5 in the Klithi Rockshelter reach. The top of this unit is c. 3.7 m above the channel bed. The fine gravel below 250 cm continues to the base. b) Photograph of this section, showing the charcoal-rich hearth and the fine-grained sediments that lie above it.

6.3.5 Aristi-Papingo Bridge Reach

This reach is located in the upstream part of the Lower Vikos Gorge, in the area of the Spiliotissa Monastery where the road from Aristi to Papingo crosses the Voidomatis (Figure 4.5; Figure 6.7). Confined by the gorge walls, the channel exhibits a meandering pattern, switching from one side of the valley floor to the other, and divides into two anabranches mid-reach around a 300 m long vegetated medial island (Figure 6.7). Several steep tributaries drain into the main channel in this reach, one of which contains a well-preserved sequence of SWDs (Figure 6.7). These tributaries have evidently supplied considerable volumes of sediment to the river, as evidenced by the poorly sorted flysch-rich alluvial fan sediments that have spread some 100 m into the valley bottom. The tributary just upstream of cross section 2 has become entrenched by over 3 m, probably due to sediment starvation and main channel incision over recent years.

The valley floor contains extensive low (2 - 6 m) fine-grained units. River cut exposures of these sediments at cross sections 2 and 3 indicate that they are similar to that dated by ^{14}C from the hearth at the previous reach (Figure 6.6). At cross sections 2 and 3 there is just one

main surface, but at cross section 1 mapping and surveying revealed five different surfaces, all of which are only 2 - 4 m above the channel bed over a distance of approximately 130 m. No sections or datable material were available from them. These features have probably formed as the river has migrated towards the left bank, progressively incising and leaving these stepped alluvial surfaces.

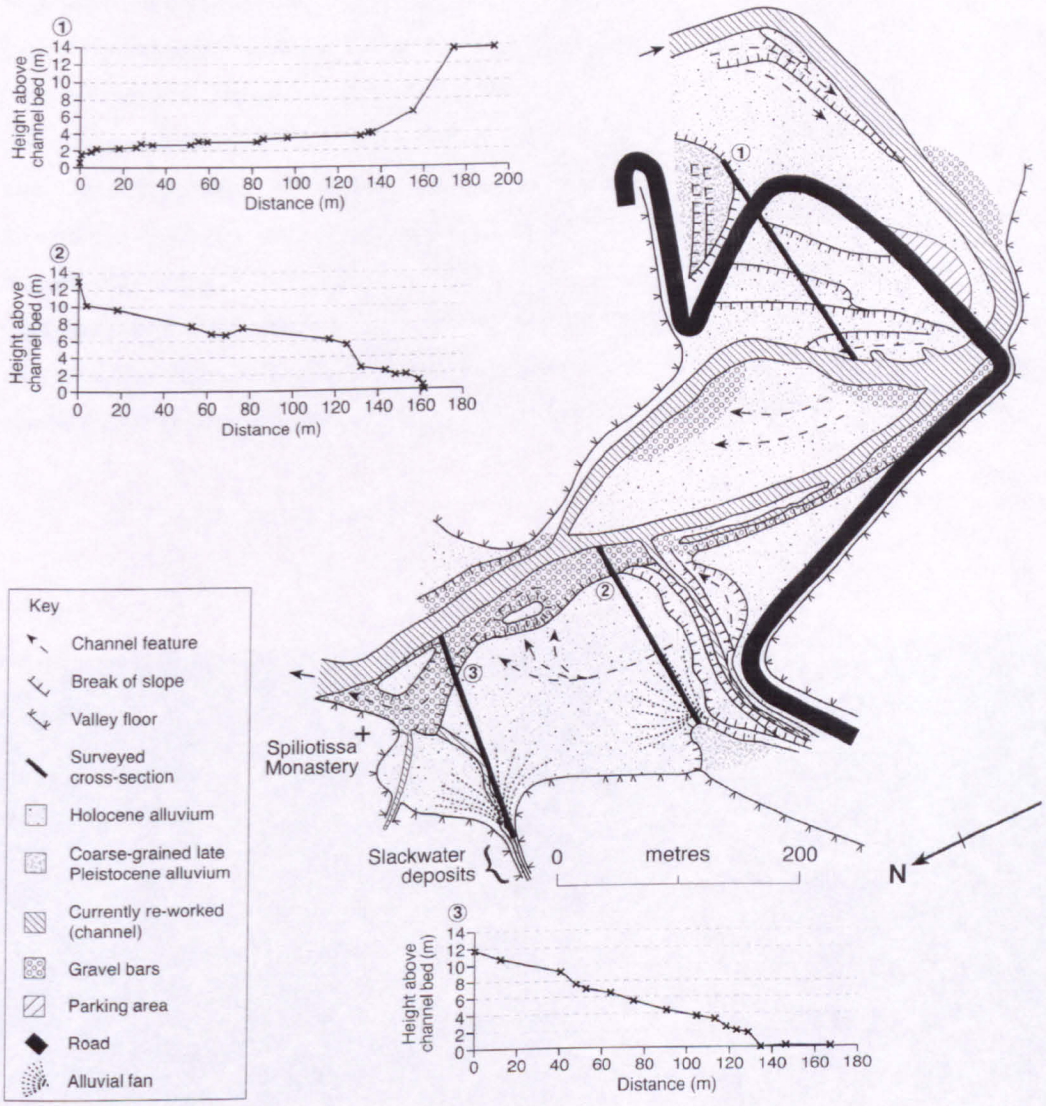

FIGURE 6.7 Geomorphological map and topographic survey results from the Aristi-Papingo Bridge reach on the Voidomatis River. All cross sections are shown viewing the section from the upstream direction, with heights relative to channel bed.

In addition to this Holocene alluvium, two exposures of high, coarse-grained alluvium are preserved some 12 - 14 m above the modern channel bed (Figure 6.7). The lithofacies of the unit at cross section 2 is very similar to the Late Pleistocene units on the Konitsa basin and at Old Klithonia Bridge, with gravels and occasional small boulders cemented in a sandy matrix. However, an attempt to date this unit by uranium-series failed as the calcite cement had

probably been hydrated very recently (S. Black, pers. comm., 1998). The facies of the high unit at cross section 1 is again fairly similar, except the clasts are not well cemented and a distinctive red soil rests above them (Figure 6.8). This was identified by Woodward *et al.* (1994) as Soil Profile A, who assigned this an estimated age of c. 85,000 years on the basis of a soil weathering index. In the absence of further dating evidence, is reasonable to assume that these exposures are contemporaneous, as they are positioned at similar heights above the channel and have a similar sedimentology. The 85,000 year age estimate is very close to the date of 80,000 ± 7000 for the 12.75 m alluvial unit on the Konitsa basin reach (Figure 6.1), and on the basis of this dating and the similar elevation of these units it seems reasonable to correlate them to this phase of sedimentation. Throughout the Lower Vikos Gorge and further onto the Konitsa basin the channel exhibits a very similar gradient (c. 0.005) (Figure 6.9), and thus it is reasonable to assume that terraces of a similar height above the channel bed may correlate. This is corroborated by Lewin *et al.* (1991), who measured the elevation of the channel bed and Aristi unit terraces using an aneroid barometer (Lewin *et al.*, 1991, Fig. 4). They found a reasonably similar bed slope and terrace height above channel bed in the study reaches discussed above.

FIGURE 6.8 Photograph of the coarse grained alluvial unit at the eastern end of cross section 1 at the Aristi-Papingo Bridge Reach. The gravel matrix is not cemented and appears quite weathered. A distinctive red soils rests on top of the alluvial deposit (*cf.* Woodward *et al.*, 1994). A water bottle is shown for scale.

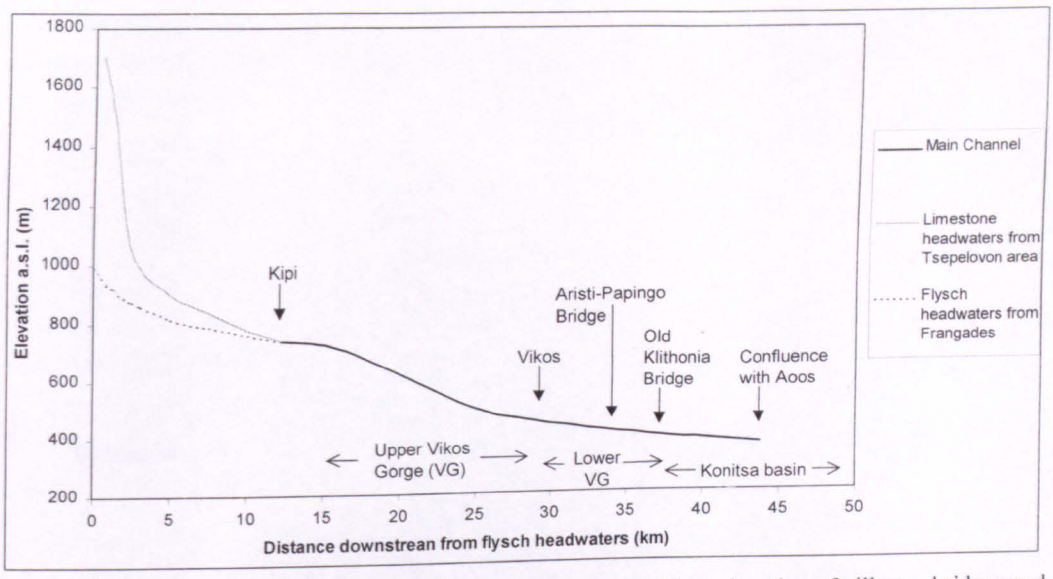

FIGURE 6.9 The long profile of the Voidomatis River, annotated with the location of villages, bridges and physiographic zones. The locations of the place names used here are shown in Figures 3.2 and 3.8.

6.3.6 Vikos Canyon Fan Reach

This is the most upstream of the study reaches on the Voidomatis discussed in this thesis, located near the middle of the Upper Vikos Gorge (Figure 4.5). Valley floor alluvial units are less common in the Upper Gorge compared to further downstream, probably as a result of the steeper gradient and more confined nature of the valley bottom (Figure 6.9 and section 3.2.1). Thus the Upper Gorge is primarily an incisional area, compared to the greater degree of aggradation in the Lower Gorge and on the Konitsa basin. However, in this reach, a steep tributary has built an alluvial fan on the northeastern (right-bank) side of the valley. Several boulder berms are also present above the modern channel (discussed in Chapter 8). The fan morphology displays three clear phases of aggradation and dissection (Figure 6.10), with the current channel incised beneath the lower surface. The upper fan surface is well cemented by calcite, which yielded a uranium-series date of 104,000 ± 9000 years. This age overlaps with the date of 113,000 ± 6000 years for the 15.5 m alluvial fill on the Konitsa basin (Figure 6.1), and the deposition of these sediments may have occurred during the same major sedimentation phase. Incision of the fan surface after that time was interrupted by two phases of sedimentation, although suitable materials were not present for these to be dated. This feature demonstrates that several major phases of Late Quaternary sedimentation have taken place in steep alluvial fan environments, where sediment delivery is largely from local bedrock weathering, as well as in the valley floor where sediments may have been supplied from a much larger catchment area.

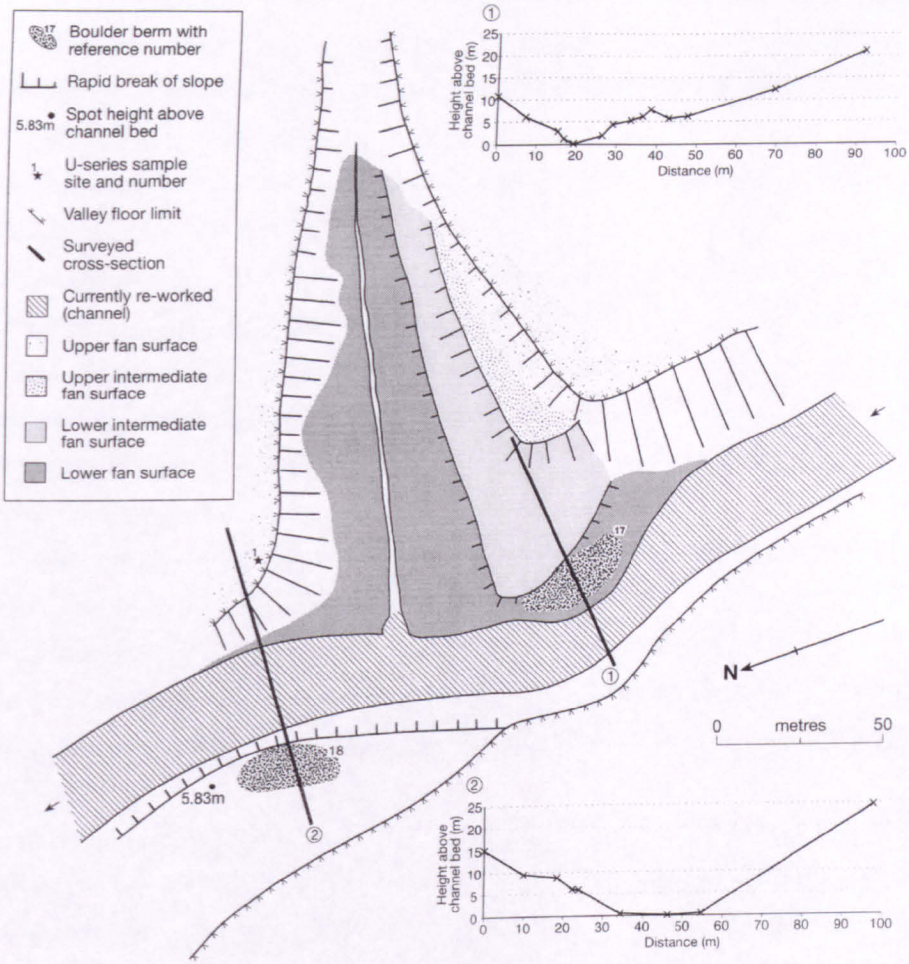

FIGURE 6.10 Geomorphological map and topographic survey results from an incised alluvial fan in the Upper Vikos Gorge. The upper fan surface now delimits the extent of the valley floor.

6.3.7 Summary of field evidence and dating results

A programme of geomorphological mapping and dating of valley fill units has revealed a dynamic history of Late Quaternary river activity in the Voidomatis Basin. Sedimentation style has shifted with the transition from Late Pleistocene to Holocene environments. Aggradation during the Late Pleistocene produced river levels typically 8 - 16 m higher than today, with widespread deposition of gravels by a braided river system. Around 8 m of net channel incision has taken place since the Last Glacial Maximum (LGM). In the Late Holocene there has been fluvial deposition more characteristic of a single thread meandering system, with extensive overbank deposition of fines on top of former gravel bedforms. This has formed a floodplain surface typically 4 m above the modern channel. There remains no evidence of Early- or Mid-Holocene alluviation (*cf.* Lewin *et al.*, 1991), which indicates that this period saw progressive incision, with any phases of sedimentation having been minor, either reworked or buried by the more significant Late Holocene accretion.

The dating results from the reach studies can be compared with climate proxy records, to examine the environmental conditions associated with each dated period of river sedimentation. Three records have been selected for this study (see Figure 6.11):

- The long pollen record from Lake Ioaninna (Tzedakis, 1994; Tzedakis *et al.*, 1997), only 30 km to the south of the Voidomatis basin, along with the more distant but higher resolution Tenaghi Phillipon record (section 3.3.2);
- An oxygen isotope record from the central Mediterranean Sea (Paterne *et al.*, 1986);
- The high resolution GRIP oxygen isotope record (GRIP Members, 1993; Thouveny *et al.*, 1994). Thouveny *et al.* (1994) have shown that the high-resolution fluctuations in the GRIP record were experienced in southern Europe, and the similar fluctuations revealed in the record of Paterne *et al.* (1986) serves as further evidence of the widespread nature of this pattern of climate change.

The uranium-series dating results in Figure 6.11 show good correspondence between reaches, with major phases of catchment aggradation dated to c. 110, 78, 55 and 25 ka. An initial comparison of these dating results with the climate proxy records shows:

1. A major phase of Late Pleistocene aggradation occurred around c. 25 ka, which on all palaeoclimate records is associated with the pronounced cold period of the LGM (Figure 6.11).
2. Earlier phases of aggradation took place around 55, 75 and 110 ka. Greater uncertainty with older dates can make correlation to environmental phases less precise, especially in view of the fluctuating and complex nature of Late Pleistocene climate change shown by the oxygen isotope records (Figure 6.11). However, it is likely that at 55 ka the area was also experiencing cold conditions (early Oxygen Isotope Stage (OIS) 3), whilst 78 and 115 ka seem to have been periods of transitional climate, changing from warmer to cooler periods (early OIS 4 and late-Oxygen Isotope Substage (OISst) 5e - 5d respectively) (Figure 6.11).

All the uranium-series dates are minimum ages, as there may be some time delay between sediment deposition and calcite cementation. To estimate the significance of this delay, it is necessary to consider the mechanism of cemenation. Nash and Smith (1998) described upper horizon calcretes in southeast Spain that are believed to be of pedogenic origin, with the carbonate probably arriving from dust inputs or surface wash. It is probable that similar processes formed the upper horizon calcretes in the Voidomatis basin. Such processes would have been effective when a soil moisture deficit prevailed, limiting the leaching of calcite down the profile (Nash and Smith, 1998). These conditions are known to have existed in Epirus during cold periods of the Late Quaternary, when moisture deficits resulted in a sparse, steppe-like vegetation (Tzedakis, 1993, 1994; Turner and Sánchez Goñi, 1997). Considering that these gravel units appear to have been deposited during cold conditions, it is reasonable to assume that the calcrete formed relatively quickly at these times, probably over no longer than 1000 to 2000 years. This assumption is supported by the highly correlated U-Th isochrons (Appendix

IX) and the short time gap between the lower ESR dates at Old Klithonia Bridge and the uranium-series date on the gravel unit above (Figure 6.4). Thus the uranium-series dates can be assumed to provide a minimum age estimate that is close to the actual age of deposition.

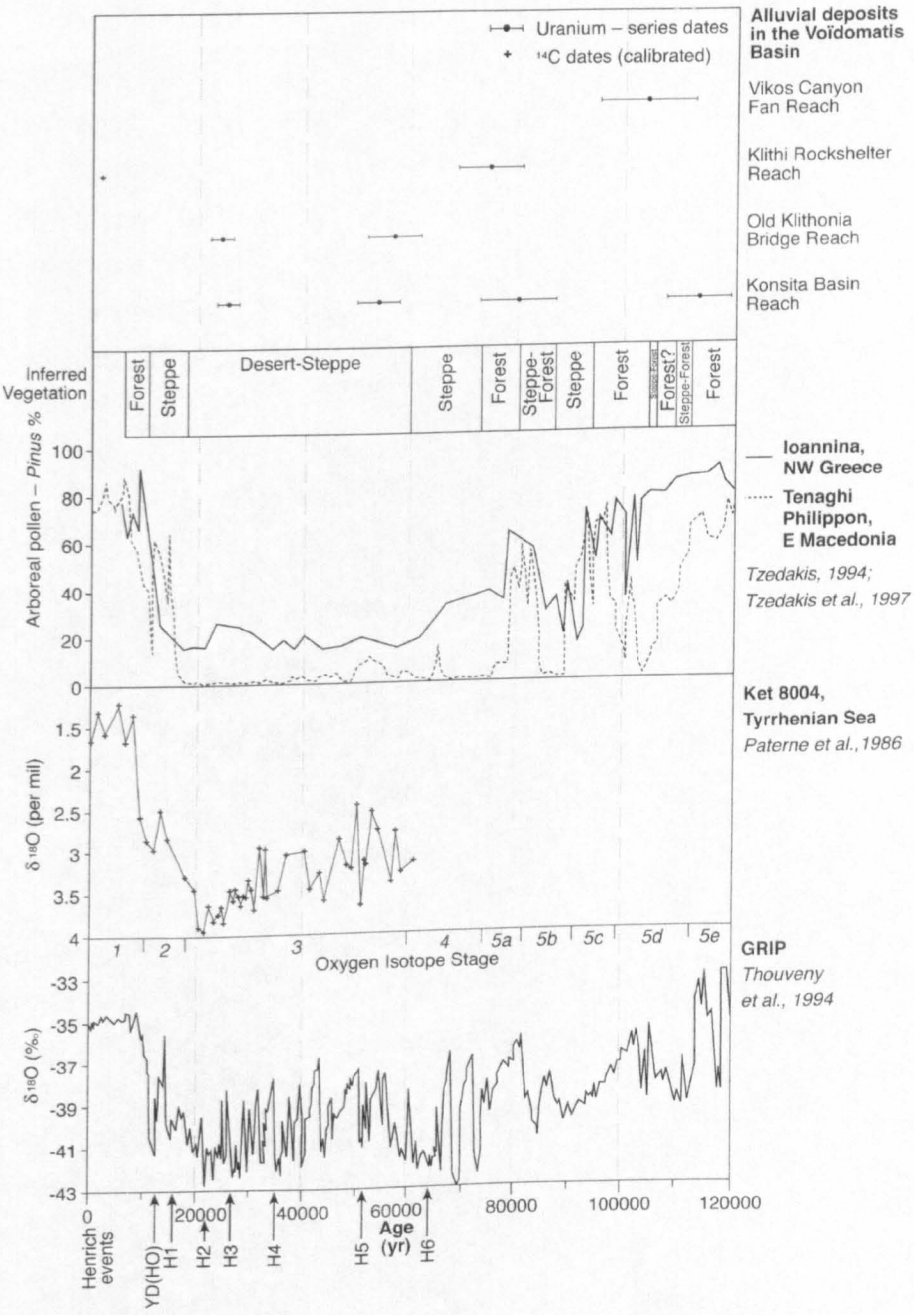

FIGURE 6.11 Climate proxy records and dating results from alluvial fill deposits in the Voidomatis basin. All results are shown in calendar years, with 2 sigma uncertainties. This only includes the results from samples collected since 1996.

The wider implications of these results in terms of extrinsic controls on river activity will be discussed further in section 6.6. However, to provide further information on long-term river activity, the next section of this chapter details the provenance of the fine sediments associated

with these sedimentary units. This allows temporal changes in fluvial sediment sources to be determined, with the aim of linking changing catchment characteristics to the genesis of these deposits.

6.4 PROVENANCE CHARACTERISTICS OF ALLUVIAL FILLS

The quantitative sediment fingerprinting technique outlined in Chapter 5 and Hamlin *et al.* (in press) was used to determine the provenance of the fine (<2 mm) sediments in the alluvial units. Section 5.1 described how information on the source of river sediments may be particularly valuable for investigating spatial and temporal changes in the nature of catchment sediment supply processes (Woodward *et al.*, 1992; Passmore and Macklin, 1994). Change in sediment supply is frequently quoted as an important mechanism in long-term river dynamics (Knighton, 1998), so direct provision of evidence regarding changes in sediment delivery processes could provide valuable information to explain the history of aggradation and incision in the Voidomatis. Samples for fingerprinting analysis were taken from most of the directly dated alluvial units, some of the undated ones, and also from contemporary fines so that the provenance of present river sediments could be determined.

6.4.1 Contemporary river sediments

Eight samples of contemporary alluvial fines (<2 mm) collected from different locations were analysed for provenance. Samples from different parts of the catchment do show some variation, which reflects local lithologies upstream of the sample point. In-channel fines in the headwater tributary that drains the flysch basin to the south of the catchment (Figure 3.8) are nearly 90% flysch. In the Upper Vikos Gorge, limestone and till, which are more immediate sediment sources (Figure 3.8), together constitute greater than 50% of the fines. In contrast, samples from the Lower Vikos Gorge tend to have a high flysch content, due to flysch delivery by local tributaries that drain the flysch beds above the Lower Gorge (Figure 3.8). However, the average pattern for all of these samples is a dominance of flysch (51%), with significant contributions of limestone (30%), till (8%) and ophiolite (5%). All other source groups comprise less than 3% (as displayed graphically in Figure 6.13). The dominance of flysch undoubtedly reflects the highly erodible nature of this lithology, which shows many signs of intense erosion today (section 3.2.1.2). The flysch outcrops occupy just over 40% of the catchment (Table 5.1), so the average of over 50% in contemporary fines indicates that the catchment is preferentially eroding fine sediments from the flysch slopes. The limestone is supplying a disproportionately lower amount, as it occupies nearly 47% of the catchment area (Table 5.1) yet contributes only c. 30% to the contemporary fine sediment flux.

6.4.2 Late Holocene floodplain sedimentation

Four samples were taken from the section shown in Figure 6.6 for fingerprinting, the results of which are shown in Figure 6.12. As might be expected, the provenance of overbank alluvium

deposited over recent centuries is similar to that of contemporary in-channel fines, with flysch dominating the fingerprints. However, flysch is even more prevalent in these overbank fines, with an average of about 80%. This may be indicative of greater flysch-derived sediment transfer over the Late Holocene in comparison to today, with more active erosion of the semi-badland flysch beds. The greater flysch proportions might also be due to grain size sorting, as these overbank deposits are of a finer texture (mean d_{50} 50 μm) compared to the in-channel contemporary sediments (mean d_{50} 435 μm). The softer flysch is comminuted to finer textures than the limestone, which may have the effect of increasing flysch concentrations in these overbank deposits. Grain size effects may also explain why limestone and till are largely absent from these fines, as coarser grains are not transported so easily overbank. Nevertheless, it is clear from Figure 6.12 that flysch has been a dominant sediment source over recent centuries. It is noticeable that, considering their low exposure in the catchment (Figure 3.8 and Table 5.1), both dolomite and ophiolite occur in surprisingly large proportions, especially mid-section, along with small amounts of terra rossa (Figure 6.12). The high ophiolite contribution indicates quite large amounts of fine sediment transfer from the eastern headwater area of the catchment where these igneous rocks outcrop. This may have resulted from historic logging activities, which have been active in the ophiolite region. In general however, the provenance characteristics of these four samples are similar which suggests that over the timecale covered by this fine sediment accumulation (probably at least the last c. 500 years), extrinsic environmental controls have not been sufficient to significantly alter the character of the fine sediment flux.

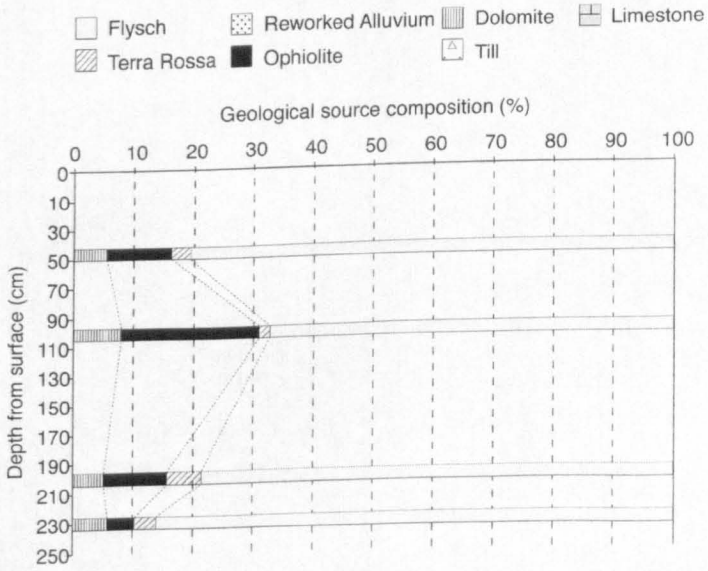

FIGURE 6.12 Provenance of four samples taken from the fine-grained valley fill in the Klithi rockshelter reach. This may be correlated with the section shown in Figure 6.6.

6.4.3 Dated Late Pleistocene alluvial units

Figure 6.13 shows the fingerprinting results from the dated Late Pleistocene alluvial units identified in the Konitsa basin reach (Figure 6.1), with the mean results for contemporary fines and Late Holocene floodplain sedimentation shown for comparison. The contemporary fines are directly comparable with the fines from the Late Pleistocene gravels units, as both of these are in-channel sediments, not altered by the possible effects of overbank sorting discussed in section 6.4.2. In contrast to these flysch-dominated contemporary deposits, the sediments dated to the cold LGM period have very different characteristics, being completely dominated by limestone and till (Figure 6.13). This dramatic contrast in sediment provenance is due to the influx of large amounts of fine sediment produced by glacial erosion in the limestone-dominated mountain headwaters. Frost weathering processes on the gorge walls may also have contributed to the limestone sand fraction of the fine sediment load during cold, glacial phases. Considering that the clast lithology of these sediments is 95% limestone (Lewin *et al.*, 1991), a significant proportion of the <2 mm limestone fraction was probably also produced from in-channel abrasion and attrition. Whilst fine sediment may have continued to be transferred from the flysch slopes, this appears to have been overwhelmed by glacial sediment supply processes from the mountainous limestone headwaters. Other sources such as ophiolite, dolomite and terra rossa, which are significant in the more recent deposits, were also suppressed at the LGM.

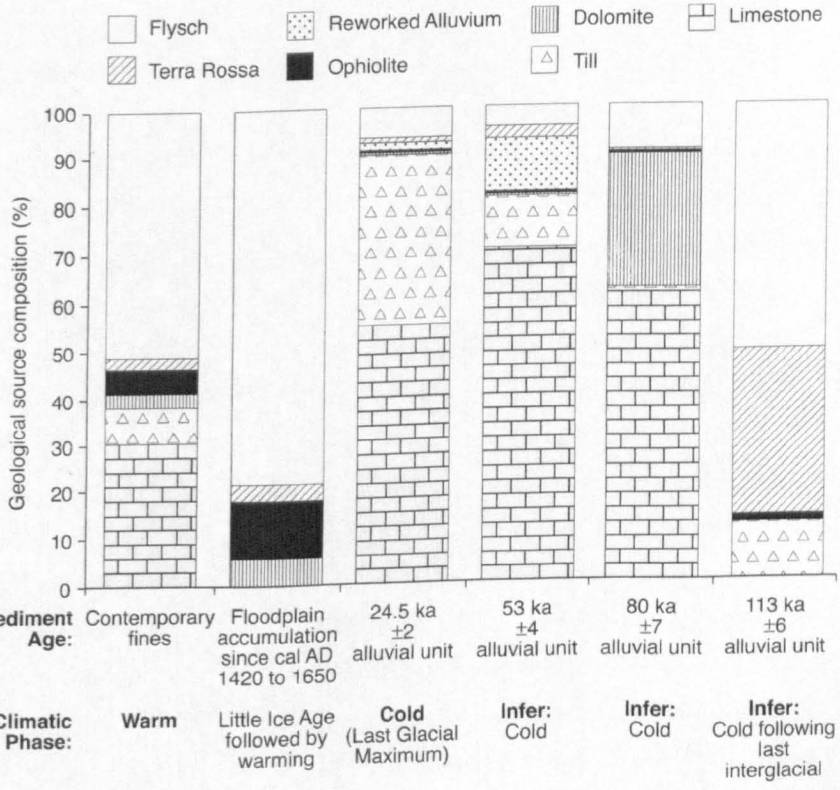

FIGURE 6.13 Provenance of valley fill units of known age in the Voidomatis basin, as determined by quantitative sediment fingerprinting. Chronological and proposed climatic information are also shown.

An understanding of varying sediment sources with changing environmental conditions can be used to aid interpretation of the older alluvial units where increasing uncertainty in dating results over longer timescales precludes exact palaeoenvironmental reconstruction.

The unit dated at 53 ±4 ka has a very similar sediment provenance signal to that of sediments at the LGM, and can therefore also be interpreted as having been deposited during a similar cold phase climate. The lower till content but greater limestone might indicate less widespread glacial outwash and instead greater bedrock breakdown by frost action. However, it should be borne in mind that till can be less reliably predicted than other sources (section 5.3.3), and it seems likely that at this time catchment conditions were similar to the LGM. Although the unit dated at 80 ±7 ka shows a significant proportion of dolomite, this must be treated with caution considering the low number of dolomite source samples (Table 5.1). It is more significant to note that limestone still dominates the fine fraction, being five times more prevalent than flysch, and therefore the catchment must also have been experiencing cold phase climate conditions.

The valley fill sediments dated to 113 ±6 ka have very different characteristics, with high levels of flysch and reworked soil material. These sediments are likely to have been deposited during cool OISst 5d, following the Last Interglacial (OISst 5e) (Figure 6.11). The extensive thickness of these sediments (Figure 6.2), and their dominantly limestone-derived coarse gravel lithofacies, point to a period of very high sediment supply, which could not have taken place during the warm, densely vegetated environment of the OISst 5e interglacial (Tzedakis, 1994). The high proportion of terra rossa, the weathered soil which occurs on the limestone, suggests that it was more widespread in the catchment at this time, which is likely considering the potential for extensive soil development during the prolonged warm interglacial conditions (van Andel and Tzedakis, 1996; Rose *et al.*, 1999). Weathering and soil development would also have occurred on the flysch outcrops. Subsequently, the rapid climatic deterioration of OISst 5d brought a large decrease in vegetation cover over this part of the Balkans (Tzedakis, 1993, 1994). This would have caused slope destabilisation, releasing the pre-existing terra rossa and weathered flysch material for entrainment into the fluvial system. These large volumes of flysch and soil could have dominated the fine fraction, whilst the cold OISst 5d conditions would have seen frost weathering of the gorge walls to supply the dominantly limestone-derived gravel which is found in this unit. This first period of major river activity following the last interglacial probably removed much of the readily available soil and flysch material from the valley slopes. This would explain why these are in low levels during subsequent Late Pleistocene aggradation periods when slopes were probably much barer. A similar pattern of Late Pleistocene terra rossa soil formation and subsequent removal and secondary deposition in alluvial environments was found by Roberts (1995) in the Konya basin, south central Turkey. In addition to climatic controls, flysch erosion at this time might have been accentuated by tectonic uplift, inducing gully incision into this softer lithology. It is also possible that the predicted terra

rossa component could in part be a secondary signal, having developed from *in situ* weathering. However, establishing the significance of any diagenetic effects would require further mineral magnetic and/or microscopic analysis, which were beyond the scope of this study.

6.4.4 Undated Late Pleistocene alluvial units

Sediment samples taken from three undated valley floor units were also fingerprinted. At the Konitsa basin reach, it was inferred that the 9.3 m unit at the northeastern section of the mapped area correlated with the slightly lower 8.3 m units at the mouth of the lower gorge, dated to an average of 24.5 ±2 ka (Figure 6.1). The small difference in elevation could be the result of 1 – 2 m of incision which has been observed since 1986 downstream of the modern weir that is located beside the Old Klithonia Bridge (J.C. Woodward, pers. comm. 1999) (Figure 6.3). The fingerprinting results for this unit show a similar provenance to the LGM sediments (Figure 6.14), with the only difference being slightly unequal proportions of limestone and till. However, it is important to remember that till is predicted less reliably than other sources and could be confused with limestone in the fingerprinting procedure (section 5.3.3). The limestone-dominated provenance indicates that this unit also originates from cold catchment conditions, and it is reasonable to assume that it corresponds to LGM aggradation.

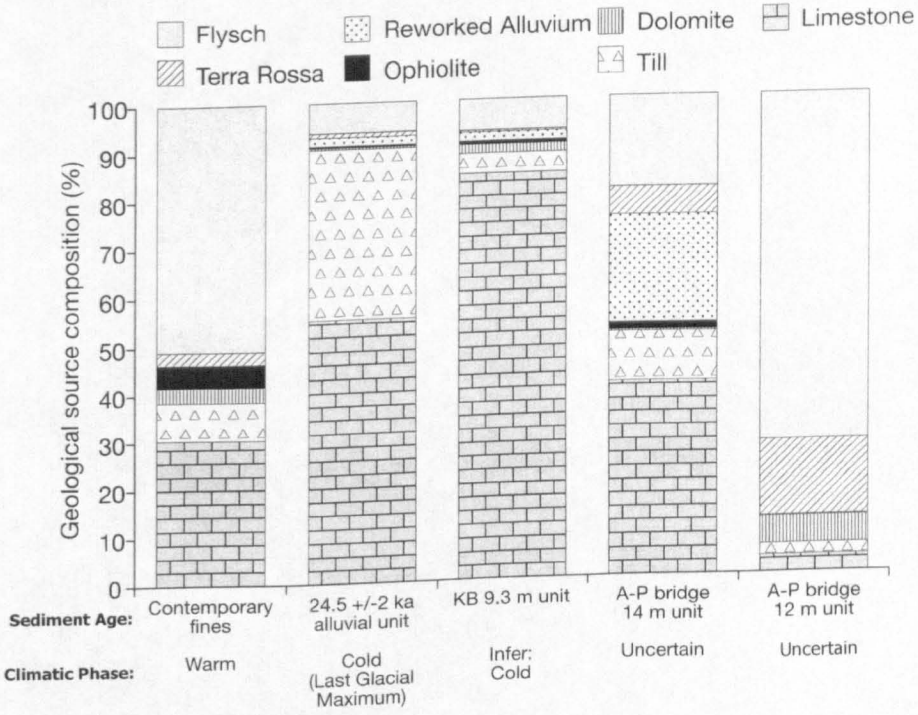

FIGURE 6.14 Provenance of undated valley fill units in the Voidomatis basin, as determined by quantitative sediment fingerprinting. The provenance characteristics of contemporary fines and the alluvial sediments dated to the LGM are shown for comparison. The palaeoclimatic characteristics of the undated sediments are proposed.

In contrast, both fragments of Late Pleistocene alluvium in the Aristi-Papingo Bridge reach (Figure 6.7) show quite different provenance characteristics to the LGM sediments (Figure

6.14). These units, which are both thought to correspond to aggradation around 80 – 85 ka (section 6.3.5), show variable provenance characteristics, with a greater significance of flysch and terra rossa compared to the LGM sediments. Factors specific to this study reach probably explain why the fine components of these units are less dominated by limestone and till compared to those in the Konitsa basin. The weathering environment and local hydrology seems to be different in the Aristi-Papingo study reach, exemplified by the fact that neither of these two units were cemented sufficiently for uranium-series dating, with their matrix appearing less 'clean'. The spatial variability in provenance between the two units, and the greater proportion of predicted flysch and terra rossa, has probably been caused by *in situ* weathering, and thus the fingerprinting results probably reflect a secondary diagenetic signal, rather than a genuine primary provenance difference. It is possible that the flysch contribution could have been somewhat higher than in the Konitsa basin due to sediment influx from several flysch-draining tributaries that join the main channel near the Aristi-Papingo Bridge. However, weathering has probably played an important role in altering the primary signal in these sediments. This demonstrates how the fingerprinting data can be less valuable in settings were alluvial sediments have suffered significant weathering, particularly over longer Late Pleistocene timescales and where only limited exposures are available.

6.5 A REAPPRAISAL OF THE VOIDOMATIS BASIN ALLUVIAL RECORD

In order to clarify current understanding of the stratigraphic record from the Voidomatis River, it is necessary to fit the new evidence presented in this chapter within the pre-existing framework of alluvial units established by Lewin *et al.* (1991) (described in section 6.2). This section provides a revised record of Late Pleistocene and Holocene sedimentation for the Voidomatis basin, integrating all of the results presented here within the context of previous work.

In general terms, the results presented in this chapter corroborate the work of Lewin *et al.* (1991), as the deposition of coarse gravel units during the Late Pleistocene (akin to Aristi unit) and overbank sedimentation during the Late Holocene (akin to Klithi unit) have been shown to be the two most significant periods of valley floor sedimentation. However, one of the principal findings of this investigation has been that the Voidomatis experienced additional phases of Late Pleistocene sedimentation to those previously recognised. At least four phases of Aristi-type Late Pleistocene aggradation can be identified, and greater geochronological data are now available for the Late Holocene sedimentation.

6.5.1 Late Pleistocene fluvial sedimentation

Through the combined application of field mapping and uranium-series dating this study has identified four phases of Late Pleistocene valley floor sedimentation (termed U4 to U7 in Table 6.2). They have all resulted from the widespread deposition of gravels by a braided channel

system, as Lewin *et al.* (1991) proposed for the Aristi sediments. Minimum ages have been obtained for these units by uranium-series techniques (Table 6.2; Figure 6.11). An 11 m surface between U6 and U5 sediments on the Konitsa basin could be evidence of a further phase of sedimentation bracketed by these two (Figure 6.1 and section 6.3.2). However, this may represent and incisional feature and in the absence of exposures or dating evidence there is insufficient evidence for a further sedimentation at present. U8 is the ancient Kipi unit described by Lewin *et al.* (1991), which is much older than the other units, having been deposited at some time before the present drainage network of the modern Voidomatis had become fully established, when the catchment extended further into the ophiolite terrain to the east.

U4 corresponds to what Lewin *et al.* (1991) considered to be the period of Aristi aggradation, greater complexity of this Aristi-type sedimentation. Lewin*et al.* (1991) identified a second, more minor Late Pleistocene unit, named the Vikos Unit (Table 6.1). This unit was differentiated from the Aristi sediments mainly via its stratigraphic position and sedimentary characteristics, with the Vikos unit clast lithology exhibiting c. 10% more flysch and c. 4% more ophiolite than the Aristi sediments (Table 6.1). A minimum age for the Vikos unit was obtained by TL date on overlying soil of 19,600 ± 3000 years (VOI24) (1 σ uncertainty (Debenham, 1997)), which was coherent with its stratigraphic position in relation to the Aristi (28,200 ± 7000 – 24,300 ± 2600 years) unit (Lewin *et al.*, 1991). Comparison of these soil-based TL dates with the uranium-series dates in this study show that the TL ages should be considered minimum age estimates for the underlying alluvial unit. This evidence comes from the discrepancy between the TL date of 28,200 ± 7000 (VOI23), which was obtained from soil overlying the 12.75 m unit on the Konitsa basin (Figure 6.1; soil profile B of Woodward *et al.*, 1994), sediments which have been show here to be at least 80,000 ± 7000 years old (Figure 6.1). It is possible that the TL date itself may be accurate, but the soil may have formed a considerable time after the deposition of the underlying alluvial sediments. This suggests that the Vikos unit TL date should be treated as a minimum age whose accuracy is uncertain. However, it does indicate another minor phase of sedimentation at some time after the main U4 LGM aggradation event. This would appear to have occurred during a period of deglaciation (Lewin *et al.*, 1991). It should be emphasised that these U3 (Vikos unit) sediments are of very limited spatial extent in the catchment, so this was probably a much less extensive phase of deposition than U7 to U4.

6.5.2 Late Holocene fluvial sedimentation

Lewin *et al.* (1991) believed that the Klithi unit was composite in nature, as sediments of this type yielded variable ^{14}C ages and exhibited differing degrees of soil development. The field mapping presented in this chapter confirms this, as a number of low, Late Holocene surfaces have been identified (e.g. Figure 6.1 and Figure 6.7). A variety of both new and previous dating results obtained from these Late Holocene sediments have been discussed section 6.3.4 (Klithi

TABLE 6.2 Summary of alluvial fill units and related sedimentation phases identified in the Voidomatis basin. Heights are quoted for the surface of the terrace above modern channel bed. All dating results are shown with 2 sigma uncertainties and the dating method is quoted in brackets. For radiocarbon dates both "cal AD" and "years BP" dates are shown. Data for U3 and U8 are from Lewin *et al.* (1991). † Denotes a minimum age. ‡ Denotes dates quoted in Bailey *et al.* (1986) and Gowlett *et al.* (1997).

Alluvial unit & Sedimentation Phase	Age: dating results shown where appropriate	Max. height (m)	Lithofacies type	Climatic conditions at time of deposition	Probable fluvial sedimentation style
U1 Present channel	Current in-channel sedimentation	-	Gravel bed	Mediterranean mountain climate: wet and warm	Incising, single thread meandering gravel bed river. Generally low suspended sediment load.
U2 Klithi unit	*Upper horizons:* deposited by semi-continuous 20th century sedimentation ($^{210}Pb_{unsupp}/^{137}Cs$). *Mid-section:* cal AD 1420 – 1650 (400 ± 120 BP) (^{14}C) *Early sedimentation:* cal AD 690-1290 (1000 ± 300 BP)‡; cal AD 1020-1400 (800 ± 200 BP)‡ (^{14}C)	4.5	Overbank fines resting on a gravel base	Minor climate change encompassing the Little Ice Age and subsequent warming	Single thread, meandering river with quite high suspended sediment loads during floods affecting vertical accretion of overbank fines.
U3 Vikos unit	19,600 ± 6000 years (soil TL date)†	9.7	Uncemented gravels	Uncertain, probably OIS 2 deglaciation	Low suspended sediment load
U4 (Aristi-type)	*End of sedimentation:* 24,000 ± 2000 years (U/Th) † 25,000 ± 2000 years (U/Th) † *Start of sedimentation:* 24,300 ± 2600; 25.000 ± 500; 26,000 ± 1900 (ESR, by R. Grün)	8.3	Gravels cemented in a sandy matrix. Both fractions are limestone dominated.	Cold Last Glacial Maximum climate, with glaciated mountain areas.	Aggrading, wide, braided floodplain with high sediment supply from glacial mountain areas and bare valley slopes. Probably high meltwater flood discharges.
U5 (Aristi-type)	53,000 ± 4000 years (U/Th) † 56,000 ± 5000 years (U/Th) †	10.0	As for U4	Cold early OIS 3 climate, glaciated (?)	As for U4.
U6 (Aristi-type)	74,000 ± 6000 years (U/Th) † 80,000 ± 7000 years (U/Th) †	12.8	As for U4	Cold OIS 4 or OISst 5b climate, glaciated (?)	As for U4.
U7 (Aristi-type)	104,000 ± 9000 years (U/Th) † 113,000 ± 6000 years (U/Th) †	15.5	As for U4	The transition to cold OIS 5d conditions following the last interglacial (OISst 5e)	Aggrading, wide, braided floodplain with streams reworking preexisting soils and weathered flysch slopes.
U8 Kipi unit	> 150,000 (TL)	56.0	Sandy gravels and thin silt beds	Uncertain. Catchment watershed extended further east.	Aggrading, low sinuosity coarse sediment river system.

Rockshelter reach). These show that Late Holocene sedimentation on stabilised floodplain areas was initiation by around 1000 years ago, and has been continuing through to the 1990s, as shown by unsupported ^{210}Pb and ^{137}Cs data presented in section 8.4. Thus, although there are different Klithi unit surfaces (e.g. at cross section 1 on Figure 6.7), these have been formed by essentially a single phase of sedimentation that has been semi-continuous over roughly the last millennium. The different surfaces are features of channel incision and lateral migration. However, the principal mode of Late Holocene sedimentation has been vertical accretion of fine sediments during floods. Thus, the Klithi unit can be retained as a name for this phase of Late Holocene river sedimentation, which is also termed U2 in this study (Figure 6.15 and Table 6.2). The new dates have enabled the timing of this Klithi unit sedimentation to be much more tightly constrained.

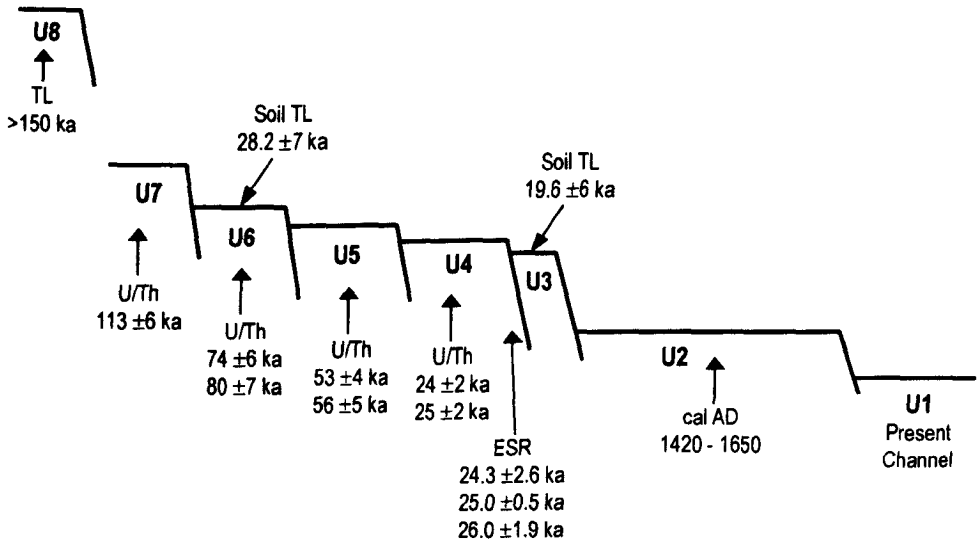

FIGURE 6.15 Schematic cross section of the Late Quaternary alluvial stratigraphy of the Voidomatis basin. The diagram shown the results of dating analysis of this study, as well as some of the dates obtained by Lewin *et al.* (1991). This diagram complements the information in Table 6.2.

6.6 PLEISTOCENE AND HOLOCENE RIVER ACTIVITY: ENVIRONMENTAL CONTROLS

Elucidating the controls on Late Pleistocene and Holocene river development in the Mediterranean has become a major topic in Quaternary geomorphology (section 2.5.3). This final section of the chapter explores the controlling mechanisms behind the alluvial record presented above, and discusses the potential role of catastrophic palaeoflood events.

6.6.1 Late Pleistocene climatic vs tectonic controls

In the absence of significant anthropogenic effects on the catchment over the Late Pleistocene, climate and tectonics are the two possible extrinsic controls on the development of the

Voidomatis River. Northwest Greece lies in one of the most tectonically active regions of the Mediterranean basin (section 3.1), and the possibility of tectonic activity controlling river behaviour needs to be evaluated.

The alluvial units identified in this study show no evidence of major tectonic disturbances of the valley floor over at least the last c. 113,000 years. Alluvial units show no signs of faulting, and there has been no deformation of the river terrace profiles. Even over large distances, the river terraces show horizontal surfaces and height correspondence with coeval deposits on opposite sides of the valley (e.g. the highest terrace on Figure 6.1, which was surveyed to 15.5 m (± 10 cm) on both the eastern and western fringes of the valley. Uniform vertical uplift could have taken place, still leaving the terraces horizontal and well preserved, but there is no evidence regarding the occurrence and timing of such activity. Over longer timescales (10^5 - 10^7 years), tectonics have undoubtedly been important in controlling the pattern of drainage and fluvial sedimentation in the rivers of Epirus (King and Bailey, 1985; Collier *et al.*, 1995; King *et al.*, 1997). Indeed, the dramatic gorges of the Voidomatis are obvious evidence of this. In addition, the ancient U8 Kipi unit sediments (*cf.* Lewin *et al.*, 1991) could well owe their abandonment to uplift of the headwater region where they are preserved, and a tectonically-induced change in watershed configuration. Unfortunately, specific evidence of long-term tectonics is difficult to obtain or quantify. The evidence presented in this chapter regarding the timing and provenance of the fluvial sedimentation phases, indicates that Late Pleistocene development of the Voidomatis River was primarily controlled by climatic fluctuations, with clear correlations between climate change and river activity. These are discussed in the following section.

6.6.2 Late Pleistocene river response to climatic change

The evidence presented in this chapter, particularly in terms of uranium-series dating (section 6.3) and fine sediment provenancing (section 6.4), indicates that river aggradation over the Late Pleistocene occurred during cold phase climatic conditions. In particular, U4, U5 and U6 have all been dated to cold periods (Figure 6.11) and show fine sediment provenance characteristics typically expected of the Voidomatis at such times (Figure 6.13). The palaeoenvironment during these cold Late Pleistocene periods was of course very different to today. An understanding of these environmental changes is important so that their effects on river activity can be understood. Pollen evidence indicates that open steppe-type vegetation dominated during cold stages, characterised by herb taxa such as *Artemisia* (wormwood) and *Chenopodiaceae* (goosefoot), and very low biomass production (Tzedakis, 1993, 1994; Turner and Sánchez Goñi, 1997). Such assemblages suggest a more arid climate during cold periods. However, this conflicts with some evidence of high lake levels during the last glacial cycle, which implies wetter conditions (Higgs *et al.*, 1967; Roberts, 1983; Harrison and Digerfeldt, 1993). A reconstruction of the palaeoclimate at this time must reconcile these two pieces of evidence.

GCM (Global Circulation Model) simulations for the LGM (e.g. COHMAP Members, 1988) have shown that the glacial climate saw a strong and fixed anticyclonic high pressure cell develop over the northern European ice sheet, and the displacement of the jet stream and westerly winds to the south. All models tend to predict summers as being cool and dry, with westerly winds blowing from the cold Atlantic having a low moisture carrying capacity. There is some disagreement over the synoptic winter configuration. Some models predict very cold, dry north-easterly airflow from the continental ice mass (e.g. Kutzbach and Guetter, 1986; COHMAP Members, 1988), which implies that year-round low precipitation coupled with low evaporation might have supported high lake levels and steppe vegetation. However, other studies have suggested that glacial winters were very cold due to strong westerly advection from the cold North Atlantic, but that winter precipitation was intense and frequent along the jet-stream which was shifted southward to Mediterranean latitudes (e.g. Broccoli and Manabe, 1987; Prentice *et al.*, 1992). This has been considered more likely to explain the palaeoclimatic evidence, as an increased seasonality of precipitation during the Last Glacial could have maintained high lake levels but could not have overcome the soil-moisture deficit, which resulted in the steppe vegetation (Prentice *et al.*, 1992). Thus a winter-rain steppe environment probably prevailed, for which there is no exact contemporary analogue (Turner and Sánchez Goñi, 1997).

Such environmental conditions have far reaching implications for river activity, as the nature of climate and vegetation dynamics can control two key fluvial geomorphic processes: sediment supply and flow regime. It is probable that the Voidomatis had an increased flow regime during the Late Pleistocene, owing to intense precipitation in winter and large glacial meltwater discharges in spring (Woodward *et al.*, 1995). This could have played a key role in the behaviour of the Voidomatis, by enabling greater volumes of sediment to be introduced into and transported through the fluvial system. This is discussed further in section 0. However, it is likely that a very high sediment supply accompanied these higher discharges to allow the thick Late Pleistocene aggradation units such as U4, U5 and U6 to have formed (*cf.* Bull, 1979, 1988). The palaeoclimatic conditions during cold Late Pleistocene phases would have generated increased sediment supply. Winter temperatures in the Mediterranean at the LGM were as much as 10°C lower (COHMAP Members, 1988), which meant that much of the increased winter precipitation may have fallen as snow (Prentice *et al.*, 1992). This combination of cold and wet winter conditions lead to the development of mountain valley glaciers in Epirus during cold Pleistocene periods (Woodward *et al.*, 1995).

Glaciation would have generated a profound increase in sediment supply from the limestone mountain areas in the Voidomatis basin due active glacial erosion processes, as evidenced by large moraines and deeply scoured glaciated valleys (section 3.2.1.1). In addition, the cold conditions would have facilitated increased mechanical rock breakdown by means of frost weathering processes, which would have been particularly effective on the limestone gorge

walls. The importance of glacial erosion and mechanical rock breakdown is demonstrated by the high limestone and till contents of U4, U5 and U6 (Figure 6.13). The fact that these provenance characteristics are associated with substantial aggradation implies that there was higher sediment supply during phases of limestone dominated sediment transfer. However, further evidence for increased sediment supply during the deposition of these units comes from the supressed levels of flysch in the fine fraction of these deposits. The relative contribution of flysch to U4, U5 and U6 is very low. This is perhaps surprising, considering that this erodible lithology would, if anything, be expected to supply greater volumes of sediment during the cold periods, when the *Artemisia*-steppe environment was characterised by a low vegetation cover, resulting in bare ground and unstable slopes with poor soil development (Turner and Sánchez Goñi, 1997). It appears that the volume of flysch inputs was swamped by a great increase in the supply of other sediment sources, primarily limestone and direct glacial inputs. Even if the *absolute volume* of flysch-derived sediment during the Late Pleistocene had only been equal to today's, other sediment sources must have liberated approximately 9 times as much fine sediment to suppress the flysch relative contribution from c. 50% today to the typical value of 10% in U4, U5 and U6. As shown in Table 6.3, this would have equated to a 550% greater supply of <2 mm sediment from other sources (mainly limestone and till) compared to today. Assuming an arbitrary 50% greater flysch sediment volumes during cold Late Pleistocene environments might be more realistic, as the barren landscape probably allowed active gully and rill erosion of the flysch. If this scenario was appropriate, a massive 725% overall increase in sediment supply would have been needed to surpress the flysch proportion to c. 10% (Table 6.3). Even 50% less flysch still implies an overall increase in sediment supply of 275% (Table 6.3). The fingerprinting data show that such sediment supply increases mainly came from the glaciated areas (Figure 6.13), where substantial volumes of limestone-derived fine sediments were produced. Confidence can be placed in these interpretations of sediment supply changes, as flysch displays very small amounts of measurement variance in the reliability assessment of fingerprinting results (section 5.3.3). It is probable that the supply of coarse (>2 mm) sediments also greatly increased. Lewin *et al.* (1991) have shown that the gravel fraction of the Late Pleistocene sediments is dominated by limestone (c. 95%), undoubtedly the result of increased glacial inputs and limestone breakdown during cold periods. Much of the large volume of scree that mantles the walls of the Upper Víkos Gorge probably formed during these cold Late Pleistocene environments (Macklin *et al.*, 1997).

The genesis of U7 is somewhat different to the other Late Pleistocene units, with much of the fine fraction derived from flysch slopes or terra rossa, but the clast lithology dominated by limestone. This phase of sedimentation is believed to have occurred during OISst 5d, a period of climatic deterioration and cooling following immediately after the Eemian interglacial (OISst 5e) (Figure 6.11). OISst 5e is believed to have extended from c. 130 - 117 ka, with warm and moist conditions in the Mediterranean region (Van Andel and Tzedakis, 1996; Rose *et al.*,

TABLE 6.3 Estimates of the change in supply of <2 mm sediment during the Late Pleistocene compared to today, based on assumptions regarding variations in the volume of flysch-derived sediment runoff.

Period	Approximate contribution of flysch to the <2 mm fraction	Ratio of flysch to other sources	Increase in total volume of sediment supply relative to today
U1: Contemporary in-channel fines	50%	1 : 1	-
U4, U5 and U6: assuming that the volume of sediments deriving from flysch areas was **the same** during the Late Pleistocene as it is today	10%	1 : 9	550%
U4, U5 and U6: assuming that the volume of sediments deriving from flysch was **50% greater** during the Late Pleistocene compared to today	10%	1 : 13½	725%
U4, U5 and U6: assuming that the volume of sediments deriving from flysch was **50% less** during the Late Pleistocene compared to today	10%	1 : 4½	275%

1999). Temperate forest vegetation cover was widespread in northwest Greece, with the early expansion of *Quercus* (oak) and to a lesser extent *Ulmus* (elm) and *Zelkova* (Caucasian elm), followed by *Carpinus* (hazel) and *Ostrya* (hornbeam), and finally *Abies* (fir) populations (Tzedakis, 1994). The forest vegetation developed in parallel to maturing soils and increasing biological diversity (Van Andel and Tzedakis, 1996), which would have resulted in stable slopes and presumably low sediment supply during the interglacial. At the end of OISst 5e, a brief double peak of *Abies, Carpinus* (hornbeam) and *Quercus* interrupted by prominent *Pinus* (pine) peak is seen in the Ioannina record, which may point to climatic instability at the end of the Eemian (Tzedakis, 1994; Van Andel and Tzedakis, 1996). Such instability could have instigated U7 sedimentation. If not, the fairly rapid deterioration of climate during the OISst 5d stadial would have certainly been sufficient, as it brought a rapid decrease in vegetation density compared to OISst 5e. Although a decrease in vegetation cover is less distinct in the Ioannina record, it is clear in the higher resolution Tenaghi Philippon record (Figure 6.11), which records a decrease in tree cover during both OISst 5d and 5b. Thus the soil and weathered flysch material that developed during the warm moist conditions of OISst 5e are likely to have become liberated for entrainment into the fluvial system following the biomass decrease and resulting slope destabilisation in OISst 5d. This would undoubtedly have caused an increased supply of fine sediments, whilst a greater supply of coarse particles from frost weathering during the cold OISst 5d conditions probably brought about an similar increase in the supply of gravel sized limestone clasts. The change in climate and slope character may also have induced higher water discharges at this time.

So far less attention has been given to the periods of more subdued river activity between the major phases of sedimentation. The nature of the stratigraphic record means that only high stands of the river bed tend to be clearly preserved. Incision over the Late Pleistocene could have arisen from a decreased sediment supply resulting from a decline in glacial activity

and the stabilisation of slopes by denser vegetation. It is also possible that tectonic uplift could have induced incision. Evidence of Late Pleistocene incision prior to the LGM comes from the section preserved at the Old Klithonia Bridge (Figure 6.4). The fine-grained sediments that immediately underlie the thick U4 gravel member, at a height of c. 3.9 - 4.4 m above the channel, are laminated and well-sorted, resembling SWDs (section 6.3.3). Such well-sorted fines could only have resulted from overbank sedimentation. Thus, between U5 and U4 the river level must have been well below the height of these fines. This implies a minimum incision depth of some c. 6 - 8 m after U5. The small difference between the ESR dates for these sands and the uranium-series date for the cemented U4 gravels suggests that following U5 the river incised to be at a low stand just prior to the onset of U4, which was a rapid phase of aggradation. Whether incision of a similar magnitude was observed between other Late Pleistocene sedimentation phases is uncertain. However, since U4 deposition there has clearly been a lowering of the river bed, which has been punctuated by the minor deposition of the U3 Vikos unit sediments. This incision has been caused due to the waning of glacial outwash and decreased rate of frost weathering as a result of climatic amelioration following the LGM. In addition, there is evidence to suggest that this Lateglacial period in the vicinity of the Voidomatis basin saw a successional development of forest vegetation, possibly becoming established as early as 15,000 year BP (Turner and Sánchez Goñi, 1997). Beaver is the third most common type of bone found at the Klithi rockshelter, providing strong evidence for considerable tree cover in the gorge between c. 16,500 and c. 13,500 years BP (Gamble, 1997). Tree cover would have stabilised slopes and decreased sediment supply. This progressive incision continued into Holocene period (section 6.6.3).

6.6.3 Holocene river activity

The influence of climatic change is complicated over the Holocene due to the increasing likelihood of landscape disturbances caused by human action. Variations in the intensity and timing of antropogenic disturbances in Mediterranean catchments mean that the relative importance of climate and human action in controlling Holocene river activity may vary considerably between catchments (section 2.5.3).

Evidence has been presented for one major phase of U2 (Klithi unit) Late Holocene sedimentation (Table 6.2). This does not necessarily mean that sedimentation was not taking place earlier in the Holocene, but the lack of preservation of any Early- to Mid-Holocene alluvial units indicates that it must have been minor in comparison the Late Holocene sedimentation. Subdued river activity during the Early- to Mid-Holocene can be attributed to a warm, moist and densely vegetated environment. At this time, eastern Mediterranean lake levels were high (Harrison and Digerfeldt, 1993) as a consequence of warmer sea surface temperatures increasing moisture availability and precipitation, and more frequent northerly migrations of tropical air masses in to the Mediterranean (Macklin *et al.*, 1995). Palynological data for this

period from northwest Greece show that vegetation cover during these humid conditions was particularly rich (Willis, 1992a, 1992b, 1992c, 1997; Turner and Sánchez Goñi, 1997). Evidence from Rezina Marsh, in the mountains above the Voidomatis (Figure 3.17), shows a rapid early Holocene expansion of a large number of woodland species from Lateglacial refugia (Willis, 1992b, 1997). This woodland continued to develop and diversify until approximately 6000 years BP, so in general this early part of the Holocene would have seen stable slopes, resulting in reduced sediment supply to the Voidomatis, which probably continued to incise through Late Pleistocene sediments.

At approximately 6000 years BP, tree species suddenly declined, probably as a result of landscape disturbance by Neolithic people (Willis, 1992c, 1997). Whilst there was some woodland recovery from about 5000 to 4000 BP, there followed a rapid decline in woodland density, with replacement by *Ericaceae* and open ground herbaceous taxa, which coincided with large-scale topsoil erosion and increased lake sedimentation (Turner and Sánchez Goñi, 1997; Willis, 1997). This woodland decline corresponds to widespread Bronze Age settlement and slope clearance throughout the Balkans, for which there is good evidence in Epirus (Gowlett *et al.*, 1997). An environment similar to today probably became established, and has remained so up to the present day, with the exception of a period between approximately 1990 and 1200 BP where a pine forest became established on the mountain slopes, either due to climatic changes or local depopulation (Willis, 1997). The question therefore arises why, considering extensive slope disturbance over the last c. 4000 years, significant valley floor alluviation is not recorded in the Voidomatis until U2 sedimentation, for which the earliest reliable date is 1000 ± 300 years BP (OxA-191) (Table 6.2). There are two possible explanations for this. Firstly, it is possible that, although anthropogenic disturbance has been prevalent since c. 4000 years BP, it has intensified since the final pine forest decline around 1200 years BP, hence producing more intensive erosion and sediment delivery than during the earlier Bronze age disturbance. Section 3.4 has shown how mountain village populations were very high from 1805 to 1880 AD, and probably started significant growth as early as 1500 AD. Thus human activities in the Voidomatis basin over the last c. 500 years may have been particularly important. The fingerprinting results suggest that there have been particularly destabilising effects on the flysch terrain (Figure 6.13), possibly due to intensified agriculture in these areas. It is also possible that ophiolite-derived sediment delivery increased over the Late Holocene (Figure 6.12), due to increased clearance in the mountain headwaters that are proximal to the small ophiolite outcrop (Figure 3.8).

A second explanation is that climatic conditions over the last 1000 years or so have been more capable of harnessing the sediment destabilised by human action, resulting in the prominent sedimentation over the last millennium. Neoglacial climatic fluctuations, including the Little Ice Age (c. 1450-1850 AD) (Grove, 1988), which occurred over the Late Holocene and recent centuries, appear to have resulted in increased flooding on Mediterranean rivers

(Benito *et al.*, 1996; Maas, 1998). In particular, historical evidence indicates increased flood frequency between 1500 to 1850 AD in the western Mediterranean (Benito *et al.*, 1996), a period which shows close correspondence with the Little Ice Age and the mid-section date for U2 sedimentation (Table 6.2). Increased storminess and flooding would not only have favoured overbank sedimentation, but would also have enhanced the delivery of fines from the flysch areas due to increased slope wash and gully erosion. Extreme rainfall can also be very important in generating sediment delivery via mass movements on slopes adjacent to the river channel. It therefore seems likely that over the last c.1000 years, and particularly during the Little Ice Age (c. 1450-1850 AD) (Grove, 1988), both anthropogenic disturbance and climatic conditions have been particularly conducive to river sedimentation. The impact of both factors in combination has probably been the environmental stimulus of prominent Late Holocene river sedimentation.

The Voidomatis currently exhibits an incised form over the majority of its length. Again, this might be explained by climatic amelioration since the Little Ice Age, weakening both sediment delivery and flow regime. Additionally, the establishment of the catchment as part of the protected Zaghori National Park in 1973 (M.I.C.C., 1994) may have lead to decreased anthropogenic slope disturbances, and certainly the last 30 years have seen decreased grazing pressure and the general spread and expansion of woodland and scrub vegetation (Bailey *et al.*, 1993).

6.6.4 Comparison with other studies in the Mediterranean

There has been a long running and often controversial debate over the timing and principal controls on Late Quaternary river development in the Mediterranean region (section 2.5.3). A major problem in resolving this debate has been the lack of reliably-dated records of sedimentation. However, with increasing application of luminescence and uranium-series disequilibria dating methods, a number of particularly well constrained records of river activity have recently been established (e.g. Fuller *et al.*, 1996, 1998; Maas, 1998; Maas *et al.*, 1998; Rose and Meng, 1999; Rose *et al.*, 1999; Hamlin *et al.*, in press.). Whilst the controls on Holocene alluviation remain strongly influenced by catchment histories and physiographies, these studies exhibit remarkable similarities for the Late Pleistocene, with strong evidence for climatic controls on river aggradation, which has been shown to have occurred during cold phase environments (section 2.5.3). Figure 6.16 and the accompanying Table 6.4 show a comparison of the alluvial chronology presented here with the results of these recent studies. The last 140 thousand years is shown, a period that encompasses the most recent interglacial-glacial cycle (Figure 6.11). For a comparison of more studies of Mediterranean alluviation, including older work and studies that have concentrated more on Holocene activity, the reader is referred to Maas (1998). Dating uncertainties, which are unfortunately frequently ignored in these comparisons, are included in Figure 6.16 to enable an informed evaluation of dating results.

Inspection of Figure 6.16 shows some clear correspondence between these different studies. In particular, the U4 sedimentation (≈ 26 - 24 ka) in the Voidomatis associated with the LGM is recorded in all other regions, with the exception of certain rivers in Crete. This suggests that this was a very important sedimentation phase in the Mediterranean. Agreement is also found further back in the Pleistocene, although the generally larger dating uncertainty with age can make correlations somewhat less precise. U5 Voidomatis sedimentation (≈ 64 - 52 ka) correlates closely with alluvial sedimentation in the small catchments of Mallorca and the records from the Guadalope basin, suggesting coeval deposition associated with cold conditions at the end of OIS 4 and the beginning of OIS 3 (Figure 6.11). The absence of this phase from the Cretan records may simply be due to a lack of preservation, or the more southerly latitude of this area meaning that less severe conditions were experienced at this time. Similarly, U7 sedimentation in the Voidomatis (≈ 102 - 116 ka), occurring during cold OISst 5d was also documented in Mallorca, and possibly at Castelserás on the Guadalope, although no sediments of this age were found by Maas (1998). There is a somewhat less clear correspondence for the U6 alluviation (≈ 86 - 72 ka), which has been shown to be related to cold conditions in either OISst 5b or early OIS 4 (section 6.4.3). The U6 sedimentation does coincide with river aggradation in Crete, which suggests that this was a significant phase of alluviation in Greece. However, the studies from Mallorca and Mas de Las Matas on the Guadalope date aggradation during this period to c. 90 ka, approximately 10 ka earlier than the Greek dates (Figure 6.16). This could reflect palaeoevnironmental differences within the Mediterranean region. Different dating techniques might also be a factor (Table 6.4), with the uranium-series dates from the Greek studies showing later dates than the Spanish luminescence-based chronologies due to a delay in the calcite cementation of alluvial units at this time. However, there is no evidence for significantly delayed cement formation in the $^{230}Th/^{234}U$ analyses in this study. It should be stressed that the precise degree of correspondence between studies over these longer time scales does become more speculative, because the error bars surrounding the dates become more significant. Figure 6.16 shows that there is considerable overlap of the age uncertainties for all of the studies at c. 80 ka, and thus it is possible that there was in fact coeval depositional at all sites around this time.

All of the studies show significant aggradation during OIS 2 (c. 20 - 10 ka), and U3 (Vikos unit) sedimentation is known to have occurred during this period in the Voidomatis basin (Table 6.2; Figure 6.15). Limited preservation of Vikos unit sediments suggest that this was a minor phases of sedimentation, which is in contrast to thick and widespread deposits of this age noted in other catchments (e.g. Maas, 1998; Rose and Meng, 1999). This difference may have been due to northwest Greece experiencing very rapid Lateglacial expansion of forest vegetation from refugia (Turner and Sánchez Goñi, 1997), which would have rapidly stabilised slopes and limited sediment availability during the glacial-interglacial transition. In addition, the seemingly quite early retreat of glaciers in the Voidomatis basin after U4 deposition at c. 24 ka, has meant

that in the absence of significant glacial activity subsequent U3 (Vikos unit) sedimentation was comparatively minor.

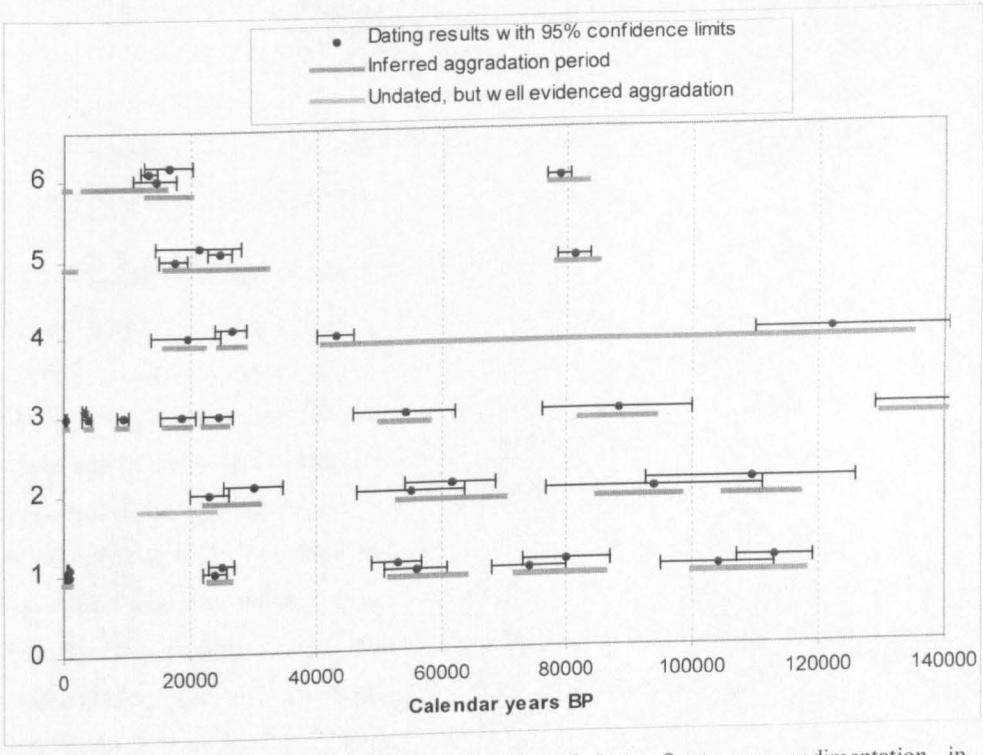

FIGURE 6.16 Comparison of selected chronologies of Late Quaternary sedimentation in the Mediterranean Region. Details of the studies included are given in Table 6.4. Inferred aggradation periods have been made on the basis of interpretations and stratigraphic information given in the original references.

TABLE 6.4 The selected studies used in Figure 6.16. * Includes cal BP ^{14}C dates for the Late Holocene.

No.	Reference(s)	Study site	Dating technique
1	*This study*; Hamlin *et al.* (in press).	Voidomatis River, NW Greece	$^{230}Th/^{234}U$ *
2	Rose and Meng (1999); Rose *et al.* (1999).	Torrente d'es Coco & Torrente de sa Telaia Freda, NE Mallorca, Spain	OSL
3	Fuller *et al.* (1996, 1998)	Mas de Las Matas, Guadalope River, NE Spain	IRSL
4	Fuller *et al.* (1996, 1998)	Castelserás, Guadalope River, NE Spain	IRSL
5	Maas (1998)	Samaria Gorge, SW Crete, Greece	$^{230}Th/^{234}U$
6	Maas (1998); Maas *et al.* (1998)	Rapanas and Omalos Rivers and the Aradena Gorge, SW Crete, Greece.	$^{230}Th/^{234}U$

In general terms, the comparison of this study with other recently obtained data from the Mediterranean reveals considerable synchronicity in river activity. Periods of aggradation have commonly occurred during recognised cold periods of the Late Pleistocene, such as OIS 5d, 5b, 4, and late-stage 3. Notable periods of limited river activity coincide with warm periods such as the last interglacial (OISst 5e; c. 130-115 ka) and mid-OIS 3 (c. 45-30 ka), which is known to have been warmer than the preceding and following full glacial conditions which generated U5 and U4 sedimentation (Fuller *et al.*, 1998; Rose *et al.*, 1999). Thus, the good correspondence of

the data shown in Figure 6.16 supports the strengthening belief that, over the Late Pleistocene, river activity was strongly controlled by climatic conditions, with reoccurring cycles of cold phase sedimentation and warm phase incision or subdued activity. It is important to note that Epirus is within one of the most tectonically active regions of the Mediterranean, yet the overriding climatic signal is still clear in the alluvial record. This indicates that even in tectonically active regions it was possible for Late Pleistocene climatic changes to maintain a dominant control on river behaviour.

6.6.5 The possible role of catastrophic flood events

Changes in sediment supply and/or flow regime are the main mechanisms by which extrinsic controls (e.g. climate, tectonics, and land-use) can bring about changes in river behaviour. Late Quaternary sediment supply fluctuations have been discussed in detail above. However, it is possible that changes in the frequency and magnitude of flooding may have been of equal, and perhaps sometimes greater importance in controlling river activity. The large volumes of coarse bedload transported by the river and stored in the valley floor, particularly during the Late Pleistocene, mean that channel change may have been episodic, and strongly influenced by the occurrence of high magnitude, *catastrophic* flood events (section 2.4.3). Catastrophic floods may bring about both massive aggradation and degradation (Table 2.5), their relative effects largely being determined by catchment conditions, as outlined in Table 6.5 (*cf.* Bull, 1979, 1988). Considering the fact that tectonic uplift has apparently had a fairly minor influence over Late Quaternary sedimentation, the effect of catastrophic floods can be simplified to being determined by the relative balance of stream power (i.e. flood magnitude) to resisting power (i.e. sediment availability) (Bull, 1979, 1988). Thus it is quite possible that extreme floods may have induced either aggradation or incision in the Voidomatis, depending on the time of their occurrence. Periods of both high and low sediment availability have been identified in sections 6.6.2 and 6.6.3, and these are likely to have controlled the impact of catastrophic flows. It is likely that the cold stage Late Pleistocene Voidomatis experienced very high spring meltwater discharges. Much of the increased winter precipitation of this may have fallen as snow (Prentice *et al.*, 1992), and therefore spring ablation from both snow packs and glaciers probably released large volumes of stored water. The archaeological evidence points to a hostile environment in the Voidomatis gorges during LGM, with the Klithi, Boila and Magalakkos rockshelters having no evidence of occupation before 20,000 cal BP (Bailey *et al.*, 1997). The braided river pattern during the sedimentation of U7 to U4 also implies high flow velocities and stream powers (*cf.* Schumm, 1977). Extreme spring discharges may therefore have been important in depositing the thick Late Pleistocene gravel units, as many of the factors that encourage net aggradation (Table 6.5) were present during the cold periods. Similarly, it has been speculated that periods of increased flooding over recent centuries may have had an important role to play in Late Holocene sedimentation, as sediment availability was also high due to anthropogenic

disturbance (section 6.6.3). However, confirmation of the occurrence and geomorphic effects of catastrophic floods requires detailed palaeoflood records for periods of river metamorphosis. These are presented in the following two chapters.

TABLE 6.5 Factors that tend to increase the likelihood of either net aggradation or degradation of a river reach upon the occurrence of a flood event (*After: Bull, 1988).*

Factors encouraging net *degradation*	Factors encouraging net *aggradation*
1. Stable hillslopes yielding minimal sediment.	1. Abundant sediment storage on hillslopes.
2. Dense hillslope vegetation.	2. Fires that remove hillslope vegetation, exposing soils to accelerated water erosion.
3. Climatic changes giving more frequent high intensity rainfall, greater annual rainfall, or a lower proportion of precipitation falling as snow.	3. Climatic changes that decrease vegetation cover or increase rainfall intensity.
4. Tectonic uplift increasing relief, drainage density, and longitudinal valley floor slope.	4. Unstable slopes prone to landslide that introduce much sediment directly into the channel.
	5. Lack of relative vertical tectonic uplift.

6.7 SUMMARY

Reach-based studies of alluvial stratigraphy have enabled a detailed history of Late Pleistocene and Holocene river activity to be reconstructed. Eight $^{230}Th/^{234}U$ dates have been obtained from cemented Late Pleistocene sandy-gravel alluvial units. The highly correlated isochrons obtained from these samples indicate the cement formed during a short period of time. The results therefore provide reliable minimum age estimates for sedimentation phases, and have relatively small dating uncertainties. The $^{230}Th/^{234}U$ method provides a valuable dating approach for deposits such as these where organics are poorly preserved and bodies of fine sediment for luminescence dating are rare. The dating results have been complemented by quantitative fine-sediment fingerprinting data. There have been systematic changes in the provenance of the fine sediment over Late Pleistocene and Holocene timescales, which can be largely explained by the effects of climate change on sediment delivery processes. The provenance of fine sediments provides a valuable indication of the catchment environment at the time of deposition. Quantitative fine sediment provenancing is therefore a valuable tool for investigating the environmental controls on long-term river activity (Hamlin *et al.*, in press).

This combination of research methods has revealed a considerable volume of new data regarding the Late Quaternary development of the Voidomatis River, which builds on the previous work of Lewin *et al.* (1991). Eight alluvial sedimentation units can now be recognised for the Late Quaternary (Table 6.2). At least four major phases of Late Pleistocene sedimentation have taken place (U4 – U7). U7 occurred during the cold phase of OISst 5d at c. 110 ka, when large volumes of weathered flysch and terra rossa, which had developed during the last interglacial, were washed through the river system. Subsequent phases of Late Pleistocene sedimentation have been dated to minimum ages of c. 78 ka (U6), c. 54 ka (U5), and a final phase coincided with the LGM at c. 25 ka (U4). The fine sediments incorporated within

these units are dominated by limestone and till, in contrast to modern and historical fine sediment fluxes which have been dominated by flysch-derived sediment. Whilst flysch probably continued to supply sediment to the river during the deposition of U6, U5 and U4, its relative contribution to these units is minor. This is due to a large increase in sediment supply, estimated to between 275% and 725% greater than today, principally from limestone areas as a result of glacial erosion, and also to some extent frost weathering and a low vegetation cover. Thus cold climate, and in particular glacial activity appears to have been the primary stimulus of Late Pleistocene river aggradation.

In between these periods of sedimentation, warmer conditions have brought either limited river activity or incision as a result of decreased sediment supply. There has been progressive incision from the LGM until the Late Holocene, as warm, high biomass conditions stabilised valley slopes. During approximately the last 1000 years U2 (Klithi unit) has been deposited, with a general sedimentation style of vertical accretion of fine sediments above a base of former in-channel gravels. Prominent sedimentation over the Late Holocene can be explained by unstable neoglacial climatic periods (principally the Little Ice Age) with high frequencies of storms and flooding coinciding with an intense period of human activity and landscape disturbance in the region. The erodible flysch lithology now provides the dominant source of fine sediments to the Voidomatis River.

This chapter demonstrates the dynamic nature of Late Quaternary river activity in Mediterranean mountain catchments such as the Voidomatis. There have been regular and systematic fluctuations between aggradation and incision. Over the Late Pleistocene the close correlation between river activity and changes in climate and vegetation provides strong evidence for climate having been the primary control upon river activity. These results show considerable similarities to other recently-developed alluvial chronologies in the Mediterranean (section 6.6.4), indicative of periods of broadly synchronous, climatically-controlled sedimentation phases in Mediterranean rivers. Climate continues to assume a significant control during the Holocene, where the combined effects of anthropogenic disturbance and unstable climate are the likely driving forces behind widespread sedimentation in the Voidomatis basin over the last c. 1000 years.

This chapter has provided a detailed account of environmental and landscape changes which have taken place in the Voidomatis basin over the Late Pleistocene and Holocene. As outlined in section 6.1 this chapter forms a very important geomorphic context for the rest of this thesis, establishing a broad framework of valley floor development within which evidence for flood events can be placed. The following chapters will present palaeoflood records that enable the relative importance of high magnitude flood events in the development of the Voidomatis River to be assessed in detail.

7. LATE PLEISTOCENE CATASTROPHIC FLOODING IN THE VOIDOMATIS BASIN

This chapter deals with the occurrence and implications of extreme magnitude Late Pleistocene floods, which have been investigated through the analysis of palaeoflood slackwater deposits (SWDs). The context of this work within the overall thesis aims is described in section 7.1. Section 7.2 deals with field descriptions of the SWDs, and section 7.3 with the dating results. Section 7.4 then presents a detailed sedimentological description of the deposits to enable a record of specific flood event occurrence and magnitude to be constructed. On the basis of these results there then follows a discussion of the environmental controls on the generation of these high magnitude floods (section 7.5) and their geomorphological impacts (section 7.6).

7.1 INTRODUCTION

It has frequently been proposed that variations in the occurrence of high magnitude flooding over long (10^3 - 10^5 years) timescales could have had an important influence on the operation and development of river systems (e.g. section 2.4.3; Rose *et al.*, 1980; Bull, 1988; Knox, 1988; Coxon *et al.*, 1996). Rivers in the Mediterranean region tend to have relatively small and steep catchments by world standards, which are prone to high magnitude flash floods (section 2.5). Studies of river activity in the Mediterranean have therefore often referred to high magnitude flooding as a potentially important geomorphic process (e.g. Grossman and Gerson, 1987; Frostick and Reid, 1989; Rose and Meng, 1999). However, a detailed demonstration of their long-term effects is frequently not possible, due to the lack of evidence for extreme flood events over such long timescales.

This chapter aims to document the occurrence, characteristics and implications of catastrophic flood events in the Voidomatis basin over the Late Pleistocene, and particularly the Late Würm (c. 25 - 10 ka). This was the most recent major climatic transition from full glacial to warm interglacial conditions, when considerable climatic and hydrological variability could have resulted in flood events of exceptional magnitude. This period also saw a major phase of landscape metamorphosis. The Voidomatis River at the Last Glacial Maximum (LGM) was an aggrading system with a braided planform transporting large volumes of sediment liberated by glacial erosion and frost weathering (Chapter 6). However, the Voidomatis in the Holocene has become deeply incised within these sediments and has adopted a single thread, gently meandering pattern, with much lower sediment yields derived mainly from the erodible flysch lithologies in the catchment (Chapter 6). This has been one of the most dynamic periods in the Late Quaternary development of the Voidomatis River, and is therefore an important timescale over which to investigate the occurrence of potentially important geomorphic processes such as

catastrophic floods, which could have played a large role in such landscape change (Section 6.6.5). Commonly, the occurrence of such flood events would simply have to either be postulated, or inferred from indirect sedimentological evidence. However, in the Voidomatis basin a number of palaeoflood slackwater deposits (SWDs) have been identified (Lewin *et al.*, 1991), which may provide direct evidence of individual flood events over this part of the Late Pleistocene. SWDs can arguably provide the most complete and accurate palaeoflood information of all sedimentary deposits, potentially yielding both reliable age and discharge information (see sections 2.3.1 to 2.3.4). By analysing the SWDs in the Voidomatis basin, this chapter provides one of the first detailed accounts of dated Late Pleistocene flood events for a river in the Mediterranean region. These data are compared to the history of river activity and landscape development that has been established in Chapter 6, to assess the geomorphological impact of catastrophic floods over this period. The timing of these flood events is also compared to climate proxy records, to investigate the likely environmental controls on the generation of extreme events over this period of climatic transition.

7.2 FINE-GRAINED PALAEOFLOOD SLACKWATER DEPOSITS: DESCRIPTION AND LOCATION

Three SWD sites have been identified adjacent to the Voidomatis River, at locations shown on Figure 4.5. The sedimentology and stratigraphic context of these deposits are discussed here.

7.2.1 Tributary site

These SWDs are located in the Lower Vikos Gorge within the Aristi-Papingo Bridge reach described in section 6.3.5. They have been deposited in the mouth of a relatively small tributary close to the Spiliotissa Monastery, as shown in Figure 6.8. The tributary has narrow channel (<2 m wide) and is quite entrenched by some 2 to 3 m below the fan/terrace surface. The SWDs are well exposed in the stream-cut tributary banks (Figure 7.1). Previous studies have shown that a tributary mouth is classic site for the deposition of SWDs (section 2.3.1), as during large floods the main channel flow encroaches up the tributary and fines are deposited due the rapid decrease in competence in this backflooded slackwater zone. The configuration of this tributary is favourable for the deposition of SWDs, as the junction angle with the main channel is nearly 90° (Figure 6.8), which is conducive to effective backflooding and sediment deposition (Baker and Kochel, 1988). In addition, the drainage area of the tributary basin is very small in comparison to the main channel, and therefore during storms this small, steep tributary basin will have peak flows well before those of the main channel, thus resulting in calmer, less disruptive hydraulic condtions in the tributary mouth when the main channel peak stage arrives.

SWDs are preserved on both sides of the tributary (Figure 7.1 and Figure 7.2). Each of these exposures was logged and photographed, as shown in Figures 7.3 to 7.5. The sediments are particularly thick on the right bank of the tributary, with over 3 m of fines at exposures 1 and

3, whilst at exposure 2 the sediments are less than half this thickness and generally exhibit much thinner sedimentary units. This reflects asymmetric deposition within the tributary mouth, which occurs due to backflooding flowing more forcefully into the downstream side of the tributary, and then circulating around the tributary mouth with reverse eddys, leaving the upstream side experiencing calmer conditions conducive to sediment deposition. The pale cream colour of the deposits (typically 2.5 Y 7/2), which suggest a considerable limestone content, confirms that they are main channel deposits, and not more locally derived sediment. The tributary, like most in the Lower Vikos Gorge, drains an area dominated by flysch outcrops (Figure 3.8), and the fines that are carried by the channel during floods are dark brown and flysch-dominated. Thus pale cream fine sediments of this nature could only have been deposited by the main channel.

The sedimentary logs show that the SWDs typically show alternating layers of medium to fine sands with medium to coarse silts, each layer generally being separated by sharp contacts. Occasionally, strings of pebbles or fine gravels occur, although this is rare. With a few exceptions, each unit is generally well-sorted and structureless, although some layers show upward fining and occasional reverse grading, whilst in places fine, within-unit laminations can be seen (Figures 7.3 to 7.5).

FIGURE 7.1 Photograph of the Tributary SWD site, looking up-tributary. SWDs are visible in the near left-hand corner (exposure 1) and 5 m further upstream on the opposite side of the channel (exposure 2). Exposure 3 is a further 12 m upstream, although this is heavily shaded in this photograph. The view is taken from the downstream end of the mapped area shown in Figure 7.2.

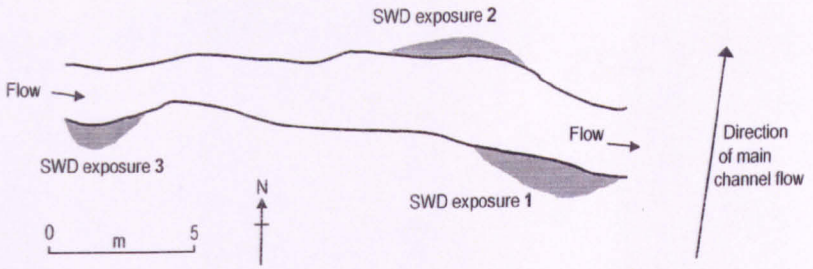

FIGURE 7.2 Map showing the location of studied stream-cut SWD exposures along the tributary channel (Tributary site). The exposures are shown in schematic view and are not to scale. This map area corresponds approximately to that labelled as slackwater deposits in Figure 6.8.

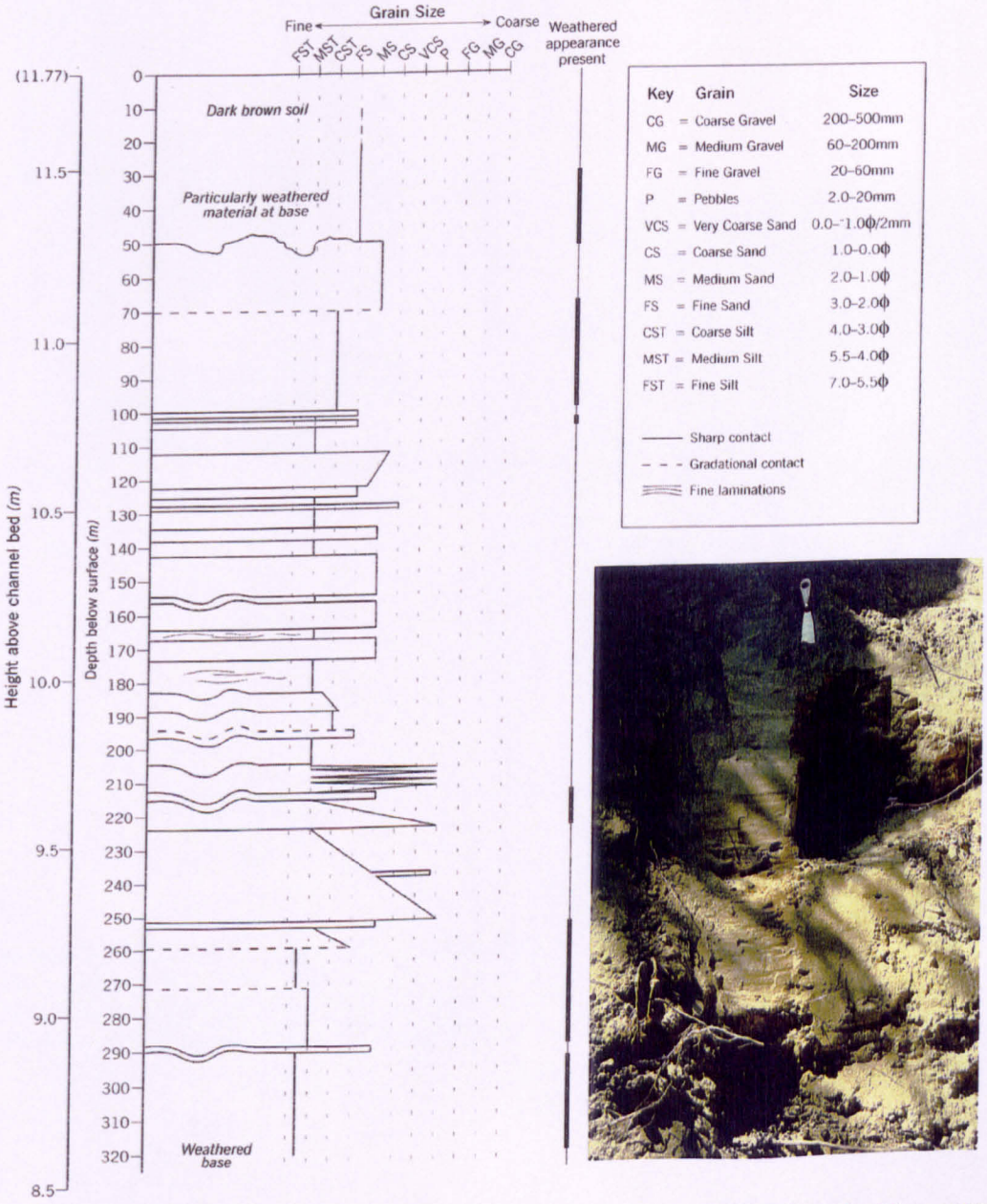

FIGURE 7.3 Sedimentary log and photograph of the SWDs at exposure 1 at the Tributary site (Figure 7.2).

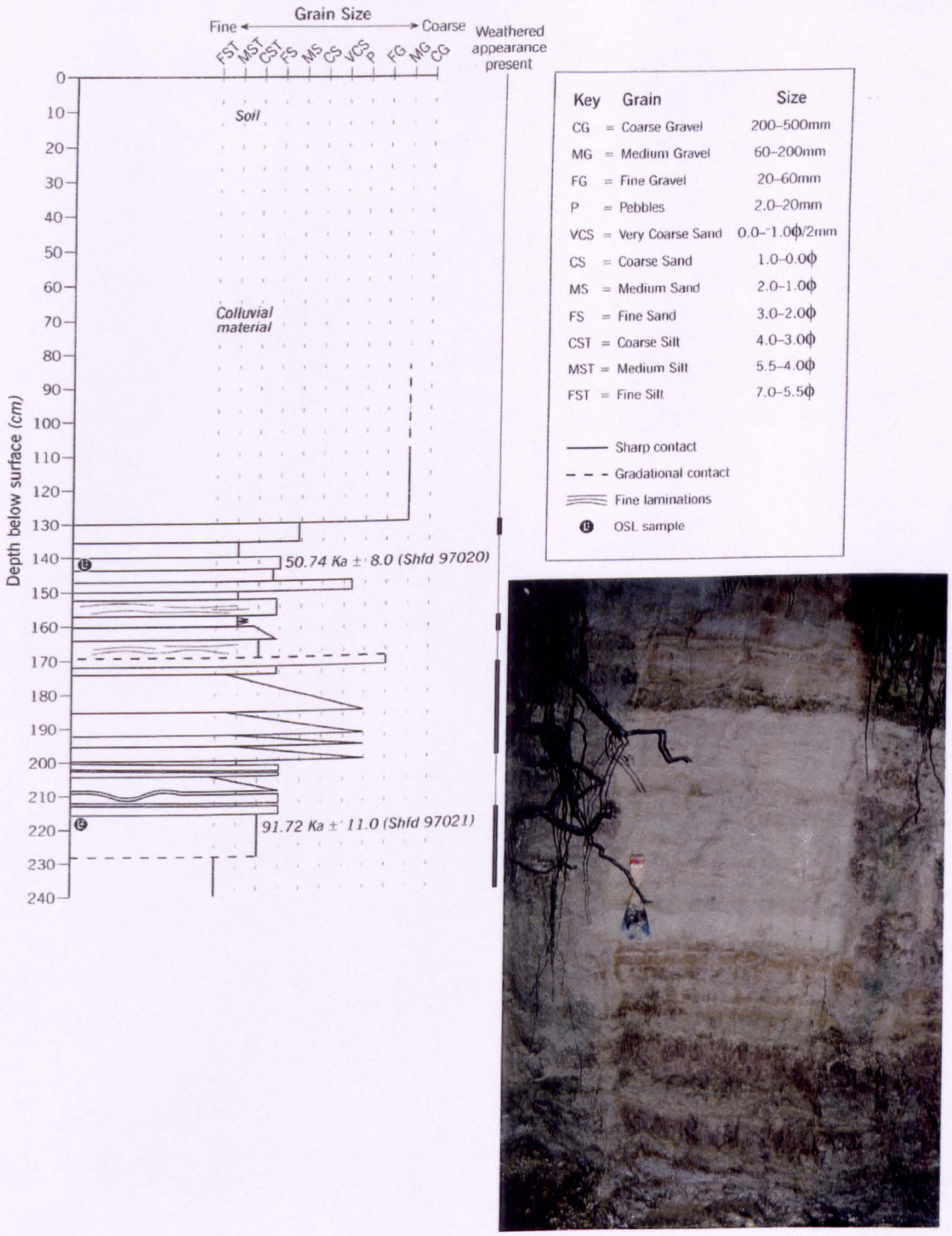

FIGURE 7.4 Sedimentary log and photograph of the SWDs at exposure 2 at the Tributary site (Figure 7.2). The sediments have notably thinner units and less overall thickness than those at exposure 1. The colour of the photograph is deceptively light due to the need for flash photography at this shaded exposure. The two dates were determined by OSL, however, they are not reliable (see section 7.3.3).

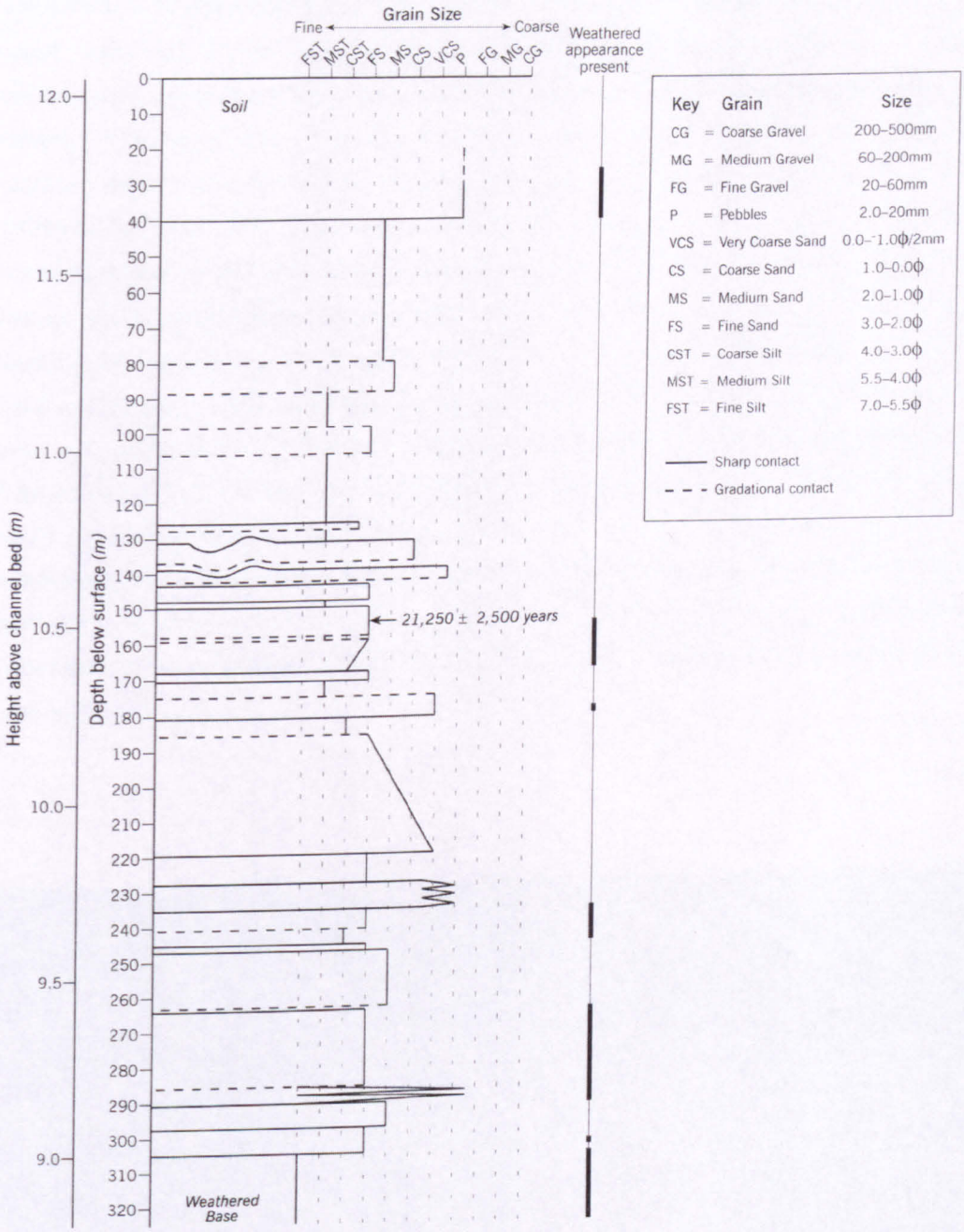

FIGURE 7.5 Sedimentary log of the SWDs at exposure 3 at the Tributary site (Figure 7.2). The section shows deposits of a similar thickness, sedimentary structure and appearance to those at exposure 1.

7.2.2 Boila rockshelter site

The Boila rockshelter is located at the mouth of the Lower Vikos Gorge, within the Old Klithonia Bridge study reach (Figure 6.4). The rockshelter is set in the north-facing gorge walls above the Late Pleistocene U4 sediments shown in Figure 6.4. The rockshelter opening is 17 m wide, whilst its floor covers c. 80 m^2 and lies c. 11 m above the modern channel bed (Figure 7.6) (Kotjabopoulou *et al.*, 1997). Excavations of the Boila rockshelter by a team of Greek

researchers took place between 1993 and 1997. The main cultural deposits are found in the upper layers and are up to 80 cm thick. Well-sorted, laminated fine-grained trunk stream sediments were discovered below the cultural layers (Figure 7.7 and Figure 7.8). These fines are clearly SWDs, laid down by large floods that overtopped the lip of the cave. Rockshelters are another common site for SWD accumulation (e.g. Patton and Dibble, 1982; O'Connor *et al.*, 1994), as the floor of the cave, offset from the main channel, provides a zone of rapid flow deceleration and hence fine sediment deposition (section 2.3.1). There appears to have been two distinct phases of SWD deposition. The upper 24 cm of the fines are inter-bedded fine sands and medium silts separated by sharp contacts (Figure 7.7). The layers are quite thin (c. 2 - 5 cm) horizontal laminae, some of which show upward fining characteristics. The deposits are of a clean pale cream colour (typically 2.5 Y 6/3), and do not show any signs of weathering (Figure 7.8). At 24 cm there is evidence for a distinct hiatus, with marked weathering features as well as small amounts of organic material (Figure 7.8). Below this point are older, more heavily weathered SWDs. They are also generally coarser, with thin bands of pebbles and coarse sands inter-bedded between coarse silt layers. The base of these fines grades into medium sized, limestone-dominated gravels set in a coarse sandy matrix which forms the bottom of the rockshelter stratigraphy.

FIGURE 7.6 Photograph of the Boila rockshelter during the summer 1997 excavations, looking upstream showing the bedrock wall.

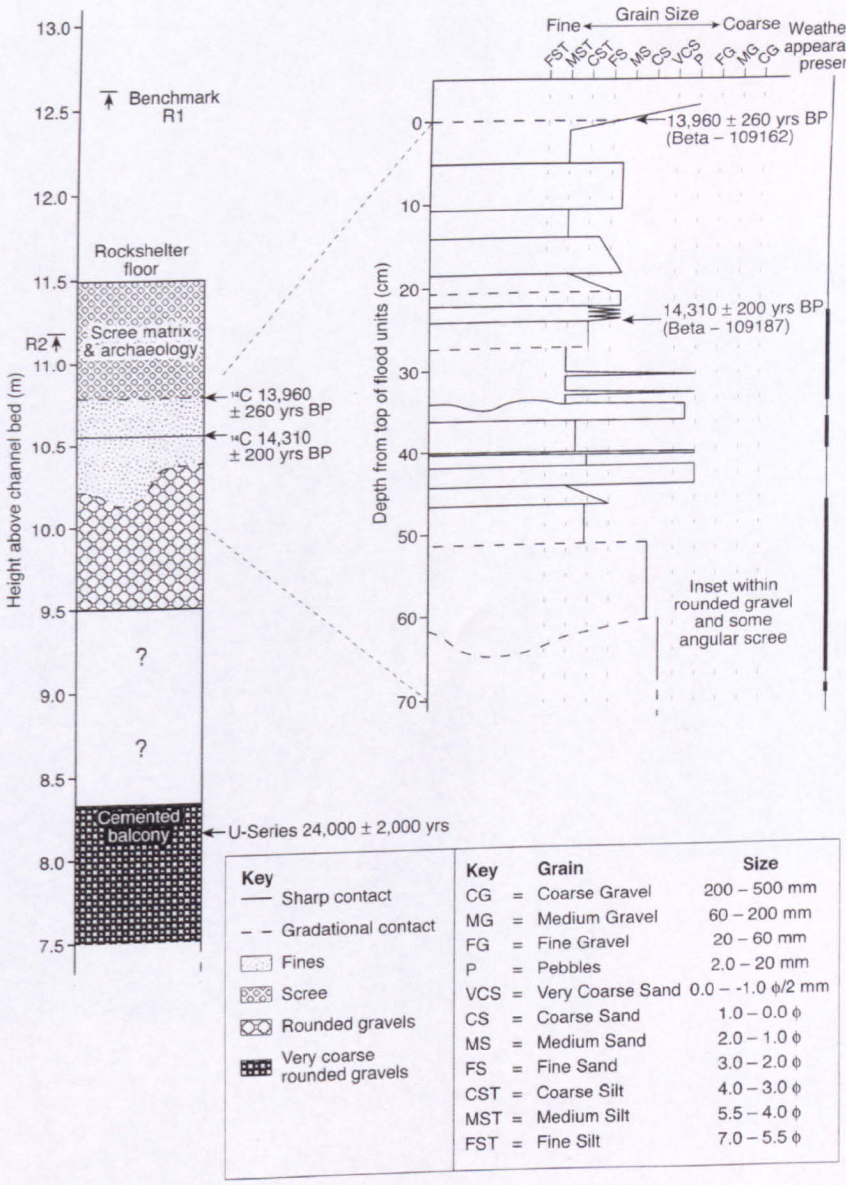

FIGURE 7.7 Section of the Boila rockshelter stratigraphy at the back trench of the rockshelter (showing the section between reference points (21,2) and (22,2) on Figure 22.3 of Kotjabopoulou *et al.*, 1997).

7.2.3 Old Klithonia Bridge site

The third SWD site is located c. 100 m from Boila, at the location of another U4 alluvial fill unit just downstream from Old Klithonia Bridge (Figure 6.4). The overall stratigraphy of the site is shown in Figure 7.9 and Figure 6.5. The main sequence of SWDs are located between 9 and 11.5 m above the modern channel, whilst a thinner band of fines also occurs below the cemented U4 sediments (Figure 7.9). The sequence of fine sediments is interrupted in many places by bands of pebbles or fine gravel throughout the sequence. Some of the sandy units have cross-bedded ripples, structures which are thought to occur due to some degree of pulsatory wave motion within the depositional environment (Kochel and Ritter, 1987; Kochel and Baker,

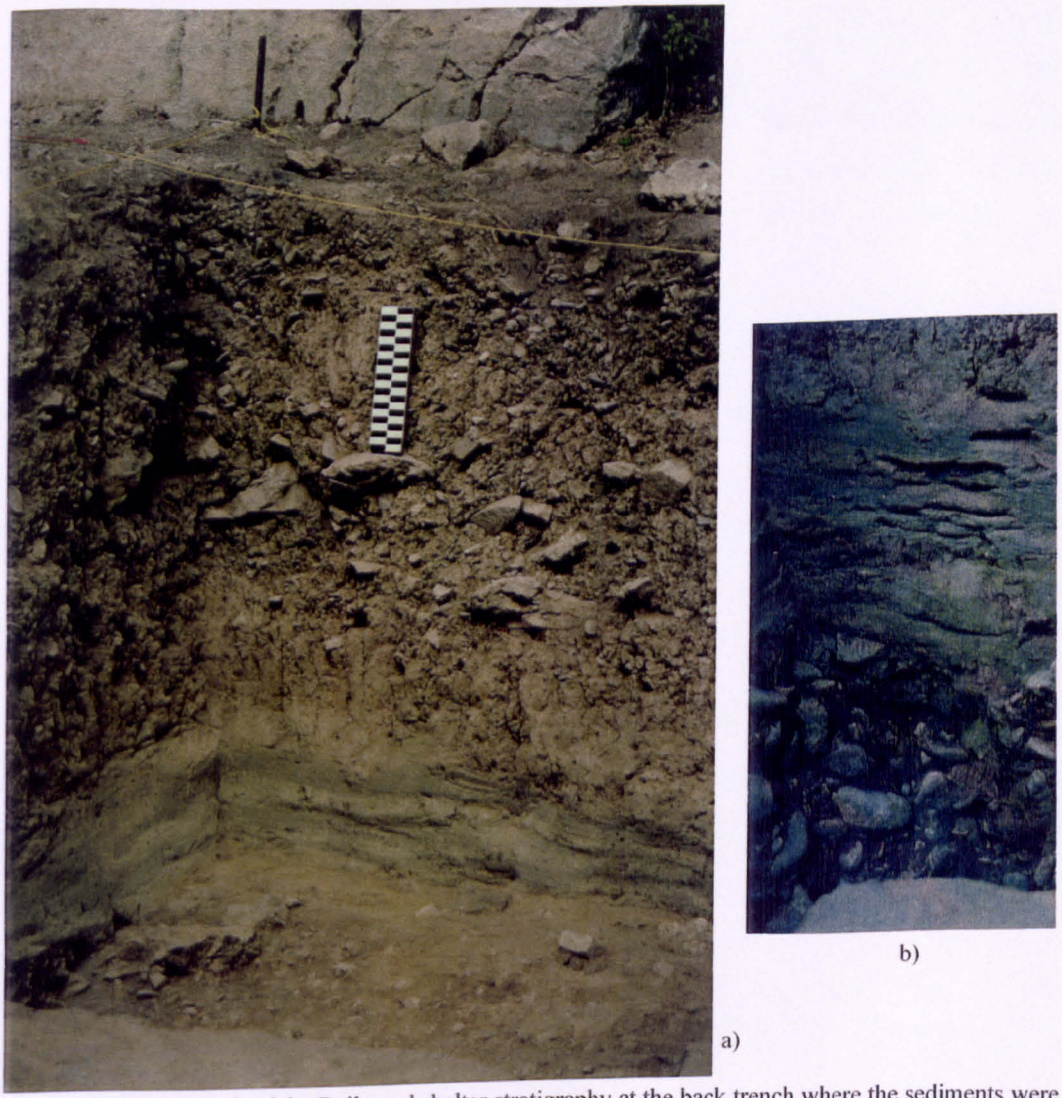

b)

a)

FIGURE 7.8 Photograph of the Boila rockshelter stratigraphy at the back trench where the sediments were examined and sampled in this study. The log for this section is shown in Figure 7.7. a) Shows the stratigraphy excavated to the point of the hiatus in sedimentation at 24 cm depth from the top of the flood units. The fine-grained SWDs are evident at the base of this section. b) Shows this same section when excavated to a deeper level, revealing the lower, less well preserved fines which are darker in colour, and overlying the gravels which fill the base of the rockshelter.

1988; Benito *et al.*, 1998). On the other hand, structureless fine-grained units are probably the result of particularly rapid deposition from suspension (Baker *et al.*, 1983a; Ely and Baker, 1985). The site is located at a point where the valley floor width increases markedly with the opening of the Lower Vikos Gorge onto the Konitsa basin. Areas of channel expansion allow slackwater zones to form in channel margin areas (section 2.3.1), which accounts for the existence of these deposits at the Old Klithonia Bridge.

7.2.4 Perspective

The SWDs are thick (>3 m at the Tributary site) and well preserved, and therefore provide the potential for palaeoflood reconstruction over the Late Pleistocene. These SWDs may have been

formed by a large number of flood events, although it may be an oversimplification to assume that all separate sedimentary layers represent individual flood events (Hattingh and Zawada, 1996). Section 7.4 provides quantitative sediment provenance information and the results of detailed textural analysis, to enable the differentiation of individual flood events within the SWD records. The dating results for these deposits are described in the following section.

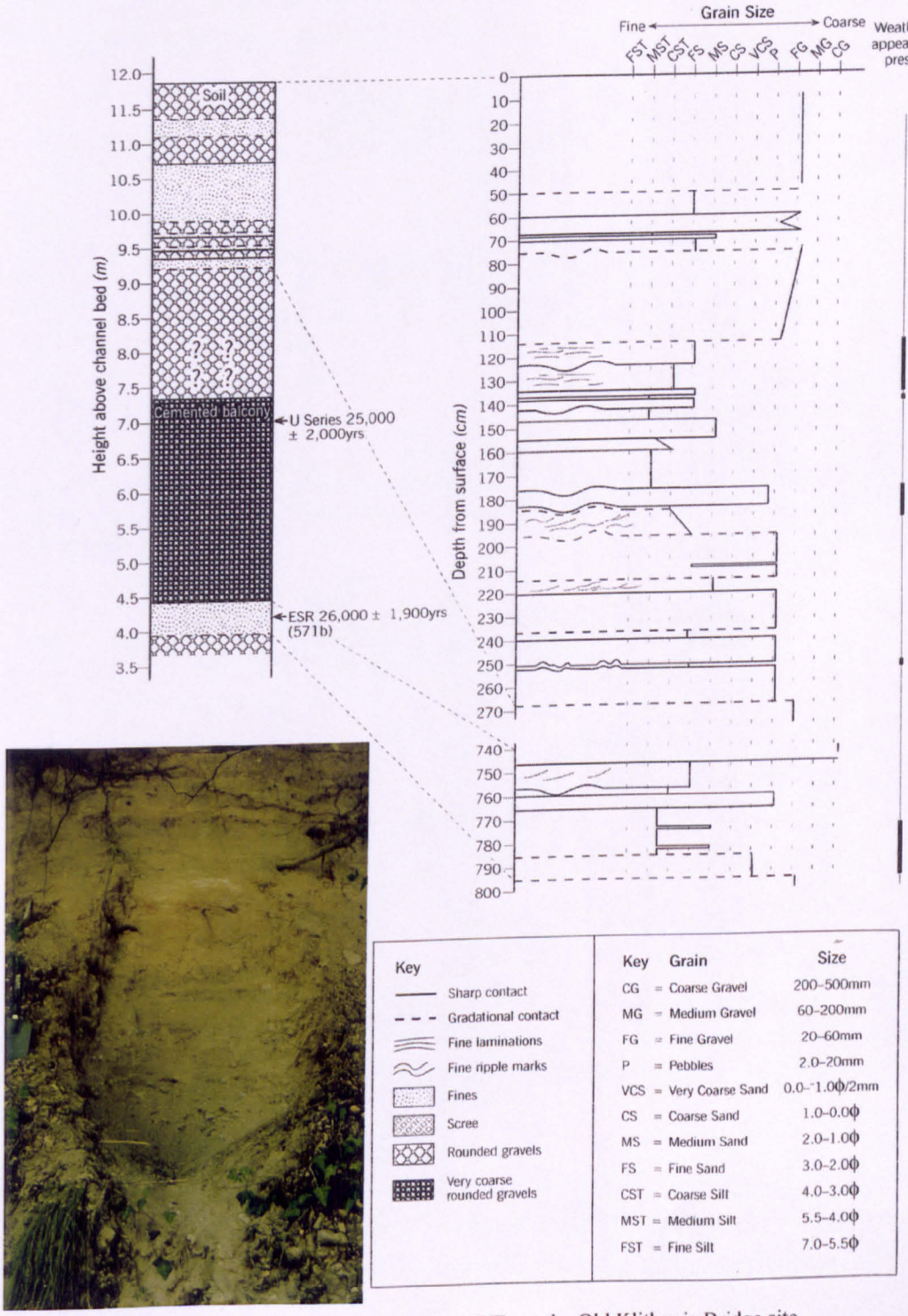

FIGURE 7.9 Sedimentary log and photograph of the SWDs at the Old Klithonia Bridge site.

Pages Missing not Available

184 + 185

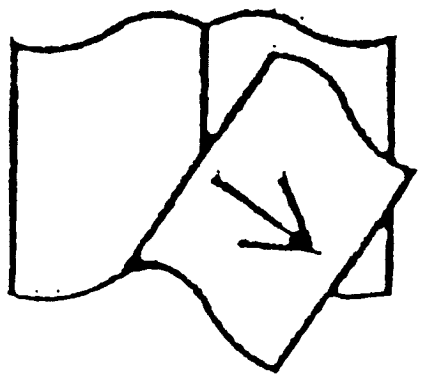

109162) and 17,297 ± 265 cal years (Beta-109187). However, neither of the two OSL ages (Table 7.1) are close to these dates. The single aliquot age estimate might be expected to be closer to the true age, as it samples only the most light sensitive traps. However, it appears to be c. 5 ka too young. The multiple aliquot determination could be taken as a maximum age estimate for the sediments, but is actually c. 8 ka too old. This provides independent confirmation that the OSL ages for this sample are unreliable, which can be accounted for by the evidence for insufficient bleaching of the sample prior to burial.

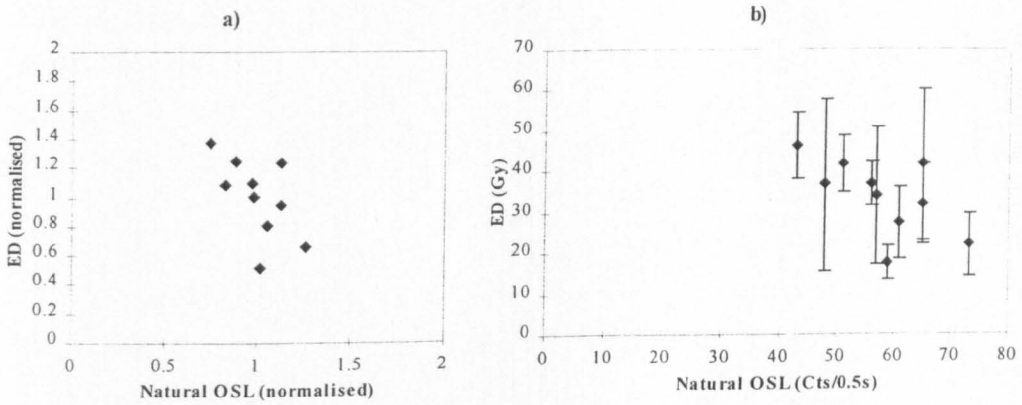

FIGURE 7.10 a) Single aliquot bleach test after Clarke (1996) for Shfd97088, the OSL sample taken from the Boila rockshelter site. b) Bleach test using the additive dose single aliquot method (after Duller, 1994) for the same sample.

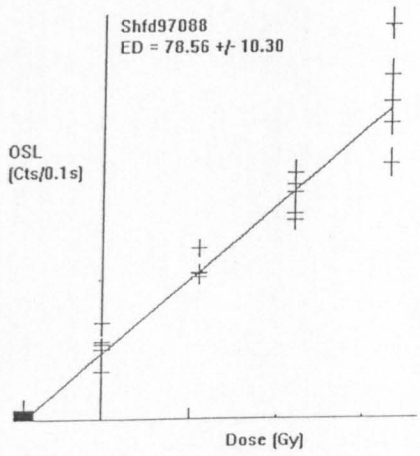

FIGURE 7.11 Additive growth curve using multiple aliquots for Shfd97088, the OSL sample taken from the Boila rockshelter site.

Similar bleaching tests were done on sample L3, taken from the fine-grained sediments described in the Klithi rockshelter reach (see section 6.3.4). These showed that this sample has been bleached more thoroughly, although probably not completely. There was still some

difference between the single and multiple aliquot estimates (Table 7.1) and the results can only be taken as maximum age estimates.

The dating results from the Tributary SWDs are also indicative of ineffective zeroing. These sediments have been deposited at the same time as those in exposure 3, which have been reliably dated in their mid-section to 21,250 ± 2500 years by uranium-series methods (section 7.3.2). However, the OSL dates from exposure 2 (Figure 7.4 and Table 7.1), although stratigraphically coherent, are much older than this, dated to c. 50 ka even in their upper horizons. These dates are far too old to agree with the uranium-series result, suggesting that the sediment was not bleached sufficiently at deposition. A period of c. 40 ka between these OSL samples, which were taken less than 80 cm apart, also seems highly unrealistic as there are no obvious signs of unconformities. Both samples exhibited large scatter around the growth curves.

There may be a variety of reasons for the unreliability of OSL dating in this study:

- The seasonally wet conditions and dense vegetation of the Voidomatis Basin may not be conducive to OSL dating, as shade in the valley floor may restrict bleaching.
- Large flood events are likely to have turbid flows, which could have impeded zeroing during transport.
- Uncertainty regarding the typical moisture content of these sediments for the time since deposition may have caused inaccuracies.

Whatever the cause, this section shows the importance of independent confirmation of OSL dating methods when being applied in new environments. It is clear that for this study, the results are unreliable, and consequently no further OSL dating has been attempted.

7.3.4 The chronology of Late Pleistocene flood deposits

The SWDs have proved quite difficult to date. OSL ages are unreliable, and cemented horizons or datable organic samples are rare. Nevertheless, direct dating has been achieved at two of the three sites. The floods which laid down the upper deposits at Boila occurred between 13,960 ± 260 (Beta-109162) and 14,310 ± 200 (Beta-109187) years BP. At some time before the latter of these dates, floods have laid down the lower SWDs at this site, which now exhibit a more weathered appearance. Flooding at the tributary site occurred around 21,250 ± 2500 years. Although not directly dated the SWDs at the Old Klithonia Bridge site were deposited either during or after U4 aggradation (c. 25 ± 2 ka), but probably no later than the flood sediments at Boila (~14 ka BP).

7.4 Reconstruction of Late Pleistocene flood events using sedimentological information

This section presents data on the grain-size characteristics, sediment provenance and thickness of sedimentary units within the slackwater sediments, with the aim of deriving detailed information about the palaeofloods recorded in the SWD stratigraphy. Following an

introduction to the data and the general characteristics of the deposits, the sedimentology of the SWDs are considered in detail to determine for each site: i) the number of flood events recorded; ii) the palaeoenvronmental conditions at the time of flooding; and iii) the magnitude of floods recorded.

7.4.1 Introduction

The basic sedimentological features of the SWDs have been described in section 7.2. Samples were taken from each sedimentary unit (section 4.3.3), and were analysed for grain size as described in section 4.5.5. Only the larger sedimentary units within each of the SWD sequences were analysed for provenance characteristics using the quantitative sediment fingerprinting technique described in Chapter 5. Provenance data were obtained for 14 units from the Tributary site, 10 from the Boila Rockshelter site and 17 from the Old Klithonia Bridge site.

Figure 7.12 shows the average d_{50} of the different SWDs, with the d_{50} range of samples at each site also shown to illustrate the variability between sedimentary units. All of the SWDs are considerably finer and better sorted than the modern in-channel fines or the fine fraction of Late Pleistocene alluvial units (Figure 7.12). The sediments at the Tributary and Boila sites are particularly fine, with median grain size only slightly higher than the U2 overbank alluvium, although they both show far greater variability between units. This variability is even greater in the SWDs at the Old Klithonia Bridge, with the range bring from less than 100 to greater than 600 microns. The coarser sedimentary units in the SWDs have probably resulted from very large floods, which have been capable of transporting sand-sized material to these high-level slackwater sites. It is clear that the Old Klithonia Bridge deposits are considerably coarser than at the other sites, suggesting a higher energy environment upon deposition.

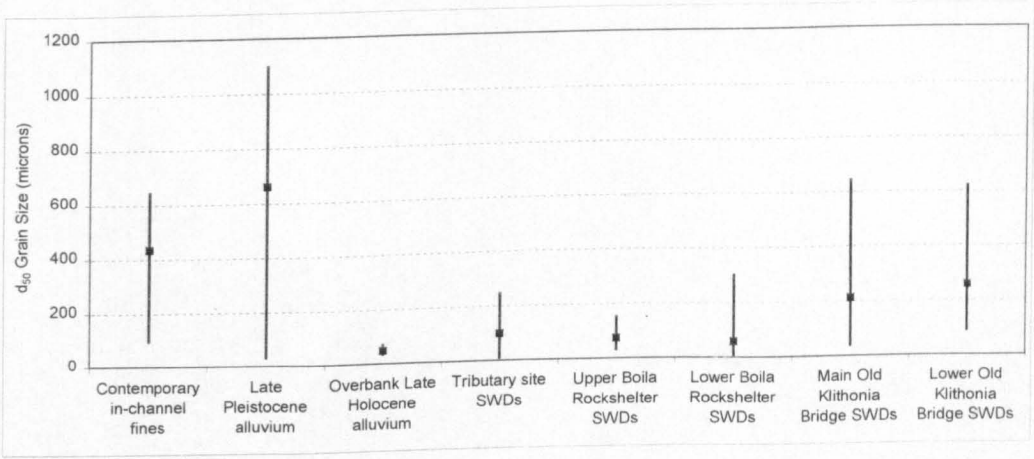

FIGURE 7.12 Graph showing the mean d_{50} of the <2 mm sediment from the different SWDs (shown by ■), with the d_{50} range from samples taken from each deposit also shown to illustrate the variability in median grain size at each site. The data for the three major types of valley fill alluvial deposits are shown for comparison. The data for Late Pleistocene alluvium is an average of samples taken from U4, U5, U6, and U7 deposits (Table 6.2).

The nature of the grain size distribution can be described through statistical parameters such as skewness and kurtosis that are determined by the shape of the distribution, and measures of central tendency, which describe the degree of sorting. The arithmetic skewness and kurtosis were calculated by the Coulter® LS™230 software using the equations described by Coulter® (1994). The standard deviation has been used as a measure of sorting within the <2 mm fraction. The % coefficient of variance is preferred by some authors (e.g. Lindholm, 1987) as it provides a relative measure of sorting scaled to the mean grain size. However, in this study it is the absolute degree of sorting within only the fine fraction that is of interest and therefore the standard deviation is the most useful sorting parameter.

These parameters are shown in Table 7.2. All of the SWDs show a general trend of a right skewed, and quite peaked leptokurtic distribution, although the strength of skewness and kurtosis varies somewhat between deposits. The degree of sorting varies significantly between the SWD sites, with the deposits at Old Klithonia Bridge, and to a lesser extent at the Tributary site, showing notably poorer sorting than those at Boila. However, in general terms, all of the SWDs have a fairly similar type of distribution. This is in contrast to the considerable variability displayed by the various types of valley fill alluvium (Table 7.2).

In the following more detailed investigation of the SWDs, the lower deposits at Old Klithonia Bridge have not been studied in detail. Their only moderate height above the modern channel (<4 m) compared to the other deposits (which are typically at 10 - 11 m) means that it is unlikely that these deposits originate from floods of an exceptionally high magnitude. They are consequently of less relevance for this study.

	Mean d_{50} (microns)	Average sorting (STD)	Average skewness (arithmetic)	Average kurtosis (arithmetic)
Contemporary in-channel fines	434.90	494.90	0.99	0.27
Late Pleistocene alluvium (<2 mm)	660.20	642.00	0.34	-1.27
Overbank Late Holocene alluvium	49.85	189.70	6.79	51.91
Tributary SWDs	99.75	205.99	2.14	5.98
Upper Boila SWDs	74.48	112.89	2.35	8.84
Lower Boila SWDs	59.04	173.97	1.59	1.91
Main OKB SWDs	212.75	257.76	2.12	7.07
Lower OKB SWDs	259.89	377.78	2.48	11.05

TABLE 7.2 Mean grain size distribution parameters for the <2 mm fraction of the SWDs and major valley fill alluvial units. The sorting parameter is the standard deviation from the mean (STD). Positive values for arithmetic skewness indicate a right skewed distribution, negative values a left skewed. Positive values for arithmetic kurtosis indicate a leptokurtic (more peaked) distribution, negative values a platykurtic (flatter). A sample with zero values for both skewness and kurtosis would display a normal distribution. The data for Late Pleistocene alluvium is an average of samples taken from U4, U5, U6, and U7 deposits (Table 6.2).

7.4.2 Identification of the number of palaeoflood events

The identification of specific flood events within SWDs is an important step in obtaining detailed palaeoflood information (section 2.3.2). Previous studies have normally differentiated flood events on the basis of sedimentary features such as abrupt vertical changes in grain size,

buried palaeosols or distinct colour changes (Baker *et al.*, 1983a; Ely and Baker, 1985; Kochel and Baker, 1988; Ely, 1997). However, in some cases accumulations of slackwater sediments can be relatively homogenous, with insufficient contrasts between sedimentary units to allow separate floods to be distinguished through visual inspection (Hattingh and Zawada, 1996). Although field logging revealed clear textural variations within each SWD in the Voidomatis basin, there was little colour change over the sections and very few distinct separating markers between flood events such as evidence of sub-aerial exposure or layers of colluvium (Figures 7.3, 7.5, 7.7 and 7.9). More detailed sedimentary analyses of the slackwater sediments was therefore undertaken to enable flood events to be distinguished with greater confidence. The results of detailed grain size analysis (Figure 7.13a, b and c), quantitative sediment fingerprinting and magnetic susceptibility measurement (Figures 7.14 to 7.16) and sedimentary logging (Figures 7.3, 7.5, 7.7 and 7.9) have been used in combination for flood event discrimination. Five flood events have been identified in the sediments at Boila, twelve at the Tributary site and nine at Old Klithonia Bridge (Figure 7.13a, b and c). The grain size data proved particularly valuable for this purpose, providing a number of objective quantitative parameters for identifying the degree textural differences between each sedimentary unit. Many commonly used grain size parameters and statistics are shown for each of the SWD sites in Figure 7.13. The amount of medium sand (0.25 to 0.5 mm) is also displayed, as Knox (1987) found that variations within this fraction were the most useful for defining the boundaries between fine-grained flood units.

Different flood layers were perhaps most distinct at Boila (Figure 7.13a). The base of the flood sediments is clearly marked by a gravel fill at 65 cm, which displays very different grain size and provenance characteristics to the overlying flood sediments (Figure 7.13a and Figure 7.14). There is also a hiatus in the record at 24 cm, below which are the darker brown lower sediments which shows signs of weathering and are predominantly flysch-derived, whilst above this are the unweathered cream-coloured sediments, which have a significant limestone component (Figure 7.14). The higher magnetic susceptibility of the lower sediments is probably a result of *in situ* weathering processes (Figure 7.14). These lower sediments contain three clear flood events, Flood B1 being separated by a band of scree, and B2 being distinctly coarser, less sorted, and having a less positively skewed and leptokurtic (peaked) distribution than the overlying B3 sediments. The contact between B2 and B3 at 34.5 cm is undulating (Figure 7.7), probably representing and uneven antecedent surface with the onset of Flood B3, or some erosion at the beginning of the flood event. The upper sediments are believed to have been deposited by two major flood events, which agrees with other detailed micromorphological investigations of the Boila sequence (Karkanas, unpublished). Sediments from Flood B4 are distinct from B5, as they are much finer in texture, have generally thinner sedimentary units, and have significantly higher flysch contents. B5 sediments are some of the coarsest in the

section, composed of 55 - 80 % sand (Figure 7.13a), and contain a much more significant limestone and dolomite component (Figure 7.14).

The identification of flood units at the other two sites was slightly more complex. Upon field inspection of the Tributary site, it was difficult to determine the base of the flood sediments. However, fingerprinting results show that the very fine-grained material below 260 cm is almost entirely flysch-derived, in contrast to the generally high limestone and till contents throughout the rest of the section (Figure 7.15). The uranium-series date from this site (21.25 ±2.5 ka; section 7.3.2) suggests that these sediments were deposited around the time of the LGM, when the main channel fine sediment flux was dominated by limestone and till (section 6.4.3). The basal flysch-dominated sediments are therefore unlikely to have originated from the main channel, but instead are probably local tributary alluvium. The tributary largely drains part of the flysch outcrops which surround the Lower Vikos Gorge (Figure 3.8), and the fine sediments are therefore dominated by this source. The oldest main channel flood at this site is therefore recorded at 260 cm depth, and slackwater sediments continue until 50 cm, where a soil with distinctly high magnetic susceptibility (>90 10^{-8} m^3 kg^{-1}) and fine texture completes the section (Figure 7.13b and Figure 7.15).

Twelve flood units have been identified, largely on the basis of grain size. The section displays a rhythmic textural pattern, with regular 'couplets' of coarser- and finer-grained sedimentary units (Figure 7.3 and Figure 7.13b). Such sand-silt rhythmites have frequently been observed in other studies of fine-grained flood sedimentation, with the coarse sediment generally believed to have been deposited more rapidly from suspension during the early stages of the flood (rising limb), and the finer sediments being deposited later during the falling limb as a fine drape or capping (Kochel and Baker, 1982, 1988; Macklin *et al.*, 1992b; Benito *et al.*, 1998). The coarse layer almost always lies at the base of the slackwater sediments at both the Tributary and Old Klithonia Bridge sites, and upper flood B5 at Boila also displays this typical fining upward pattern (Figure 7.13a, b and c). The fine sediment layers typically have a d_{50} of over 50% less than the basal sandy layer, and have more positively skewed and more leptokurtic (peaked) distributions (Figure 7.13b and c). These fining-upward rhythmites have formed the basis for distinguishing the majority of the flood units for the Tributary site. The provenance of these flood units is fairly similar. However, T2, T5 and T11 had much larger flysch proportions than sediments above and below, confirming the likelihood that they have originated from

---

FIGURE 7.13 (following pages) Grain size parameters for the slackwater sediments which have been used to identify specific flood events within the SWDs at a) the Boila rockshelter site, b) the Tributary site and c) the Old Klithonia Bridge site. A sample was taken from each sedimentary unit at each site, with the analytical results presented for the depth that each unit covered. The medium sand % refers to the 0.25 - 0.50 mm fraction. The sorting parameter shown is the standard deviation (STD), which identifies absolute degrees sorting within the <2 mm fraction. The skewness and kurtosis are both arithmetic parameters calculated as described in Coulter® (1994).

a) Boila Rockshelter site slackwater sediments

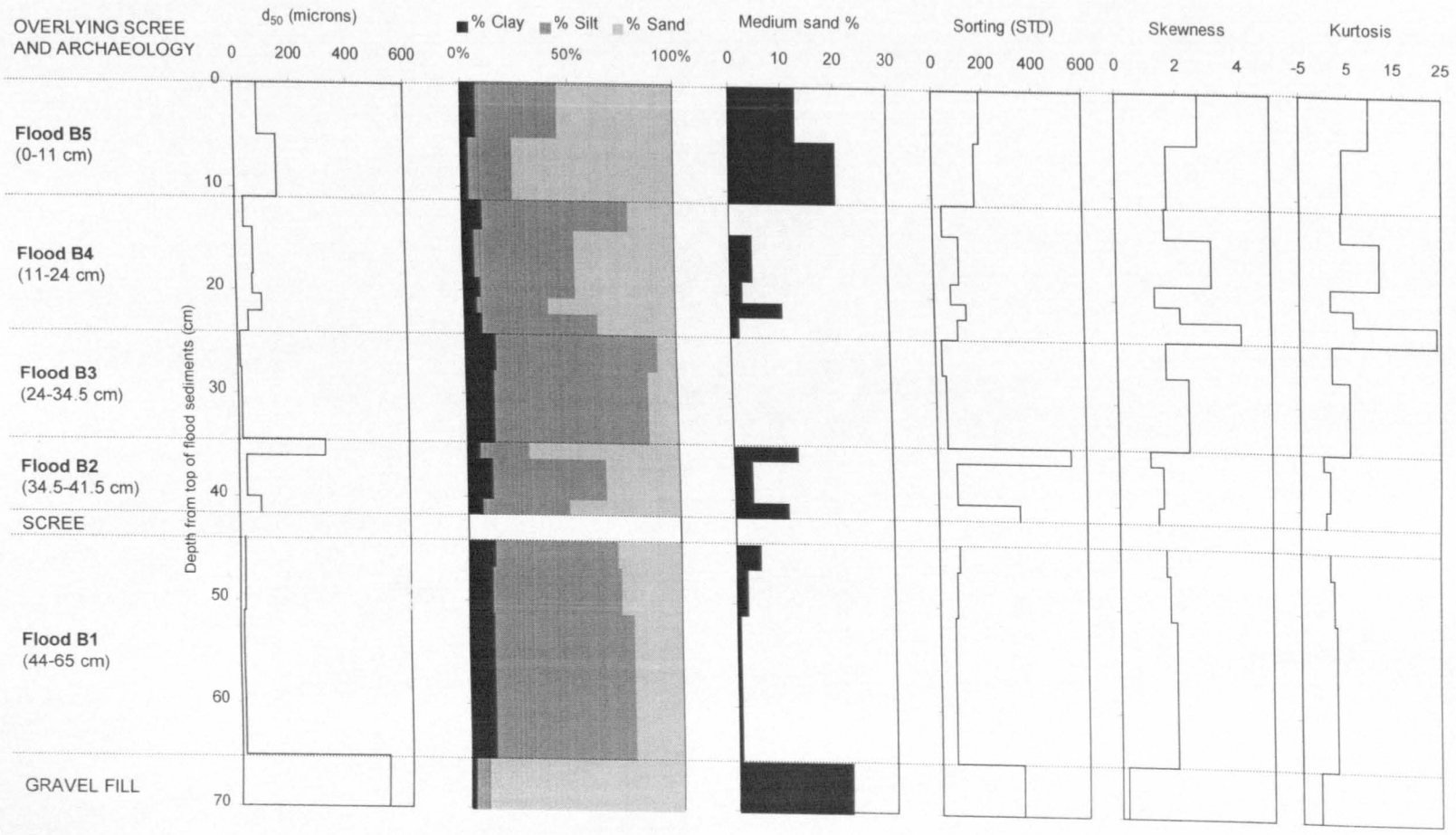

b) Tributary site slackwater sediments

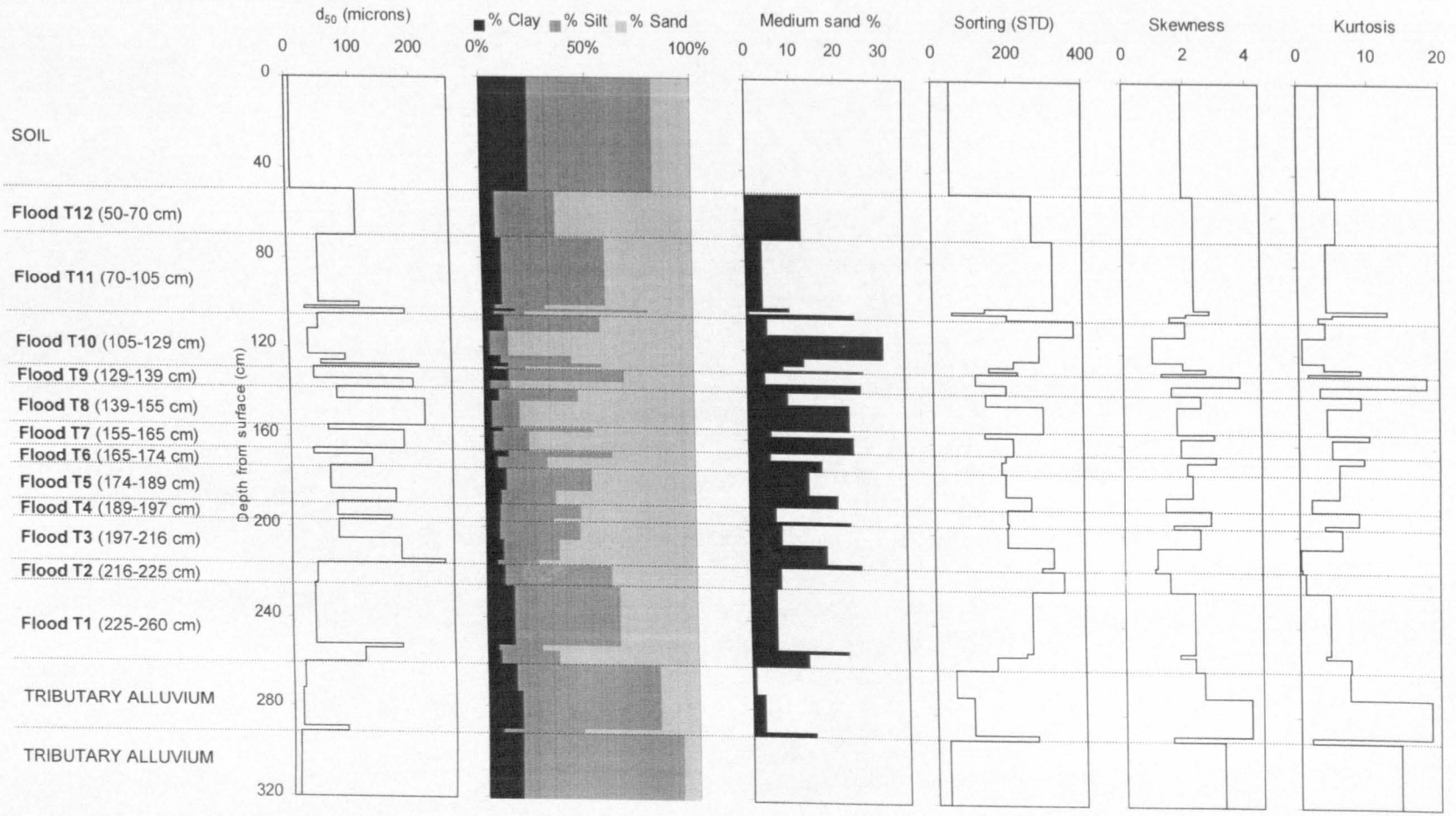

c) Old Klithonia Bridge site slackwater sediments

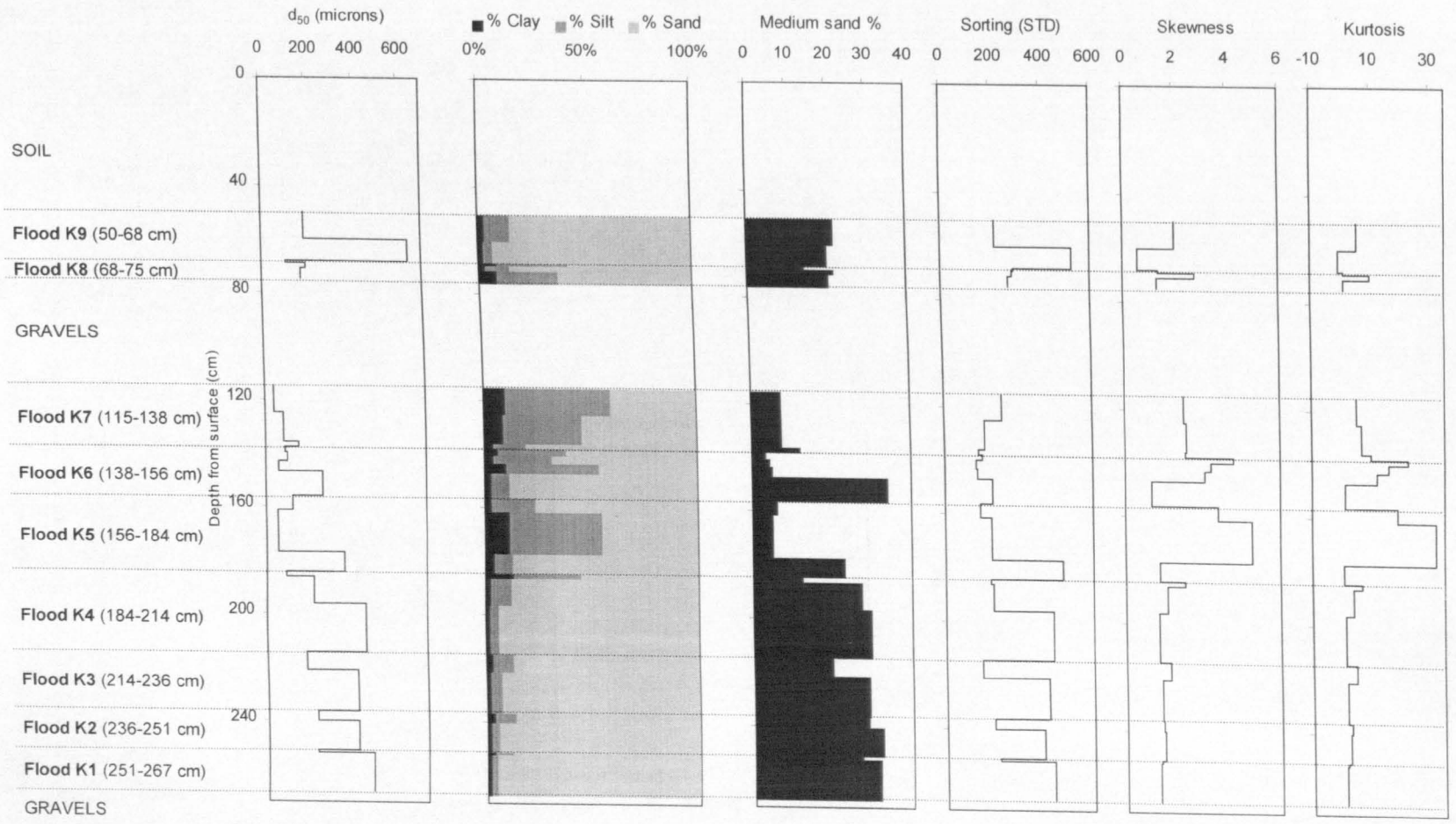

different flood events (Figure 7.15). T2 (216 - 225 cm) was also distinct as a separate fining upward unit on the sedimentary log (Figure 7.3).

Flood events at the Old Klithonia Bridge site have mainly also been differentiated using coarse-fine couplets identified from grain size analysis (Figure 7.13c). Nine floods have been distinguished, all showing this fining upward nature. A 40 cm layer of gravels in the upper part of the section serves as a clear separator of flood K7 and K8. The upper layer of flood unit K7 may have been sub-aerially exposed for a significant period, as the top layer of this unit has a relatively high magnetic susceptibility (>40 10^{-8} m^3 kg^{-1}) and contains a significant amount of terra rossa (Figure 7.16), both of which may have formed by *in situ* weathering. Other than this layer, these flood sediments have very similar provenance characteristics, except for variations in the relative amounts of limestone and till. The relative amount these two sources seems to be related to grain size, the coarser basal layers having less till and more limestone than the finer cappings. Thus with each flood having a progressive decrease in the limestone:till ratio, the fingerprinting results also depict the separate flood units. This pattern is to be expected, particularly if these sediments were deposited during periods of glacial sediment transfer, as the fine matrix of till is typically of a very silty nature, whereas limestone may have been originating more from frost weathering of bedrock and thus more likely to be associated with the coarser sand fraction. It should be noted that whilst not all of the flood unit divides occur at sharp sedimentary contacts on Figure 7.9, this does not mean that they are incorrectly placed. Sharp contacts suggest non-erosional flows entered the site (Benito *et al.*, 1998), but gradational contacts could equally mark the break between flood units if the depositing flow slightly eroded the pre-flood surface, as has been observed in previous studies (Hattingh and Zawada, 1996).

7.4.3 Sedimentological evidence regarding the timing of palaeofloods

In section 7.4.2 the sediment fingerprinting data have been of considerable value for interpreting the slackwater sediments. They have served to effectively differentiate main channel flood sediments from more local sources, whilst both inter- and intra-flood variations in provenance have proved valuable for distinguishing individual flood events. However, the fingerprinting data are also useful for palaeoenvironmental interpretation, as was described in Chapter 5 and applied to the alluvial fill sediments in Chapter 6. This could be particularly valuable considering the complexities in obtaining a large number of reliable dates for the SWDs (section 7.3). The following two sections discus both inter- and intra-site provenance features.

7.4.3.1 Inter-site provenance comparisons

In Figure 7.17 the average source characteristics of samples taken from sedimentary units at each SWD site are shown, with the fingerprints for sediments deposited during warm (present) and cold phase (LGM) climate included for reference. The provenance data shown for the Boila site is an average of the samples taken from the upper unweathered deposits, which are

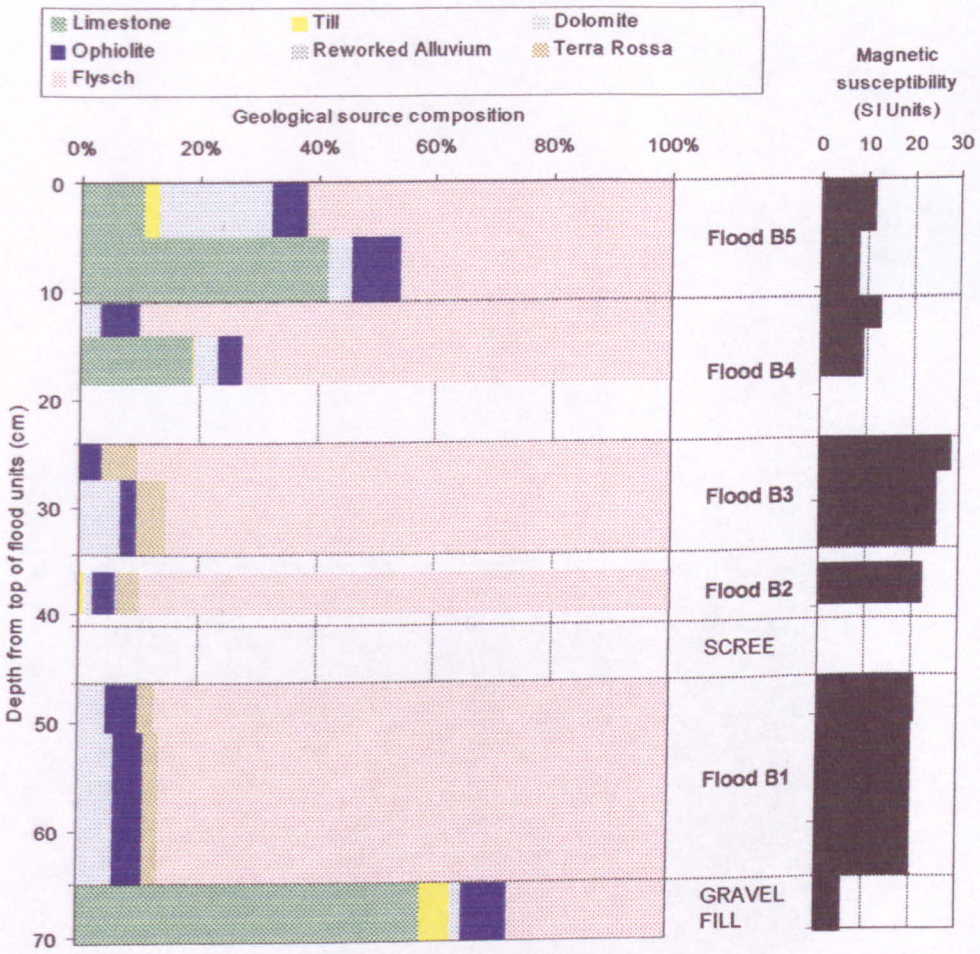

FIGURE 7.14 Fine sediment fingerprinting results and mass-specific low-frequency magnetic susceptibility for the slackwater sediments at the Boila rockshelter site. The fingerprinting results have been determined as described in Chapter 5. The magnetic susceptibility is shown in SI Units ($10^{-8}m^3kg^{-1}$).

bracketed between the two ^{14}C dates on Figure 7.7. There are clear contrasts between the different sites. The SWDs at Boila show very similar characteristics to the sediments that are typical of the modern warm phase climate, with a large proportion of flysch and very little limestone or till (Figure 7.17). This would suggest that at c. 14,000 years BP (c. 17,000 cal years), when these flood sediments were deposited, glacial sediment inputs had waned following the Last Glacial Maximum (LGM), and that environmental conditions in the catchment may have been similar to those today. Such provenance characteristics are coherent with the dating results for this site, which indicate that these floods occurred a considerable time after the LGM. They are also consistent with the sedimentological sequence from Klithi (core Y25), which shows increased flysch accumulation over the Lateglacial (Woodward, 1997). The characteristics of the sediments in both the Old Klithonia Bridge and Tributary SWDs are very

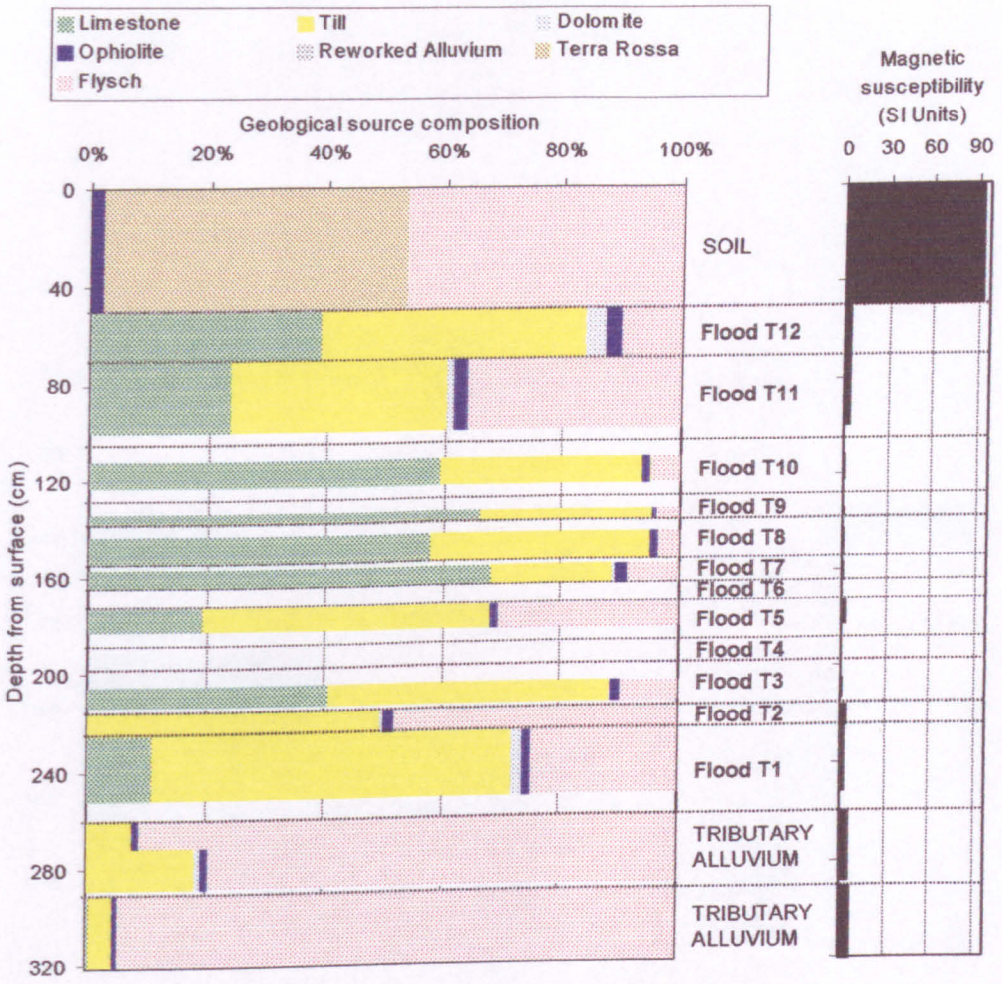

FIGURE 7.15 Fine sediment fingerprinting results and mass-specific low-frequency magnetic susceptibility for the slackwater sediments at the Tributary site. The fingerprinting results have been determined as described in Chapter 5. The magnetic susceptibility is shown in SI Units (10^{-8} m^3 kg^{-1}).

different, with a dominance of limestone and till that is comparable to that of the alluvial unit deposited at the LGM (Figure 7.17). This suggests cold phase deposition of these flood sediments, which is consistent with the date of 21,250 ± 2500 years at the Tributary site. The sediments at Old Klithonia Bridge show very similar source characteristics to the Tributary site and, given their stratigraphic context discussed in sections 7.2 and 7.3, it is probable that they have been deposited during the same period.

7.4.3.2 Intra-site provenance variations

Fine-grained sediments that have accumulated over time, such as these SWDs, may contain valuable information regarding changes in environmental conditions during that period. For example, sedimentological analysis of fines accumulated in the Klithi rockshelter has enabled changes caused by the Last Glacial-Interglacial Transition to be detected in this stratigraphy

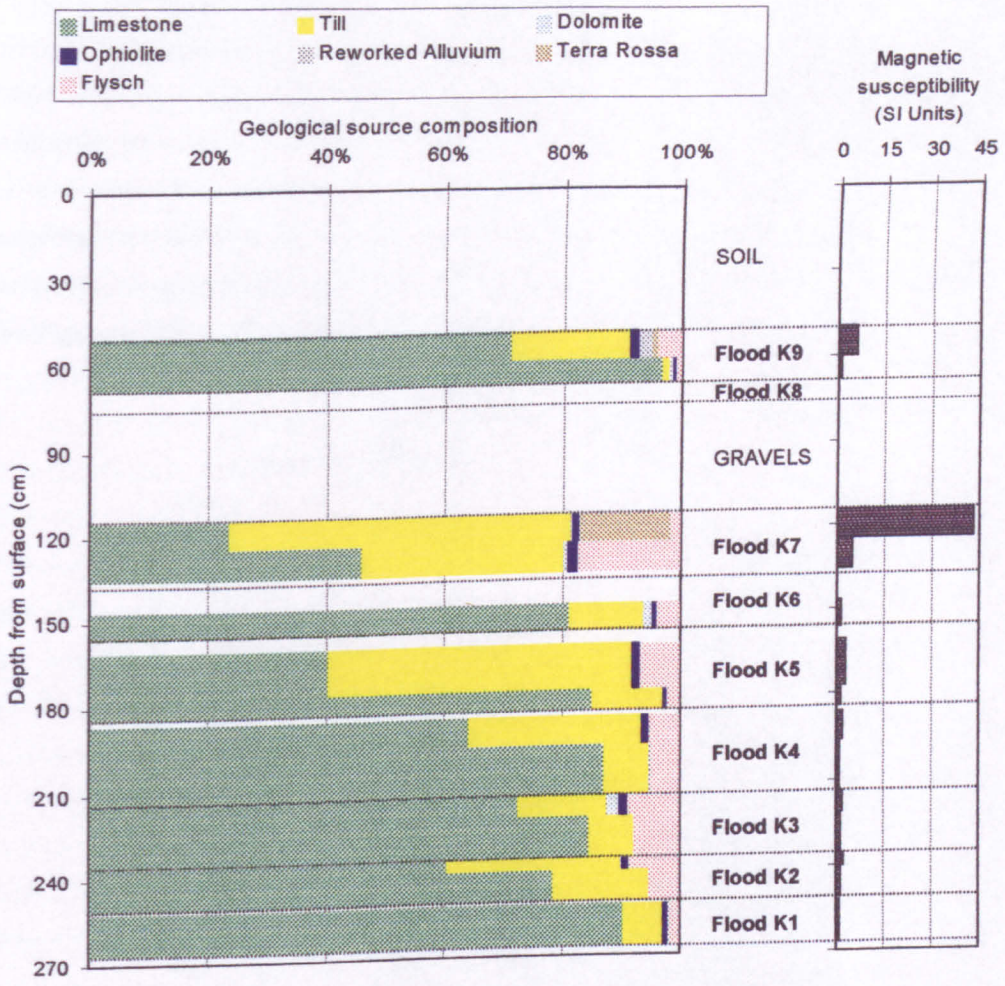

FIGURE 7.16 Fine sediment fingerprinting results and mass-specific low-frequency magnetic susceptibility for the slackwater sediments at the Old Klithonia Bridge site. The fingerprinting results have been determined as described in Chapter 5. The magnetic susceptibility is shown in SI Units (10^{-8} m^3 kg^{-1}).

(Woodward, 1997). Variations in provenance at each SWD site could contain important information regarding the timescale encompassed by the successive flood events at each site. The fingerprinting results regarding the cold phase flood sedimentation at the Tributary and Old Klithonia Bridge sites are shown in Figure 7.15 and Figure 7.16. The Tributary sediments may contain more till due to their finer texture, with till-derived materials being more commonly associated with silts and clays and limestone with the sand fraction during the period of cold phase sediment transfer. These grain size effects probably account for the increase in till between floods K1 to K7 at Old Klithonia Bridge (Figure 7.13c), and the lesser amounts of limestone in finer units at the top and bottom of the flood sequence at the Tributary site (Figure 7.13b). Another difference is that the Tributary site deposits contain significantly more flysch. A good deal of confidence can be placed in the prediction for flysch as this has been shown to be one of the most reliably predicted sources in the fingerprinting procedure (section 5.3.3).

However, this difference may be due to the incorporation of a minor component of local flysch-dominated tributary fines during flooding. The mouth of this tributary during a contemporary flood is shown in Figure 2.8, where the mixing of dark brown flysch fines from the tributary with paler main channel suspended sediments can clearly be seen. Thus the difference in the amount of flysch between the two sites does not necessarily mean that the sediments were deposited at a different time. It should also be borne in mind that the amount of tributary sediments incorporated in the SWDs could vary between each flood event, which could explain the slight variations in flysch content between flood events at the Tributary site (Figure 7.15).

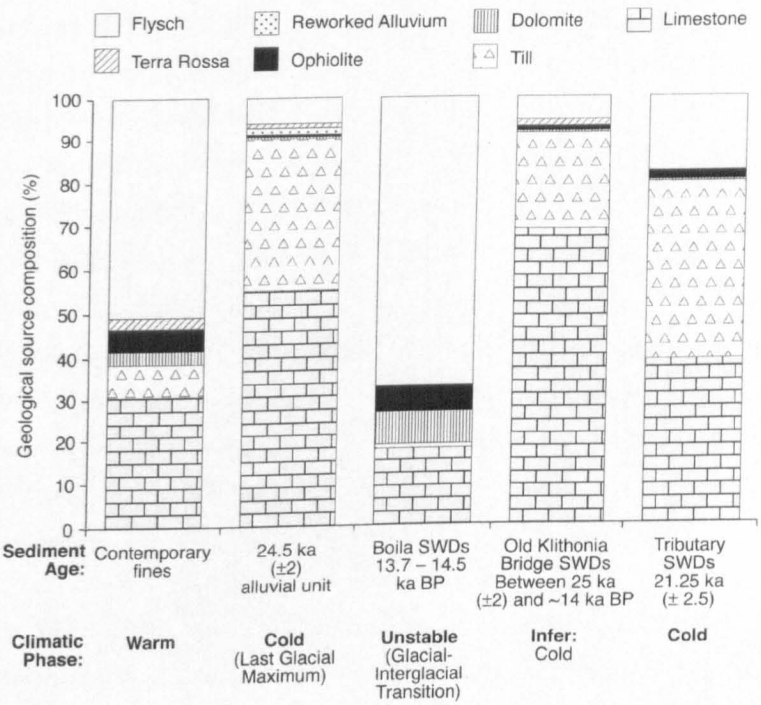

FIGURE 7.17 Sediment fingerprinting results from the palaeoflood slackwater deposits at the three sites. The sediment provenance signatures described in Chapter 6 for contemporary fines and U4 alluvium deposited at the LGM are shown for comparison. Chronological data and proposed climatic conditions are also shown.

Aside from these variations, the general pattern at both sites is one of broadly similar provenance between each of the flood events. The provenance of every flood event is dominated by a combination of limestone and till, the main components of glacial sediment transfer. Throughout each SWD sequence there is no consistent change which could have been caused by changing catchment conditions. Even though the Old Klithonia Bridge deposits show evidence for a hiatus at the top of flood unit K7 (section 7.4.2 and Figure 7.15), K8 and K9 still show very similar characteristics to the earlier flood events. Overall, it seems that the series of floods at both sites has probably occurred over a relatively short period of time during the Lateglacial, when catchment conditions did not change significantly. In the absence of direct dating of the

Old Klithonia Bridge deposits, it remains unclear whether some of the floods at the two sites may be contemporaneous.

There are greater contrasts within the Boila flood sediments (Figure 7.14). The sediments below the 24 cm hiatus point are very homogenous in terms provenance, and perhaps surprisingly dominated by between 80 to 90% flysch. This is in stark contrast to the fine matrix of the gravel fill which show characteristics associated with cold phase sedimentation, and probably relates to U4 or even earlier deposition (Table 6.2). However, micromorphological evidence (Karkanas, unpublished) and the anomalously high proportion of terra rossa and magnetic susceptibility measurements compared to surrounding sediments (Figure 7.14), indicates that these sediments have been substantially altered by *in situ* diagenesis, which has distorted the primary sediment source signal. The upper (above 24 cm) flood sediments are, in contrast, relatively free of weathering features. Floods B4 and B5 do show some sediment source differences, with the later unit having lower flysch proportions but larger amounts of limestone and dolomite. However, this difference is likely to be related to some differences in the source of sediment runoff during each flood event, which has been observed in contemporary river systems (e.g. Collins *et al.*, 1998), rather than a wholesale change in catchment environment. There may also again be some grain size effects on the provenance of these deposits. However, in every sedimentary unit, flysch is the dominant sediment source, so the indication of a relatively warm (non-glacial) catchment environment prevails nonetheless (Figure 7.14). There is no evidence for a significant hiatus between these two flood events, and thus the catchment environment was probably comparable during each event.

The discussion in this section serves to demonstrate the value of quantitative fingerprinting for interpreting the timing of palaeoflood slackwater sediment deposition. It is perhaps surprising that this is only the second SWD provenance study in the literature, the first being Saynor and Erskine (1993). Even without being able to obtain dates for all of the deposits, the fingerprinting has enabled an interpretation of the timing of Late Pleistocene flood events and the nature of the catchment environment during each period of flooding. In combination with uranium-series and ^{14}C dating, the fingerprinting shows that between the flooding of the Tributary/Old Klithonia Bridge sites and the Boila Rockshelter site, a major change in the environment of the Voidomatis catchment took place. The Tributary site has been shown to be flooded by 12 events during a relatively short period of time around 21,250 ± 2500 years, a minimum age date obtained for the mid-section of the deposits (Figure 7.5), probably equating to floods T7 or T8. Thus many of the Tributary site floods, and particularly those in the mid- and upper-section, probably occurred several thousand years after the peak of sediment supply at the Last Glacial Maximum and the period of U4 valley floor sedimentation which has been dated to a minimum age of 24,000 ± 2000 years (Table 6.2). Discussion in section 6.6 and Macklin *et al.* (1997) have postulated that there was an earlier expansion and retreat of valley glaciers in the Voidomatis

basin compared to the main LGM recognised elsewhere in Europe. However, the Tributary flood sediments (and those at Old Klithonia Bridge) still strongly resemble cold phase glacial sediment transfer, with large amounts of both limestone and till. Thus during many of the Tributary site floods (c. 21,250 ± 2500 years) the Voidomatis was probably experiencing the onset of 'paraglacial' conditions. This refers to the state when the availability and flux of sediment continues to reflect glacial conditions even though glacial activity has waned to disproportionately low or absent levels (Church and Ryder, 1972). Instead, sediments delivered by former glacial action are being redistributed through the catchment. The length of this postglacial relaxation time, which can be termed the 'paraglacial cycle', may vary from a few thousand years for upland basins on Baffin Island (Church and Ryder, 1972) to tens of thousands of years for large basins in British Columbia (Church and Slaymaker, 1989). The contrasting fingerprinting results for the upper deposits at Boila appear to constrain the timing of the end of the paraglacial cycle in the Voidomatis basin. These flood sediments are dominated by flysch to an extent akin to modern environmental conditions (Figure 7.17). The upper Boila floods B4 and B5 occurred at c. 14,000 years BP (c. 17,000 cal years), by which time cold phase glacial style sediment fluxes had diminished and a larger component of the sediment yield was being delivered from the erodible flysch slopes. Thus the analysis of these flood deposits has given an unusually detailed insight into landscape changes associated with the transition to interglacial conditions during the Late Würm. This period saw a fairly short paraglacial cycle (c.7000 years at most) and consequently a quite rapid transition to the type of sediment fluxes that would be expected for non-glacial catchment conditions. The geomorphological implications of these results are discussed further in section 7.6.

7.4.4 Reconstruction of palaeoflood magnitude

The most common palaeoflood magnitude reconstruction approach is to use the height of the SWD as a palaeostage indicator (PSI), and then use step-backwater models such as HEC-2 to estimate the palaeodischarge (section 2.3.3). For this approach to be appropriate, several important assumptions must be valid (see section 2.3.3.1). One of these is that the geometry of the study reach has not changed significantly, with a stable channel cross section and no significant aggradation or incision. The validity of this assumption has been assessed in this study through a comprehensive investigation of river terraces and valley fill sediments located in study reaches encompassing the SWD sites (Figure 4.5). The results of this work have been described in Chapter 6 for the purposes of investigating the long-term development of the Voidomatis River. This information can be used here to evaluate the stability of the channel over time.

In Chapter 6, six phases of aggradation were identified in the Voidomatis River during and since the Late Pleistocene (Table 6.2). The coarse-grained Late Pleistocene sediments (U7-U4) represent former in-channel gravels, therefore providing an approximation of the position

of the river bed at the time. The gravel base of fine-grained Late Holocene floodplain unit U2 serves a similar purpose, as these are also former channel bed sediments which have subsequently been buried by overbank sedimentation. This record of bed level changes is summarised in Figure 7.18, which shows data for alluvial deposits whose height and age are accurately known. The dated Late Pleistocene units U4 to U7 are shown, along with the hearth date for Late Holocene U2 alluviation. Figure 7.18 also includes the ESR date of 26,000 ± 1900 (571b) from SWDs beneath the U4 sediments at Old Klithonia Bridge (Lewin *et al.*, 1991) (Figure 6.5), which indicates that the river bed was no higher than c. 4 m above the modern channel bed at this time. Rapid aggradation of LGM U4 sediments was followed by progressive incision, which may have been interrupted at some point by aggradation of the poorly constrained U3 sediments (Table 6.2). The implications of this alluvial record are that the times of major SWD deposition, as shown by the dates from the Tributary and Boila sites on Figure 7.18, the height of the river bed was probably very different to that of today. Since the high stand of the LGM U4 aggradation, both the height of the channel bed and the overall channel geometry will have changed a great deal, with massive volumes of Late Pleistocene alluvium having been reworked to lower the channel to its current position. The assumption of no changes in the valley floor configuration is therefore invalid.

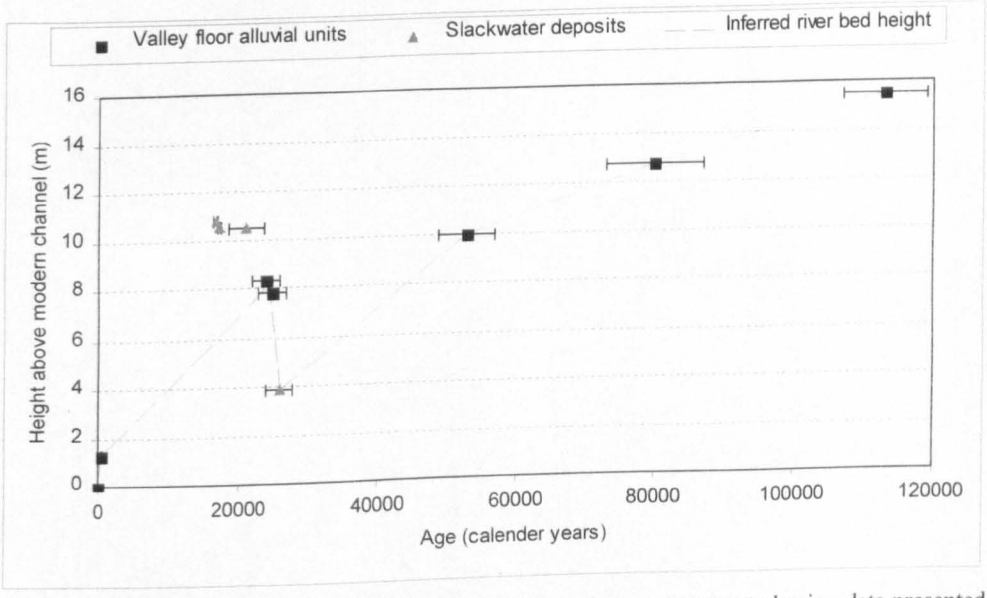

FIGURE 7.18 Dated Late Pleistocene and Holocene bed level changes constructed using data presented in Chapter 6, compared with SWD date and stratigraphic positions. See text for further explanation. The inferred river bed height is merely an estimate, assuming progressive linear incision between dated alluvial units whose height provides a guide to the position of the river bed. 2 sigma uncertainties are shown for all dating results, though for the Late Holocene units these are smaller than the plotted points.

There are other reasons for not using the HEC-2 procedure, especially the fact that the reliability of the SWDs as PSIs cannot be verified. Section 2.3.3 discussed the problem with this other fundamental assumption, and described how the points where SWDs pinch-out ideally need to

be identified. This would have been particularly relevant at the Tributary site, but unfortunately pinch-outs could not be found as exposures were only available in the lower part of the tributary, where most flood units had not thinned to their pinched-out point. Thus the reliability of each flood layer as a PSI cannot be guaranteed. In addition, section 2.3.3 discussed numerous other limitations of the HEC-2 method, such as those related to sediment transport and erosion, which provide further reasons to reject this approach.

It may possible to obtain at least relative estimates of variations in palaeoflood magnitude from the sedimentary characteristics of the deposits. The largest flood within an SWD can be expected to produce the thickest and coarsest unit (Kochel, 1988a), thus both deposit thickness and grain size could be used as relative palaeoflood magnitude indicators. In a detailed consideration of these parameters, Kochel and Baker (1988) found sediment thickness varied directly with flood duration and peak stage, so it can be used for this purpose *at-a-site*, but not between sites as it is then complicated by the geometry of the accumulation area. Although grain size could also be useful at-a-site, it can be expected to show a weaker relationship to discharge, being influenced by variability in the characteristics of different flood events, their sediment sources and the antecedent conditions (Kochel and Baker, 1988; Walling and Moorehead, 1989). In addition to these parameters, the presence of sedimentary structures such as cross-bedding or ripple marks can be indicative of greater discharges (Kochel and Ritter, 1987; Benito *et al.*, 1998). The Pecos River in Texas provides a good example of the behaviour of these parameters, where in 1954 the largest recorded flood (Figure 2.10) deposited the thickest, coarsest and most heavily cross-bedded SWD of the last 10,000 years in the Arenosa shelter (Figure 2.2) (Patton and Dibble, 1982). Knox (1987) also found that the largest historic flood on the Mississippi in SW Wisconsin produced the thickest and coarsest fine-grained sedimentation. Thus, although the relationship between discharge and these sedimentary parameters may be complex, they may nevertheless provide a useful at-a-site guide to the relative magnitude of these extreme floods

Figure 7.19 shows a selection of these sedimentological parameters. The Boila site shows some interesting variations (Figure 7.19a). Little is known about floods B1 to B3, as the sediments are heavily weathered and undated. However, floods B4 and B5 are of more interest, as their age has been accurately constrained (Figure 7.7). The three parameters show a varying trend for these two floods, with the maximum sedimentary unit thickness and d_{50} grain size suggesting B5 was a larger event, whilst the thickness of the flood units suggests the opposite (Figure 7.19a). Micromorphological investigations of these sediments by Karkanas (unpublished) have shown that B4 displays preferred orientation of the limestone particles in the coarse fraction, and was characterised by low rates of sedimentation compared to B5, where the orientation of limestone particles is absent to weak which is probably due to higher rates of sedimentation and a higher energy environment. Thus B5 was almost certainly a larger event, and thus maximum sedimentary unit thickness, and in particular grain size would appear to be

the more reliable palaeodischarge indicators at this site. Certainly the much greater influx of sand sized particles into the site during B5 compared to B4 (Figure 7.13a) can be most sensibly explained by considerably higher flood discharges in the B5 event. The actual thickness of the flood unit could be less representative. If a lower magnitude flood had a relatively long duration and a multi-peaked hydrograph, this could result in the deposition of a thick flood unit composed of numerous thin sedimentary units, which would probably also be quite fine-grained.

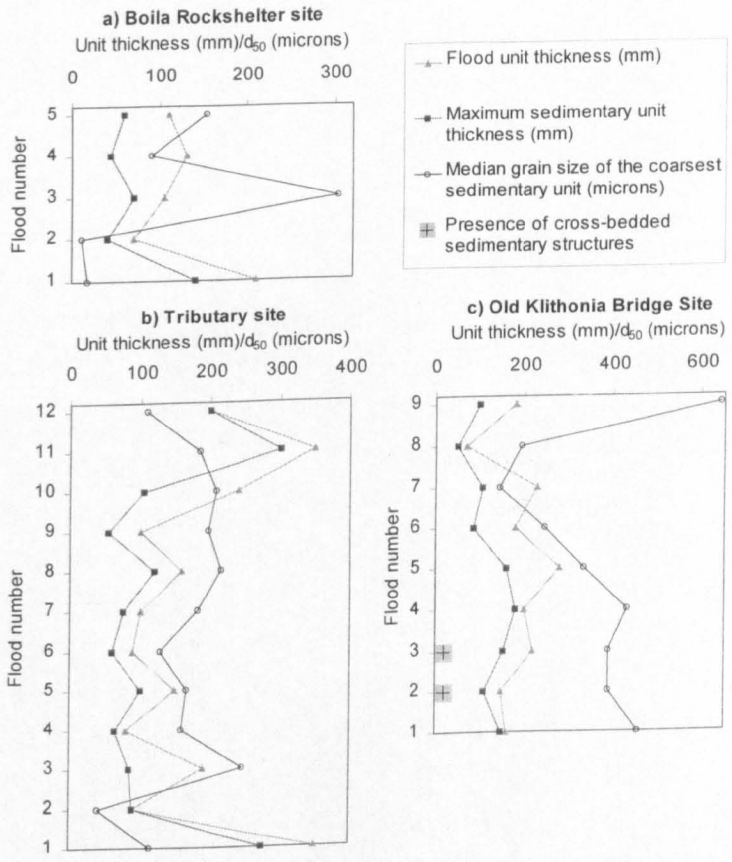

FIGURE 7.19 Sedimentological indicators of relative palaeoflood magnitudes. These include both the thickness of the flood unit as a whole and the thickness of the largest sedimentary unit associated with each flood. The median grain size (d_{50}) of the coarsest sedimentary unit in each flood unit is displayed, and floods where sedimentary units show cross-bedded features are also identified.

There are certain trends visible in both the Tributary and Old Klithonia Bridge records. Concentrating on the grain size and sedimentary unit thickness, particularly large floods at the Tributary appear to have been T1, T3 and T11, although all of flood units T7 to T11 show relatively coarse grain size characteristics (Figure 7.19b and Figure 7.13b). Whist there may therefore have been several larger floods earlier in the sequence, these parameters point to more moderate magnitudes for floods T4 to T6 before a return to higher flood magnitudes in the upper part of the sequence. The Old Klithonia Bridge SWDs show more consistent variation between all three parameters (Figure 7.19c). Floods K1 to K4 all appear to have been of a relatively high magnitude. Cross-bedding features within K2 and K3 (Figure 7.9) also indicate

that these were high magnitude floods. The middle part of the sequence shows a progressive decrease in flood magnitude, with K7 and K8 probably being the lowest magnitude events. The lower magnitudes for K5 to K8 are also evidenced in Figure 7.13c, which shows a far greater component of silt and clay sized particles in these flood units. However, the last flood recorded at the site (K9) appears to have reversed this decreasing trend, this flood being of a magnitude perhaps comparable to or even greater than floods K1 to K4.

It is far more difficult to attempt a comparison of the different flood magnitudes between sites, as local hydraulic settings have a strong influence on the calibre and thickness of sediment deposition (Kochel and Baker, 1988). For example, the generally much coarser SWDs at the Old Klithonia Bridge (Figure 7.12 and Figure 7.13) could be explained by higher magnitude floods depositing sediments there, but could equally result from the hydraulic configuration and proximity to the channel of the site which may have been more conducive to the deposition ofcoarse sediment. All of the sites are at a similar height above the channel (between c. 9.0 and 11.5 m above the modern channel), so if the progressive incision since U4 LGM sedimentation is assumed as shown on Figure 7.18, it would follow that there were greater flow depths during the flooding of Boila in comparison with the Tributary site. However, bed level changes between the dated alluvial units may well have shown a very different pattern to this inferred linear rate, and so such flow depth interpretations can only be very tentative.

As the HEC-2 approach is inappropriate for this study, absolute estimates of flood magnitude are not possible. However, it is believed that these deposits reflect flood events of exceptional proportions. The deposits show very many similarities with previously documented SWDs, which have been shown to have resulted from floods of catastrophic magnitude (e.g. Patton and Dibble, 1982; Baker *et al.*, 1983a; Gillieson *et al.*, 1991; Greenbaum *et al.*, 1998). The fact that these deposits have been preserved in such high-level parts of the valley floor (over 10 m above the modern channel) indicates that subsequent flood events have not been of sufficient magnitude to either rework the SWDs, or deposit further, more recent flood sediments at these sites. For example, the stratigraphy at Boila indicates that since the relatively high magnitude flood B5, which occurred shortly before 13,960 ± 260 years BP (16,834 ± 345 cal years) (Beta – 109162), there appears to have been no subsequent flood sedimentation at the site, and certainly not during the c. 4000 year Palaeolithic occupation of Boila (Figure 7.7, Kotjaboupoulou *et al.*, 1997). This suggests that these floods were rare events.

7.5 INFLUENCES OF ENVIRONMENTAL CHANGE ON THEOCCURRENCE LATE PLEISTOCENE CATASTROPHIC FLOODS

Figure 7.20 shows the available dates for the SWDs and phases of valley floor sedimentation over the last 30,000 years compared with the GRIP oxygen isotope record (GRIP Members, 1993; Thouveny *et al.* 1994). U4 sedimentation coincided with the coldest conditions of the last glacial, ending at c. 24,000 years. The GRIP record shows that a slow but progressive warming

trend was initiated at c. 22,000 years. This continued through to c. 13,000 years, after which there followed the Younger Dryas cool phase before rapid warming with the onset of the Holocene just before 10,000 years. Floods at the Tributary and Boila sites both date to the period of climatic transition which occurred from c. 22,000 to c. 13,000 years (Figure 7.20). This part of the Late Würm is known to have been characterised by highly fluctuating, unstable climatic conditions (Bond *et al.*, 1992; Taylor *et al.*, 1993; Thouveny *et al.*, 1994; Stein *et al.*, 1996).

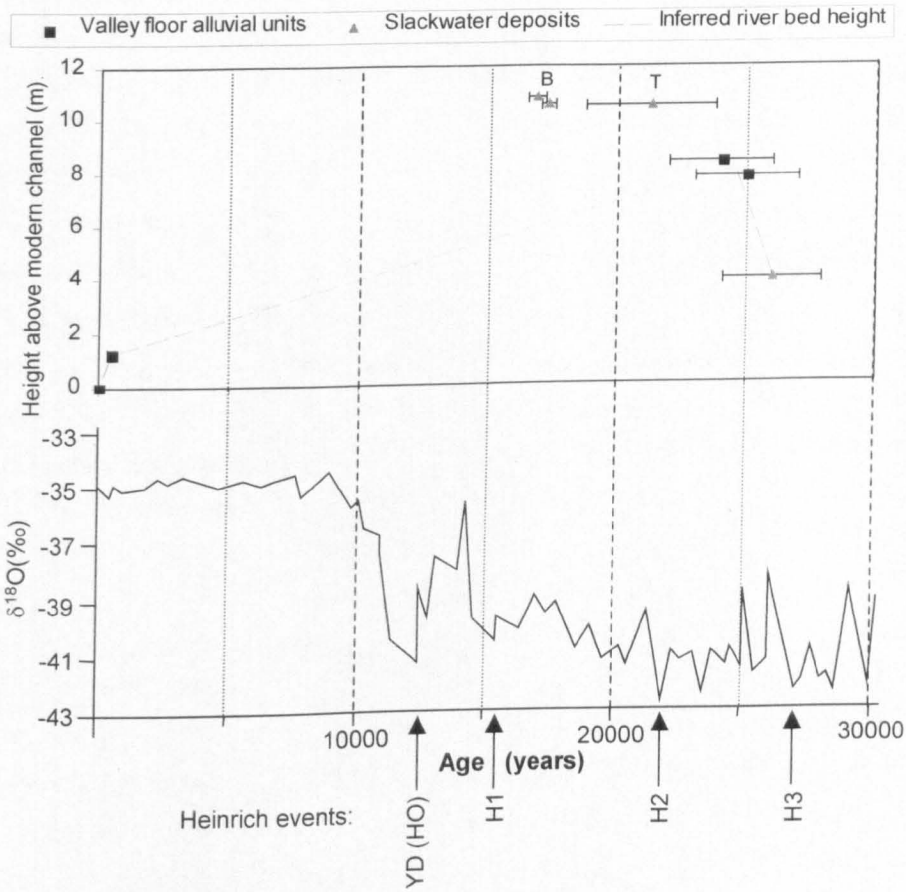

FIGURE 7.20 Dated alluvial deposits in the Voidomatis basin over the last 30,000 years (upper graph, all dates shown as cal. years) compared with the GRIP oxygen isotope record (lower graph) (GRIP Members, 1993; Thouveny *et al.* 1994). For a description of the dates shown on the upper graph see section 7.4.4. T labels the date for floods at the Tributary site, whist B labels the dates from Boila which bracket the upper flood sediments. The inferred river bed height is merely an estimate, assuming progressive linear incision between dated alluvial units whose height provides a guide to the position of the river bed. 2 sigma uncertainties are shown for all dating results, although for the Late Holocene units these are smaller than the plotted points.

The most striking periods of rapid climatic variability during this time have been 'Heinrich events', which are labelled on Figure 7.20. These are sudden periods of cooling, which occurred with a drop in sea surface temperatures and salinity and saw massive, short-lived discharges of icebergs into the North Atlantic from eastern Canada (Bond *et al.*, 1992; Grimm *et al.*, 1993).

There is actually a reasonably close correspondence between Heinrich events H1 and H2 and flooding at the Boila and Tributary sites respectively (Figure 7.20). Although on the GRIP record H1 does occur slightly later than the dates from Boila, different proxy climate records do show slightly different dating constraints for these Heinrich events. For example, Bond *et al.* (1992, Fig. 2) present uncalibrated ^{14}C dates which bracket the H1 event to between 13,490 ± 220 and 14,590 ± 230 years BP, which shows a remarkably precise correspondence with ^{14}C dates which bracket the upper floods at Boila (Figure 7.7). Heinrich events in southern Europe probably showed a very similar timing and occurrence to those evident in the north Atlantic and Greenland records (Thouveny *et al.*, 1994). It is certainly conceivable that these sudden, intense cooling periods could have generated extreme flood events. As discussed in section 6.6.2, during cold Late Pleistocene conditions it has been argued that the eastern Mediterranean received increased winter precipitation from more frequent storms due to a southward shifted jet stream (Prentice *et al.*, 1992). Cold conditions result in the latitudinal temperature gradient becoming steepened, which favours a more extended and southward shifted jet stream along which warm and cold air is mixed, resulting in climatic instability (Lamb, 1982; Rumsby and Macklin, 1994). Such increased storm frequency and winter precipitation could equally have been expected to have occurred during the cool Heinrich events as well as at the LGM, the period that Prentice *et al.* (1992) specifically consider. Thus the floods at Boila may have been rainfall-generated due to increased precipitation, perhaps associated with H1. If the precipitation fell as snow, spring melt of heavy winter snowfalls could have been the flood generating mechanism. As the Tributary site floods may have occurred under somewhat cooler conditions, it seems more likely that they will have been generated by snowmelt, possibly accentuated by heavy snowfalls during H2. These floods may also have received significant glacial meltwater contributions, as occurring within only a few thousand years of the LGM, decaying glaciers may still have been present in the Voidomatis basin. This seems particularly likely considering the high limestone and till content of the SWDs at the Tributary site, which would typically be expected for the suspended sediments of glacial outwash (Figure 7.15). Low vegetation cover at the time of the Tributary site floods would also have enhanced flooding, with rapid runoff from the bare headwater slopes.

Whether either set of flood deposits are directly related to Heinrich events or not, the generally transitional and variable nature of climate over this period is likely to have been a key factor in generating these catastrophic floods. Not only would glacial meltwater have been intense with climatic amelioration after the LGM, but also transitional periods such as this tend to have greater hydrological variability, and have been recognised as important periods for high magnitude flood occurrence in previous studies (*cf.* Ely *et al.*, 1993). In the Mediterranean high discharges have been documented for the Po basin into the Adriatic Sea between c. 14,500 to 13,500 years BP, and c. 12,200 to 11,200 years BP, which is also accounted for climatic transition and unstable, variable hydrological conditions (Zonneveld, 1996; Zonneveld and

Boessenkool, 1996). Clearly the Late Würm may have been conducive to high magnitude flooding on many Mediterranean rivers, both due to glacial meltwater and increased precipitation regimes. The dates from SWDs in the Voidomatis basin show a striking coherence with Heinrich events, however more local, high-resolution climate proxy records would be required before such possible causal links can be established with greater confidence.

7.6 GEOMORPHOLOGICAL IMPLICATIONS OF LATE PLEISTOCENE CATASTROPHIC FLOODING

Chapter 6 described the Late Pleistocene and Holocene development of the Voidomatis basin, considering in particular variability in sediment supply mechanisms a control over river activity. Whilst changes in sediment availability have undoubtedly been very important, high magnitude flood events may also have played a significant role in the development of the catchment, as discussed in section 6.5.6. There has been a dramatic transformation of the Voidomatis River with the transition from the LGM to the Holocene. This period saw wholesale changes in sedimentation style, channel planform, the degree of bed aggradation and the volume and source of fluvial sediment transfers (Chapter 6). The cold stages of the Late Pleistocene resulted in thick aggradations of coarse-grained sediments by a braided channel. The change to the Holocene brought incision and reworking through these sediments and the rationalisation of the channel into a predominantly single-thread meandering river with much lower fluxes of both coarse and fine sediment. Whilst such changes could be accounted for by decreased sediment supply, section 6.5.6 discussed how the coarse, partially-cemented Late Pleistocene bedload would have presented a quite high resistance to channel change. Geomorphological changes could therefore have been more episodic, with potentially a relatively large amount of work being carried out by high magnitude events. The impact of such events would be largely controlled by the relative balance of stream power to sediment availability (Table 6.5) (*cf.* Bull, 1979, 1988).

The sediment fingerprinting results provide particularly valuable information for interpreting the likely impact of the floods that are recorded in the SWDs. Most, if not all of the floods at the Tributary site probably occurred after the end of U4 sedimentation and the peak of glacial sediment availability (Figure 7.20). However, the flood units still contain large amounts of glacial style sediment sources, which implies that they occurred when the Voidomatis basin was under early 'paraglacial' conditions (section 7.4.3). The floods at the Tributary site may therefore have eroded large volumes of slope and near-channel sediments which were originally produced by glacial erosion and frost weathering, especially from the glaciated mountain headwaters where such sediment availability would have been particularly high. These floods are also likely to have reworked substantial amounts of Late Pleistocene alluvium deposited during U4 and earlier sedimentation phases. Both processes would have resulted in the dominance of limestone and till as fine sediment sources during these flood events, as is

observed in Figure 7.15. Although the age of floods at the Old Klithonia Bridge site is poorly constrained, it is probable that these events had a similar effect, as they too are dominated by limestone and till (Figure 7.16). It is difficult to establish whether this would have resulted in significant amounts of incision or aggradation. Major aggradation by the post-LGM floods cannot have taken place, otherwise the U4 sediments would have been buried. However, following the principles of Bull (1979, 1988) (Table 6.5), large amounts of incision also seem unlikely as reasonably high sediment availability would have remained during paraglacial conditions. Therefore, bed level may not have changed significantly during these floods, but the key geomorphic effect would have been extensive downstream transport and clearance of glacially-generated fine sediments. This active sediment 'flushing' would explain why the length of the paraglacial cycle in the Voidomatis appears to have been relatively short (c. 7000 years at most) (section 7.4.3). By floods B4 and B5 at Boila glacial sediment sources appear to have been far less significant (Figure 7.14), suggesting that glacially-supplied fine sediments may largely have been removed from the catchment by earlier events. Some reasonably high limestone amounts in the base of the B5 sediments may be explained by the higher magnitude of this event (section 7.4.4), which would have made it more capable of reworking the remaining U4 or older Late Pleistocene alluvium. The completion of the paraglaical cycle may also have been aided by warmer environmental conditions (Figure 7.20) allowing woodland expansion as early 15,000 – 14,000 years BP at Lake Tseravinas and Lake Ziros (Turner and Sánchez Goñi, 1997, locations shown on Figure 3.17). The earliest woodland expansion at Rezina Marsh and Lake Gramousti (Figure 3.17) is less well dated, but appears to have occurred a little later, probably around 13,000 - 11,000 years BP (Willis, 1992a, 1992b, 1992c, 1997). The similarity in sediment provenance of the upper Boila floods to the contemporary Voidomatis sediments (Figure 7.17), would suggest reasonably similar controls on sediment delivery, and hence it seems likely that some denser vegetation has become established by this point.

The influence of both early woodland expansion and prior flushing of glacial sediment through the catchment would both have resulted in a lower sediment availability during floods B4 and B5 in comparison to the Tributary and Old Klithonia Bridge floods. Following the principles of Bull (1979, 1988) (Table 6.5), it can be therefore be expected that the Boila floods would have caused river channel incision. There has been approximately 8 m of bed level lowering since the LGM (Figure 7.20), and floods B4 and B5 may have resulted in a significant amount of this downcutting occurring at c. 14,000 years BP. Following B5 there is no further evidence for fluvial sedimentation at Boila, so incision during B5 may have lowered the bed level substantially, leaving the rockshelter too high to be inundated again by the river. Such a conclusion would be consistent with the archaeological evidence from the rockshelter. There is no significant evidence for human occupation of the site prior to the B5 flood (Figure 7.7; Kotjabopoulou *et al.*, 1997). Instead, use of the site by humans occurred from c. 13,240 ± 220 to c.10,190 ± 260 years BP, as recorded in the cultural sediments above the B5 flood unit

(Kotjabopoulou *et al.*, 1997). Floods B4 and especially B5, through lowering the river level, may have made Boila a viable site for human occupation, free from the risk of inundation and higher above the ground surface to give improved views for the hunter-gatherer occupants. Ongoing analysis of the Boila stratigraphy and archaeology will enable the use of the site in comparison to others such as Klithi to be elucidated in more detail (Kotjabopoulou*et al.*, 1997). However, this study shows an encouraging consistency between the sedimentological and archaeological records, and demonstrates how extreme flood events could have played an important role in making rockshelter sites in the Voidomatis basin attractive for Palaeolithic occupation. Such possibilities emphasise the importance of considering low frequency, high magnitude landscape events as potential influences on Palaeolithic geographies. Considering the earlier flood events, the relatively regular high magnitude, high sediment flux, Lateglacial flooding of the Tributary and Old Klithonia Bridge sites would have provided a hostile, dangerous environment in Vikos gorges. This may have influenced why the Klithi, Boila and Magalakkos rockshelters show no evidence of occupation before 20,000 cal years (Bailey, 1997a).

Whilst the above discussion has so far considered sediment redistribution and river incision, an alternative hypothesis for the earliest floods at the Tributary site and the poorly constrained sequence of floods at the Old Klithonia Bridge site should also be discussed. Allowing for dating uncertainties associated with these deposits (Figure7.20), it is possible that some of these SWDs were deposited during the latter periods of U4 sedimentation as overbank fines during high magnitude flood events. The sediment provenance signatures of the Old Klithonia Bridge SWDs and the early floods in the Tributary site show a very similar provenance to the fine matrix of U4 sediments (Figure 7.17), allowing for some extra flysch at the Tributary site due to local influx of flysch fines from the tributary catchment. If these floods did occur over this period, they would almost certainly have resulted in river aggradation (Table 6.5), due to the high sediment availability associated with the LGM (section 6.6.2). Thus these floods could have played a significant role in the U4 alluviation. Confirmation of these effects would require improved dating of the lower floods at the Tributary site and the SWD sequence at Old Klithonia Bridge, which did not prove possible in this study due to the lack of preserved organics and unreliability of OSL (section 7.3). What is clear from this chapter is that preserved in the stratigraphic record are two distinct periods of Late Pleistocene catastrophic flooding in the Voidomatis basin. The first saw as many as 12 major flood events occur at c. 21,250 years (Figure 7.20), with particularly large events early and later in the sequence (section 7.4.4). These floods resulted in widespread erosion and reworking of sediments supplied during the glacial conditions. They probably served to shorten the length of the paraglacial cycle in the Voidomatis basin, so that by the second phase of extreme flooding, with two events at c. 14,000 years BP (c. 17,000 cal years), paraglacial conditions has ended and sediment availability was much reduced. This probably meant that these two floods, and particularly the latter high

magnitude B5 event, resulted in considerable incision of the river channel, lowering the bed level closer to its modern position. Thus both periods of extreme floods recorded in the SWD record have probably been of considerable significance in the Lateglacial transformation of the Voidomatis valley floor. The modern geometry of the Voidomatis River shows a clear imprint of the fluvial processes that took place over the Late Würm. In general, the modern floodplain is deeply entrenched 8 - 10 m below Late Pleistocene alluvial units, which still mantle the margins of the valley floor in many places. This downcutting of the river could only have occurred with the reworking of large amounts of Late Pleistocene alluvium, a significant proportion of which was probably transported through the river system by catastrophic floods during the Late Würm.

7.7 SUMMARY

Whilst high magnitude floods over the Late Pleistocene are likely to have been important geomorphic events in Mediterranean mountain environments such as the Voidomatis basin, their occurrence and effects have rarely been described in detail, as direct evidence for such events is often not preserved in the stratigraphic record. However, through the analysis of palaeoflood slackwater deposits, this chapter has presented direct evidence for specific catastrophic flood events over the Late Würm. Two main periods of catastrophic flooding occurred during this capricious climatic and hydrological period. The precise timing of these events may have been driven by the occurrence of sudden cool conditions during Heinrich events. It is likely that these floods played a significant role in the metamorphosis of the Voidomatis valley floor. This chapter serves to emphasise the importance of considering the effects of extreme events, even over Late Pleistocene timescales, in shaping the modern fluvial landscapes of Mediterranean mountain rivers.

8. CATASTROPHIC FLOODING AND FLOOD VARIABILITY IN THE VOIDOMATIS AND AOOS BASINS OVER THE LAST 200 YEARS.

This chapter presents a flood history for the Voidomatis and Aoos Rivers for approximately the last two centuries. The aims and context of the chapter are described in section 8.1. Data on flood occurrence and magnitude have been obtained from three sources (systematic hydrological data, boulder berms and overbank flood sediments) and are presented in sections 8.2 to 8.4. Section 8.5 brings these results together to discuss the implications of this extended flood record for understanding occurrence and geomorphological significance of extreme flood phenomena in this environment.

8.1 INTRODUCTION

Palaeoflood investigations can provide important information of relevance to the following:

1. Attempts to estimate the frequency and magnitude of extreme flood events (section 2.4.1).
2. Improving our understanding of the environmental conditions that are conducive to catastrophic flooding (section 2.4.2).
3. Developing an improved understanding of the geomorphological effects of catastrophic floods and their role in landscape development (section 2.4.3).

In Chapter 7, the second and third of these issues were considered in detail for catastrophic flooding over the Late Pleistocene. However, the need to improve flood frequency estimations was not addressed, as the SWDs represent flood events beyond the timescale relevant to modern hydrological planning. However, providing frequency and magnitude estimations for extreme floods is particularly important for Mediterranean mountain rivers such as the Voidomatis and Aoos, where flow records are of a poor spatial and temporal coverage, yet extreme flood events occur with reasonable regularity (section 3.5.3). Catastrophic floods are one of the major environmental problems facing the Mediterranean region (Poeson and Hooke, 1997). They cause damage to life and property and massive amounts of erosion, but their rarity and flashy nature mean that they are hard to predict and mitigate against. The last 200 years is a suitable timescale for furthering knowledge regarding recent catastrophic flooding (section 1.4.2). Flood records for this period are suitable for assessing the recurrence of large, potentially catastrophic floods in contemporary environments and over the foreseeable future. This period also incorporates the climatic amelioration from the final cold phase of the Little Ice Age (Grove, 1988; Bradley and Jones, 1992), which may provide a useful analogue for the possible effects of future climate change on flood occurrence (Rumsby and Macklin, 1996). Anthropogenic landscape disturbances have also been important over this period (section 3.4.2), and their effects on the production of catastrophic floods also needs to be evaluated. The geomorphic

effects of rare floods over this timescale are also of great importance in understanding, and hence managing, the dynamics of Mediterranean mountain rivers such as the Voidomatis and Aoos. Relatively little is known about the geomorphic impact of extreme floods in Mediterranean river environments (Poesen and Hooke, 1997). By focusing on the last 200 years, this chapter will therefore address the three main areas identified above as key applications of palaeoflood data (section 2.4).

Gauged streamflow records are the obvious starting point for investigating flooding over the last two centuries, as these provide the most reliable and detailed flood records available. Systematic hydrological data have been collected for the Voidomatis and Aoos basins (section 4.2), and the basic features of these records have been described in section 3.5. These data are analysed in more detail in this chapter to determine flood frequency and magnitude estimations, temporal trends in flood hydrology and the control of large scale atmospheric conditions in producing extreme flood events. However, the records only cover the last 30 to 40 years (section 4.2), and are therefore not long enough to assess fully the recurrence of catastrophic floods, which by their nature are likely to be rare, occurring perhaps only once every 50 or 100 years. In the absence of documentary records, wall marks or anecdotal evidence recording large flood events, palaeoflood hydrological techniques provide a promising means of extending the flood record to cover a timespan of the last 200 years or so which is necessary to assess catastrophic flooding. The combined use of systematic hydrological data and palaeoflood data can be a profitable research approach, as the gauged records provide a characterisation of the recent flood-producing systems of the river, which is valuable context for palaeoflood investigations (e.g. Jarrett and Costa, 1988; Ely, 1997). Palaeoflood data have been obtained from two sources; i) boulder berms, and ii) overbank flood sedimentation. The systematic and palaeoflood data are described in turn.

8.2 FLOODING RECORDED IN SYSTEMATIC HYDROLOGICAL DATA

In section 3.5 it was demonstrated how the Voidomatis and Aoos basins can receive intense storm precipitation in excess of 150 mm in 24 hours (Table 3.3). Additionally, both rivers were shown to exhibit flashy storm hydrographs, and have experienced large flood events in the recent past (section 3.5.3). This section goes on to explore the flood hydrology of the Voidomatis and Aoos basins in more detail.

8.2.1 Flood frequency estimations

It is standard hydrological practice to analyse gauged streamflow records to calculate the magnitude of floods with different return intervals. In particular, one of the most frequently required flood frequency estimations is the 100-year flood. Such estimations are of great importance, being used in flood risk analyses and management and in structural engineering projects within the floodplain such as dam and bridge design and construction (section 2.4.1). It

is therefore important to estimate flood frequency and magnitude on the basis of the gauged records, to provide a guide to frequency and magnitude of rare floods on the Voidomatis and Aoos Rivers. These estimates may then be assessed in the light of the palaeoflood records (sections 8.4 and 8.3) which provide flood data over much longer timescales, and are therefore more likely to include rare, catastrophic floods.

There remains no clear consensus over which method of flood frequency analysis is preferable. The U.S. Water Resources Council recommends the adoption of the log Pearson III distribution, but this method has often proved unpopular, as it has various drawbacks including a particular sensitivity to outlying large flood events (Costa, 1978b). Probably the most common method amongst European hydrologists is the Gumbel distribution, which plots annual maximum floods according to their recurrence probability. Probabilities are typically calculated using the Gringorten or Weibull formulae, which produce very similar results (Shaw, 1988). These are well-established methods that are relatively simple to apply. Flood frequencies have therefore been calculated using Gumbel's extreme value distribution (Type 1) with the annual maximum flood series. Probabilities were plotted according to the Gringorten formula as recommended and described by Shaw (1988). The formula is:

$$P(X) = \frac{r - 0.44}{N + 0.12} \qquad (8.1)$$

where P(X) is the probability P that an annual maximum flood equals or exceeds a given magnitude X, r is the rank of X and N is the total number of data values. Table 8.1 shows the results for various stations whose locations are shown on Figure 3.1, and the estimated Voidomatis record[1]. The estimates from Bourazani Bridge and Doukas Bridge are the most reliable as they are based on comprehensive daily flow measurements. The estimated Voidomatis record is less reliable, as it is a shorter and not directly gauged[1]. Estimates for other stations are much less reliable as they are based on less frequent flow measurements. There are generally large confidence intervals around the estimates (Table 8.1), caused by large variability in the annual maximum flood series.

The predicted magnitude of rare floods on the Voidomatis and Aoos differ considerably. The main stations on the Aoos upstream of the confluence with the Voidomatis are Konitsa and Doukas Bridge, which are less than 4 km apart (Figure 3.1). Estimates for these nearby stations show good correspondence, with the 100-year event for this area of the Aoos estimated to around 400 m^3s^{-1} (Table 8.1). The 100-year event at on the Aoos at Bourazani Bridge, downstream of the Voidomatis confluence (Figure 3.1), is some 4 to 5 times greater, estimated to around 1800 m^3s^{-1} (Table 8.1). The flood predictions for the estimated Voidomatis record are even greater than at Bourazani Bridge, as a result of some very high annual

[1] Not directly gauged, but determined by subtracting the discharge of the River Aoos upstream of the confluence with the Voidomatis with that downstream of it (see section 3.5.3 for details).

maximum discharges being recorded in only a 12 year record. This may not be entirely realistic, as one would expect larger floods at Bourazani Bridge, which also incorporates the waters of the Aoos (Figure 3.1). However, this attests to the propensity for higher magnitude flooding on the Voidomatis compared to the Aoos, as was identified in section 3.5.3.

TABLE 8.1 Selected discharge (m^3s^{-1}) estimates from the Gumbel (Type 1) flood frequency distribution for floods of various return periods, with the 95% confidence limits shown. † Denotes the number of years where there were a sufficient number of flow readings to make flood frequency analysis possible.

Return Period (years)	Bourazani Bridge	Doukas Bridge	Voidomatis (estimated)	Konitsa	Vovoussa	Kokkoris Bridge	Tsep-elovon
200	2007 ±631	409 ±131	2202 ±800	467 ±165	128 ±48	36 ±9	13 ±5
100	1815 ±552	369 ±115	1974 ±701	417 ±145	114 ±42	33 ±8	11 ±4
50	1627 ±476	330 ±99	1750 ±604	367 ±125	100 ±36	31 ±7	10 ±4
20	1361 ±370	262 ±77	1434 ±470	298 ±97	79 ±28	23 ±6	9 ±3
5	956 ±218	192 ±45	954 ±276	188 ±57	49 ±16	17 ±3	6 ±2
Maximum recorded flood (m^3s^{-1})	1779	432	1627	420	135	23	8
Length of record (yrs)†	27	24	12	28	25	17	15

The major limitation of these estimates is the short length of flow records on which they are based, being typically 20 to 30 years (Table 8.1). This means that the prediction of floods for long return periods such as the 100-year flood involves extrapolation beyond the limits of the observed probabilities. Such estimates must be treated with caution (Shaw, 1988), as for a 20 year record for example, there is only a 26% probability that a 100-year event has been recorded, and only a 33% probability that a 50-year flood is included in the measurements (Smith and Ward, 1998). It is not known whether during the time period not covered by these systematic records much larger floods might have occurred which in turn would serve to increase the 100-year flood estimates. There is therefore a need to extend the timescale of the flood record. Section 8.5.2 will discuss the use of palaeoflood data for this purpose.

8.2.2 Regional flood envelope curves

Mimikou (1984a, 1984b) has developed of a series of increasing power functions relating drainage area to a range of hydrological parameters for western and northwestern Greek catchments. The relationships between catchment area and the maximum recorded flood discharge (Figure 8.1) are especially relevant to this study. These discharges are based on the gauged records of major rivers in western and northwestern Greece, which are typically of 25 - 30 years duration. The two regions have considerable climatological and physiographical differences, and thus separate flood envelope curves are drawn for each region (Figure 8.1). The rivers studied in the northwest include the Aoos at Konitsa and Vovoussa, and presumably the envelope curve should be relevant to the Voidomatis, as it is intended as a means of estimating maximum floods in ungauged or poorly gauged catchments.

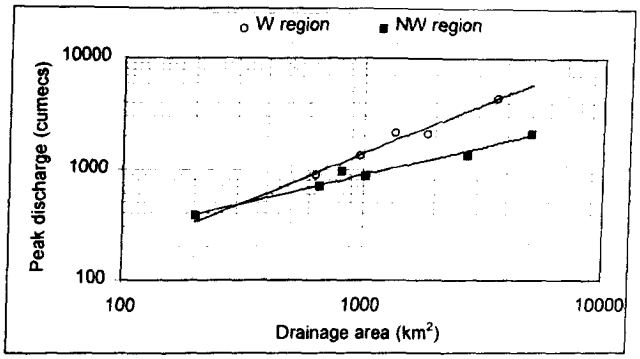

FIGURE 8.1 Envelope curves for maximum flood discharges recorded in systematic gauged record for western and northwestern Greece. *(Source: Mimikou, 1984a).*

There is some conflict between the systematic data used in this study and the predicted maximum flood discharges of Mimikou (1984a). If the envelope curve is valid the Voidomatis, being a smaller basin the Aoos, should have lower maximum flood flows (Figure 8.1). However, the Voidomatis has experienced greater flood magnitudes than the Aoos at Doukas Bridge and Konitsa, in spite of its smaller drainage area (Table 8.2). Furthermore, the Bourazani Bridge record deviates from this relationship, as recorded floods are well in excess of the envelope curve limits (Table 8.2). In contrast, the data for the Aoos at Doukas Bridge and Konitsa are within the limits of the envelope curve. In fact, it may be that the curve actually overpredicts the maximum discharge for the Aoos at these stations (Table 8.2). A simple relationship between drainage area and extreme flood magnitude may therefore be an oversimplification. The data in this study indicate that there are other important factors that can influence extreme flood magnitudes, such as basin morphometry. These limit the value of simple drainage area - flood envelope curves in moderate-sized mountain catchments such as these, which are prone to less predictable extreme flood magnitudes. The envelope curves also suffer from the problem that they are based on a gauged data set that is of inadequate duration to properly represent catastrophic floods (section 2.5.1). Maximum floods from envelope curves only have a return period equivalent to the length of the flood record (Mimikou, 1987). Envelope curves may be of greater value when based on longer gauged records (which are more likely to incorporate rare flood events), and for larger lowland rivers where maximum flood events might show less inter-catchment variability.

TABLE 8.2 Comparison of theoretical maximum flood flows determined for the Voidomatis and Aoos basins from the work of Mimikou (1984a) with floods contained within the systematic records obtained in this study. The Aoos at Konitsa is the only station used by Mimikou (1984a). † Denotes an estimated record, obtained from the difference in discharge upstream and downstream of the Aoos confluence. ‡ Denotes that these drainage areas are maximum estimates obtained from 1:50 000 maps.

Basin	Drainage area (km^2)	Predicted maximum flood discharge from envelope curve (m^3s^{-1})	Maximum gauged discharge in this study (m^3s^{-1})
Aoos (at Konitsa)	665	724	420
Aoos (at Doukas Bridge)	c.850‡	821	432
Aoos (at Bourazani Bridge)	c.1250‡	1000	1779
Voidomatis (at Aoos confluence)†	384	547	1627

8.2.3 Trends in flood hydrology over the last c. 40 years

Although the systematic records only cover approximately the last 40 years, they do enable the timing of high magnitude flooding over this timescale to be investigated. This section investigates temporal trends in both the precipitation and streamflow records.

8.2.3.1 Precipitation

The general and seasonal patterns in precipitation have been described in section 3.5. In terms of flood variability it is important to know which years have seen the greatest precipitation. The monthly rainfall totals, shown in Figure 8.2 and Figure 8.3 provide a useful guide to temporal variations. The seasonality is displayed here, with the monthly totals in winter reflecting the intense precipitation possible in this area (section 3.5). It is common to see a winter month with over 300 mm precipitation, and 765 mm was recorded at Skamnelli for January 1979 (Figure 8.2). There is marked inter-year variability in precipitation. Intense monthly rainfall occurred over the winters of 1969-70, 1978-79, 1981-82, 1985-86, and 1990-91 (Figure 8.2). Wet periods around the turn of the decades from the 1960s-70s and 1970s-80s are particularly prominent. In addition, the earlier Konitsa record shows that very wet periods also occurred prior to 1968, with 1962-3 and 1966-7 having greater totals than the post-1968 period at this station (Figure 8.3).

Trends in precipitation can be detected more clearly by means of various statistical analyses (e.g. Giakoumakis and Baloutsos, 1997). Here z scores have been calculated for the data in a similar fashion to Kutiel *et al.* (1996). This is a useful but simple method for showing temporal trends and for identifying years that were particularly wet or particularly dry. The formula used for calculating z scores is:

$$z = \frac{x_i - x}{\sigma} \qquad (8.2)$$

where x_i is the annual value, x is the average annual value, and σ is the annual or seasonal standard deviation. Hydrological years (September - August) were again used in this analysis, so as not to split the rainy season. Following Kutiel *et al.* (1996), years with z scores greater than 0.5 can be considered *wet* years, and where z is greater than 1.5, *extremely wet.* Conversely, where z is less than -0.5 the year can be described as *dry*, and when z is less than -1.5, *extremely dry.*

The z scores for annual precipitation are shown in Figure 8.4. From 1968-69 onwards, all of the stations generally exhibit similar variability over time. For the 1955-1968 period, only the Konitsa record exists. This trend analysis highlights many of the variations identified in the discussion of monthly totals above. This 1955-1992 period has experienced regular variations between wet and dry periods (Figure 8.4). The Konitsa record shows that 1962-63 and 1966-67 were extremely wet, and far wetter than any subsequent years in the Konitsa record (1954-1981). The annual mean z score for 1968-69 to 1991-92 never quite reaches extremely wet

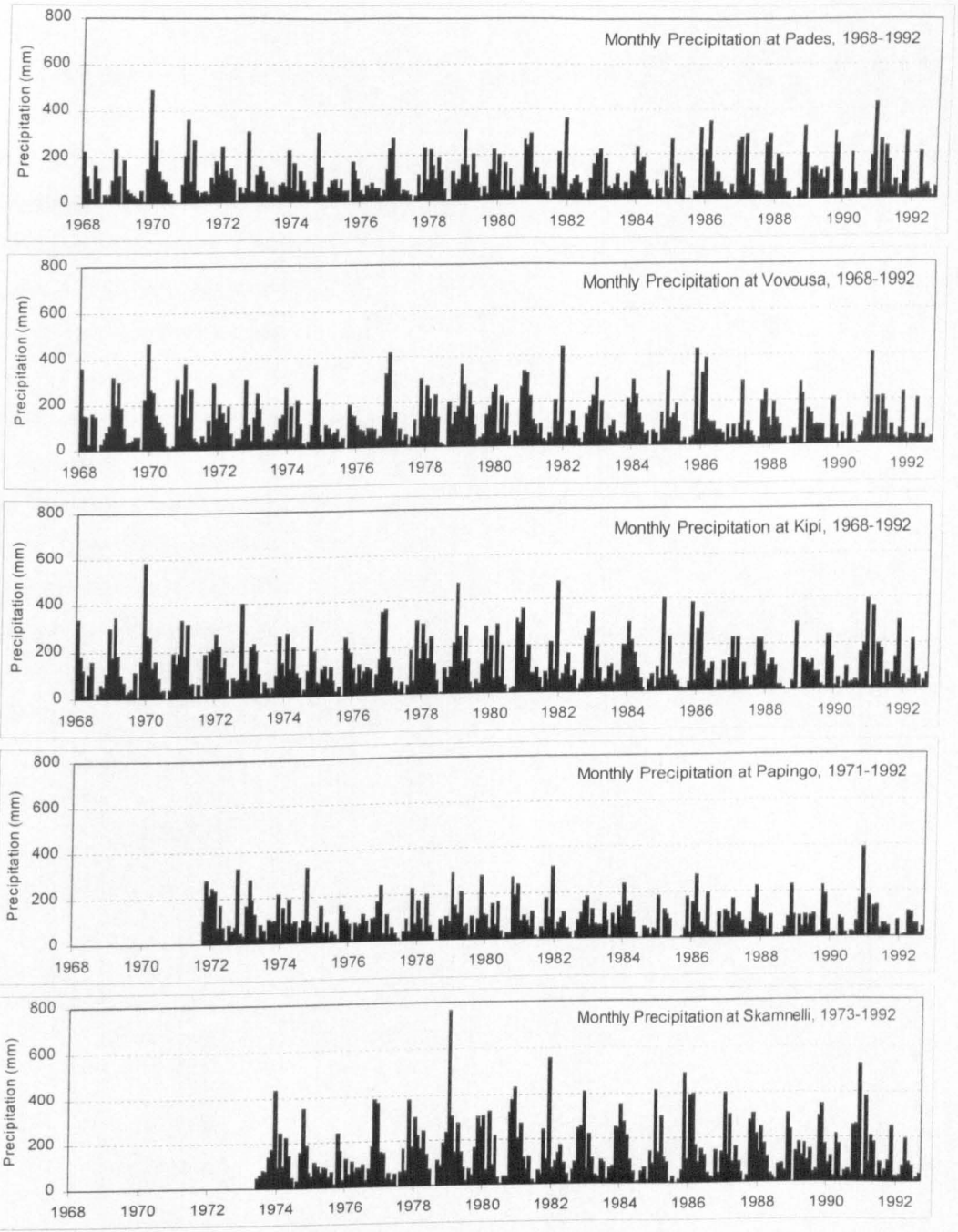

FIGURE 8.2 Monthly precipitation totals at stations in the Voidomatis and Aoos basins, shown for the period 1968 - 1992. Locations of these stations are shown in Figure 3.1.

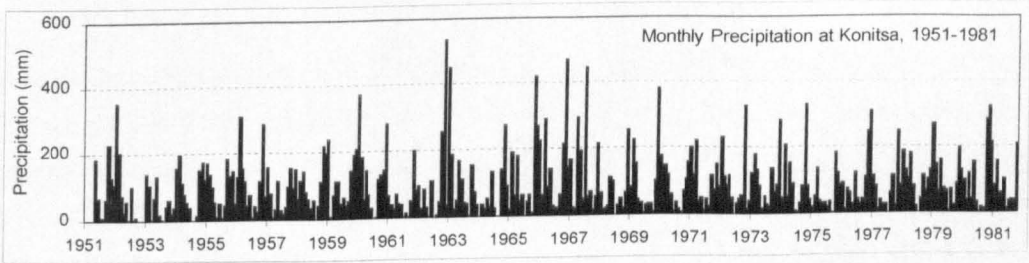

FIGURE 8.3 Monthly precipitation totals at Konitsa, 1951 - 1981.

proportions, although extremely wet years have been experienced at specific stations over this period (Figure 8.4). A series of wet periods are seen in 1969-70, 1978-79, 1980-81, 1985-86 and 1990-91. Dry conditions have occurred between the wet periods, most notably in 1975-76, 1984-85 and 1989-90. Drier conditions are more common over recent years, which may reflect drier conditions in the eastern Mediterranean more generally since the mid-1970s (Kutiel *et al.*, 1996) and particularly during the 1980s (Maheras and Kolyva-Machera, 1990; Maheras *et al.*, 1992, 1994). The year of 1978-79 seems to have been particularly wet, with 3 of the 6 stations recording precipitation classed as extremely wet. Again, generally wetter conditions around the turn of the decades 1960s-70s and 1970s-80s are evident, and the most recent decade change from the 1980s-90s was also very wet, extremely so at Pades. In fact, post-1968-69 there is to some extent a cyclical variation on a 10-year timescale, with wet conditions at the transition of each decade, and gradual drying trend during the decade until wetter conditions return 10 years later (Figure 8.4). Giakoumakis and Baloustsos (1997) also found very similar decadal cycles in hydrological time series for the Evinos catchment in Greece. This variation could be a feature of the eastern Mediterranean region.

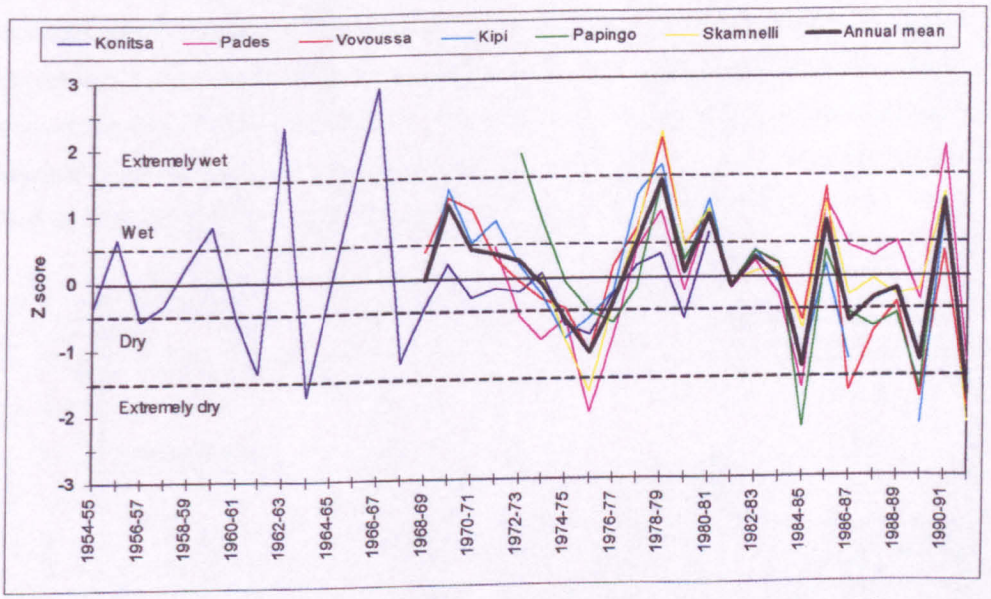

FIGURE 8.4 Trends in annual (Sept.-Aug.) precipitation over the study area as determined by z scores. Z >0.5 is defined as a wet year, z >1.5 being extremely wet. z <-0.5 is defined as a dry year, z <-1.5 being extremely dry.

It is clearly important to focus attention on periods of extreme precipitation which is important in generating rare, high magnitude flash floods (Doswell *et al.*, 1996). Variation in the number of days of very heavy precipitation each year (defined here as >40 mm (section 4.2.1)) is shown by the z scores in Figure 8.5, where using a similar procedure as with the annual precipitation data, storm occurrence can be described as either *frequent* or *infrequent*. The data follow a

broadly similar pattern to that of annual precipitation (Figure 8.4), so in general increased storm frequency was observed during the wetter years.

To assess the temporal variability in potentially catastrophic rainfall events, it is relevant to look at trends in the most intense precipitation received each year. Therefore, z scores have again been calculated, this time for the maximum 24 hour precipitation total recorded each year. Again, using a similar procedure, the z scores can be used to determine whether these storms were *intense* or *light* (Figure 8.6). These results show different patterns to the previous graphs. By far the most intense storm precipitation occurred during 1970-71, with all but one of the stations recording an extremely intense downpour. This year, although shown as being wetter than average, was surprisingly not one of the wettest years on record (Figure 8.4). After 1970-71, there is considerable inter-station variability. Certain stations show intense storms in 1976-77, 1978-79 and 1980-81, but the average pattern is for only moderate storm events until 1985-86, which had on average the most intense storms since 1970-71 (Figure 8.6). The year 1989-90 also witnessed intense precipitation, particularly at both Pades and Skamnelli, despite it being quite a dry year overall (Figure 8.4). Therefore, very wet years have not always experienced more intense, rare precipitation events. Of course, for some years this does hold true, most notably during the 1960s when the Konitsa record shows that 1962-63 and 1966-67 were both extremely wet years and which did experience extremely intense storm events. However, the post-1968 results illustrate the greater spatial variability in extreme precipitation compared to the annual totals. The following section identifies trends in the river flow records, which as expected have been strongly influenced by these variations in precipitation.

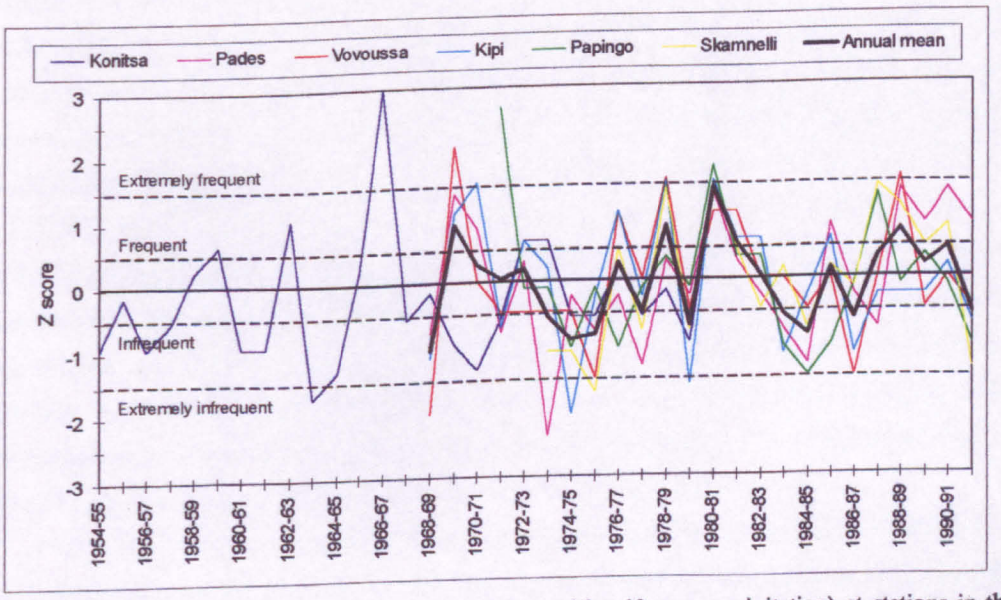

FIGURE 8.5 Trends in storm frequency (number of days with >40 mm precipitation) at stations in the Voidomatis and Aoos basins. z >0.5 is defines as frequent storminess, z >1.5 being extremely frequent. z <-0.5 is defined as relatively infrequent storminess, z <-1.5 being extremely infrequent.

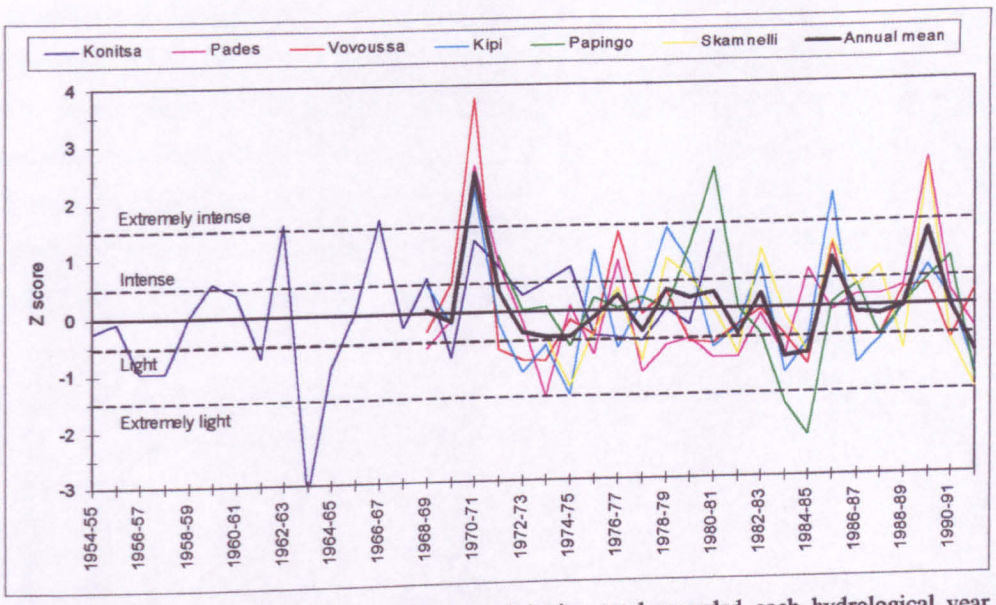

FIGURE 8.6 Trends in the maximum 24 hour precipitation total recorded each hydrological year at stations in the Voidomatis and Aoos basins. z >0.5 is defined as a relatively intense storm, z >1.5 being extremely intense. z <-0.5 is defined as a relatively light storm, z <-1.5 being extremely light.

8.2.3.2 River Flow

The general character of flow on the Voidomatis and Aoos Rivers has been described in section 3.5.3, where the records of daily flow at Bourazani Bridge and Doukas Bridge have been presented (Figures 3.23 and 3.24) along with the estimated record for the Voidomatis (Figure 3.25). At Bourazani Bridge there were very few large floods in the 1950s (Figure 3.23). This changed during the following decade, with 1962-63 and 1965-66 both having a number of large events which exceeded 1000 m^3s^{-1}. However, 1970-71 saw the highest discharges on all of the three records, with two very large flood events around November and the end of December. The latter event was particularly severe on the Voidomatis and at Bourazani Bridge, with discharges of 1627 and 1779 m^3s^{-1} respectively. The 1970s saw further years of reasonably high flooding in 1973-74, 1976-77 and 1978-79, although these again appear to have been more pronounced on the Voidomatis and at Bourazani Bridge. 1978-79 saw notably high river levels sustained over the entire year at Bourazani Bridge, in response to the generally very wet conditions at this time (Figure 8.4). After the 1970-71 event, the Doukas Bridge record generally shows less variability in flooding, with reasonably similar peak discharges each year. However, larger floods did occur during 1986-87, and also more recently during the 1990s, with the discharge of 202 m^3s^{-1} near the end of 1996 being the second highest discharge on record.

The variability in extreme flooding over the period of record can de depicted through inspection of the annual maximum flood series. Figure 8.7 presents these values divided by the mean annual flood at each station to reveal years of above or below average flooding. This emphasises the extreme magnitude of the 1970-71 floods at these sites. This year experienced very intense precipitation at all but one station in the study area. This widespread distribution of

extremely intense precipitation will have been important in generating such high discharges, as subsequent years have only received more localised intense precipitation (Figure 8.6). The next most severe years of flooding were probably during 1962-63 and 1965-66, which were also generally very wet years (Figure 8.4) and saw very intense precipitation recorded at Konitsa (Figure 8.6). Other years of above average flooding occurred during the 1970s and in 1996-97, however these are all overshadowed by the magnitude of the 1970-71 floods. The 1950s and mid- to late-1980s have been notable periods of low flood magnitudes.

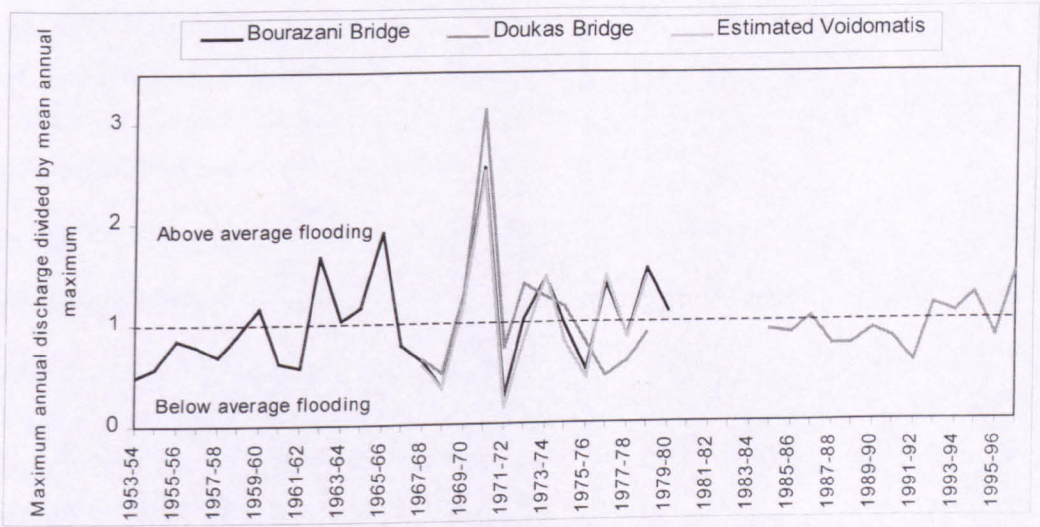

FIGURE 8.7 Maximum discharge recorded in daily flow records for the Voidomatis and Aoos Rivers. The data have been divided so that above (>1) or below (<1) average flooding is depicted.

8.2.4 Atmospheric circulation and extreme floods

To fully understand the flood-producing system, it is important to examine climatic influences on variations in the frequency and magnitude of flooding (section 2.4.2). Such research has been termed flood hydroclimatology (Hirschboeck, 1988). An important part of this work has involved investigating the influence of large-scale atmospheric circulations on flood hydrology, in an attempt to understand the synoptic weather conditions which are conducive to storms and flooding (e.g. Knox, 1984; Haydon, 1988; Hirschboeck, 1987, 1988, 1991; Rumsby and Macklin, 1994; Ely, 1997). This can provide valuable information for flash flood forecasting procedures (Doswell *et al.*, 1996). However, these studies have mainly focused on the U.S. and the U.K. Whilst some work has been done into the flood hydroclimatology of the Iberian Peninsula (Benito *et al.*, 1996), in the eastern Mediterranean the influence of atmospheric circulation has generally only been considered in the context of rainfall (e.g. Maheras and Kolyva-Machera, 1990; Kutiel *et al.*, 1996), and rarely in terms of flood frequencies and magnitudes. The hydrological data collected in this study present an opportunity to investigate flooding in the context of atmospheric circulation. This has been achieved in two ways and each is described here in turn.

8.2.4.1 Annual and seasonal flood hydroclimatology

The approach taken here is to compare the z score values for precipitation and flow data to zonal and meridional indices calculated for a suitable area of Europe. This approach has been used successfully by Kutiel *et al.* (1996) in assessing extreme rainfall conditions in the eastern Mediterranean, and in Rumsby and Macklin's (1994) investigation of flooding in Northern England. Zonal and meridional indices are frequently used to characterise regional atmospheric circulation, being calculated according to the atmospheric pressure gradients between different latitudes and longitudes. For this study the region used is delimited at 35°N and 55°N, and 5°E and 30°E (Figure 8.8). This area is a suitable size to characterise large-scale atmospheric circulation over the relevant part of the Mediterranean, being similar to that used by Kutiel*et al.* (1996). The indices are calculated as shown below. As examples, data for mean winter pressures (December to February inclusive) are shown with the resulting indices:

ZI (zonal index) = (P_{35N}) - (P_{55N}) e.g. Winter 1989 = 1020.1-1009.4 mb = ZI of 11.5 (8.3)

MI (meridonal index) = (P_{5E}) - (P_{30E}) e.g. Win. 1989 = 1017.1-1018.5 mb = MI of −1.3 (8.4)

where P_x refers to the pressure P at latitude/longitude x. Figure 8.9 provides a guide to interpret the ZI and MI. Positive ZI values indicate westerly flows, whereas negative ZI values mean easterly flow. Similarly, positive MI values mean southerly flows, whilst negative MI values indicate northerly flows.

It is thought that the equator-to-pole temperature gradient controls the characteristics of circumpolar flow (Lamb, 1982). During cooler periods in the middle and lower latitudes of the Northern Hemisphere, the latitudinal temperature gradient is steepened, which weakens the strength of westerly winds (zonal flow) and favours more frequent occurrences of meridional (north-south) flow (Rumsby and Macklin, 1994). Figure 8.10 shows many of the links that would be expected between regional temperature and the strength of zonal airflow. During the late-19th and early-20th century, quite low temperatures at Athens were accompanied by fairly weak zonal flow (and hence stronger meridional circulation). This was particularly clear for the period c. 1903 - 1913, which saw a drop in both temperatures and ZI. Immediately after this time a gradual increase in temperature, and hence weakening of the latitudinal temperature gradient, saw the ZI increase to a peak in 1926-27, coinciding with the warmest year on record at Athens. A gradual cooling trend from 1930 onwards brought weaker westerly zonal flow during the rest of the 20th century. Interestingly, the period of weakest zonal flow occurred during a cold period around 1970-71, the time of the largest floods on the Voidomatis and Aoos Rivers. These atmospheric changes may therefore have had very significant effects in terms of flood production. It is clear for this region that temperature has a significant influence on nature of large scale atmospheric circulation. Kozuchowski and Marciniak (1988) have observed a similar trend for southern Europe as a whole, with cooler winter temperatures occurring with increasing meridional flow.

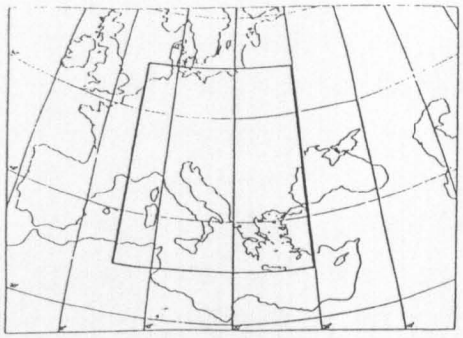

FIGURE 8.8 Map showing the limits of the region for which zonal and meridional indices were calculated, with the location of the study area in northern Greece identified. The area is a suitable size to characterise the direction of circumpolar airflow affecting the eastern Mediterranean.

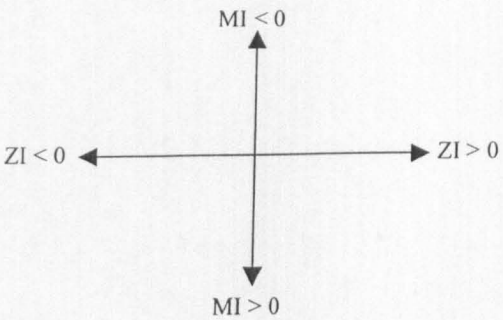

FIGURE 8.9 Illustration showing the prevailing circulation according to various ZI or MI values. *(Source: Kutiel et al., 1996).*

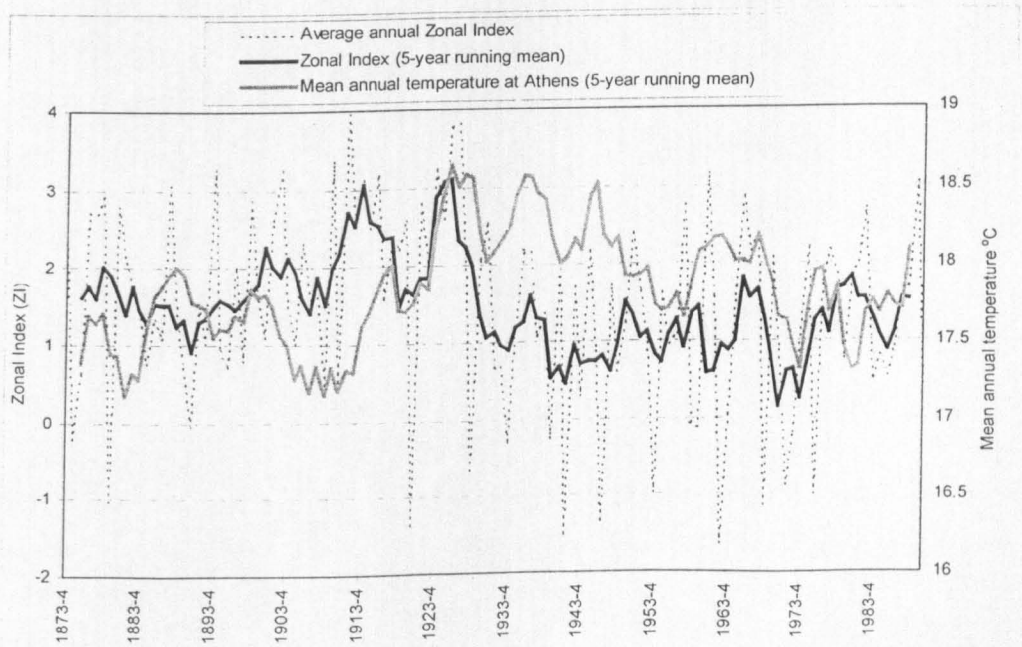

FIGURE 8.10 Variation in the Zonal Index (ZI) from 1873 to 1990, compared with the mean annual temperature at Athens. The zonal index is that from the region shown in Figure 8.8.

To allow a precise comparison between flood hydrology and prevailing atmospheric circulation, z scores for precipitation and river discharge have been correlated with ZI and MI. Spearman's rank correlation coefficients for precipitation and stage have been calculated as the data did not display normal distributions so a non-parametric test was required.

There is generally a negative relationship between precipitation and ZI, statistically significant at the 95% confidence level for both winter and summer (Table 8.3). This points to a lower ZI (a weakening of westerly airflow) being more conducive to precipitation. In autumn and spring the relationship seems less apparent (Table 8.3). Correlations with MI also tend to be negative, though generally less significant than with ZI. This suggests wetter conditions with decreasing MI (a weakening of southerly flow), although in summer this tendency may be reversed. Again, the correlations are only weak in autumn and spring (Table 8.3). Overall this suggests that wetter conditions generally occur with northeasterly meridional flows, although wetter conditions in summer may occur with southeasterly meridional flow. Certainly weakening zonal flow generally produces increased precipitation. This phenomenon is consistent with the findings of many recent climatological studies in the Mediterranean region (Kozuchowski and Marciniak, 1988; Maheras, 1988; Maheras and Kolyva-Machera, 1990; Kutiel *et al.*, 1996). The weakening of zonal flow allows expansion of the polar front and latitudinal mixing of warm and cold air, which leads to unsettled weather (Winstanley, 1973; Perry, 1981).

TABLE 8.3 Correlation coefficients between precipitation z scores and zonal and meridonal indices (ZI and MI). The period 1954-55 until 1990-91 uses z scores for Konitsa until 1968-69, after which mean z scores for all available stations are used. Correlation was subsequently carried out on the latter period alone. Figures in bold are significant at the 0.05 level, those in italics at the 0.1 level. R_s is the Spearman's rank correlation coefficient, and N is the number of years in the record.

		Annual		Autumn		Winter		Spring		Summer	
		R_S	N	R_S	N	R_S	N	R_S	N	R_S	N
1954-1991	ZI	-0.09	37	-0.27	37	-0.36	37	+0.02	37	**-0.56**	37
	MI	-0.21	37	-0.10	37	**-0.50**	37	-0.01	37	+0.08	37
1968-1991	ZI	-0.02	23	-0.11	23	**-0.47**	23	-0.20	23	**-0.72**	23
	MI	-0.10	23	-0.17	23	*-0.39*	23	-0.12	23	+0.27	23

The results of correlations between both mean and maximum discharge and ZI and MI are shown in Table 8.4. These show notably lower correlation coefficients than for precipitation, suggesting that river flow may be more strongly affected by factors other than regional meteorology. Correlations with mean annual and seasonal discharge show no discernible trend (Table 8.4a). The maximum discharge at Bourazani Bridge is generally higher with weaker MI (greater northerly flow), however this pattern is not observed at Doukas Bridge (Table 8.4b). To see if a clearer pattern was exhibited by periods of particularly high, separate correlations were carried out on those years where z is greater than 0.5 (Table 8.5). More significant correlations were found here, although there appears to be no consistent trend in the data, with great

variability in the strength and direction of these relationships. This may partly be related to the low number of high and low flow years available, with such small samples being less suitable for correlation analysis. However, this may also reflect considerable complexity in general annual and seasonal relationships between river flow and atmospheric conditions. Whilst precipitation shows a consistent relationship with ZI and MI (Table 8.3), river flow may be affected by many other factors such as antecedent soil moisture conditions, the intensity and duration of rainfall experienced and the timing of snowmelt. For specific flow maxima it may also be more significant to investigate the atmospheric conditions at the specific time of the flood event, rather than the annual or seasonal average airflow. Therefore the following section explores the synoptic daily atmospheric conditions associated with some of the largest floods on record.

TABLE 8.4 Correlation coefficients between zonal and meridional indices (ZI and MI) and; a) mean river discharge z scores, and b) maximum river discharge z scores. Discharge was selected for years with complete flow records at Bourazani Bridge (1954-55 to 1978-79) and Doukas Bridge (1967-68 to 1974-75; 1978-79; and 1984-85 to 1990-91). Figures in bold are significant at the 0.05 level, those in italics at the 0.1 level. R_s is the Spearman's rank correlation coefficient, and N is the number of years in the record.

a) Mean Discharge		Annual		Autumn		Winter		Spring		Summer	
		R_S	N	R_S	N	R_S	N	R_S	N	R_S	N
Bourazani Bridge	ZI	+0.07	25	-0.17	25	-0.04	25	+0.03	25	-0.16	25
	MI	-0.15	25	+0.17	25	-0.22	25	-0.25	25	+0.23	25
Doukas Bridge	ZI	-0.21	17	+0.19	17	-0.08	17	-0.33	17	0.12	17
	MI	+0.05	17	+0.37	17	-0.28	17	-0.19	17	0.16	17

b) Maximum Discharge		Annual		Autumn		Winter		Spring		Summer	
		R_S	N	R_S	N	R_S	N	R_S	N	R_S	N
Bourazani Bridge	ZI	+0.07	25	+0.10	25	-0.05	25	-0.03	25	+0.09	25
	MI	-0.23	25	+0.00	25	-0.22	25	**-0.51**	25	-0.05	25
Doukas Bridge	ZI	+0.18	17	-0.06	17	-0.20	17	-0.14	17	0.29	17
	MI	+0.41	17	+0.30	17	+0.02	17	-0.37	17	0.18	17

TABLE 8.5 Correlation coefficients between zonal and meridional indices (ZI and MI) and mean and maximum river discharge z scores only for years of *high* flow (where z>0.5). The discharge years used were the same as in Table 8.4. Figures in bold are significant at the 0.05 level, those in italics at the 0.1 level. R_s is the Spearman's rank correlation coefficient, and N is the number of years in the record.

a) Mean Discharge HIGH FLOW YEARS		Annual		Autumn		Winter		Spring		Summer	
		R_S	N	R_S	N	R_S	N	R_S	N	R_S	N
Bourazani Bridge	ZI	+0.50	3	-0.20	4	-0.80	4	+0.80	4	+0.50	3
	MI	**+1.00**	3	-0.40	4	+0.40	4	**-1.00**	4	**+1.00**	3
Doukas Bridge	ZI	+0.43	6	+0.40	4	+0.80	4	+0.54	6	**+1.00**	3
	MI	+0.14	6	-0.80	4	**-1.00**	4	-0.31	6	+0.50	3

b) Maximum Discharge HIGH FLOW YEARS		Annual		Autumn		Winter		Spring		Summer	
		R_S	N	R_S	N	R_S	N	R_S	N	R_S	N
Bourazani Bridge	ZI	-0.29	7	-0.20	6	-0.29	7	+0.37	6	+0.10	5
	MI	-0.14	7	-0.49	6	+0.64	7	-0.54	6	+0.50	5
Doukas Bridge	ZI	-	2	-0.50	3	-0.80	4	+0.11	4	+0.21	5
	MI	-	2	+0.50	3	-0.20	4	+0.31	4	+0.41	5

8.2.4.2 Single event flood hydroclimatology

The most intense precipitation and flooding recorded in the Voidomatis and Aoos basins occurred during the New Year period of 1970-71 (section 8.2.3). Investigation of the synoptic meteorological conditions recorded in archive sources for this time shows the atmospheric configuration that gave rise to this extreme event. Before the flooding on the 29th December, a large frontal system was positioned across the eastern Mediterranean and pressure was 1020 mb over northern Greece (Figure 8.11). A low near the Iberian Peninsula on the 29th deepened and moved east to be located to the north of Italy on the 30th. Although there are no precipitation records for this day, the study area must have experienced intense precipitation as river discharge rapidly increased to over 1000 m^3s^{-1} at Bourazani Bridge (Figure 8.11). This day saw intense meridional air mixing, with pressure dropping to 1008 mb over Epirus, and rain probably fell due to the uplift of warm air associated with the cold front. By the 31st December this low pressure system had continued to move east towards Russia, but northern Greece remained close to the frontal system, just in the lee of the cold front. This brought daily precipitation of over 100 mm at all stations, and the Aoos at Bourazani Bridge and the Voidomatis both reached their peak discharge ever recorded. The 1st January 1971 saw a low pressure system deepen and move eastward from the central Mediterranean, so that northern Greece remained dominated by low pressure and atmospheric instability. Intense precipitation continued, probably still influenced by the uplift of warm air at the cold front to the east. Although discharges began to wane on the Voidomatis and at Bourazani Bridge, the maximum discharge at Doukas Bridge occurred at this time (Figure 8.11).

It is clear that this extreme event of 1970-71 was generated by particularly unstable large-scale atmospheric conditions. This four-day period saw intense mixing of warm air from the lower latitudes with cold arctic air, with the jet stream showing an extended, sinuous course over Europe. This meridional air movement gave rise to a number of anticyclonic depression systems, with warm air being forced above denser, cooler air. Particularly intense rainfall occurred just in the lee of a cold front, which only moved slowly over Epirus resulting in persistent heavy rainfall. This would undoubtedly have been aided by orographic uplift of relatively warm and moist winds coming from the Ionian Sea. If this rain fell on snow lying on the mountains this stored water may also have been released and 'rain-on-snow' effects may have contributed to the extreme discharges.

The lee of a cold front frequently gives heavy rainfall in the eastern Mediterranean, as shown in Figure 8.12 for a more recent period of intense storms in 1996. On the 27th November 1996, just five days before the chart shown in Figure 8.12, the largest flood on record at Doukas Bridge since the New Year 1970-71 event occurred (Figure 3.24). On this day the atmospheric configuration was very similar to that shown in Figure 8.12, with a cold front having just passed over northern Greece as part of a large low pressure system. Thus another very large flood occurred when Greece was positioned in the lee of a cold front. Cold fronts are by far the most

common type of front experienced across the Mediterranean region, contributing 70 - 80% of all frontal systems (Flocas, 1984). Considering the 1970-71 and 1996 events, it is likely that cold fronts are very important in generating extreme floods. Inspection of synoptic charts for other large flood events in the systematic records provides an interesting comparison with these two events. The second largest flood on record at Bourazani Bridge occurred on the 13th January 1966, when several low pressure cells and anticyclonic systems were centred over the eastern Mediterranean, and again the study area lay at the boundary between warm and cold air masses (Figure 8.13). The close proximity to two low pressure systems would have produced very unstable weather conditions. The third largest flood at Bourazani Bridge occurred several years earlier, on the 19th January 1963. This day saw a large, deep, single low pressure frontal system over the whole of the Mediterranean region, with winds blowing from the south (Figure 8.14). Instead of a close cold front as with the charts shown in Figure 8.11, this day saw the leading warm front of the depression positioned over northern Greece. Thus exactly the same synoptic atmospheric conditions do not always occur at the time of largest floods. This probably explains the poor correlations between ZI and MI and the years and seasonal or maximum flows.

However, a number of features are common in the weather charts at the times of the major flood events on the Voidomatis and Aoos. All of these days saw northern Greece lying in close proximity to low pressure cells passing over the Mediterranean region., the centre of which is almost always at a latitude just north of northwest Greece (c. 40 - 45°N). The majority of the largest floods occurred when quite well developed frontal systems were affecting the region, providing very unstable atmospheric conditions. Two of the largest events, and in particular the most extreme event in 1970-71, saw northwest Greece positioned just in the lee of a cold front which was migrating to the east as the following tail of large depression. This was particularly severe during the New Year of 1970-71 as the cold front and low pressure exhibited very slow movement and therefore remained close to the study area, giving sustained and intense rainfall for several days (Figure 8.11). Slow moving, persistent weather systems are known to increase the likelihood for high magnitude flash flooding, both in the Mediterranean region (Doswell *et al.*, 1998) and elsewhere (Doswell *et al.*, 1996).

FIGURE 8.11 (Following page) Daily hydrological data and weather charts for the period 29th December 1970 to 1st January 1971 which saw high flood magnitudes on the Voidomatis and Aoos Rivers. † Denotes that these are indirect discharge estimates[1]. *(Weather charts from The Times).*

29th December 1970

River Discharge (m^3s^{-1}):	
Bourazani Br.	85.3
Voidomatis†	81.1
Doukas Br.	4.2
Precipitation (mm):	
No records	

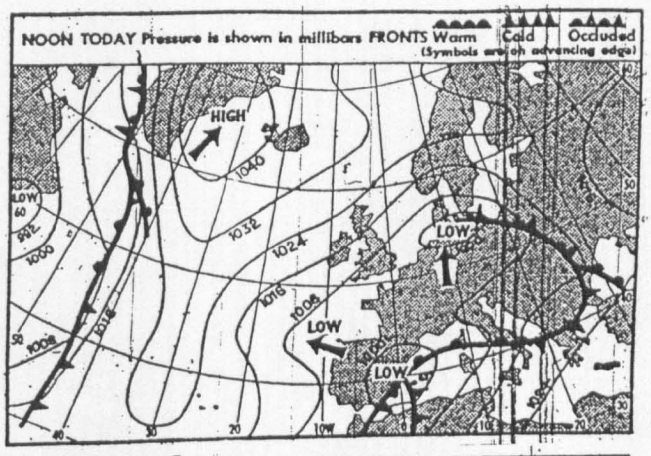

30th December 1970

River Discharge (m^3s^{-1}):	
Bourazani Br.	1005.3
Voidomatis†	987.7
Doukas Br.	17.5
Precipitation (mm):	
No records	

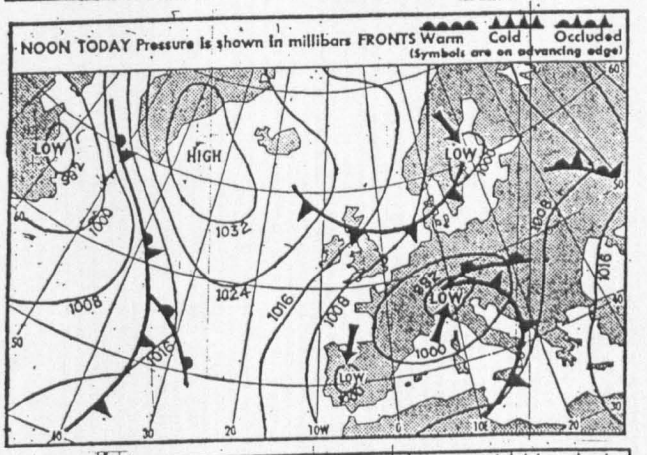

31st December 1970

River Discharge (m^3s^{-1}):	
Bourazani Br.	1779.4
Voidomatis†	1627.1
Doukas Br.	152.3
Precipitation (mm):	
Vovoussa	161.9
Pades	113.5
Kipi	102.5

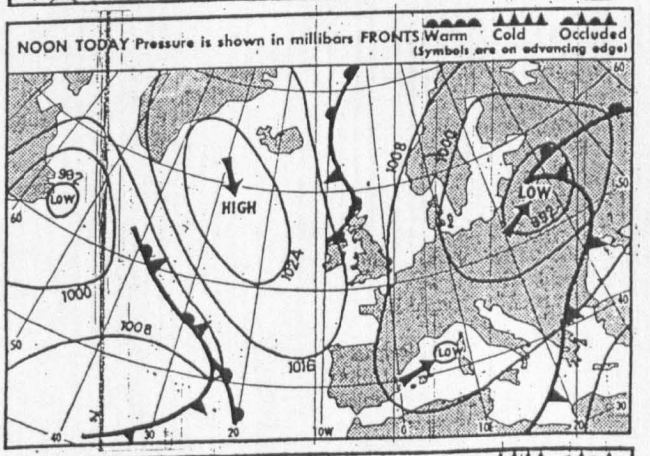

1st January 1971

River Discharge (m^3s^{-1}):	
Bourazani Br.	808.2
Voidomatis†	592.5
Doukas Br.	215.7
Precipitation (mm):	
Vovoussa	153.4
Pades	148.4
Kipi	89.5

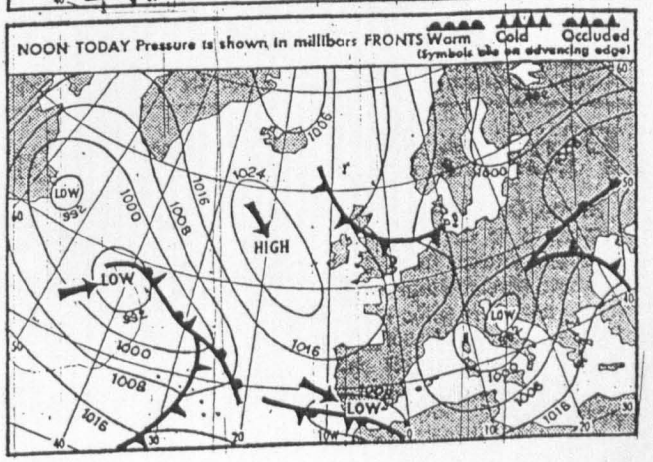

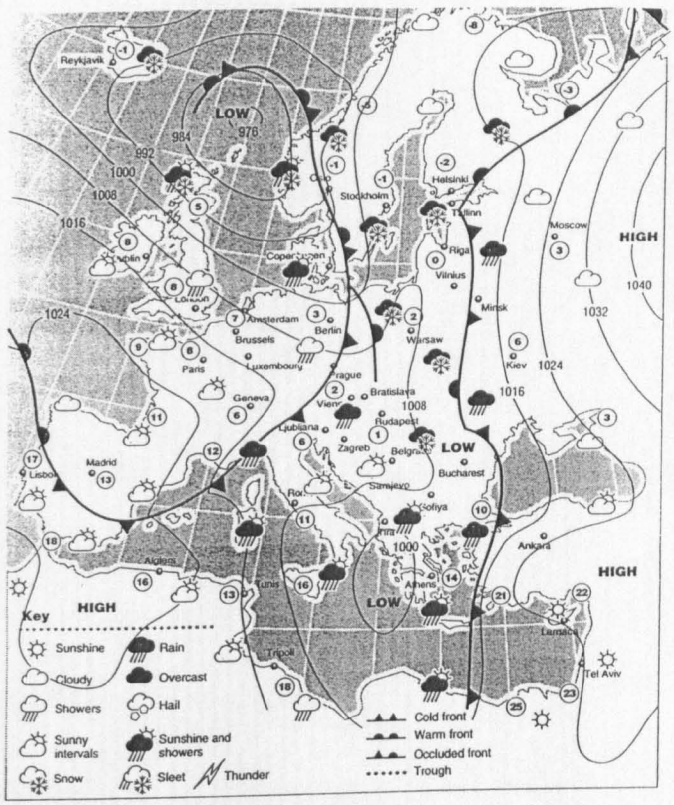

FIGURE 8.12 Weather chart for the 2nd December 1996. This period saw very heavy rain in the Voidomatis and Aoos basins, as witnessed by the author whilst on fieldwork, and high river discharges (as recorded in the Doukas Bridge record). Greece lay in an area of low pressure, just in the lee of a cold front. This is a similar situation to the New Year flooding of 1970-71, shown in Figure 8.11. Behind the cold front warm air is being undercut by cold air, and therefore forced to rise, cool and condense. This brought wet weather across the whole of the eastern Mediterranean at this time. *(Source: The Guardian, 2/12/96).*

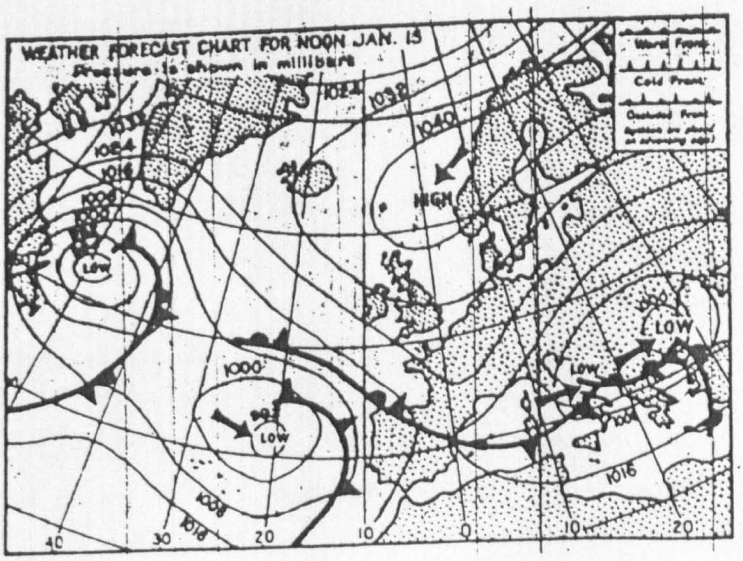

FIGURE 8.13 Weather chart for the 13th January 1966. *(Source: The Times, 13/1/66).*

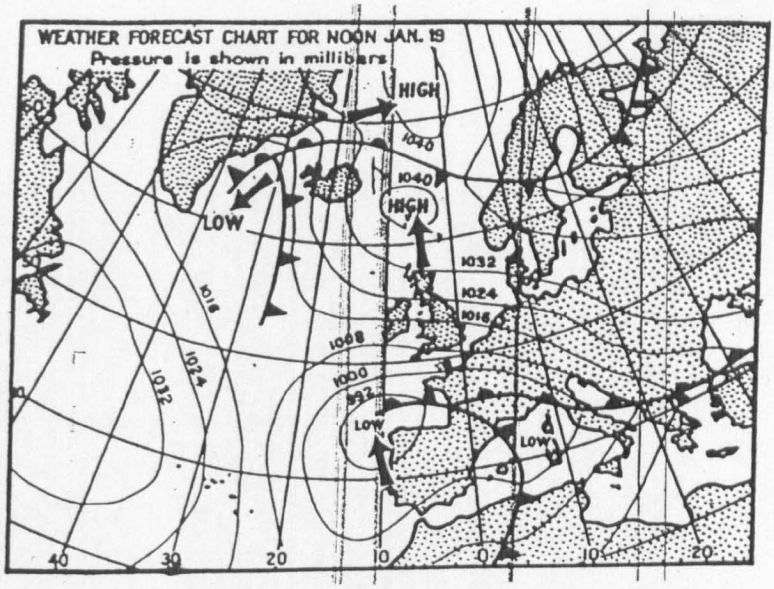

FIGURE 8.14 Weather chart for the 19th January 1963. *(Source: The Times, 19/1/63).*

8.2.4.3 Implications for extreme flood occurrence and prediction

A comparison of ZI and MI with precipitation and discharge has enabled the broad climatic conditions that are likely to produce wet weather and floods to be identified. The generation of the most severe flood events have been investigated in more detail, to explore the atmospheric configurations that have given rise to high magnitude flooding. Wetter conditions occur with a weakening of westerly zonal circulation, and an increase in northeasterly meridional flows, although wetter conditions in summer may occur with southeasterly meridional flow (Table 8.3). River flow shows less consistent relationships with general airflow directions, although inspection of daily synoptic charts at the time of major flood events has confirmed the importance of meridional mixing of warm and cold air masses in low pressure systems for generating the most intense rainfall and flood events.

The comparison of hydrological patterns with large-scale atmospheric circulation should not be expected to reveal simple reproducible patterns (Doswell *et al.*, 1996, 1998; Romero *et al.*, 1998). The synoptic climatology of flood-producing conditions is quite variable, with differing wind directions and atmospheric conditions inducing large flood events. The Mediterranean climate is complex, and similar circulation may give very different weather at different places and different times (Maheras *et al.*, 1994). In addition, whilst atmospheric configurations may control general trends in flood frequency and magnitude, there will be other more local influences determining the nature of rainfall-runoff conversion at a certain point in space and time (Hirshboeck, 1988; Maheras and Kolyva-Machera, 1990). Numerous other studies in the Mediterranean have identified this complexity in the occurrence and timing of

certain weather conditions, but have also concluded that large scale atmospheric circulation remains a very important controlling factor (Winstanley, 1973; Kuzuchowski and Marciniak, 1988; Maheras and Kolyva-Machera, 1990; Maheras *et al.*, 1992, 1994; Kutiel, 1996; Reddaway and Bigg, 1996; Doswell *et al.*, 1998).

The results in this section are consistent with other studies, as they have illustrated the important influence of large-scale atmospheric instability in generating extreme floods on the Voidomatis and Aoos Rivers. Such information is very important for successful and informed flash flood prediction, as whilst there is complexity and variability in the flood-producing system, certain common features between extreme flood events can normally be identified (Doswell *et al.*, 1996). These are what Doswell *et al.* (1996) have termed the 'ingredients' of flash flooding, and they are very important to recognise if flash flood prediction is to be successful. The key ingredients for extreme floods identified in this study are; (1) deep low pressure systems invading close to the area of interest, allowing the convection of warm, moist air; (2) orographic effects are always likely to accentuate convection; (3) flooding is intensified by slow moving weather systems which bring persistent heavy rainfall; (4) particularly intense precipitation falls in the lee of a cold front.

8.2.5 Perspective

The investigation of the systematic hydrological data in this section has determined the nature of recent changes in flood hydrology and has given a detailed insight into the flood producing system. This provides a valuable basis upon which to extend the flood records with palaeoflood data.

8.3 BOULDER BERMS: IDENTIFICATION, DESCRIPTION AND CHRONOLOGY

The use of coarse-grained flood deposits such as boulder berms in palaeoflood reconstruction has been reviewed in section 2.2. Boulder berms are open-framework accumulations of gravels and boulders that have been deposited across or adjacent to the river channel during flood events (Costa, 1984). This section describes the results from the analysis of boulder berms in the Voidomatis and Aoos basins.

8.3.1 Description and location of boulder berm study reaches

A reconnaissance study of the Voidomatis and Aoos Rivers found that boulder berms were not present throughout the catchments. Instead, distinct boulder berms only occurred in the Upper Vikos Gorge and the Aoos Ravine. Widespread lichen growth on the boulders enabled these deposits to be dated by lichenometry (section 8.3.2). Boulder berms were investigated in three study reaches where they were common and well preserved.

8.3.1.1 Vikos Canyon Boulder Berm Reach

This c. 2 km reach is located at the downstream end of the Upper Vikos Gorge, just below the village of Vikos (Figure 4.5). The valley floor is confined to less than 100 m wide in places, due to the narrowness of the gorge the large talus cones which run down close to the river itself (Figure 3.11). Although the floodplain is largely composed of extensive areas of near-channel benches covered in gravels, there are numerous small segments of both Late Pleistocene and Holocene alluvium preserved around the edge of the valley floor (Figure 8.15a). The channel itself is steep gradient (0.022), with margins of exposed bedrock and large boulders. Eight small boulder berms are preserved at the upstream end of the reach, whilst one large berm is preserved at the downstream end (Figure 8.15a).

8.3.1.2 Aoos Ravine Boulder Berm Reach

This reach is roughly 1.5 km long, located at the mouth of the Aoos Ravine just upstream of Konitsa (Figure 4.6). In contrast to the above reach in the Vikos Canyon, there are no clear river terraces, but instead much of the valley floor is occupied by large areas of recent gravel which are partially stabilised by vegetation (Figure 8.15b; and general view of the area in Figure 3.16). Seven distinct boulder berms have been identified in this reach preserved in near-channel floodplain areas.

8.3.1.3 Vikos Canyon Fan Reach

Two boulder berms were studied in in the shorter Vikos Canyon fan reach (Figure 4.5). This reach has been described in section 6.3.6 and a geomorphological map displayed in Figure 6.10. These two prominent berms lie above the main channel banks at heights of over 5 m above the channel bed (Figure 6.10).

A number of reasons explain why boulder berms are only found within these large gorges. Previous authors have suggested that local hydraulic conditions may be the most important control on the location of boulder deposits, assuming that a reasonable volume of coarse sediment is available throughout the river (Carling, 1989; Wohl, 1992b). Clearly overbank boulder deposition can only result from quite exceptional localised flow conditions. River channels in the Upper Vikos Gorge and Aoos Ravine follow a relatively straight course through a steepland area, and consequently have high channel gradients (Lewin *et al.*, 1991). During floods this produces high velocity, deep flows in these narrow bedrock and boulder bed gorge environments. Such conditions can result in exceptionally high stream powers (Baker, 1984, 1988; Baker and Costa, 1987; Baker and Kale, 1998) capable of depositing coarse gravels and boulders overbank, leaving berms after the flood. In other areas of the catchments, where the channel gradient is less steep and the valley floor wider, the stream powers generated during floods will be much lower. Extensive boulder deposits are also encouraged by increased coarse

sediment availability (Grimm *et al.*, 1995; Cenderelli and Cluer, 1998), and this is very high in these canyons, where colluvium supplies large rock clasts to the river (Figure 3.12 and 3.16).

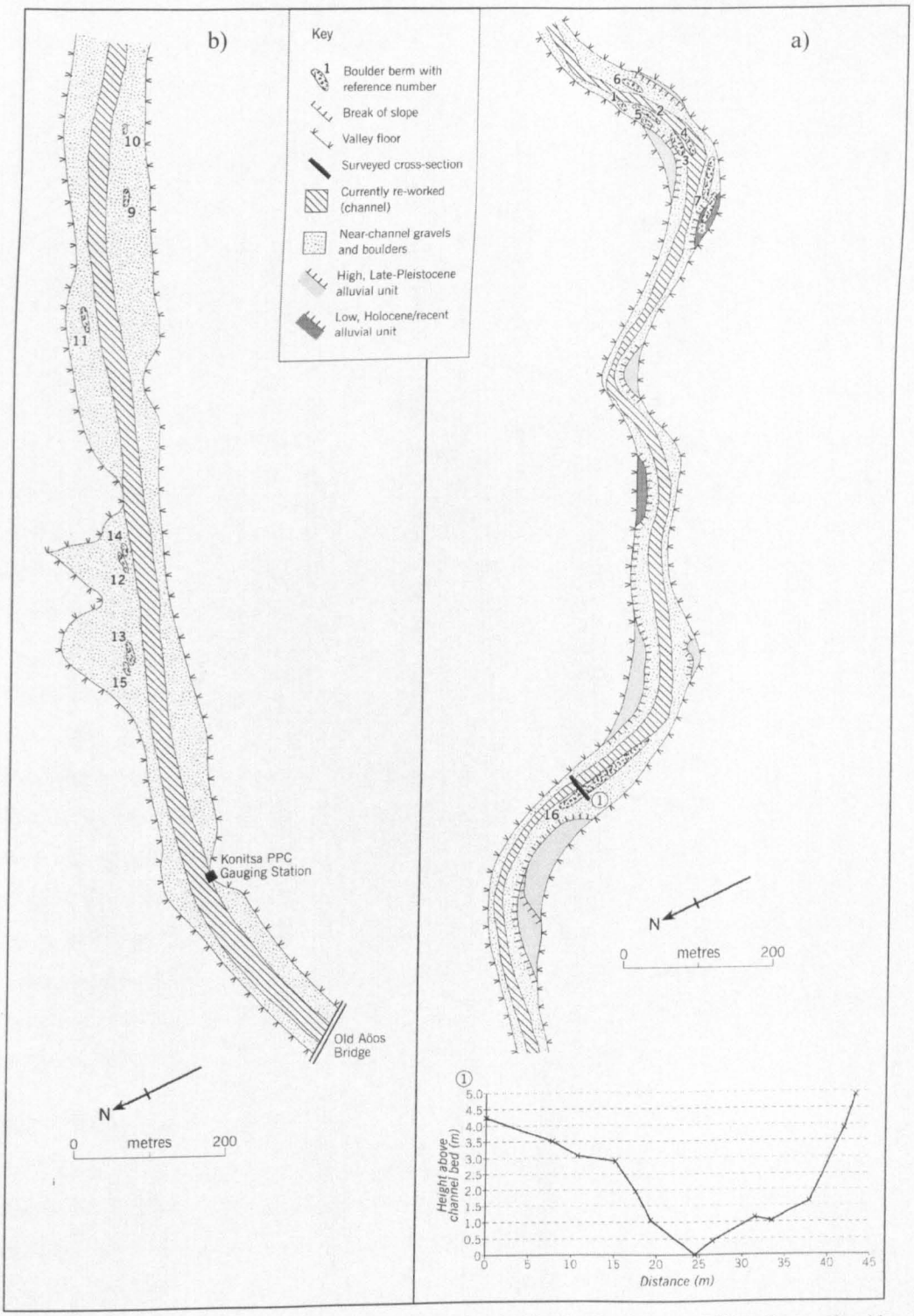

FIGURE 8.15 Geomorphological map and topographic survey results from; a) the Vikos Canyon boulder berm reach on the Voidomatis River; and b) the Aoos Ravine boulder berm reach on the Aoos River. The cross section is shown viewing the section from the upstream direction, with heights relative to channel bed. The Late Pleistocene and Holocene alluvium are identified by means of the distinctive lithofacies and height above channel. The location of these reaches is shown in Figure 4.5.

When using boulder berms in palaeoflood reconstruction it is important to establish that they were deposited by Newtonian (water) flows, rather than non-Newtonian flows such as debris flows (section 2.2.2). There are a number of criteria for discriminating these types of deposits (section 2.2.2.2). In this study emphasis has been placed on four of the most reliable indicators of Newtonian transport and deposition:

1. Berms lack a fine sediment matrix between the boulders (Mears, 1979; Costa, 1984; Cenderelli and Cluer, 1998). This is probably the most useful diagnostic feature (section 2.2.2.2).
2. It is normal for berms to be aligned in the direction of river flow (Carling, 1987, 1989).
3. Boulder alignment: berms normally have a fairly consistent clast alignment parallel or perpendicular to the direction of flow (Carling, 1987; Costa, 1988), and clast imbrication may also be evident (Costa, 1984).
4. Berms often result in a floodplain trough on the distal side from the channel (Carling, 1989).

These characteristics were investigated by field observations and geomorphological mapping of reaches containing boulder deposits. Mapping provides a clear indication of whether their alignment and location is indicative of a water flood deposit, isolated from major tributary or colluvial inputs. Deposits were not studied unless they at least conformed to criteria 1, 2 and 3 above. If the deposits showed any of the features of debris flows described in section 2.2.2 they were discounted. The maps of the boulder berm reaches show that all of the berms are aligned in the direction of river flow and at locations where flow separation may have occurred, facilitating deposition (*cf.* Carling, 1987, 1989). For example, in Figure 8.15a berms are identified on the inside of a meander just before the bend apex and on the outside of the bend a little downstream of the apex. Closer inspection of the deposit serves to further confirm their water-flood origin. For example, Figure 8.16 shows berm 17 in the Vikos Canyon fan reach (Figure 6.10). The berm is distinct because it is free of a fine-grained matrix, and is aligned in the downstream direction. This berms also displays the classic trough on the far side from the modern channel (Figure 8.16). Using the above four criteria, 18 berms were identified in these three study reaches. The deposits were then analysed to determine the age and the magnitude of the floods that deposited them, as described in the following sections.

8.3.2 Lichenometric dating

Of the various possibilities for dating boulder berms (see section 2.2.3), lichenometry was selected as being the most appropriate for these deposits (section 4.1). This technique uses the size of lichen thalli as a measure of the age of the substrate upon which they are growing (see section 4.4.2). The common occurrence of *Aspicilia calcaria (L.) Mudd* on the majority of rock surfaces around the study area meant that it was possible to use this lichen species for dating purposes. The lichen measurement procedures have been described in section 4.4.2.2. There are two stages to the dating procedure. Firstly, a lichen growth curve must be constructed for the

FIGURE 8.16 The foreground shows berm 17 in the Vikos Canyon fan reach (Figure 6.10). This view is looking upstream, the main channel sweeping around the berm to the right. The boulders, which are nearly all over 1 m in diameter, are free of interstitial fines, and some show imbrication and alignment in the downstream direction. A distal floodplain trough is also evident on the left of the photograph where a number of small trees are growing.

local region. This growth curve can subsequently be used to determine the age of the berms on the basis of the size of lichen growing upon the boulders.

The growth curve was constructed by measuring the largest lichen growing on independently dated surfaces, such as monuments, bridges, walls and buildings (Appendix XI). The growth curve, shown in Figure 8.17 shows an exceptionally good correlation between age and lichen size ($R^2 = 0.923$). Most of the independent age measurements were taken at sites within the study basins, and even the most distant were no further than 8 km outside the watersheds. This restricted the number of calibration points on the growth curve to 17. However, spatial restrictions were important as they ensured that the growth curve only reflects the local environmental conditions, and does not include data from more distant areas where even small environmental differences could distort growth rates (section 4.2). The region of Epirus, like many mountain regions, has been shown to have steep environmental gradients (section 3.1) and therefore lichen growth rates could vary considerably over a larger area. Using the linear growth curve relationship, lichen size can be converted to age. The regression relationship shown in Figure 8.17 has a low degree of scatter around the fitted line and is significant at the 99.9% confidence level, which suggests that the growth curve provides a reliable means of age estimation from lichen size. Additional confidence can be draw from the

fact that the regression line almost exactly crosses the y axis at zero, as would be expected (zero years should equal zero lichen growth) (Figure 8.17). The growth rate of 0.63 mm yr^{-1} is quite similar to that of 0.83 mm yr^{-1} for this species determined in southwest Crete (Maas, 1998; Maas *et al.*, 1998), the slightly slower rate in Epirus probably being explained by generally cooler temperatures than Crete.

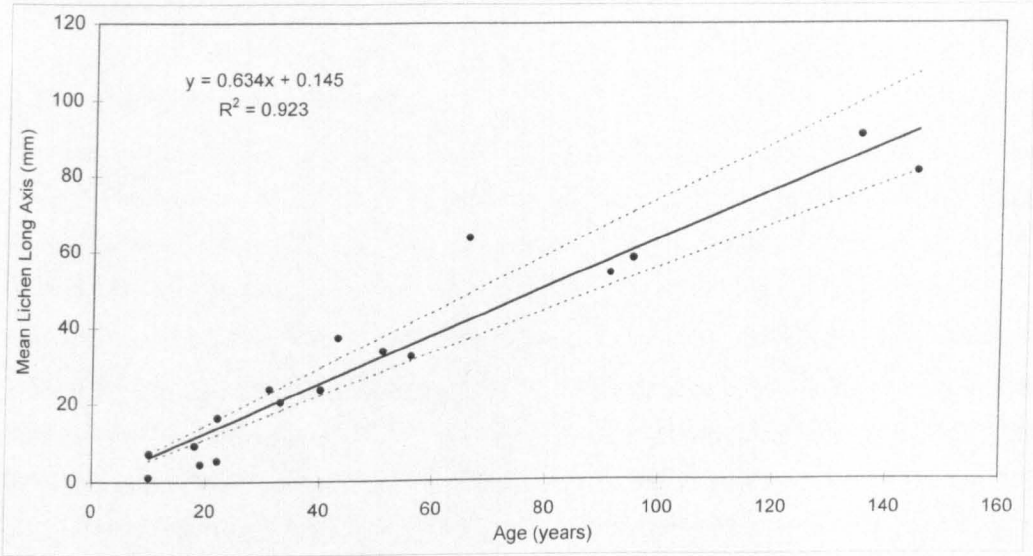

FIGURE 8.17 Growth curve for *Aspicilia calcaria (L.) Mudd* constructed for the Voidomatis and Aoos basins. The mean of the five largest lichen long axes (mm) is taken as a measure of substrate age (section 4.4.2.2). Following the approach of Maas *et al.* (1998), upper and lower quartile growth rate envelope lines (dotted lines) provide maximum and minimum age estimates. For the conversion of lichen sizes to age, the two parameters in the growth curve were regressed on the opposite axes to obtain a linear regression equation that was used for this purpose.

To test the reliability of the growth curve it is important to check that there are no significant environmental influences on lichen growth, such as altitude or precipitation, which could result in unequal growth rates on different boulder berms. Previous workers have attempted to assess environmental effects on lichen growth by correlating lichen size data with a range of environmental factors (Macklin *et al.*, 1992a; Merrett and Macklin, 1999). However, this relies on the age of independently dated substrates being the same in different places, which is unlikely to be the case. Instead, it is more meaningful to correlate lichen *growth rates* with environmental variables. Table 8.6 shows that neither precipitation nor elevation has a significant effect on lichen growth, whereas the relationship between lichen size and substrate age is significant at the highest conventional significance levels. Field investigations also found there was no detectable influence of aspect on lichen growth. Therefore, around the Voidomatis and Aoos basins the growth of *Aspicilia calcaria (L.) Mudd* can be expected to be relatively uniform, and consequently provides a valuable dating tool. The dating results for the berms are discussed in combination with flood magnitude data in subsequent sections.

TABLE 8.6 Spearman's rank correlation coefficients (n=17) between various lichen data used in the growth curve and environmental parameters. Precipitation was determined from the mean annual precipitation at the closest station and ranged from 1079 – 1484 mm. Elevation was estimated from topograpic maps and ranged from 300 – 1300 m asl. There is no significant relationship between growth rate and either precipitation or elevation.

	R_s
Lichen size v age	+0.947†
Growth rate v precipitation	+0.091
Growth rate v elevation	-0.241

† Significance level is <0.001.

8.3.3 Palaeodischarge estimations

The most common approach for determining palaeodischarge from coarse-grained flood deposits has been to apply sediment transport equations to relate the size of boulders within a deposit to the magnitude of flow which deposited them (e.g. Costa, 1983; Williams, 1983). Section 2.2.4 discussed how these approaches often only provide quite rough flow estimates, as they are only based on a fairly limited knowledge of flow during extreme floods due to the difficulties in observing or measuring such events. However, for this study they provide the only clear method available for estimating palaeodischarge from boulder berms. The results have been assessed where possible through independent flow measurements.

Palaeodischarge estimates were calculated using the methods of Costa (1983) and Williams (1983), which determine the flow from the size of the boulders in each berm, as described in section 2.2.4. The assumption that the few largest boulders measured are proportional to the flood magnitude is reasonable in this study, as a very large range of boulder sizes are available for transport in both the Upper Vikos Gorge and The Aoos Ravine (e.g. Figures 3.12 and 3.16). The b-axis of boulders in the berms was measured in the field to the nearest centimetre using a tape measure (see Table 8.7), whilst cross sections and channel slope were determined from surveying, 1:50 000 topographic maps and geomorphological mapping.

Some other approaches were considered, but rejected. The basic Manning's approach of Mears (1979) was found to produce unrealistic results. The approach of Carling (1986) was not adopted as these equations are site-specific and not suitable for general application (Komar, 1987). Equations presented by Bathurst *et al.* (1987) are only calibrated for medium to fine gravels, which means that their application to the large boulders found in these berms (Table 8.7) would have been inappropriate.

The results of the palaeodischarge estimations are shown in Figure 8.18. The equations of Williams (1983) are intended to determine the *minimum* flow required to transport clasts of a certain size, whilst Costa's equations are aimed at determining the exact flow magnitude. This explains why the results of the Williams (1983) procedure are consistently lower than those of Costa (1983). Williams (1983, p.240) admits that, "the actual transporting flow could have been much higher than this minimum". In contrast, the approach of Costa (1983) has been criticised for having a tendency to overestimate discharges (Carling, 1986; Reid and Frostick, 1987;

Komar, 1988, 1989). Thus it is likely that the true discharge actually lies between these two estimates.

TABLE 8.7 Lichen size, boulder size and estimated age data for the 18 boulder berms studied. The mean of the five largest lichen was selected as a suitable measure of lichen size for lichenometry (section 4.4.2). The mean of the 10 largest boulders has been used to represent clast size in boulder berms for the palaeodischarge calculations using the method of Williams (1983). Dates have been calculated using the lichen growth curve shown in Figure 8.17. The estimated minimum and maximum dates are determined from the upper and lower quartile growth rate envelope lines (after Maas *et al.*, 1998).

Berm no.	Location	Mean of the five largest lichen (mm)	Mean of the ten largest boulders (mm)	Date (AD)	Estimated date range
1	Upper Vikos Gorge	50	808	1919	1909-1931
2	Upper Vikos Gorge	53	1416	1914	1903-1926
3	Upper Vikos Gorge	47	1065	1924	1914-1934
4	Upper Vikos Gorge	21	1150	1966	1962-1970
5	Upper Vikos Gorge	93	1005	1851	1831-1872
6	Upper Vikos Gorge	23	860	1963	1958-1968
7	Upper Vikos Gorge	71	1650	1887	1872-1903
8	Upper Vikos Gorge	101	1630	1839	1818-1862
9	Aoos Ravine	19	980	1969	1965-1973
10	Aoos Ravine	13	815	1977	1975-1980
11	Aoos Ravine	13	1070	1978	1975-1981
12	Aoos Ravine	22	950	1964	1959-1969
13	Aoos Ravine	10	1443	1983	1981-1985
14	Aoos Ravine	No lichen	878		
15	Aoos Ravine	53	1125	1915	1904-1927
16	Upper Vikos Gorge	127	2150	1798	1771-1827
17	Upper Vikos Gorge	137	2210	1782	1753-1813
18	Upper Vikos Gorge	No lichen	1900		

Assessment of these results is possible for berms found in the Aoos Ravine reach, due to the proximity of the Konitsa gauging station (Figure 8.15b), for which fairly regular daily discharge readings are present from the late-1960s until the late-1980s (Appendix I). Additionally, the Doukas Bridge station is only 4 km further downstream (Figure 3.1). Berms 9, 10, 11 and 13 yielded ages which indicate that they were deposited during the period of systematic measurements (Table 8.7), therefore their palaeodischarge estimations can be compared to the gauged records. The largest recorded discharge within the dated range for each of these berms is shown in Figure 8.18. Each corresponds very closely to the Williams (1983) palaeodischarge estimations, which results in discharge values close the to maximum recorded floods at Konitsa and Doukas Bridge (Table 8.1). However, inspection of some of the results for other berms suggest that the Williams (1983) estimate is probably much less than the actual discharge. For example, berm 17 was one of the most impressive berms in the field, consisting of a large number of clasts, 9 of which were over 2 m in diameter, arranged in a typical berm deposit some 6 m above the modern channel bed (Figure 8.16). It was therefore expected that this berm would produce one of the highest flow estimates. However, the Williams (1983) procedure gives a discharge of just over 100 m^3s^{-1}, whilst the Costa (1983) procedure yields one of the highest discharges for any of the berms, which seems more sensible. Considering the estimated

maximum discharge for the Voidomatis catchment from systematic data is 1627 m^3s^{-1}, some of the palaeodischarge estimates from the Williams (1983) method for berms in the Upper Vikos Gorge do seem rather low. The very large clasts that constitute these berms (Table 8.7) suggest that they have been deposited by some of the most extreme flood events over recent times. Thus, in some cases, the Costa (1983) method might be more appropriate. In addition, it is important to appreciate that the gauged discharge records at Konitsa are only partial records and the peak flood flow may not always have been recorded, since these readings are generally only recorded once or twice a week at best. In view of the very flashy nature of the flood hydrographs in this area (section 3.5.3), discharge readings should ideally be taken hourly to ensure that the maximum flood discharge is recorded. Thus whilst the systematic data compares well with the Williams (1983) calculations in Figure 8.18, the peak flood discharges could have been considerably higher.

In summary, the Williams (1983) method has been shown to provide reliable *minimum* discharge estimations, but in some cases these are probably unrealistically low. The Costa (1983) method produces results that are more consistent with field interpretations of the berms, but this method frequently overestimates discharge (Carling, 1986; Reid and Frostick, 1987; Komar, 1988, 1989). The Costa (1983) method may therefore provide a *maximum* discharge estimate, with the actual value lying somewhere between the two methods. Given the limitations of these rather simplistic flow competence approaches as discussed in section 2.2.4, these calculations should be treated as only general flow estimates.

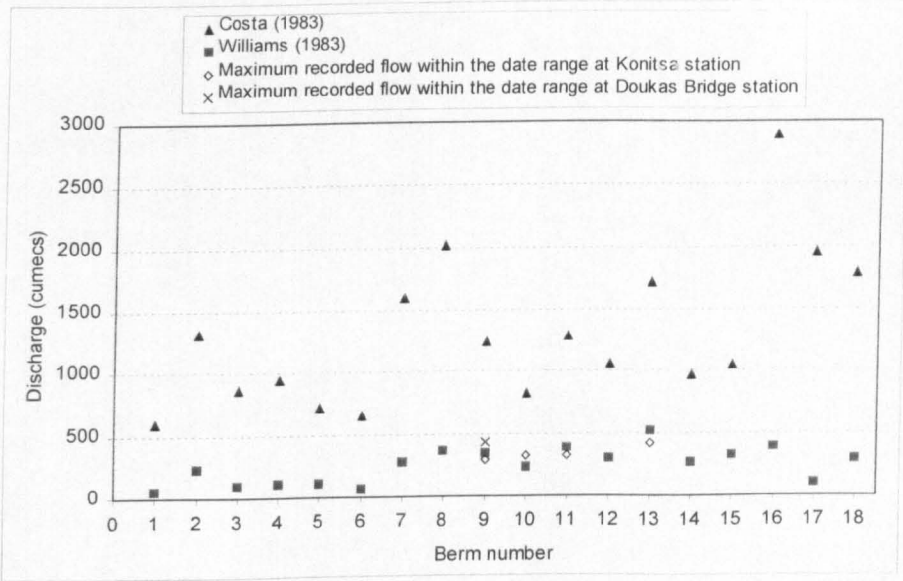

FIGURE 8.18 Palaeodischarge estimates determined from the size of boulders in each berm. The method of Costa (1983) uses the mean of the five largest boulders, whilst the mean of the 10 largest was used for the approach of Williams (1983). These palaeodischarge estimates are compared with large floods recorded at Konitsa and Doukas Bridge gauging stations during the estimated date range for berms 9, 10, 11 and 13. There were large floods at the Konitsa station at all of these times except berm 13, whose age is estimated to between 1981 and 1985. A large flood that is recorded during early 1987 (Appendix I) is therefore shown for this berm. The Doukas bridge record is only relevant for berm 9. See Table 8.7 for berm locations and boulder size data.

8.3.4 Flooding recorded in the boulder berm record

The boulder berms studied here are valuable for recording probably the most extreme flood events over the last 200 years, as only catastrophic flows are capable of transporting such large clasts overbank. This is reaffirmed by the fact that even minimum palaeodischarge estimates for some of these berms are comparable to the maximum recorded flood events at gauging stations. The flood occurrence and magnitude data determined from the boulder berms are presented in Figure 8.19. The dating shows that extreme flooding over the last 200 years has been clustered during specific periods, particularly 1780-1800, 1910-1930 and 1960-1990 (Figure 8.19a). Interestingly, four berms are dated to around 30 years ago (Figure 8.19b) and may have been deposited during the extreme magnitude event of 1970-71 (discussed in section 8.2). Extreme floods also occurred around the 1830s, 1850s and 1880s. Dating of the oldest berms required extrapolation of the lichen growth rate beyond the oldest point in the growth curve (145 years) (Figure 8.17). However, considering the low scatter shown on the curve there is no reason to believe that growth rates should be any different between 145 and c. 200 years. Nevertheless, it is important to recognise that there is a significant level of uncertainty in all of these age estimates (Figure 8.19b). There are no berms dated from about 60 to 40 years ago, which may indicate that any floods between 1940 and 1960 were of a lower magnitude compared to earlier and later periods in the 20th century.

When interpreting the boulder berm record it is important to recognise that over time major floods may destroy pre-existing deposits, especially in these narrow gorges, and therefore the sequence of flood deposits may not fully represent the sequence of past floods (Helley and LaMarche, 1973). There is likely to be less extensive evidence for older floods yet abundant evidence for the most recent extreme flood. Thus the large number of young berms in Figure 8.19 does not necessarily mean there more frequent flooding around the 1960s and 1970s compared to other dated periods of berm deposition. It may simply reflect that more berms have been preserved from recent floods. When interpreting the berms dates it is more appropriate to discuss the *occurrence* of extreme floods rather than rather than possible changes in flood *frequency*.

Changes in extreme flood magnitude over time can either be interpreted using the size of clasts in the berms (Figure 8.19b) or by using the palaeodischarge estimates described in section 8.3.3 (Figure 8.19c). Due to the numerous limitations of the palaeodischarge estimation methods, some authors have chosen to use boulder size as a simple proxy for flood magnitude (e.g. Macklin et al., 1992; Merrett and Macklin, 1999). The two rivers show a significantly different temporal trend. The Voidomatis displays a clear decreasing magnitude of extreme floods over the last 200 years, with the size of boulders and the palaeodischarge estimates decreasing by at least 50% over this timescale (Figure 8.19b and c). This trend is supported by the fact that most of the berms in the two Vikos Canyon reaches predate the catastrophic New Year flood of 1970-71 (described in section 8.2) (Figure 8.19b). Floods that deposited these

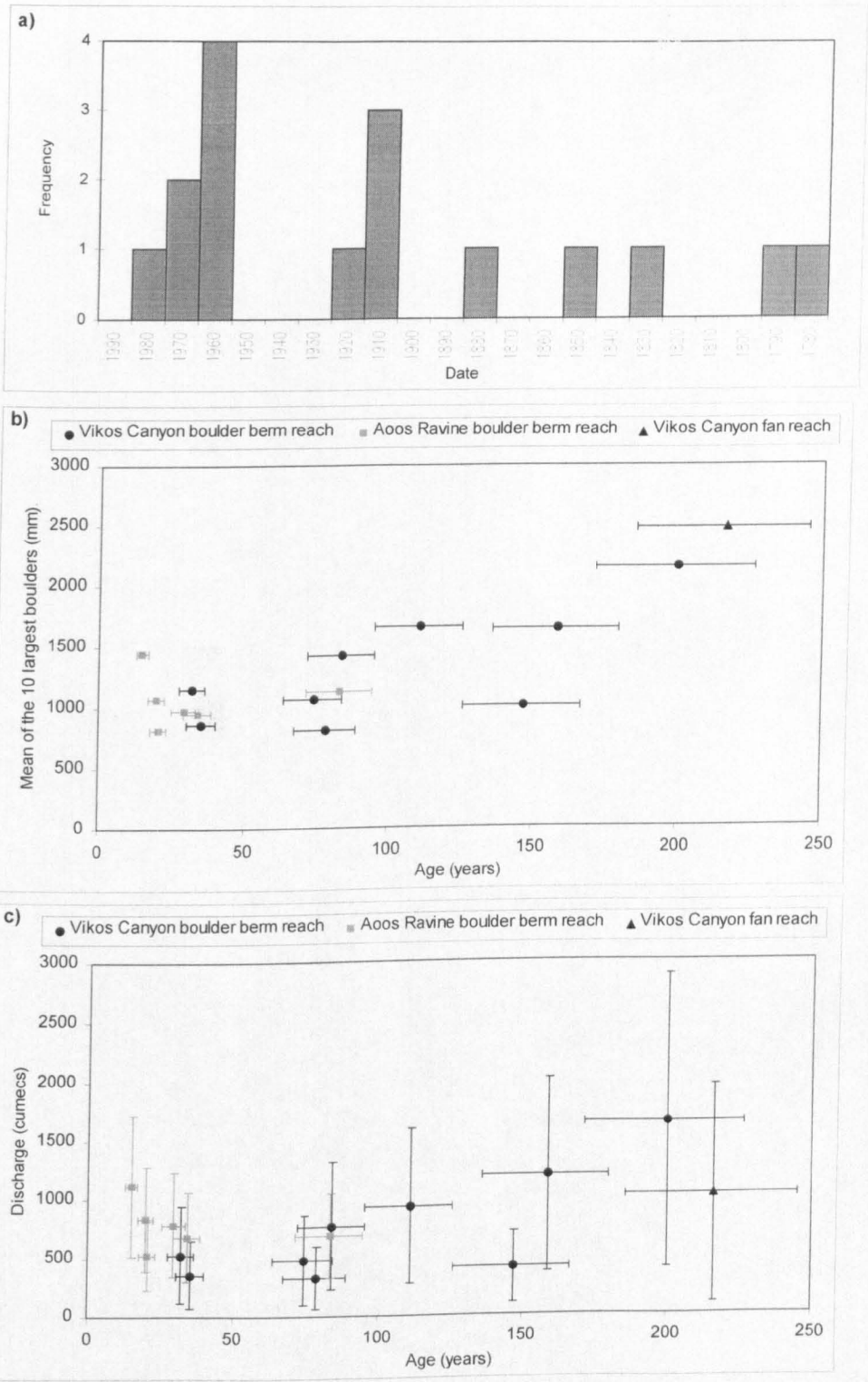

FIGURE 8.19 a) Histogram showing the timing of floods as determined by lichenometric dating of the boulder berms. b) Variation of clast size for boulder berms of different age. The estimated minimum and maximum ages are determined from the upper and lower quartile growth rate envelope lines (after Maas *et al.*, 1998). c) Variation in palaeodischarge estimates for boulder berms of different age. Age data are shown as in Figure 8.19b. The plotted palaeodischarge is the mean of the estimates determined using the methods of Costa (1983) and Williams (1983). The lower limit is the Williams (1983) palaeodischarge estimate and the upper limit is from the approach of Costa (1983).

older berms must have been of equal or greater magnitude to the 1970-71 event, as otherwise they are unlikely to have been preserved. The Aoos berms only cover the 20th century, and it is unclear whether flood magnitudes were also higher during the 19th century. Over approximately the last 100 years flood magnitudes have not changed significantly, with means of the 10 largest boulders in the range of 800 to 1500 mm and discharge estimates in the approximate range of 300 to 1300 m^3s^{-1}.

8.4 OVERBANK FLOOD SEDIMENTATION OVER THE LAST CENTURY

Dating floodplain sedimentation using a ^{210}Pb and ^{137}Cs chronology (section 4.4.1) has the potential to yield valuable palaeoflood information covering approximately the last century (section 2.3.5; section 8.1). This approach is adopted here in an attempt to bridge the gap between the high resolution but short gauged records, and the longer yet lower resolution lichenometric berm record.

8.4.1 Study site location and context

A core was sampled from U2 (Klithi unit) (Table 6.2) fine-grained alluvium and analysed for radionuclides as described in section 4.4.1 It was collected from location B within the Klithi rockshelter study reach in the Lower Vikos Gorge (see Figure 4.5 and Figure 6.6). This site was 20 m further round the meander bend from where the historic hearth, described in section 6.3.4, was found, as here the alluvium contained a greater proportion of fine-grained material and hence was more suitable for radionuclide analysis (Figure 8.20). The well developed vegetation on the floodplain surface suggests that the alluvium has not experienced significant surface erosion and consequently should contain a relatively complete, undisturbed record of historic overbank sedimentation.

FIGURE 8.20 The site of the floodplain core (point B, Figure 6.6) which was used for radionuclide analysis for dating overbank flood sedimentation. The lower half of the core is still *in situ*.

8.4.2 Dating results

The unsupported ^{210}Pb profile for the floodplain core is shown in Figure 8.21. There are four distinctly different parts to the profile exhibiting different rates of unsupported ^{210}Pb decay with depth, indicating different rates of sedimentation within the dating range (Rowan *et al.*, 1999). A range of sedimentation dating models are available for unsupported ^{210}Pb (section 4.4.1.1). The non-linear profile in Figure 8.21 meant that a model which accommodated varying sedimentation rates was required. The CRS (constant rate of supply) model (Appleby and Oldfield, 1978; Oldfield and Appleby, 1984b) was used as it does not assume a constant sedimentation rate, and therefore allows variable accumulation to be reconstructed which is important for obtaining reliable chronologies (Ivanovich and Harman, 1992). When applied to the unsupported ^{210}Pb measurements, the CRS model results suggest that the two periods of increased flood sedimentation identified in Figure 8.21 occurred between approximately 1893-1928, and post-1979. Measurements of ^{137}Cs were carried out to assess the reliability of the CRS model ages. Detectable ^{137}Cs was found within the upper 6 cm of the core (Figure 8.22). The prominent peak in the profile approximately corresponds to maximum ^{137}Cs fallout around 1963 (section 4.4.1.2), and the base of the profile can be approximated to 1950 which is a satisfactory estimate for the earliest significant ^{137}Cs fallout levels (Ely *et al.*, 1992).

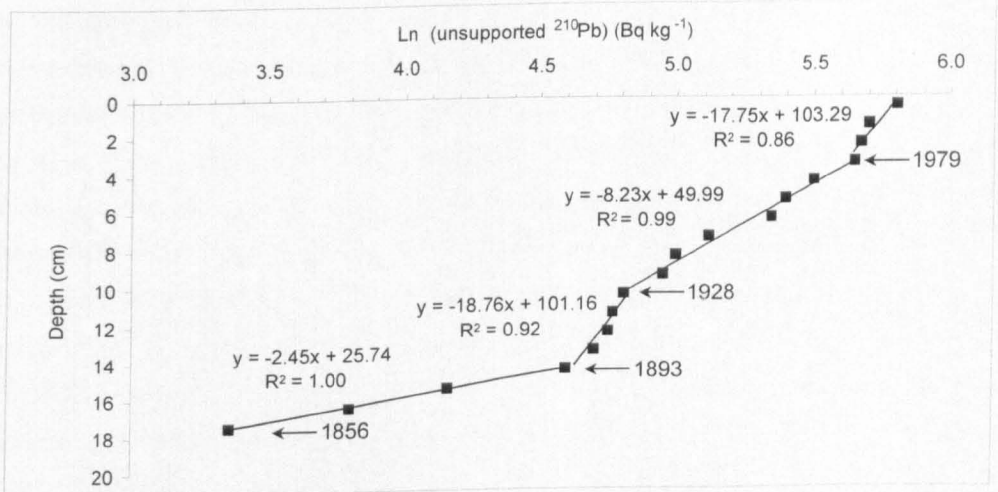

FIGURE 8.21 Unsupported ^{210}Pb profile from the floodplain core. Four zones with different rates of unsupported ^{210}Pb decay are identified. The dates are determined by the CRS model (Appleby and Oldfield, 1978).

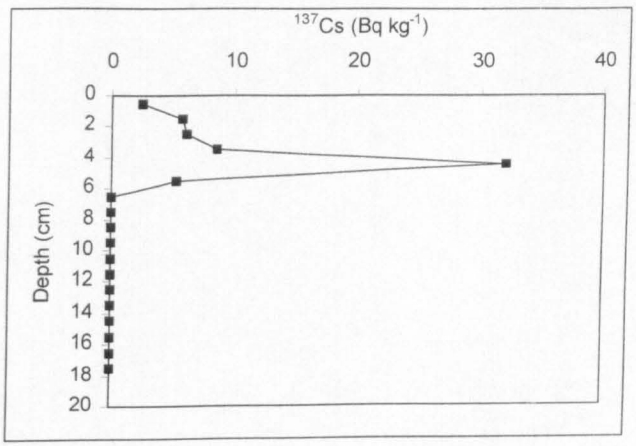

FIGURE 8.22 ^{137}Cs profile for the floodplain core.

The unsupported ^{210}Pb and ^{137}Cs dating results are plotted together in Figure 8.23. In general, the two dating methods correspond closely, indicating the CRS model is producing reliable ages. It is possible that the unsupported ^{210}Pb ages are slightly too young near the top of the core due to a slight lack of coherence with the 1960s ^{137}Cs peak, although the difference is only slight and the small depth of detectable ^{137}Cs means that this peak could realistically date to any time during the 1960s. As reflected in the unsupported ^{210}Pb profile, there are two distinct periods of increased flood sedimentation where accumulation rates are approximately 100% greater than the intervening period (Figure 8.23). These occurred between c. 1915 and 1942, and from c. 1979 to present. Considering the slight incoherence with the ^{137}Cs for the 1960s, it is possible that the latter phase of increased sedimentation could be a response to the to the 1970-71 event and other above average flood events during the 1970s (Figure 8.7). The period around the 1920s also coincides with large flood events identified in the boulder berm record (Figure8.19). The lower flood sedimentation indicated for the late-19th century must be treated with caution, as beyond 100 years the dating uncertainty greatly increases due much lower levels of unsupported ^{210}Pb (Figure 8.23). The ^{14}C dated hearth in these sediments at point A in the Klithi Rockshelter reach (Figure 6.6) can be used to estimate rates of flood sedimentation beyond the dating range of the unsupported ^{210}Pb. The hearth, at 157-165 cm profile depth, was dated to AD 1420 – 1650 (Beta – 109186) (see Figure 6.7). The unsupported ^{210}Pb shows that over approximately the last century (1893 - present), there has been 14.5 cm of accretion, equating to a sedimentation rate of 0.14 cm yr^{-1} (Figure 8.23). Assuming a constant sedimentation rate from the dated hearth to the dated 14.5 cm layer (1893 AD ±11 years) yields a mean sedimentation rate from the 157 – 15 cm depth in the profile of between 0.61 and 0.29 cm yr^{-1}. The much higher flood sedimentation rates points to higher flood frequencies and magnitudes between the hearth date and the late-19th century. This can only be a tentative conclusion since there will have been an increasing threshold of deposition over time as sediments accreted (Knox, 1987; O'Connor *et al.*, 1994), and the river also appears to have become incised recently which would

have further limited overbank sedimentation. However, it should be noted that in the hearth section there are a number of gravel lenses interdigitated within the fine-grained alluvium (e.g. 29 - 41 cm and 83 - 99 cm in Figure 6.7). Overbank deposition of fine gravel such as this has frequently been used as evidence of high magnitude floods (Costa, 1974; Ritter, 1975; Knox, 1979, 1988), and provides strong supporting evidence to the sedimentation rates for high magnitude pre-20th century floods.

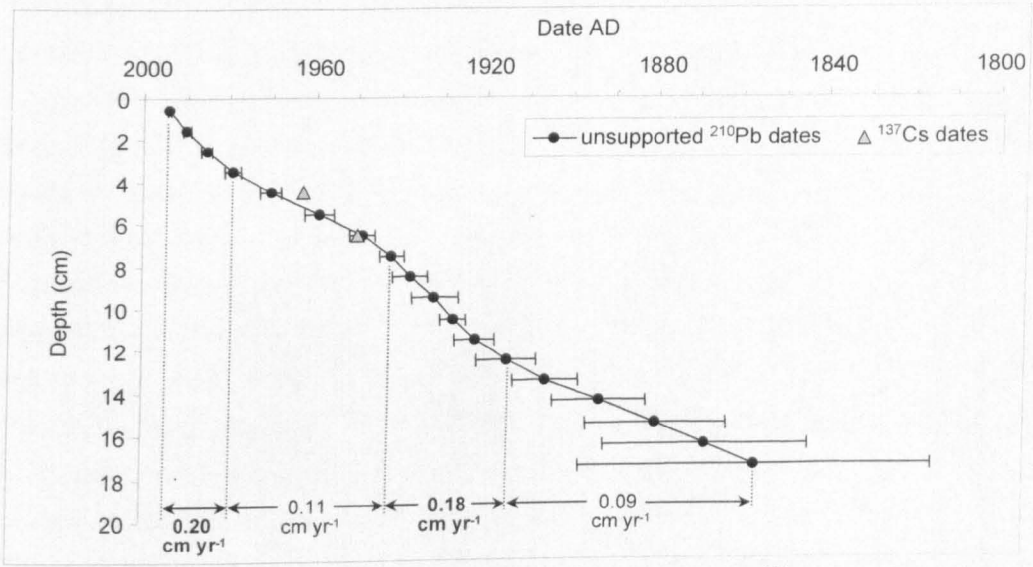

FIGURE 8.23 Age-depth results from the floodplain core from unsupported ^{210}Pb determined using the CRS model, with error bars shown for the 95% confidence limits. The peak of the ^{137}Cs (corresponding to about 1963) and the base of the ^{137}Cs profile (corresponding to about 1950) are also shown. In a similar fashion to Figure 8.21, four periods of different sedimentation rate are identified.

8.5 SYNTHESIS OF FLOODING OVER THE LAST 200 YEARS

The results obtained from the analysis of systematic data, floodplain sedimentation and the boulder berm record have been described in sections 8.2 to 8.3. This section aims to bring these results together to present a combined record of flooding for the last 200 years, and to discuss the wider implications of these results.

8.5.1 Environmental controls

For effective management of river systems, it is important to be able to understand (and hence predict) the impact of environmental changes, particularly on extreme phenomena such as catastrophic floods (section 2.4.2). The last 200 years has not only been a very important period of landscape disturbance by human action in Epirus (section 3.4.2), but has also seen significant environmental changes with a general warming in climate following the Little Ice Age (c. 1450 - 1850) (Grove, 1988). Of the successive Neoglacial cold phases which are collectively termed the Little Ice age, the final phase brought particularly severe conditions from c. 1700-1850 (Bradley and Jones, 1992), which were experienced extensively throughout the world including in southern Europe (Serre-Bachet *et al.*, 1992). It has been suggested that climatic warming

since this period may provide a useful analogue for the effects of future climate change on flood occurrence (Rumsby and Macklin, 1996). This section assesses the relative importance of climatic and anthropogenic controls on flood occurrence, and whether catastrophic floods are becoming more or less frequent and intense.

The occurrence of high magnitude flood events determined from the systematic and palaeoflood data is shown in Figure 8.24a. The gauged flood data are taken from Figure 8.7. The two periods of higher flood sedimentation identified on Figure 8.23 are shown, along with probable higher flood sedimentation rate earlier in the 19th century as discussed in section 8.4.2. All 16 of the dated boulder berms are shown. It is important to remember that there is a degree of error around the palaeoflood dates (as shown in Figure 8.19 and Figure 8.23), although for clarity these are not repeated in Figure 8.24a. On the basis of the three information sources, seven periods of catastrophic flooding have been identified (shaded in Figure 8.24). There is considerable coherence between the different records, giveing confidence in the reliability of the data. The flood record is compared with available environmental data (temperature, zonal index and local population dynamics) to investigate the potential influence of these environmental controls on flood occurrence. The closest long temperature records are those from Athens, which show a close agreement with general temperature trends identified for the Mediterranean region by Metaxas *et al.* (1991) and Reddaway and Bigg (1996). Athens is therefore a useful climate record for this study. As well as annual temperature, the mean winter temperature is also shown on Figure 8.24, as winter is the most common season for high magnitude flooding on these rivers (section 3.5.3).

The environmental conditions associated with catastrophic flooding of 1970-71, identified separately on Figure 8.24, have been discussed at length in section 8.2.4.2, which showed the importance of persistent low pressure systems and weak zonal flow in generating the flood. The very low zonal index at this time is apparent in Figure 8.24. Major high magnitude flooding also occurred during the mid-1960s and around the turn of the decade from the 1970s to 1980s (Figure 8.24). Both of these periods saw wet and stormy conditions in Zaghori (Figure 8.4 and Figure 8.5), and have been recognised as wet, high discharge phases for the Evinos River in Greece by Giakoumakis and Baloustos (1997). The temperature records show significant drops in winter temperature during these periods. The timing of flooding in relation to the zonal index is less clear than in 1970-71, although flooding during the early 1960s coincides with the weakest annual zonal flow on record. Looking back in the flood history, the next major period of high magnitude flooding occurs from c. 1912 - 1926, as evidenced by both floodplain sedimentation and boulder berms. This appears to have been a quite variable climatic period although it does centre on some particularly low zonal index conditions (Figure 8.24). Maheras and Kolyva-Machera (1990) and Maheras *et al.* (1992) have identified this as a particularly wet period over the central and eastern Mediterranean. This period also follows major local depopulation, and the effects of land abandonment may have

enhanced flood generation. A single boulder berm dates an earlier catastrophic flood to c. 1887. This was a cool, low zonal index period but also coincided with some of the largest populations in the catchments. Thus not only may climatic factors have been important, but also the significant deforestation at this time (section 3.4) would have decreased interception and increased rates of overland flow. The two earliest periods of catastrophic flooding in the record are c. 1780 - 1800 and c. 1836 - 1853 (Figure 8.24). The earlier of these was before the most significant historic anthropogenic landscape disturbances (section 3.4). Both periods coincide with the last cold stage of the Little Ice Age (Bradley and Jones, 1992).

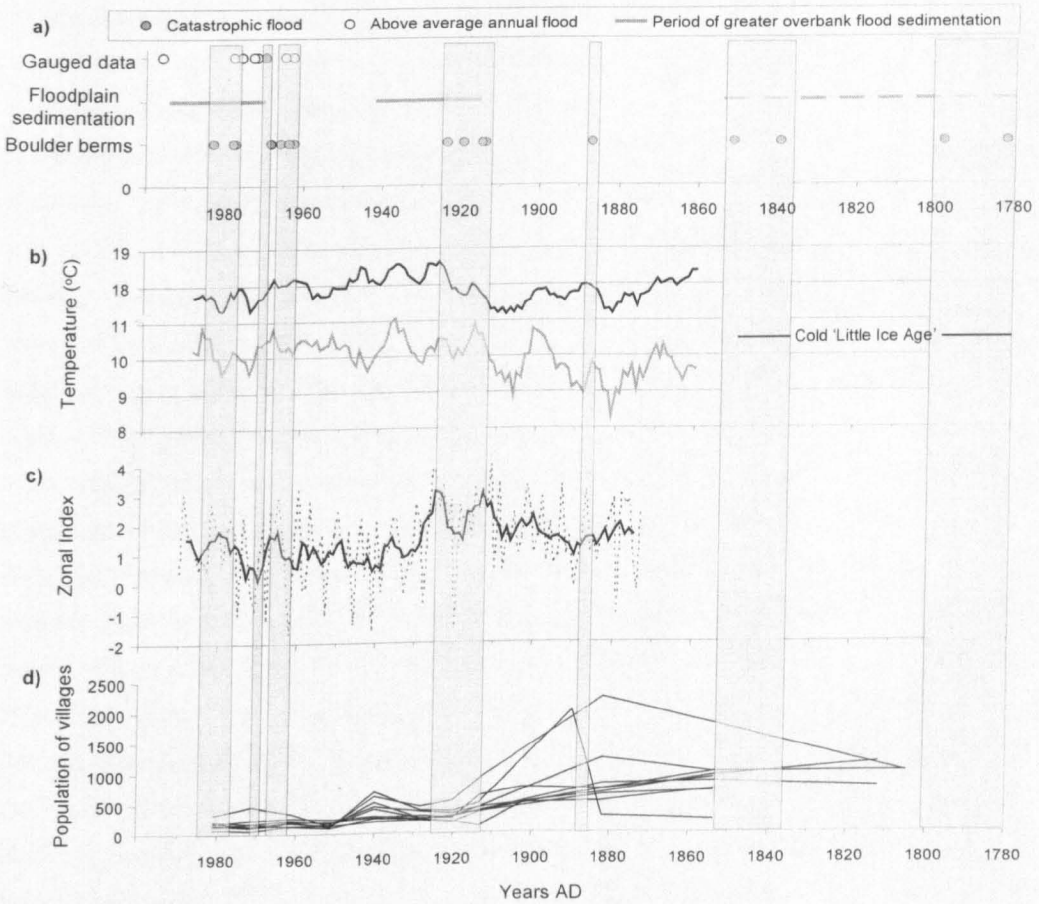

FIGURE 8.24 Combined evidence for high magnitude flooding and environmental changes from 1780 AD to present. a) The timing of flood events determined in this chapter. b) 5-year running means of the annual (black line) and winter (grey line) temperature at Athens, 1860-1987 (World Climate Disk, 1992). c) Annual mean (dotted line) and 5-year running mean (solid line) of the zonal index, calculated as discussed in section 8.2.4.1. d) Population of local villages from 1805 - 1981 (McNeil, 1992). The colour plot where individual villages are identified is shown in Figure 3.18. All systematic data are shown for hydrological years (Sept.-Aug.) with the labelled year on the diagram referring to the start of the hydrological year. Palaeoflood data were not of sufficient resolution to allow conversion to hydrological years.

Determining the relative importance of climatic and anthropogenic effects on flood generation can be difficult as both environmental parameters frequently vary simultaneously (Figure 8.24). However, there are various features of the data that indicate that climatic controls are far more

important. There have been important phases of high magnitude flooding between c. 1962 - 1983, which was long after the major phase of anthropogenic activities in the 19th century. Conversely, Epirus has seen a respite in landscape disturbance since the 1960s and the general spread of woodland and scrub vegetation (Bailey *et al.*, 1993). Numerous high magnitude floods over this period therefore conflicts with the hypothesis of anthropogenic controls being dominant. Section 8.2.4 has shown that these floods have been generated by particular climatic conditions that have induced intense rainfall and runoff. The oldest boulder berms in the record also indicate the greater importance of climatic conditions, as these occurred before the most intense human activities in the catchments (section 3.4), yet they were probably deposited by the largest discharges of the last 200 years or more (Figure 8.19). Cold Little Ice Age conditions were probably more important in their generation. Thus climatic effects have been the most important control on high magnitude flood occurrence. Anthropogenic effects have played a much more minor role, although they may have accentuated the magnitude of flood events during the late-19th and early-20th centuries.

The nature of these climatic controls has been discussed with reference to recent flooding in section 8.2.4, where it was concluded that in general flooding would be encouraged by meridional air flow (low zonal index) and slow moving low pressure atmospheric systems. It is therefore reasonable to argue that extreme flood events would have occurred under conditions conducive to this type of atmospheric behaviour over the last 200 years. As discussed in section 8.2.4.1, cooler periods in the middle and lower latitudes of the Northern Hemisphere steepen the latitudinal temperature gradient, which tends to weaken the strength of westerly winds (zonal flow) and favour more frequent meridional flow (Lamb, 1982; Rumsby and Macklin, 1994). Inspection of the flood record in Figure 8.24 does often show the occurrence of catastrophic floods with cool low zonal index conditions, particularly in c. 1887, c. 1920, c. 1962 and the 1970-71 flooding. However, a precise link between these dates and the climatic data is difficult because of errors involved in the palaeoflood dating and the variability of the climate over time. Convincing evidence for greater flooding during cold conditions comes from the two oldest phases of flooding, and particularly the period around 200 years ago. These floods deposited by far the coarsest boulder berms, with the mean of the 10 largest boulders averaging over 2000 mm, and have been calculated to have had the highest palaeodischarges on record, with maximum estimates of over 2500 m^3s^{-1} (Figure 8.19). These catastrophic floods indicate non-stationarity in the boulder berm flood record with decreasing magnitudes of extreme floods through time, which is particularly clear when the Voidomatis is considered alone (Figure8.19). This is supported by the investigations of floodplain sedimentation, where prior to the 20th century a number of extreme flood events have deposited gravel overbank where normally only sands and silts accumulate (section 8.4). A similar study of boulder berms in southwest Crete by Maas (1998) revealed a similar pattern, with generally decreasing palaeoflood magnitudes over the last c. 150 years. Flood events dated prior to c. 1850 AD in this study coincide with the final

cold phase of the Little Ice Age, where low temperatures would have encouraged meridional airflow and the frequent development of low pressure weather systems. Whilst there is less palaeoflood data for the Aoos, the Voidomatis has certainly seen a progressive decrease in extreme flood magnitudes with warmer conditions during the late-19th and throughout the 20th century. This trend is also in agreement with many other studies of flooding in the mid-latitudes, which have found greater flood magnitudes during cool, low zonal index periods (Knox, 1984; Hirschboeck, 1987, 1988; Rumsby and Macklin, 1994; Ely, 1997). For studies in the Mediterranean region, both Pavese *et al.* (1992) and Benito *et al.* (1996) also found that the early part of the 19th century had particularly high flood frequencies and magnitudes. Although most studies concentrate on atmospheric circulation, another important climatic factor encouraging catastrophic flooding during cold periods in these mountainous catchments may be the degree of winter snow cover, since most of the high magnitude floods in the systematic record have occurred during the winter months (section 3.5.3). By modelling of the hydrological impacts of climate change on mountain rivers in northern Greece, Mimikou *et al.* (1991) identified snow as the most significant determining factor of basin response to climatic change. Cooler winters would bring greater meridional airflow and increased precipitation, a greater proportion of which would fall and be stored as snow. The melting of large volumes of snow, probably caused by a period of warmer winter temperatures and rain-on-snow events, could potentially give massive winter discharges. Thus the apparent decrease in flood magnitudes since the Little Ice Age on the Voidomatis could also be related to lower snowpack volumes during winter.

These patterns of extreme flooding through climatic changes have important implications for the influence of global warming on catastrophic flood occurrence. In view of the large number of catastrophic floods recently reported in the Mediterranean region (section 1.3), it has been speculated that catastrophic flooding may be increasing in frequency, perhaps in response to global climatic changes. However, there is no clear evidence for catastrophic floods on the Voidomatis and Aoos Rivers becoming increasingly common over the last decade or so. The flood record actually shows that the last 15 years have *not* been a period of significant catastrophic flooding, yet the 1960s and 1970s saw far more frequent extreme flow events (Figure 8.24). In terms of changes in flood magnitude, the last century has probably seen a similar magnitude of extreme floods (Figure 8.19), but when the record is viewed over the last 200 years there is clear non-stationarity for the Voidomatis River record, with larger floods occurring during the 19th century. This decreasing magnitude is the result of warming since the end of the Little Ice Age (c. 1850). With future global warming, such a decrease in the magnitude of extreme winter floods could be expected to continue. However, it is possible that other flood producing mechanisms, such as summer thunderstorms or heavy autumn rains, could become more frequent as continued global warming may alter weather systems in less predictable ways (Palutikof and Wigley, 1996; Smith and Ward, 1998). In addition, it should be

emphasised that the catastrophic floods have occurred regularly over the last 200 years, as ultimately the characteristics of the Voidomatis and Aoos basins make them inherently prone to extreme flooding (section 3.5). Thus whilst climatic changes may have lessened the severity of catastrophic floods, the problem of reoccurring extreme flows remains.

8.5.2 Implications for flood recurrence estimations

Systematic hydrological records for the Voidomatis and Aoos basins, like many other areas of the Mediterranean, are of insufficient length to fully assess the recurrence of rare, catastrophic flood events. They have proven valuable in this chapter to assess changes in flood hydrology over roughly the last 40 years, and catastrophic flooding during 1970-71 has been identified. Whilst magnitude-frequency estimations for the 100- or 200-year flood have been made from these short records, there is considerable uncertainty associated with these predictions (section 8.2.1). This is problematic considering that reliable estimations of rare floods are crucial for valley floor engineering projects and flood risk analyses (section 2.4.1).

The extended stream record presented in this study shows that the 1970-71 flooding in the Voidomatis and other events during the mid-1960s have been the largest floods for roughly the last 70 years (Figure 8.19 and Figure 8.24). On the Aoos, 3 boulder berms have been dated to around 1980, a second period of recent extreme flooding which is not recorded on the Voidomatis (Figure 8.19). The combined flood record (Figure 8.19 and Figure 8.24) shows that flooding of a comparable or greater magnitude to the 1970-71 flood has occurred on average approximately once every 40 to 50 years. Floods of this magnitude may be somewhat more frequent on the Aoos considering the evidence for high magnitude flooding in the late-1970s and early-1980s. This allows an assessment of the flood frequency estimates shown in 8.2.1. For the estimated Voidomatis record, the maximum recorded flood of 1970-71 is in close agreement with the 50-year flood (see Table 8.1). For Bourazani Bridge, the 50-year flood appears to be an underestimate of some 150 m^3s^{-1}. Both the floods at Doukas Bridge and Konitsa are significantly larger than the 50-year flood, which again suggests these flood magnitudes are underestimates. It is likely that all of the other less reliable records (Vovoussa, Kokkoris Bridge and Tsepelovon) are underestimates as the infrequency of flow measurements at these sites mean that large floods are probably underrepresented. The seeming underestimation of flood frequency predictions on the Aoos could have some serious implications for management of this river. There are a series of HEP stations (weirs and a headwater dam) upstream of Konitsa (section 3.2.2), and flood estimates from these gauging stations have probably been used in the design of these structures. The palaeoflood data suggest that the conventional flood frequency predictions based on short records like this should be treated as conservative estimates.

It is more difficult to assess what is a realistic 100- or 200-year flood estimate, due to the considerable uncertainty associated with the boulder berm palaeodischarge methods (Figure 8.19c). However, the boulder berm record does suggest that much larger floods than those

recorded in the systematic data have occurred on the Voidomatis, particularly around 200 years ago. If the mean of the Williams (1983) and Costa (1983) methods are taken as reasonable discharge estimates, this would suggest floods of roughly three times the magnitude of those within the systematic data have occurred in the Vikos Canyon over the last 200 years (Figure 8.19c). Certainly much coarser boulders were deposited earlier compared to later in the record. However, the 200-year flood estimates for the Voidomatis and Bourazani Bridge records are far less than three times the maximum recorded discharge during the 1970-71 event. Thus on the basis of the palaeoflood record, the 200-year flood prediction seems to be a gross underestimate. Rare flood estimates such as these can be very important, particularly in dam construction (Poesen and Hooke, 1997). However, section 8.5.1 has discussed how the record of extreme floods on the Voidomatis over the last 200 years displays non-stationarity, with climatic conditions inducing changes in the flood-producing system. Whether floods of such magnitude could occur under current environmental conditions is open to question. However, this emphasises the need to view the flood record within a reasonably long history of climatic changes, as these can greatly influence the magnitude of rare floods (Knox, 1984). Palaeoflood data provide a valuable means of assessing what might be the maximum expected flood (e.g. Enzel *et al.*, 1993). This is more reliable than regional flood envelope curves (e.g. Mimikou, 1984a) which have been shown to be unrealistic (section 8.2.2). The fact that the Voidomatis has experienced even higher discharges than the 1970-71 event might need to be incorporated in planning and engineering projects.

8.5.3 Geomorphic effects

Many features of the Voidomatis and Aoos basins suggest that high magnitude flood events are of considerable geomorphic importance, including flashy hydrographs and relatively high Flash Flood Magnitude Indices (FFMIs), and coarse bedload and resistant channel boundaries that present high thresholds to change (Chapter 3). The palaeoflood evidence allows a consideration of the geomorphic effects of rare flood events. This section also makes use of field observations on the Voidomatis River between the 27th November and the 2nd December 1996, which saw the largest flooding of that winter recorded in the Doukas Bridge flow record (Figure 3.24). This is believed to be a reasonable estimate of the scale of mean annual flood flows. The precise impacts of floods depend on the river setting considered, with large, narrow bedrock canyons such as the Upper Vikos Gorge or the Aoos Ravine showing different responses to catastrophic floods than gorges with wider valley floors and less coarse bedload such as the Lower Vikos Gorge.

In the large bedrock canyons low and moderate flows are confined in a narrow, incised 'inner channel', with exposed bedrock and gravel benches occupying the majority of the floodplain, interspersed with occasional boulder berms and preserved fragments of alluvium (e.g. Figure 8.15). Inner channels are common in bedrock fluvial systems (Baker, 1988), and are

believed to progressively evolve due to bedrock erosion initiated during high magnitude events (Shepherd and Schumm, 1974). At only a few metres depth (e.g. Figure 3.12 and Figure 6.10), these inner channels are not as pronounced as in many true bedrock systems (e.g. Wohl, 1992a), probably due to the significant boulder and cobble bedload in the Voidomatis and Aoos canyons. However, the inner channel is important because it contains the flow up to considerable discharges. During flows approximating to the annual mean flood, as observed during 1996 flooding, river flow was at around bankfull level in the inner channel. With this degree of flooding there is significant transport of fine sediments and probably fine gravels, although this transfer is largely limited to within the inner channel. Only catastrophic floods fully escape from the inner channel to inundate the wider valley floor, as evidenced by the large number of boulder berms in the Vikos Canyon and Aoos Ravine. When not restricted to the inner channel, extreme floods can entrain boulders and gravel from the valley slopes and near channel areas as well as the bed itself. Undercutting of valley slopes may lead to the failure of scree and rock slopes. Berms and gravel splays are deposited in near channel areas. The high stream powers during catastrophic floods are necessary to transport the very coarse sediment in these canyon settings. It is also commonly recognised that it is the highest stream powers that accomplish the most significant bedrock erosion (Baker and Costa, 1987; Baker, 1988; Baker and Kale, 1998). Catastrophic floods are therefore very important geomorphic agents, as it is the coarse gravel and boulders as well as the bedrock that dictate the form of these channels. The investigation of boulder berms has demonstrated that the depositional features of catastrophic floods which occurred as much as 200 years ago still dominate the near channel morphology in parts of the modern river (e.g. Figure 8.16). These are persistent features, which will require a flood of equal or greater magnitude to significantly readjust the floodplain morphology. The palaeoflood record indicates that this would require at least a 200-year event.

The different physical characteristics of the Lower Vikos Gorge mean that floods have different effects. At lower flows, the river gently wanders within the channel margins and around large gravel bars, repeatedly flowing over prominent riffles into deep pools, (e.g. Figures 3.7, 6.6 and 6.8). Few significant geomorphic effects occur during these flows. However, during annual floods the channel is filled by floodwaters, although overbank flooding is limited (Figure 8.25). U2 (Klithi unit) terraces are rarely inundated (Figure 8.26), which supports results from the floodplain core analysis that revealed only quite low rates of vertical sedimentation on U2 surfaces over the last century (Figure 8.23). The gravel bars probably see some small scale adjustment in form during these floods, although their overall position and shape probably does not change as many remain partly emergent during annual floods and vegetation plays an important role in stabilising their basic form (Figure 8.26 and Figure 8.27). During catastrophic floods, the floodplain core analysis shows that the bars and Late Holocene alluvium do become inundated, with sedimentation on stabilised floodplain areas and probably major adjustment of gravel bar forms, in the manner observed by Wohl (1992b). As the outside of meander bends

frequently comprise the bedrock gorge walls (e.g. Figure 8.25), high flow stages in these settings can only be accommodated by a straightening of the thalweg (Nanson, 1986). This has resulted in erosion of the inside of some mender bends, as found at the upstream end of the Aristi-Papingo Bridge reach (Figure 6.8) and in the surveyed part of the Klithi rockshelter reach (Figure 6.6). At both points the inside corner of the meander bend appears to have been lowered or stripped. Evidence of this is shown in Figure 8.28. This area of partially exposed gravels set in a fine-grained matrix appears to be the former gravel base of U2 (Klithi unit) sediments, with the overlying fine-grained alluvium having been stripped in a similar fashion to that observed by Nanson (1986) and Baker (1988). This stripping may have been caused by some of the older catastrophic floods in the 200 year record as tree and lichen growth show this surface has been exposed for a considerable number of years.

The changing effects of high magnitude floods through time may be particularly important in the Lower Vikos Gorge. The three earliest phases of flooding identified in Figure 8.24 probably coincided with high sediment availability as mechanical rock breakdown would have been greater during the Little Ice Age and 19th century human activities may have destabilised slopes and increased sediment availability. Consequently, these floods were probably important aggradational events (*cf.* Bull, 1979, 1988), producing considerable vertical accretion of U2 (Klithi unit) sediments, resulting in the thick sedimentary beds displayed in exposed sections of this unit (Figure 6.7). Subsequent catastrophic floods during the 20th century have occurred under warmer conditions and less active anthropogenic landscape disturbances. This would have effected lower sediment availability and hence these floods would generally have caused channel incision (*cf.* Bull, 1979, 1988), lowering the river further from the height of the U2 terrace. This would explain the incised form of the modern Voidomatis River. Catastrophic floods are likely to cause the majority of incision as even in the Lower Gorge the bedload is still typically coarse gravels which can only be entrained under particularly high stream powers.

To summarise, it is clear that in both the large, narrow bedrock canyons and lower, wider, more meandering bedrock gorges catastrophic floods are very important geomorphic events. In the former they cause by far the most widespread erosion and deposition, leaving transient landforms such as boulder berms which persist for hundreds of years. In the latter they determine the shape and position of gravel bedforms, periodically strip the inside of meander bends, bring about the most vertical accretion, and have played an important role in generating Late Holocene aggradation and incision. In both settings the narrow valleys prohibit lateral adjustments and energy dissipation by meandering and braiding, so flood events can attain very high stream powers and stages (Nanson, 1986; Wohl, 1992a). In determining the effects of any flood, the relationship between this erosive force and resistance to change is crucial (e.g. Baker, 1977; Gupta, 1983; section 2.4.3). In the Voidomatis and Aoos rivers the bedload is very coarse, and substantial areas of bedrock also border the channel, and therefore it is often only very high

FIGURE 8.25 The Lower Vikos Gorge near the Klithi Rockshelter study reach during the flooding of late November 1996, which probably approximates to the mean annual flood. There is no significant floodplain inundation, but floodwaters are confined to the modern channel. The photograph was taken from the Klithi rockshelter looking downstream.

FIGURE 8.26 View of the Aristi-Papingo Bridge study reach (Figure 6.8), looking downstream from the bridge itself during the 1996 flooding. The large mid-channel island remains stabilised by dense vegetation. A U2 alluvial unit on the right of the photograph remains free of inundation.

FIGURE 8.27 A gravel bar in the Aristi-Papingo Bridge study reach (Figure 6.8), just upstream from the bridge itself. This was also taken during the 1996 flooding. The top of the bar remains emergent from the flow, stabilised by woody vegetation that is resistant to the floodwaters. The basic form of the bar did not appear to significantly change during the flood event

FIGURE 8.28 A near-channel area in the Lower Vikos Gorge just upstream of the Aristi-Papingo study reach. The area where J.C. Woodward is standing appears to be a segment of U2 alluvium that has been stripped of its upper fine-grained sediment (*sensu* Nanson, 1986), leaving the gravel base exposed. The exposed roots of the trees over this area are also indicative of this process. The gravels grade into a more stabilised area to the right side of the photo which survived stripping, and retains it upper fines.

erosional forces can overcome the resistance to change of most of the valley floor landforms. This study has shown that the effects of large floods can be variable over time, with the modern morphology of these rivers containing many transient features formed under significantly different environmental conditions to today. Catastrophic floods are therefore fundamental geomorphic processes for the past, present, and future dynamics of these river systems.

8.6 SUMMARY

This chapter has used systematic gauged and palaeoflood data to explore in detail the occurrence, production and effects of catastrophic floods over the last 200 years. Catastrophic flooding occurred at the following times: 1780-1800, 1836-1853, 1887, 1912-1926, 1962-1966, 1970-71, and 1977-1983. Climate has been shown to be the primary control on catastrophic flood occurrence. Extreme floods in the systematic record have been generated by unstable atmospheric conditions associated with meridional airflow, and slow moving low pressure weather systems which bring prolonged and intense storm precipitation to upland northwest Greece. As most extreme floods have occurred in winter, it seems likely that snowmelt and rain-on-snow processes have accentuated runoff during these storms. Catastrophic floods over the last 200 years have often coincided with cool, low zonal index conditions, which would have been conducive to these mechanisms of flood production. A general climatic warming over the last 200 years has seen a progressive decrease in catastrophic flood magnitudes in the Voidomatis basin, resulting from less frequent meridional airflow and a decreased snowpack volume. The geomorphic impacts of these floods have varied through time. Catastrophic floods coinciding with high sediment availability during the 19th century produced thick floodplain sedimentation and raised gravel bedforms. During the 20th century sediment availability has progressively decreased, and extreme floods have lowered the channel bed giving these rivers their current incised form. Catastrophic floods are very important geomorphic processes in these river environments, as they have sufficient stream powers to overcome the high thresholds to change of the coarse bedload and bedrock channel margins.

In the Voidomatis and Aoos basins, catastrophic floods have been shown to occur at least once every 40 to 50 years. Thus short gauged records of 20 to 30 years, which are typical for Mediterranean rivers, are of insufficient duration to fully represent these rare events. Many flood frequency calculations for rare floods such as the 100-year event based on these systematic records are underestimates, because the data do not include the full range of possible discharges. Extended flood records over the last 200 years allow flood recurrence estimates to be assessed and provide a valuable indication of how environmental changes influence catastrophic flooding. In areas such as the Mediterranean region where extreme floods present a major environmental threat, extended flood records of the type presented in this chapter are potentially of considerable value.

9. CONCLUSIONS AND RECOMMENDATIONS

This thesis has explored the occurrence and effects of catastrophic flooding in two steepland river basins in the Mediterranean region. Palaeoflood hydrology has been used to construct flood records that extend over a much longer timescale than the short (c. 30 year) gauged record, providing a flood series of sufficient length to adequately represent rare, extreme flow phenomena. Two timescales were chosen for the palaeoflood investigations: i) the last 200 years; ii) the Late Würm (c. 25 - 10 ka) (section 1.4.2). A central aim of the research has been to establish both the geomorphic effects of catastrophic floods and the influence of environmental change on their occurrence and magnitude. This required an investigation of the Late Pleistocene and Holocene alluvial stratigraphy of the Voidomatis basin (Chapter 6), so that evidence for specific catastrophic flood events could be evaluated within a history of landscape dynamics and fluvial response to environmental change. Detailed analysis of palaeoflood slackwater sediments has provided evidence for extreme flows during the Late Würm (Chapter 7), and emphasised the importance of such events in the long-term development of the Voidomatis River. The successful development of a quantitative fine sediment fingerprinting technique applicable over long (10^2 - 10^5 years) timescales (Chapter 5) greatly enhanced the interpretation of the Late Pleistocene alluvial sediments. Flood records covering the last 200 years have been constructed by combining systematic hydrological data with palaeoflood studies of boulder berms and floodplain sedimentation (Chapter 8). Whilst also enabling geomorphic impacts and potential relationships with environmental change to be explored, these flood data are relevant for the management and prediction of modern extreme flood events.

This chapter outlines the main conclusions that can be drawn from this thesis. A final section discusses the key benefits and limitations of this work, and by doing so identifies some areas and directions for future research.

9.1 CONCLUSIONS

- A quantitative fingerprinting technique has been successfully applied to fine-grained fluvial sediments of Late Pleistocene and Holocene age. Quantitative information on sediment sources has provided a valuable complement to the geochronological data. The approach provides evidence of changes in sediment delivery processes driven by environmental variations. It has been demonstrated that in the Voidomatis basin, sediment sources have been strongly influenced by climatic controls, and therefore fingerprinting provides a valuable tool for understanding the effects of environmental change on river behaviour.
- During the Late Pleistocene the Voidomatis River experienced at least four major phases of aggradation by a coarse-garined braided channel, between which were periods of incision

and more subdued river activity. Periods of sedimentation have been shown to end at approximately 108, 78, 54 and 25 ka, and in addition there is evidence for a minor phase of aggradation during the Lateglacial period (Vikos unit). The timing of these sedimentation phases has been primarily controlled by climatic conditions. Aggradation occurred during cold phase climate, almost certainly as a result of increased sediment supply from glacial erosion with a lesser contribution from frost weathering processes. Since alluviation associated with the Last Glacial, there has been progressive river incision into the Holocene.

- Subdued river activity and predominant incision continued through much of the Holocene in the Voidomatis basin, although over approximately the last 1000 years an important phase of sedimentation was been initiated, which was well established by c. 1420 - 1650 AD. This Late Holocene sedimentation is predominantly in the form of vertical accretion by a gently meandering gravel bed river. It is believed to have been stimulated by increased flooding during the Little Ice Age coinciding with an intense period of human activity and landscape disturbance.
- Two periods of catastrophic flooding within the Voidomatis basin have been identified during the Late Würm. The first period saw as many as 12 major flooding events in fairly rapid succession around 21.25 ka, followed by a second period of two catastrophic floods at c. 14 ka BP (c. 17 cal ka). Flooding at c. 21.25 ka probably coincided with the early stages of deglaciation, when massive meltwater discharges from the mountain glaciers and the snowpack were probably the main flood-generating mechanisms. The later floods probably occurred due to heavy storm precipitation that may have occurred during this period of hydrological instability and transition. Both periods of flooding show a close correspondence with Heinrich events, which may have provided conducive conditions for Late Pleistocene catastrophic flooding across the Mediterranean region.
- Catastrophic floods over the Late Würm had significant effects on the behaviour of the Voidomatis river system at the end of the Pleistocene. The earlier floods were important paraglacial sediment flushing events, reworking colluvium and alluvium that had been generated during the LGM. By the second period of flooding, it is likely that the paraglacial cycle of the Voidomatis had ended, and much lower sediment availability prevailed. The floods would have contributed to the postglacial incision of the Voidomatis channel, which has been of the order of 8 - 10 m since the Last Glacial Maximum. This serves to emphasise the importance of considering the effects of extreme events, even over Late Pleistocene timescales, in shaping the present day fluvial landscapes of Mediterranean mountain rivers.
- There have been repeated catastrophic flood events in both the Voidomatis and Aoos basins over the last 200 years. The combined record of gauged flows and palaeoflood data shows important periods of extreme flooding around 1780-1800, 1836-1853, 1887, 1912-1926, 1962-1966, 1970-71, and 1977-1983. Over the last two centuries climate has been the primary control on catastrophic flood occurrence. Extreme floods are generated during cool,

low zonal index conditions, which are conducive to the frequent passage of depressions over the Mediterranean region. There is no evidence in these catchments for catastrophic floods becoming larger and more frequent in recent years due to the speculated effects of global warming. Over the last 200 years, a general trend of warming since the Little Ice Age has induced a progressive decrease in catastrophic flood magnitudes in the Voidomatis basin, resulting from less frequent meridional airflow and a decreased extent of the winter snowpack. If this area does experience warmer conditions in the future, the magnitude of extreme floods during winter can be expected to decrease, although possible increases in the importance of other flood-producing mechanisms cannot be ruled out.

- There are common features to the meteorological conditions which have produced catastrophic floods recorded in the gauged record; (1) close, deep low pressure weather systems; (2) orographic effects accentuate convection; (3) flooding is intensified by slow moving weather systems which bring persistent heavy rainfall; (4) particularly intense precipitation falls in the lee of a cold front. These can be considered the meteorological 'ingredients' of catastrophic flash flooding on these rivers.
- Extending flood records over the last 200 years using palaeoflood hydrology has considerable potential value for the management and prediction of extreme floods. Over the last two centuries, phases of catastrophic flooding have occurred at least every 40 to 50 years. The Voidomatis and Aoos basins have gauged records of roughly 20 to 30 years duration, which are therefore insufficient to fully represent the full range of major flood events. Flood frequency estimations and flood envelope curves based on these instrumented data have been shown to frequently underestimate rare, extreme floods. Palaeoflood studies are therefore required to fully understand extreme flood phenomena in catchments of this type.
- The geomorphic impacts of floods over the last 200 years have varied through time. Catastrophic floods during the 19th century produced thick floodplain sedimentation and raised the relative heights of gravel bedforms. Due to lower sediment availability during the 20th century, extreme floods have resulted in channel incision, producing the current incised form. Catastrophic floods are very important geomorphic processes in these river environments, as they have sufficient stream powers to overcome the high thresholds to change which result from the very coarse bedload and resistant bedrock channel margins.

9.2 RECOMMENDATIONS FOR FUTURE RESEARCH

There are a number of opportunities to build on the research techniques and results presented in this thesis. The principal areas are outlined below:

- Further work is required in a range of Mediterranean environments to assess the degree of spatial variability, both in terms of catastrophic flood occurrence and the timing and controls over longer-term landscape development. Advances in the application of

$^{230}Th/^{234}U$, optical luminescence and other dating techniques over the last decade means that the potential exists to greatly improve our understanding of the Late Quaternary development of Mediterranean rivers. However, reliable alluvial histories need to be compiled for a wide range of locations and settings to enable well-founded regional assessments to be made.

- Quantitative fine sediment fingerprinting is recommended as a tool for future studies of Late Quaternary river activity, particularly where dating results alone may not be conclusive. However, fingerprinting should only be used in appropriate contexts and further work is required to allow differentiation between primary and secondary sediment source signals.
- Further study of river activity over the Late Holocene is recommended. There are few well-dated chronologies of Mediterranean river activity over this period, particularly the last 1000 years, yet this has the greatest relevance for applied geomorphological purposes. This and other studies have shown that it was a dynamic period, with considerable variations in river sedimentation and flood occurrence. Radiometric $^{210}Pb/^{137}Cs$ dating can be particularly valuable in Late Holocene studies, but is currently under-used in the Mediterranean, but. In steepland catchments, emphasis should be given to the occurrence of large floods over this period, as they are important geomorphological processes whose magnitude has been shown to be sensitive to minor Late Holocene climatic changes.
- Further research is required to develop more suitable palaeodischarge reconstruction methods. In this study it has proved difficult to obtain accurate and precise palaeodischarge estimates from palaeoflood deposits. For slackwater deposits this arises due to the considerable variability in channel geometry through time, which precludes the application of step-backwater flow modelling procedures. The major limitation with boulder berms is the lack of accurate and widely applicable flow competence equations for large clasts (Carling and Tinkler, 1998). Advances in this area would enhance the value of these palaeoflood deposits.
- Catastrophic floods are by their nature rare, exceptional flows, which can be hard to predict and difficult to mitigate against. However, this study has shown that there are some common features and trends to catastrophic flood occurrence. Considering the damage to life and property that is regularly caused by catastrophic floods in the Mediterranean region, the wider application of palaeoflood studies is recommended. The approach allows an estimation of the likely return interval of these events, assessment of the scale of the probable maximum flood, and an understanding of the environmental factors that cause variability in the flood producing system. Such data can be integrated in land-use planning and engineering design, flood risk analyses and catastrophic flood management and prediction procedures.

APPENDIX Ia: Konitsa discharge record, 1964-1993. The start of January and July each year are labelled. Gaps are where there were no readings taken.

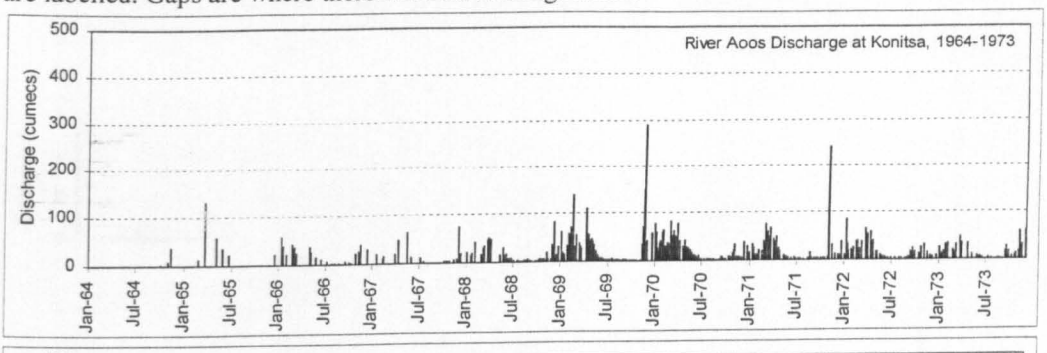

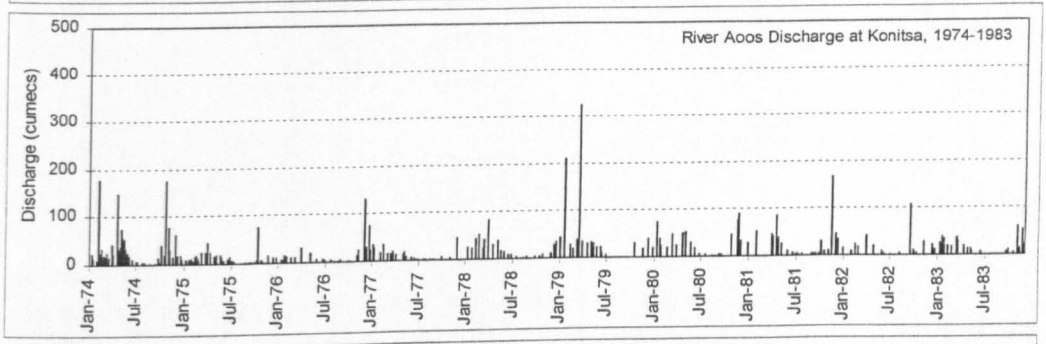

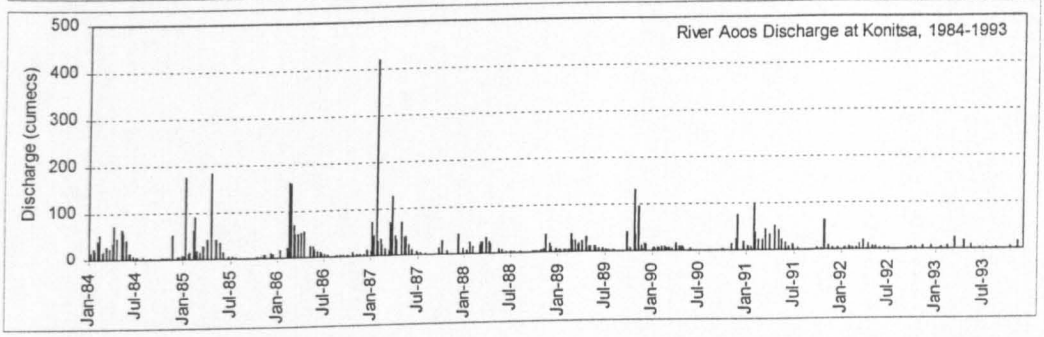

APPENDIX Ib: Occasional discharge readings at Kokkoris Bridge, 1961-1980. The start of January each year is labelled. Gaps are where there were no readings taken.

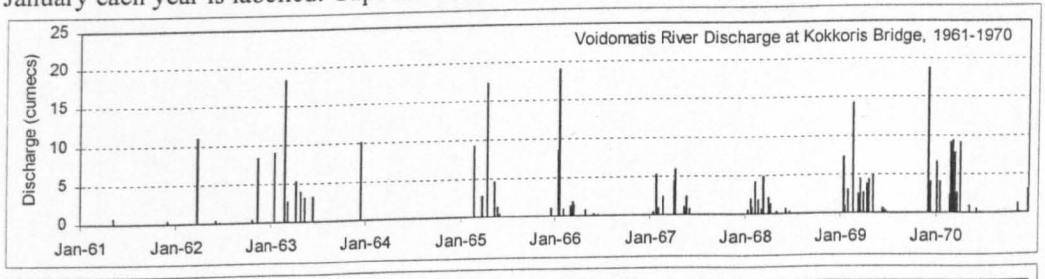

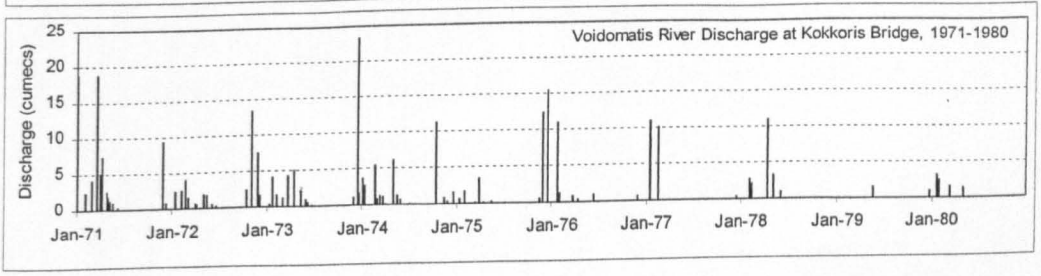

APPENDIX Ic: Occasional discharge readings at Kokkoris Bridge, 1970-1987. The start of January each year is labelled. Gaps are where there were no readings taken.

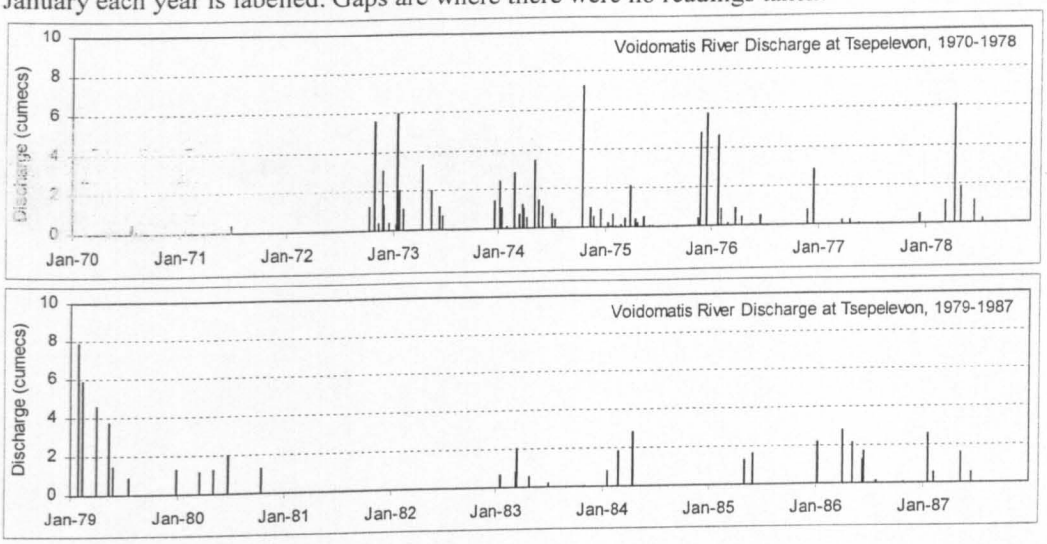

APPENDIX Id: Vovoussa discharge record, 1967-1993. The start of January and July each year are labelled. Gaps are where there were no readings taken.

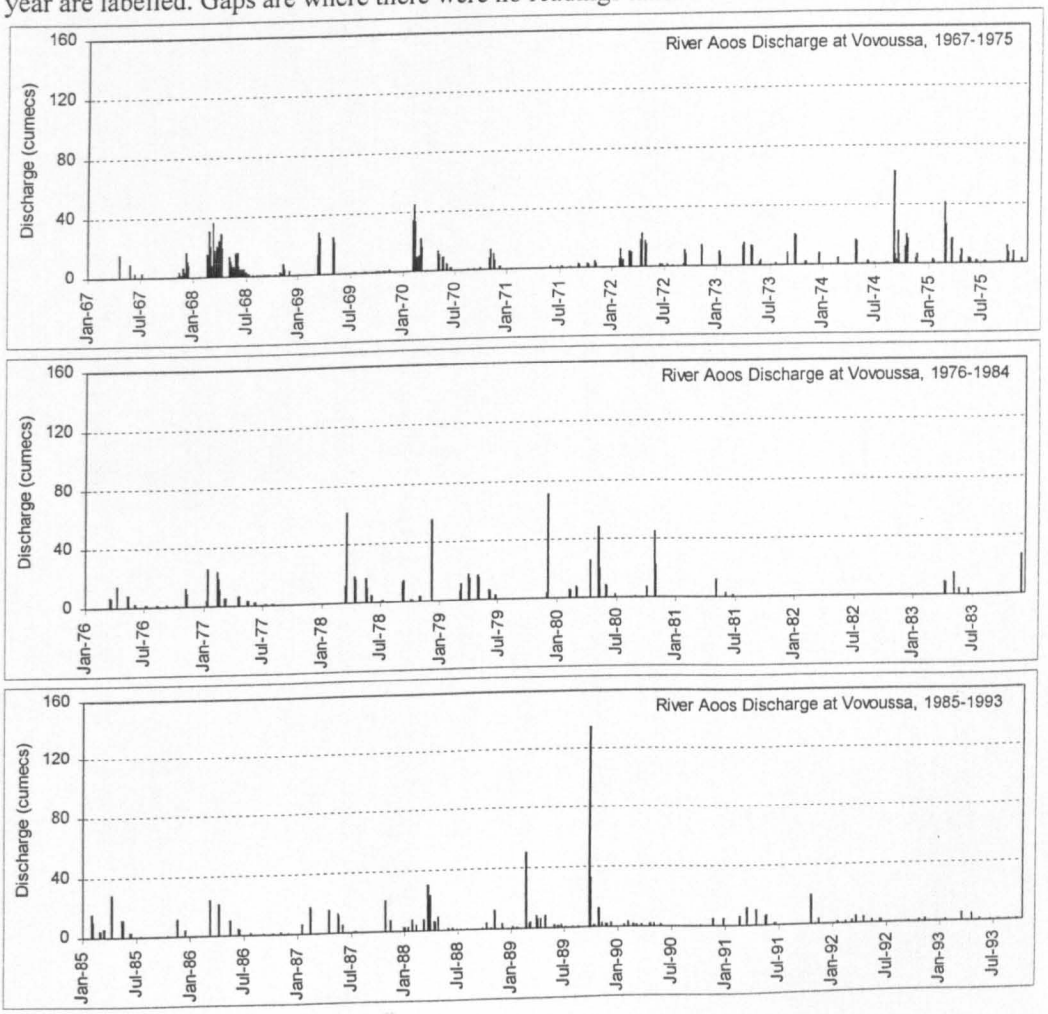

APPENDIX II: Trace element geochemistry (determined by XRF) of the sediment source samples used in the sediment fingerprinting procedure. †DE Flysch refers to 'dolomite enriched flysch'. All data are in ppm.

Sample code	Sediment source type	Ba	Cr	Cu	La	Ni	Nd	Pb	Rb	Sr	V	Y	Zn	Zr
V42	Flysch	381	343	56	29	211	37	24	133	76	171	29	112	152
V15	Flysch	383	285	52	28	186	38	18	141	152	179	26	108	146
V93	Flysch	336	241	52	12	196	30	15	135	219	163	25	111	117
V75	Flysch	359	372	53	39	215	47	18	134	83	160	34	105	172
V40	Flysch	352	292	58	24	213	24	19	129	130	166	27	105	142
V4	Flysch	345	308	55	24	201	13	18	132	126	174	28	114	149
V9	Flysch	388	296	57	29	176	18	17	156	130	185	29	114	160
V5	Flysch	228	239	18	20	102	11	10	45	218	85	17	41	123
V16	Flysch	288	233	23	7	103	7	14	58	190	114	21	65	193
V20	Flysch	238	220	16	9	97	11	12	44	221	70	19	46	143
V21	Flysch	188	222	13	10	84	17	9	33	241	45	15	29	95
V25	Flysch	240	201	17	17	90	4	11	49	261	74	19	45	128
V41	Flysch	293	297	31	13	167	23	15	69	155	98	23	86	169
V44	Flysch	317	216	24	22	107	20	13	67	221	95	22	64	162
V74	Flysch	200	315	19	12	142	17	16	46	220	61	17	67	126
V16D	Flysch	299	200	23	24	88	17	13	56	223	86	19	58	145
V92	Flysch	303	248	35	22	138	18	15	80	197	115	23	78	155
V10	Flysch	292	249	32	13	142	4	18	67	132	128	21	96	178
V99	DE flysch†	793	142	78	16	183	3	16	94	729	97	19	93	65
V100	DE flysch†	1274	51	33	10	97	14	8	43	1214	41	11	51	12
V13	Limestone	35	12	12	10	9	0	3	2	398	9	7	7	0
V17	Limestone	42	12	16	7	13	1	5	4	844	28	7	12	0
V19	Limestone	24	8	12	5	10	0	6	4	896	10	5	6	0
V52	Limestone	23	6	9	0	11	4	5	2	767	15	4	7	0
V53	Limestone	25	5	11	0	13	1	5	3	686	9	7	15	0
V54	Limestone	11	9	8	4	8	0	6	2	691	17	3	6	0
V61	Limestone	13	6	6	0	5	2	5	3	360	16	0	4	0
V62	Limestone	38	5	8	0	8	0	3	2	446	15	1	9	0
V81	Limestone	27	5	7	0	10	0	5	3	432	16	3	7	0
V82	Limestone	48	6	9	8	11	2	7	4	394	18	7	10	0
V84	Limestone	92	10	4	0	7	5	1	2	320	10	4	6	0
V86	Limestone	53	4	7	0	8	0	5	3	375	9	1	5	0
V87	Limestone	67	5	7	0	8	0	3	3	386	15	2	6	0
V96	Till	98	35	24	3	43	0	7	22	527	27	11	27	25
V97	Till	140	65	26	4	64	6	7	31	434	48	11	37	41
V101	Till	142	54	25	8	58	0	8	30	441	41	12	34	39
V102	Till	94	38	22	3	43	1	8	21	526	29	10	27	23
V12	Dolomite	964	13	16	19	11	4	4	11	203	14	11	19	12
V78	Ophiolite	27	2974	19	4	2588	2	2	2	0	81	0	46	2
V79	Ophiolite	19	2727	19	0	2243	0	0	1	0	73	0	42	2
V23	Ophiolite	27	2791	20	0	2214	4	0	1	0	63	0	43	3
V50	Terra Rossa	449	580	74	58	292	76	23	103	74	143	55	120	218
V51	Terra Rossa	450	614	66	59	274	49	25	103	77	135	53	112	220
V95	Terra Rossa	425	258	120	68	308	62	31	94	222	119	70	125	155
V55	Terra Rossa	394	362	95	72	218	89	31	112	111	168	75	144	224
V56	Alluvium	102	49	24	0	59	14	8	22	537	35	8	28	10
V57	Alluvium	102	33	21	0	42	7	5	17	526	25	8	24	8

APPENDIX II continued.

Sample code	Sediment source type	Ba	Cr	Cu	La	Ni	Nd	Pb	Rb	Sr	V	Y	Zn	Zr
V58	Alluvium	81	58	20	0	59	13	7	18	548	31	10	25	10
V59	Alluvium	106	63	24	15	66	2	8	21	513	29	10	33	16
V65a	Alluvium	102	52	29	5	52	13	8	23	482	42	10	38	20
V65b	Alluvium	87	49	29	4	51	2	7	22	482	38	10	38	19
V67a	Alluvium	347	28	17	4	35	3	6	12	507	27	8	27	7

APPENDIX III: Low-frequency mass-specific magnetic susceptibility (χ) and percentage frequency-dependent magnetic susceptibility ($\%\chi_{fd}$) of the sediment source samples used in the sediment fingerprinting procedure. †DE Flysch refers to 'dolomite enriched flysch'. Low-frequency mass-specific magnetic susceptibility is in 10^{-8} m^3 kg^{-1}.

Sample code	Sediment source type	χ	$\%\chi_{fd}$
V42	Flysch	14.9	2.5
V15	Flysch	13.7	2.2
V93	Flysch	13.4	-0.8
V75	Flysch	25.3	6.7
V40	Flysch	11.2	0.9
V4	Flysch	11.1	0.8
V9	Flysch	14.1	0.4
V5	Flysch	8.5	2.0
V16	Flysch	11.7	2.5
V20	Flysch	9.9	1.3
V21	Flysch	14.1	0.9
V25	Flysch	9.9	1.3
V41	Flysch	10.2	0.5
V44	Flysch	13.3	-0.4
V74	Flysch	9.9	0.0
V16D	Flysch	11.3	1.2
V92	Flysch	13.9	0.0
V10	Flysch	13.2	0.3

Sample code	Sediment source type	χ	$\%\chi_{fd}$
V99	DE flysch	12.0	1.3
V100	DE flysch	26.1	0.0
V13	Limestone	0.5	0.0
V17	Limestone	0.7	6.7
V19	Limestone	0.5	-36.4
V52	Limestone	1.4	3.2
V53	Limestone	0.4	-12.5
V54	Limestone	0.5	0.0
V61	Limestone	0.6	6.7
V62	Limestone	4.1	1.1
V81	Limestone	2.2	6.0
V82	Limestone	0.7	6.7
V84	Limestone	7.5	-1.1
V86	Limestone	1.0	8.3
V87	Limestone	0.1	100.0
V96	Till	3.8	4.1
V97	Till	3.4	1.5
V101	Till	3.5	0.0
V102	Till	3.6	4.4

Sample code	Sediment source type	χ	$\%\chi_{fd}$
V12	Dolomite	1.4	0.0
V78	Ophiolite	61.1	0.7
V79	Ophiolite	58.6	-1.0
V23	Ophiolite	30.8	-0.1
V50	Terra Rossa	300.4	10.3
V51	Terra Rossa	259.3	9.4
V95	Terra Rossa	244.6	8.3
V55	Terra Rossa	240.9	9.7
V56	Alluvium	4.5	0.0
V57	Alluvium	3.1	0.0
V58	Alluvium	3.4	-4.0
V59	Alluvium	14.5	4.0
V65a	Alluvium	5.5	4.0
V65b	Alluvium	5.5	6.5
V67a	Alluvium	2.8	0.0

APPENDIX IV: Trace element geochemistry (determined by XRF) of fine (<2 mm) sediments from alluvial fills which were analysed for the sediment fingerprinting procedure. KB = Konitsa basin; OKB = Old Klithonia Bridge; SWDs = Slackwater deposits; APB = Aristi-Papingo Bridge Reach; KR = Klithi Rockshelter; CF = Contemporary fines. All data are in ppm.

Sample code	Field Description	Ba	Cr	Cu	La	Ni	Nd	Pb	Rb	Sr	V	Y	Zn	Zr
V56	9.3 m alluvial unit, KB reach	102	49	24	0	59	14	8	22	537	35	8	28	10
V57	9.3 m alluvial unit, KB reach	102	33	21	0	42	7	5	17	526	25	8	24	8
V58	10 m alluvial unit, KB reach	81	58	20	0	59	13	7	18	548	31	10	25	10
V59	10 m alluvial unit, KB reach	106	63	24	15	66	2	8	21	513	29	10	33	16
V65a	8.3 m alluvial unit below OKB SWDs	102	52	29	5	52	13	8	23	482	42	10	38	20
V65b	8.3 m alluvial unit below OKB SWDs	87	49	29	4	51	2	7	22	482	38	10	38	19
V67a	12.75 m alluvial unit, KB reach	347	28	17	4	35	3	6	12	507	27	8	27	7
V67b	12.75 m alluvial unit, KB reach	702	51	23	5	48	24	6	18	493	33	8	37	14
V73a	15.5 m alluvial unit, KB reach	314	343	58	44	206	57	22	84	219	121	37	101	182
V73b	15.5 m alluvial unit, KB reach	313	329	58	47	211	59	21	84	220	110	37	99	180
V90a	12 m alluvial unit, APB reach	350	235	55	30	195	35	30	80	146	122	24	113	98
V90b	12 m alluvial unit, APB reach	341	219	56	25	195	41	24	82	138	121	25	113	105
V48	14 m alluvial unit, APB reach	175	217	42	18	133	17	12	43	272	66	22	58	61
V49	14 m alluvial unit, APB reach	129	60	27	6	58	0	7	22	329	69	21	44	23
Hrth 1	Late Holocene alluvium, KR reach	305	500	28	14	156	20	14	74	78	110	20	60	192
Hrth 2	Late Holocene alluvium, KR reach	283	659	23	11	136	11	13	62	73	100	17	52	258
Hrth 3	Late Holocene alluvium, KR reach	306	463	29	19	147	14	13	73	100	111	20	58	192
Hrth 4	Late Holocene alluvium, KR reach	332	373	33	19	167	21	16	76	123	115	23	66	176
V1	CF (winter), APB reach	259	422	25	11	157	11	11	57	187	86	74	52	154
V2	CF (winter), KR reach	67	22	14	7	22	0	4	8	565	15	8	12	2
V3	CF (winter), KR reach	271	304	25	20	149	6	12	57	235	79	16	53	111
V7	CF (winter) limestone headwaters near Kipi	272	519	29	11	211	13	14	69	137	107	18	62	132
V8	CF (winter) flysch headwaters nr. Kipi	372	346	44	29	168	18	18	100	127	145	27	91	173
V11	CF (winter), Vikos Canyon	211	181	28	6	142	2	13	53	348	74	16	53	89
V47	CF (summer), APB reach	194	151	20	11	93	0	9	33	400	50	11	35	60
V83	CF (summer), Vikos Canyon	218	189	27	12	130	17	11	48	370	66	15	50	77

APPENDIX V: Trace element geochemistry (determined by XRF) of the slackwater deposit fine (<2 mm) sediments which were analysed for the sediment fingerprinting procedure. OKB = Old Klithonia Bridge. The sedimentary logs are shown in Chapter 7. All data are in ppm.

Sample code	Site	Depth on sedimentary log (cm)	Ba	Cr	Cu	La	Ni	Nd	Pb	Rb	Sr	V	Y	Zn	Zr
okb1.4	Boila	14.0-18.3	268	310	28	15	174	15	12	65	128	90	17	57	111
okb1.5	Boila	10.9-14.0	314	425	32	18	194	18	14	83	94	114	23	72	181
okb1.6	Boila	5.0-10.9	196	357	22	11	127	0	10	42	231	62	13	39	71
okb1.7	Boila	0.0-5.0	379	337	33	15	156	0	12	56	186	82	17	56	101
okb1.8	Boila	24.0-27.3	352	371	53	39	215	37	19	98	113	140	37	105	200
okb1.9	Boila	27.3-34.3	369	325	52	27	211	41	16	77	162	113	30	85	170
okb1.11	Boila	36.2-40.2	303	356	38	19	177	18	14	67	148	97	24	67	140
okb1.14	Boila	46.6-51.0	337	403	45	25	197	31	16	79	135	115	28	81	161
okb1.15	Boila	51.0-65.0	370	386	48	18	190	40	17	78	148	112	28	83	162
okb1.16	Boila	410-base	131	293	19	12	84	17	8	27	342	41	12	36	74
okb2.1	OKB	50-60	60	68	16	3	39	0	6	14	498	21	8	18	15
okb2.2	OKB	60-67	50	22	15	4	23	8	9	8	542	14	7	12	2
okb2.6	OKB	115-125	150	143	46	17	90	6	10	33	320	43	15	38	69
okb2.7	OKB	125-136	118	118	19	5	68	0	8	27	392	36	11	30	53
okb2.12	OKB	147-156	74	45	17	5	36	5	7	10	504	21	7	17	10
okb2.14	OKB	161-177	88	81	20	9	50	7	7	21	431	30	11	27	40
okb2.15	OKB	177-184	46	31	15	9	27	0	6	11	536	18	6	16	11
okb2.17	OKB	185-196	76	67	18	6	46	9	8	14	511	27	8	20	19
okb2.18	OKB	196-214	58	58	16	14	29	1	4	9	530	17	6	13	14
okb2.19	OKB	214-220	92	78	20	13	46	2	8	14	497	23	7	18	20
okb2.20	OKB	220-236	67	78	16	3	33	0	6	11	521	19	6	15	16
okb2.21	OKB	236-240	66	77	19	8	47	5	7	17	472	24	8	19	31
okb2.22	OKB	240-251	50	79	17	13	38	0	5	11	521	20	8	18	16
okb2.24	OKB	252-267	39	49	14	1	25	0	6	7	553	16	6	12	5
okb2.25	OKB	747-757	88	86	20	3	40	4	6	16	491	24	9	20	31
okb2.28	OKB	775-795	143	151	23	6	77	8	8	30	403	41	14	34	75
okb2.29	OKB	795-804	69	57	17	10	40	11	7	13	520	21	8	21	21
trib1.*	Tributary	0-50	358	412	73	54	286	76	23	118	77	175	54	136	159
trib1.1	Tributary	50-70	134	120	24	6	71	8	8	26	402	34	12	32	58
trib1.2	Tributary	70-100	174	186	35	15	104	18	11	41	257	62	18	50	108
trib1.7	Tributary	112-123	56	71	20	6	40	11	6	15	479	24	9	26	24
trib1.12	Tributary	134-138	70	51	16	2	36	3	6	13	500	22	9	23	19
trib1.14	Tributary	143-155	75	67	17	6	41	7	6	16	480	23	8	19	25
trib1.16	Tributary	157-165	81	96	16	3	46	9	7	15	473	27	9	23	31
trib1.19	Tributary	173-183	155	142	25	17	81	10	10	40	346	49	16	41	73
trib1.24	Tributary	205-214	104	95	21	12	54	14	9	22	450	31	11	26	44
trib1.26	Tributary	215-224	210	203	30	16	118	1	12	55	216	71	19	55	121
trib1.27	Tributary	224-252	168	141	27	12	88	20	9	38	357	50	17	43	89
trib1.30	Tributary	260-272	275	272	42	26	136	34	18	73	180	111	28	76	164
trib1.31	Tributary	272-289	271	255	42	32	134	29	15	72	203	96	31	74	155
trib1.33	Tributary	290-base	281	271	42	37	157	39	12	82	175	110	33	82	163

APPENDIX VI: Low-frequency mass-specific magnetic susceptibility (χ) and percentage frequency-dependent magnetic susceptibility ($\%\chi_{fd}$) for fine (<2 mm) sediments from the alluvial fills and slackwater deposits. The field context for these sample codes is given in Appendix IV and V. Low-frequency mass-specific magnetic susceptibility is in 10^{-8} m^3 kg^{-1}.

Sample code	χ	$\%\chi_{fd}$
V56	4.4	0.0
V57	3.1	0.0
V58	3.4	-4.0
V59	14.5	4.3
V65a	5.5	4.0
V65b	5.5	6.5
V67a	2.8	0.0
V67b	3.6	6.1
V73a	102.5	7.2
V73b	94.2	5.1
V90a	50.8	7.3
V90b	51.8	6.9
V48	21.0	8.3
V49	21.0	10.0
Hrth 1	23.9	7.3
Hrth 2	25.0	6.8
Hrth 3	30.1	7.4
Hrth 4	22.6	7.1
V1	15.6	4.0
V2	0.8	16.7
V3	15.3	5.2
V7	21.2	2.5
V8	35.7	6.5
V11	16.5	5.4
V47	13.4	-126.0
V83	15.3	5.0

Sample code	χ	$\%\chi_{fd}$
okb1.4	9.5	1.0
okb1.5	13.2	1.1
okb1.6	8.1	1.8
okb1.7	11.6	-0.8
okb1.8	28.6	0.7
okb1.9	25.2	1.8
okb1.11	22.4	4.3
okb1.14	20.9	-0.5
okb1.15	20.3	1.1
okb1.16	5.7	-4.2
okb2.1	6.0	7.3
okb2.2	1.0	18.8
okb2.6	43.2	9.2
okb2.7	4.8	3.9
okb2.12	1.2	-4.0
okb2.14	2.9	4.9
okb2.15	1.3	14.3
okb2.17	2.1	4.7
okb2.18	0.9	-5.0
okb2.19	1.9	-7.3
okb2.20	1.2	-7.7
okb2.21	2.4	8.5
okb2.22	1.3	-4.2
okb2.24	1.0	-7.7
okb2.25	2.7	1.7
okb2.28	4.3	-10.0
okb2.29	1.8	-2.6
trib1.*	94.3	11.1
trib1.1	4.9	2.9
trib1.2	5.5	1.7
trib1.7	2.0	4.9
trib1.12	1.7	8.3
trib1.14	1.9	7.3
trib1.16	2.3	2.0
trib1.19	4.1	-1.1
trib1.24	2.2	0.0
trib1.26	5.4	-1.7
trib1.27	3.8	42.0
trib1.30	7.5	3.7
trib1.31	6.8	1.4
trib1.33	8.1	2.4

APPENDIX VII: Data from radiocarbon dating analysis. 1 sigma (68%) uncertainties are reported here. Analysis performed by Beta Analytic Inc., Miami, USA.

Sample Code	Analysis	Measured 14C age	13C/12C ratio	Conventional 14C age
Beta-109186	Radiometric-standard	400 ± 60 BP	-25.0 o/oo	400 ± 60 BP
Beta-109162	Standard-AMS	14000 ± 110 BP	-27.6 o/oo	13960 ± 130 BP
Beta-109187	Standard-AMS	14270 ± 100 BP	-22.6 o/oo	14310 ± 100 BP

APPENDIX VIII: Further data from OSL analysis, in supplement to the data presented in Table 7.1

Sample Code	Uranium (ppm)	Thorium (ppm)	Potassium (ppm)	Cosmic Dose (Gy/ka)	Total Dose (Gy/ka)
Shfd97020	0.6 ± 0.03	1.5 ± 0.08	0.50 ± 0.03	0.161 ± 0.008	0.911 ± 0.03
Shfd97021	0.8 ± 0.04	2.2 ± 0.11	0.65 ± 0.03	0.144 ± 0.007	0.899 ± 0.03
Shfd97086: sample:	2.1 ± 0.1	9.4 ± 0.5	1.53 ± 0.08	0.155 ± 0.008	2.50 ± 0.18
Overlying sediment:	2.2 ± 0.1	7.4 ± 0.4	1.57 ± 0.08		
Underlying sediment:	2.0 ± 0.1	7.5 ± 0.4	1.48 ± 0.07		
Shfd97088: sample:	2.1 ± 0.1	7.3 ± 0.4	1.82 ± 0.09	0.185 ± 0.009	2.99 ± 0.20
Overlying sediment:	1.9 ± 0.1	6.8 ± 0.4	1.76 ± 0.09		
Underlying sediment:	2.6 ± 0.1	9.8 ± 0.5	2.12 ± 0.11		

APPENDIX IX: Data from the U-Th analysis used in the isohcron age determination (explained in section 4.4.4). The R squared value for the fitted line is shown with the sample number. A, B, C, D, and E refer to sub samples of the sample itself, whilst 'Calcite' is hand-picked pure calcite cement surrounding the clasts.

Sample	$(^{234}U/^{232}Th)$	$(^{230}Th/^{232}Th)$	$(^{234}U/^{238}U)$	U (ppm)	Th (ppm)
#1 (R^2 = 0.992)					
A	5.53	6.1432	1.087	1.697	1.022
B	7.9	7.08	1.17	2.168	0.976
C	14.92	12.9	1.015	9.047	1.887
D	11.01	10.003	1.099	1.81	0.554
#2 (R^2 = 0.999)					
A	6.601	6.034	1.302	8.37	5.06
B	15.502	12.16	1.286	11.05	2.81
C	12.682	10.033	1.292	9.99	3.12
Calcite	31.793	22.25	1.266	20.01	0.797
#3 (R^2 = 0.994)					
A	14.66	10.9	1.14	1.401	0.334
B	6.25	7.8	1.198	0.192	0.113
C	13.01	10.5	1.178	2.82	0.784
D	7.011	7.9	1.213	1.249	0.663
#4 (R^2 = 0.997)					
A	8.61	5.888	1.211	7.21	3.11
B	17	7.109	1.232	13.41	2.98
C	12.15	6.511	1.268	9.97	3.19
D	4.015	5.552	1.221	2.51	2.34
#5 (R^2 = 0.995)					
A	8.036	7.403	1.321	7.4	3.73
B	20.156	9.763	1.217	17.34	3.21
C	6.269	6.889	1.274	3.17	1.98
D	14.035	8.459	1.221	9.59	2.56
#6 (R^2 = 0.936)					
A	3.325	2.949	1.113	0.221	0.227
B	3.265	2.929	1.222	0.773	0.887
C	2.45	2.636	1.249	0.789	1.234
D	3.801	3.003	1.223	0.775	0.764
E	4.503	3.501	1.334	1.468	1.334

APPENDIX IX: Continued.

Sample	($^{234}U/^{232}Th$)	($^{230}Th/^{232}Th$)	($^{234}U/^{238}U$)	U (ppm)	Th (ppm)
#7 ($R^2 = 0.996$)					
A	1.949	3.345	1.236	0.284	0.553
B	1.895	3.704	1.191	0.393	0.758
C	4.056	4.404	1.177	0.861	0.766
D	5.045	5.069	1.199	2.076	1.513
#8 ($R^2 = 0.989$)					
A	8.905	7.232	1.193	4.028	1.654
B	7.034	6.034	1.21	3.378	1.781
C	5.567	5.298	1.171	3.864	2.492
D	4.057	4.567	1.157	3.413	2.984

APPENDIX X: The results of radionuclide analysis of the floodplain core collected from U2 (Klithi unit) sediments in the Lower Vikos Gorge.

Depth (cm)	CRS Age (years)	Date of Deposition	137Cs (Bq kg^{-1})	Incremental ^{210}Pb inventory below section (Bq m^{-2})	Dry mass (g)	Cum. Dry Mass (kg m^{-2})	Ln unsupported ^{210}Pb
0.5	4.093	1994	2.485	11843.012	11.533	4.854	5.804
1.5	8.374	1990	5.761	10364.918	11.750	9.800	5.700
2.5	12.977	1986	6.080	8980.846	11.281	14.548	5.675
3.5	19.060	1979	8.566	7431.118	12.951	19.999	5.650
4.5	27.983	1971	32.113	5628.298	17.505	27.367	5.500
5.5	39.441	1959	5.275	3939.314	18.110	34.989	5.401
6.5	49.612	1949	0	2869.980	12.130	40.095	5.345
7.5	56.465	1942	0	2318.456	7.831	43.391	5.120
8.5	60.767	1938	0	2027.809	4.653	45.349	5.000
9.5	66.581	1932	0	1691.970	5.652	47.728	4.950
10.5	70.970	1928	0	1475.837	4.184	49.489	4.810
11.5	75.989	1923	0	1262.305	4.302	51.300	4.770
12.5	83.677	1915	0	993.580	5.524	53.625	4.750
13.5	92.823	1906	0	747.332	5.321	55.865	4.700
14.5	105.440	1893	0	504.531	5.799	58.305	4.600
15.5	118.714	1880	0	333.719	6.334	60.971	4.160
16.5	130.330	1868	0	232.429	5.384	63.237	3.800
17.5	142.021	1856	0	161.502	5.853	65.701	3.360

APPENDIX XI: Lichen growth data for independently dated substrates used in the construction of the lichen growth curve.

Surface	Date	Years from present (1998)	Largest lichen (mm)	Other 4 largest individuals on surface (mm)				Mean of 5 largest (mm)	Estimated elevation (m a.s.l.)	Mean annual precipitation (mm)
Kipi Bridge	1853	145	86	84	80	78	78	81.2	300	1484
Ano Pedina church wall	1863	135	96	95	92	89	83	91.0	800	1484
Water Memorial: edge of Aristi	1903	95	68	63	54	53	53	58.2	1200	1079
Monument floor in Papingo	1907	91	67	62	50	46	46	54.2	1200	1079
Memorial in Vasiliko	1932	66	79	74	61	54	50	63.6	350	1148
Monument base in Aristi	1942	56	35	33	32.5	32	30	32.5	1200	1079
Mesovounion War memorial	1947	51	37	33	33	33	33	33.8	1000	1079
Memorial on road near Papingo	1955	43	38	38	37	37	37	37.4	1100	1079
School Tower in Papingo	1958	40	28	26	25	16		23.8	1300	1079
Monument near Bourazani	1965	33	24	17				20.5	300	1148
Monastery wall near Molivdoskapasto	1967	31	28	26	24	21	21	24.0	300	1148
Memorial Box: edge of Aristi	1976	22	19	17.5	17	15	15	16.7	1200	1079
Monument wall in Konitsa	1976	22	8.5	7	5	4	3.5	5.6	500	1148
Wall in Vasiliko	1979	19	6	5	3			4.7	350	1148
Wall of house in Papingo	1980	18	12	10	9	8	8	9.4	1250	1079
Monument in Elafotopos	1988	10	2.1	1.2	1.1	1.05	0.9	1.3	1100	1079
Monument near Geroplatanos	1988	10	8.5	8.5	7	6.5	6.5	7.4	500	1148

APPENDIX XII: Lichen and boulder size data for the 18 boulder berms studied. Reference numbers are those used in Chapter 8.

Berm no.	Location	Largest lichen (mm)	Other 4 largest individuals on surface (mm)				Mean of 5 largest (mm)	Age calibrated from growth curve †	Date (AD)
1	Upper Vikos Gorge	54	54	50	47	45	50.0	79	1919
2	Upper Vikos Gorge	65	52	50	50	50	53.4	84	1914
3	Upper Vikos Gorge	66	52	46.5	39	33	47.3	74	1924
4	Upper Vikos Gorge	22	19				20.5	32	1966
5	Upper Vikos Gorge	118	114	101	73	61	93.4	147	1851
6	Upper Vikos Gorge	26	25	22	21	19	22.6	35	1963
7	Upper Vikos Gorge	94	69	68	63	59	70.6	111	1887
8	Upper Vikos Gorge	116	111	105	94	78	100.8	159	1839
9	Aoos Ravine	21	19	19	18	17	18.8	29	1969
10	Aoos Ravine	15	14	13	12	12	13.2	21	1977
11	Aoos Ravine	14	14	13	13	10	12.8	20	1978
12	Aoos Ravine	26	23	22	21	17	21.8	34	1964
13	Aoos Ravine	10	10	10	9	9	9.6	15	1983
14	Aoos Ravine	No lichen							
15	Aoos Ravine	70	65	50	40	40	53.0	83	1915
16	Upper Vikos Gorge	130	129	127	125	124	127.0	200	1798
17	Upper Vikos Gorge	146	145	135	131	130	137.4	216	1782
18	Upper Vikos Gorge	Lichen are too old: coalescing							

† Years before 1998

Berm no.	Intermediate axis of the 10 Largest Boulders (cm)										Mean of 5 largest (mm)	Mean of 10 largest (mm)
1	1300	1060	1000	850	820	650	630	620	600	550	1006	808
2	1900	1700	1700	1600	1530	1300	1200	1150	1080	1000	1686	1416
3	1500	1500	1400	1300	1000	1000	900	850	700	500	1340	1065
4	1600	1600	1300	1300	1300	1200	1000	800	700	700	1420	1150
5	1450	1300	1000	950	950	900	900	900	850	850	1130	1005
6	1300	1300	1100	800	800	700	700	700	600	600	1060	860
7	2200	1700	1700	1700	1600	1600	1500	1500	1500	1500	1780	1650
8	2300	2200	1900	1600	1600	1500	1400	1400	1200	1200	1920	1630
9	1500	1200	1000	1000	950	900	900	850	800	700	1130	980
10	1050	850	850	800	800	800	800	750	750	700	870	815
11	1300	1200	1100	1100	1100	1000	1000	1000	1000	900	1160	1070
12	1300	1200	1100	1000	900	900	750	700	700		1100	950
13	1700	1600	1600	1400	1400	1300	1100				1540	1443
14	1200	1200	1100	900	800	800	700	600	600		1040	878
15	1200	1200	1100	1000							1125	1125
16	2900	2400	2200	2200	2200	2000	1900	1900	1900	1900	2380	2150
17	2700	2500	2400	2300	2200	2100	2000	2000	2000	1900	2475	2244
18	2900	2300	2100	2000	1900	1900	1700	1600	1300	1300	2240	1900

REFERENCES CITED

Abbot, J.T. and Valastro, S. Jnr. (1995), The Holocene alluvial records of the chorai of Metapontum, Basilicata and Croton, Calabria, Italy, in: Lewin, J., Macklin, M.G. and Woodward, J.C. (eds.) *Mediterranean Quaternary River Environments*, Balkema/ Rotterdam/ Brookfield, pp. 195-205.

Abrahams, A.D. and Cull, R.F. (1979), The formation of alluvial landforms along New South Wales Coastal Streams, *Search,* 10 (5), pp. 187-188.

Aitken, M.J. (1985), *Thermoluminescence Dating,* Academic Press: London and New York.

Aitken, M.J. (1990), *Science-based Dating in Archaeology,* Longman: London and New York, 274 pp.

Aitken, M.J. (1992), Optical Dating, *Quaternary Science Reviews,* 11, pp. 127-131.

Alonso, A. and Garzón, G. (1994), Quaternary evolution of a meandering gravel bed river in central Spain, *Terra Nova,* 6, pp. 465-475.

Appleby, P.G. and Oldfield, F. (1978), The calculation of Lead-210 dates assuming a constant rate of supply of unsupported ^{210}Pb to the sediment, *Catena,* 5, pp. 1-8.

Armstrong, R.A. (1975), The influence of aspect on the pattern of seasonal growth in the lichen *Parmelia glabratula* ssp *fuliginosa* (Fr. ex Duby) Laund, *New Phytologist,* 75, pp. 245-251.

Armstrong, R.A. (1975), The response of lichen growth to transplantation to rock surfaces of different aspect, *New Phytologist,* 75, pp. 245-251.

Attendorn, H.-G. and Bowen, R.N.C. (1997), *Radioactive and Stable Isotope Geology,* Chapman & Hall: London, 508pp.

Aubouin, J. (1959), Contribution à l'étude géologique de la Grèce septrionale; les confins de L'Epire et de la Thessalie, *Annales Géologiques* des pays Hélleniques, 10, pp. 1-483.

Bagnold, R.A. (1966), An approach to the sediment transport problem from general physics, *U.S. Geological Survey Professional Paper,* 422-I, pp. 11-137.

Bailey, G.N. (ed.) (1997a), *Klithi: Palaeolithic Settlement and Quaternary Landscape in northwest Greece, Volume 1: Excavation and intra-site analysis at Klithi,* McDonald Institute, pp. 1-317.

Bailey, G.N. (ed.) (1997b), *Klithi: Palaeolithic Settlement and Quaternary Landscape in northwest Greece, Volume 2: Klithi in its local and regional setting,* McDonald Institute, pp. 318-699.

Bailey, G.N. (1997c), The Klithi Project: History, aims and structure of investigations, in Bailey, G.N. (ed.), *Klithi: Palaeolithic Settlement and Quaternary Landscape in northwest Greece. Volume 1: Excavation and intra-site analysis at Klithi,* McDonald Institute, pp. 3-26.

Bailey, G.N., Lewin, J., Macklin, M.G. and Woodward, J.C. (1990), The "Older Fill" of the Voidomatis Valley, North-west Greece and its relationship to the Paleolithic archaeology and glacial history of the region, *Journal of Archaeological Science,* 17, pp. 145-150.

Bailey, G.N., Gamble, C.S., Higgs, H.P., Roubet, C., Webley, D.P., Gowlett, J.A.J., Sturdy, D.A. and Turner, C. (1986), Dating results from Palaeolithic sites and environments in Epirus (North-west Greece). In: Gowlett, J.A.J. and Hedges, R.E.M. (eds.), *Archaeological results from accelerator dating,* (Monograph 11) Oxford: Oxford University Committee for Archaeology, pp. 99-107.

Bailey, G.N., Papagonstantinou, V. and Sturdy, D.A. (1992), Asprochaliko and Kokkinopilos: TL dating and reinterpretation of Middle Palaeolithic sites in Epirus, north-west Greece, *Cambridge Archaeological Journal,* 2, pp. 136-144.

Bailey, G.N., King, G. and Sturdy, D. (1993), Active tectonics and land-use strategies: a Palaeolithic example from northwest Greece, *Antiquity,* 67, pp. 292-312.

Bailey, G.N., Turner, C., Macklin, M.G., Woodward, J.C. and Lewin, J. (1997), The Voidomatis Basin: An introduction, in: Bailey, G.N. (ed.) *Klithi: Palaeolithic Settlement and Quaternary Landscape in northwest Greece. Volume 2: Klithi in its local and regional setting,* McDonald Institute, pp. 321-346.

Bailiff, I.K. (1992), Luminescence dating of alluvial deposits, in: Needham, S. and Macklin, M.G. (eds.) *Alluvial Archaeology in Britain,* Oxbow Monograph 27, Oxford, Oxbow Press, pp. 27-35.

Baker, V.R. (1977), Stream channel response to floods, with examples from central Texas, *Geol. Soc. of Am. Bull.,* 88, pp. 1057-1071.

Baker, V.R. (1984), Flood Sedimentation in bedrock fluvial systems, in: Koster, E.H. and Steel, R.J. (eds.) *Sedimentology of Gravels and Conglomerates, Canadian* Society of Petroleum Geologists, Memoir 10, pp. 87-98.

Baker, V.R. (1987), Palaeoflood hydrology and extraordinary flood events, *Journal of Hydrology,* 96, pp. 79-99.

Baker, V.R. (1988), Flood erosion, in: Baker, V.R., Kochel, R.C. and Patton P.C. (eds.) *Flood Geomorphology,* John Wiley: New York, pp. 81-95.

Baker, V.R. (1989), Magnitude and frequency of paleofloods, in: Beven, K. and Carling, P. (eds.) *Floods: Hydrological, Sedimentological and Geomorphological Implications,* John Wiley & Sons Ltd., pp. 171-183

Baker, V.R. (1993), Learning from the past, *Nature,* 361, pp. 402-403.

Baker, V.R. and Ritter, D.F. (1975), Competence of rivers to transport coarse bedload material, *Geological Society of America Bulletin,* 86, pp. 975-978.

Baker, V.R., Kochel, R.C. and Patton, P.C. (1979), Long-term flood frequency analysis using geological data, in: *The Hydrology of Areas of Low Precipitation,* Scientific Publication of the International Association of Hydrologists, 128, pp. 3-9.

Baker, V.R., Kochel, R.C., Patton, P.C., and Pickup, G. (1983a), Paleohyrologic analysis of Holocene flood slack-water sediments, *Special Publication of the International Association of Sedimentologists,* 6, pp. 229-239.

Baker, V.R., Pickup, G. and Polach, H.A. (1983b), Desert paleofloods in central Australia, *Nature,* 301, pp.502-504.

Baker, V.R. and Bunker, R.C. (1985), Cataclysmic Late Pleistocene flooding from Glacial Lake Missoula: a review, *Quaternary Science Reviews,* 4, pp. 1-41.

Baker, V.R., Pickup, G. and Polach, H.A. (1985), Radiocarbon dating of flood events, Katherine Gorge, Northern Territory, Australia, *Geology,* 13, pp.344-347.

Baker, V.R. and Costa, J.E. (1987), Flood power, in: Mayer, L. and Nash, D. (eds.) (1987), *Catastrophic Flooding,* Allen & Unwin: Boston, pp. 1-21.

Baker, V.R. and Pickup, G. (1987), Flood geomorphology of the Katherine Gorge, Northern Territory, Australia, *Geological Society of America Bulletin,* 98, pp. 653-646.

Baker, V.R., Ely, L.L., O'Connor, J.E. and Partridge, J.B. (1987), Paleoflood hydrology and design applications, in: Singh, V.P. (ed.) *Regional Flood Frequency Analysis,* D. Reidel, Norwell, Mass., pp. 339-353.

Baker, V.R. and Kochel, R.C. (1988), Flood Sedimentation in bedrock fluvial systems, in: Baker, V.R., Kochel, R.C. and Patton P.C. (eds.) *Flood Geomorphology,* John Wiley: New York, pp. 123-137.

Baker, V.R., Kochel, R.C. and Patton P.C (1988), Part III: Floods, climate, landscape, in: Baker, V.R., Kochel, R.C. and Patton P.C. (eds.) *Flood Geomorphology,* John Wiley: New York, pp. 167-168.

Baker, V.R. and Kale, V.S. (1998), The role of extreme floods in shaping bedrock channels, in: Tinkler, K.J. and Wohl, E.E. (eds.) *Rivers Over Rock: Fluvial Processes in Bedrock Channels,* Geophysical Monograph 107, American Geophysical Union, pp. 153-165.

Ballais, J.L. (1995), Alluvial Holocene terraces in eastern Maghreb: climate and anthropogenic controls, in: Lewin, J., Macklin, M.G. and Woodward, J.C. (eds.), *Mediterranean Quaternary River Environments*, Balkema/Rotterdam/Brookfield, pp. 183-194.

Bard, E., Hamelin, B., Fairbanks, R.G. and Zinder, A. (1990), Calibration of the ^{14}C timescale over the past 30,000 years using mass spectrometric U-Th ages from Barbados corals, *Nature*, 345, pp. 405-410.

Bard, E., Fairbanks, R.G., Arnold, M., and Hamelin, B. (1992), $^{230}Th/^{234}U$ and ^{14}C ages obtained by mass spectrometry on corals from Barbados (West Indies), Isabela (Galapagos) and Mururoa (French Polynesia). In: Bard, E. and Broecker, W.S. (eds.) *The Last Deglaciation: Absolute and Radiocarbon Chronologies*, Springer-Verlag: Berlin, Heidelberg, pp. 103-110.

Bard, E., Arnold, M., Fairbanks, R.G. and Hamelin, B. (1993), ^{230}Th-^{234}U and ^{14}C ages obtained by mass spectrometry on corals, *Radiocarbon*, 35 (1), pp. 191-199.

Batalla, R.J. and Sala, M. (1995), Effective discharge for bedload transport in a subhumid Mediterranean sandy gravel-bed river (Arbucies, north-east Spain), in: Hickin, E.J. (ed.) *River Geomorphology*, John Wiley & Sons, Chichester, pp. 93-104.

Bateman, M.D. and Catt, J.A. (1996), An absolute chronology for the raised beach deposits at Sewerby, E. Yorkshire, UK, *Journal of Quaternary Science*, 11, pp. 389-395.

Bathurst, J.C. (1987), Critical conditions for bed material movement in steep, boulder-bed streams, in: Beschta, R.L *et al.* (eds.) *Erosion and Sedimentation in the Pacific Rim*, IAHS Publication No. 165, pp. 309-318.

Bathurst, J.C., Graf, W.H. and Cao, H.H. (1983), Initiation of sediment transport in steep channels with coarse bed material, in: Multlu Summer, A. and Muller, A. (eds.) *Mechanics of Sediment Transport"*, Proceedings of Euromech 156, A.A. Balkema: Rotterdam, pp. 207-213.

Bathurst, J.C., Graf, W.H. and Cao, H.H. (1987), Bed load discharge equations for steep mountain rivers, in: Thorne, C.R., Bathurst, J.C. and Hey, R.D. (eds.) *Sediment Transport in Gravel-bed Rivers*, pp. 453-?.

Beard, L.R. (1975), Generalized evaluation of flash flood potential, *Texas University Centre Research Water Resources Technical Report*, CRWR-124, 27 pp.

Becker, B. and Kromer, B. (1993), The continental tree-ring record – absolute chronology, ^{14}C calibration and climatic change, *Palaeogeography, Palaeoclimatology, Palaeoecology*, 103, pp. 67-71.

Benito, G. (1997), Energy expenditure and geomorphic work of the cataclysmic Missoula flooding in the Columbia River Gorge, USA, *Earth Surface Processes and Landforms*, 22, pp. 457-472.

Benito, G., Gutiérrez, M. and Sancho, C. (1992), Erosion rates in badland areas of the central Ebro basin (NE-Spain), *Catena*, 19, pp. 269-286.

Benito, G., Machado, M.J. and Pérez-González, A. (1996), Climate change and flood sensitivity in Spain, in: Branson, J., Brown, A.G. and Gregory, K.J. (eds.) *Global Continental Changes: the Context of Paleohydrology*, Geological Society Special Publication No. 115, pp. 85-98.

Benito, G., Machado, M.J., Pérez-González, A. and Sopeña, A. (1998), Palaeoflood hydrology of the Tagus River, central Spain, in: Benito, G., Baker, V.R. and Gregory, K.J. (eds.), *Palaeohydrology and Environmental Change*, John Wiley & Sons, Chichester, pp. 317-333.

Beshel, R.E (1950), Flechten als Altersmasstab rezenter Moränen, *Z. Glerscherkd. Glazialgeol.* 1, pp. 152-161.

Beshel, R.E. (1961), Dating rock surfaces by lichen growths and its application to glaciology and physiology (lichenometry). In: Raasch, G.O. (ed.) *Geology of the Arctic*, Vol. II. University of Toronto press, Toronto, pp. 1044-1062.

Beshel, R.E. (1973), Lichens as a measure of the age of recent moraines, *Arctic and Alpine Research*, 5 (4), pp. 303-310.

Birman, J.H. (1968), Glacial Reconnaissance in Turkey, *Geological Society of America Bulletin,* 79, pp. 1009-1026.

Bischoff J. L., Julia, R. and Mora, R. (1988), Uranium-series dating of the Mousterian occupation at Abric Romani, Spain, *Nature,* 332, pp. 68-70.

Bischoff J. L. and Fitzpatrick, J. A. (1990), U-series dating of impure carbonates: An isochron technique using total-sample dissolution, *Geochimica et Cosmochimica Acta,* 55, pp. 543-554.

Black, S., Macdonald, R., and Kelly, M. (1997), Crustal Origin for Peralkaline Rhyolites from Kenya: Evidence from U-series Disequilibria and Th-Isotopes, *Journal of Petrology,* 38, pp. 277-297.

Black, S., Howard, A.J. and Macklin, M.G. (1998), U-series dating of cemented river gravels and tufa deposits in upper Wharfedale, between Kettlewell and Grassington, in: Howard, A,J, and Macklin, M.G. (eds.), *The Quaternary of the Eastern Yorkshire Dales: Field Guide. The Holocene Alluvial Record.* Quaternary Research Association, London, pp. 31-44.

Blintliff, J.L. (1975), Mediterranean alluviation: New evidence from archaeology, *Proceedings of the Prehistoric Society,* 41, pp. 78-84.

Blong, R.J. and Gillespie, R. (1978), Fluvially transported charcoal gives erroneous ^{14}C ages for recent deposits, *Nature,* 271, pp.739-741.

Bloom, A.L. (1991), *Geomorphology: a Systematic Analysis of Late Cenozoic Landforms,* 2nd Edition, Englewood Cliffs (NJ): Prentice Hall.

de Boer, D.H. and Crosby, G. (1995), Evaluating the potential of SEM/EDS analysis for fingerprinting suspended sediment derived from two contrasting topsoils, *Catena,* 24, pp. 243-258.

Bond, G., Heinrich, H., Broeker, W., Labeyrie, L., McManus, J., Andrews, J., Huon, S., Jantschik, R., Clasen, S., Simet, C., Tedesco, K., Klas, M., Bonani, and Ivy, S. (1992), Evidence for massive discharges of icebergs into the North Atlantic during the last glacial period, *Nature,* 360, pp. 245-249.

Boon, P.J., Calow, P. and Petts, G.E. (1992), *River Conservation and Management,* Wiley: Chichester.

Bottema, S. (1974), *Late Quaternary Vegetation History of Northwestern Greece,* Gröningen: Gröningen University Press.

Bøtter-Jenson, L. and Duller, G.A.T. (1992), A new system for measuring optically stimulated luminescence from quartz samples, *Nuclear Tracks and Radiation Measurements,* 20, pp. 549-553.

Bradley, R.S. and Jones, P.D. (eds.) (1992), *Climate Since A.D. 1500,* Routledge, London.

Bradley, W.C. and Mears, A.I. (1980), Calculations of flows needed to transport coarse fraction of Boulder Creek alluvium at Boulder, Colorado, *Geological Society of America Bulletin,* 91 , pp. 1057-1090.

Brandt, C.J. and Thornes, J.G. (1996), *Mediterranean Desertification and Land Use,* John Wiley & Sons, Chichester, 554 pp.

Braudel, F. (1972), *The Mediterranean and the Mediterranean World in the Age of Phillip II,* Volumes I & II, Collins, London.

Bretz, J.H. (1929), Valley deposits immediately west of the Channeled Scabland of Washington, *Journal of Geology,* 37, pp. 393-427, 505-541.

Broccoli, A.J. and Manabe, J. (1987), The influence of continental ice, atmospheric CO2, and land albedo on the climate of the last glacial maximum, *Climate Dynamics,* 1, pp. 87-99.

Brodo, I.M. (1973), Substrate ecology, in: Ahmadjian, V. and Hale, M.E. (eds.), *The Lichens,* New York: Academic Press, pp. 401-441.

Broecker, W.S. and Ku, T.-L. (1969), Caribbean cores P6304-8 and P6304-9: new analysis of absolute chronology, *Science,* 66, pp. 404-406.

Brookes, A. (1987), River channel adjustments downstream from channelization works in England and Wales, *Earth Surface Processes and Landforms,* 12, pp. 337-351.

Brookes, A. (1995), River channel restoration: Theory and practice, in: Gurnell, A. and Petts, G. (eds.) *Changing River Channels,* John Wiley & Sons, Chichester, pp. 369-388.

Brookes, I.A. (1987), A medieval catastrophic flood in central west Iran, in: Mayer, L. and Nash, D. (eds.), *Catastrophic Flooding,* Allen & Unwin: Boston, pp. 225-246.

Brunsden, D. and Thornes, J.B. (1979), Landscape sensitivity and change, *Transactions of the Institute of British Geographers,* NS4, pp. 463-484.

Bull, W.B. (1979), Threshold of critical power in streams, *Bulletin of the Geological Society of America,* 90, pp. 453-464.

Bull, W.B. (1988), Floods; degradation and aggradation, in: Baker, V.R., Kochel, R.C. and Patton P.C. (eds.) *Flood Geomorphology,* John Wiley: New York, pp.157-165.

Butzer, K. (1969), Changes in the land, *Science,* 4 July 1965, vol. 165.

Cambray, R.S., Cawse, P.A., Garland, J.A., Gibson, J.A.B., Johnson, P., Lewis, G.N.J., Newton, D., Salmon, L., and Wade, B.O. (1987), Observations on radioactivity from the Chernobyl accident, *Nuclear Energy,* 26, pp. 77-101.

Carling, P.A. (1983), Threshold of coarse sediment transport in broad and narrow natural streams, *Earth Surface Processes and Landforms,* pp. 1-18.

Carling, P.A. (1986), The Noon Hill flash floods; July 17th 1983. Hydrological and geomorphological aspects of a major formative events in an upland landscape, *Transactions of the Institute of British Geographers,* N.S. 11, pp. 105-118.

Carling, P.A. (1987), Hydrodynamic interpretation of a boulder berm and associated debris-torrent deposits, *Geomorphology,* 1, pp. 53-67.

Carling, P.A. (1989), Hydrodynamic models of boulder berm deposition, *Geomorphology,* 2, pp. 319-340.

Carling, P.A. (1995), Flow-separation berms downstream of a hydraulic jump in a bedrock channel, *Geomorpholpgy,* 11, pp. 245-253.

Carling, P.A. and Grodek, T. (1994), Indirect estimation of ungauged peak discharges in a bedrock channel with reference to design discharge selection, *Hydrological Processes,* 8, pp. 497-511.

Carling, P.A. and Tinkler, K. (1998), Conditions for the entrainment of Cuboid boulders in bedrock streams: An historical review of literature with respect to recent investigations, in: Tinkler, K.J. and Wohl, E.E. (eds.) *Rivers Over Rock: Fluvial Processes in Bedrock Channels,* Geophysical Monograph 107, American Geophysical Union, pp. 19-34.

Carrara, P.E. and Andrews, J.T. (1973), Problems and application of lichenometry to geomorphic studies, San Juan Mountains, Colorado, *Arctic and Alpine Research,* 5 (4), pp. 373-384.

Cenderelli, D.A. and Cluer, B.L. (1998), Depositional processes and sediment supply in resistant boundary channels: examples from two case studies, in: Tinkler, K.J. and Wohl, E.E. (eds.) *Rivers Over Rock: Fluvial Processes in Bedrock Channels,* Geophysical Monograph 107, American Geophysical Union, pp. 105-131.

Chadwick, A. and Morfett, J. (1993), *Hydraulics in Civil and Environmental Engineering,* E & FN Spon: London, 557 pp.

Chorley, R.J. (1962), Geomorphology and general systems theory, *U.S. Geol. Survey Prof. Paper,* 500-B, 10pp.

Chow, V.T. (1959), *Open Channel Hydraulics,* McGraw-Hill: New York, 690pp.

Church, M. and Ryder, J.M. (1972), Paraglacial sedimentation: a consideration of fluvial processes conditioned by glaciation, *Geological Society of America Bulletin,* 83, pp. 3059-3071.

Church, M. and Slaymaker, O. (1989), Disequilibrium of Holocene sediment yield in glaciated British Columbia, *Nature,* 337, pp. 453-454.

Clarke, M.L. (1996), IRSL dating of sands: Bleaching characteristics at deposition inferred from the use of single aliquots, *Radiation Measurements,* 26, pp. 611-620.

Clews, J.E. (1989), Structural controls on basin evolution: Neogene to Quaternary of the Ioanian zone, Western Greece, *Journal of the Geological Society, London,* 146, pp. 447-457.

COHMAP Members (1988), Climatic observations of the last 18,000 years: observations and model simulations, *Science,* 241, pp. 1043-1052.

Collier, R.E.Ll., Leeder, M.R. and Jackson, J.A. (1995), Quaternary drainage development, sediment fluxes and extensional tectonics in Greece, in: Lewin, J., Macklin, M.G. and Woodward, J.C. (eds.) (1995), *Mediterranean Quaternary River Environments,* Balkema/Rotterdam/Brookfield, pp. 31-44.

Collins, A.L., Walling, D.E. and Leeks, G.J.L. (1997a), Source type ascription for fluvial suspended sediment based on a quantitative composite fingerprinting technique, *Catena,* 29, pp. 1-27.

Collins, A.L., Walling, D.E. and Leeks, G.J.L. (1997b), Use of the geochemical record preserved in floodplain deposits to reconstruct recent changes in river basin sediment sources, *Geomorphology,* 19, pp. 151-167.

Collins, A.L., Walling, D.E. and Leeks, G.J.L. (1998), Use of composite fingerprints to determine the provenance of the contemporary suspended sediment load transported by rivers, *Earth Surface Processes and Landforms,* 23, pp. 31-52.

Conchon, O. (1986), Quaternary glaciations in Corsica, *Quaternary Science Reviews,* 5, pp. 429-432.

Costa, J.E. (1974a), Stratigraphic, morphologic, and pedologic evidence of large floods in humid environments, *Geology,* 2 (6), pp. 301-303.

Costa, J.E. (1974b), Response and recovery of a Piedmont watershed from tropical storm Agnes, June 1972, *Water Resources Research,* 10, pp. 106-112.

Costa, J.E. (1978a), Colorado Big Thompson flood: Geologic evidence of a rare hydrologic event, *Geology,* 6, pp. 617-620.

Costa, J.E. (1978b), Holocene stratigraphy in flood frequency analysis, *Water Resources Research,* 14 (4), pp. 626-632.

Costa, J.E. (1983), Paleohyraulic reconstruction of flash-flood peaks from boulder deposits in the Colorado Front Range, *Geological Society of America Bulletin,* 94, pp. 986-1004.

Costa, J.E. (1984), Physical geomorphology of debris flows, in: Costa, J.E. and Fleisher, P.J. (eds.) *Developments and Applications of Geomorphology,* Springer-Verlag: Berlin, pp. 343-367.

Costa, J.E. (1988), Rheologic, geomorphic, and sedimentologic differentiation of water floods, hyperconcentrated flows, and debris flows, in: Baker, V.R., Kochel, R.C. and Patton P.C. (eds.) *Flood Geomorphology,* John Wiley: New York, pp. 113-122.

Costa, J.E. and Jarrett R.D. (1981), Debris flows in small mountain stream channels of Colorado and their hydrologic implications, *Bulletin of the Ass. of Engineering Geologists,* 18 (3), pp. 309-322.

Coulter® (1994), *Coulter LS Series Product Manual,* Coulter Corporation, Miami, Florida.

Coxon, P., Owen, L.A. and Mitchell, W.A. (1996), A Late Pleistocene catastrophic flood in the Lahul Himalayas, *Journal of Quaternary Science,* 11, pp. 495-510.

Dalrymple, T. and Benson, M.A. (1967), Measurement of peak discharge by the slope-area method, *Tech. Water Resources Division (U.S. Geol. Survey) Book 3,* Ch. A-2, pp. 1-12.

Davidson, D.A. (1980), Erosion in Greece during the first and second millennia BC, in: Cullingford, R.A., Davidson, D.A. and Lewin, J. (eds.) *Timescales in Geomorphology,* pp. 143-158.

Davis, W.M. (1899), The geographical cycle, *Geographical Journal,* 14, pp. 481-504.

Davis, P.T. (1985), Neoglacial moraines on Baffin Island, pp. 682-719, In: Andrews, J.T. (ed.) *Quaternary environments: eastern Canadian Arctic, Baffin Bay, and western Greenland,* Allen & Unwin: Boston.

De Ploey, J. (1989), *Soil Erosion Map of Western Europe,* Cremlington-Destedt: Catena Verlag.

De Ploey, J. (1992), Gullying and the age of badlands: an application of the erosional susceptibility model, Es. *Catena* Supplement 23, pp. 31-45.

Dearing, J.A. (1992), Sediment yields and sources in a Welsh upland catchment during the past 800 years, *Earth Surface Processes and Landforms,* 17, pp. 1-22.

Dearing, J.A. (1994), *Environmental Magnetic Susceptibility: Using the Bartington MS2 System,* Chi Publishing: Kenilworth, 104 pp.

Debenham, N. (1997), Thermoluminescence dating of sediment from Epirus, in: Bailey, G.N. (ed.), *Klithi: Palaeolithic Settlement and Quaternary Landscape in northwest Greece. Volume 2: Klithi in its local and regional setting,* McDonald Institute, pp. 681-682.

Dedkov, A.P. and Mozzherin, V.I. (1992), Erosion and sediment yield in mountain regions of the world, in: Walling, D.E., Davies, T.R. and Hasholt, B. (eds.) *Erosion, Debris Flows and Environment in Mountain Regions (proceedings of the Chengdu Symposium, July 1992),* IAHS Publication No. 209, pp. 37-40.

Dewey, J.F., Pitman III, W.C., Ryan, W.B.F. and Bonnin, J. (1973), Plate tectonic and the evolution of the Alpine system, *Geological Society of America Bulletin,* 84, pp. 3137-3180.

Douglas, M.S.V., Smol, J.P. and Blake Jr., W. (1994), Marked post-18th Century environmental change in High-Arctic ecosystems, *Science,* 266, pp. 416-419.

Doswel III, C.A., Brooks, H.E. and Maddox, R.A. (1996), Flash flood forecasting: an ingredients-based methodology, *Weather and Forecasting,* 11, pp. 560-581.

Doswel III, C.A. (1998), A diagnostic study of three heavy precipitation episodes in the western Mediterranean region, *Weather and Forecasting,* 13, pp. 102-124.

Duller, G.A.T. (1994), Luminescence dating of sediments using single aliquots: new procedures, *Quaternary Geochronology (Quaternary Science Reviews),* 13, pp. 149-156.

Duller, G.A.T. (1996), Recent developments in luminescence dating of Quaternary sediments, *Progress in Physical Geography,* 20 (2), pp. 127-145.

Easton, R.M. (1995), Lichens and rocks: a review, *Geoscience Canada,* 21 (2), pp. 59-76.

Ely, L.L. (1997), Response of extreme floods in the southwestern United States to climatic variations in the late Holocene, *Geomorphology,* 19, pp. 175-201.

Ely, L.L. and Baker, V.R. (1985), Reconstructing palaeoflood hydrology with slackwater deposits: Verde River, Arizona, *Physical Geography,* 5 (2), pp. 103-126.

Ely, L.L., Enzel, Y., O'Connor, J.E. and Baker, V.R. (1991), Paleoflood records and risk assessment: examples from the Colorado River basin, in: Ganoulis, J. (ed.) *Water Resources and Engineering Risk Assessment,* Springer-Verlag: New York, pp. 105-112.

Ely, L.L., Webb, R.H. and Enzel, Y. (1992), Accuracy of post-bomb ^{137}Cs and ^{14}C in dating fluvial deposits, *Quaternary Research,* 38, pp. 196-204.

Ely, L.L., Enzel, Y., Baker, V.R. and Cayan, D.R. (1993), A 5000-year record of extreme floods and climate change in the Southwestern United States, *Science,* 262, pp. 410-412.

Enzel, Y., Ely, L.L., House, P.K., Baker, V.R., Duckstein, L. and Weber, J. (1991), The contribution of long-term records of hydrologic extremes to risk analyses, in: Ganoulis, J. (ed.) *Water Resources and Engineering Risk Assessment,* Springer-Verlag: New York, pp. 97-104.

Enzel, Y., Ely, L.L., House, P.K., Baker, V.R. and Webb, R.H. (1993), Paleoflood evidence for a natural upper bound to flood magnitudes in the Colorado River Basin, *Water Resources Research*, 29 (7), pp. 2287-2297.

Ergenzinger, P. (1988), Regional erosion: rates and scale problems in the Buonamico basin, Calabria, *Catena Supplement 13*, pp. 97-107.

Ergenzinger, P. (1992), A conceptual geomorphic model for the development of a Meditteranean river basin under neotectonic stress (Buonamico basin, Calabria, Italy, in: *Erosion, Debris Flows and Environment in Mountain Regions*, Proceedings of the Chengdu Symposium, Italy, July 1992, IAHS Publication no. 209, pp. 51-60.

Erskine, W.D. (1993), Erosion and deposition produced by a catastrophic flood on the Genoa River, Victoria, *Australian Journal of Soil and Water Conservation*, 6 (4), pp. 35-43.

Erskine, W.D. (1994), Sand slugs generated by catastrophic floods on the Goulburn River, New South Wales, *Variability in Stream Erosion and Sediment Transport*, Proceedings of the Canberra Symposium, December 1994, IAHS Publication no. 224, pp. 143-151.

Erskine, W.D. and Saynor, M.J. (1996), Effects of catastrophic floods on sediment yields in southeastern Australia, in: *Erosion and Sediment Yield: Global and Regional Perspectives*, IAHS Publication No. 236, pp. 381-388.

Erskine, W.D. and Livingtone,, E.A. (1999),In-channel benches: the role of floods in their formation and destruction on bedrock-confined rivers, in: Miler, A.J. and Gupta, A. (eds.) *Varieties of Fluvial Form*, John Wiley & Sons, pp. 445-475.

Everett, J.R., Morisawa, M. and Short, M.N. (1986), Tectonic landforms, in: Short, N.M. and Blair, R.W. (eds.) *Geomorphology from Space: a Global Overview of Regional Landforms*, NASA: Washington (DC), pp. 27-185.

F.A.O. (1959), *F.A.O. Mediterranean Development Project: The integrated development of Mediterranean Agriculture and Forestry in relation to economic growth. A Study and Proposals for Action*, F.A.O., 213 pp.

Fairchild, I., Hendry, G., Quest, M. and Tucker, M. (1988), Chemical analysis of sedimentary rocks, in: Tucker, M. (ed.) *Techniques in Sedimentology*, Blackwell Scientific Publications: Oxford, pp. 274-354.

Farmer, J.G. (1978), The determination of sedimentation rates in Lake Ontario using the ^{210}Pb dating method, *Canadian Journal of Earth Science*, 15, pp. 431-437.

Farmer, J.G. and Lovell, A. (1984), Massive diagenetic enhancement of manganese in Loch Lomond sediments, *Environmental Technology Letters*, 5, pp. 257-262.

Faure, G. (1977), *Principles of Isotope Geology*. Wiley & Sons: New York London.

Feldman, A.D. (1981), HEC models for water resource system simulation: Theory and experimence, in: Chow, V.T. (ed.) *Advances in Hydroscience*, vol. 12, New York: Academic Press, pp. 297-423.

Ferguson, R.I. (1993), Understanding braiding processes in gravel-bed rivers: progress and unsolved problems, in: Bristow, C.S. and Best, J.L. (eds.) *Braided Rivers*, Geological Society of London, Special Publication no. 75, pp. 73-88.

Ferrari, E., Gabriele, S. and Villani, P. (1993), Combined regional frequency analysis of extreme rainfalls and floods, in: Kundzewicz, Z.W., Rosbjerg, D., Simonovic, S.P. and Takeuchi, K. (eds.) *Extreme Hydrological Events: Precipitation, Floods and Droughts*, IAHS Publication No. 213, pp. 333-346.

Fitton, G. (1997), X-ray fluorescence spectrometry, in: Gill. R. (ed.) *Modern Analytical Geochemistry*, Longman, pp. 87-115.

Flocas, A.A. (1984), The annual and seasonal distribution of fronts over central-southern Europe and the Mediterranean, *Journal of Climatology*, 4, pp. 255-267.

Foley, M.G., Doesburg, J.M. and Zimmerman, D.A. (1984), Palaeohydrologic techniques with environmental applications for siting hazardous waste facilities, in: Koster, E.H. and Steel, R.J. (eds.) *Sedimentology of Gravels and Conglomerates, Canadian* Society of Petroleum Geologists, Memoir 10, pp. 99-108.

Foster, I.D.L., Lees, J.A., Owens, P.N. and Walling, D.E. (1998), Mineral magnetic characterization of sediment sources from an analysis of lake and floodplain sediments in the catchments of the Old Mill Reservoir and Slapton Ley, South Devon, UK, *Earth Surface Processes and Landforms,* 23, pp. 685-703

Foucault, A. and Stanley, D.J. (1989), Late Quaternary palaeoclimatic oscillations in East Africa recorded by heavy minerals in the Nile Delta, *Nature,* 339, pp. 44-46.

Friedman, G.M. and Sanders, J.E. (1978), *Principles of Sedimentology,* Wiley: New York.

Frostick, L.E. and Reid, I. (1989), Climatic versus tectonic controls of fan sequences: lessons from the Dead Sea, Isreal, *Journal of the Geological Society,* 146, pp. 527-538.

Fuller, I.C., Wintle, A,G, and Duller, G.A.T. (1994), Test of the partial bleach methodology as applied to the IRSL of an alluvial sediment from the Danube, *Quaternary Geochronology (Quaternary Science Reviews),* 13, pp. 423-427.

Fuller, I.C., Macklin, M.G., Passmore, D.G., Brewer, P.A., Lewin, J. and Wintle, A.G. (1996), Geochronologies and environmental records of Quaternary fluvial sequences in the Guadalope basin, northeast Spain, based on luminescence dating, in: Branson, J., Brown, A.G. and Gregory, K.J. (eds.) *Global Continental Changes: the Context of Paleohydrology,* Geological Society Special Publication No. 115, pp. 99-120.

Fuller, I.C., Macklin, M.G., Lewin, J., Passmore, D.G. and Wintle, A.G. (1998), River response to high frequency climate oscillations in southern Europe over the last 200,000 years, *Geology,* 26, pp. 275-278.

Furlan, D. (1977), The climate of southeast Europe, in: Wallen, C.C. (ed.) *Cliamtes of Central and Southern Europe,* World Survey of Climatology Volume 6, Elsevier: Amsterdam.

G.B. Meteorological Office (HMSO) (1962), *Weather in the Mediterranean: Volume 1 (Second Edition) General Meteorology,* London: Her Magesty's Stationary Office, pp. 1-6, 179-189, 358-360.

Gascoyne, M., Schwarcz, H.P. and Ford, D.C. (1983), Uranium-series ages of speleothem from northwest England: correlation with Quaternary climate, *Philosophical Transactions of the Royal Society of London,* B301, pp. 143-164.

Giakoumakis, S.G. ans Baloutos, G. (1997), Investigations of trend in hydrological time series of the Evinos River basin, *Hydrological Sciences Journal,* 42 (1), pp. 81-88.

Gillieson, D., Ingle Smith, D., Greenaway, M. and Ellaway, M. (1991), Flood history of the limestone ranges in the Kimberly region, Western Australia, *Applied Geography,* 11, pp. 105-123.

Godwin, H. (1962), Half-life of Radiocarbon, *Nature,* 195, pp. 242-244.

Goodwill, P. and Rowan, J.S. (in press), Uncertainty in the quantification of contemporary suspended sediment sources, Wyresdale Park lake catchment, Lancashire, UK, in: Foster, I.D.L. (ed.) *Tracers in Geomorphology,* John Wiley & Sons: London.

Gordon, D., Smart, P.L., Ford, D.C., Andrews, J.N., Atkinson, T.C., Rowe, P.J. and Christopher, N.S.T. (1989), Dating of Late Pleistocene interglacial and interstadial periods in the United Kingdom from Speleothem growth frequency, *Quaternary Research,* 31, pp. 14-26.

Gottesfield, A.S. (1996), British Columbia flood scars: maximum flood stage indicators, *Geomorphology,* 14, pp. 319-325.

Gowlett, J., Hedges, R. and Housley, R. (1997), Klithi: the AMS radiocarbon dating programme for the site and its environs, in Bailey, G.N. (ed.), *Klithi: Palaeolithic Settlement and Quaternary Landscape in northwest Greece. Volume 1: Excavation and intra-site analysis at Klithi,* McDonald Institute, pp. 27-40.

Greenbaum, N., Margalit, A., Schick, A.P., Sharon, D., and Baker, V.R. (1998), A high magnitude storm and flood in a hyperarid catchment, Nahal Zin, Negev Desert, Israel, *Hydrological Processes*, 12 (1), 1-24.

Greenbaum, N., Schick, A.P. and Baker, V.R. (in press), The paleoflood record of a hyperarid catchment, Nahal Zin, Negev Desert, Isreal, *Earth Surface Processes and Landforms.*

Greenland Ice-core Project (GRIP) Members (1993), Climate instability during the last interglacial period recorded in the GRIP ice core, *Nature*, 364, pp. 203-207.

Gregory, K.J. (1976), Lichens and the determination of river channel capacity, *Earth Surface Processes*, 1, pp. 273-285.

Grenon, M. and Batisse, M. (1989), ***Futures for the Mediterranean Basin: The Blue Plan,*** Oxford University Press.

Grimm, E.C., Jacobson, G.L. Jnr., Watts, W.A., Hansen, B.C.S. and Maasch, K.A. (1993), A 50,000-Year record of climate oscillations from Florida and its temporal correlation with the Heinrich events, *Science*, 261, pp. 198-200.

Grimm, M.M., Wohl, E.E. and Jarrett, R.D. (1995), Coarse-sediment distribution as evidence of an elevation limit for flash flooding, Bear Creek, Colorado, *Geomorphology*, 14, pp. 199-210.

Grimshaw, D.L. and Lewin, J. (1980), Source identification for suspended sediments, *Journal of Hydrology*, 47, pp. 151-161.

Grossman, S. and Gerson, R. (1987), Fluviatile deposits and morphology of alluvial surfaces as indicators of Quaternary environmental changes in the southern Negev, Isreal, in: Frostick, L. and Reid, I. (eds.) *Desert Sediments: Ancient and Modern,* Geological Society Special Publication No. 35, pp. 17-29.

Grove, A.T. (1988), *The Little Ice Age,* London, Methuen.

Grove, A.T. (1997), Classics in physical geography revisited, *Progress in Physical Geography*, 21, pp. 251-256.

Gupta, A. (1975), Stream Characteristics in eastern Jamaica, an environment of seasonal flow and large floods, *American Journal of Science*, 275, pp. 825-847.

Gupta, A. (1983), High-magnitude floods and stream channel response, *Special Publication of the International Association of Sedimentologists*, 6, pp. 219-227.

Gupta, A. and Fox, H. (1975), Effects of high-magnitude floods on channel form: a case study in Maryland Piedmont, *Water Resources Research*, 10, pp. 499-509.

Gupta, A., Kale, V.S. and Rajaguru, S.N. (1999), The Narmada River, India, through space and time, in: Miler, A.J. and Gupta, A. (eds.) *Varieties of Fluvial Form,* John Wiley & Sons, pp. 113-143.

HMGS (1985), ***1:50 000 Tpographic Map of Greece: Metsovon Sheet.***

Hallet, B., Hunter, L. and Bogen, J. (1996), Rates of erosion and sediment evacuation by glaciers: A review of field data and implications, *Global and Planetary Change*, 12, pp. 213-235.

Hamlin, R.H.B., Woodward, J.C., Black, S. and Macklin, M.G. (in press), Sediment fingerprinting as a tool for interpreting long-term river activity: the Voidomatis basin, NW Greece, in: Foster, I.D.L. (ed.) *Tracers in Geomorphology,* John Wiley & Sons: London.

Hammond, N.G.L. (1967), *Epirus,* Oxford Clarendon Press, 847 pp.

Hardy, R. and Tucker, M. (1988), X-ray powder diffraction of sediments, in: Tucker, M. (ed.) *Techniques in Sedimentology,* Blackwell Scientific Publications: Oxford, pp. 191-228.

Harrison, S.P. and Diggerfeldt, G. (1993), European lakes as palaeohydrological and palaeoclimatic indicators, *Quaternary Science Reviews*, 12, pp. 233-248.

Harvey, A.M. (1984a), Geomorphological response to an extreme flood: a case from southeast Spain, *Earth Surface Processes and Landforms*, 9, pp. 267-279.

Harvey, A.M. (1984b), Aggradation and dissection sequences on Spanish alluvial fans: influence on morphological development, *Catena,* 11, pp. 289-304.

Harvey, A.M. (1996), The role of alluvial fans in the mountain fluvial systems of southeast Spain: implications of climatic change, *Earth Surface Processes and Landforms,* 21, pp. 543-553.

Harvey, A.M., Alexander, R.W., and James, P.A. (1984), Lichens, soil development and the age of Holocene valley floor landforms: Howgill Fells, Cumbria, *Geografiska Annaler,* 66A, pp. 353-366.

Harvey, A.M. and Wells, S.G. (1987), Response of Quaternary fluvial systems to differential epeirogenic uplift: Aguas and Feos river systems, southeast Spain, *Geology,* 15, pp. 689-693.

Hattingh J. and Zawada, P.K. (1996), Relief peels in the study of palaeoflood slack-water deposits, *Geomorphology,* 16, pp. 121-126.

Haughton, P.D.W., Todd, S.P. and Morton, A.C. (1991), Sedimentary provenance studies, in Morton, A.C., Todd, S.P. and Haughton, P.D.W. (eds.) *Developments in Sedimentary Provenance Studies,* Geological Society Special Publication No. 57, The Geological Society: London, pp. 1-13.

Haydon, B.P. (1988), Flood climates, in:Baker, V.R., Kochel, R.C. and Patton P.C. (eds.) *Flood Geomorphology,* John Wiley: New York, pp. 13-26.

He, Q. and Walling, D.E. (1996), Use of fallout Pb-210 measurements to investigate longer-term rates and patterns of overbank sediment deposition on the floodplains of lowland rivers, *Earth Surface Processes and Landforms,* 21, pp. 141-154.

Hedges, R.E.M. (1991), AMS dating: Present status and potential applications, In: Lowe, J.J. (ed.) *Radiocarbon Dating: Recent Applications and Future Potential,* Quaternary Proceedings No. 1, Quaternary Research Association, Cambridge, pp. 5-10.

Helley, E.J. (1969), Field measurement of the initiation of large bed particle motion in Blue Creek near Klamath, California, *U.S. Geological Survey Professional Paper,* 562-G, 19 pp.

Helley, E.J. and LaMarche, V.C. Jnr (1973), Historic flood information for northern California streams from geological and botanical evidence, *U.S. Geological Survey Professional Paper,* 485-E, pp. 1-16.

Higgs, E.S. (1963), Epirus: Palaeolithic survey, *Archaiologikon Deltion, Chronika,* 18, pp. 157-158.

Higgs, E.S. (1966), Excavations at the Rockshelter of Asprochaliko, *Archaiologikon Deltion, Chronika,* 21, pp. 292-294

Higgs, E.S. and Vita-Finzi, C. (1966), The climate, environment and industries of Stone Age Greece, part II, *Proceedings of the Prehistoric Society,* 32, pp. 1-29.

Higgs, E.S., Vita-Finzi, C., Harris, D.R. and Fagg, A.E. (1967), The climate, environment and industries of Stone Age Greece, part III, *Proceedings of the Prehistoric Society,* 33, pp. 1-29.

Hillaire-Marcel, C. and Causse, C. (1989), The late Pleistocene Laurentide glacier: Th/U dating of its major fluctuations and $\delta^{18}O$ range of the ice, *Quaternary Research,* 32, pp. 125-138.

Hirshboeck, K.K. (1987), Catastrophic flooding and atmospheric circulation anomalies, in: Mayer, L. and Nash, D. (eds.) (1987), *Catastrophic Flooding,* Allen & Unwin: Boston, pp 23-56.

Hirshboeck, K.K. (1988), Flood Hydroclimatology, in: Baker, V.R., Kochel, R.C. and Patton P.C. (eds.) *Flood Geomorphology,* John Wiley: New York, pp. 27-49.

Hirshboeck, K.K. (1991), Hydrology of floods and droughts: Climate and floods, *U.S. Geological Survey Water-Supply Paper 2375,* National Water Summary 1988-89 - Floods and Droughts: HYDROLOGY, pp. 67-88.

Hoang, C.T. and Taviani, M. (1991), Stratigraphic and tectonic implications of uranium-series-dated coral reefs from uplifted Red Sea islands, *Quaternary Research,* 35, pp. 264-273.

Holmgren, K., Lauritzen, S.-E. and Possnert, G. (1994), $^{230}Th/^{234}U$ and ^{14}C dating of a Late Pleistocene stalagmite in Lobatse II Cave, Botswana, *Quaternary Science Reviews,* 13, pp. 111-119.

Hooke, J.M., Harvey, A.M., Miller, S.Y. and Redmond, C.E. (1990), The chronology and stratigraphy of the alluvial terraces of the River Dane valley, Cheshire, N.W. England, *Earth Surface Processes and Landforms,* 15, pp. 717-737.

Houghton, J. (1997), *Global Warming: The Complete Briefing,* Second Edition, Cambridge University Press, 251 pp.

Hua S.-Q. (1987), A general survey of flood-frequency analysis in China, *Journal of Hydrology,* 96, pp. 15-25.

Hunt, C.O. and Gilbertson, D.D. (1995), Human activity, landscape change and valley alluviation in the Feccia Valley, Tuscany, Italy, in: Lewin, J., Macklin, M.G. and Woodward, J.C. (eds.) *Mediterranean Quaternary River Environments,* Balkema/ Rotterdam/ Brookfield, pp. 167-176.

Huntley, D.J., Godfrey-Smith, D.I. and Thewalt, M.L.W. (1985), Optical dating of sediments, *Nature,* 313, pp. 105-107.

Hutchinson, S.M. (1995), Use of magnetic and radiometric measurements to investigate erosion and sedimentation in a British upland catchment, *Earth Surface Processes and Landforms,* 20, pp. 293-314

Hütt, G. and Jungner, H. (1992), Optical and TL dating on glaciofluvial sediments, *Quaternary Science Reviews,* 11, pp. 161-163.

Hupp, C.R. (1987), Botanical evidence of floods and palaeoflood history, in Singh, V.P. *Regional Flood Frequency Analysis,* D. Reidel, Norwell, Mass., pp. 371-390.

Hupp, C.R. (1988), Plant ecological aspects of flood geomorphology and paleoflood history, in: Baker, V.R., Kochel, R.C. and Patton P.C. (eds.) *Flood Geomorphology,* John Wiley: New York, pp. 335-356.

Hydrologic Engineering Centre (1982), *HEC-2 water surface profiles: program user's manual,* Davis, Calif.: US Army Corps of Engineers.

IGME (1970), *1:50 000 Geological Map of Greece: Doliana Sheet.*

IGME (1970), *1:50 000 Geological Map of Greece: Tsepelovon Sheet.*

IGME (1987), *1:50 000 Geological Map of Greece: Konitsa Sheet.*

Inbar, M. (1987), Effects of a high magnitude flood in a Mediterranean climate: A case study in the Jordan River Basin, in: Mayer, L. and Nash, D. (eds.) (1987), *Catastrophic Flooding,* Allen & Unwin: Boston, pp. 333-353.

Inbar, M. (1992), Rates of fluvial erosion in basins with a Mediterranean type climate, *Catena,* 19, pp. 393-409.

Innes, J.L. (1985a), An examination of factors affecting the largest lichen on a substrate, *Arctic and Alpine Research,* 16 (2), pp. 233-244.

Innes, J.L. (1985b), Lichenometry, *Progress in Physical Geography,* 9, pp. 187-254.

Innes, J.L. (1985c), Moisture availability and lichen growth: the effects of snow cover and streams on lichenometric measurements, *Arctic and Alpine Research,* 17 (4), pp. 417-424.

Innes, J.L. (1986), Dating exposed rock surfaces in the arctic by lichenometry: the problem of thallus circularity and its effect on measurement errors, *Arctic,* 39 (3), pp. 253-259.

Ivanovich, M. and Harmon, R.S. (eds.) (1992), *Uranium-Series Disequilibrium: Applications to Earth, Marine and Environmental Sciences,* 2nd Edition, Clarendon Press: Oxford.

Ivanovich, M., Latham, A.G. and Ku, T.-L. (1992), Uranium-series disequilibrium applications in geochronology, in: Ivanovich, M. and Harmon, R.S. (eds.) *Uranium-Series Disequilibrium: Applications to Earth, Marine and Environmental Sciences,* 2nd Edition, Clarendon Press: Oxford, pp. 62-94.

Jackson, R.G. (1978), Preliminary evaluation of lithofacies models for meandering alluvial streams, in: Miall, A.D. (ed.) *Fluvial Sedimentology,* Can. Soc. Petrol. Geol. Mem., 5, pp. 543-577.

Jaeger, J.M., Nittrouer, C.A., Scott, N.D. and Millilman, J.D. (1998), Sediment accumulation along a glacially impacted mountainous coastline: north-east Gulf of Alaska, *Basin Research,* 10, pp. 155-173.

Jarrett, R.D. (1984), Hydraulics of high gradient streams, *Journal of Hydraulic Engineering,* 110, pp. 1519-1539.

Jarrett, R.D. (1987), Errors in slope-area computations of peak discharges in mountain streams, *Journal of Hydrology,* 96, pp. 53-67.

Jarrett, R.D. (1990a), Hydrologic and hydraulic research in mountain rivers, *Water Resources Bulletin,* 26 (3), pp. 419-429.

Jarrett, R.D. (1990b), Paleohydrologic techniques used to define the spatial occurrence of floods, *Geomorphology,* 3, pp. 181-195.

Jarrett, R.D. (1991), Paleohydrology and its value in analyzing floods and droughts, *U.S. Geological Survey Water-Supply Paper 2375 (1991),* National Water Summary 1988-89-Floods and Droughts: Hydrology, pp. 105-116.

Jarrett, R.D. and Costa, J.E. (1988), Evaluation of the flood hydrology in the Colorado Front Range using precipitation, streamflow, and paleoflood data for the Big Thompson River basin, *U.S. Geological Survey Water-Resources Investigations Report 87-4117,* Denver, Colorado, pp. 1-37.

Jetfić, L., Kečkeš,S. and Pernetta, J.C. (1996), Implications of future climatic changes for the Mediterranean coastal region, in: Jetfić, L., Kečkeš,S. and Pernetta, J.C. (eds.) *Climatic Change in the Mediterranean Volume 2,* Arnold: London, pp. 1-26.

Jochimsen, M. (1973), Does the size of the largest thalli really constitute a valid measure for dating glacial deposits?, *Arctic and Alpine Research,* 5 (4), pp. 417-424.

Jones, G. and Robertson, A.H.F. (1991), Tectono-stratigraphy and evolution of the Mesozoic Pindos ophiolite and related units, northwest Greece, *Journal of the Geological Society, London,* 148, pp. 267-288.

Kale, V.S., Ely, L.L., Enzel, Y. and Baker, V.R. (1994), Geomorphic and hydrologic aspects of monsoon floods on the Narmada and Tapi Rivers in central India, *Geomorphology,* pp. 157-168.

Karkanas, P. (unpublished), *Description of the alluvial sequence at Boila.*

Karlen, I., Olsson, I.U., Kalkberg, P. and Kilicci, S. (1966), Absolute determination of the radioactivity of two ^{14}C dating standards, *Arkiv Geofysik,* 6, pp. 465-471.

King, G. and Bailey, G. (1985), The palaeoenvironment of some archaeological sites in Greece: the influence of Accumulated Uplift in a seismically active region, *Proceedings of the Prehistoric Society,* 51, pp. 273-282.

King, G.C.P., Tselentis, A., Gomberg, J., Molnar, P., Roecker, S.W., Sinvhal, H., Soufleris, C. and Stock, L.M. (1983), Microearthquake seismicity and active tectonic of northwestern Greece, *Earth and Planetary Science Letters,* 66, pp. 279-288.

King, G., Sturdy, D. and Bailey, G. (1997), The tectonic background to the Epirus landscape, in: Bailey, G.N. (ed.), *Klithi: Palaeolithic Settlement and Quaternary Landscape in northwest Greece. Volume 2: Klithi in its local and regional setting,* McDonald Institute, pp. 541-558.

Knighton, D. (1998), *Fluvial Forms and Processes: A New Perspective,* Arnold: London, 383 pp.

Knox, J.C. (1979), Geomorphic evidence of frequent and extreme floods, in: Henry, W.P. (ed.) *Improved Hydrological Forecasting - Why and How,* Proc. Eng. Found. Conf., Am. Soc. Civ. Eng., New York, pp. 220-238.

Knox, J.C. (1984), Fluvial responses to small scale climate changes, in: Costa, J.E. and Fleisher, P.J. (eds.) *Developments and Applications of Geomorphology,* Springer-Verlag: Berlin, pp. 318-342.

Knox, J.C. (1985), Responses of floods to Holocene climatic change in the Upper Mississippi Valley, *Quaternary Research,* 23, pp. 287-300.

Knox, J.C. (1987), Stratigraphic evidence of large floods in the Upper Mississippi Valley, in: Mayer, L. and Nash, D. (eds.), *Catastrophic Flooding,* Allen & Unwin: Boston, pp. 155-180.

Knox, J.C. (1988), Climatic influence on upper Mississippi valley floods, in: Baker, V.R., Kochel, R.C. and Patton P.C. (eds.) *Flood Geomorphology,* John Wiley: New York, pp. 279-300.

Knox, J.C. (1993), Large increases in flood magnitude in response to modest changes in climate, *Nature,* 361, pp. 430-432.

Knox, J.C. (1995), Fluvial systems since 20,000 years BP, in: Gregory, K.J., Starkel, L. and Baker, V.R. (eds.), *Global Continental Palaeohydrology,* Wiley: Chichester, pp. 87-108.

Kochel, R.C. (1988a), Extending stream records with slackwater paleoflood hydrology: examples from west Texas, in: Baker, V.R., Kochel, R.C. and Patton P.C. (eds.) *Flood Geomorphology,* John Wiley: New York, pp. 377-391.

Kochel, R.C. (1988b), Geomorphic impact of large floods: review and new perspectives on magnitude and frequency, in: Baker, V.R., Kochel, R.C. and Patton P.C. (eds.) *Flood Geomorphology,* John Wiley: New York, pp. 169-187.

Kochel, R.C. and Baker, V.R. (1982), Paleoflood hydrology, *Science,* 215, pp. 353-361.

Kochel, R.C. and Ritter, D.F. (1987), Implications of flume experiments for the interpretation of slackwater paleoflood sediments, in Singh, V.P. *Regional Flood Frequency Analysis,* D. Reidel, Norwell, Mass., pp. 371-390.

Kochel, R.C. and Baker, V.R. (1988), Paleoflood analysis using slackwater deposits, in: Baker, V.R., Kochel, R.C. and Patton P.C. (eds.) *Flood Geomorphology,* John Wiley: New York, pp. 357-376.

Komar, P.D. (1988), Sediment transport by floods, in: Baker, V.R., Kochel, R.C. and Patton P.C. (eds.) *Flood Geomorphology,* John Wiley: New York, pp. 97-111.

Komar, P.D. (1989), Flow-competence evaluations of the hydraulic parameters of floods: an assessment of the technique, in: Beven, K. and Carling, P. (eds.) *Floods:Hydrological, Sedimentological and Geomorphological Implications,* John Wiley & Sons Ltd., pp. 107-134.

Kominz, M.A., Heath, G.R., Ku, T.-L. and Pisias, N.G. (1979), Brunhes time scales and the interpretation of climatic change, *Earth and Planetary Science Letters,* 45, pp. 394-410.

Kosmas, C. *et al.* (1997), The effects of land use on runoff and soil erosion rates under Mediterranean conditions, *Catena,* 29, pp. 45-59.

Kotjaboupoulou, E., Panagopoulou, E. and Adam, E. (1997), The Boila Rockshelter: a Preliminary Report, in: Bailey, G.N. (ed.) *Klithi: Palaeolithic settlement and Quaternary Landscapes in northwest Greece. Volume 2: Klithi in its local and regional setting.* McDonald Institute, Cambridge, pp. 427-438.

Kozuchowski, K. and Marciniak, K. (1988), Variability of mean monthly temperatures and semi-annual precipitation totals in Europe in relation to hemispheric circulation patterns, *Journal of Climatology,* 8, pp. 191-199.

Ku, T., Bull, W.B., Freeman, S.T. and Knauss, K.G. (1979), Th^{230}-U^{234} dating of pedogenic carbonates in gravelly desert soils of Vidal Valley, southeastern California, *Geol. Soc. of Am. Bull.,* 90 pt I, pp. 1063-1073.

Kurashige, Y. and Fusejima, Y. (1997), Source identification of suspended sediment from grain size distributions: I. Application of nonparamteric statistical tests, *Catena,* 31, pp. 39-52.

Kutiel, H., Maheras, P. and Guika, S (1996), Circulation and extreme rainfall conditions in the eastern Meditteranean during the last Century, *International Journal of Climatology,* 16, pp. 73-92.

Kuzbach, J.E. and Geutter, P.J. (1986), The influence of changing orbital parameters and surface boundary conditions on climate simulations for the past 18,000 years, *Journal of Atmospheric Sciencs,* 43, pp. 1729-1759.

Kuzucuoglu, C. (1995), River response to Quaternary tectonics with examples from northwestern Anatolia, Turkey, in: Lewin, J., Macklin, M.G. and Woodward, J.C. (eds.), *Mediterranean Quaternary River Environments,* Balkema/ Rotterdam/ Brookfield, pp. 45-53.

Kuzucuoglu, C., Pastre, J-F., Black, S., Ercan, T., Fontugne, M., Guillou, H., Hatté, C., Karabiyikoglu, M., Orth, P. and Türkecan, A. (1998), Identification and dating of tephras from Quaternary sedimentary sequences of inner Anatolia, *Journal of Volcanology and Geothermal Research,* 85, pp. 153-172.

Lamb, H.H. (1982), *Climate, History and the Modern World,* Methuen, London, 387 pp.

Lane, W.L. (1987), Palaeohydrologic data and flood frequency estimation, in: Singh, V.P. (ed.) *Regional Flood Frequency Analysis,* D. Reidel, Norwell, Mass., pp. 287-298.

Lees, J. (1997), Mineral magnetic properties of mixtures of environmental and synthetic materials: linear additivity and interaction effects, *Geophysics Journal International,* 131, pp. 335-346.

Leopold, L.B., Wolman, M.G. and Miller, J.P. (1964), *Fluvial Processes in Geomorphology,* Freeman, San Francisco, 522 pp.

Lewin, J. (1989), Floods in fluvial geomorphology, in: Beven, K. and Carling, P. (eds.) *Floods:Hydrological, Sedimentological and Geomorphological Implications,* John Wiley & Sons Ltd., pp. 265-284.

Lewin, J., Macklin, M.G. and Woodward, J.C. (1991), Late Quaternary fluvial sedimentation in the Voidomatis basin, Epirus, Northwest Greece, *Quaternary Research,* 35, pp. 103-115.

Lewin, J., Macklin, M.G. and Woodward, J.C. (eds.) (1995a), *Mediterranean Quaternary River Environments,* Balkema/Rotterdam/Brookfield.

Lewin, J., Macklin, M.G. and Woodward, J.C. (1995b), Mediterranean Quaternary River Environments - some future research needs, in: Lewin, J., Macklin, M.G. and Woodward, J.C. (eds.), *Mediterranean Quaternary River Environments,* Balkema/Rotterdam/Brookfield, pp. 99-102.

Lewis, D.W. and McConchie, D.M (1994), *Analytical Sedimentology,* Chapman & Hall: New York, London., 197 pp.

Libby, W.F. (1955), *Radiocarbon Dating,* 2nd Edition, University of Chicago Press, Chicago.

Lindholm, R. (1987), *A Practical Approach to Sedimentology,* Allen & Unwin.

Locke, W.W. III, Andrews, J.T. and Webber, P.J. (1979), *A manual for lichenometry,* British Geomorphological Research Group Technical Bulletin 26, 47 pp.

López-Avilés, A. (1998), *Flood Regime and Quaternary Sedimentation Style in the Guadalope Basin, northeast Spain,* unpublished PhD Thesis, University of Leeds.

Lowe, J.J. and Walker, M.J.C. (1997), *Reconstructing Quaternary Environments,* 2nd Edition, 433 pp.

Luo, C.-Z. (1987), Investigation and regionalization of historical floods in China, *Journal of Hydrology,* 96, pp. 41-51.

Luo, S. and Ku, T-L. (1991), U-series isochron dating: A generalized method employing total-sample dissolution, *Geochimica et Cosmochimica Acta,* 55, pp. 555-564.

Maas, G.S. (1998), *River Response to Quaternary Environmental Change, Southwestern Crete, Greece.* Unpublished PhD Thesis, University of Leeds.

Maas, G.S., Macklin, M.G. and Kirkby, M.J. (1998), Late Pleistocene and Holocene river development in Mediterranean steepland environments, S.W. Crete, Greece, in: Benito, G., Baker, V.R. and Gregory, K.J. (eds.), *Palaeohydrology and Environmental Change,* John Wiley & Sons, Chichester, pp. 153-165.

Macklin, M.G., Rumsby, B.T. and Heap, T (1992a), Flood alluviation and entrenchment: Holocene valley-floor development and transformation in the British uplands, *Geol. Soc. of Am. Bull.*, 104, pp. 631-643.

Macklin, M.G., Rumsby, B.T. and Newson, M.D. (1992b), Historical floods and vertical accretion of fine-grained alluvium in the Lower Tyne valley, Northeast England, in: Billi, P., Hey, R.D., Thorne, C.R. and Tacconi, P. (eds.) *Dynamics of Gravel Bed Rivers*, John Wiley & Sons Ltd., pp. 574-589.

Macklin, M.G., Passmore, D.G., Stevenson, A.C., Davis, B.A. and Benavente, J.A. (1994), Responses of rivers and lakes to Holocene environmental change in the Alcañiz Region, Terual, North-East Spain, in: Millington, A.C. and Pye, K. (eds.) *Environmental Change in Drylands: biogeographical and Geomorphological Perspectives*, John Wiley & Sons, pp.113-130.

Macklin, M.G., Lewin, J. and Woodward, J.C. (1995), Quaternary fluvial systems in the Mediterranean basin, in: Lewin, J., Macklin, M.G. and Woodward, J.C. (eds.) (1995), *Mediterranean Quaternary River Environments*, Balkema/ Rotterdam/ Brookfield, pp. 1-25

Macklin, M.G. and Lewin, J. (1997), Channel, floodplain and drainage basin response to environmental change, in: Thorne, C.R., Hey, R.D. and Newson, M.D. (eds.), *Applied Fluvial Geomorphology for River Engineering and Management*, John Wiley & Sons, Chichester, pp. 15-44.

Macklin, M.G., Lewin, J. and Woodward, J.C. (1997), Quaternary river sedimentary sequences of the Voidomatis basin, in: Bailey, G.N. (ed.), *Klithi: Palaeolithic Settlement and Quaternary Landscape in northwest Greece. Volume 2: Klithi in its local and regional setting*, McDonald Institute, pp. 347-336.

Magilligan. F.J., Phillips, J.D., James, L.A. and Gomez, B. (1998), Geomorphic and sedimentological controls on the effectiveness of an extreme flood, *Journal of Geology*, 106, pp. 87-95.

Maheras, P. (1988), Changes in precipitation conditions in the western Mediterranean over the last Century, *Journal of Climatology*, 8, pp. 179-189.

Maheras, P. and Kolyva-Machera, F. (1990), Temporal and spatial characteristics of annual precipitation over the Balkans in the Twentieth Century, *International Journal of Climatology*, 10, pp. 495-504.

Maheras, P., Balafoutis, Ch. and Vafiadis, M. (1992), Precipitation in the central Mediterranean during the last Century, *Theor. Appl. Climatol.*, 45, pp. 209-216.

Maheras, P., Rossetti, R. and Guika, S. (1994), Dry and wet seasons, years and periods along the Adriatic and Ionian Sea during the last century, *'The Atmospheric Physics and Dynamics in the Analysis and Prognosis of Precipitation Fields'*, University of Rome, 15th – 18th November 1994.

Maizels, J.K. (1983), Palaeovelocity and palaeodischarge determination for coarse gravel deposits, in: Gregory, K.J. (e.d.) *Background to Palaeohydrology*, John Wiley & Sons Ltd., Chichester, pp. 101-139.

Maizels, J.K. (1987), Large-scale flood deposits associated with the formation of coarse-grained, braided terrace sequences, in: Ethridge, F.G., Flores, R.M. and Harvey, M.D. (eds.) *Recent Developments in Fluvial Sedimentology*, Society of Economic Paleontologists and Mineralogists, Special Publication No. 39, pp. 135-148.

Martínez-Goytre, J., House, P.K., Baker, V.R. (1994), Spatial variability of small-basin paleoflood magnitudes for a southeastern Arizona mountain range, *Water Resources Research*, 30 (5), pp. 1491-1501.

Mather, A.E., Silva, P.G., Goy, J.L., Harvey, A.M. and Zazo, C. (1995), Tectonics versus climate: an example from late Quaternary aggradational and dissectional sequences of the Mula basin, southeast Spain, in: Lewin, J., Macklin, M.G. and Woodward, J.C. (eds.) *Mediterranean Quaternary River Environments*, Balkema/ Rotterdam/ Brookfield, pp. 77-87.

Matthews, J.A. (1975), Experiments on the reproducibility and reliability of lichenometric dates, Storbreen gletschervorfeld, Jotenheim, Norway, *Norsk Geografisk Tidsskrift*, 29, pp.97-109.

Matthews, J.A. (1977), A lichenometric test of the 1750 end-moraine hypothesis, Storbreen gletschervorfeld, Jotenheim, Norway, *Norsk Geografisk Tidsskrift,* 31, pp. 129-136.

Mayer, L. and Nash, D. (1987), Preface, *Catastrophic Flooding,* Allen & Unwin: Boston, pp vii-viii.

McAlister, J.J. (1996), Analytical techniques for the examination of building stone, in: Smith, B.J. and Warke, P.A. (eds.) *Processes of Urban Stone Decay,* Donhead Publishing Ltd., pp. 171-193.

McManus, J. (1988), Grain size determination and interpretation, in: Tucker, M. (ed.) *Techniques in Sedimentology,* Blackwell Scientific Publications: Oxford, pp. 63-85.

McNeil, J.R. (1992), *The Mountains of the Mediterranean World: An Environmental History,* Cambridge University Press, 423 pp.

McQueen, K.C., Vitek, J.D. and Carter, B.J. (1993), Paleoflood analysis of an alluvial channel in the south-central great plains: Black Bear Creek, Oklahoma, *Geomorphology,* 8, pp.131-146.

Mears, A.I. (1979), Flooding and sediment transport in a small alpine drainage basin in Colorado, *Geology,* 7, pp. 53-57.

Mejdahl, V. (1987), Thermoluminescence dating of sediments, *Radiation Protection Dosimetry,* 17, pp. 219-227.

Meko, D., Hughes, M. and Stockton, C. (1991), Climate change and climatic variability: The paleo record, in: *Managing Water Resources in the West Under Conditions of Climate Uncertainty,* Proceedings of a colloquium, November 1990, Scattsdale, Arizona, National Academy Press, Washington. D.C., pp. 71-100.

Merrett, S.P. and Macklin, M.G. (1998), Historic floods and valley floor transformation, Upper Coverdale, Yorkshire Dales, in: Howard, A,J, and Macklin, M.G. (eds.), *The Quaternary of the Eastern Yorkshire Dales: Field Guide. The Holocene Alluvial Record.* Quaternary Research Association, London, pp. 5-10.

Merrett, S.P. and Macklin, M.G. (1999), Historic river response to extreme flooding in the Yorkshire Dales, nothern England, in: Brown, A.G. and Quine, T.A. (eds.) *Fluvial Processes and Environmental Change,* John Wiley & Sons: Chichester, pp. 345-360.

Messerli, B. (1967), Die Eiszeitliche und die gegenwartige Vergletscherung im Mettelmeermaum, *Geographica Helvetica,* 22, pp. 105-228.

Metaxas, D.A., Bartzokas, A. and Vtsas, A. (1991), Temperature fluctuations in the Mediterranean area during the last 120 years, *International Journal of Climatology,* 11, pp. 897-908.

Miller, A.J. and Cluer, B.L. (1998), Modeling considerations of flow in bedrock channels, in: Tinkler, K.J. and Wohl, E.E. (eds.) *Rivers Over Rock: Fluvial Processes in Bedrock Channels,* Geophysical Monograph 107, American Geophysical Union, pp. 61-104.

Miller, A.J. and Gupta, A. (eds.) (1999), *Varieties of Fluvial Form,* John Wiley & Sons, Chichester, 521 pp.

Miller, G.H. (1973), Late Quaternary glacial and climatic history of Northern Cumberland Peninsula, east Baffin Island, N.W.T., Canada, *Quaternary Research,* 3, pp. 561-583.

Milliman, J.D. and Syvitiski, J.P.M. (1992), Geomorphic/tectonic control of sediment discharge to the ocean: the importance of small mountain rivers, *Journal of Geology,* 100, pp. 525-544.

Mimikou, M. (1984a), Envelope curves for extreme flood events in north-western and western Greece, *Journal of Hydrology,* 67, pp. 55-66.

Mimikou, M. (1984b), Regional relationships between basin size and runoff characteristics, *Hydrological Sciences Journal,* 29, pp. 63-73.

Mimikou, M. (1987), Regional treatment of flood data, in: Singh, V.P. (ed.) *Regional Flood Frequency Ananlysis,* D. Reidel, Norwell, Mass., pp. 91-101.

Mimikou, M. and Gordios, J. (1989), Predicting the mean annual flood and flood quantities for ungauged catchments in Greece, *Hydrological Sciences Journal,* 34, pp.169-184.

Mimikou, M., Kouvopolous, Y., Cavadias, G. and Vayianos, N. (1991), Regional hydrological effects of climate change, *Journal of Hydrology,* 123, pp. 119-146.

Municipality of Ioannina Cultural Centre (M.I.C.C.) (1994), *Epirus,* Yerasimos Douvalis – Eleftherios Apostolou Press, Ioannina.

Molina Sempere, C.M., Vidal-Abarca, M. and Suárez, M.L. (1994), Floods in arid south-east Spanish areas: a historical and environmental review, in: Rossi, G., Harmancioglu, N. and Yevjevich, V. (eds.) *Coping with floods,* Dordrecht, Kluwer Academic, pp. 271-78.

Mook, W,G, (1986), Recommendations/resolutions adopted by the Twelfth International Radiocarbon Conference, *Radiocarbon,* 28 (2A), pp. 799.

Murray, A.S. (1996), Developments in optically stimulated luminescence and photo-transferred thermoluminescence dating of young sediments: Application to a 2000-year sequence of flood deposits, *Geochimica et Cosmochimica Acta,* 60 (4), PP. 565-576.

Nanson, G.C. (1986), Episodes of vertical accretion and catastrophic stripping: A model of disequilibrium flood-plain formation, *Geological Society of America Bulletin,* 97, pp. 1467-1475.

Nash, D.J. and Smith, R.F. (1998), Multiple calcrete profiles in the Tabernas Basin, southeast Spain: their origins and geomorphic implications, *Earth Surface Processes and Landforms,* 23, pp. 1009-1029.

Newson, M.D. (1992), Geomorphic thresholds in gravel-bed rivers – Refinement for an era of environmental change, in: Billi, P., Hey, R.D., Thorne, C.R. and Tacconi, P. (eds.) *Dynamics of Gravel-bed Rivers,* John Wiley & Sons Ltd, pp. 3-15.

Newson, M.D. (1997), *Land, Water and Development: Sustainable management of river basin systems,* Routledge: London and New York, 420 pp.

O'Connor, J.E. and Webb, R.H. (1988), Hydraulic modeling for paleoflood analysis, in: Baker, V.R., Kochel, R.C. and Patton P.C. (eds.) *Flood Geomorphology,* John Wiley: New York, pp. 393-402.

O'Connor, J.E., Ely, L.L., Wohl, E.E., Stevens, L.E., Melis, T.S., Kale, V.S. and Baker, V.R. (1994), A 4500-year record of large floods on the Colorado River in the Grand Canyon, Arizona, *The Journal of Geology,* 102, pp. 1-9.

Oldfield, F. (1983), The role of magnetics studies in palaeohydrology, in: Gregory, K.J. (ed.) *Background to Palaehydrology,* John Wiley and Sons Ltd., pp. 141-165.

Oldfield, F. (1991), Environmental magnetism – a personal perspective, *Quaternary Science Reviews,* 10, pp. 73-85.

Oldfield, F. and Appleby, P.G. (1984a), A combined radiometric and mineral magnetic approach to recent geochronology in lakes affected by catchment disturbance and sediment redistribution, *Chemical Geology,* 44, pp. 67-83.

Oldfield, F. and Appleby, P.G. (1984b), Empirical testing of ^{210}Pb-dating models for lake sediments, in: Haworth, E.Y. and Lund, J.W.G. (eds.) *Lake Sediments and Environmental History,* Leicester University Press, pp. 93-123.

Oldfield, F., Maher, B.A., Donoghue, J. and Pierce, J. (1985), Particle-size related, mineral magnetic source sediment linkages in the Rhode River catchment, Maryland, USA, *Journal of the Geological Society,* 142, pp. 1035-1046.

Oldfield, F. and Thompson, R. (eds.) (1986), Special Issue: Mineral Magnetic Studies, *Physics of the Earth and Planetary Interiors,* 42 (1-2).

Olley, J.M., Murray, A.S., Mackenzie, D.H. and Edwards, K. (1993), Identifying sediment sources in a gullied catchment using natural and anthropogenic radioactivity, *Water Resources Research,* 29 (4), pp. 1037-1043.

Palmentola, G., Acquafredda, P. and Fiore, S. (1990), A New Correlation of the glacial moraines in the Southern Apennines, Italy, *Geomorphology,* pp. 1-8.

Palutikof, J.P. and Wigley, T.M.L. (1996), Developing climate change scenarios for the Mediterranean region, in: in: Jetfić, L., Kečkeš,S. and Pernetta, J.C. (eds.) *Climatic Change in the Mediterranean Volume 2,* Arnold: London, pp. 27-56.

Partridge, J. and Baker, V.R. (1987), Palaeoflood hydrology of the Salt River, Arizona, *Earth Surface Processes and Landforms,* 12, pp. 109-125.

Passmore, D.G. and Macklin, M.G. (1994), Provenance of fine-grained alluvium and late-Holocene land-use change in the Tyne basin, northern England, *Geomorphology,* 9, 127-142.

Paterne, M., Guichard, F., Labeyrie, J., Gillot, P.Y. and Duplessy, J.C. (1986), Tyrrhenian tephrochronology of the oxygen isotope record for the past 60,000 years, *Marine Geology,* 72, pp. 259-285.

Patton, P.C. (1988), Drainage basin morphometry and floods, in: Baker, V.R., Kochel, R.C. and Patton P.C. (eds.) *Flood Geomorphology,* John Wiley: New York, pp. 51-64.

Patton, P.C. and Baker, V.R. (1977), Geomorphic response of central Texas streams to catastrophic rainfall and runoff, in: Doehring, D.O. (ed.) *Geomorphology in Arid Regions,* Proceedings of the 8th Annual Geomorphology Symposium at Binghampton, September 1977, pp. 189-217.

Patton, P.C., Baker, V.R. and Kochel, R.C. (1979), Slackwater deposits: a geomorphic technique for the interpretation of fluvial paleohydrology, in: Rhodes, D.D. and Williams, G. (eds.) *Adjustments of the Fluvial System,* Kendall-Hunt Publishing Co., Iowa, pp. 225-252.

Patton, P.C. and Dibble, D.S. (1982), Archeologic and geomorphic evidence for the paleohydrologic record of the Pecos River in West Texas, *American Journal of Science,* 282, pp. 97-121.

Patton, P.C. and Boison, P.J. (1986), Processes and rates of Holocene terrace formation in Harris Wash, Escalante River Basin, southcentral Utah, *Geological Society of America Bulletin,* 97, pp. 369-378.

Pavese, M.P., Banzon, V., Colacino, M. Gregori, G.P. and Pasqua, M. (1992), Three historical data series on floods and anomalous climatic events in Italy, in: Bradley, R.S. and Jones, P.D. (eds.) *Climate Since A.D. 1950,* Routledge: London and New York, pp. 155-170.

Peart, M.R. and Walling, D.E. (1986), Fingerprinting sediment source: the example of a drainage basin in Devon, UK, in: Hadley, R.F. (Ed.), *Drainage Basin Sediment Delivery,* IAHS Publication No. 174, IAHS Press, Wallingford, pp. 41-55.

Penning-Rowsell, E.C., Parker, D.J. and Harding, D.M. (1986), *Floods and Drainage: British policies for hazard reduction, agricultural improvement and wetland conservation,* Allen & Unwin: London, 199 pp.

Perkins, N.K. and Rhodes, E.J. (1994), Optical dating of fluvial sediments from Tattershall, UK, *Quaternary Geochronology (Quaternary Science Reviews),* 13, pp. 517-520.

Perry, A. (1981), Mediterranean climate - a synoptic reappraisal, *Progress in Physical Geography,* 5, pp. 107-113.

Petts, G.E. (1979), Complex response of river channel morphology subsequent to reservoir construction, *Progress in Physical Geography,* 3, pp. 329-362.

Phillips, J.D. (1991), Multiple modes of adjustment in unstable river channel cross sections, *Journal of Hydrology,* 123, pp. 39-49.

Phillips, J.D. (1992), The end of equilibrium? in: Phillips, J.D. and Renwick, W.H. (eds.), Geomorphic Systems, *Geomorphology,* 5, pp. 195-201.

Pilcher, J.R. (1991a), Radiocarbon dating, in: Smart, P.L. and Frances, P.D. (eds.) *Quaternary Dating Methods - A Users Guide,* QRA Technical Guide No. 4: Cambridge, pp. 16-36.

Pilcher, J.R. (1991b), Radiocarbon dating for the Quaternary scientist, In: Lowe, J.J. (ed.) *Radiocarbon Dating: Recent Applications and Future Potential,* Quaternary Proceedings No. 1, Quaternary Research Association, Cambridge, pp. 27-33.

Poesen, J.W.A. and Hooke, J.M. (1997), Erosion, flooding and channel management in Mediterranean environments of southern Europe, *Progress in Physical Geography,* 21 (2), pp. 157-199.

Pope, K.O. and Van Andel, T.H. (1984), Late Quaternary alluviation and soil formation in the southern Argolid: its history, causes and archaeological implications, *Journal of Archaeological Science,* 11, pp. 281-306.

Popp, C.J., Hawley, J.W., Love, D.W. and Dehn, M. (1988), Use of radiometric (Cs-137, Pb-210), Geomorphic, and stratigraphic techniques to date recent oxbow sediments in the Rio Puerco drainage grants uranium region, New Mexico, *Environmental Geology and Water Science,* 11 (3), pp. 253-269.

Prentice, I.C., Guiot, J. and Harrison, S.P. (1992), Mediterranean vegetation, lake levels and palaeoclimate at the Last Glacial Maximum, *Nature,* 360, pp. 658-660.

Prescott, J.R. and Hutton, J.T. (1994), Cosmic ray contributions to dose rates for luminescence and ESR dating: large depths and long-term time variations, *Radiation Measurements,* 2/3, pp. 497-500.

Quick, M.C. (1991), Reliability of flood discharge estimates, *Canadian Journal of Civil Engineering,* 18, pp. 624-630.

R.E.S.A. (Road Editions S.A.) (1995), *Epiros/Thessaly,* 1:250000 sheet, Athens, Greece.

Ramsey, M.H. (1998), Sampling as a source of measurement uncertainty: techniques for quantification and comparison with analytical sources. *Journal of Analytical Atomic Spectrometry,* 13, pp. 97-104.

Ramsey, M.H., Thompson, M. and Hale, M. (1992), Objective evaluation of precision requirements for geochemical analysis using robust analysis of variance. *Journal of Geochemical Exploration,* 44, pp. 23-36.

Reddaway, J.M. and Bigg, J.R. (1996), Climatic change over the Mediterranean and links to the more general Atmospheric circulation, *International Journal of Climatology,* 16, pp.651-661.

Reid, I. and Frostick, L.E. (1987a), Toward a better understanding of bedload transport, in: Ethridge, F.G., Flores, R.M. and Harvey, M.D. (eds.) *Recent Developments in Fluvial Sedimentology,* Society of Economic Paleontologists and Mineralogists, Special Publication No. 39, pp. 13-19.

Reid, I. And Frostick, L.E. (1987b), Flow dynamics and suspended sediment properties in arid zone flash floods, *Hydrological Processes,* 1, pp. 239-253.

Richter, D., Mariolakos, I. and Risch, H. (1978), The main flysch stages of the Hellenides, in: Closs, H. (ed.) *Alps, Appennines and Hellenides,* Vertagsbuch, Stuttgart: Schweizerbart, pp. 434-438.

Ritchie, J.C., McHenry, J.R. and Gill, A.C. (1973), Dating recent reservoir sediments, *Limnology and Oceanography,* 18, pp. 254-263.

Ritchie, J.C., Hawks, P.H. and McHenry, J.R. (1975), Deposition rates in valleys determined using fallout Ceasium-137, *Geological Society of America Bulletin,* 86, pp. 1128-1130.

Ritchie, J.C. and McHenry, J.R. (1990), Application of radioactive fallout Ceasium-137 for measuring soil erosion and sediment accumulation rates and patterns: a review, *Journal of Environmental Quality,* 19, pp. 215-233.

Ritter, D.F. (1975), Stratigraphic implications of coarse-grained gravel deposited as overbank sediment, southern Illinois, *Journal of Geology,* 83, pp. 645-650.

Robbins, J.A. (1978), Geochemical and geophysical applications of radioactive lead, in: Nriagu, J.O. (ed.) *The Biogeochemistry of Lead in the Environment,* Elsevier: Amsterdam, pp. 286-283.

Robbins, J.A. and Edgington, D.N. (1975), Determination of recent sedimentation rates in Lake Michigan using Pb-210 and Cs-137, *Geochimica et Cosmochimica Acta,* 39, pp. 285-304.

Roberts, N. (1983), Age, palaeoenvironments, and climatic significance of Late Pleistocene Konya Lake, Turkey, *Quaternary Research,* 19, pp. 154-171.

Roberts, N. (1995), Climatic forcing of alluvial fan regimes during the late Quaternary in the Konya basin, south central Turkey, *in:* Lewin, J., Macklin, M.G. and Woodward, J.C. (eds.), *Mediterranean Quaternary River Environments,* Balkema/ Rotterdam/ Brookfield, pp. 207-217.

Robinson, S.G. (1997), *Beginning Environmental Magnetism: An Introduction to the Theoryand Techniques of Applied Rock-Magnetism For Environmental Studies,* unpublished book, School of Geography, University of Manchester.

Rodier, J.A. and Roche, M. (1984), *World Catalogue of Maximum Observed Floods,* IAHS-AISH Publication no. 143, 355 pp.

Romero, R., Ramis, C. and Alonso, S. (1998), Mesoscale model simulations of three heavy precipitation events in the western Mediterranean region, *Monthly Weather Review,* 126 (7), pp. 1859-1881.

Rose, J. (1984), Contemporary river landforms and sediments in an area of equatorial rain forest, Gulong Mulu National Park, Sarawak, *Transactions of the Institute of British Geographers,* N.S. 9, pp. 345-363.

Rose, J., Turner, C., Coope, G.R. and Bryan, M.D. (1980), Channel changes in a lowland river over the last 13,000 years, *in:* Cullingford, R.A., Davidson, D.A. and Lewin, J. (eds.), *Timescales in geomorphology,* John Wiley & Sons, New York, pp. 159-175.

Rose, J. and Meng, X. (1999), River activity in small catchments over the last 140 ka, North-east Mallorca, Spain, in: Brown, A.G. and Quine, T.A. (eds.) *Fluvial Processes and Environmental Change,* John Wiley & Sons: Chichester, pp. 91-102.

Rose, J., Meng, X. and Watson, C. (1999), Palaeoclimate and palaeoenvironmental responses in the western Mediterranean over the last 140 ka: evidence from Mallorca, Spain, *Journal of the Geological Society, London,* 156, pp. 435-448.

Rowan, J.S., Higgit, D.L. and Walling, D.E. (1993), Incorporation of Chernobyl-derived radiocaesium into reservoir sedimentary sequences, in: McManus, J. and Duck, R.W. (eds.) *Geomorphology and Sedimentology of Lakes and Reservoirs,* John Wiley & Sons: Chichester, pp. 55-71.

Rowan, J.S., Black, S. and Schell, C. (1999), Floodplain evolution and sediment provenance reconstructed from channel fill sequences: The Upper Clyde basin, Scotland, in: Brown, A.G. and Quine, T.A. (eds.) *Fluvial Processes and Environmental Change,* John Wiley & Sons: Chichester, pp. 223-240.

Ruiz-Flaño, P., García-Ruiz, J.M. and Ortigosa, L. (1992), Geomorphological evolution of abandoned fields. A case study in the central Pyranees, *Catena,* 19, pp. 301-308.

Rumsby, B.T. and Macklin, M.G. (1994), Channel and floodplain response to recent abrupt climate change: the Tyne basin, northern England, *Earth Surface Processes and Landforms,* 19, pp. 499-515.

Rumsby, B.T. and Macklin, M.G. (1996), River response to the last neoglacial (the 'Little Ice Age') in northern, western and central Europe, in: Branson, J., Brown, A.G. and Gregory, K.J. (eds.) *Global Continental Changes: the Context of Paleohydrology,* Geological Society Special Publication No. 115, pp. 217-233.

Sala, M. (1983), Fluvial and slope processes in the Fuirosos basin, Catalan Ranges, north east Iberian coast, *Zeit. F. Geomorph. N.F.,* 27 (4), pp. 393-411.

Sala, M. (1988), Slope runoff and sediment production in two Mediterranean mountain environments, *Catena Supplement 12,* pp. 13-29.

Sala, M. and Inbar, M. (1992), Some hydrologic effects of urbanization in Catalan Rivers, *Catena,* 19, pp. 363-378.

Saynor, M.J. and Erskine, W.D. (1993), Characteristics and implications of High-level slackwater deposits in the Fairlight Gorge, Nepean River, Australia, *Australian Journal of Marine and Freshwater Research*, 44, pp. 735-747.

Schell, C., Black, S. and Hudson-Edwards, K. (in press), Sediment source characteristics of the Río Tinto, Huelva, SW Spain, in Foster, I.D.L. (ed.), *Tracers in Geomorphology,* John Wiley & Sons: London.

Schumm, S.A. (1973), Geomorphic thresholds and the complex response of drainage systems, in: Morisawa, M. (ed.) *Fluvial Geomorphology,* State University of New York, Binghampton, pp. 473-485.

Schumm, S.A. (1977), *The Fluvial System,* John Wiley & Sons, New York, 338 pp.

Schumm, S.A. (1979), Geomorphic thresholds: the concept and its applications, *Transactions of the Institute of British Geographers*, NS4, pp. 483-515.

Schumm, S.A. and Lichty, R.W. (1965), Time, space and causality in geomorphology, *American Journal of Science,* 263, pp. 110-119.

Schwarcz, H. and Gascoyne, M. (1984), Uranium-series dating of Quaternary deposits, in: Mahaneu, W.C. (ed.) *Quaternary Dating Methods,* Elsevier: Amsterdam, pp. 31-51.

Schwartz, H.E., Emel, J., Dickens, W.J., Rogers, P. and Thompson, J. (1990), Water quality and flows, in: Turner, B.L. *et al.,* (eds.), *The Earth as Transformed by Human Action,* Cambridge University Press, Cambridge, pp. 253-270.

Scott, K.M. and Gravlee, G.C. (1968), Flood surge on the Rubicon River, California – Hydrology, hydraulics and boulder transport, *U.S. Geological Survey Professional Paper,* 422-M, 40 pp.

Serre-Bachet, F., Guiot, J. and Tessier, L. (1992), Dendroclimatic evidence from southwestern Europe and northwestern Africa, in: Bradley, R.S. and Jones, P.D. (eds.) (1992), *Climate Since A.D. 1500,* Routledge, London, pp. 349 – 365.

Shaw, E.M. (1988), *Hydrology in Practice,* Second Edition, Chapman & Hall, 539 pp.

Shepherd, R.G. and Schumm, S.A. (1974), Experimental study of river incision, *Geological Society of America Bulletin,* 85, pp. 257-268.

Shi, F., Yi, Y. and Han, M. (1987), Investigation and verification of extraordinarily large floods on the Yellow River, *Journal of Hydrology,* 96, pp. 69-78.

Shields, A. (1936), Andwendung der ahnlichkeits-mechanik und der turbalenzforschung auf die geschiebebewungung, *Mitteilung der preussischen Versuchsanstatt für Wasserbau und Schiffbau*, pt. 26.

Sigafoos, R.S. (1964), Botanical evidence of floods and floodplain deposition, *Geol. Surv. Prof. Pap. (U.S.) 485-A,* pp. 1-35.

Sirvent, J., Desir, G., Gutierrez, M., Sancho, C. and Benito, G. (1997), Erosion rates in badland areas recorded by collectors, erosion pins and profilometer techniques (Ebro Basin, NE-Spain), *Geomorphology,* 18, pp. 61-75.

Smart, P.L. (1991), Uranium Series Dating, in: Smart, P.L. and Frances, P.D. (eds.) *Quaternary Dating Methods - A Users Guide,* QRA Technical Guide No. 4: Cambridge, pp. 45-83.

Smith, A.G. and Moores, E.M. (1974), Hellenides, in: Soencer, R.A. (ed.) *Mesozoic and Cenozoic Orogenic Belts,* Special Publication 4, Geological Society of London, pp. 159-185.

Smith, A.G., Woodcock, N.H. and Naylor, M.A. (1979), The structural evolution of a Mesozoic continental margin, Othris Mountains, Greece, *Journal of the Geological Society of London,* 136, pp. 589-603.

Smith, B.W., Rhodes, E.J., Stokes, S., Spooner, N.A. and Aitken, M.J. (1990), Optical dating of sediments: initial quartz results from Oxford, *Archaeometry,* 32 (1), pp. 19-31.

Smith, G.R., Woodward, J.C., Heywood, D.I., and Gibbard, P.L. (1998), Mapping glaciated karst terrain in Mediterranean mountain environments using SPOT and TM data, in: *Proceedings of the 24th Annual*

Conference and Exhibition of the Remote Sensing Society, The University of Greenwich, 9-11 September 1998, 457-463.

Smith, K. and Ward, R. (1998), *Floods: Physical Processes and Human Impacts,* John Wiley & Sons: Chichester, 382 pp.

Stedinger, J.R. and Cohn. T.A. (1986), Flood frequency analysis with historical and paleoflood information, *Water Resources Research,* 22, pp. 785-793.

Stedinger, J.R. and Baker, V.R. (1987), Surface water hydrology: historical and paleoflood information, *Reviews of Geophysics,* 25 (2), pp.119-124.

Stein, R., Nam, S.-L., Grobe, H. and Hubberten, H. (1996), Late Quaternary glacial history and short-term ice-rafted debris fluctuations along the East Greenland continental margin, in: Andrews, J.T., Austin, W.E.N., Bergsten, H. and Jennings, A.E. (eds.) *Late Quaternary Palaeoceanography of the North Atlantic Margins,* Geological Society Special Publication No. 111, pp. 131-151.

Stokes, S. (1992), Optical dating of young (modern) sediments using quartz: results from a selection of depositional environments, *Quaternary Science Reviews,* 11, pp. 153-159.

Stuiver, M. and Polach, H.A. (1977), Discussion of reporting ^{14}C data, *Radiocarbon,* 19 (3), pp. 355-363.

Stuiver, M., Long, A., Kra, R.S. and Devine, J.M. (eds.) (1993), *Radiocarbon: Calibration 1993,* 35 (1).

Sturdy, D.A., Webley, D. and Bailey, G. (1997), The Palaeolithic geography of Epirus, in: Bailey, G.N. (ed.), *Klithi: Palaeolithic Settlement and Quaternary Landscape in northwest Greece. Volume 2: Klithi in its local and regional setting,* McDonald Institute, pp. 587-614.

Talma, A.S. and Vogel, J.C. (1993), A simplified approach to calibrating ^{14}C dates, *Radiocarbon,* 35 (2), pp. 317-322.

Taylor, K.C., Lamorey, G.W., Doyle, G.A., Alley, R.B., Grootes, P.M., Mayewski, P.A., White, J.W.C. and Barlow, L.K. (1993), The flickering switch of Late Pleistocene climate change, *Nature,* 361, pp. 432-436.

Thomas, D.S.G., Bateman, M.D., Mehrshahi, D. and O'Hara, S.L. (1997), Development and environmental significance of an aeolian sand ramp of the Last-Glacial Age, Iran, *Quaternary Research,* 48, pp. 155-161.

Thompson, A. and Jones, A. (1986), Rates and causes of proglacial river terrace formation in south east Iceland; an application of lichenometric dating techniques, *Boreas,* 15, pp. 231-246.

Thompson, R. and Oldfield, F. (1986), *Environmental Magnetism,* Allen & Unwin: London, 219 pp.

Thouveny, N., de Beaulieu, J.-L., Bonifay, E., Creer, K.M., Guiot, J., Icole, M., Johnsen, S., Jouzel, J., Reille, M., Williams, T. and Williamson, D. (1994), Climate variations in Europe over the past 140 kyr deduced from rock magnetism, *Nature,* 371, pp. 503-506.

Trieste, D.J. (1992), Evaluation of supercritical/subcritical flows in a high-gradient channel, *Journal of Hydraulic Engineering,* 118, pp. 1107-1118.

Trieste, D.J. and Jarrett, R.D. (1987), Roughness coefficients of large floods, in: James, L.G.and English, M.J. (eds.), Irrigation and Drainage Division Speciality Conference, *Irrigation Systems for the 21st Century,* Portland, Oregon, 1987, Proceedings: New York, American Society of Engineers, pp. 32-40.

Tropeano, D. (1991), High flow events and sediment transport in small streams in the 'Tertiary Basin' area in Piedmont (Northwest Italy), *Earth Surface Processes and Landforms,* 16, pp. 323-339.

Turner, C. and Sánchez Goñi, M.-F. (1997), Late glacial landscape and vegetation in Epirus, in: Bailey, G.N. (ed.) *Klithi: Palaeolithic Settlement and Quaternary Landscape in northwest Greece. Volume 2: Klithi in its local and regional setting,* McDonald Institute, pp. 559-585.

Tzedakis, P.C. (1993), Long-term tree populations in northwest Greece through multiple Quaternary climatic cycles, *Nature,* 364, pp. 437-440.

Tzedakis, P.C. (1994), Vegetation change through glacial-interglacial cycles: a long pollen sequence perspective, *Philosophical Transactions of the Royal Society, London,* Series B, 345, pp. 403-432.

Tzedakis, P.C., Andrieu, V., de Beaulieu, J.-L., Crowhurst, S., Follieri, M., Hooghiemstra, H., Magri, D., Reille, M., Sadori, L., Shackleton, N.J. and Wijmstra, T.A. (1997), Comparison of terrestrial and marine records of changing climate of the last 500,000 years, *Earth Science and Planetary Science Letters,* 150, pp. 171-176.

U.S. National Research Council (1985), *Safety of Dams; Flood and Earthquake Criteria,* National Academy Press, Washington, D.C., 176 pp.

van Andel, T.H., Runnels, C.N. and Pope, K.O. (1986), Five thousand years of land use and abuse in the southern Argolid, Greece, *Hesperia,* 55, pp. 103-128.

van Andel, T.H., Zangger, E. and Demitrack, A. (1990), Land use and soil erosion in Prehistoric and Historical Greece, *Journal of Field Archaeology,* 17, pp. 379-396.

van Andel, T.H. and Tzedakis, P.C. (1996), Palaeolithic landscapes of Europe and environs, 150,000 - 25,000 years ago: an overview, *Quaternary Science Reviews,* 15, pp. 481-500.

Verrucchi, C. and Minisale, A. (1995), Multivariate statistical comparison of Northern Apennines Paleozoic sequences: a case study for the formations of the Monti Romani (Southern Tuscany - Northern Latium, Italy), *Applied Geochemistry,* 10, pp. 581-598.

Vita-Finzi, C. (1963), Carbon-14 dating of Medieval alluvium in Libya, *Nature,* 198, pp. 880.

Vita-Finzi, C. (1964), Synchronous stream deposition throughout the Mediterranean area in hisorical times, *Nature,* 202, pp. 1324.

Vita-Finzi, C. (1969), *The Mediterranean Valleys: Geological Changes in Historical Times,* Cambridge University Press, Cambridge.

Vita-Finzi, C. (1976), Diachronism of Old World alluvial sequences, *Nature,* 263, pp. 218-9.

Vogel, J.C., Fuls, A., Visser, E. and Becker, B. (1993), Pretoria calibration curve for short lived samples, *Radiocarbon,* 35 (1), pp. 73-86.

Wagstaff, J.M. (1981), Buried assumptions: some problems in the interpretation of the "Younger Fill" raised by recent data from Greece, *Journal of Archaeological Science,* 8, pp. 247-264.

Wainwright, J. (1996), Hillslope response to extreme storm events: The example of the Vaison-La-Romaine Event, in: Anderson, M.G. and Brooks, S.M. (eds.) *Advances in Hillslope Processes,* Volume 2, John Wiley & Sons, Chichester, pp. 997-1026.

Walling, D.E., Peart, M.R., Oldfield, F., and Thompson, R. (1979), Suspended sediment sources identified by magnetic measurements, *Nature,* 281, pp. 110-113.

Walling, D.E. and Moorehead, P.W. (1989), The particle size characteristics of suspended sediment: an overview, *Hydrobiologica,* 176/177, pp. 125-149.

Walling, D.E. and Woodward, J.C. (1992), Use of radiometric fingerprints to derive information on suspended sediment sources, *Erosion and Sediment Transport Monitoring Programmes in River Basins* (Proceedings of the Oslo Symposium, August 1992). IAHS Publ. no. 210, pp. 153-164.

Walling, D.E., Woodward, J.C. and Nicholas, A.P. (1993), A multi-parameter approach to fingerprinting suspended sediment sources, *Tracers in Hydrology* (Proceedings of theYokohama Symposium, July 1993) IAHS Publ. no. 215, pp. 329-328.

Walling, D.E. and He, Q. (1993), Towards improved interpretation of ^{137}Cs profiles in lake sediments, in: McManus, J. and Duck, R.W. (eds.) *Geomorphology and Sedimentology of Lakes and Reservoirs,* John Wiley & Sons: Chichester, pp. 31-53.

Walling, D.E. and He, Q. (1994), Rates of overbank sedimentation on the floodplains of several British rivers during the past 100 years, *Variability in Stream Erosion and Sediment Transport* (Proceedings of the Canberra Symposium, December 1994). IAHS Publication No. 224, pp. 203-210.

Walling, D.E. and Woodward, J.C. (1995), Tracing sources of suspended sediment in River Basins: a case study of the River Culm, Devon, UK, *Marine Freshwater Research*, 46, pp. 327-336.

Walling, D.E. and He, Q. (1997), Use of fallout ^{137}Cs in investigations of overbank sediment deposition on river floodplains, *Catena*, 29, pp. 263-282.

Walling, D.E., Owens, P.N. and Leeks, G.J.L. (1997), The characteristics of overbank deposits associated with a major flood event in the catchment of the River Ouse, Yorkshire, UK, *Catena*, 31, pp. 53-75.

Ward, R.C. (1978), *Floods: A Geographical Perspective*, Macmillan: London.

Webb, R.H. and Baker, V.R. (1987), Changes in hydrologic conditions related to large floods on the escelante River, South-Central Utah, in: Singh, V.P. (ed.) *Regional Flood Frequency Ananlysis*, D. Reidel, Norwell, Mass., pp. 309-323.

Webber, P.J. and Andrews, J.T. (1973), Lichenometry: A Commentary, *Arctic and Alpine Research*, 5 (4), pp. 295-302.

Wells, L.E. (1990), Holocene history of the El Niño phenomenon as recorded in flood sediments of northern coastal Peru, *Geology*, 18, pp. 1134-1137.

Wentworth, C.K. (1922), A scale of grade and class terms for clastic sediments, *Journal of Geology*, 30, pp. 377-392.

Wijmstra, T.A. (1969), Palynology of the first 30 metres of a 120 m deep section in northern Greece, *Acta, Bot. Neerl.*, 18, pp. 511-527.

Wijmstra, T.A. and Groenhart, M.C. (1983), Record of 700 000 years vegetational history in Eastern Macedonia (Greece), *Rev. Acad. Colomb. Ciencis Exactas, Fisi. Nat.*, 15, pp. 87-98.

Williams, G.P. (1983), Paleohydrological methods and some examples from Swedish fluvial environments: I cobble and boulder deposits, *Geografiska Annaler*, 65A pp. 227-243.

Williams, G.P. and Costa, J.E. (1988), Geomorphic measurements after a flood, in: Baker, V.R., Kochel, R.C. and Patton P.C. (eds.) *Flood Geomorphology*, John Wiley: New York, pp.

Williams, R.W., Collerson, K.D., Gill, J.B. and Deniel, C. (1992), High U/Th ratios in subcontinental lithospheric mantle: mass spectrometric measurements of Th isotopes in Gaussberg lamproites, *Earth and Planetary Science Letters*, 111, pp. 257-268.

Willis, K.J. (1992a), The Late Quaternary vegetational history of northwest Greece, I. lake Gramousti, *New Phytologist*, 121, pp. 101-117.

Willis, K.J. (1992b), The Late Quaternary vegetational history of northwest Greece, II. Rezina Marsh, *New Phytologist*, 121, pp. 119-138.

Willis, K.J. (1992c), The Late Quaternary vegetational history of northwest Greece, III. A comparative Study of two contrasting sites , *New Phytologist*, 121, pp. 139-155.

Willis, K. (1997), Vegetational history of the Klithi environment: a palaeoecological viewpoint, in: Bailey, G.N. (ed.), *Klithi: Palaeolithic Settlement and Quaternary Landscape in northwest Greece. Volume 2: Klithi in its local and regional setting*, McDonald Institute, pp. 395-414.

Windley, B.F. (1984), *The Evolving Continents*, John Wiley & Sons, Chichester.

Winstanley, D. (1973), Rainfall patterns and general atmospheric circulation, *Nature*, 245, pp. 190-194.

Wintle, A.G. (1977), Detailed study of a thermoluminescent mineral exhibiting anomalous fading, *Journal of Luminescence*, 15, pp. 385-393.

Wintle, A.G. (1991), Luminescence dating, in: Smart, P.L. and Frances, P.D. (eds.) *Quaternary Dating Methods - A Users Guide,* QRA Technical Guide No. 4: Cambridge, pp. 108-127.

Wise, S.M. (1980), Ceasium-137 and lead-210: a review of techniques and some application is geomorphology, in: Cullingford, R.A., Davidson, D.A. and Lewin, J. (eds.), *Timescales in geomorphology,* John Wiley & Sons, New York, pp. 109-127.

Wise, S.M., Thornes, J.B. and Gilaman, A. (1982), How old are the badlands? A case study from south-east Spain, in: Bryan, R.B. and Yair, A. (eds.) *Badland Geomorphology and Piping,* Norwich: Geobokks, pp. 259-277.

Wohl, E.E. (1992a), Bedrock benches and boulder bars: floods in the Burdekin Gorge of Autralia, *Geological Society of America Bulletin,* 104, pp. 770-778.

Wohl, E.E. (1992b), Gradient irregularity in the Herbert gorge of northeastern Australia, *Earth Surface Processes and Landforms,* 17, pp. 69-84.

Wohl, E.E., Fuertsch, S.J., and Baker, V.R. (1994), Sedimentary records of late Holocene floods along the Fitzroy and Margaret Rivers, Western Australia, *Australian Journal of Earth Sciences,* 41, pp. 273-280.

Wolman, M.G. (1967), A cycle of sedimentation and erosion in urban river channels, *Geografiska Annaler,* 49A, pp. 385-395.

Wolman, M.G. and Leopold, L.B. (1957), River flood plains: Some observations on their formation, *U.S. Geological Survey Professional Paper,* 282-c, pp. 87-109.

Wolman, M.G. and Miller, J.P. (1960), Magnitude and frequency of forces in geomorphic processes, *Journal of Geology,* 68, pp. 54-74.

Woman, M.G. and Gerson, R. (1978), Relative scales of time and effectiveness of climate in watershed geomorphology, *Earth Surface Processes and Landforms,* 3, pp. 89-208.

Wood, P.A. (1978), Fine-sediment mineralogy of source rocks and suspended sediment, Rother catchment, West Sussex, *Earth Surface Processes,* 3, pp. 255-263.

Woodward, J.C. (1990), *Late Quaternary Sedimentary Environments in the Voidomatis Basin, northwest Greece,* unpublished PhD thesis, Darwin College: Cambridge, 217 pp.

Woodward, J.C. (1995), Patterns of erosion and suspended sediment yield in Mediterranean river basins, in: Foster, I.D.L., Gurnell, A.M. and Webb, B.W. (eds.) (1995), *Sediment and Water Quality in River Catchments,* John Wiley & Sons Ltd., pp. 365-389.

Woodward, J.C. (1997), Late Pleistocene rockshelter sedimentation at Klithi, in: Bailey, G.N. (ed.), *Klithi: Palaeolithic Settlement and Quaternary Landscape in northwest Greece. Volume 2: Klithi in its local and regional setting,* McDonald Institute, pp. 361-376.

Woodward, J.C., Lewin, J. and Macklin, M.G. (1992), Alluvial sediment sources in a glaciated catchment: the Voïdomatis basin, Northwest Greece, *Earth Surface Processes and Landforms,* 17, pp. 205-216.

Woodward, J.C., Macklin, M.G. and Lewin, J. (1994), Pedogenic weathering and relative-age dating of Quaternary alluvial sediments in the Pindus Mountains of Northwest Greece, in: Robinson, D.A. and Williams, R.B.G. (eds.) *Rock Weathering and Landform Evolution,* John Wiley & Sons Ltd., pp. 259-283.

Woodward, J.C., Lewin, J. and Macklin, M.G. (1995), Glaciation, river behaviour and Palaeolithic settlement in upland northwest Greece, in: Lewin, J., Macklin, M.G. and Woodward, J.C. (eds.) (1995), *Mediterranean Quaternary River Environments,* Balkema/Rotterdam/Brookfield, pp. 115-129.

World Climate Disk (1992), Global Climate Change Data, Chadwick-Healey.

Worsley, P. (1990), Lichenometry, In: Goudie, A. (ed.) *Geomorphological Techniques* (2nd Edition), pp. 422-428.

Yanosky, T.M. (1982), Effects of flooding upon woody vegetation along parts of the Potomac River Floodplain, *U.S. Geological Survey Professional Paper,* 1206, pp. 1-21.

Yanosky, T.M. (1983), Evidence of floods on the Potomac River from anatomical abnormalities in the wood of floodplain trees, *U.S. Geological Survey Professional Paper,* 1296, pp. 1-46.

York, D. (1969), Least squares fitting of a straight line with correlated errors, *Earth and Planetary Science Letters,* 5, pp. 320-324.

Yu, L. and Oldfield, R. (1989), A multivariate mixing model for identifying sediment source from magnetic measurements, *Quaternary Research,* 32, pp. 168-181.

Yu, L. and Oldfield, R. (1993), Quantitative sediment source ascription using magnetic measurements in a reservoir-catchment system near Nijar, S.E. Spain, *Earth Surface Processes and Landforms,* 18, pp. 441-454.

Zawada, P.K. (1997), Palaeoflood hydrology: method and application in flood-prone South Africa, *South African Journal of Science,* 93, pp. 111-132.

Zonnefeld, K.A.F. (1996) Palaeoclimatic reconstruction of the last deglaciation (18-8 ka BP) in the Adriatic Sea region; A land-sea correlation based on palynological evidence, *Palaeogeography, Palaeoclimatology, Palaeoecology,* 1, pp. 89-106.

Zonnefeld, K.A.F. and Boessenkool, K.P. (1996), Palynology as a tool for land-sea correlation: an example from the eastern Mediterranean region, in: Andrews, J.T., Austin, W.E.N., Bergsten, H. and Jennings, A.E. (eds.) *Late Quaternary Palaeoceanography of the North Atlantic Margins,* Geological Society Special Publication No. 111, pp. 351-357.